ITER TECHNICAL REPORT

iter
china eu india japan korea russia usa

REPORT NO.

ITR-24-005

TITLE

ITER Research Plan within the Staged Approach (Level III – Final Version)

AUTHOR/AUTHORS

D.J. Campbell, A. Loarte, D. Boilson, X. Bonnin, P. de Vries, L. Giancarli, Y. Gribov, S.H. Kim, M. Lehnen, T. Luce, I. Nunes, A.R. Polevoi, S.D. Pinches, R.A. Pitts, R. Reichle, M. Schneider, J. van der Laan, G. Vayakis

AUTHOR EMAIL(S)

alberto.loarte@iter.org

DATE

10th April 2024

ITER Research Plan within the Staged Approach (Level III - Final Version)

D.J. Campbell[1], A. Loarte[1], D. Boilson[1], X. Bonnin[1], P. de Vries[1], L. Giancarli[1], Y. Gribov[1], M. Henderson[1,2], S.H. Kim[1], Ph. Lamalle[1,3], M. Lehnen[1], T. Luce[1], I. Nunes[1], A.R. Polevoi[1], S.D. Pinches[1], R.A. Pitts[1], R. Reichle[1], M. Schneider[1], J. Snipes[1,4], J. van der Laan[1], G. Vayakis[1], and ITER IRP contributors
(see Annex A and Annex B).

[1] ITER Organization, Route de Vinon-sur-Verdon, CS90046, 13067 St Paul-lez-Durance, France
[2] Present institution: United Kingdom Atomic Energy Authority, Culham Centre for Fusion Energy, Culham Science Centre, Abingdon, Oxon OX14 3DB, United Kingdom
[3] Present Institution: LPP-ERM/KMS, avenue de la Renaissance, 30, B-1000 Brussels, Belgium
[4] Present Institution: Princeton Plasma Physics Laboratory, PO Box 451, Princeton, NJ 08543-0451, United States of America
E-mail: campbell-dj@t-online.de

Contents

Glossary and Acronyms

2016-FP	ITER First Plasma planned in the FP phase of the 2016-IRP
2016-IRP	Staged Approach Baseline 2016 ITER Research Plan (2XUY9N)
AFP	Augmented First Plasma
AP	Assembly Phase
ASDEX	Axially Symmetric Divertor Experiment
Be	Beryllium
CIS	Central Interlock System
CPS	Coil Protection System
CQ	Current Quench of a disruption
CSS	Central Safety System
CS	Central Solenoid
CXN	Charge-Exchange Neutrals
DD	Deuterium Deuterium
DEMO	Demonstration power plant
DBC	Disruption Budget Consumption
DMS	Disruption Mitigation System
DNB	Diagnostic Neutral Beam
DT	Deuterium-Tritium
EAST	Experimental Advanced Superconducting Tokamak
ECRH	Electron Cyclotron Resonant Heating
ECWC	Electron Cyclotron Wall Conditioning
ELM	Edge Localized Mode
EO	Engineering Operation
FEP	Fuel Enrichment Plant
FP	First Plasma
FPE	First Plasma Exhaust System
FPO	Fusion Power Operation
FPPC	First Plasma Protection Components
FW	First Wall
FWP	First Wall Panel
GDC	Glow Discharge Cleaning
GIS	Gas Injection System
HC	Hot Cell
HCCB	Helium-Cooled Ceramic Breeder
HCS	Helium Cooling System
HFS	High Field Side
HNB	Heating Neutral Beam
HV	High Voltage
IC	Integrated Commissioning

I&C	Instrumentation & Control System
ICH	Ion Cyclotron Heating
ICRF	Ion Cyclotron Range of Frequencies
ICWC	Ion Cyclotron Wall Cleaning
ILW	ITER-like Wall (Be) installed at JET
IRP	ITER Research Plan
ISS	Isotope Separation System
ITER ELMCC	ITER ELM control coil
ITER RAMI	Reliability, Availability, Maintainability and Inspectability
ITPA	International Tokamak Physics Activity
ITR	ITER Technical Report
JET	Joint European Torus
LCFS	Last Closed Flux Surface
LFS	Low Field Side
LTM	Long Term Maintenance
MFC	Micro-Fission Chamber
MHD	Magnet Hydro Dynamic
NAS	Neutron Activation System
NBI	Neutral Beam Injection
NBMFRS	Neutral Beam Magnetic Field Reduction System
Ne	Neon
n_{GW}	Greenwald density limit
NTM	Neoclassical Tearing mode
OMP	Outer Mid Plane
PCS	Plasma Control System
PF	Poloidal field
PF	Pipe Forest
PFC	Plasma-Facing Components
PFPO	Pre-Fusion Power Operation
PFPO-2	Pre-Fusion Power Operation 2
PMA	Particular Material Appraisal
RAFM	Reduced Activation Ferritic-Martensitic
RE	Runaway Electrons
RH	Remote-Handling
RMS	Root Mean Square
RoX	Return on Experience
SCD	Single Crystal Diamond
SNU	Switching Network Units
SOL	Scrape Off Layer
SPND	Self-Powered Neutron Detector
SQRS	Simplified Q2 Recycling System
STM	Short Term Maintenance

TAS	Tritium Accountancy System
TBM	Test Blanket Module
TBS	Test Blanket Systems
TES	Tritium Extraction System
TF	Toroidal Field
TFTR	Tokamak Fusion Tet Reactor
TORE SUPRA	Torus Superconductor Tokamak
TPR	Tritium Production Rate
TQ	Thermal Quench of a disruption
VDE	Vertical Displacement Event
VV	Vacuum Vessel
W	Tungsten
WCCB	Water-Cooled Ceramic Breeder
WCLL	Water-Cooled Lithium-Lead
WCS	Water Cooling System
WEST	W-Environment in Steady-State Tokamak
XGC	Gyrokinetic modelling code

Abstract

The goals of the ITER Research Plan (IRP) are to provide a guide to the overall program of research activities to be undertaken within the framework of the ITER Project and to develop a strategy towards the attainment of the level of physics and technology performance required to meet the ITER mission goals. The current version of the IRP was developed within the revised ITER baseline schedule, referred to as the 'Staged Approach', and focusses on research activities to be implemented during the ITER Operations Phase, in particular, on fusion plasma physics R&D and on the R&D and testing program of (tritium breeding) Test Blanket Modules (TBM). It also makes recommendations on the preparatory R&D required to support routine and reliable operation of the ITER tokamak in hydrogen, helium, deuterium and deuterium-tritium plasma scenarios. The staged expansion of the operational capabilities of the ITER tokamak and facility is described and the implications for the phasing of the experimental program towards the achievement of high fusion power are discussed. A detailed analysis of the progressive development of plasma scenarios satisfying the specified operational milestones for the successive experimental campaigns is developed and the potential for physics studies of fusion plasmas under conditions relevant to fusion power production and, in particular, in burning plasmas is detailed. Key challenges in the development of suitable plasma scenarios for the production of several hundred MW of fusion power at high fusion gain in both inductive and non-inductive plasma scenarios are presented and the current approaches to their resolution are reviewed. The perspective for the longer-term evolution of the ITER research program in the context of developing the physics and technology basis for DEMO is also outlined. This is the final version of the Level III IRP and has been revised to reflect the final planning for the evolution of the ITER Plant Configuration within the Staged Approach.

Keywords: Tokamak, ITER, DT experiments, Tritium breeding, H-mode, Steady-state operation

---

This ITER technical report describes at Level III the ITER Research Plan consistent with the 2016 Staged Approach Baseline and the associated tokamak machine and ancillary systems' configurations adopted in its various phases. This is an evolution from the ITER Research Plan within the Staged Approach (Level III - Provisional Version) (ITR-18-003) in which several options for the tokamak machine and ancillary systems' configurations were considered in some phases. For the options maintained in the 2016 Staged Approach both this new ITER Technical Report and ITR-18-003 describe very similar plans with the details given in ITR-18-003 remaining valid. In addition, this new ITER Technical Report provides a major update of the required R&D to support the ITER Research Plan which has guided the International Tokamak Physics Activity R&D programme in the recent years and will further guide in the future for the many issues which are common between the 2016 Staged Approach ITER Baseline and the 2024 New ITER Baseline.

1. Introduction

The overall programmatic objective of the ITER project [1], 'to demonstrate the scientific and technological feasibility of fusion energy for peaceful purposes', is defined by a series of scientific and technical goals designed to establish the physics basis and much of the technological basis for design and construction of DEMO device(s) capable of electricity production from deuterium-tritium fusion. The scientific goals, defined in terms of plasma fusion performance, are:

- The device should achieve extended burn in inductively driven plasmas with the ratio of fusion power to auxiliary heating power, Q, of at least 10 ($Q \geq 10$) for a range of operating scenarios and with a duration sufficient to achieve stationary conditions on the timescales characteristic of plasma processes.
- The device should aim at demonstrating steady-state operation using non-inductive current drive with the ratio of fusion power to input power for current drive of at least 5.
- In addition, the possibility of controlled ignition should not be precluded.

Technical goals are:

- The device should demonstrate the availability and integration of technologies essential for a fusion reactor (such as superconducting magnets and remote maintenance).
- The device should test components for a future reactor (such as systems to exhaust power and particles from the plasma).
- The device should test tritium breeding module concepts that would lead in a future reactor to tritium self-sufficiency, the extraction of high-grade heat and electricity production.

The primary aim of the ITER Research Plan (IRP) is to define the plan of research and development and of facility exploitation necessary to meet these ITER mission goals. The research and development program includes activities directly related to specification of performance requirements for ITER components as well as R&D required from other facilities, so as to provide a solid physics and technology basis for the efficient exploitation of ITER. In its final form, the IRP will define the full range of R&D activities to be implemented in pursuit of the detailed scientific and technical goals. The emphasis in this version of the IRP is on the definition of the research program which will be implemented to satisfy the key scientific goals, while the discussion of technology activities is limited to the Test Blanket Module (TBM) testing program. While this latter element satisfies a key technical mission goal, future developments of the IRP are expected to extend the discussion of technology R&D activities to encompass the wide-ranging research which will be undertaken on ITER tokamak, auxiliary and plant systems in pursuit of the full scope of the project's technical mission goals.

The IRP also aims to provide an analysis of the ITER facility's capability to fulfil its mission and considers possible upgrade paths which may be required to address science and technology issues supporting the achievement of specific mission goals. The current version outlines options for such upgrades and indicates the potential impact of these upgrades on the project's scientific research program during the Operations Phase. In addition, a risk analysis has been carried out in which the likelihood and consequences of negative R&D outcomes are assessed, identifying, where appropriate, possible risk mitigation measures.

The Research Plan is organized around a series of key thematic research areas, which are integrated to form an exploitation plan for the facility. This exploitation plan has been embedded within the 'Staged Approach' strategy developed during the revision of the ITER project schedule in 2015 - 2016, e.g., [2]. The implications of this strategy for the overall structure of the IRP and for the scheduling of the key activities within the research program, including the transition to operation with deuterium-tritium fuel leading to significant fusion power production, are outlined in section 2.

Within the Staged Approach, operation of the ITER device is foreseen to develop in a series of experimental campaigns interspersed with major enhancements to the hardware capabilities providing access to more extensive experimental activities and leading, after approximately 10 years of operation, to the first studies of DT plasmas. Thereafter, the focus of the research program will be the optimization of burning plasma operation towards high fusion power production in a range of operational scenarios. Within a longer term perspective, the burning plasma experiments would address science and technology issues influencing design and operational issues for DEMO-class devices, exploiting a range of potential upgrades which would enhance the DEMO-relevance of the research program. The experimental program foreseen for the operational campaigns in hydrogen, helium, deuterium and deuterium-tritium plasmas during the preparation for and demonstration of significant fusion power in long-pulse operation is detailed in section 3.

The testing of prototypical tritium-breeding modules for DEMO devices is a central mission goal of the ITER technology research program and a unique capability of the ITER facility. A structured program on the testing of several candidate breeding blanket technologies developed by the ITER Members, ultimately testing their capability for tritium breeding and the extraction of high-grade heat under long-pulse exposure to high fusion power will be performed within the TBM program, as discussed in section 4.

Identifying key physics issues requiring further R&D in advance of ITER operation, to support the efficient scientific exploitation of the ITER device and to ensure its routine and robust operation, has provided a significant motivation for the development of the IRP well in advance of the ITER Operations Phase. The principal issues which should be addressed within the international fusion research program on existing experimental devices and the implications of these issues for ITER's exploitation are outlined in section 5.

The discussion of the IRP presented in this paper is an abridgement of the preliminary Level III IRP document, available as [3], focusing on the main themes in fusion science and technology research developed there, but revised to reflect the final planning for the evolution of the ITER Plant Configuration within the Staged Approach. This latter incorporates a series of appendices which discuss detailed issues relating to the implementation of the research program and to the phasing of heating and current drive and diagnostic systems associated with the implementation. To avoid repetition of this material here, where necessary these appendices will be referred to in the form, e.g., [3-Appendix A].

2. ITER Research Plan: Aims and Structure

2.1 Objectives

Initial development of the IRP was launched within the scope of the ITER Design Review, which was conducted in the period 2007 - 2008 to verify the suitability of the ITER facility design to meet the project's mission goals. Developed as a collaboration involving the ITER Organization (IO), the ITER Domestic Agencies (DAs) and experts from the International Tokamak Physics Activity (ITPA) and ITER Members' fusion communities, the resulting analysis, referred to as IRP-v1.0, was valuable in providing guidance to the capabilities required to support the implementation of a scientific research program which could address, and indeed fulfil, the project's key scientific mission goals. As a result of subsequent evolution in the construction and installation strategy, e.g., the facility configuration for First Plasma, several revisions of the IRP were prepared to reflect the impact on the implementation of and time schedule for the scientific research program. The comprehensive revision of the ITER Baseline, performed in the period 2015 - 2016 in response to a request from the ITER Council, stimulated a wide-ranging re-analysis of the IRP in support of the development of the revised strategy for the overall project schedule (the Staged Approach).

The revised IRP presented here has again drawn on the wide-ranging expertise in fusion research and tokamak operational experience within the IO, DAs, ITPA and Members' fusion communities. The collaboration analyzed the key activities required to develop the research program following First Plasma, aligning the experimental activities with the planned hardware configuration within the Staged Approach (see figure 1) so as to: (i) commission all required auxiliary systems with plasma to full performance (with pulse durations appropriate to the program requirements); (ii) develop the experimental capability required to achieve initial DT fusion power production at levels of several hundred MW; and (iii) propose a program of experiments in DT plasmas aimed at meeting the project's key mission goals in both inductive and non-inductive plasma scenarios, incorporating also the needs of the TBM testing program. These studies also addressed:

- Whether requirements for system availability were consistent with the planned experimental program;
- Estimates of the operational time required for the various experimental activities within the program;
- Experimental or operational issues which would require further analysis within the ITER R&D program to support the future development of the Research Plan;
- Risks to the Research Plan and possible mitigation measures;
- Possible upgrades which could be incorporated later in the Operations Phase to expand the experimental capabilities, to improve plasma performance and to address specific aspects of the physics and technology basis for DEMO-class devices.

The results discussed in the following reflect the outcome of the analysis developed in response to the questions outlined above. The resultant research program reflects the constraints on the availability of operational capabilities associated with the Staged Approach. A key aim within each experimental campaign is the rapid commissioning and exploitation of the installed

hardware capabilities to advance the level of plasma performance and to lay the basis for successive operational phases, identifying, where necessary, preferred options for later upgrades.

An attempt has also been made to assign estimates of durations to the various elements of the experimental program within the IRP, but these are necessarily uncertain and become more so as the IRP progresses towards fusion power production, involving the study and optimization of burning plasmas, an entirely new regime of laboratory plasma research to which ITER will provide access. Nevertheless, these estimates have been developed to assess the feasibility of accomplishing the major milestones for each phase of the research program within the foreseen project timescale. A more important output of the plan, at this stage of its development, is the logical sequence developed for the programmatic activities and the identification of the necessary prerequisites for the implementation of the major activities, in terms both of auxiliary hardware availability and of output from previous steps in the plan.

2.2 ITER Baseline Schedule: the Staged Approach

In response to a request from the ITER Council, during the period 2015 - 2016 the ITER project management developed a revised resource-loaded long-term schedule for the ITER project. The revised baseline schedule, which was endorsed by the ITER Council in November 2016, was aimed towards ensuring successful completion of construction and entry into operation of the ITER facility as rapidly as possible within the Members' resource constraints. The Staged Approach strategy which guided the revision of the project schedule foresees phasing of the completion and installation of various hardware elements so as to allow plasma operation to be launched at the earliest feasible date, while supporting a gradual expansion of the operational capabilities and the scope of the experimental program. The Research Plan has been adapted to the new strategy with the overall aim of exploiting the available experimental capability to prepare the transition to nuclear operation in the most effective way from a schedule perspective.

A schematic of the structure of the revised baseline schedule, covering the initial years of ITER operation leading to the launching of DT fusion power production, is shown in figure 1, while a more detailed discussion of the gradual increase in operational capabilities associated with the phased installation is given in section 2.3. Within the four stages of the revised operational schedule (including the longer-term extension of the final stage to an extensive development program of DT fusion power production in long-pulse DT scenarios and a research program in burning plasma studies), the principal goals are:

- **First Plasma (FP):** achievement of the First Plasma milestone of plasma breakdown in hydrogen or helium with at least 100 kA of plasma current for at least 100 ms; during the subsequent Engineering Operation phase for commissioning of the Magnet systems to full current, operation with circular limiter plasmas of up to 1 MA is not excluded.
- **Pre-Fusion Power Operation 1 (PFPO-1):** extensive 'commissioning with plasma' activities will be undertaken to establish diverted plasma operation in hydrogen/helium up to at least 7.5 MA/5.3 T, supported by a program of plasma control, diagnostics, Electron Cyclotron Resonant Heating (ECRH) commissioning and the systematic development of a disruption management/ mitigation capability to prepare for operation at higher currents; exploration of H-mode access and sustainment with toroidal fields of up to 2.65 T supported

by ECRH; this may involve operation at a toroidal field of 1.8 T if plasma initiation at this field value can be robustly demonstrated.

- **Pre-Fusion Power Operation 2 (PFPO-2):** initial emphasis would be given to commissioning of the Heating Neutral Beam (HNB), Diagnostic Neutral Beam (DNB) and Ion Cyclotron. Resonance Frequency (ICRF) heating systems to full power, together with the necessary plasma control capability, to support the subsequent program; development of H-mode operation in hydrogen up to, at least, 7.5 MA/2.65 T, with helium as back-up if this is not possible, incorporating reliable edge localized mode (ELM) control and divertor heat flux control would be a major thrust during this period of the research program; a further key goal would be the development of high-power L-mode operation to demonstrate the full technical capability of the device (i.e. operation at 15 MA/5.3 T); systematic studies of plasma-wall interactions and issues such as plasma-facing component erosion, redeposition, dust production, fuel retention and fuel removal would also be pursued in preparation for the nuclear phase. If 1.8 T plasma operation were feasible, hydrogen and helium H-modes would be possible at this stage, providing a physics basis to compare H-modes in H and He, which could be very important if hydrogen H-modes are not possible at higher fields during this period. In addition, if H-mode operation at 1.8 T had been achieved in PFPO-1, this would allow the evaluation of the effects of the 3-D fields created by the TBMs, by comparing PFPO-1 (no TBMs) plasmas with those of PFPO-2 (with TBMs), and the development of mitigation schemes for such effects beyond basic error field correction, if required.
- **Fusion Power Operation (FPO)**: building on the experimental capabilities acquired during the previous operational phase, the initial aim of this campaign would be to demonstrate operation of high-power H-modes in deuterium to prepare plasma scenarios for DT operation; beginning with trace tritium experiments, a gradual transition to full DT operation would be undertaken as the fuel reprocessing throughput of the Tritium Plant increased; the goal of the first campaign of DT operation would be to demonstrate fusion power production of several hundred MW for at least 50 s at $Q \geq 5$. In subsequent experimental campaigns, the fusion gain would be optimized to achieve $Q \geq 10$, the pulse duration in inductive plasma scenarios would be extended towards the goal of 300 - 500 s burn required by the ITER *Project Specification*, and hybrid and fully non-inductive scenarios would be developed to achieve burn durations in the range 1000 - 3000 s with $Q \sim 5$.

The plan for each of the exploitation phases is based on a series of key research issues around which an experimental program has been developed to commission systems with plasma, to develop certain control capabilities, to establish specific plasma scenarios, to address uncertainties in the physics of plasmas at the ITER scale and in the burning plasma regime, and finally to perform detailed scientific studies of burning plasmas while optimizing their fusion performance. There is greater uncertainty, of course, in relation to the details of later phases of the Research Plan, since the results derived from earlier phases are expected to dominate the final planning of subsequent phases and, in addition, ITER is the first experiment which will provide access to the study of burning plasmas.

2.3 Assumptions on phasing of ITER operational capabilities

The central concept of the revised ITER schedule within the Staged Approach is the phased installation of the operational capability of the ITER tokamak and of the ITER facility. The framework for the evolution of the baseline 'Plant Configuration' for each stage in the revised construction and operations schedule was developed as a balance between the available resources for completion of major tokamak and facility elements and the capabilities required to support the achievement of specific scientific and technical milestones within the Research Plan. Figure 2 provides a schematic overview of this evolution in plant configuration during the Staged Approach. The major elements impacting on the implementation of the experimental program are summarized here for ease of reference. A more detailed discussion of the key considerations relating to the phasing of the H&CD systems and to the sequence of Diagnostic installation is presented in [3-Appendix G] and [3-Appendix H] respectively.

The following evolution of the auxiliary systems has been agreed to support the experimental programs discussed in sections 3 and 4:

(I) First Plasma (H/He):

- Initial set of poloidal field (PF) coil/ central solenoid (CS) power converters;
- First Plasma Protection Components (FPPC) to provide required protection of in-vessel systems and vacuum vessel;
- Central Control System fully operational;
- H&CD installed power: P_{ECRH} = 8 MW from 1 upper launcher (allowing 5.8 MW to be coupled to the plasma from 7 of the 8 available gyrotrons due to constraints on the dimensions of the inboard wall ECRH mirrors);
- A limited subset of the baseline Diagnostic capability, essentially to characterize plasma breakdown and to provide limited plasma control and machine protection;
- Fuelling: gas injection capability;
- Vacuum: 6 cryopumps incorporating activated charcoal;
- Vacuum Vessel baking and preliminary Glow Discharge Cleaning system.

(II) Pre-Fusion Power Operation (H/He) 1:

- PF/CS converters upgraded to full performance;
- Shielding blanket/beryllium first wall and all-tungsten divertor;
- H&CD installed power: P_{ECRH} = 20 MW (5 launchers);
- A subset of the baseline Diagnostic capability, with the emphasis on plasma control and machine protection;
- Fuelling: full gas injection capability and at least 2 pellet injectors;
- Disruption mitigation system: hardware commissioned;
- Error field correction coils: hardware commissioned;
- Vertical stabilization coils: hardware commissioned;
- In-vessel viewing system; hardware commissioned;
- An appropriate Be handling capability will be provided;

- H-mode operation in hydrogen in this phase would require an upgrade of, at least, 10 MW to the ECRH system; this has been evaluated to be technically feasible, but no decision regarding its implementation has been made.

(III) Pre-Fusion Power Operation (H/He) 2:

- H&CD installed power: P_{NB} = 33 MW (870 keV H^o), P_{ECRH} = 20 MW (30 MW if upgrade option were implemented in PFPO-1), P_{ICRF} = 20 MW (2 antennas);
- Diagnostic Neutral Beam (DNB) system;
- An extended set of Diagnostics for advanced control and physics studies;
- Fuelling: 2 additional pellet injectors;
- ELM control coil system: hardware commissioned;
- First set of TBM modules (PFPO-2-TBM) installed for initial phase of testing program;
- Tritium Plant undergoing integrated non-active commissioning.

(IV) Fusion Power Operation (D/DT):

It should be expected that essentially all elements of the tokamak and its auxiliary systems will have been brought into operation during the PFPO phase in order to allow the efficient implementation of the D and DT phases of the program. Significant new capabilities that would be available for the nuclear phase include NBI with 1 MeV D^o, the measurement capability for 14.1 MeV neutrons, since this aspect of the neutron calibration will be scheduled just prior to the start of the nuclear phase of operations, and a range of fusion product diagnostics (see [3-Appendix H]). A principal goal of the PFPO phase is to ensure that all of the H&CD capability is commissioned to full power for durations of at least ~100 s before the nuclear phase and that all elements of the fuelling systems are operational with all required gases except deuterium and tritium. As will be discussed in section 3.2.1, key aims of the PFPO phase include commissioning of all aspects of magnetic control, several aspects of kinetic control (e.g., control of divertor heat exhaust), demonstration of reliable and effective disruption mitigation (including runaway electron mitigation), and demonstration of ELM suppression/ control. Thus, essentially all of the plant and ancillary systems should be in an advanced state of operation by the beginning of the nuclear phase. The major plant commissioning activity that would proceed in parallel with nuclear operation would be the expansion of the processing throughput of the Tritium Plant. This would rise gradually during the deuterium experiments and into the initial period of DT operation. In addition, if essential upgrades have been identified during PFPO to achieve the Q = 10 goal, it is likely that these will be implemented either before, or in the early stages of, FPO. Upgraded systems may require dedicated commissioning time.

2.4 Structure of the Research Plan

An essential element in the integration of the ITER Research Plan into the Staged Approach is the link between the hardware capabilities of the ITER facility (the Plant Configuration) at each stage of the Operations Phase and the corresponding objectives. As noted previously, a balance has been struck between the project-level constraints on the procurement schedule and the operational requirements to fulfil overall objectives for the PFPO phase which would support a timely transition to DT operation. This understanding has been derived from the development of the Research Plan in parallel with ITER construction and additional experience gained through

the physics R&D programs in the Members' fusion communities, which have provided insight on the experimental time that will probably be required to progress from FP to a level of plasma performance and operational efficiency in ITER which would: (i) confirm that the tokamak systems were performing satisfactorily, (ii) provide confidence that an adequate level of plasma performance had been achieved in ITER, and (iii) that the necessary level of experimental expertise (integration and control of plasma scenarios) had been demonstrated to justify the transition to DT operation and fusion power production. The resultant schedule towards DT operation incorporates both project level and scientific/ technical considerations on the path towards DT operation.

In addition to the logical structure defining the steps necessary to progress from FP to full performance in DT plasmas, the Research Plan makes estimates of the duration of each of the steps within the experimental program to obtain an overall estimate of the operational time required for successive phases of the program. This analysis is clearly subject to substantial uncertainties so far in advance of ITER exploitation. Nevertheless, on the basis of discussions with fusion community experts, a first estimate of the experimental time required by the principal activities within the IRP has been assembled and this forms the basis of the estimates given in the tables accompanying the detailed discussion of each experimental campaign.

The Research Plan experimental program within the Staged Approach begins with 3 experimental phases (including FP) in hydrogen/helium (i.e., non-activating fuels) in which all of the tokamak, plant and auxiliary systems are commissioned with plasma to high performance (not all aspects of system performance can be commissioned to the highest level in advance of fusion power production). Following the transition to the use of D/DT fuels, an initial campaign is designed to achieve significant fusion power production as rapidly as possible, and this is followed by a sequence of experimental campaigns on a two-yearly cycle. In these campaigns, in which the ITER scientific and technical mission goals are pursued (including the TBM testing program), burning plasma physics is studied in detail, and the physics basis for DEMO design and operation is developed. The present Plan develops the exploration of the DT phase within the achievement of the principal scientific mission goals and so limits the time horizon related to the elaboration of the program to the first 3 experimental campaigns in DT plasmas, as illustrated in figure 3. The broad aims of each phase of this experimental program have been outlined in section 2.2, and these are expanded in some detail in sections 3.2.1 and 3.3.1.

The resultant structure of the experimental program, illustrated in figure 3, therefore consists of:

- **First Plasma Campaign:** ~1 month, plus 6 months of Engineering Operation including, possibly, some plasma operation;
- **Pre-Fusion Power Operation 1:** 18 months of H/He plasmas;
- **Pre-Fusion Power Operation 2**: 21 months of H/He plasmas;
- **Fusion Power Operation 1:** 16 months of initially D and subsequently DT plasmas
- **Fusion Power Operation 2:** 16 months of DT plasmas;
- **Fusion Power Operation 3:** 16 months of DT plasmas.

It should be emphasized that although the schematic representation of the Research Plan shown in figure 3 highlights the milestones associated with the achievement of specific fusion power and plasma performance goals, wide-ranging accompanying research on all aspects of burning plasma

physics will be a central component of the research conducted during the FPO campaigns, including:

- Waves and energetic particle physics;
- Fuel mixture control and helium exhaust;
- Self-heating and thermal stability;
- Macroscopic stability physics and control;
- Multi-scale transport physics;
- Physics of the plasma-boundary interface;
- Integrated burning plasma scenario development.

Additional key physics issues for advanced modes include current profile control and MHD control at pressures near the no-wall β-limit. These studies will not only address issues related to the ITER core mission, but also leverage the unique capabilities that ITER provides within the worldwide fusion program. Examples of such capabilities include operation at low normalized gyroradius, operation with a low collisionality pedestal coupled with a high-density divertor, and operation with a large population of isotropic energetic particles.

Beyond this sequence of experimental campaigns which is the subject of the analysis presented in succeeding sections, the ITER experimental program would, of course, be expected to implement extensive scientific and technical R&D in pursuit of its overall mission goal to demonstrate the scientific and technological feasibility of fusion energy for peaceful purposes and to provide key information for the further development of DEMO. However, this longer-term development of the ITER program is beyond the scope of this version of the Research Plan.

As a point of reference, an estimate of the maximum number of experimental days available in PFPO-1, PFPO-2 and FPO (per campaign) is given in Table 1. The basis for this estimate is derived from the assumptions developed in the ITER RAMI (Reliability, Availability, Maintainability and Inspectability) analysis [4]: in 2-shift operation, which forms the basis of operational planning within the Staged Approach, it is assumed that the operational pattern is 12 days of experimental operation and 2 days of short-term maintenance within a 14-day cycle.

As required by the *Project Requirements*, ITER shall be capable of executing the next pulse after a duration not exceeding three times the duration of the previous pulse or 1800 s whichever is longer. This implies that within a 2-shift operational day, a 30-minute pulse repetition time should be maintained for pulses with an overall duration of less than ~ 600 s allowing, in principle, 32 plasma pulses. When corrected for the 60% 'Inherent Availability' assumed for the RAMI analysis, and the loss of time associated with disruptions/disruption recovery, a total of 13 'good' plasma pulses (i.e., plasmas contributing fully to the ITER Research Plan) per day results. Later in the FPO phase, as pulses with durations beyond 600 s are developed, the number of pulses per day will, of course, be reduced with a minimum number of pulses determined by the pulse repetition rate described above. However, this reduction in 'good' pulses per day for long pulse operation will be compensated, to some extent, by a reduction in the frequency of disruptions; this will necessarily be substantially lower in the FPO phase than in the PFPO phase as a result of the progress made in disruption management, as outlined in later sections, and of the need to avoid significant loss of experimental time due to the impact on in-vessel components of disruptions at high fusion power.

The estimates given in Table 1 are, of course, likely to be an upper bound to the number of days actually available to the experimental program, since the system performance assumed in the RAMI analysis relates to the operation of mature systems, but they nevertheless provide a basis for comparison with the estimates of the experimental time required for the main activities within the Research Plan presented in more detailed tables for each experimental campaign presented later.

The transition from the PFPO phase, during which non-activating fuels are used, to the FPO phase, where deuterium and deuterium-tritium plasmas form the basis of the experimental program, is, of course, a key step in the Research Plan. Within the Staged Approach, this is planned to occur following Integrated Commissioning IV. In preparation for supporting the experimental program following this transition, it is planned that the Tritium Plant will take the significant step of embarking on the commissioning of its operation with tritium in parallel with PFPO operations (see figure 3). It is expected that early in FPO campaign 1, the T-Plant will be able to supply trace tritium amounts for the ITER experimental program. In the course of FPO-1, a fraction of the Isotope Separation System (ISS) will be operational and will be able to provide pure tritium for ITER operation, reaching a daily fuel throughput of the order of 10% of the final throughput (the final throughput is specified as 200 Pam^3s^{-1} (~10^{23} D/T atoms.s^{-1}) for a 300 - 500 s $Q = 10$ plasma with a repetition time of 1800 s). The initial throughput will be sufficient to allow an expanding program of DT experiments to be developed during the latter half of the first FPO campaign, leading to significant fusion power production of several hundred megawatts during the campaign. This framework for the commissioning and operational start-up of the Tritium Plant forms the basis for the development of the FPO program presented in section 3.3.

2.5 Physics issues influencing the IRP development

The physics basis for the design of the ITER device was first formalized by the ITER Experts Groups in 1999 [5] and updated by their successors, the ITPA[1] Topical Physics Groups, in 2007 [6]. Since the key elements of fusion plasma physics determining the ITER design which were developed in some detail in these reviews shared a wide acceptance within the fusion research community, they have, inevitably, also influenced much of the planning for the exploitation phase of ITER. Nevertheless, there has been a process of continuous updating of the community's understanding of the physics determining fusion plasma performance through the ongoing research programs within the project Members' communities and, in particular, through the extensive interactions between the ITER project and the international fusion community mediated and coordinated by the activities of the ITPA.

The research program outlined in later sections of the paper is designed to address successive challenges in preparing robust scenarios for DT fusion power production while simultaneously exploring the physics processes determining plasma performance at the ITER scale and in the parameter regime relevant to thermonuclear plasmas. There are several aspects of these studies which emerge as overarching constraints on the development and implementation of the

[1] ITPA: International Tokamak Physics Activity - a collaboration among the magnetic fusion research communities of the ITER Members (and latterly including Australia) which, since 2008, has operated under the auspices of the ITER Agreement.

experimental program, and these are introduced in the following sections to establish the framework within which the IRP has been elaborated. Open R&D issues in these areas are discussed in some detail in section 5.

2.5.1 H-mode Access

While significant progress has been made in understanding of the physics processes generating the H-mode transition in recent decades (e.g., [7, 8]), the absence of a quantitative prediction for the H-mode access conditions derived from first principles motivates the use ofscaling predictions for the H-mode threshold power recommended by the ITPA [9] as the basis for assessing the conditions for H-mode operation in ITER. Nevertheless, due to the large scatter in the ITPA database underpinning the L-H power threshold scaling, the 95% confidence interval gives a wide range of possible values for the L-H transition power in ITER: from 0.54 to 1.86 times the central value derived from the Martin scaling [9],

$$P_{th,D} = 0.049 \times \overline{n_e}^{0.72} B_T{}^{0.8} S^{0.94}, \qquad (1)$$

with $P_{th,D}$ the threshold power prediction for deuterium plasmas, $\overline{n_e}$ (10^{20}m^{-3}) the line-averaged density, B_T (T) the toroidal field value at the magnetic axis and S the plasma surface area at the separatrix (taken as 683 m^2 in ITER). This introduces significant uncertainties on the range of plasma conditions over which the H-mode will be achievable in ITER with the baseline heating schemes. This has an impact not only on the planning for DT operation, but even more so for the initial (PFPO) phases of operation in H and He plasmas. The uncertainties in the scaling reflect the impact of divertor geometry, input torque, Z_{eff}, etc., on the power required to access the H-mode. Some of them are expected to lead to lower threshold power in ITER than predicted by the scaling (lower Z_{eff} than in devices using carbon plasma-facing components (PFC), lower torque input than in present NBI-heated plasmas, etc.) while others could lead to a significantly increased threshold power (divertor geometry, impact of the temperature profile at the target and the associated edge electric field, E_r, etc.).

Hydrogenic isotope mass is known to have a significant impact on the threshold power, as demonstrated by experiments in H, D, DT, and T plasmas in JET, where $P_{th} \propto M^{-1}$ was observed [10], with M the average mass number of the fuel isotope(s). Comparisons between H and D plasmas in other devices have confirmed this trend, though the precise value of the isotope mass exponent shows some variation with plasma parameters. H-mode access conditions in helium plasmas have also been studied in several devices (e.g., JET [11]. AUG [12], and DIII-D and C-Mod [13]) in some experiments using carbon-based, in others metal-based PFCs. Comparison between the power threshold for D and He plasmas showed that, in some cases, the H-mode could be accessed at input power levels which were a factor of 1 - 1.5 greater than in D plasmas, although at some densities this factor approached 2. In view of the limited heating power available in the PFPO phase of ITER operation, which is likely to make H-mode access in H plasmas problematic, an option for H-mode exploration in He plasmas has been incorporated in the PFPO phase of the IRP. Figure 4 compares the predicted H-mode threshold power derived from the Martin scaling as a function of plasma current (implicitly as a function of toroidal field with q_{95} = 3) for H, He and D plasmas, and for two normalized values of plasma density. For the He cases, a range of values is shown for each value of normalized density, corresponding to, $P_{th,He}$ = [1 - 1.5]×$P_{th,D}$.

It should also be noted that experiments from JET, ASDEX-Upgrade and DIII-D show that small amounts of a heavier hydrogen isotope or specie (He) into a lighter hydrogen isotope plasma can significantly reduce the H-mode threshold [14, 15, 16], although this impact may be restricted to specific density ranges [17]. This would be particularly advantageous in preparing for later experiments in the FPO phase, since the confinement and ELM behaviour of predominantly H plasmas might mimic those of D and DT plasmas more closely than would the behaviour in He plasmas. This option therefore remains open for implementation on ITER based on further experimental studies with such isotope mixtures for which the R&D needs are discussed in section 5.3.1.

It is well recognized that the threshold power scaling of Eq. (1) is valid only above a certain minimum density, below which the threshold power is observed to rise with decreasing density. The position of this minimum density is reported to range from 20% to 40% of the Greenwald density [9]. Analysis of experimental results from AUG have revealed that the density minimum, $n_{e,min}$, is determined by the role of the edge ion heating in triggering the L-H transition, and a scaling for its value has been derived in terms of global plasma parameters [18]. When mapped to ITER parameters for $q_{95} = 3$, this scaling yields, $n_{e,min} \approx 0.4 \times n_{GW}$ (with $n_{GW} = I_p/\pi a^2$ (10^{20}m^{-3}) the Greenwald density, I_p (MA) the plasma current and a (m) the plasma minor radius). This is of particular significance in the PFPO phases of ITER operation, during which the limited baseline power is expected to constrain the plasma parameters, in particular, B_t and hence I_p, for H-mode operation to relatively low values, perhaps 50% of the design values. This will limit the density range over which H-mode operation can be sustained, which, in turn, can have implications for neutral beam shine-through (impacting the first wall power loading) and electron-ion coupling (with potential implications for sustainment of the H-mode edge conditions). These considerations underline the importance of demonstrating robust H-mode operation as early as possible in ITER operation, the challenges that must be addressed in achieving this goal (see, in particular, section 3.2.4.5) and the R&D needs that should be pursued in the ongoing fusion physics research program (see section 5.3.1).

Ferromagnetic inserts within the vacuum vessel interspace are used to compensate for the toroidal field ripple arising from the 18 TF coil configuration in ITER. At maximum toroidal field (5.3 T at a major radius, R, of 6.2 m), this results in an estimated maximum value of TF ripple, δ_{TF}, of +0.34% at the nominal outboard plasma separatrix, while at 2.65 T the estimated maximum value of δ_{TF} is -0.54% (i.e., the inserts overcompensate the intrinsic ripple, producing a ripple with the opposite phase to the intrinsic ripple) and at 1.8 T the estimated maximum value of δ_{TF} increases to -1.3% [3]. Experimental results from JET [19], JT-60U [20] and DIII-D [21] indicate, however, that the H-mode threshold power is insensitive to TF ripple within this range (though H-mode confinement is more sensitive to TF ripple [22, 23]). On the other hand, in ELM control experiments in AUG, MAST and DIII-D (e.g., [13]), strong resonant components in the resonant magnetic perturbation (RMP) spectrum have been shown to increase P_{th} for RMP fields above a critical threshold (i.e., for $\delta B/B_t$ above $\sim 3 \times 10^{-4}$). There is a need to frame this criterion in a form which allows a reliable extrapolation to ITER plasma conditions, but it nevertheless highlights a requirement to design the ELM control spectrum for ITER with care to minimize the impact of the ELM control perturbation spectrum on the H-mode access conditions. Specific open R&D issues for ITER requiring further studies in current devices are discussed in section 5.7.

Further factors observed to influence the H-mode threshold power in current experiments include: the divertor geometry, including factors such as the use of vertical vs horizontal target [24], X-point height [19, 21] and degree of divertor closure [25, 26]; the use of metallic, rather than carbon-based, PFCs [27, 28], where the change in P_{th} might be associated with changes in the core plasma impurity content (as characterized by Z_{eff} [29, 30, 31]); and variations in input torque [32]. Variations induced by some of these elements might already be reflected in the large uncertainty associated with the 'Martin' scaling noted above.

Overall, therefore, managing the time evolution of plasma scenarios to ensure access to robust H-modes will be a significant theme throughout ITER operation, but particularly in early experiments with non-active fuels (H, He) and limited auxiliary heating power, as discussed in some detail [33, 34] and developed further in later sections. These considerations emphasize the importance of achieving H-mode operation in ITER at the earliest opportunity to test the validity of the nominal scaling, characterize where ITER plasma operation lies within the extrapolation uncertainties and determine whether H&CD upgrade(s) might be required to ensure reliable H-mode access in advance of the transition to fusion power production.

2.5.2 Integration of scenario requirements with edge/plasma-wall Interaction requirements

The use of all-metal, water-cooled PFCs (Be first wall, W divertor targets), high stationary heat loads during reference DT scenarios, significant transient heat loads associated with MHD instabilities (ELMs, disruptions) and long-pulse operation under burning plasma conditions (up to 3000 s) are indicative of the demanding environment within which ITER plasma scenarios must be sustained. A series of core-edge/plasma-wall interaction (PWI) challenges, in both physics and technology, must be addressed in developing a successful experimental program towards the production of high fusion power for periods of several hundred to several thousand seconds. Key considerations related to the principal core-edge/PWI integration challenges are summarized in the following to provide the background against which the experimental program has been developed. Specific PWI issues are discussed in the following section.

Helium Operation: As noted above, He plasmas may constitute a significant element of PFPO experiments if this proves necessary to allow early access to H-mode operation because of associated lower H-mode threshold power. Nevertheless, some edge-core integration issues may be more complex in He plasmas due to the higher sputtering of W than in H plasmas that may render He H-mode scenarios difficult to develop and control in ITER. The actual level of W sputtering in these scenarios may be impacted by the possible coverage of the W divertor by a Be layer due to increased main wall erosion in He plasmas compared to H ones, as is observed with boron in He and D plasmas in AUG [35]. Further open R&D issues in the area of He operation are discussed in section 5.4.

For these, and other reasons associated with W PWI behaviour discussed later, the IRP during PFPO gives priority to the exploration of the operational range of hydrogen (or predominantly hydrogen) H-mode plasmas and if, these turn out not to be viable, the pursuit of He H-mode plasma scenarios for H-mode characterization and the development of H-mode specific control schemes. It should be noted that, in terms of density control, no major differences are expected between H and He plasmas, since the ITER cryopumps have a similar performance for H and He, unlike most of the cryopumping systems in present fusion experiments, which generally apply

the Ar frosting technique to have sufficient capability to pump He plasmas. Despite this, significant differences in some of the edge-core integration processes that need to be controlled in FPO H-mode scenarios imply that the experience acquired in helium H-mode plasmas will not to be fully applicable to later experimental phases. For instance, the dynamics of plasma detachment are sufficiently different between He- and H-fuelled plasmas, due differences in atomic and molecular processes [36 - 38], that power load control techniques developed in the former (e.g., by extrinsic impurity seeding) may have limited applicability to the latter. On the other hand, from the operational perspective, the additional divertor radiation obtained in He plasmas should allow operation at higher input power before divertor detachment control is required (see [3-Appendix C]).

Given these issues, the IRP PFPO plan minimizes operation with He plasmas to that needed to support H-mode scenario development for FPO, while additional exploration of helium H-mode plasma behaviour in ITER remains very limited.

Stationary power load control: Power load control in FPO is an essential ingredient for core-edge integration, and understanding of this issue in ITER, together with the development of control schemes, is essential during FPO. A key ingredient is the understanding of the radial profile of parallel power flow in both the near- and far-scrape-off layer (SOL), which is critical for predicting the requirements for acceptable divertor power loading in ITER and for the analysis of first wall heat and particle fluxes - the latter has implications for first wall power handling and material erosion/migration, as well as for ICRF antenna coupling. For the near-SOL stationary power profile (i.e., between ELM perturbations), the most recent scaling derived from IR thermographic observations in a range of devices [39] extrapolates to a value of $\lambda_{q,near} \sim 1$ mm in ITER 15 MA plasmas, a factor of ~3 lower than assumed in previous analysis which scoped out the operational window of the ITER divertor. This scaling, in which $\lambda_{q,near} \propto 1/I_p$, is supported by analytic modelling based on neoclassical magnetic drift theory [40], although recent gyro-kinetic (XGC) and fluid (BOUT++) simulations at the ITER scale find a strong major radius dependence, yielding $\lambda_{q,near} \sim 5$ - 6 mm in 15 MA H-mode plasmas [41, 42, 43]. Therefore, early characterization of the real value of $\lambda_{q,near}$ and its parametric dependence will be a key issue for the initial phases of ITER operation both in L-mode and, later, in H-mode. The IRP is based on the assumption that initial plasma operation in PFPO-1 up to, at least, 7.5 MA in L-mode and 5 MA in H-mode (resulting in $\lambda_{q,near} > 3$ mm) with additional heating levels in the range of 20 - 40 MW will be compatible with toroidally averaged power loads below 10 MWm^{-2} at the divertor [34, 44] without the need for strong extrinsic impurity radiation [3-Appendix C]. Exploitation of these scenarios is foreseen in the IRP to develop power load control schemes that will be applied in later phases of PFPO and FPO in which higher current and additional heating power operation in both L- and H-mode is performed.

Note, however, that the use of extrinsic impurity radiation may be required to control divertor W sputtering because of the limited operational density range in H-mode during PFPO [34] and, thus, the control of impurities in early H-mode operation in the IRP may be more demanding in terms of edge-core integration than power load control by itself. Open R&D issues regarding core-edge integration in PFPO are discussed in detail in section 5.4.

In relation to FPO operation, a very narrow $\lambda_{q,near}$ reduces the operational range for high-Q operation, in terms of separatrix density and edge impurity concentration, for which toroidally

averaged power loads at the divertor can be maintained under 10 MWm^{-2}, as analysed in [45]. This not only poses operational restrictions but also raises challenges to detachment control schemes, since loss of detachment implies divertor power loads that can only be sustained by the divertor for very short durations (<1 s). Power load control in ITER will require the extensive use of extrinsic impurity seeding (Ne is currently foreseen with the optional use of Ar and, if needed, N_2), implying a necessity for the development of associated control schemes. The effectiveness of gas fuelling and impurity seeding for power load control is well established (see e.g., [5, 6, 46, 47, 48, 49]). The majority of studies of exhaust power dissipation via impurity seeding in devices with all-metal PFCs have exploited N_2 as the seeded impurity due to initial results exhibiting superior H-mode energy confinement than in H-modes seeded with Ne. However, more recent experiments and modelling studies (e.g. [50, 51] indicate that, at ITER parameters, Ne is expected to provide effective detachment control with acceptable energy confinement, and these results motivate an increased emphasis on the use of Ne impurity seeding for exhaust power dissipation in ITER. Experimental studies of detachment using seeded impurities have been accompanied by developments in real-time feedback control, and techniques for maintaining stable detachment based on a variety of diagnostic measurements have been reported, *inter alia*, from JET [52], DIII-D [53], EAST [54], AUG [55] and TCV [56]. It is therefore assumed in the IRP that schemes of this type will be used routinely in ITER for operational with high power additional heating and that this technique will be able to address the challenges described above. To account for this, the IRP includes a large number of intermediate steps, together with the associated experimental time, in the expansion of the FPO operational space towards high Q and high plasma current.

Open R&D issues relating to power load control and associated edge-core compatibility in this area are described in sections 5.4, 5.9 and 5.12.

The quantitative characterization of power and particle fluxes in the far-SOL, which has important implications for the magnitude of first wall heat and particle fluxes and, therefore, for power handling, material erosion/ migration and ICRF coupling, remains uncertain, despite multi-machine studies and model developments [57 - 59]. Eventually, these fluxes may impact the clearance between the plasma separatrix and the wall, which can influence plasma performance, first wall lifetime and fuel retention (through erosion/ deposition of beryllium). For this reason, adoption of plasma configurations with relatively large wall clearances has been selected as the reference for the execution of the IRP. Indeed, characterization of such fluxes is included in the earlier phases of ITER operation to determine the optimum trade-off between the processes involved and to monitor how this trade-off changes as the plasma operational range expands.

Application of 3-D magnetic fields for ELM control has a significant impact on stationary power load control. The structure of the edge plasma changes from 2- to 3-D, leading to power being deposited at (radial) distances potentially far from the plasma strike point at the divertor, and also at the first wall at specific toroidal locations [60]. Of specific importance for the IRP is the achievement of a radiative divertor condition with low power loads across the divertor target, which has specific features regarding off-separatrix loads [61, 62]. The ITER ELM control coil (ELMCC) system has the capability to modify the structure of the applied field by varying the currents applied to the coils with frequencies of up to 5 Hz providing flexibility to cope with localized heat fluxes at the divertor and the first wall [63]. However, routine application of such schemes can impact the lifetime of both the control coils and the PFCs, and should thus be limited

to a minimum. Open issues related to core-edge integration in the presence of 3-D fields for ELM control in ITER are discussed in section 5.12.

Transient ELM power load control: ELM power/ particle loads are expected to cause significant PFC erosion/ damage ELM-generated impurity influxes. Present understanding of ELM divertor target heat fluxes [64] indicates that melting of the W divertor (including gaps in between W monoblocks) will not occur in H-modes with plasma currents of up to 5 MA [65]. Above this current level, gap edge melting may occur, while melting of the front face of the monoblocks occurs only at much higher currents [65, 66]. The IRP therefore assumes that it will be possible to develop H-mode scenarios at low plasma current (≤5 MA), where ELM control will not be necessary, and that such scenarios can then be exploited for the development of ELM control schemes before expanding H-mode operation to higher currents and high Q in FPO.

Similarly, control of impurities in H-mode (including ELM-generated influxes) may differ significantly in ITER from that in present experiments. This is due to the impact of the high edge density operation required in ITER for radiative divertor operation in H-mode at high current/ additional heating power levels [67, 68]. In common with ELM power fluxes, these impurity exhaust differences between present experiments and ITER are expected to develop as H-mode scenarios are extended towards higher plasma current levels within the IRP, allowing a gradual development of the associated control schemes, namely the transit from ELM mitigation at low currents to ELM suppression at high currents. Open R&D issues associated with ELM control are discussed further in sections 5.12 and 5.13.

In ITER, interactions of ELM transients with the first wall could produce significant erosion under certain conditions, due notably to the much lower melting temperature of Be compared with that of W. Depending on the characteristics of the ELM filaments, SOL transport and the design of the magnetic equilibrium (e.g., [69]), which determines the fraction of ELM energy reaching the walls, melting could occur in the secondary X-point region. This is not expected to be a problem until burning plasma operation [70], though detailed calculations of gap loading between first wall castellations have not yet been attempted. Nevertheless, as the plasma has a higher tolerance for Be, than for W, impurities and since stationary handling of power fluxes on the first wall is not as critical as for the divertor, gap melting on the Be tiles, should it occur, is expected to be less problematic than on the divertor W tiles.

2.5.3 Plasma-Wall Interaction issues

Helium Operation: Operation with He plasma to promote H-mode access in PFPO gives rise to certain PWI issues that are not present in H plasmas. This is due to specific effects of He in metals arising from the strong trapping of He exhibited by most metals and to the tendency of He to cluster and form bubbles, which leads to strong morphology changes. Moreover, He-induced embrittlement has been observed for W materials, which leads to a reduced threshold for surface cracking. These effects are strongly temperature dependent and may not materialize during initial operational phases of the IRP. Nevertheless, monitoring of PFC surface conditions during He operation in PFPO will be required to ensure that such operation does not have long term impact on the divertor lifetime during later phases with higher stationary heat loads. Section 5.4 discusses open R&D issues associated with He-related PWI interactions during PFPO and FPO.

Tungsten-related material issues: While tungsten's high melting temperature is considered a significant advantage in its application as a plasma-facing material, recrystallization/ grain growth

can occur at substantially lower temperatures, resulting in strong changes in the material mechanical properties and, in particular, a reduction in strength/hardness and shock resistance despite an increase in ductility. Appearance of macro-cracks in W during high heat flux testing at 20 MWm^{-2} is indeed attributed to exhaustion of ductility of recrystallized W - the temperature being high enough for recrystallization to occur [71, 72]. To avoid the deleterious effects associated with recrystallization, an operational budget for the IRP will need to be defined accounting for the time/ temperature dependence of the recrystallization process to ensure that divertor lifetime is sufficient for its execution. Present evaluations of this operational budget [45, 73] indicate that it should be sufficient for the achievement of the project's fusion power production goals according to the IRP (i.e., up to FPO-3), but monitoring of divertor target and adjustment of operational conditions will be required during the execution of the IRP to ensure that this lifetime is preserved.

The impact of transient loads (e.g., ELMs and disruptions) on this operational budget and the impact of synergetic effects of simultaneous particle/ power fluxes on W divertor target lifetime raise more complex questions [73]. Open issues concerning behaviour of W PFCs under plasma exposure and the impact on ITER operation of degraded PFC components will be discussed in the section 5.4.

Of specific importance are power loads on the W divertor monoblocks. For feasibility reasons, the ITER monoblock design adopts a simple toroidal bevel to protect against misalignment of toroidally adjacent units in the high heat flux areas [74], but does not protect loading of gaps running in the toroidal direction between poloidally neighbouring blocks. This choice has been the result of extensive design and physics studies [65, 74 - 76] and results in the reduction of the effective divertor area for power deposition by about 40% compared to a non-shaped solution. The toroidal gaps can be protected with the addition of a further, poloidal, bevel, but this is effective only at the outer target in ITER and would add an additional penalty on the allowable stationary parallel heat flux densities [75].

As already described in the context of edge-core integration, power fluxes to these gaps are expected to determine the maximum ELM power fluxes that can be tolerated by the divertor without W melting. Therefore, careful attention will have to be paid to power loading in these gaps as the ITER operational space expands during the execution of the IRP. Gap edge loading occurs on the ion Larmor radius scale, typically on the order of a few hundred microns, so that only the high resolution divertor IR systems, which view a small region of the vertical targets at a single toroidal location, will be appropriate for the detection of these interactions. The lower resolution, machine protection, IR systems will, however, be capable of detecting the stationary top surface loading on a substantial fraction of the individual monoblocks in the strike-point areas.

Radio-frequency-assisted wall conditioning techniques: Given the limitations on cycling of the superconducting magnets which generate ITER's toroidal field, it is likely that glow discharge cleaning (GDC) will be a viable surface conditioning method only during the commissioning phases preceding the major experimental campaigns when the superconducting magnet systems are not energized [77]. Ion cyclotron wall conditioning (ICWC) or electron cyclotron wall conditioning (ECWC) are alternative techniques that can operate in the presence of high toroidal fields and so can, in principle, be applied for fuel and impurity removal between plasma pulses. Both methods use the conventional heating antennas to produce low temperature magnetized

discharges. ICWC is a non-resonant technique which relies on collisional absorption of RF waves by electrons [78] and so can be applied at essentially any value of toroidal field.

Both schemes are expected to be used in ITER for conditioning between pulses (for instance to recover from disruptions or from the application of disruption mitigation) and for control of the in-vessel T inventory. Schemes for optimum ICWC and ECWC thus need to be developed for application in ITER so that the impact of conditioning on the IRP can be minimized. We note that, since ICRF will not be available in PFPO-1, ECWC is the only conditioning scheme that can operate with TF field on in this phase. This optimization requires modelling studies [79] and experimental demonstration [80 - 83]. Open R&D issues related to the application of ECWC and ICWC in ITER are described in section 5.6.

2.5.4 Disruption Management

Plasma disruptions can generate substantial heat loads to the divertor and the first wall, high electromagnetic loads on in-vessel components and on the vacuum vessel itself, and may also lead to the formation of runaway electrons (REs) that can potentially cause water leaks due to very localized deposition of energy on first wall panels or divertor PFCs. Operation of ITER will have to focus strongly in achieving a high success rate for disruption avoidance while mitigating those disruptions for which avoidance techniques fail [84 - 87]. The IRP incorporates this requirement, and significant operational time for commissioning and optimizing the disruption mitigation system (DMS) and for establishing appropriate disruption forecasting and avoidance techniques and schemes, linked closely to basic and advanced control systems, is reserved in all three operational phases, PFPO-1/-2 and FPO. This research is explained in greater detail in later sections. When possible, the IRP aims to commission each system one operational period before it is needed. Figure 5 shows the various limits for PFC melting associated with thermal and electromagnetic loads during ITER disruptions. The assessment of thresholds for PFC melting or for a possible failure of cooling channels after runaway impact is an ongoing R&D activity and limits cannot be represented in a simple way in figure 5. R&D required to firm-up the evaluation of such limits for ITER is discussed in section 5.2. Nevertheless, it is the role of the DMS, when mitigating disruptions, to ensure RE avoidance by an appropriate choice of the injected gas species and quantity.

Given the high impact of disruptions on component lifetime and machine availability, an appropriate management scheme must be in place to allow the timely achievement of the IRP objectives. The disruption loads and their consequences determine the allowable disruption rates (and consequently the necessary avoidance rates) and mitigation success rates for the various phases of operation, with increasing thermal and magnetic energies towards the $Q = 10$ baseline scenario. To define these rates, a disruption budget consumption (DBC) that represents the ‘costs’ of a disruption at a specific magnetic and thermal energy has been introduced [85]. This DBC can be attributed to any disruption impact that is cumulative, or for which an occurrence probability can be defined. Specifying the DBC values with a reliable physics basis is a prerequisite for establishing a robust strategy for disruption management. Improving the physics basis for the definition of the DBC in ITER is a continuous process and R&D is required to support this refinement (see section 5.2). During operation, the forecasting and the accounting of the DBC will have to be updated, based both on the post-disruption assessment of the actual impact that has occurred and on scalings for disruption loads that will be established via experimental

measurements. This careful accounting will allow identification of deviations from the planned budget consumption and, if required, adjustment of the operational plan. It is also important to note that mitigated disruptions can contribute to the DBC, for example, by radiation flash heating of first wall components, or by consumption of fatigue lifetime of in-vessel components. A further significant risk to the successful execution of the IRP arises from the unintended generation of runaway electrons during disruption mitigation. Since extrapolation from one plasma current level to the next involves substantial uncertainties, runaway avoidance during disruption mitigation has to be carefully validated throughout the approach to 15 MA operation and the IRP includes dedicated experimental time towards the achievement of this goal.

Following the activation of the DMS, recovery of a suitable vacuum quality for plasma operation will be required. This includes pump-down of the injected (by the DMS) material and, if needed, in-vessel conditioning. The target duration for these activities is one hour (with a maximum duration of three hours). Although the highest priority is to mitigate the direct consequences of a disruption, optimization of the DMS must also consider the impact of the mitigation action on the pulse rate and possibly also on the performance of the subsequent pulse. Therefore, disruption rates - and also DMS triggering rates during the early phase of operation - will have to be limited. Moreover, the injected quantities will also have to be optimized with a view to preventing the injection of an excessive mass of material, which would cause operational delays due to longer vessel pump-out times. Early verification of the impact of injecting high quantities of material on vacuum systems, such as cryopumps and gas handling systems, will be essential. Following unmitigated disruptions, but prior to further operation at high plasma performance, a conditioning sequence (including ECWC/ICWC and low performance plasma) might be required in case of degradation of the operational conditions (vacuum quality, divertor/first wall localized melting, etc.). These losses of operational time must be accommodated and will contribute to the definition of targets for disruption rates. Such considerations will also necessitate minimizing of the number of disruption mitigation events in plasma parameter ranges for which no damage to PFCs is expected. Equally, targets for the false alarm rates of the disruption predictor must reflect the need to minimize the associated loss of operational time.

3. Research Program during Operations

3.1 First Plasma

The operational activities surrounding the production of First Plasma in ITER, targeted within the Staged Approach for December 2025, consist of 3 main phases: Integrated Commissioning (IC), First Plasma and Engineering Operation (EO).

3.1.1 Integrated Commissioning

As installation of the various ITER plant and auxiliary systems is completed, each of the systems will undergo instrumentation and control (I&C) integration with ITER’s Control Data Access and Communication (CODAC) and system commissioning. This should ensure that each system satisfies those design requirements that can be tested in the absence of plasma in advance of their integration into the tokamak operations framework. Following completion of the

construction of the tokamak core, a first period of Integrated Commissioning, lasting ~11 months, will occur, with the achievement of high vacuum conditions in the vacuum vessel (VV), cooling of the superconducting magnets and demonstration of a significant level of performance, together with the commissioning of all major tokamak subsystems required to support plasma operation. Of particular importance is the qualification of the VV as nuclear pressure equipment by a hydrostatic pressure test which will be performed in this campaign. A schematic of the sequence of events and estimates of time required for the various commissioning activities in shown in figure 6.

A detailed analysis of this phase of operations has been undertaken in order to develop estimates of the time required for completion of the various activities and to confirm the detailed sequence of commissioning. The major activities determining the critical path through Integrated Commissioning are illustrated in the figure: the cryostat is evacuated and leak detection is undertaken at room temperature (this includes leak detection of in-cryostat coolant and cryogenic circuits, including those of the superconducting magnets); subsequently the superconducting coils and power supplies are tested to high voltage, the vacuum vessel is evacuated and the cooling water circuits and VV are leak tested; the cryostat and vacuum vessel are then vented and the hydrostatic pressure test is performed by pressurizing the vacuum vessel interspace using the primary VV cooling water system. Pump-down of the VV, pump-down of the cryostat and cooldown of the cryostat and its internal components, including the superconducting coils, to cryogenic temperatures follow. The VV and all in-vessel components are then baked at high temperature, a second leak detection is performed and (in advance of the energization of the TF coils) glow discharge cleaning of the vacuum components is carried out to the extent necessary to achieve reliable plasma operation; following the ‘warm’ testing of the superconducting coil systems and their power supplies in earlier steps in the integrated commissioning procedure, energizing and charging of the coils to approximately 50% of their maximum current is performed - this involves extensive operation of the coils individually and then as an integrated system, together with commissioning of the protection systems and validation of the corresponding coil and tokamak electromagnetic models.

Integrated commissioning of control and auxiliary systems required for FP is also performed during this period, as far as possible in parallel with the critical path activities. The Gas Injection System (GIS) is the first auxiliary system to undergo integrated commissioning, since it is used during glow discharge cleaning of the VV. A subset of Diagnostics has been identified as essential for FP (see Table 2) and these must be fully commissioned to be ready to take data during the FP campaign - the magnetics diagnostic will be critical to the implementation of this campaign, and calibration and extensive measurement consistency tests will be an essential activity to be carried out in parallel with the commissioning of the superconducting coil systems. In addition, specific measurements to determine the structure of the TF magnetic field are planned for this phase and these will be used to support the alignment of the blanket modules (shield blocks and first wall panels) in Assembly Phase II that precedes PFPO-1. The scope of the diagnostic measurement capability will be gradually expanded concomitant with the demands of the experimental program, as discussed in later sections (see also Tables 3, 7 and 10).

The Plasma Control System (PCS), Central Interlock System (CIS) and Central Safety System (CSS) will also undergo integrated testing under CODAC during this period (PCS control of the poloidal field (PF) and central solenoid (CS) coil currents will be implemented during magnet

commissioning). Following offline commissioning of the ECRH power sources and transmission lines, the ECRH system will be integrated into the operational systems and short-pulse injection (up to 100 ms) will be used to condition one upper launcher.

The culmination of the Integrated Commissioning activity would be a 'dress rehearsal' for plasma operation of the tokamak without gas injection, in which all tokamak, plant and auxiliary systems are operated under CODAC control (where relevant, via PCS) and shown to satisfy the respective requirements for plasma operation.

3.1.2 First Plasma Campaign

The FP campaign, scheduled nominally for a duration of 1 month, essentially constitutes a demonstration of the successful integration of the tokamak core and principal plant systems (magnets, power supplies, cooling, cryogenics, vacuum, etc.) and is the conclusion of the first phase of integrated commissioning of the ITER facility. The achievement of FP will provide confirmation that all core tokamak systems (excluding major in-vessel components) have been commissioned successfully and that the device is capable of supporting plasma operation. During the FP campaign, none of the main in-vessel components will be installed, in particular no blanket/first wall modules or divertor cassettes. Therefore, the vacuum vessel, in-vessel wiring, diagnostics and other installed in-vessel components will be protected by the First Plasma Protection Components (FPPC), consisting principally of 4 poloidal limiters, most likely with a stainless-steel PFC, capable of supporting plasma operation at up to 1 MA at 2.65 T. The FPPC also include a divertor replacement structure that protects the bottom of the vessel, preventing plasma from reaching the divertor region. These structures are illustrated in figure 7.

The essential parameters for FP will be:

I_p ~ 100 kA

t_{pulse} ~ 100 ms

P_{aux} < 5.8 MW (for breakdown/burn-through assist).

The achievement of FP requires the optimization of the magnetic configuration to provide a suitable magnetic field null before and during CS discharge, of the gas injection to achieve the required neutral pressure and uniformity within the torus, and of the electron cyclotron power to ensure (if necessary) adequate pre-ionization. For the last-mentioned, up to 5.8 MW of injected EC power will be available. Optimization of the magnetic configuration requires detailed validation of the models for the PF/CS, power supplies, magnetic diagnostics, cryostat tokamak components, tokamak building electromagnetic models, etc., since stray magnetic fields and eddy currents produced during the CS discharge have a substantial impact on plasma start-up. The EC power will be injected through one upper launcher and reflected by a set of mirrors located at the High Field Side (HFS) of the tokamak, crossing the null where gas will be ionized, and will subsequently be absorbed by an optical dump installed in an equatorial port to avoid multiple reflections of scattered mm-wave power within the VV, avoiding potential damage to those in-vessel components already installed.

The optimization described above is particularly complex in ITER because of the large VV dimensions, the low absorption efficiency of injected EC heating by the neutral gas at 2.65 T (170 GHz corresponds to 2nd harmonic heating at 2.65 T), the low value of the electric field induced by the discharge of the PF/CS coil system and the large eddy currents in the VV induced at plasma start-up (see, e.g., [88]). Despite the extensive integrated commissioning activities

previously undertaken, it is considered that of order 1 month of dedicated ‘plasma optimization’ may be required to accomplish the FP objective.

Optimization of the initial plasma breakdown will be guided by the results of extensive simulations of FP scenarios, including simplified electromagnetic models of the VV, and their comparison to the available experimental measurements, chiefly VV currents, measured magnetic fields, neutral pressure, plasma line integrated density, visible spectroscopy and interactions of the plasma with the FP protection components (FPPC). In the optimization process to be followed in achieving FP, particular attention will be given to the avoidance of slide-away/runaway electron formation at plasma start-up, since this can lead to significant localized power fluxes on the FPPC. This will require careful adjustment of the GIS, EC and PF/CS waveforms. In parallel with plasma operation, parasitic commissioning of some diagnostics is expected to take place, and testing of PCS feedback loops (most likely in open loop) using diagnostic input signals will also be performed.

While the target plasma parameters for FP, a current of at least 100 kA for a duration of at least 100 ms, require only partial burn-through, if a successful plasma start-up occurs, including full burn-through, higher plasma currents could be achieved. This is strongly dependent on the levels of impurities in the plasma resulting both from vacuum conditions and from the interactions of the plasma with the FPPC that are difficult to predict in advance. Since the FPPC are designed to withstand plasma disruption loads for currents of up to 1 MA at 2.65 T, PCS will implement plasma terminations to ensure that this level of plasma current is not exceeded in this experimental phase.

The FP campaign has been developed around a plasma scenario at 2.65 T, for which EC-assist can be used, but ohmic plasma initiation will also be explored, even if EC-assisted plasmas are successful. This would be important, both to assess the influence of EC-assist on plasma start-up and to determine the robustness of ohmic start-up in ITER with a view to the exploration of H-mode plasma operation at 1.8 T, as foreseen within the research plan for the PFPO phase. If FP experiments show that robust ohmic plasma start-up is not expected in PFPO, maintaining the option to explore H-mode plasma operation at 1.8 T would require the procurement of several additional gyrotrons operating at ~100 GHz to support reliable plasma breakdown at 1.8 T in PFPO.

Following the demonstration of FP, or if plasma breakdown at 2.65 T proves unsuccessful due to issues such as those described above (e.g., high impurity levels prevent partial burn-through, 2nd harmonic ECH provides insufficient pre-ionization at 2.65 T), the program will transition to the Engineering Operation phase, which may include additional plasma initiation studies at toroidal fields of up to 5.3 T, if required.

3.1.3 Engineering Operation

Commissioning of the superconducting magnet systems to full current will form the core activity during Engineering Operation, to which 6 months of operational time has been allocated. This program will be implemented by operating the CS, TF and PF coils to their maximum operating currents individually and in the combination(s) required to demonstrate the capability for 15 MA/5.3 T operation. The magnet integrated commissioning activities foreseen include performance verification of the magnets as the current levels are increased and the acquisition of the ‘as-built’ data for the magnets, including measurements of coolant flow, steady-state heat

loads, AC losses, mechanical responses, thermal data (specially temperature gradients among components) and eddy currents. In parallel with these activities, further commissioning of PCS, CSS and CIS will be performed as required by the expansion of the magnet operational space. This will be accompanied by dedicated operation to calibrate the magnetic diagnostics and to validate the tokamak and system models, as already performed in the integrated commissioning phase, but now extended to the nominal current levels for the PF/CS and up to 5.3 T for the TF. Additional measurements to determine the structure of the TF magnetic field may also be obtained, if required.

Following completion of the magnet integrated commissioning, additional studies of ohmic plasma start-up may be performed, with an emphasis on low TF values (1.8 T). The scope of this program will depend on the outcome of the FP campaign. It is most likely that these studies will be performed if an EC-assisted FP had been demonstrated at 2.65 T, but ohmic plasma breakdown had not, unless the results of the FP program were considered to provide conclusive evidence that ohmic start-up is not possible in ITER at low TF values.

Should the FP campaign not have achieved its primary goal due to limitations associated with 2.65 T operation, experiments to establish reliable plasma breakdown during the Engineering Operation phase will take place when TF values of up 5.3 T will be available. At this TF value the absorption of EC power in the neutral gas is much more efficient (170 GHz corresponds to 1st harmonic absorption at $R \sim 5.4$ m for 5.3 T), leading to a higher degree of pre-ionization, which would favour plasma start-up. A similar optimization of the plasma breakdown scenario to that described for the dedicated FP campaign would be performed, but at 5.3 T, leading to the demonstration of FP. As indicated for the campaign at 2.65 T, it is possible that once a successful plasma start-up is generated, including full burn-through, higher levels of plasma current than the nominal 100 kA might be achieved. This is more likely at 5.3 T, since the better EC absorption increases the likelihood of overcoming radiation losses during impurity burn-through. Since the FPPC are designed to withstand plasma disruption loads for currents of up to 0.5 MA at 5.3 T, during these experiments the PCS will implement plasma terminations to ensure that this level of plasma current is not exceeded for 5.3 T operation.

Alternatively, if a satisfactory demonstration of FP is indeed achieved during the dedicated FP campaign and there remains operational time in the Engineering Operation campaign after having achieved all of the primary objectives, further short pulse limiter operation with the FPPC (limited to a maximum plasma current of 1 MA at 2.65 T) could be performed, if this is considered an effective means of advancing the commissioning of the PCS and diagnostics with plasma.

3.1.4 Experimental Risks

The main physics/operation risk for First Plasma is that plasma start-up is not achieved at 2.65 T with a partially charged CS. It is expected that ohmic start-up will be very marginal for FP in ITER (very small pre-fill neutral pressure operational window) [88]. In addition, ECH pre-ionization provided by the available power of 5.8 MW is not expected to be particularly efficient at 2.65 T, since this corresponds to second-harmonic absorption. Mitigation for this risk of unsuccessful breakdown at 2.65 T is already included as an option in the Engineering Operation plan: FP attempts would be repeated at 5.3 T (with a fully charged CS, if needed) and supported by ECH pre-ionization. A field of 5.3 T corresponds to first harmonic ECH absorption in the pre-

fill gas, which is expected to be much more efficient than second harmonic absorption at 2.65 T, thus facilitating plasma start-up.

A further risk is that plasma-start up is obtained but impurity burn-through does not occur; this may limit the level of plasma current that can be demonstrated in the FP phase. This is a lower level risk for FP than inefficient pre-ionization, since impurity burn-through is not strictly required to be demonstrated for FP at 2.65 T [88]. The same mitigation strategy as for start-up above is considered in the IRP, namely further experimentation during Engineering Operation at 5.3 T using ECH-assisted start-up, since the increased absorbed power with first harmonic operation also facilitates impurity burn-through.

It should be noted, however, that in relation to start-up and burn-through issues, the gas/plasma composition (i.e., impurity species and concentrations) has a profound impact on such processes, and these are likely to be very different during FP and EO (stainless steel temporary plasma facing components and, probably, elevated oxygen levels) than from PFPO-1 onwards (Be/W plasma facing components with low oxygen levels). Similarly, the level of installed ECH power that can be coupled to the plasma for FP (5.8 MW) is significantly lower than for PFPO-1 and subsequent campaigns (20 MW). Therefore, if these risks materialize and difficulties are eventually found in demonstrating FP in this initial phase (FP+EO), it is considered unlikely that this will be an issue for operation from PFPO-1 onwards. Further details on open R&D issues for plasma start-up in ITER are discussed in section 5.5.

3.2 Pre-Fusion Power Operation Phase (PFPO)

3.2.1 Objectives for PFPO

During the Pre-Fusion Power Operation phase, operation of the ITER tokamak with the majority of the systems required to achieve the Project's goals will be demonstrated. This includes commissioning of the H&CD systems, Fuelling systems, Plasma Control System, Diagnostics, etc., which are required to provide routine operation up to the nominal plasma current/toroidal field (15 MA/5.3 T) in L-mode and up to (approximately) 7.5 MA/2.65 T in H-mode. These aims will be pursued by developing plasma scenarios that satisfy all the operational requirements in this phase, including those of core-edge plasma integration (ELM control, divertor power load control, etc.). In addition, development of control schemes and integration issues required to meet the needs of DT high-Q operation (including long-pulse/steady-state goals) will be investigated. Insofar as possible, the experimental program will be carried out in hydrogen plasmas, though helium plasma operation may be necessary should H-mode access prove problematic in hydrogen.

In advance of the PFPO campaigns, all in-vessel components will have been installed, in particular the divertor, with tungsten PFCs, the first wall/ shielding blanket modules with beryllium PFCs, and the ELMCC. Following this installation phase, full performance of the magnet coil systems (superconducting and conventional) will be available with the exception of the ELMCC power supplies. PFPO will be subdivided into PFPO-1, which will exploit up to 20 MW of ECRH power launched from an equatorial and 4 upper port plugs (with an option, which remains under review, for a further 10 MW of ECRH power), and PFPO-2, which will develop all three of the auxiliary H&CD systems to reach injection levels of 20 MW of ECRH power, 20 MW of ICRF power (from 2 antennas), and 33 MW of NBI power (from 2 beam-lines), in preparation for the Fusion Power Operation (FPO) phase.

Further improvements to the operational capability in preparation for PFPO-1 will include installation of the full DMS, enhancement of the Fuelling systems with the addition of 2 (continuous) pellet injectors and expansion of the diagnostic systems, with a subset of the final Diagnostic set available that emphasizes plasma control and machine protection (see Table 3). In addition to the upgraded H&CD capability available in PFPO-2, the Diagnostic systems will be further expanded, with additional scope for physics studies, including a Diagnostic Neutral Beam (DNB) system, a further 2 pellet injectors will be installed and the full set of ELMCC power supplies will be available. Although not a central element of the operational plans in the PFPO phase, the first set of 4 test blanket modules (TBMs) will be installed in advance of PFPO-2 to allow initial commissioning, including electromechanical and thermal tests, to be conducted in parallel with tokamak operation (see section 4).

The main objectives of PFPO-1 operation are:

- Commissioning of the plasma control, interlock and safety (specifically the Fusion Power Shutdown System partial commissioning) systems with plasma to levels supporting the experimental program (at least 7.5 MA L-mode and 5 MA H-mode);
- Commissioning of installed diagnostic systems, validation of data and integration into control/ interlock systems;
- Establishing robust plasma initiation over the range in toroidal field of 2.65 - 5.3 T;
- Commissioning and exploitation of the (in-vessel) Vertical Stabilization (VS) coils and the external Error Field correction coils (EFCC) to at least 7.5 MA/5.3 T;
- Commissioning and routine deployment of basic plasma control functions required to support the foreseen range of plasma scenarios for PFPO-1, including: (i) plasma current, position and shape control; (ii) vertical stability control incorporating the in-vessel coil circuit; (iii) density control with gas and pellet fuelling; (iv) $(n = 1)$ error field control; (v) ECRH power control; (vi) first wall and divertor power flux control;
- Demonstration of routine plasma operation with the final configuration of water-cooled in-vessel components and PFCs;
- Characterization of error fields without TBMs and demonstration of effective error field correction over the full range of plasma scenarios explored;
- Optimization of the current ramp-up/ ramp-down limiter phases and characterization of limiter power loads;
- Commissioning and routine operation of the ECRH system to the installed power level (20 MW injected) for at least 50 s in both O- and X-mode;
- Establishment of routine and robust (i.e., low disruptivity) diverted plasma operation in L-mode to at least 7.5 MA with up to 20 MW of ECRH power for durations of at least 50 s;
- Commissioning and routine application of disruption prediction, avoidance and disruption/runaway electron mitigation systems, and characterization of disruption loads to in-vessel components and the vacuum vessel at plasma currents of up to (at least) 7.5 MA and toroidal fields of 5.3 T; unmitigated disruption loads to be characterized to the extent possible;
- Determination of auxiliary (ECRH) power requirements to access and sustain the high confinement plasma regime in hydrogen and/or helium plasmas at toroidal fields of up to 2.65 T;

- Exploration of H-mode operation in hydrogen and/or helium plasmas, expansion of H-mode operation insofar as possible, characterization of ELM power loads and investigation of ELM control schemes at toroidal fields of up to 2.65 T;
- Initial physics characterization of core and edge plasmas (energy and particle confinement, plasma-wall interactions etc.) in ohmic, L-mode and H-mode regimes.

The main objectives of PFPO-2 operation are:

- Commissioning of the PCS, CIS and CSS with plasma to the nominal ITER operational values (15 MA/5.3 T) in L-mode and up to at least 7.5 MA/2.65 T in H-mode);
- Establishing routine error field correction with TBMs and commissioning with plasma of the Neutral Beam Magnetic Field Reduction System (NBMFRS);
- Commissioning of the in-vessel VS coils to 15 MA/5.3 T in L-mode and of the ELMCC up to at least 7.5 MA/2.65 T in H-mode;
- Establishing robust plasma initiation up to the maximum CS premagnetization current over the range in toroidal field of 2.65 - 5.3 T;
- Commissioning of the additional Diagnostic systems, in tandem with H&CD systems where appropriate, validation of data and integration into control/ interlock systems as required to support the PFPO-2 program;
- Commissioning and exploitation of the H&CD systems (HNB (33 MW), ICRF (20 MW), ECRH (20 MW), DNB) in plasma operation to their installed power level for at least 100 s;
- Extension of the capability for disruption prediction, avoidance and mitigation to 15 MA/5.3 T in L-mode plasmas and 7.5 MA/2.65 T in H-mode;
- Commissioning and routine implementation of the control functionality required to support the PFPO-2 experimental program in L-mode plasmas at up to 15 MA/5.3 T and in H-mode plasmas up to at least 7.5 MA/2.65 T: (i) plasma current, position and shape control; (ii) vertical stability control incorporating the in-vessel coil circuit; (iii) density control with gas and pellet fuelling; (iv) (n = 1) error field control in the presence of TBMs and NBMFRS; (v) ELM control using in-vessel coils and pellet pacing; (vi) ECRH, ICRF and NBI auxiliary power control; (vii) first wall and divertor power flux control to the highest P_{aux} (= 73 MW); (viii) impurity and heating minority control;
- Development and optimization of the current ramp-up/ ramp-down and H-mode entry/exit phases in L-mode plasmas at up to 15 MA/5.3 T and in H-mode plasmas up to at least 7.5 MA/2.65 T;
- Characterization of electromechanical and thermal disruption loads to in-vessel components and the vacuum vessel during mitigated and unmitigated disruptions and vertical displacement events (VDEs), allowing extrapolation to 15 MA/5.3 T;
- Determination of the effectiveness of the DMS to reduce disruption-induced electromechanical and thermal loads and to avoid/mitigate runaway electrons up to the nominal current and field values of 15 MA/5.3 T;
- Establishing H-mode plasma operation up to at least 7.5 MA/2.65 T (in H/He, as the power threshold allows), determination of the H-mode access conditions and development of a reliable ELM control capability;
- Demonstration of routine and robust (i.e., low disruptivity) L-mode operation in diverted plasmas up to the nominal field and current values of 15 MA/5.3 T, with auxiliary heating

of up to 20 MW ECRH, 20 MW ICRF and 33 MW NBI for at least 100 s (maximum auxiliary power level might deviate from 73 MW);

- Demonstration of routine and robust (i.e., low disruptivity) H-mode operation in diverted plasmas up to at least 7.5 MA/2.65 T, with auxiliary heating of up to 20 MW ECRH, 20 MW ICRF and 33 MW NBI for at least 100 s (using at least 2 auxiliary heating systems simultaneously);
- First characterization of the current drive capabilities of the ECRH and NBI systems under stationary conditions for plasma scenarios with 4.5 - 6.5 MA/2.65 T;
- Exploration of the capabilities of the ECRH system to control neoclassical tearing modes (NTMs);
- Physics characterization of core and edge plasmas (energy and particle confinement, plasma-wall interactions etc.) of ohmic, L-mode and H-mode plasmas at the highest achievable parameters in terms of plasma current/magnetic field and input power in H/He plasmas;
- Characterization of key aspects of plasma-wall interactions in the ITER environment, e.g., hydrogenic fuel retention, dust production, PFC erosion/ redeposition, evaluation of the efficiency of conditioning schemes and specific plasma operation to facilitate removal of in-vessel fuel with the aim of refining the strategy for T inventory control to be implemented during the FPO campaigns;
- Time allowing, initial attempt at long-pulse (~1000 s) H-mode operation at 7.5 MA/2.65 T.

Together with these high-level objectives, the operational experience and experimental results are expected to provide key information regarding required upgrades to ITER systems which might be needed to support the achievement of the high-*Q* goals in DT.

3.2.2 Assumptions for PFPO

In the following analysis, it is assumed that the FP campaign was successful in achieving full integrated commissioning of the operational ITER plant systems, including a plasma of at least 100 kA for at least 100 ms duration at 2.65 T in H and/or He, and that the CS, PF, TF, and CC magnets were subsequently commissioned to their fully specified operating voltage and current values without plasma. It is also assumed that the first 8 gyrotrons of the ECRH system have been fully commissioned, at least for short pulse operation (<1 s duration) at 170 GHz through one upper launcher. The PCS, CIS, and CSS should all have been fully commissioned for the functions required for FP and all commissioning of plant systems and diagnostics required for the subsequent operation phase that can be performed without plasma should have been carried out successfully during the Integrated Commissioning II phase just prior to the restart of plasma operations.

Both ELM and VS in-vessel coils will be installed prior to PFPO-1 but only the latter will be equipped with power supplies. Installation of the ELMCC power supplies will take place during Assembly Phase III, preceding PFPO-2. Although a temporary GDC system will be installed for FP, the permanent system will be installed and commissioned in preparation for PFPO-1 plasma operation. Similarly, the shielding blanket modules, including the beryllium first wall, and the divertor with tungsten PFCs will be installed. The additional diagnostic systems required for PFPO-1 will be installed during Assembly Phase II. Table 3 lists the diagnostic set and

corresponding measurement capability which will be available during PFPO-1. The remainder of the GIS, one cask with two pellet injectors (PIS) and the DMS will also be installed. Finally, the three additional upper ECRH launchers and one equatorial launcher, together with the remaining 16 gyrotrons and their transmission lines, will be installed to provide the full 20 MW (injected) ECRH power during PFPO-1.

During Assembly Phase III, between the PFPO-1 and the PFPO-2 phases, a number of additional systems will be installed and these will be integrated into the operational environment during Integrated Commissioning III, prior to PFPO-2. This extended operational capability will include: the ICRF system (incorporating two antennas) to provide a total of 20 MW (injected) ICRF heating; the diagnostic neutral beam (DNB) and two heating neutral beam (HNB) systems to provide 33 MW (injected) neutral beam power; additional diagnostics (see Table 7 in section 3.2.5.1); a further pellet injector cask with 2 additional pellet injectors; the ELMCC power supplies and the first 4 Test Blanket Module (TBM) systems, incorporating ferromagnetic structural materials. During PFPO-2, it is planned to commission the three baseline auxiliary H&CD systems up to the full injected power capability of 73 MW. With a total of 4 pellet injectors, high fuelling capabilities to full performance, as well as ELM pacing, will be possible. The influence of the ferromagnetic TBMs on the required error field corrections to avoid low density locked modes, as well as their impact on H-mode performance, will form one component of the experimental activity in PFPO-2.

3.2.3 Plasma scenarios for H and He

During the PFPO phase of operation, plasma fuelling will be limited to hydrogen or helium. It is expected that, whenever possible, preference will be given to H plasmas, since the overall fuelling, transport and recycling properties will be similar to those of D and T, and since there is some remaining uncertainty about the impact of He plasmas on plasma-facing materials. Nevertheless, given that the H-mode power threshold is expected to be a factor of ~1.5 - 2 lower in He than in H, He operation may be unavoidable in order to obtain a high quality H-mode enabling ELM control and mitigation tests to be undertaken during the PFPO phase. For these reasons, and given the uncertainties on the actual H-mode threshold in ITER, scenarios have been designed for both H and He plasmas.

In subsequent sections details of the most relevant plasma scenarios are presented, including steps towards 15 MA operation, with an emphasis on H&CD conditions and on capabilities for long-pulse operation. In view of several operational options that have been identified in the Research Plan analysis following the development of the revised schedule within the Staged Approach, both baseline and optional scenarios are described.

The steps towards 15 MA operation described in the present document may be adjusted during the experimental campaigns according to actual observations and achievements. These steps will be progressive in magnetic field and plasma current, with some deviations from operation at $q_{95} \sim 3$ to allow the approach to the nominal 15 MA/5.3 T scenario to investigate carefully the issues and risks associated with disruptions. Figure 8 shows an estimate of the operational range for each H&CD system (EC, IC, NBI) for different values of magnetic field and plasma current. Due to the resonance conditions associated with the absorption of EC and IC waves, their operational ranges in toroidal magnetic field are constrained by the requirement that the power is absorbed sufficiently close to the plasma centre. The operational range of the HNB system is

constrained by the minimum plasma density required to limit shine-through power losses to an acceptable level. Steps foreseen towards 15 MA operation are displayed as points on this figure.

The availability of H&CD systems to support the experimental program is summarized in Table 4, indicating also the possibility of an early upgrade of 10 MW to the ECRH power.

Scenarios in the non-active phase can be grouped in six main categories (see also [33, 34, 89]):

- First plasma: 100 kA/2.65 T
- First divertor plasma: 3.5 MA/2.65 T
- First q_{95} = 3 plasma: 7.5 MA/2.65 T
- First H-mode plasma: 5.0 MA/1.8 T
- Progressive steps: 7.5 - 9.5 MA/3.3 T,
  9.5 - 10.5 - 12.5 MA/4.5 T,
  12.5 MA/5.3 T
- First 15 MA plasma: 15 MA/5.3 T

These scenarios represent ‘reference points’ around which the experimental program will be developed during the PFPO phase, but this does not exclude the use of additional scenarios, e.g., at $q_{95} > 3$, to facilitate progress towards these reference plasmas. For all these cases, it is likely that H plasmas will be developed first, followed by He plasmas where operation in He is necessary, e.g., only if a good H-mode cannot be achieved in H plasmas with the available H&CD power. Further details of these scenarios follow.

First divertor plasma in PFPO-1: The first divertor plasma will be in H in L-mode at a magnetic field of 2.65 T with a plasma current of 3.5 MA. The goal is to establish initial divertor operation at the lowest possible plasma current, with a flat-top duration of at least 10 s, as a target for the commissioning of various systems, such as PCS, diagnostics, interlock systems and DMS. The choice of 3.5 MA is based on an analysis indicating that this is just above the minimum current allowing reliable magnetic control with a full bore divertor configuration. The currents in the CS coils can be varied from 12 kA/turn to 30 kA/turn, leading to a flat-top duration between 10 s and 200 s. Plasma heating in this scenario would rely entirely on the foreseen ECRH (injected) power of up to 20 MW.

First q_{95} = 3 plasma in PFPO-1 and PFPO-2: The first q_{95} = 3 scenarios will use H and He plasmas at a magnetic field of 2.65 T with a plasma current of 7.5 MA. At this I_p/B_t combination, H plasmas are likely to remain in L-mode, while current expectations for the H-mode threshold scaling in He plasmas (see figure 4) indicate that H-mode operation should be achieved with the H&CD power available in PFPO-2, and there is some possibility of achieving helium H-mode operation at 2.65 T in PFPO-1 (hydrogen H-mode operation would require a 10 MW power upgrade). The maximum flat-top can reach several hundred seconds with a CS coil current varying from 30 kA/turn to 45 kA/turn. Operation above 40 kA/turn will consume the CS coil fatigue lifetime, and hence long-pulse operation will be addressed during the PFPO phase if operational time permits and long pulses of interest can be produced without significant consumption of the CS fatigue life.

While the baseline H&CD power will be limited to 20 MW during PFPO-1, the full range of baseline H&CD capabilities will be available in PFPO-2 following commissioning with plasma. However, the ability to exploit this power will depend on details of the plasma scenario, in

particular, on the toroidal magnetic field value, the plasma fuel ion and the plasma density [89]. Second harmonic heating at 170 GHz will allow efficient coupling of the full ECRH power. Equally, in helium plasmas, fundamental H-minority heating (using an H concentration of 2 - 8%) at 40 MHz should provide single pass absorption (SPA) of almost 100% of the injected ICRF power. In H plasmas, however, the ICRF heating options at 2.65 T are poor and the highest coupled power is predicted to be achieved using the second harmonic heating of ^{4}He-minority (at ~20% concentration), with a predicted SPA of ~50%.

The full HNB power of 33 MW at a neutral hydrogen injection energy of 870 keV will be available in PFPO-2, but constraints set by the tolerable shine-through power load on the first wall (in fact, exposed areas of the shielding blanket) will necessitate a trade-off among the beam poloidal injection angle, the injected ion energy, E_b (and hence injected power - $P_{NB} \sim E_b^{2.5}$), the plasma fuel species and the plasma density [90]. Thus, at low densities (~2×10^{19} m^{-3}) in H, beam injection would be limited to ~500 keV/8 MW, while operation in He at such densities would allow the injection of ~660 keV/17 MW. Injection at 870 keV/33 MW would be possible at densities above 3×10^{19} m^{-3} in He and 4.5×10^{19} m^{-3} in H. Thus, the total available power for development of these scenarios, including both accessing and sustaining the H-mode, will range from ~40 MW to 73 MW, implying (see figure 4) that H-mode access in He should be possible at 2.65 T, but that in H plasmas H-mode access might be marginal.

5 MA/1.8 T scenarios in PFPO-1 and PFPO-2: 5 MA/1.8 T scenarios are designated as first H-mode plasmas in the context of the PFPO-1 phase, since they are designed to enable H-mode operation in this phase with very limited auxiliary heating with ECRH (20 MW with a possible upgrade to 30 MW under discussion). However, these scenarios will be investigated both in PFPO-1 and PFPO-2, and both in H and He plasmas. Maximum sustainable flat-top durations for these scenarios extend from ~200 s to ~1400 s for CS coil current values varying from 20 kA/turn to 45 kA/turn. However, scenarios exploiting operation at CS coil currents below 30 kA/turn, implying negligible consumption of the CS coil lifetime, would allow flat-tops of up 700 s [33] and would be adequate for initial assessments of long-pulse operation. Operation at such low field leads to an overcompensation of the magnetic field ripple by ferromagnetic inserts, inducing a ripple at the plasma separatrix of -1.3% (as described in detail in [3-Appendix F]). If this ripple level is found to be critical for H-mode performance or ripple induced losses when NBI or ICRF is applied in PFPO-2, it can be reduced to -0.55% by increasing the plasma-wall distance [91]; doing so will strongly degrade ICRF coupling performance.

The low densities and temperatures associated with the ohmic and L-mode phases of 5 MA/1.8 T plasmas entail specific issues for the application of both ECRH and NBI power. Specifically, 3X heating at 170 GHz must be used and, particularly in PFPO-1, the low initial absorption of electron cyclotron waves leads to substantial (>50%) shine-through power incident on the first wall. However, scenario modelling [33, 34] indicates that the rapid rise in electron temperature, even with low initial ECRH power absorption, produces an increase in SPA to beyond 90% in less than 1 s, i.e., much shorter than the allowed duration of 5 s set by first wall power flux limits. NB injection energy and power are more severely constrained than at 7.5 MA, with the injection energy and power limited to ~500 keV/9 MW in hydrogen and ~660 keV/17 MW in helium.

Analysis of possible ICRF heating scenarios has shown that in both H and He plasmas second harmonic heating of hydrogen (in the case of He plasmas, as an injected minority at ~7% concentration) using a frequency in the range 52 - 54 MHz provides efficient plasma heating, allowing the injection of 20 MW of ICRF power [33]. This assumes, however, that it will be possible to operate with the nominal plasma-antenna gap of 23 cm. As noted above, the high value of TF ripple at the plasma separatrix in the nominal plasma scenario could cause excessive fast ion losses, an issue which is still to be evaluated, and could also influence the H-mode and ELM behaviour [34]. A slimmer plasma, with a plasma-antenna gap of up to 63 cm, would reduce the edge TF ripple by more than a factor of 2, but would severely degrade the antenna coupling resistance, reducing the coupled power by more than an order of magnitude. Thus, in PFPO-2, if the nominal plasma shape is found suitable to allow ICRF heating, a total injected power of up to ~49 MW (20 MW ECRH, 20 MW ICRF, 9 MW NB) might be available in 5 MA/1.8 T H plasmas, while up to 57 MW (20 MW ECRH, 20 MW ICRF, 17 MW NB) might be available in 5 MA/1.8 T He plasmas. Otherwise, if ICRF cannot be coupled, these values are reduced to 29 and 37 MW, respectively. These provide headroom over a wide range of plasma densities relative to the predicted H-mode threshold power for helium plasmas (see figure 4) and, if ICRF can be coupled, also for hydrogen plasmas.

Progressive steps towards full current in PFPO-1 and PFPO-2: Steps in magnetic field and plasma current beyond 7.5 MA/2.65 T are illustrated in figure 8 (see also [89]). They have not all been modelled in detail, and so their definition will possibly evolve further. These steps are foreseen in H plasmas; He plasmas would also be considered if appropriate for the further expansion of the H-mode operational range in PFPO-2. The H plasmas will likely be in L-mode, since H&CD capabilities are reduced at intermediate values of field and current, as shown in the operational ranges of figure 8.

High values of SPA, with heating localized within $\rho < 0.5$, should be achieved for ECRH over a significant fraction of the toroidal field range in question, though at higher toroidal fields, $4.1 \leq B_t \leq 5.3$ T, the 1O heating mode must be used, rather than the 2X mode valid for the range $2.65 \leq B_t \leq 3.4$ T. Since neither of these heating modes allows central deposition of power at intermediate values of B_t, as is clear from figure 8, the intermediate scenario foreseen at $B_t \sim 4$ T might be performed at lower input power, or the operating point relocated to just beyond $B_t \sim 4.1$ T, depending on the operational experience gained during this progression. As noted previously, the injected energy and power of the beams must be adjusted to the plasma density in each scenario to limit the shine-through power on the shielding blanket modules. Based on the analysis in [90], which errs on the conservative side, in H plasmas the allowable injection energy ranges (linearly) from 500 to 870 keV as the plasma density is increased from 2.4 to 5.6×10^{19} m^{-3}, while in He plasmas the corresponding density range runs from 1.5 to 3.5×10^{19} m^{-3}. Appropriate programming of the ECRH, ICRF and NBI power within the development of the plasma scenario allows effective exploitation of these constraints to maximize the permissible NBI injection power at each point in the (I_p, B_t) progression [90]. From the analysis of losses of neutral beam fast ions for 5.3 T plasmas and the expected level of ripple at these fields, it is expected that ripple-induced losses will be within the specified first wall power loading limits [92].

Within the lower field range, $B_t < 3.6$ T, efficient ICRF power coupling is predicted in He plasmas using fundamental H-minority heating, but, as discussed above in the context of the

development of the 7.5 MA/2.65 T scenario, ICRF heating options for H plasmas are predicted to have limited heating efficiency. More advanced, 3-species, heating scenarios are found to be applicable to plasmas in the TF range 3 - 3.3 T (e.g., H plasmas with minority concentrations of ^{4}He and ^{3}He) [93] that may allow exploration of hydrogen H-mode operation if the presence of helium decreases the H-mode threshold. A more detailed analysis of this option is in progress to explore the integration of such a scenario into the progression foreseen for this aspect of the program. In the higher TF range, above 4 T, the favoured ICRF scheme for the PFPO-2 phase would be fundamental heating of a ^{3}He minority for both H and He plasmas. If adaptation of the resonant RF heating systems to this approximately constant q_{95} progression ($3 \leq q_{95} \leq 4$) proves problematic, due to the need to readapt the scenario evolution to the changing heating scenarios (including, for example, the impact on impurity transport), an alternative progression at constant B_t = 5.3 T would be implemented (as discussed in section 3.2.5.7).

First full current plasma in PFPO-1 and PFPO-2: The first 15 MA/5.3 T (L-mode) plasmas will be developed in PFPO-2 as the end-point of the progression discussed above, since it is not considered likely that there will be sufficient operational time available in PFPO-1 to develop the scenario and to commission reliable operation of the disruption detection and mitigation systems to this level of plasma performance. However, performing full field/low current discharges is foreseen during PFPO-1 to develop disruption mitigation capabilities with respect to runaway avoidance before applying the DMS to higher currents.

For the 15 MA/5.3 T scenario, the H-mode power threshold in H is expected to be well beyond the level of installed heating power and access to H-mode is expected to be marginal in He, even with 73 MW of additional heating. Given the risks associated with operating such high current plasmas just above the H-mode threshold, the development and demonstration of 15 MA plasmas during the PFPO-2 phase will be carried out in the hydrogen L-mode regime. The flat-top duration can vary from ~10 s in ohmic plasmas to ~100 s with full auxiliary power (73 MW), for a CS coil current of 45 kA/turn. The experience gained in the optimization of H&CD scenarios during the (I_p, B_t) progression discussed above would determine the final heating program and total applied power for these plasmas.

3.2.4 Pre-Fusion Power Operation 1 (PFPO-1)

3.2.4.1 PFPO-1 Overall Plan

As noted previously, the installation of the beryllium blanket and tungsten divertor prior to PFPO-1 will initiate the exploration of a wide range of plasma configurations with currents greater than 1 MA and plasma durations beyond several seconds, and the specific objectives for this campaign have been detailed in section 3.2.1. Plasma initiation will need to be re-established in H at 2.65 T with the new first wall conditions. This will be followed by the development of limited low elongation plasmas at currents of up to 2 - 3 MA, together with the development of disruption and runaway electron (RE) mitigation. Plasma magnetic control of the current, position, and shape, including vertical stability control of elongated plasmas will lead up to 3.5 MA diverted plasma operation. A significant part of the initial operation program will be devoted to the commissioning of ECRH, fuelling, control and diagnostic systems with plasma. For the last, in particular, the calibration and determination of the measurement capabilities of the installed diagnostics, as well as the resolution of possible inconsistencies among the measurements of

plasma parameters, are essential to allow an efficient progress of the experimental program. Routine operation will then be developed up to 7.5 MA to provide a suitable plasma configuration for the commissioning of diagnostics and the ECRH power up to the full 20 MW for at least 50 s duration. Effective disruption and RE mitigation will have to be progressively established as the plasma current is gradually increased. The toroidal field and plasma current will also be increased in steps beyond 7.5 MA/2.65 T up to 7.5 MA/5.3 T and, if time allows, possibly up to 10 MA. An important goal of the program, once these operational elements have been established, will be the initial exploration of H-mode operation in H and He plasmas at fields in the range 1.8 - 2.65 T. Time permitting, and depending on the progress of the experimental program, the pulse duration may be extended to beyond 100 s at lower plasma currents to qualify auxiliary systems, particularly the ECRH system, for longer pulse operation in PFPO-2. Table 5 provides a summary of the main experimental activities foreseen for the PFPO-1 campaign, including estimates of the associated experimental time requirements, to provide a guide for the subsequent discussion.

3.2.4.2 Establishing routine operation with diverted plasmas to 3.5 MA

Commissioning robust plasma initiation: Commissioning and optimization of the plasma initiation and burn-through will be an essential prerequisite for efficient implementation of the subsequent experimental program. A robust operating space needs to be determined and the control of the plasma formation needs to be commissioned. ECRH and ohmic start-up will be explored and, if a robust breakdown/ burn-through strategy without EC-assist can be established, the routine use of ohmic breakdown would be the preferable approach.

For operation up to 3.5 MA a CS precharge of 20 kA is sufficient. The plan envisages starting operation at 2.65 T at maximum loop voltage using ohmic breakdown with prefill scans and PF coil bias scans for a first optimization of the timing of the plasma formation. This will provide the basis for the application of the EC breakdown assist, to obtain plasma formation (in case ohmic breakdown is not successful) and to expand the operation window for reliable breakdown. The use of EC-assist requires commissioning of the injection of EC waves into vacuum due to the potentially high stray radiation (implying interlock commissioning).

The operational domain for plasma formation should be documented in terms of gas dosing range (prefill), PF coil bias, timing of the gas and bias with respect to the loop voltage evolution, and the timing of the EC power waveform. It would be advantageous to commission the plasma formation over a range of CS precharge currents (10 - 30 kA).

For this first phase, the commissioning of plasma initiation at 5.3 T and the use of He is optional and can be implemented later when required by the experimental program, since full field operation during this early phase of PFPO-1 would require the additional commissioning of EC wave injection in O-mode. Helium operation could, in principle, be achieved following plasma formation in H should difficulties in plasma breakdown with He be found [94].

Limiter operation to 2 MA: The first demonstration of plasma magnetic control is planned at low currents of $I_p \sim 2$ MA and in limiter configuration, with a flat-top phase of several seconds. For shape measurement, the computed plasma boundary from magnetic data needs to be validated against other diagnostics such as (infra-red) camera images of the blanket modules and probe measurements. Magnetic control commissioning will proceed in several stages, from mainly pre-programmed plasma formation, I_p control, boundary flux control (or centroid control), tests of VS

at low elongation (natural elongation, κ, ~1.5) and verification of control gaps in limiter operation.

A first assessment of heat loads on the blanket first wall panels will be performed, although estimates of the PFC power loads during PFPO-1 indicate that power loads on PFCs during this period should be within their design limits [95]. Additional time will be required for validating the wall protection techniques. Corrective actions need to be identified and tested on real pulses, in case limiting conditions are reached, as part of the event handling development (see section 3.2.4.3).

Correction of error fields with toroidal mode number $n = 1$ will be performed using the external EFCC, and, during the initial operation phase, algorithms for error field reduction will be developed. The DMS must also be commissioned during early plasma operation to start the documentation of initial disruption forces (unmitigated, mitigated) and RE assessment in limiter plasmas, as outlined in section 3.2.4.6.

Commissioning of the plasma density control will be performed in two stages: a first stage using only the gas valves and a second stage with both the gas valves and pellet injectors. Density control with gas injection in various limiter phases, including current rise, flat-top (at 2 MA) and current ramp-down, will be commissioned. Density limits and fuelling limits will need to be documented. For He operation, planned later in PFPO-1, density control will need to be re-optimized and the density achievable in He assessed.

Limiter operation to 3.5 MA: Following completion of the initial commissioning at 2 MA and assessment of the disruption forces, operation will be expanded to 3.5 MA in limiter configuration with low natural elongation. Vertical stability control will be commissioned with and without in-vessel VS coils by gradually increasing the plasma elongation until plasmas with a near-divertor configuration are established. Tuning and optimization would include, if possible, reduction of low frequency noise in the dz/dt diagnostic signal used in the feedback stabilizing loop.

As soon as plasmas with an electron temperature of several hundred eV are achieved, more extensive commissioning of the ECRH system can be launched. The principal issues to be addressed are the beam polarization and the launcher angles. Operation of EC at 2.65 T is planned, injecting X-mode and heating at the second harmonic resonance. For the equatorial launcher (EL), in particular, this approach is potentially hampered by strong absorption in the 3rd harmonic (X3 heating) towards the plasma edge on the low field side (LFS). Potential cross polarization (O-mode) may be strongly absorbed at the 2nd harmonic resonance (O2 heating). These additional absorption processes may complicate verification of the wave polarization and the location of deposition. As X3 and O2 heating make significant contributions at higher temperatures and densities, it may be necessary to perform the polarization tests at the lowest currents for which a diverted plasma can be achieved. This requires further analysis using beam tracing codes, but it can be noted here that X3 heating can be avoided by increasing the toroidal field for this intermediate operational point from 2.65 T to 2.75 T, so as to move the corresponding 3rd harmonic layer just beyond the last closed flux surface (LCFS) on the outboard side of the plasma.

In parallel, a further assessment of the DMS system will be carried out for limiter operation up to 3.5 MA, together with the documentation of the disruption loads and the potential for creating REs (as discussed in section 3.2.4.6). Heat loads to blanket modules, error field correction and density control may also need further assessment and optimization at 3.5 MA.

Diverted operation at 3.5 MA: Magnetic control of a diverted plasma configuration at low plasma current (3.5 MA) is challenging in ITER. However, disruptions at low current present a reduced risk of localized damage to PFCs, allowing optimization of the plasma magnetic control, optimization of the plasma-wall gaps, strike-point control and stabilization of plasma vertical displacements in the divertor configuration, both with and without the in-vessel VS coils. An important aspect of divertor operation is the additional validation of the plasma configuration derived from other diagnostics (than magnetics), e.g., to confirm the location of strike-points, plasma/wall separation etc. First diverted plasmas at 3.5 MA will be established at lower elongation ($\kappa \sim 1.5$) to allow tests with and without in-vessel VS coils. Operation will be extended to full bore at full elongation once control of the plasma boundary, control of the strike-point location and vertical stability control have been commissioned.

As soon as plasmas with an electron temperature of several hundred eV are achieved, more extensive commissioning of the ECRH system can be launched. The principal issues to be addressed are the beam polarization and the launcher angles. EC operation at 2.65 T is planned, injecting X-mode and heating at the second harmonic resonance. This will include assessment of the impact of higher harmonics at the edge (X3) and of residual cross polarization in the beam (O mode with O2 absorption). The peripheral X3 effect may be significant as the edge temperature increases and this may require tuning of the toroidal field value to position the secondary resonance layer beyond the last closed flux surface (LCFS) on the outboard side of the plasma (i.e. by a small increase of the toroidal field beyond 2.65 T).

Full plasma scenarios will be developed, with current ramp-up, X-point formation and ramp-down in divertor configuration using feedback control of plasma current, plasma-wall ‘gaps’ and strike-point positions. In addition, scenarios with varying rates of current ramp-up (with/without ECRH) and ramp-down will be explored. This will also allow validation/adaptation of the plasma transport models used in simulations describing these transient phases.

Commissioning of event handling and ramp-down, or shut-down, strategy/logic is important during the initial divertor operation phase, laying the basis for routine divertor operation in ITER. Commissioning of basic wall protection could be performed at much lower limits or by means of artificially triggered events to commission the PCS response. Density control needs to be tuned for divertor operation using both gas dosing and pellet fuelling. Once pellets are being produced and injected, plasma operation will be required to validate the quality of the pellets entering the chamber. Tests will also be necessary for pellets of various sizes. Substantial commissioning of the DMS system will be performed during 3.5 MA divertor operation, as outlined in section 3.2.4.6. As detailed in the following section, commissioning of the ECRH, which will have been restricted to plasma initiation and burn-through in the early phase of operation, will also be undertaken to provide a capability for optimization of the plasma initiation and current rise in this phase.

3.2.4.3 Commissioning Activities for Control, Data Validation, and Heating and Current Drive

Validation of diagnostic data and demonstration of measurement consistency: As discussed in section 3.1.1, diagnostic calibration and validation activities will be initiated during Integrated Commissioning (e.g., magnetics, neutral pressure, etc.). Magnetic measurements will be used to determine the (toroidal) magnetic axis of the toroidal field to align the blanket modules, which

will already require validation and demonstration of the measurement consistency of the magnetic field measurements with modelling of the field in the absence of eddy currents. With FP, there will also be the opportunity to validate and demonstrate the measurement consistency between the magnetic diagnostics and modelling, including eddy currents in the conducting structures. As was the case during the Integrated Commissioning preceding FP, there will be extensive commissioning activities for diagnostic systems in preparation for plasma operation. A particularly important activity, which will assume greater significance during PFPO-2 (see discussion in section 3.2.5.2), concerns the in-situ calibration of the 2.5 MeV neutron measurement systems.

From early in PFPO-1, as each of the diagnostics is commissioned, their measurements must be validated and the consistency between various measurements will need to be demonstrated, particularly for control and investment protection functions. This validation and consistency process will continue throughout all the operational phases as the installed diagnostic capability expands. Once routine operation is underway, the process for data validation for the majority of systems will not require dedicated plasma time. Nonetheless, some dedicated pulses for diagnostic commissioning are included in the planned run-time estimates, and progress to the target plasma scenario will be performed in steps only after diagnostic validation.

Diagnostics required for investment protection will also have to be rigorously validated and checked for consistency across multiple measurements. Plasmas with reduced risk for investment protection will be used until accurate data validation and consistency have been established. For example, the plasma shape will be cross-checked with visible camera images that provide the contact points during the limiter phase and the strike-point locations during diverted operation.

During PFPO-1, as additional diagnostics are brought on-line and general plasma conditions (including duration) improve, diagnostic data validation will work towards applying automatic procedures and more sophisticated models of the plasma behaviour within the Integrated Modelling and Analysis Suite (IMAS) to validate measurement consistency. Establishing the validity and consistency of the measurement and analysis chain (including, for example, particle and energy transport models) as early as possible is essential to ensuring reliable operation in later phases of the experimental program and to providing the analysis capability necessary to develop a detailed understanding of physics processes in burning plasmas. This activity will therefore be important in preparation of subsequent high plasma performance operation and fusion power experiments.

Commission control, interlock and safety functions: During initial operation in PFPO-1, all of the basic control functions will be commissioned, as well as commissioning/ verification of the PCS supervisory monitoring functions, event handling logic, and the interaction with the CIS. All technical commissioning that can be carried out without plasma for PCS control of the actuators, the communications among plant systems, supervisory systems, and the PCS failure monitoring will be performed before plasma operation.

The strategy for PCS commissioning in PFPO-1 will be aligned with the overall logic of the Research Plan, consisting of three stages with two options for further development:

1) commissioning of magnetic control up to robust diverted operation at 3.5 MA/2.65 T;
2) commissioning of magnetic control up to 5 MA/2.65 T;
3) commissioning of magnetic control up to 7.5 MA/2.65 T.

The first option for further development involves H-mode operation at 5 MA/1.8 T, both to demonstrate H-mode access and to commission initial ELM control techniques. The second option relates to commissioning of magnetic control up to ~10 MA/5.3 T, initiating the development towards 15 MA L-mode operation. Pursuit of the latter option would rely on demonstrating satisfactory progress in the development of disruption and RE mitigation and on having sufficient experimental time beyond the achievement of the essential goals for PFPO-1.

Commissioning activities will initially establish adequate control of plasma current, position and shape with limited plasmas, followed by demonstration of reliable vertical stability control at high elongation, allowing the transition to diverted plasmas. Equilibrium reconstruction will be required in the first phase, as well as error field control, particularly to correct for $n = 1$ error fields. Density control will be commissioned for both gas and pellet fuelling. ECRH breakdown assist will need to be recommissioned with the beryllium first wall and divertor, and ECRH control will also need to be commissioned for burn-through, heating during the plasma current flat-top and during the ramp-down. If the H-mode threshold is within the available power of 20 MW, first H-mode operation may be developed at 5 MA/1.8 T, allowing first tests of ELM control with pellet pacing. Initial forecasting and event handling schemes will be developed to anticipate controllability boundaries and to allow evasive actions, to optimize plasma operation and avoid disruptions. Depending on the development of disruption and RE mitigation techniques, magnetic control commissioning could be extended up to ~10 MA at 5.3 T towards the end of PFPO-1.

The investment protection system incorporates both dedicated Plant Interlock Systems (PIS) and the Central Interlock System, and is designed to prevent operational limits being exceeded, as well as to ensure that the systems and components are protected against self-induced faults, faults generated by other systems and unintended consequences of plasma operation. After thorough technical commissioning, the relevant interlocks will have to be tested with plasma. These may include interlocks to impose lower limits on plasma current, density, or electron temperature (in case of X3 or O2 heating). Stray radiation monitoring with a large number of ECRH sniffer probes at various poloidal and toroidal locations is planned. The in-vessel elements of the ITER ECRH system will be similar in many respects to those of the W7-X system already in operation (10 MW, 2000 s) [96]. Transfer of operational experience from W7-X would therefore be beneficial for the preparation of these ITER commissioning activities.

Real-time recognition of off-normal events, such as the development of a significant population of runaway electrons or approaching the predicted boundary for vertical stability, and the automated initiation of counter measures, including discharge termination, should be validated and incorporated into the operational framework as soon as practical. Real-time protection for critical PFCs will need to be commissioned as a prerequisite for sustaining reliable operation in subsequent experimental phases, in which the power and energy input will increase. These functions will be included in PCS, but an additional level of protection will be included in CIS to protect against plasma events with a high level of integrity.

While PCS will act as the first line of defence for investment protection, CIS will always provide the ultimate investment protection response, even for complex functions during plasma operation, including first wall and divertor heat load protection. To ensure a robust operation of the investment protection framework, dedicated experimental time for commissioning of first

wall and divertor protection is included in the estimated run-time for each step in I_p and H&CD power.

For ITER, a set of use cases has been identified in which the plasma is either involved in, or affected by, safety functions. It is then mandatory to demonstrate that the safety events (formally 'protection important' events) are detected and the corresponding actions are performed. At present the only safety-related event in which plasma operation is implicated is the activation of the Fusion Power Shutdown System (FPSS). The system must therefore be tested during dedicated plasma operation, probably at reduced performance to avoid the risk of damage to internal components. Additionally, the critical event detection, namely the protection important measurement of the plasma current, must be validated and tested similarly to the approach expected for the investment protection functions.

ECRH commissioning in plasmas at up to 7.5 MA/2.65 T: Each H&CD system will require commissioning periods with and without plasma, but the discussion here and in later sections focusses on commissioning activities during plasma operation. Initial ECRH commissioning must be undertaken prior to FP and has been described briefly in section 3.1.1. The PFPO-1 phase will benefit from the full ECRH power capabilities, i.e., the set of 24 gyrotrons delivering a total EC power of 20 MW at 170 GHz. All gyrotrons are assumed to have been conditioned up to the torus windows in advance of plasma operation. ECRH commissioning should demonstrate the following capabilities:

- Demonstration of local deposition (correct polarization, separately for each gyrotron) with an appropriate launcher control. This process checks for several potential sources of uncertainty in the location of the power deposition (launcher angles, X3 parasitic absorption, ray tracing parameters, equilibrium, mapping routines, analysis of ECE data, etc.);
- Launching of 20 MW in short pulses via the equatorial launcher (EL) and/or the upper launchers (ULs). Short pulse conditioning of all beam lines and parallel operation of all gyrotrons (screening against magnetic field interference) and power supplies must be demonstrated, together with the full power capability of launchers;
- The effect of X3 heating at 2.65 T for the equatorial launcher must be checked. If crucial, the magnetic field may need to be increased by 2-4% or the EL polarization changed from X- to O-Mode;
- For the O1 heating scheme at 5.3 T, the X1 reflection must be shown to be lower than 1%: first harmonic heating (i.e., at high fields in ITER) requires O-mode injection, but any cross-polarized radiation will be reflected at the X-mode cut-off and focussed on the LFS first wall. A cross-polarization fraction of 1% has been assumed, corresponding roughly to a power density of 1 - 10 MWm^{-2} at the location of the first reflection on the outer wall. This estimate forms the basis for the window design - windows are typical components at risk from incompletely absorbed EC radiation (note that, in current devices, cross-polarization has been demonstrated to be below 3%, close to the resolution limit);
- Long-pulse heating above 50 s must be achieved. The entire ECRH system and the ITER vessel are cooled, but while some plasma facing areas are efficiently cooled by proximity to cooling channels, more distant regions are cooled by temperature gradients. Any anisotropy of the surface heating of order 1 MWm^{-2}, corresponding to the average neutron

power deposition in the wall, may increase these gradients on long time scales, leading to hot spots. These potential issues need to be detected and counter-measures implemented prior to significant fusion power production. This is equally true for 'spill-over' losses due to large asymmetric mode content (mode impurity of up to 5% is allowed, which can generate beam shapes with 2 maxima);

- The power modulation capability must also be tested within the commissioning activities.

Commissioning of the full ECRH system (i.e., 24 gyrotrons, the EL and 4 ULs) will be performed in 7.5 MA/2.65 T plasmas, using 2X ECRH absorption, which requires a low density and modest temperature ($n_e \sim 10^{19}$ m^{-3} and $T_e \sim 1$ keV) to achieve full absorption of the ECRH power. The commissioning period could be combined with other aspects of plasma commissioning or experimentation.

Further ECRH commissioning time will probably be necessary as the toroidal field is raised towards 5.3 T, for which the heating scheme would be fundamental O-mode absorption. As plasma scenarios are developed towards higher current and field, it will be necessary to switch from the 2X heating scheme to the 1O scheme. At the other extreme, the option for operating at $B_t = 1.8$ T would require a further allocation of ECRH commissioning time.

Advanced control commissioning in PFPO-1: Once routine plasma operation is achieved and robust basic magnetic and kinetic control schemes allow standard plasma scenarios to be reproduced reliably, more advanced control functions can be commissioned. In this context, 'advanced control' refers to control functions beyond those required for basic plasma current, position, and shape control, basic density control and basic heating system control - the functions involved are likely to have an important role in supporting plasma scenarios required to satisfy ITER's fusion power and fusion gain missions. The more advanced control functions include kinetic control functions such as: first wall and divertor protection, β and stored energy control, rotation profile control, and minority species control; MHD and error field control functions such as: ELM, NTM, dynamic error field and resistive wall mode (RWM), and sawtooth control; and supervisory control functions including exception handling and more advanced actuator management functions. Although some dedicated time is foreseen for commissioning of this functionality within PCS, the full development of these functions to the point at which they provide a robust control capability is likely to require further run-time as part of the physics program.

Plasma kinetic control: First wall protection is an early commissioning priority to ensure that it is routinely (and reliably) available before expected first wall heat loads exceed the power handling capability of the beryllium first wall panels. The first wall shaping has been designed on the basis of a heat flux e-folding length scaled to ITER from current experiments with the requirement that the dedicated first wall 'limiter' (i.e., high heat flux) panels can withstand stationary limiter plasma operation up to ~5 MA with an additional ECRH power satisfying P_{ECRH} (MW) ≤ I_p (MA) (see [95] for more details). However, due to uncertainties in the scaling to ITER, it is currently considered prudent to avoid limiter plasma operation beyond about 3.5 MA, a current level at which diverted plasmas should be achievable (this guideline might be revised once experimental data from ITER is available). Several discharges with special equilibrium shapes and plasma currents between 3.5 and 5 MA will be needed to fully commission first wall heat flux control and to investigate heat loads due to plasma contact at

various points along the first wall, in particular, to compare the protection of the high heat flux panels and the standard heat flux panels. Once the plasma current is raised beyond 5 MA, whether in PFPO-1 or PFPO-2, a robust first wall protection functionality must be demonstrated in both PCS and CIS.

Divertor protection will not be required in PFPO-1 since there will be only 20 MW (at most 30 MW) of auxiliary heating power, and the divertor is not expected to be overloaded for auxiliary heating levels under 40 MW [3-Appendix C]. However, it will be important to begin to develop divertor protection during PFPO-1 before it becomes essential for investment protection. Although it may not be possible to fully demonstrate effective divertor heat flux control with limited auxiliary heating power, initial tests of divertor heat flux control algorithms can begin once routine diverted plasma operation is achieved.

Development of effective β control should also begin in PFPO-1 to prepare for the exploitation of high auxiliary power in PFPO-2. As plasma parameters approach $q_{95} = 3$ at 7.5 MA/2.65 T, β control will be an important capability to assure overall control of MHD stability and to sustain quasi-stationary plasma conditions, in particular, to achieve longer pulse durations at nearly full auxiliary heating power. Relatively simple proportional-integral-derivative (PID) control algorithms, or more sophisticated physics model-based controllers [97] can be implemented, with a variety of sensors available.

A further, more advanced, control capability that could be commissioned in PFPO-1 relates to the mixture ratio of different plasma fuelling species. Diagnostics available in PFPO-1 that can at least provide some information on the minority content and species mixture include the visible H_α system and the vacuum ultraviolet system. With only H and He fuel available in PFPO-1, fuel mixture control may not be required in this phase, except possibly for certain H-mode experiments. It would, nevertheless, be valuable to begin to develop fuel mixture control experiments even in this phase as part of H/He changeover experiments.

Magnetohydrodynamics (MHD) and error field control: With the EFCC and the ECRH&CD system commissioned in PFPO-1, it will be possible to begin to develop advanced control schemes for several MHD instabilities and for error field correction. Depending on the level of error fields found in ITER due to coil manufacturing and installation tolerances, it may already be necessary to correct for error fields with the EFCC at low plasma current to avoid low density locked modes in the current rise [98, 99]. The correction of small, non-axisymmetric magnetic fields in a tokamak generated by the real three-dimensional, non-toroidally-continuous nature of device components is important to maximize plasma performance and yield superior plasma stability. These ‘error fields’ can change in time throughout the plasma pulse. The plasma itself can amplify such fields, and such amplification can itself be dynamic in nature (time varying in amplitude and toroidal phase). Typically, the most deleterious error fields have toroidal mode number $n = 1$, with varied poloidal field spectra. Since the EFCC are designed primarily for the correction of quasi-static error fields, control of ‘dynamically amplified’ error fields will be possible only when the ELMCC system is operational in PFPO-2.

With at least two pellet injectors installed, it should be possible to begin to develop ELM control techniques in PFPO-1 if suitable H-mode regimes can be established. It is not anticipated that ELM control will be required in PFPO-1, since the predicted heat loads for the relevant plasmas with lower plasma current and limited auxiliary power are not expected to be severe. Nevertheless, the development of ELM control techniques as soon as H-mode operation is

obtained will be valuable preparation for higher performance operation and to explore the strategy to prevent accumulation of tungsten in the core plasma in H-modes. After the ECRH system and the pellet injection systems are fully commissioned in PFPO-1, H-mode operation will be attempted, as described in section 3.2.4.5. If ELMy H-modes are achieved, then ELM control techniques with both pellet pacing [100, 101] and vertical plasma oscillations [102 - 104] will be tested.

Once the ECRH system is fully commissioned, initial tests of NTM control could already be attempted in PFPO-1, well before it will be required to avoid disruptions at higher plasma performance. Even at the low plasma performance expected in PFPO-1, classical tearing modes are likely to be driven unstable under some conditions allowing their control using ECRH to be attempted. Although there is an extensive background on the implementation of NTM control in existing devices [105 - 113], the specific conditions in ITER will require significant run-time to fully develop a reliable NTM control capability.

Sawtooth control is also a potential application of ECRH/ ECCD in PFPO-1, i.e., prior to high-I_p/low-q operation in PFPO-2, when such control might be essential. At 7.5 MA/2.65 T (i.e., q_{95} ~ 3), plasmas might exhibit relatively large sawteeth (particularly if 30 MW of auxiliary heating is available in PFPO-1), providing a good scenario for initial sawtooth control commissioning. Extensive studies have been performed to develop an understanding of sawtooth control and to demonstrate the technique on existing devices with both ECRH and ICRF heating, establishing a basis for the modelling of sawtooth control on ITER [114 - 120].

Supervisory control: A key feature of the ITER PCS is advanced supervisory control, which includes both exception handling, i.e., when a plant system or plasma event occurs that requires a real-time change in control, and shared actuator management, which attempts to optimize a limited number of actuators for multiple simultaneous or consecutive control functions. Initial elements of exception handling are already required from FP to monitor operation limits and take action if prescribed thresholds are approached, e.g., for coil protection. Exception handling is also used to perform real-time tuning or changes of controllers via comparison with expected performance based on prior modelling. Exception handling is an essential part of the PCS as the first line of defence for investment protection. Optimization of the available run-time will steadily increase the requirements for exception handling as plasma performance increases. Some aspects of this technique are already implemented on JET and ASDEX Upgrade, and the functionality is incorporated in the ITER PCS design [118, 119].

Initial commissioning of actuator management can begin once the ECRH system can routinely deliver ~20 MW to the plasma. This will include automatic switching of power from the equatorial to one of the upper launchers, as well as switching power between the upper and lower steering mirrors (USM, LSM) of each upper launcher. The control is straightforward, but the timescales for switching (~3 s) must be included in the algorithms and the consequent dead time must be reflected in the shared actuator control schemes such as sawtooth and NTM control. Descriptions of the PCS architecture requirements and of the approach to shared actuator management can be found in [118, 120].

Advanced control commissioning deliverables (PFPO-1):

- H-mode operation in plasmas at 5 MA/1.8 T including handling of L-H and H-L transitions;
- Initial ELM control with pellet pacing and vertical plasma oscillations;

- Initial first wall and divertor heat load protection;
- Initial β and stored energy control;
- Initial NTM and sawtooth control as plasmas parameters allow;
- Development of more advanced actuator management functions;
- Initial forecasting and event handling schemes to anticipate controllability boundaries and to take evasive action to optimize plasma operation and avoid disruptions;
- Magnetic control at plasma parameters of up to ~10 MA/5.3 T, depending on the development of disruption and runaway mitigation.

3.2.4.4 Development of reliable operation to 7.5 MA/2.65 T

Establishing 7.5 MA/2.65 T divertor plasmas with ECRH: Following the development of routine diverted plasma operation up to 3.5 MA and 2.65 T and the commissioning of disruption and RE mitigation, diagnostics, plasma control, interlock, and safety systems and initial commissioning of ECRH&CD at modest plasma current levels, plasma scenarios will be developed up to 7.5 MA at 2.65 T in L-mode. These plasma scenarios will be initially developed in H, but operation in He may also be required, in particular, to explore H-mode operation if the H-mode threshold is within the available power limit.

This development will consists of steps in plasma current with a first step at 4 MA at 2.65 T and with further development of plasma current, shape, and position control in H plasmas towards 7.5 MA in subsequent steps of ~0.5 - 1 MA. The first small step to 4 MA ensures that scenario development should be straightforward to quickly ensure robust magnetic and density control, as well as improved disruption and RE mitigation. As current increases beyond 4 MA, the likelihood of PFC melt damage during disruptions increases (the threshold for this is presently evaluated to be in the range of ~ 7 MA for the current quench [124]). Therefore, monitoring and assessment of first wall heat loads following disruptions will be routinely performed. Moreover, with increasing current level the likelihood of disruption melt damage and RE generation increases. Thus, operational time will need to be allocated to developing robust disruption and RE mitigation techniques.

At every current level, further development of plasma current, position, and shape control will be required, including robust vertical stability control to avoid the occurrence of VDEs. Similarly, plasma termination scenarios for both standard ramp-down and for emergency terminations will need to be developed at each current level before moving to the next step, with particular attention to impurity accumulation and vertical stability control in the ramp-down phase. Depending on the level of error fields found due to coil manufacturing and installation tolerances, error field correction may also require further development with every step in plasma current.

Once robust scenarios have been developed to a level of 6 - 7 MA, including disruption avoidance and mitigation as required, a plasma scenario at 7.5 MA/2.65 T, the first ITER scenario at q_{95} = 3, would be developed. Such plasmas are expected to be more susceptible to disruption-inducing MHD phenomena, implying appropriate care would need to be taken in their development, particularly in establishing robust equilibrium control (i.e., plasma current, position, shape and, in particular, vertical stability control). Core fuelling with pellet injection may be required at this current level. Central electron heating with ECRH should be developed, to control impurity accumulation in the core, and sawtooth control should also be pursued, as

large sawteeth are expected at lower values of q_{95}. Additional first wall and initial divertor heat flux control should be developed in parallel. These scenarios will also incorporate elements of the advanced control and disruption mitigation activities discussed in sections 3.2.4.3 and 3.2.4.6. Further development of plasma termination scenarios will be necessary to avoid impurity accumulation and ensure vertical stability in the ramp-down.

Routine operation of 7.5 MA/2.65 T plasmas would be a key milestone from this phase of experimentation. The pulse duration of these scenarios would then be extended out to ~50 s to provide a standard ITER scenario for development of the heating schemes. Since this scenario is the half current, half field equivalent of the baseline 15 MA/5.3 T scenario, development of robust operation at 7.5 MA/2.65 T is required to commission all systems in PFPO-1.

Limiter heat load characterization: As in many tokamaks, plasma current ramp-up in ITER will begin in limiter configuration on the first wall. This will be the case for all plasmas, in all operational phases, with the only difference being the range of B_t which will be explored in each phase. The First Wall Panels (FWPs) are designed such that start-up can be on either the outboard or inboard equatorial regions, with enhanced heat flux (EHF) panels installed there to handle perpendicular heat loads up to ~4.5 MWm^{-2} [125]. For a number of reasons [126], inboard start-up is preferred and the majority of start-up scenarios developed for ITER favour this route. So far, all ramp-down scenarios bring the plasma down into a limiter configuration on outboard panels those in the lower part of the poloidal cross-section at low I_p.

In recent years, a great deal of work has been invested in the R&D community, led through the ITPA Divertor and SOL Topical Group, to properly characterize start-up limiter heat loads. This was stimulated by the first measurements on the JET ILW Be main chamber protection limiters [127, 128] which found strong evidence for a very narrow feature (of width $\lambda_{q,near}$), in the SOL parallel heat flux at the LCFS of inboard limiter plasmas, followed by the normal 'broader SOL' (of width $\lambda_{q,main}$), which had previously been assumed for the design of the ITER FWPs to be the only structure of limiter SOLs. In fact, multi-device studies [126] have revealed that $\lambda_{q,near}$ scales with $1/I_p$ in the same way as for the near-SOL in diverted H-modes (see [3-Appendix C]). It has also been shown [129] to be reasonably well matched by the heuristic drift model developed for the H-mode [40].

In the light of the JET findings, a very extensive multi-machine database has been constructed for the inboard limiter $\lambda_{q,main}$ [130] to try and confirm the original assumptions for the broad SOL width made for the ITER wall design which were based on very sparse data. The new scalings, derived from the JET data complemented with a database from extensive sets of experiments in smaller devices (see references in [126]), for both $\lambda_{q,near}$ and $\lambda_{q,main}$ have been used to redefine the toroidal shape of the ITER inner wall FWPs [126] since the previous major release of the ITER Research Plan (the outer wall panel shape remains unchanged). This new shape takes into account the presence of a double exponential structure in the SOL parallel heat flow.

A great deal more information is now also available regarding the accuracy with which the blanket can be mechanically aligned [and it is now even more important than before that the IRP foresees adequate operational time for limiter heat load verification to carefully validate FWP heat loads, given the penalties that must be introduced to account for blanket misalignments and the fact that the real design of the FWP contour is only an approximation to the ideal shape defined by physics [131].

Dedicated limiter heat load studies will be required in PFPO-1 at all major toroidal field values to be used for scenario design and DMS commissioning. Part of these experiments can be conducted during the commissioning phases that must be performed to establish routine limiter operation, as detailed in section 3.2.4.2. The first stages will be at lower I_p (2 MA), followed by a step to near 3.5 MA, which is the approximate plasma current at which a divertor configuration can be formed according to current scenario design. This commissioning will also include development of ECRH heating scenarios; this is important for limiter heat load testing which requires additional power. The early tests, probably starting at lower B_t, will permit a first crude look at the influence of FWP misalignment on the power distribution (using the wide angle main chamber IR viewing diagnostics) and a cross check of the magnetic axis measurements [95] which will have been performed following the FP attempts and prior to full blanket installation.

The FWP shape design has been optimized for $\lambda_{q,main}$ = 15 mm and 50 mm for outboard and inboard limiter plasmas respectively and $\lambda_{q,near}$ = 4 mm for inboard limiter configurations (the narrow feature is not present for plasmas limited on the outboard). The chosen values for $\lambda_{q,main}$ fall within the inner wall limiter multi-machine database scatter at for I_p up to 5 MA, the highest plasma current considered in the FWP design [132]. Regression analysis of the database finds a best fit engineering parameter scaling for inboard limiter plasmas of $\lambda_{q,main} \propto (P_{IN}/V)^{-0.4}\kappa^{1.3}$ with P_{IN} the total input power, and V the plasma volume. For inner wall limiter configurations, a second parameter also plays an important role in the new shape design: the effective ratio, R_q, of power transported in the near and main SOL regions of the profile. This has been fixed at R_q = 4 for the ITER inner FWP [126], but is uncertain since the data from the multi-machine experiments are more scattered and a scaling cannot yet be defined. There is, however, some flexibility here since the chosen toroidal shaping allows for a range of possible R_q before power overload, although this will be sensitively dependent on the degree of FWP misalignment [95] and must be carefully checked.

Thus, according to current best scalings, there is no explicit B_t dependence in either $\lambda_{q,main}$, or $\lambda_{q,near}$, a relatively clear $\lambda_{q,near} \propto 1/I_p$ dependence and uncertainty in the variation of R_q, though there is some evidence for a direct scaling with P_{IN} [133], so that both $\lambda_{q,main}$ and R_q are likely to be input power dependent. Detailed assessment of the FWP power handling during design phases was conducted assuming B_t = 5.3 T, so that the safety factor at the LCFS (q_{LCFS}) will be lower at a given I_p for ramp-ups with 1.8 T and 2.65 T (e.g., for near full bore limiter plasmas at $\kappa \sim 1.5$ and I_p = 3.0 MA, $q_{LCFS} \sim 10$ (5.3 T), 5 (2.65 T) and 3.5 (1.8 T)). For a given plasma shape, this is unfavourable for FWP loading since higher pitch angles at lower field mean that field line penetration may occur in regions not anticipated in the original design. Detailed field line mapping for all configurations to be tested, incorporating basic SOL heat flow models, will need to be performed before any dedicated power loading experiments. The very first attempts at low I_p can be used to calibrate the models and tools now being put in place to perform these assessments. It should be noted, however, that the main chamber IR systems, which are the primary diagnostics for this experiment, will not be sensitive to very low surface temperatures and so at very low input power, limiter heat flux patterns may not be easy to measure.

Once limiter plasma and ECRH power commissioning are satisfactorily completed at each given B_t, dedicated limiter heat load characterization in PFPO-1 should include the following main elements, conducted for both inboard and outboard limiter configurations:

- Elongation scan at fixed I_p and P_{IN};
- Power scan at fixed shape (elongation) and I_p;
- I_p scan at fixed elongation and P_{IN};
- Density scan over the range possible at fixed I_p, P_{IN} and elongation.

The experiments should be performed in H plasmas since He sputtering will be higher and impurity distributions different to those in hydrogenic plasmas. Moreover, if the narrow feature width scales with ion orbit width, this will be different in H and He. Similar experiments could be run, if required, in He plasmas to expand the limiter loading database, but this should not be a priority in the Research Plan.

A simple criterion was adopted for the FWP shape design to define the maximum power fluxes during limiter phases [126, 129]: $P_{limiter}$ [MW] < I_p [MA], so that at the highest specified I_p (7.5 MA), a total of 7.5 MW of heating power (ohmic plus additional heating) is assumed. This allows for a reasonable margin for ECRH heating, though as mentioned above, detailed wetted area and power flux density calculations will be required prior to any limiter plasma work at higher input powers. The lower power commissioning stages will have permitted any gross FWP panel misalignments to be quantified and this will also set the limits to what can be done during the full heat load characterization, both with respect to input power and plasma shape variation. The maximum values of P_{IN} and, in particular I_p, will need to be chosen for these experiments once the first commissioning results are available and will be dependent on progress with disruption mitigation (see section 3.2.4.6).

Experiments on JET with Be limiters performed long before the ITER-Like Wall installation found no runaway generation during unmitigated disruptions up to 5 MA at high toroidal magnetic field [134], but the limiter configuration is more favourable for runaway appearance when mitigation is deployed [135]. However, thermal loads during the current quench of unmitigated disruptions at higher currents can be prohibitive due to conversion of magnetic energy into thermal power flux and subsequent melt damage to the first wall [124, 136]. The choice of maximum I_p for the limiter heat load characterization will therefore primarily be determined by the status of DMS testing. If feasible, maximum target values would be ~4 MA at 1.8 T and ~6 MA at 2.65 T. Nearly circular plasmas will likely be restricted at the higher current and powers due to unacceptable field line penetration. These are in any case of lower interest, other than to test the shaping design, since nearly circular plasmas will only ever occur at very low I_p (hence low power) in the very early ramp-up phases.

The aim of these limiter heat load validation experiments is to set the limits on what is acceptable with regard to first wall power loading, to check if the input physics assumptions defining the wall shape are applicable at the ITER scale, to benchmark field line tracing and wall shape parameters and to test wall heat load protection algorithms. The full main chamber IR diagnostic (WAVS: Visible/IR) system must be in place to conduct this validation - experience from JET [127] demonstrated how important it is to be able to see as much of the limiter surface as possible. For the actively cooled FWPs, steady state power handling is achieved in several seconds, so that the experiments should guarantee phases of this duration for each of the chosen scenarios. The active cooling is advantageous in the sense that several experimental points can in principle be obtained in a single discharge, depending on the maturity of plasma shape control. Once experiments have been performed at the first chosen value of B_t, it should be relatively

straightforward to repeat the scans, or a subset, at higher toroidal field and less dedicated experimental time should be required.

Heat loads and detachment control during divertor operations: A proper determination of heat loads to main chamber and first wall PFCs during diverted operation and demonstration of their control, particularly in the divertor, is a key element of the PFPO phases, in preparation for nuclear operation, when robust power flux control will be mandatory for ITER to achieve its mission goals. Providing as comprehensive a database as possible in the early operational phases will also allow years of model development to be validated, hopefully improving confidence that the physics of divertor power dissipation and SOL transport in ITER is well understood. The main issues to be addressed require experimental time both in the L-mode development program and in the H-mode exploration discussed in detail in section 3.2.4.5, but are gathered here to provide a self-consistent overview of this aspect of the PFPO-1 research program. Specific experimental studies required are (see also sections 2.5.2 and 2.5.3):

- Scaling of the near SOL L-mode and inter-ELM H-mode heat flux width;
- Characterization of the far-SOL width for power and particles (main chamber interactions) in L-mode and inter-ELM H-mode;
- Assessment of upper FWP power handling;
- Understanding divertor detachment behaviour;
- Effects of 3-D magnetic fields for ELM control on divertor target power distribution;
- Assessment of ELM transient divertor and main wall power loading.

Many of the required measurements will naturally be obtained during commissioning and development of scenarios in the early phases and only a relatively small number of dedicated plasmas are likely to be required, particularly in PFPO-1, when power levels will be low. As shown in [3-Appendix C, 43], steady state power loads at the divertor do not challenge the heat handling capacity of the divertor monoblocks for $P_{SOL} \lesssim 40$ MW, which cannot be achieved until PFPO-2, and even then the heat load is only problematic at low divertor neutral pressure (high divertor plasma temperature), at which W ingress may in any case be prohibitive. It is also the case that for the maximum input power available in PFPO-1, L-mode and ELMy H-mode loads to the upper FWP in the secondary X-point point region for the baseline equilibrium at $q_{95} = 3$ are also far below (at least a factor 3) the maximum power handling capability of the EHF FWP #8,9 located in this area, even for $\Delta r_{sep} = 4$ cm, the lowest (outer midplane) primary to secondary separatrix separation allowed during the burning plasma phase.

In PFPO-1, therefore, PFC power loads will be well within their design limits, so that active control is not required beyond the usual (accurate) control of the plasma shape (wall gaps, strike-point positions, etc.) and the respect of operational limits (see e.g., section 3.2.4.6). Specific heat load studies in this phase can therefore be pursued without concern for PFC damage, provided the DMS has been adequately commissioned. Experiments will rely heavily on main chamber and divertor IR cameras, including the high resolution divertor systems viewing the inner and outer targets at a single toroidal location.

The following studies are to be performed, if possible, in this phase:

- *L-mode divertor heat load characterization in H and He at the different toroidal fields to be used, including:*
  - Power and density scans;

  - Current scans from the minimum (~3.5 MA) to the maximum foreseen at each B_t (e.g., 5 MA at 1.8 T, 7.5 MA at 2.65 T).

  In reality, there will be a limit to the lowest input power or highest density which can be explored since the ITER divertor is highly dissipative and too low a power or too high a density will result in strong detachment and operation too close to disruption boundaries. The best power load measurements will be obtained with low density/high power and with the divertor more attached. The aim is to obtain the L-mode scaling of $\lambda_{q,near}$ and estimates of the divertor power flux spreading parameter. Different combinations of B_t and I_p will also allow characterization of the divertor wetting as a function of total incidence angle.

- *H-mode divertor heat load characterization at 1.8 T:* a first look at the inter-ELM $\lambda_{q,near}$ and fast IR measurements of unmitigated ELM heat loads, hopefully providing information on potential issues of monoblock gap edge loading and first data for comparison with ELM energy density scalings ([3-Appendix C]).
- *Assessment of upper FWP heat loads and far-SOL power and particle widths using the upper chamber viewing IR and main chamber visible spectroscopy, including:*
  - Scans in Δr_{sep} up to double null in L-mode and to Δr_{sep} ~ 4 cm in H-mode for primary combinations of I_p, B_t;
  - Density scans up to close to the density limit at fixed power in hydrogen L-modes to investigate SOL density profile broadening. Similar observations are also of value in H-mode, but the available parameter range is likely to be restricted in PFPO-1.

Power levels will, in general, be too low in PFPO-1 to provide serious tests of divertor heat flux control using extrinsic seeding, except at the lowest densities (and thus high divertor plasma temperatures) when the relevance of such seeding is questionable. At more reasonable densities, the addition of even small quantities of impurities is likely to result in strong detachment. Prior to any detachment control tests, an important first goal will be to characterize as best as possible the divertor plasma itself, even in simple L-modes, to provide a database for model benchmarking to ensure that the basic detachment behaviour in simple situations is properly understood. The diagnostic tools necessary to constitute this database should be mostly available in PFPO-1 (e.g., divertor target Langmuir probes, fast in-vessel pressure gauges, divertor target IR, divertor bolometry and spectroscopy).

Some aspects of the divertor heat flux control methods developed at this stage can, nevertheless, be trialled in PFPO-1, in addition to tests, for example, of divertor reattachment provoked by local modifications to divertor gas fuelling and due to the effect of asymmetric toroidal gas injection. In this respect, H plasmas are more appropriate since detachment behaviour in He is very different (see section 2.5.2) and, depending on the control sensors used, He plasmas would not be a good testbed for later operation at high power with hydrogen isotopes as fuel. If impurity seeding is to be tried, a key question to be addressed would be to determine whether Ne is effective in satisfying both the requirements of exhaust power dissipation and of maintaining acceptable confinement. If this were not the case and it were necessary to use N_2 seeding at this time, it would be important to assess ammonia formation rates, since this impacts later phases of the IRP (see also sections 2.5.2, 3.2.4.7 and 3.2.5.8).

Development of a 'raised strike-points' scenario: Current predictions indicate that co-deposition of Be and T in the divertor will mainly occur on the upper part of the vertical targets and on the baffle area. Given the possible limitations in the efficiency of the divertor bake for tritium removal from thick co-deposits [137], and the fact that divertor baking is a time-consuming activity, which can probably not be executed too often during a campaign, it is of interest to explore techniques capable of accessing the fuel trapped in these co-deposits. Besides inter-pulse ECWC, one possibility (recently tested in the context of fuel removal from JET [83] is to run a plasma discharge with strike-points located further up the vertical targets or even on the baffle region. This would allow a local heating of the co-deposits, together with isotopic exchange and, possibly, some physical sputtering of the co-deposits if the local T_e is high enough.

The possibility of running ITER plasmas with raised strike-points was examined in [138] in the context of the original divertor strategy with carbon in the strike-point regions - the idea was to position strike-points on a W region extending down from the baffle region to gain early experience operating on W targets. Since that time, the CFC/W divertor was eliminated in favour of the full-W variant. The study found that for strike-points raised to just below the current transition region from the straight to curved parts of the vertical W divertor targets, high current ($I_p \geq 10$ MA) L-mode plasmas would be controllable in terms of vertical stability, similar to the maximum plasma currents envisaged to be attempted in PFPO-1.

Material migration studies: Initial studies of material (mainly Be) migration in ITER can be performed during PFPO-1. Visible spectroscopy in the main chamber and the divertor will be available during this phase. Monitoring the evolution of the main chamber and impurity sources requires that a standard (or reference) monitoring discharge is executed regularly during the campaign so as to provide reproducible and identical plasma conditions. Such a reference pulse would also be useful other purposes such as diagnostic calibration, verification of the PFC thermal response, verification of the wall conditions, etc. (see [3-Appendix D]). The pulse will consist of several phases such as limiter, L-mode, H-mode, with scans of the separatrix location and outer wall gap distance, allowing the study of Be transport in different plasma configurations. The discharge will evolve with the machine capabilities, and during PFPO-1 will probably consist only of the limiter and L-mode phases. Absolute calibration of the spectroscopic diagnostics will be required, together with regular monitoring of the transmission of the optical path, to be able to convert the measured signal into photon fluxes which can then be compared to the signals calculated by synthetic diagnostics of edge plasma codes.

In addition, a set of first wall samples will be installed during the assembly/maintenance phase prior to each operation phase. They will be installed in slots between FWPs at different toroidal and poloidal locations and will be shadowed from direct plasma impact. The aim is to evaluate the first wall erosion caused by fast charge-exchange (CX) neutrals. The sample surface will be made of Be with marker layers to provide high resolution erosion measurements. After PFPO-1, some (or all) of the samples will be retrieved and analysed in a dedicated laboratories. The data from these samples will provide useful information to validate the edge plasma/migration models used to predict material migration.

Studies of off-axis ECRH at 7.5 MA/2.65 T: As discussed later in section 3.2.5.7, the plan to expand L-mode operation from 7.5 MA/2.65 T to 15 MA/5.3 T in H plasmas in PFPO-2 relies on several intermediate I_p/B_t steps with q_{95} = 3 - 4. This is also the basis for the development of L- and H-mode plasmas in FPO, as described in sections 3.3.2.3, 3.3.2.4 and 3.3.3. For several of

the scenarios in the development sequence it will not be possible to ensure that the ECRH power is deposited centrally and, for some extreme cases in this step ladder, the peak of the ECRH deposition profile will lie around half-radius (ρ_{ECRH} ~ 0.5). This raises the question as to whether W accumulation might occur in such L-mode plasmas, potentially increasing disruptivity. If this were the case, some steps in the initially proposed step-ladder will be omitted at the cost of larger changes of I_p/B_t between consecutive steps.

Due to the significant implications of this issue for the further development of scenarios in the IRP, an assessment is included in PFPO-1. In general, in current experiments the problem of W accumulation with off-axis heating is found to be more serious for H-mode conditions (including exit phases) with NBI heating (and core fuelling) than in stationary L-modes, due to the reduced edge transport in the former. It is therefore possible that by ensuring that the W divertor influx remains low in ITER (low sputtering and high prompt redeposition as discussed in [3-Appendix C]), W accumulation might not occur in L-mode plasmas, even when ECRH heating is not fully on-axis.

The assessment will consist of a series of L-mode discharges at 7.5 MA/2.65 T with ECRH at the level of ~14 - 20 MW and a range of plasma densities ($<n_e> = 0.2 - 0.8 \times n_{GW}$) using pellet fuelling and gas fuelling. In these conditions the injection angle of the ECRH equatorial launcher will be adjusted to vary the EC power deposition profile from dominant central heating (ρ_{ECRH} ~ 0.2) to off-axis heating (ρ_{ECRH} ~ 0.5) while the W density, divertor plasma parameters and W influxes are measured. The aims of the experiments are:

i. to determine the level of off-axis ECRH heating that, if exceeded, causes W accumulation, and
ii. to determine if this level depends on divertor plasma conditions (influenced by the separatrix density) and/or core density profiles (modified by pellet fuelling compared to gas fuelling).

3.2.4.5 Options for H-mode operation

Summary of plasma scenarios: Experience operating ITER with H-mode plasmas in this phase would provide critical information for optimizing the exploitation of H-mode operation during PFPO-2, when the full complement of H&CD systems will be available. The primary goals of the H-mode operation campaign in PFPO-1 are:

i. to validate the predictions of the L-H threshold power and its scaling with density and, as far as possible, with toroidal field;
ii. to provide the first assessment of the energy and particle confinement properties of (dominantly electron heated) H-mode plasmas in ITER;
iii. to perform initial tests of alternative ELM control schemes using pellet pacing or vertical plasma oscillations (as plasma conditions allow) in plasma conditions for which unmitigated type-I ELMs are not expected to cause melting of the W divertor monoblocks;
iv. to validate projections of the H-mode SOL power flux width in preparation for higher power H-mode operation in later phases;
v. to provide reference ITER H-mode plasma conditions, which would establish a critical baseline for the evaluation of the possible influence of TBMs on H-mode performance at 1.8 T. This influence will be explored in PFPO-2 together with the optimization of the mitigation of the TBM effects with the ex-vessel EFCC and the in-vessel ELMCC.

With this motivation, the plan for H-mode operation in the PFPO-1 phase can be summarized as follows:

- **Highest priority and first H-mode attempts (if hydrogen H-mode operation is successful):** H-mode operation in H dominated plasmas at 5 MA/1.8 T;
- **Operation to provide conditions for H-mode exploration if H-mode in hydrogen is unsuccessful:**
  H-mode operation in He plasma at 5 MA/1.8 T;
- **Assessment of the L-H power threshold dependence on B_t:** H-mode operation in He plasma up to 7.5 MA/2.65 T.

Consistent with the Staged Approach plan, it is assumed that ECRH operating at up to 20 MW will be the only H&CD system available in PFPO-1, with a possible upgrade to 30 MW under discussion. A scenario for which the L-H power threshold is less than 20 MW is therefore required to achieve H-mode. Projections of the L-H threshold powers for ITER plasmas operated at one-third of the maximum current and field (5 MA and 1.8 T) indicate that 20 MW should exceed the threshold for He plasmas, while it would likely be marginal for H plasmas, assuming, of course, that all the available heating power can be coupled efficiently to these plasmas and that the plasma density is set to the value required to minimize the threshold power (as discussed in more detail in [3-Appendix B]). At half current and field (7.5 MA and 2.65 T) the 20 MW available in PFPO-1 would be marginal with respect to the threshold power in He plasmas, and below the predicted threshold for H.

The detailed operational plan for H-mode plasmas in PFPO-1 depends on whether the 5 MA/1.8 T H plasmas provide appropriate H-mode performance to meet the main required goals of the experiments (H-mode characterization and exploration of ELM control) or He plasmas are required. Details of the expected deliverables from this initial H-mode exploration phase in PFPO-1 and the rationale for the prioritization of these first H-mode attempts are given below. The associated R&D that could be undertaken during ITER construction to address the outstanding issues for H-mode operation is described in section 5.3, while technical issues and detailed physics issues associated with 5 MA/1.8 T operation in ITER are described in [3-Appendix F] and section 5.3.

Note that a transition from L- to H-mode will change the plasma inductance and β. These changes will require adjustments to poloidal field currents in gap control to preserve the plasma boundary shape and strike-point positions. The response of the control system needs to be commissioned for L-H and H-L transitions in flat-top, or during current ramp-up and ramp-down phases. Limitations on CS and PF coil currents for shape control in H-mode need to be commissioned and PCS must be further optimized to cope with a sudden loss of auxiliary heating. Standard plasma ramp-down scenarios following the H-mode phase need to be developed and plasma termination scenarios for fault conditions during H-modes need to be commissioned. The response of the plasma control system to H-modes and ELMs, in particular VS, needs to be optimized and the limitations documented using the lowest possible value of I_p, to ensure that disruptions due to loss of vertical stability of the plasma do not cause melting of PFCs.

Motivation for low-field (1.8 T) operation in PFPO-1: There are several beneficial aspects of establishing initial H-modes in ITER at low toroidal field:

(i) Lower power threshold for H-mode access: As discussed in more detail below, as well as in [3-Appendix B] and [3-Appendix F], operation at one-third field should allow H-mode operation early in the experimental program, even for the limited ECRH power (20 MW) assumed to be available in PFPO-1. This is particularly true for He plasmas, where P_{th} from the reference scaling is predicted to lie the range of 10 - 15 MW;

(ii) Investment protection during commissioning: For events that can lead to melting of plasma-facing components, such as ELMs, disruptions, and runaway electrons, the commissioning of control and mitigation systems should start in plasma operating regimes where unmitigated events pose a low risk for melting. This is achieved by minimizing the stored energy in the equilibrium (hence minimizing the plasma thermal energy and the poloidal field energy), implying the lowest possible values of I_p and B_t, while still matching key plasma parameters, such as q_{95}, to those foreseen for high performance operation. At the same time, the intention would be to approach, as closely as possible, the parameter range known to affect ELM behaviour (e.g., plasma collisionality). Evaluation of the expected ELM energy densities for these plasma current levels in ITER [139] based on EPED pedestal pressure predictions and empirical scalings from experiment (mostly based on ASDEX-Upgrade and JET [64]) show that uncontrolled ELMs at 5 MA/1.8 T in ITER will not cause melting of the top surface nor the edges of the divertor W monoblocks in the high heat flux areas of the vertical targets, even for the most conservative assumptions for the pedestal plasma pressure (same pressure for hydrogen and helium H-modes as for DT plasmas) and divertor ELM energy density (largest value within experimental scatter and considering largest in/out ELM deposition asymmetries) [75]. In addition, 5 MA H-mode plasmas are inside the zone of acceptable operation with respect the avoidance of melting during unmitigated disruptions, as described in section 2.5.3;

(iii) Operation at $q_{95} = 3$: The ratio of plasma current to toroidal magnetic field near the edge of the plasma core ($\sim q_{95}$) is a key operating parameter for ELM control via 3-D fields, since the currents in the control coils need to be carefully tuned for a particular value of q_{95}. The reference value of the baseline $Q = 10$ H-mode inductive scenario at 15 MA/5.3 T corresponds to $q_{95} = 3$ and this can be matched by operating at 5 MA/1.8 T. A plasma current of 5 MA is also comfortably above the 3.5 MA lower limit for good plasma position control in diverted operation in ITER, as discussed in section 3.2.4.2;

(iv) H-mode operation at 1.8 T in the PFPO-2 campaign: if H-mode experiments at 1.8 T in the PFPO-1 campaign prove successful, this would open the possibility of robust H-modes in H plasmas in the PFPO-2 campaign (if this is marginal in PFPO-1 for H), as higher levels of additional heating will also be available, thus allowing the possibility of comparing hydrogen and helium H-modes for the same I_p/B_t. This would also permit the evaluation of the impact of ferromagnetic material in TBMs on H-mode performance by comparing similar H-mode plasmas at 1.8 T in PFPO-1 (no TBMs) and in PFPO-2 (with TBMs). This is an important ingredient in guiding optimization of the mitigation of the possible effects of TBMs on H-mode plasmas using the EFCC and ELMCC.

Experimental plan for H-mode operation in PFPO-1: As discussed in [3-Appendix F], operation at 1.8 T in ITER raises a series of issues related to the specifics of the parameter space in which these experiments would be performed. Considerations related to the heating schemes for such operation and to the physics associated with the resultant H-mode plasmas have therefore

been explored in some detail in [33, 34] and the results of these analyses give confidence as to the viability of the proposed experimental program. Physics R&D activities which could facilitate the experimental program in 1.8 T plasmas are reviewed in section 5.3. The research program developed in the following discussion will be preceded by the completion of commissioning of the ECRH system to full power with heating pulse lengths of up to ~50 s.

(a) first H-mode studies: initial H-mode operation in hydrogen plasmas at 3.5- 5 MA/1.8 - 2,65 T:

H-mode plasmas will be produced by applying the maximum available power to 5 MA/1.8 T plasmas. The first magnetic configuration to be explored will have the standard ITER shape and a (separatrix) TF ripple of ~ -1.3%. Initial focus of these experiments will be the achievement of an L-H transition at $n_e \sim 0.4 \times n_{GW}$ and an exploration of the density dependence of the H-mode threshold to determine the minimum density for H-mode access. These experiments will involve auxiliary power ramps to maximum power on timescales of ~20 s followed by a constant power phase of ~30 s to determine whether type-I ELMy H-mode conditions can be sustained. As well as producing the first H-mode plasmas in ITER, these experiments will also provide the first measurements of the evolution of plasma parameters following the L-H transition (important to define the details of H-mode experiments in PFPO-2).

It is expected that within this time-window some evidence of H-mode access in H plasmas will have been obtained and the required power for this access versus separatrix TF ripple value (via variation of the separatrix-first wall separation) and plasma density will have been characterized. If H-mode access in H is not achieved at this stage, the remainder of the research on H-mode and ELM control in PFPO-1 will be performed with He plasmas, which will require the research discussed in sub-section (c) below to be performed at this stage.

Even if H-mode access in H plasmas is achieved, stationary type-I ELMy H-modes might not be sustained due to the low margin of power over threshold predicted for H. If so, He will be introduced via the gas introduction system (targeting small concentrations, ~10%) to test whether this can provide additional margin for stationary type-I ELMy H-mode operation via the reduction of the H-mode threshold, as observed in JET [15] and DIII-D [16]. In addition to He concentration scans, this will require a series of density scans and separatrix-first wall separation scans analogous to those performed for pure H plasmas.

Assuming that either pure H plasmas or mixed H-He plasmas provide stationary type-I ELMy H-modes, the remainder of the studies on type-I ELMy H-mode characterization and control will continue with H-dominated plasmas. If this is not successful the research will refocus on helium H-modes and the studies discussed in sub-section (b) will be performed in He.

This phase will conclude with an assessment of stationary type-I ELMy H-mode characteristics of 1.8 T H-modes with heating pulses of up to ~50 s, including a range of currents from 3.5 to 5 MA, approximately covering the range, $q_{95} = 3.0 - 4.3$, which is relevant for ITER high-Q reference scenarios. It is expected that some properties of these H-modes will have been assessed during the initial experiments to determine H-mode access, as described above. These dedicated experiments will prioritize power and density scans (ideally over $n_e \sim 0.2 - 0.9 \times n_{GW}$) to determine the operational range of type-I ELMy H-modes, their confinement properties, ELM behaviour and associated power/particle fluxes to PFCs. An initial assessment of the effects of plasma fuelling schemes on type-I ELMy H-modes will also be performed by comparing gas-fuelled hydrogen H-modes with pellet-fuelled plasmas (two pellet injectors will be available in PFPO-1)

at several plasma density levels. Due to the low margin of the available heating power above the L-H power threshold, the ranges of these scans are expected to be limited. However, it would be important to perform this characterization of stationary type-I ELMy H-modes at this stage because these 1.8 T H-modes will define reference plasmas around which the effects of TBMs will be evaluated and mitigated during PFPO-2. The experimental measurements in these scans will provide the first indication of the scaling with plasma current of divertor power fluxes in type-I ELMy H-modes, both between and during ELMs. They will also provide the first characterization of the pedestal plasma parameters and of the overall energy confinement of H-modes in ITER, which will be important for the detailed planning of H-mode experiments in PFPO-2.

As discussed in [74], at this level of additional heating ($P_{input} \leq 20$ MW) no active measures are expected to be necessary to mitigate the divertor power loads in 5 MA/1.8 T plasmas. However, some degree of control of the divertor plasma temperature may be required to avoid excessive W sputtering. This could limit the lower range of plasma densities to be explored and/or may require the use of impurity seeding in these conditions. The precise value of the divertor plasma temperature with acceptable W net influx will be determined by the effectiveness of W prompt redeposition in these plasmas and thus will be an issue which must be assessed during the experiments.

(b) First ELM control experiments at 3.5 - 5 MA/1.8 - 2.65 T:

Assuming that the experiments discussed above deliver stationary type-I ELMy H-modes in H dominated plasmas, the next step will be to investigate ELM control in these conditions. Otherwise, the experiments in He plasmas in sub-section (c) below will take place first and the ELM control experiments in this section will then follow, also in He plasmas.

ELM control experiments will be performed in plasma conditions which are optimum for the achievement of stationary type-I ELMy H-modes at 5 MA/1.8 T (e.g., optimum plasma density and separatrix-wall distance). Since installation of the ELMCC power supplies is, at present, planned for Assembly Phase III, PFPO-1 experiments would focus on evaluating the performance of back-up ELM triggering techniques, i.e., vertical plasma oscillations and pellet injection. This study is important at this stage because these techniques are expected to be applied when expanding the operational range of type-I ELMy H-modes to higher currents and fields to avoid melting of the W divertor (see section 3.2.5.5). In fact, from preliminary estimates (to be further refined), the requirements for the back-up ELM triggering techniques are not expected to be very demanding for 5 MA/1.8 T H-modes. For vertical plasma oscillations, it is estimated that the current required in each of the in-vessel vertical stability coils to provide a 20 Hz vertical oscillation of the plasma position by ±4 cm, which is expected to be sufficient to trigger ELMs in ITER [140], is ±27 kA, i.e., less than 50% of their design limit of 60 kA. Similarly, the pellet size required for ELM triggering at this level of plasma current is expected to be 1/3 of that required to trigger ELMs for 15 MA/5.3 T $Q = 10$ plasmas (2.0×10^{21} D atoms/ pellet [141]) and, thus, about an order of magnitude lower than the maximum pellet size that can be provided by the pellet injectors (6.2×10^{21} D atoms/pellet). The two pellet injectors available in PFPO-1 provide a combined pellet injection frequency of up to 32 Hz, allowing a controlled increase of the ELM frequency by more than an order of magnitude compared to that of uncontrolled ELMs [63].

As far as possible, the plasma parameters of the stationary type-I ELMy H-modes will be scanned by varying input power, plasma density and fuelling scheme (gas versus pellets) and the characteristics of the applied control techniques (i.e., vertical plasmas oscillations or pellet pacing parameters) will be re-tuned to maintain the same level of ELM control. The results obtained during this phase will be essential for the validation of models for ELM control and for the detailed planning of H-mode experiments in PFPO-2 at higher current levels, where ELM control may already be required to avoid divertor melting and W accumulation in higher power/ higher current H-modes.

(c) H-mode in helium at 3.5 - 5 MA/1.8 - 2.65 T:

The extent of H-mode operation in helium plasmas in this phase of PFPO-1 will depend on how successfully experiments discussed above can deliver reliable stationary type-I ELMy H-mode plasmas in H plasmas. If the higher H-mode threshold of H plasmas prevents such a regime being established, initial experiments to characterize type-I ELMy H-modes in plasmas at up to 5 MA/2.65 T, and the associated ELM control experiments, will be performed in He plasmas.

Operation in He plasmas in PFPO-1 will require additional experimental time to determine the H-mode threshold in 3.5 - 5 MA/1.8 - 2.65 T H-modes and its scaling with density, as well as to determine the influence of TF ripple on helium H-mode access and on the sustainment of type-I ELMy H-mode conditions. The experiments would be analogous to those in the first part of sub-section (a). Studies of He plasmas in PFPO-1 allow the possibility of an early evaluation of the scaling of the H-mode threshold power in PFPO-1 by comparing results of the power required to access the H-mode in 1.8 T and 2.65 T plasmas, as discussed in sub-section (d) below.

In view of the arguments above and the likely need to perform the type-I ELMy H-mode characterization in He plasmas for 7.5 MA/2.65 T in PFPO-2 (see also section 3.2.5.5), for which reference scenarios at 5 MA/1.8 T helium H-mode operation in the range 3.5 - 5 MA/ 1.8 - 2.65 T are included in PFPO-1. It should be noted that the period dedicated to helium H-mode operation in PFPO-1 may ultimately be significant if the initial H-mode development in H plasmas is not successful.

(d) Determination of the H-mode power threshold in helium plasmas at ~2.65 T:

The H-mode power threshold for He plasmas at 7.5 MA/ 2.65 T is predicted to be in the range of 19 - 28 MW (at $n_e = 0.4 \times n_{GW}$), while 37 MW is predicted for H plasmas. The available heating power might therefore be sufficient to attempt the determination of the H-mode threshold scaling in He plasmas at ~2.65 T. The ECRH heating power at 170 GHz will be near central, operating in the 2X mode, while the ripple at the plasma separatrix would be 0.55% at this toroidal field value and, thus, ripple-related issues are not expected to be important in these conditions (see [3-Appendix B]).

These experiments will involve auxiliary power ramps to maximum power in timescales of ~20 s followed by a ~30 s constant power phase (to determine if type-I ELMy H-mode conditions can be sustained) for a range of L-mode target densities (ideally $n_e \sim 0.2$ - $0.9 \times n_{GW}$, or the highest value achievable by gas puffing) and restricted scans of the toroidal field (~15%), to reduce the H-mode power threshold, if this is found to be marginal, while maintaining predominantly central heating.

As these experiments will necessarily operate near the H-mode threshold, long ELM-free periods might occur that could cause W accumulation and sudden, disruption-prone, H-mode terminations [142, 143]. To avoid such events, the ELM back-up triggering schemes discussed in sub-section (b) (vertical plasma oscillations and H_2 pellet injection) will be applied. Both techniques are expected to be effective in triggering ELMs at this level of current and field [140, 63] within the design specifications of both the vertical stability coils/power supplies and of the pellet injectors. This will be further verified by the demonstration of these schemes with 5 MA/1.8 T H-modes, as outlined above. It is not expected that stationary type-I ELMy H-modes will be achieved in this phase even if the ELM back-up triggering schemes are applied. In particular, the continuous injection of H_2 pellets to trigger ELMs in He plasmas will increase the H-mode threshold towards that in H plasmas and will eventually lead to an H-L transition. However, the quantitative percentage of H in He at which this will actually occur in ITER remains uncertain [14 - 17].

Key deliverables from the H-mode experimental program in PFPO-1:

(a) *Quantification of the power required for H-mode access:* The operating scenarios and planned experiments are designed to assess the L-H transition threshold power (P_{LH}) as soon as possible in the experimental program. This will provide an initial assessment of H-mode access in ITER over a range of species (H and He and H-He mixtures), densities and fields (1.8 T and 2.65 T). This is essential, both for the detailed planning of H-mode operation in PFPO-2 and to determine if an upgrade of the baseline heating power level of 73 MW will be required to ensure successful DT operation. There are significant differences between ITER plasma regimes and the database from present tokamaks, from which P_{LH} predictions for ITER are made, that are known to affect the required power to access the H-mode. Therefore, a confirmation of the actual level of power required to access the H-mode in ITER is essential for the planning of the later experimental program and also to plan H&CD upgrades. The latter would mitigate the consequences of discovering that the H-mode threshold was higher than predicted, a result that could otherwise impact the start of FPO operation in ITER.

(b) *Determination of the confinement properties of H-mode plasmas and pedestal plasma characteristics:* This initial plasma operation will provide the first experimental evidence for the performance of type-I ELMy H-mode plasmas in ITER and of the limits to the edge plasma parameters imposed by MHD stability in ITER. The specific aspects of ITER plasmas that will be characterized concern: stiffness of the core temperature profiles in electron heated H-modes with no torque input (albeit at high T_e/T_i), particle transport with low core sources and gas versus pellet fuelling of ITER H-modes, edge MHD stability of collisionless pedestal plasmas in ITER (the expected pedestal collisionality of 5 MA/1.8 T H-modes at $n_e = 0.4 \times n_{GW}$ in ITER is lower by a factor of 2.5 than for 15 MA/5.3 T $Q = 10$ plasmas).

(c) *Characterization of ELMs (energy and particle losses and power fluxes to PFCs) and demonstration of their control:* The initial H-mode plasmas in PFPO-1 will produce the first type-I ELMs in ITER and their features will be investigated over a restricted range of plasma currents, input powers and plasma densities. These experiments will be used to validate predictions for uncontrolled ELM energy losses, ELM power fluxes, and impurity exhaust (including W). These

are key to determining the range in plasma current over which uncontrolled ELMs will be acceptable in ITER and, thus, for developing the strategy for expanding the range of type-I ELMy H-modes towards higher plasma currents in PFPO-2.

(d) *Investigation of the backup ELM control capabilities and of the effects on H-mode access and confinement:* ELM triggering back-up schemes (vertical plasma oscillations and pellet pacing) will be demonstrated and their effect on ELMs and on the H-mode plasmas will be investigated. Validation of the effectiveness for ELM control of these back-up schemes is important for the detailed planning of H-mode operation in PFPO-2 at higher field and current, for which uncontrolled ELMs could lead to melting of the W divertor monoblocks.

(e) *Establish reference H-mode performance without the influence of TBMs:* PFPO-1 will provide reference conditions regarding H-mode access and type-I ELMy H-mode performance at 1.8 T without the TBMs. This information is key to evaluate the effect of the TBMs on H-mode access and performance in PFPO-2. If a sizeable influence were established, the immediate consequence would be the development of mitigation schemes utilizing the EFCC and ELMCC within the PFPO-2 program. A potential issue with this strategy is that, given the available (limited) power in PFPO-1, the assessment of the TBM effects will have to be performed at 1.8 T in PFPO-2, as the reference plasmas will have been at established at this field. As discussed above, the level of TF ripple at 1.8 T is much higher than at 2.65 T or 5.3 T (factors of 2.5 - 4) and the TBMs themselves create a ripple which varies with the toroidal field. Therefore, specific experiments and analysis will be required to separate the quantitative influence of the two sources of ripple when comparing plasmas at 1.8 T without TBMs in PFPO-1 and with TBMs in PFPO-2. To facilitate this, an assessment of the effect of TF ripple on H-mode plasmas is included in PFPO-1 (possibly in He plasmas).

(f) *Initial validation of predictions of power fluxes in ITER H-modes:* The H-mode experiments in PFPO-1 are planned to cover a range of currents from 3.5 - 5.0 MA. This will provide the first evidence for the magnitude of the divertor power fluxes in ITER type-I ELMy H-modes and of the scaling of their fall-off length with current, which is expected to scale inversely with plasma current [39, 144]. Initial tests of the back-up ELM control techniques should also provide information on their influence on power fluxes during and between mitigated ELMs.

Assessment of diagnostic capabilities to perform H-mode research during PFPO-1: The main objective of the PFPO-1 H-mode research program is the determination of the access conditions (heating power, density etc.) to H-mode and the characterization of the properties of uncontrolled and mitigated type-I ELMy H-modes. The diagnostic set considered for PFPO-1 (see Table 3) can provide an appropriate set of measurements to determine:

- Key core plasma parameters in these experiments such as n_e, T_e, T_i, toroidal plasma rotation and impurity levels (including W);
- Power and particle fluxes to plasma-facing components as well as the influxes of recycled species and impurity influxes.

It is likely that the time resolution of these diagnostics will not meet the requirements for 15 MA/5.3 T operation, as discussed in [3-Appendix H], but the expected time resolution is considered to be adequate for the objectives of this phase. Regarding edge plasma characterization, the situation is less clear. For electron parameters, it depends on whether some

of the diagnostics planned to be available to provide experimental measurements in PFPO-2 will already be functional towards the end of PFPO-1, when the H-mode experiments will be performed. Of particular interest (discussed in [3-Appendix H]) is the early availability (towards the end of PFPO-1) of the edge Thomson scattering system, as this would allow measurements of both electron temperature and density profiles in the edge and hence the determination of edge pressure gradients. In addition, and as a risk mitigation measure, the ECE system could be used to determine the pedestal temperature in PFPO-1, but this is expected to require incorporation of a new radiometer to measure 2nd harmonic ECE into the baseline configuration. This, together with a peripheral density measurement from the interferometer, could provide a measurement of the electron pressure at the pedestal, although not of its gradient at the plasma edge. Given that the HNB and DNB systems will be unavailable in PFPO-1, all ion temperature measurements will rely on the X-ray spectrometer for the core and on the X-ray crystal spectrometer for the edge, and these are expected to provide good quality measurements, given the high electron temperatures (core and edge) expected in these 5 MA/1.8 T H-mode plasmas (see [3-Appendix F]).

3.2.4.6 Disruption and mitigation research program

This section describes the experimental program required with respect to disruption prediction, avoidance, mitigation and loads. It is important to note that the program elements described here are strongly interlinked with each other and with other elements of the Research Plan. Scenario development and the gradual increase in plasma current, in particular, will have to go hand in hand with the disruption alleviation activities listed here.

Disruption Mitigation System (DMS) commissioning/ optimization: The present design of the DMS results in a multi-dimensional parameter space for the mitigation scheme. Multiple injectors in several locations with different injection quantities and species compositions for thermal load mitigation and for runaway electron suppression will be available [145 - 147]. It is expected that by the time the commissioning work with plasma starts, the parameter space will be narrowed down with the experience gained from present devices. Nevertheless, it is highly likely that achieving all disruption mitigation goals will only be possible with fine adjustments of the injection parameters during ITER operation and therefore a substantial number of dedicated pulses to disruption studies will be required in PFPO-1 and PFPO-2. Moreover, the risk involved if mitigation is not complete during the optimization activities requires a careful, and thus pulse intensive approach.

Commissioning and optimization of the DMS aims at: (a) thermal load mitigation, (b) electromagnetic (EM) load mitigation, and (c) RE avoidance validation. The commissioning work in PFPO-1 will start at low current and 2.65 T to reduce risks during the initial phase of DMS use. The commissioning program will be strongly interlinked with the gradual increase in plasma current when developing plasma scenarios. For validation of runaway suppression, it will also be important to run at toroidal field of 5.3 T and low plasma current early in PFPO-1.

<u>(a) Thermal load mitigation</u>

Thermal loads are caused both by the plasma thermal energy loss during the thermal quench (TQ) and by conductive losses of the magnetic energy in weakly radiating current quenches (CQ). In both cases, the mitigation strategy aims at radiating a large fraction of these energies. Whereas

the high-Z quantities required to radiate the magnetic energy on the timescale of the current quench is expected to be low and compatible with EM load limits, the number of particles required for the thermal quench is uncertain and might be in conflict with allowable current decay times. In both cases, the quantities have to be validated and the injection scheme has to be adapted, if required. The compatibility of the thermal load mitigation scheme with the runaway avoidance scheme is mandatory. The margin to runaway formation must be kept large enough while optimizing thermal load mitigation.

The following milestones must be achieved in PFPO-1:

(i) Confirmation of CQ heat load mitigation for 7.5 MA operation - a prerequisite to run 7.5 MA scenarios.

Experimental strategy:

- Confirm mitigation in target plasmas of varying magnetic energy, starting at low plasma currents;
- Confirm required quantities and injection scheme to achieve ~ 100% radiated power fraction during the CQ;
- Validate compatibility of heat load mitigation with RE avoidance scheme.

(ii) Confirmation of thermal quench heat load mitigation in L-mode - a prerequisite to run at thermal energies above melt thresholds.

Experimental strategy:

- Confirm mitigation in target plasmas of varying thermal energy in L-mode;
- Confirm required quantities and injection scheme to achieve high radiation fractions during the TQ;
- Validate compatibility of heat load mitigation with RE avoidance scheme and EM load mitigation scheme.

(b) EM load mitigation

EM load mitigation aims at reducing the halo current amplitude and asymmetry during VDEs while keeping the CQ sufficiently slow to avoid exceeding limits on eddy current forces on in-vessel components. Model predictions must be validated to allow projecting requirements towards higher energies.

The following milestones must be achieved in PFPO-1:

(i) Confirmation of EM load mitigation scheme for 7.5 MA operation - a prerequisite to run 7.5 MA scenarios.

Experimental strategy:

- Confirm mitigation in target plasmas with varying magnetic energy, both in vertically stable plasmas and in plasmas with deliberate VDEs;
- Confirm dependency of CQ rates on injected quantities, species and on the injection scheme;
- Validate electromagnetic forces and halo current mitigation goals;
- Validate compatibility with RE avoidance scheme.

The DMS commissioning activities, as well as the validation of EM loads during disruptions, will require operation at 5.3 T as early as possible, and preferably in the early phase of

PFPO-1, during limiter operation with I_p of up to 3.5 MA and during X-point operation at up to 7.5 MA.

(c) RE avoidance validation

Establishing a mass injection scheme that guarantees the suppression of runaways to acceptable limits is of high priority during DMS commissioning. Due to the severe energy loads that can be produced in the case of substantial RE formation, the initial tests of the operational space of the DMS with respect to RE generation must be performed at currents of the order of 2-3 MA. Operation at high B_t in a limiter configuration will provide the most favourable conditions for RE formation and are thus the worst-case testbed [135]. As extrapolation from these conditions to higher currents has non-negligible uncertainties, further tests to validate the mitigation scheme with respect to REs will need to be performed at higher currents: the need to proceed in small current steps has been taken into account in the required number of pulses for DMS commissioning.

The following milestones must be achieved in PFPO-1:

(i) Confirmation of the injection scheme with maximum margin to RE formation - a prerequisite for using DMS in closed-loop operation.

Experimental strategy:

- Gradual increase of B_t to 5.3 T at 3.5 MA in limiter configuration;
- Variation of injection species and injection scheme towards thresholds for RE formation.

(ii) Confirmation of the margin to RE generation in diverted configuration - a prerequisite for using DMS in closed-loop operation above 3.5 MA in the divertor configuration.

Experimental strategy:

- Target plasma of 3.5 MA at 2.65 T in divertor configuration;
- Variation of injection species and injection scheme towards thresholds for RE formation starting from confirmed scheme for limiter configuration.

Disruption Load Validation: Validation of the heat loads and their scaling with plasma parameters is essential to define the requirements for mitigation in terms of mitigation efficiency, but also in relation to the prediction of success rates and false alarm rates of the disruption prediction and detection system which will be responsible for triggering of the DMS within PCS. Establishing scalings of electromagnetic loads on the VV and BMs is a prerequisite for advancing to higher plasma currents within the progressive start-up approach. Disruption models will help to achieve a high accuracy towards higher currents and to reduce the number of experimental data points needed to establish the scaling. Model validation will therefore be an integral part of this work. Validated models will be especially important if thermal and electromagnetic loads impose the necessity of limiting the maximum current for unmitigated disruptions to avoid unacceptable damage to the first wall or divertor and ensure that, at most, category II electromagnetic loads are experienced by the VV when operating at high plasma current.

The following milestones must be achieved in PFPO-1:

(i) Confirmation of EM load scaling models - a prerequisite to increase current beyond 7.5 MA.

Experimental strategy:

- Variation of plasma current at 2.65 T over a range sufficient for projecting to 15 MA, but considering possible melt damage at higher current levels;

- Measurements of halo currents and forces/ displacements on components, including the VV, during deliberate VDEs;
- Confirm predicted asymmetry and determine dynamic behaviour;
- Confirm impact of plasma parameters, e.g., internal inductance, elongation and plasma current.

(ii) Confirmation of melt thresholds for thermal loads during the CQ - a prerequisite to increase the plasma current above the expected critical current for melting (in the range of 5 to 7.5 MA).

Experimental strategy:

- Monitoring of first wall heat fluxes during upward and downward VDEs with increasing plasma current.

(iii) Confirmation of melt thresholds for the divertor - a prerequisite to increase the plasma thermal energy beyond the predicted critical energy of 25 MJ.

Experimental strategy:

- Monitor divertor loads during major disruptions and downward VDEs with increasing thermal energy.

(iv) Confirmation of melt thresholds for the first wall - a prerequisite to increase the thermal energy beyond the predicted critical energy of 50 MJ.

Experimental strategy:

- Deliberate upward and downward VDEs with gradually increasing thermal energy;
- Possibly conduct post-TQ mitigation if higher currents are required to achieve 50 MJ, in order to prevent excessive CQ heat loads.

It is important to note that the details of the above R&D program in terms of maximum current, toroidal field and plasma thermal energy depend on the actual threshold for first wall and divertor PFC degradation (e.g., melting) and the forces experienced by the VV. No significant consumption of first wall and divertor PFC lifetime should take place during the execution of this R&D and loads on the VV should remain within category I.

Disruption Mitigation System (DMS) trigger generation: Achievement of the target disruption rates requires the development of avoidance and prevention strategies, while the ability to attain the target mitigation rates depends on the development of reliable prediction schemes. In early operation, disruption prediction is expected to start with basic threshold-based indicators such as mode amplitudes. As operation moves to more complex scenarios, the predictor will have to be adapted and more input signals will need to be added. The requirements on the mitigation success rate for the loads during the current quench are extremely demanding when 15 MA operation is approached. These rates will be achieved by incorporating indicators that a disruption is ongoing, such as the vertical plasma position or the current spike at the TQ [148].

Schemes to provide the trigger to the DMS are presently under development (see section 5.2.3) and being tested in multi-machine efforts. It is anticipated that such schemes will be sufficiently developed to be available for testing in early ITER operation, with subsequent application in PFPO-1, and should complement threshold-based techniques.

The disruption predictor within PCS is a module with the single function of deciding when to trigger the DMS. A range of material injection schemes can be chosen to optimize the mitigation

action for various disruption situations. PCS will also be responsible for selecting the most appropriate injection scheme based on plasma parameters, plant system status and DMS status. Note that CIS can, upon input from plant systems or from the plasma current measurement, also initiate a mitigated disruption by triggering the DMS. In that case the injection sequence will either be the latest issued by PCS or a default sequence. Testing and defining the injection sequences constitute an aspect of the DMS commissioning activity.

Targets for disruption rates and mitigation success rates must be defined, as mentioned in section 2.5.4, when making steps in plasma current or thermal energy. However, confirming that these targets are achieved before taking the next step in performance cannot be implemented by a statistical approach, since this would require many pulses or disruptions in ITER. It will therefore be mandatory to assess the effectiveness of the chosen prediction algorithms by dedicated tests accompanied by modelling validation, which is included in the plan.

The following milestones must be achieved in PFPO-1:

(i) Disruption detection ready for high current operation - a prerequisite for further increasing current; the required reliability depends on the expected loads and might vary for different plasma currents (c.f. section 2.5.4).

Experimental strategy:

- Establish algorithms for detecting the TQ, the start of the CQ and a vertical displacement;
- Test the algorithms during low current operation and deliberate disruptions, if necessary.

(ii) TQ prediction sufficient for L-mode operation - a prerequisite for running high energy L-mode beyond the melt threshold; the required reliability depends on the expected loads and might vary for different thermal energies (c.f. section 2.5.4).

Experimental strategy:

- Establish threshold-based algorithm for predicting the TQ;
- Implement statistical methods and physics model-based methods in parallel;
- Perform dedicated disruption studies to optimize the predictor, if necessary;
- Implement and test decision schemes in PCS for the material injection sequence;
- Test algorithms during low current operation with disruptions, if necessary.

(iii) Injection sequences ready for higher current operation

Experimental strategy:

- Establish injection sequences for early injection before the TQ and for late injection into the CQ;
- Verify RE avoidance and CQ mitigation efficiency.

(iv) Injection sequences ready for elevated thermal energies - a prerequisite for running high energy L-mode plasmas beyond the melt threshold.

Experimental strategy:

- Establish injection sequences for pre-TQ injection;

Verify RE avoidance, TQ and CQ mitigation efficiency.

3.2.4.7 Edge physics and PWI studies

As indicated in Table 5, significant time will be allocated to the studies of divertor heat loads and plasma-wall interactions during PFPO-1. Several aspects of these studies have been discussed

in section 3.2.4.4, though experimental time will also be dedicated within the H-mode program of section 3.2.4.5. Here, studies relating to more 'generic' aspects of PWI which may not require significant experimental time within the research program are summarized.

Wall conditioning and cleaning: Glow discharge cleaning (GDC), is one of the primary conditioning techniques, together with baking of the vacuum vessel and blanket/first wall at 200 °C and 240 °C respectively, which ITER will use to prepare in-vessel component surfaces prior to tokamak start-up and subsequently in preparation for plasma operations following maintenance procedures requiring in-vessel access. The efficiency of GDC, i.e., its ability to efficiently desaturate wall surfaces and remove medium-*Z* impurities (adsorbed oxygen, water or carbon) must be assessed in H_2 (possibly in He) before the start of PFPO-1.

The continuous follow-up of wall conditions by means of optical emission spectroscopy and mass spectrometry, and the impact of impurity levels on plasma operation and performance during PFPO-1 will not require dedicated operational time but will be particularly important to define further conditioning needs after the initial GDC and bake-out pre-PFPO-1. This should include routine monitoring of impurity sources in reference pulses (see [3-Appendix D]).

Radio-frequency-assisted wall conditioning techniques (ECWC for PFPO-1) also need to be developed for the conditioning of the first wall surfaces between pulses, i.e., when the toroidal magnetic field is on. Among the questions to be addressed in PFPO-1, but which are common to all operation phases, is the ability of such magnetized low temperature plasmas to efficiently remove intrinsic (oxygen, water or carbon) and extrinsic (nitrogen, neon, argon) impurities, thus allowing/ easing plasma initiation (burn-through), recovery from disruptions, and control of density in long-pulse discharges with the ITER material mix. This requires the development of ECWC scenarios for each of the main toroidal field values that are expected to be used routinely in PFPO-1. For $1.8 \leq B_t \leq 3.3$ T and $f = 170$ GHz, ECWC plasmas will be produced at the 2nd or the 3rd harmonic of the EC resonance frequency, and it is unclear what the single pass absorption will be in these discharges. Since coupling of the power in ICWC (available from PFPO-2) is mainly non-resonant, discharges can be produced at very low B_t. The so-called high harmonic ($n \sim 10$) ICWC scenario, successfully operated in ASDEX-Upgrade [149] and in the JET-ILW [150], may even therefore be envisioned in later operation phases in the case of failure or unavailability of GDC in ITER.

Schemes for optimization of the cleaning efficiency are common to both techniques, proceeding first with variations of pressure and power. Due to the relatively high densities of ICWC/ECWC plasmas (in comparison with GDC), a very large fraction of the desorbed flux is immediately re-ionized and re-implanted into wall surfaces and only a small fraction is exhausted through the pumping system. The discharge duty cycle must therefore be adapted to mitigate this. Finally, the poloidal field patterns need to be optimized in both discharges at each frequency/toroidal field combination (f/B_t) to increase uniformity, wall coverage and efficiency. As for GDC, qualitative and quantitative assessment of the exhaust gas will require the use of the tokamak pressure measurement RGAs. Spectroscopy and visible cameras can be used to assess the areas wetted by the discharge, whereas interferometry and ECE will permit the evaluation of basic plasma parameters and discharge uniformity.

Fuel retention management: Most of the dust/tritium retention/erosion diagnostics will become available during PFPO-2. The focus of PFPO-1 will therefore be on commissioning and testing fuel management related systems, as well as on obtaining first estimates of fuel retention

and removal efficiency in H plasmas. These may be later refined and validated during PFPO-2 through a dedicated migration/retention experiment.

Gas balance in hydrogen: The most widely used technique for the evaluation of in-vessel fuel retention is the so-called 'gas balance' technique, which consists of a precise accounting of the amount of injected and exhausted fuel species. Based on measurements from all metal devices, and in particular from the JET-ILW [81], the expected retention rate will be lower than 1% of the injected fuel, so that careful calibrations of the gas injection system and of the pumping speeds of the different sub-systems will be required.

The most accurate method is to perform PVTc (Pressure-Volume-Temperature-composition) measurements on gas tanks connected to both the gas injection system and the tokamak exhaust. Part of the required hardware will be available for PFPO-2 to allow for ^{3}He recycling (ICRF minority). A small upgrade is required to enable gas balance analyses, consisting mainly of the installation of a dedicated gas container connected to the gas injection. Making this system available for PFPO-1 is technically possible and there appears to be no showstopper in terms of schedule. Resources will, however, have to be identified to purchase the required hardware and ensure timely installation before PFPO-1.

No dedicated operation time will be required for gas balances in PFPO-1 and measurements will be performed parasitically when H discharges are carried out, requiring regeneration of the divertor cryopumps to recover the pumped hydrogen. Gas balance in He is not relevant for fuel retention studies, but monitoring of the exhaust gas composition during He discharges will provide indications on the background H sources and their evolution with time over a campaign. Note that gas balance analysis should, if possible, be performed at least each time a reference discharge is performed (see [3-Appendix D]) providing information on the evolution of the wall conditions and the retention rates. Time will be required to determine the pumping speeds of the different systems, and perform a calibration of the gas injection system, but this can probably be done during short-term maintenance periods.

Baking studies: Relatively low Be erosion and co-deposition rates are predicted during the low power discharges of PFPO-1 [151]. To first order these rates depend on the wall particle flux, itself related to the edge plasma density/temperature. The thickness of the hydrogen-containing co-deposits formed during PFPO-1 will therefore be much lower than that expected during later high-power operations. First indications of the hydrogenic release behaviour during a bake-out of the PFCs can, however, be obtained if a bake is executed at the end of PFPO-1 (assuming that it ends with H plasmas). In addition to providing data on the release kinetics of retained gases as the PFC temperature is increased, such baking will allow a first validation of the global migration (including diffusion/ trapping) models used to predict T-retention in later nuclear operations. Since baking is a time-consuming activity, possible only when the magnetic field is off, these studies are best executed at the end of PFPO-1, before the start of the subsequent assembly phase.

3.2.4.8 Experimental Risks in PFPO-1

The main physics/operational risks to the PFPO-1 program and their mitigation can be identified according to the main four areas addressed in this campaign.

Commissioning of systems with plasma: Commissioning of systems required for plasma operation, control and investment protection accrues risks associated with the operation of such systems with plasma for the first time. These risks are mitigated in the IRP by a gradual expansion

of the operational range of systems (e.g., gradual increase of power levels and duration of ECRH, commissioning of PCS at low current prior to operation at higher currents, etc.), so that any possible issue can be detected before it poses a risk to investment protection as discussed previously in relation to the development of the PFPO-1 campaign. In addition, and this is a general strategy throughout the IRP from FP onwards, control and protection systems are, as far as possible, commissioned one campaign in advance of that for which they are needed to support implementation of the IRP. This commissioning is performed with plasma scenarios such that the malfunctioning of the control and protection systems does not have implications for investment protection (e.g., commissioning of the divertor power control system in scenarios with divertor power fluxes that cannot exceed a peak stationary value of 10 MWm^{-2}). This ensures that the control and protection systems will function correctly when needed for execution of the IRP and/or intervention of their investment protection action.

Expansion of operational space in L-mode to at least 7.5 MA/5.3 T: The expansion of the operational space to at least 7.5 MA/5.3 T has as an intrinsic risk that the consequences of plasma disruptions (thermal loads to plasma facing components and electromagnetic loads to vessel and in-vessel components) increase with increasing plasma current and energy. This risk is minimized in line with the logic explained above, i.e., by a gradual expansion of the operational range to ensure that disruptivity is minimized and that the consequences of disruptions are not serious. Specific examples of this strategy described in previous sections are: (a) the start of diverted plasma operation at low elongation ($\kappa = 1.5$), for which in-vessel coils are not required to reliable ensure vertical position control; (b) the expansion of the diverted configuration operational space in steps of 0.5 - 1 MA; (c) the study of the impact on W accumulation of off-axis ECRH at 7.5 MA/2.65 T before the toroidal field is increased towards 5.3 T (with corresponding increases in plasma current), thus confirming that central ECRH heating is not required for intermediate values of the TF, etc.

Although excessive W accumulation for off-axis ECRH is not considered likely in ITER, should this risk materialize, it will have a significant impact on the entire IRP program. This risk would therefore be retired by performing the initial operational space expansion only at fields that ensure central ECRH heating (namely ~2.65 and 5.3 T), instead of the gradual plasma current/toroidal field expansion adopted for the IRP reference strategy (the alternative approach implies that q_{95} decreases from 6 to 3 when increasing the plasma current from 7.5 to 15 MA at 5.3 T), and this strategy would be complemented, from PFPO-2 onwards, by the exploitation of ICRF to provide central heating for intermediate values of the TF.

Disruption mitigation: The assessment of the mitigation capabilities of the DMS is a major outcome of the PFPO-1 experimental program. From the operational perspective, the risks associated with this assessment concern the loads associated with the initial use of DMS for disruption mitigation in ITER (local radiation loads on PFCs, generation of REs, etc.). To minimize these risks the same strategy as for the expansion of the operational space is followed, with DMS studies performed at low plasma current/toroidal field/energy, where the risk of generating large loads and REs is very low, and then gradually increasing the range, as described in section 3.2.4.6.

From the point of view of the overall IRP development strategy, the main risk in this area is that the DMS may not demonstrate the level of mitigation efficiency required for the implementation of the IRP. Such a risk might materialize because: (a) PFPO-1 experiments show

that the mitigation efficiency is not adequate beyond a given level of plasma current/toroidal field level/plasma energy, or (b) PFPO-1 results reveal that the expected requirements for efficient disruption mitigation in PFPO/FPO exceed the DMS baseline capabilities installed for PFPO-1. The mitigation to such a risk foreseen in the IRP involves the installation of an upgrade of the DMS between PFPO-1 and PFPO-2. The nature of the upgrade depends on how the risk materializes: (a) if the issue identified is that the injected quantities foreseen for disruption mitigation or injection symmetry are insufficient for PFPO-2/ FPO, an additional set of 6 shattered pellet injectors could be installed at port 11, requiring the re-allocation of the impacted diagnostic systems; (b) if the issue is that the delivery provided by the DMS shattered pellet injectors is insufficient for effective mitigation in PFPO-2/FPO, these could be replaced by another delivery system (to be developed before PFPO-1) before further expansion of the operational space proceeds in PFPO-2. Specific open R&D issues related to disruption mitigation are described in section 5.2.2.

Exploration of H-mode operation up to 2.65 T: H-mode exploration in PFPO-1 implies operation near the L-H transition, involving intrinsic operational risks. These are typically associated with the occurrence of long ELM-free periods that can lead to W accumulation, terminating with large ELMs and increasing disruptivity. To mitigate such risks the initial H-mode operation in PFPO-1 incorporates current levels (≤5 MA) for which there should be no degradation of PFCs under ELM loads together with the use of ELM triggering schemes (pellet injection and vertical position oscillations), as described in section 3.2.4.5.

From the perspective of the overall IRP development strategy, the major risk is associated with the assessment of the power required to operate in H-mode, which is intended to be carried out in this phase. If this assessment convincingly shows that the baseline power level foreseen for PFPO-2 (20 MW ECRH, 20 MW ICRF, 33 MW NBI) is likely to be insufficient to demonstrate the FPO fusion goals, an upgrade of the baseline heating systems would have to be initiated at this stage. It is unlikely that such an upgrade would be operational for PFPO-2, which would restrict the H-mode operational range to be explored in this phase, but it would ensure that the IRP program planned for FPO could proceed as foreseen. It should be noted that a conclusive demonstration that the power required for reliable H-mode operation in ITER is significantly higher than that estimated from the reference scaling (equation (1)) is not simple at this stage, given that only 20 MW of ECRH power will be installed and that the H-mode threshold for PFPO-1 plasmas is predicted to be >10 MW for the plasma conditions considered. Specific open R&D issues related to H-mode operation in PFPO-1 are described in section 5.3.1.

3.2.5 Pre-Fusion Power Operation 2 (PFPO-2)

3.2.5.1 PFPO-2 overall aims

Table 6 provides a summary of the main experimental activities foreseen for the PFPO-2 campaign, including estimates of the associated experimental time requirements, to provide a guide for the subsequent discussion. Operation at the full design parameters of 15 MA/5.3 T is essential in this phase, *inter alia*, to ensure that all critical systems have been commissioned prior to nuclear operation. In addition, operation in H-mode at 7.5 MA/2.65 T permits key physics and control issues related to H-mode operation in DT to be addressed, reducing the risk for D and DT

operation in FPO. On the other hand, H-mode operation at 5 MA/1.8 T allows the identification of TBM effects on H-modes and the development of mitigation schemes, if required.

Routine operation of the HNB system at 33 MW for at least 100 s is necessary to support the physics program envisioned for this and later operational phases. This includes commissioning of the magnetic field reduction system and the protection systems specific to shine-through (first wall) and fast ion loss (first wall and divertor). Both of these issues are especially important for H-mode operation because they are the most likely factors to limit the use of the HNBs in hydrogen (and to a lesser degree, helium) H-mode plasmas. Due to the high shine-through power fraction in H plasmas, operation in hydrogen H-modes will most likely be restricted to short periods (~10 s) and to a very narrow density range. Thus, a proper evaluation and protection of the first wall against excessive shine-through loads is essential to carry out the H-mode research program. On the other hand, both MHD instabilities and the application of 3-D fields for ELM control can potentially increase the fast ion losses from NBI and lead to localized power fluxes on the PFCs. It is therefore essential that, together with the increase in NBI power injected into the ITER plasmas and the development of H-mode operation, the PFC power loads associated with fast particle losses are measured and maintained under control.

Routine operation of the ICRF system at 20 MW for at least 100 s is necessary to support the physics program envisioned for this and later operational phases. This requires simultaneous commissioning of both antennas in suitable H and He plasmas. The ECRH system will have already been commissioned and will be applied in the development of scenarios. Specific commissioning activities will be required for the application of the system to NTM control in H-modes, if NTMs are found to be unstable in the PFPO-2 scenarios.

During PFPO-2, the installed diagnostic set will be very close to its final configuration for DT operation; the additional measurement requirements for the PFPO-2 campaign and associated diagnostic systems to be installed prior to PFPO-2 are listed in Table 7. These additional requirements expand considerably the range of physics studies that will be possible and also provide access to expanded control capabilities, for example in relation to current drive and current profile control. Therefore, significant effort will be dedicated to the commissioning with plasma of the newly available diagnostics, as well as to their calibration and to the resolution of possible inconsistencies among plasma measurements. In this phase, plasma parameters are expected to approach comparable values to those in DT plasmas and, therefore, the demonstration of the diagnostic capabilities to support the operational program, as well as the accompanying research program, at this stage of operation is a major objective of PFPO-2.

Since this is the last operational phase before the machine will become activated, it is important to commission all systems required for DT operation as thoroughly as possible, so that any required changes can be performed during the pre-nuclear shutdown between the PFPO-2 and the FPO phases. This includes commissioning all required control, interlock, and safety functions.

The TBMs will be introduced during this operational phase and, therefore, specific experiments will be performed to characterize the resultant error fields, to evaluate the effects on L-mode and H-mode plasmas, and to develop mitigation schemes. It is essential, if sizeable effects are found, that effective mitigation schemes are developed at this stage to ensure low disruptivity and high energy confinement of H-mode plasmas before the plasma current, toroidal field and input powers are increased to their nominal baseline values later in PFPO-2. This will require the re-optimization of error field correction with the EFCC and, possibly, additional support from the

ELMCC, if required. Similarly, to characterize the effect of error fields on H-modes, specific experiments to compare H-mode performance at 5 MA/1.8 T in PFPO-1 (no TBMs) with that obtained in PFPO-2 (with TBMs) are included in this phase, together with the development of mitigation schemes at this field (minimization of error fields with EFCC and ELMCC), if required. The magnetic field reduction systems for the NBIs will produce additional sources of error fields, which may also require a re-optimization of the error field correction to be carried out in this phase to mitigate their effects.

The H-mode research program in PFPO-2 will provide the physics basis and control schemes on which to base H-mode scenario operation in FPO. By the exploration of H-modes at two toroidal fields (1.8 T and 2.65 T) and over the range $q_{95} \approx 3$ - 5 (I_p = 3.5 - 5 MA for 1.8 T and 5 - 7.5 MA for 2.65 T) in H/He plasmas, the following objectives will be fulfilled:

- Determination of the H-mode threshold in H and He over a density, toroidal field and q_{95} range allowing the evaluation of the expected power required for H-mode access in DT operation;
- Demonstration of fully integrated H-mode scenarios including power load control, ELM control, fuelling, core W control, which are key to the development of similar scenarios in FPO;
- Optimization of ELM control, divertor power load control and heating power mix for H-mode plasma performance;
- Demonstration of shape, ELM control and power load control on entry to and exit from H mode phases;
- Development of robust current ramp-up/down scenarios, including response to off-normal events.

On the other hand, the L-mode program in H plasmas to 15 MA/5.3 T will demonstrate the capabilities of the ITER tokamak and its ancillary systems to operate at their nominal design parameters, including heating, fuelling and the capability of the diagnostic and control systems to provide robust (disruption-free) plasma operation. Expanding the current range beyond 7.5 MA will require qualification of the DMS in a careful step-wise fashion. Commissioning of predictive systems for disruptions with avoidance strategies, further development of an algorithm to trigger the mitigation system, and qualification of the mitigation system at each specific current step will be performed. The proposed step-ladder approach from 7.5 MA/2.65 T to 15 MA/5.3 T follows a q_{95} = 3 - 4 band with changes of both I_p and B_t. This implies some variation in the heat deposition profile that can move off-axis (up to $\rho = 0.5$) for some steps, if NBI is not used (which is likely at the lower currents due to the high shine-through density limit in H plasmas). Therefore, W accumulation will have to be carefully monitored and controlled; specifically, the interplay between divertor conditions (W sputtering source) and core W control will need to be assessed. If the installed heating systems (chiefly ECRH and ICRF) are shown to be insufficient to provide W accumulation control, some of the specific values of the I_p/B_t step-ladder will have to be adjusted or, eventually, a constant 5.3 T route may have to be chosen for this development. This is less desirable because q_{95} changes from 6 to 3 along this route, so that MHD stability can change significantly at each step in I_p, and it can become more complicated to ensure stability as I_p approaches 15 MA. In addition to the operational experience, the L-mode plasmas obtained through this development will provide first experimental evidence of core transport physics of

plasmas with parameters not far from those at $Q = 10$, which are essential to validate the understanding of transport physics at the ITER scale and to plan D and DT operation in FPO.

If experimental time allows, it would be desirable to extend the operation of the H&CD systems to several hundred seconds, allowing long-pulse H-mode operation to be developed. This would provide initial experimental evidence of long time-scale behaviour of ITER H-mode plasmas in preparation for DT operation.

In addition to this long pulse demonstration, specific issues related to long-pulse operation in DT will already be assessed at this stage. This includes target q-profile development in the current ramp-up and sustainment for several tens of seconds (limited by NBI shine-through) in the flat-top, and assessment of the current drive capabilities of the ITER H&CD systems, particularly NBI and ECRH, in H-mode plasmas that can provide an initial assessment of possible issues related to the application of these schemes in FPO long-pulse operation (e.g., triggering of Alfvén eigenmode (AE) instabilities which could reduce NB current drive) and allow the development of schemes to mitigate them, if required.

It would also be desirable to demonstrate core MHD instability control, even if this may not be required at this stage in the development of the Research Plan, to ensure that the required schemes are developed in advance of their application in FPO and to ensure that the necessary upgrades are launched at this stage, if the baseline capabilities are found to be insufficient. Such studies would focus on the control of sawteeth and tearing modes primarily by the application of focussed ECRH/ECCD.

Finally, as discussed in section 3.2.1, the wide range of experimental conditions and plasma parameters expected in PFPO-2, in particular the high power and long-pulse operation aspects, will provide access to studies of key PWI and heat load management issues in preparation for the significantly more challenging edge and divertor parameters expected at high fusion power during FPO.

3.2.5.2 PFPO-2 plasma restart and commissioning activities

Plasma restart in PFPO-2 should aim to re-establish routine plasma operation at 7.5 MA/2.65 T as rapidly as possible. The restart will use hydrogen and should re-establish plasma initiation at 2.65 T, with further optimization when required. It should include plasma initiation at the full CS precharge of 45 kA at 5.3 T, in preparation of operation at 15 MA/5.3 T later in PFPO-2. PCS should demonstrate routine operation at 7.5 MA/2.65 T during the restart by recommissioning plasma shape control, VS control, density control with gas and pellets, and event handling. In parallel, the DMS system should be recommissioned using reference pulses from PFPO-1, and any changes to DMS hardware or control implemented during Assembly Phase III should be commissioned.

The interlocks for the H&CD systems should be retested and the ECRH system should re-establish heating power at >50% of maximum power for > 5 s. Restart targets for systems already available in PFPO-1 will have to be defined to show readiness for commissioning of new systems. Recommissioning of routine operation at 7.5 MA/2.65 T will allow a rapid start to commissioning of the H&CD systems installed during Assembly Phase III: the further development of the research program relies heavily on the availability of a reliable H&CD capability at a significant power level.

Documenting effect of TBMs: The newly installed TBMs may influence magnetic measurements, plasma rotation, the plasma response to error fields and overall plasma performance, particularly in H-mode. The effect on magnetic measurements can be documented without plasma operation during the integrated commissioning phase prior to plasma operation. However, the effect of the TBMs on error fields and the associated requirements for correction will have to be determined by assessing the lower density limit for plasma operation (error field locked modes) and the effect on plasma rotation. Error field correction (commissioned in PFPO-1) will almost certainly have to be re-optimized at an early stage of operation to include the effect of the TBMs. This re-optimization should also address possible additional error fields produced by the NB Magnetic Field Reduction system. The effect of the TBMs on overall plasma performance can probably be assessed most readily by repeating H-mode pulses from PFPO-1. Although these will be low performance H-modes (i.e., with up to 20 MW input power at 1.8 T), the effect on pedestal parameters or plasma rotation could be uniquely documented from these experiments.

H&CD Commissioning: The commissioning of the H&CD systems to full power and pulse lengths of at least 100 s (or longer, as experimental time and priorities permit) is a key goal for the PFPO-2 campaign to allow access to H-mode operation and to demonstrate the operational capability of the H&CD systems before the transition to fusion power production. For NBI, operating with H^0 at 870 keV during PFPO, extensive commissioning of the beamline components without plasma is foreseen during Integrated Commissioning III. Commissioning with injection into plasmas can start after pre-commissioning of the NB Magnetic Field Reduction system (Active Compensation and Correction Coils) to decrease the residual magnetic fields to acceptable limits (~0.1 mT in the region between the grounded grid and the neutralizer). This is necessary to limit the beam deflection and to ensure maximum beam transmission with minimal losses due to direct interception. In addition, stable operation of a standard full-bore plasma with a flat-top diverted phase having a density above the minimum shine-through density threshold must be well established and critical diagnostics for protection against unacceptable shine-through heat load on the first wall panels must operate routinely as real-time monitors (i.e., density, impurity, and IRTV viewing the relevant first wall panels). This capability will therefore need to be integrated into PCS and the beam interlock system. Error field correction will then have to be re-optimized taking into account the error field produced by the NB Magnetic Field Reduction system.

Most of the ECRH commissioning will have been undertaken during IC-I and PFPO-1. All beamlines must be reconditioned to full power for a duration of at least 100 s in PFPO-2. The ECRH heating interlocks will also need to be re-established: all gyrotrons and launchers should be reconditioned at their nominal power levels.

Some ICRF commissioning will be carried out in vacuum prior to plasma operation. Antenna conditioning at high voltage in vacuum is necessary to: (i) confirm the operational strategy for avoidance of multipactoring conditions; and (ii) to condition the system progressively to high RF voltage, using trains of short pulses of increasing voltage, to establish the reliable maximum operating voltage for all foreseen operating frequencies.

Commissioning of the ICRF system with plasma will initially take place at half-field. Part of this commissioning does not need a particularly efficient ICRF heating scheme: it can be launched

in H and continued in He plasmas[2]. ICRF system commissioning will mainly be performed in L-mode, but additional time will be required in H-mode plasmas. The commissioning can be split into early and advanced commissioning: early commissioning, relating to tests of antenna coupling, matching systems, arc detection systems, antenna phasing, real-time frequency sweeping (±1 MHz) and power modulation capability, requires 5 - 20 s of dedicated pulse time; the more advanced aspects of ICRF commissioning, involving a gradual increase in power and heating pulse length, RF coupling control via gas puffing and plasma-antenna gap control[3], determination of the influence of impurity seeding for exhaust power control and of 3-D fields for ELM control on coupling, assessment of ICRF impurity generation and the determination of cross-talk limits when operating 2 antennas simultaneously, require dedicated periods of up to 60 s, implying that they will be implemented as the extension in plasma pulse length allows. Activities within the latter category are discussed further in section 3.2.5.5, since some activities imply L-H transition capabilities. The ICWC capability of the system must also be commissioned, of course.

Additional commissioning time could be required for 1.8 T scenarios, where 2nd harmonic H heating would provide the ICRF heating scheme, both in H and He plasmas [33], if this heating scheme were to be used for 1.8 T operation, which is not the reference choice for the IRP.

Commissioning of the HNB and DNB systems will be carried out at half-field in H or He plasmas, using H^0 beams with energies of up to 870 keV (HNB) and 100 keV (DNB). The density above the minimum shine-through density threshold must be well established. The initial shine-through assessment is illustrated in figure 9 for various densities and plasma currents in H and He plasmas. Once suitable plasma conditions are established allowing injection of the beam systems, the operational time need not be exclusively allocated to this activity. In addition, the short pulses (0.1 - 1 s) required for initial beam duct conditioning could be sequenced throughout individual plasma pulses. Once beam duct conditioning/degassing is completed, the duration of beam injection into plasmas would be gradually extended, with the target duration of ~100 s being developed within the specific IRP programmatic activities. Key aspects of commissioning with plasma include the commissioning of injection at a range of bean energies, commissioning at several (poloidal) injection angles and testing of the power modulation capabilities. These elements will provide the necessary operational flexibility to support the further development of the IRP during PFPO-2.

Table 6 summarizes the anticipated time allocation to auxiliary system commissioning, primarily for H&CD systems, while figure 8 summarizes the overall operational range of the H&CD, including low toroidal magnetic field (1.8 T) scenarios.

[2] In H plasmas at 2.65 T, the envisaged ICRF heating scheme relies on direct electron heating by the fast magnetosonic wave, for which wave absorption is less efficient than with the minority heating schemes available in other plasmas or at higher magnetic fields. In He plasmas at 2.65 T, the envisaged ICRF scenario is fundamental H-minority heating, which is an efficient heating scheme.

[3] RF coupling is usually better in L-mode than in H-mode due to smaller density gradients. Optimizing the matching algorithm settings for the L-to-H transition, during which the coupling varies rapidly, will require due attention, as H-mode access will be impacted by the coupled ICRF power. Acquisition of sufficient experimental data will allow optimization of the algorithm by better anticipation of the transition. Fine-tuning of the matching will be undertaken during commissioning, and a database of matched configurations should be established based on this commissioning phase.

Diagnostics Commissioning and Validation: Core and edge diagnostics capabilities will be significantly enhanced in advance of PFPO-2 (see Table 7) and, in particular, the HNB and DNB will allow MSE and CXRS measurements to be implemented. This will provide significantly improved measurements in the higher performance plasmas to be performed in this phase, but will require substantial commissioning and validation of the measurements. Several dedicated plasma sessions will be required, not only for the commissioning of the new diagnostics, but (due to an expanded range in plasma parameters and conditions) also for the calibration of some of those previously installed.

As mentioned in section 3.2.4.3, calibrated 2.5 MeV neutron diagnostic measurements will be available from the start of the PFPO-1. Although experiments in both PFPO campaigns will be carried out in H and He plasmas, this measurement capability assumes particular importance during PFPO-2 to monitor neutron production resulting from the reactions of Be impurity ions with highly energetic protons produced by ICRF and NBI heating. Analysis of possible nuclear reactions involving Be and fast protons, including reaction chains involving secondary products of nuclear reactions, indicate that neutron emission of up to $\sim 5\times10^{14}$ s^{-1} is possible in 'worst case' scenarios [152]. Although this is several orders of magnitude lower than would be produced in the highest performance D plasmas ($\leq 10^{18}$ s^{-1}), ITER, as a nuclear facility, must account for such emission. Verification and validation of the neutron emission measurements will therefore be an important activity in preparation for high power heating experiments.

3.2.5.3 Advanced Control Commissioning in PFPO-2

With the additional systems available in PFPO-2, numerous advanced control schemes will need to be commissioned as soon as the measurement and actuator systems required for their implementation are operational. It will be important to commission and exploit as many advanced control schemes as possible so that any changes in the hardware and software can be carried out prior to FPO, in which the tokamak structures will rapidly become activated. Table 6 provides an estimate of the dedicated experimental time required for commissioning of advanced control functions, but development of the physics R&D needed to develop robust control is likely to require continuing experimental studies within the physics program. The main actuators introduced in this phase include the ICRF and NBI systems, the ELMCC power supplies and additional pellet injectors, both for fuelling and pellet pacing. As noted previously, the installation of the first four (ferromagnetic) TBMs will necessitate recommissioning of error field correction. The development of more sophisticated actuator sharing, event handling, integrated control, and forecasting techniques will also be required in this phase.

(a) Magnetic control: The development of plasma current, position, shape, and vertical stability control will have to be extended during the PFPO-2 phase up to 15 MA and 5.3 T. While this will build on the magnetic control developed during PFPO-1, at currents of perhaps up to 10 MA, the increased risk of damage to in-vessel components at higher plasma current implies that caution will have to be exercised in raising the plasma current gradually to 15 MA while ensuring the effectiveness of disruption and runaway mitigation techniques. Increased attention will also need to be paid to ensuring robust plasma shape and position control at higher plasma current.

(b) Plasma kinetic control: While first wall protection will have been developed in PFPO-1 at auxiliary heating powers of up to 20 MW and at plasma currents of at least 7.5 MA, during PFPO-

2 this capability must be developed towards total auxiliary heating powers of 73 MW and plasma currents of 15 MA. First wall protection against NB shine-through must also be developed in the course of the HNB commissioning. This will be carried out via gradual increases in NB energy (and power) and pulse length. The plasma current will be gradually raised to 15 MA and the first wall protection will include the additional ohmic heat flux at low q_{95}.

Although initial commissioning of divertor protection is scheduled during PFPO-1, the relatively low level of auxiliary heating power is not expected to challenge the divertor: only above 40 MW of auxiliary heating power is the divertor heat flux protection expected to be required. As the H&CD systems are commissioned to full power in PFPO-2, divertor protection will become essential, requiring further experimental time, as indicated in Table 6. Further details are given in sections 3.2.5.5, 3.2.5.7, and [3-Appendix C].

Sensors providing input to plasma stored energy and β control in PFPO-2 are expected to remain the same as those commissioned during PFPO-1. However, the actuators will change substantially, since HNB and ICRF will be added. Algorithms that allocate the mix of H&CD systems used (i.e., ECRH, ICRF and HNB) will need to be formulated, implemented, and tested. Any model-based algorithms implemented in the PFPO-1 period will need to be upgraded to include all three H&CD system actuators and to commission H&CD system actuator sharing.

Initial temperature and pressure profile control will be commissioned during PFPO-2 since the necessary profile diagnostics (i.e., profiles of plasma temperatures, densities and effective charge, Z_{eff}) and full H&CD systems will be available, allowing control of the heating profile. A real-time evaluation of the plasma pressure profile can more sensitively determine instability thresholds for MHD modes such as ELMs, NTMs, kinks, or RWMs than can a simple evaluation of plasma β. The real-time evaluation of the pressure profile peaking factor $p(0)/\langle p \rangle$, together with a model of the real-time profile measurement, might be sufficient initially. Control algorithms could range from the application of simple limits to temperature and pressure gradients, suitably normalized to yield improved estimates of instability limits, to the implementation of more comprehensive physics stability models that are still computable in real-time. Other possibilities include the application of precomputed ‘stability maps’ that can be evaluated simply and real-time application of neural networks in PCS.

Rotation profile control is a further advanced control technique which could be assessed, since it is a potential tool both for MHD stability control and for influencing plasma performance. In this context, the physical phenomenon of neoclassical toroidal viscosity (NTV) [153] is of particular interest, since it has been established as a technique to alter the plasma rotation in a tokamak in a controlled fashion when a largely non-resonant, weak, 3-D magnetic field is applied [154] - in ITER, this 3-D field would be produced by the ELMCC. The effect has been used in tokamak devices, primarily to slow the plasma rotation by providing drag, but the effect can also accelerate the plasma from near-zero values, originally found to provide rotation in the direction counter to the plasma current [155].

Based on this concept, therefore, the ELMCC in ITER, might then be used either under open or closed-loop control to influence the plasma rotation, as determined by sensors such as the real-time evaluation of the plasma rotation profile from the charge exchange diagnostic, which exploits the DNB and HNB systems. Nevertheless, details of any rotation profile control algorithm will remain uncertain until adequate experimental observations are obtained in ITER plasmas: it is

expected that the intrinsic plasma rotation drive will increase with plasma current and toroidal field, but modelling predicts that the NBI system will not provide sufficient torque on the plasma to be used as an actuator. The possibility of controlling the rotation profile in the presence of a variety of competing physics processes will therefore remain an R&D issue during the research program.

Initial current density profile control will be commissioned in PFPO-2 by exploiting the auxiliary H&CD systems, in particular the neutral beam current drive (NBCD) capability, and the current density profile diagnostics that will become available once the HNB is in routine operation. This could, for example, allow tailoring of the current density profile late in the current rise (to limit, or avoid, NB shine-through), e.g., to provide some control of the radial locations of the $q = 1.5$ and $q = 2$ surfaces to enhance the potential for NTM control.

Once all three heating systems have been commissioned, it will be possible to simulate fusion burn control by using one heating system as an actuator to simulate fusion power. Such experiments have been carried out on several existing tokamaks [156 - 160], providing a strong basis for similar simulation experiments at ITER.

(c) MHD and error field control: With a second pellet injector cask containing two additional pellet injectors, the full set of ELMCC power supplies and the full heating power, as well as additional diagnostics to measure ELMs, it will be possible to advance the commissioning of ELM control techniques in PFPO-2. The availability of 4 pellet injectors will allow pellet pacing with two injectors while fuelling with the other two injectors. Installation of the ELMCC power supplies will allow implementation of the $n = 3$ and $n = 4$ configurations of the ELMCC and permit rotation of the ELM coil perturbations to spread the ELM heat flux. With the full 73 MW auxiliary heating power, it should be possible to obtain type-I ELMy H-modes in He in PFPO-2.

The correction of device-generated error fields (referred to as ‘dynamic error field correction’, DEFC), or of those caused by plasma amplification of these fields, as well as those due to global plasma modes, such as the RWM (whether it be stable, or unstable), has been well-established in tokamak experiments using both PID and model-based control techniques [161, 162]. As the typical unstable, global MHD mode that appears in this situation is the RWM, the approach is typically named RWM control. Unstable RWMs are not expected in ITER until high performance plasmas are produced, most likely in the FPO phase of operation. However, the control algorithms, sensors, and actuators used for DEFC and RWM control are the same, so that commissioning of the control system for these tasks can be performed at the same time. The only difference that may occur for RWM control is that control of faster growing unstable RWMs may require faster power supplies than will be available in PFPO-2 for the ELMCC.

The sensors for DEFC and RWM control are relatively low frequency (<1 kHz) magnetic sensors, typically partial saddle loops, that are positioned toroidally to allow real-time discrimination of $n = 1$ magnetic field perturbations. Discrimination of higher-n numbers will be required to correct higher-n error fields and modes, but correction of fields with $n > 3$ may not be important. Many such sensors will be available for PFPO-2 and later operational periods. The actuators to be used for DEFC are the external EFCC (for nearly static error field components) and the internal ELMCC (for dynamic error field components, plasma amplification of the error field, or plasma mode activity rotating faster (toroidally) than the EFCC can track).

Once the H&CD systems are commissioned to full power, it will be possible to use the HNB and ICRF systems to increase the plasma β while using the ECRH system for NTM control. While

the expected β values will be moderate (≤ 1.5) and possibly too low to demonstrate full NTM control in PFPO-2, it is likely that classical tearing modes will appear in the current rise as well as in the flat-top, which will allow additional commissioning of NTM control techniques. Although extensively studied in existing devices [105 - 113], NTM control is not yet a routine tool for disruption prevention/delay and may require significant further development with ITER plasmas. This is partially due to the complexity of the control concept, but also to the over-subscription of ECRH systems (i.e., the variety of simultaneous demands on ECRH power) in present devices. Additionally, the temperature at the $q = 2$ surface on existing devices is rather low compared to that expected in ITER, requiring large power levels to drive the necessary current. The concepts for control have been successfully demonstrated, but there remains room for significant optimization. In addition, existing schemes are, to some extent, specific to the launcher geometry of each device.

With the full additional heating power and, in particular, the ability to drive fast ions with both ICRF and NBI, it will be possible to excite AEs, both in the current rise and in the flat-top. While AE control techniques are still the subject of R&D on existing devices, it is expected that current density and pressure profile control techniques will also allow some control of AEs. Some control, or influence, of ECRH on Reversed Shear Alfvén eigenmodes (RSAEs) and Toroidal Alfvén eigenmodes (TAEs) has been observed on existing devices [163, 164] and should be further developed for future use on ITER. The fast ion populations in PFPO-2 will be significant and will enable to initiate commissioning of AE control techniques before they are required in the FPO phase. While no dedicated operational time has been allocated explicitly to AE control in the present plan, it is expected that such experiments could be carried out during the current density and pressure profile control experiments in PFPO-2.

(d) Supervisory control and exception handling: As additional actuator and diagnostic systems are commissioned and plasma performance increases in PFPO-2, it will be necessary to perform further commissioning of advanced supervisory control within PCS as the ‘first line of defence’ in investment protection and to support management of shared actuators across multiple control functions. Additional exception handling commissioning will be required, for example, to deal with potential plant system faults and plasma events, as the number of plant systems and the plasma performance increase. With 73 MW of auxiliary power available, under some circumstances a fault in one H&CD system could be mitigated by using another system for some control functions. Similarly, a fault in one diagnostic channel, or system, could be mitigated by using a redundant channel or another diagnostic system. Actions in responds to plasma events such as an H-L transition, to prepare for the resulting drop in plasma β and radial shift in plasma position, must also be commissioned within the exception handling routines [122].

To meet the needs of the more extensive range of plasma scenarios which will be developed in PFPO-2 by making use of the expanded operational capabilities and, in particular, the range in auxiliary heating power (and heating mechanisms) available from the three H&CD systems, more sophisticated actuator sharing techniques will need to be commissioned in PFPO-2. With increasing plasma performance, a wider range of MHD instabilities is likely to appear, implying that simultaneous ‘advanced’ control schemes with multiple actuators must be developed. Preparation for simultaneous control of NTMs at $q = 1.5$ and $q = 2$, as well as sawtooth control and central electron heating for impurity control, may well be necessary in PFPO-2. As each of

these control schemes is commissioned, it will also become necessary to develop shared actuator control with priorities adjusted in real-time for each control function.

The deliverables for advanced control commissioning during the PFPO-2 phase include:

- Plasma current, position, shape, and vertical stability control to 15 MA/5.3 T;
- Density control with gas and pellet injection up to 15 MA/5.3 T;
- Disruption avoidance, detection, and prediction schemes to 15 MA (see section 3.2.5.4);
- First wall and divertor heat flux control to full auxiliary heating power;
- All H&CD systems operating simultaneously at injected powers of up to 73 MW and with pulse lengths of at least 100 s;
- Actuator sharing, event handling, and forecasting systems;
- H-mode operation with L-H and H-L transition control;
- ELMCC and pellet pacing for ELM control;
- Error field correction in the presence of the TBMs;
- Error field correction in the presence of the NB Magnetic Field Reduction system;
- Sawtooth and NTM control;
- β and pressure profile control;
- Temperature, density, impurity, rotation, and current density profile control.

Several of the latter deliverables will depend on the extent to which the achievement of the IRP performance goals and require development of the relevant control capability in advance of FPO.

3.2.5.4 Disruption management and mitigation research program in PFPO-2

The disruption program in PFPO-2 will focus mainly on adapting disruption prediction, avoidance and forecasting capabilities, and optimizing the mitigation schemes for high current and for H-mode operation. The DMS will be optimized towards higher currents and higher thermal energies, including assessment of eddy current forces during fast current quenches. The latter will aim at maximizing - within the load limits - the radiated power fraction during the thermal quench in preparation of thermal load mitigation and runaway suppression. Thermal load mitigation must be confirmed for VDEs and major disruptions (MD), and scalings for thermal energy, impurity species and impurity quantity need to be established. Radiation peaking must be reduced to stay below melting thresholds when extrapolating towards full performance pulses. This will necessitate, *inter alia*, optimization of the sequence of all injectors.

RE avoidance has the highest priority when approaching high current operation and the material injection schemes must ensure sufficient margin against RE seed formation during the TQ. However, testing this margin carries significant risks at high currents. Therefore, the constraints on injection quantities and sequences will have to rely to a great extent on modelling validated previously at lower current levels. Nevertheless, uncertainties will be high due to the exponential growth in avalanche multiplication when increasing the plasma current.

DMS reliability needs will increase with current and energy. This will require more focus on robust injection schemes that also consider failure of an injector during the injection sequence and possible recovery scenarios. The PCS algorithms must also be updated to react to any loss of DMS injectors during the plasma pulse, either by changing the pulse schedule or by choosing back-up injectors.

The following milestones must be achieved in PFPO-2:

(i) Confirmation of EM and thermal load mitigation during the CQ at 15 MA (a prerequisite for operation at 15 MA).

Experimental strategy:

- Monitor mitigation performance during 'natural' mitigated disruptions;
- (possibly) Perform deliberate mitigated disruptions at currents above 7.5 MA if the database is not sufficient to allow scaling to the next current level; note that significant PFC lifetime should not be consumed and electromagnetic loads should remain within category I in these experiments.

(ii) Confirmation of TQ heat load mitigation in H-mode (a prerequisite for routine operation with H-mode thermal energy levels).

Experimental strategy:

- Produce target plasmas with varying thermal energy in H-mode;
- Confirm, or adapt, required quantities and injection scheme to achieve high radiation fractions during the TQ;
- Validate compatibility with RE avoidance scheme and EM load mitigation scheme.

The majority of the dedicated studies on disruption load validation is expected to be undertaken in PFPO-1. However, load scalings are important for defining target values for disruption rate and mitigation rate and so certain aspects of heat load validation may require further measurements in H-mode or at higher currents. Establishing a reliable scaling for thermal loads occurring during the TQ at higher stored thermal energies in L-mode during VDEs and MDs may also require operation at higher currents. Finally, additional unmitigated disruptions may have to be performed if the accuracy of the electromagnetic load scalings derived from operation at up to 7.5 MA is insufficient, provided that this can be performed without significant PFC degradation and with electromagnetic loads remaining in category I range.

Development of H-mode operation will require adaptation of disruption prediction, and possibly also detection, schemes to assure reliable generation of DMS triggers. The algorithms within PCS determining the appropriate injection sequence in each phase during a pulse will also have to be adapted to the new plasma scenarios. Tests of prediction or detection schemes that include deliberate disruptions must be performed using the DMS. Extended diagnostic capabilities will have to be incorporated and exploited for the prediction algorithms. The required mitigation rates will also depend on the tendency of unmitigated disruptions to form runaway electrons. For higher thermal energies, impurity influxes, especially from the divertor, can lead to faster thermal and current quenches, facilitating RE formation.

The following milestones must be achieved in PFPO-2:

(i) Thermal quench prediction in preparation for FPO (a prerequisite for FPO operation - the required reliability depends on the expected loads and might vary for different thermal energies (c.f. sections 2.5.4 and 3.2.4.6)).

Experimental strategy:

- Monitor the performance of disruption prediction algorithms;
- (if required) Expand threshold and physics model-based algorithms for predicting the TQ during H-mode operation and implement statistical methods in parallel;
- Perform dedicated mitigated disruptions, if required to optimize the disruption predictor;

- Implement and test decision schemes in PCS for the injection sequence.

(ii) Injection sequences ready for FPO (a prerequisite for FPO operation).
Experimental strategy:

- Optimize injection sequences for pre-TQ injection;
- Verify RE avoidance, TQ and CQ mitigation efficiency.

3.2.5.5 H-mode studies in PFPO-2

Summary of scenarios: The development of the remaining aspects of H-mode operation in the non-active phase will be completed during PFPO-2. This will be a more extensive experimental program (a factor of ~3 times longer) than in PFPO-1 because of the substantial improvement of the capabilities of ITER for H-mode operation and improved diagnostics. These include the full complement of the baseline heating systems, the power supplies for the ELMCC and improved diagnostics for edge plasma parameters (e.g., reflectometers and edge Thomson scattering, if not already operational towards the end of PFPO-1) and ion temperature (e.g., charge-exchange spectroscopy), as shown in Table 7. To minimize the risks of initial H-mode operation in FPO, it is important that both operational and physics issues of H-mode operation in ITER are addressed at a plasma current level of up to 7.5 MA. This would allow H-mode operation in FPO to start at this level of current and proceed upwards in D and then DT.

The main goals of H-mode studies during the PFPO-2 phase are:

- confirm the predictions of the H-mode power threshold and power required for sustainment of high confinement type-I ELMy H-modes over a range of I_p, B_t, plasma densities and species (H and, most likely, He);
- establish stationary type-I ELMy H-modes over a range of I_p, B_t, plasma densities and powers in order to: a) characterize the scaling of H-mode energy and particle confinement in ITER;
  b) characterize ELM power fluxes to plasma-facing components;
  c) characterize effects of ELMs on W production and impurity exhaust that may establish limitations to the uncontrolled ELM energy loss/frequency;
  d) to complete the initial assessment of the scaling of the SOL power flux with a wider range of toroidal fields, plasma currents, densities and input powers; and e) to extend their duration to identify possible issues related to long-pulse operation such as long timescale recycling issues or transport changes due to the global relaxation of the current profile;
- demonstrate ELM control over a range of $q_{95} > 3$ (possibly up to 4.5) with 3-D magnetic fields for both ELM transient power exhaust and impurity exhaust and to assess the potential of the back-up ELM triggering schemes for $I_p > 5$ MA H-mode operation;
- determine the effects of the TBMs on H-mode plasma and performance by comparison with PFPO-1 experiments and, if sizeable effects are observed, to mitigate their effects by the application of correcting fields with the EFCC and the ELMCC, firstly at 1.8 T and then at 2.65 T.

The corresponding experimental plan can be summarized as follows:

- *H-mode operation to connect with PFPO-1, evaluating/mitigating TBM effects and extending H-mode operation at 1.8 T:* This will require the use of the same species as in

PFPO-1 (H or He) and currents (mostly 5 MA) plus additional experiments to exploit the increased additional heating, enhanced ELM control capabilities and improved diagnosis of the plasma;

- *Expansion of H-mode operation towards 7.5 MA/ 2.65 T:* This will include an exploration of H-mode H plasma operational range at 2.65 T with currents of up to 7.5 MA, including the use of small proportions of He and impurities to expand this range, followed by the characterization of H-mode plasmas and optimization of ELM control. The latter will be performed in He plasmas if the stationary H-mode development in H proves unsuccessful. Alternatively, assuming that R&D in present experiments confirms that this is a viable solution for ITER, other options for H operation at 3.0 - 3.3 T with ICRF three ion heating (^{3}He + ^{4}He) would be possibly considered to replace He plasmas;
- *Development of long-pulse H-modes:* this will require H-mode plasmas in H at 1.8 T or 2.65 T depending on the outcome of the research in PFPO-2.

To a large degree, the plasma conditions to be explored in PFPO-2 will be determined by the power that can be coupled to the plasma over the range of fields that will be investigated in H-mode and by the H-mode power threshold of the plasmas to be explored.

For ICRF heating of H plasmas there is a good scenario with strong SPA for 1.8 T (second harmonic H-majority) but not for 2.65 T, while for He plasmas there is a good scenario with strong SPA at 2.65 T (first harmonic H-minority) and, possibly (this will be assessed in PFPO-1), at 1.8 T (second harmonic H-minority). As mentioned above, other ICRF schemes with strong SPA in H plasmas are possible by using the novel three-ion [165] scheme demonstrated in JET, Alcator C-Mod and ASDEX Upgrade [93]. This may be viable at 3.0 or 3.3 T in ITER, although it will imply strongly off-axis ICRF power deposition profiles. For these reasons, this possibility is considered as an option at present and, if found viable for ITER, may be explored within PFPO-2 instead of the 2.65 T H and He plasmas considered in the reference operational plan below.

The application of NB heating to low density H-modes in this phase will be limited by shine-through loads on the blanket shield module that intersects the beams at the outer first wall, which is required to have a lifetime of at least 30,000 pulses. Two approaches can be taken to circumvent this issue: one is to shorten the HNB pulse and the other to decrease the HNB energy, although this implies a reduction of the HNB power with $E_{HNB}^{2.5}$ due to the perveance matching constraint [90]. Detailed studies have been carried out to determine the power levels that can be applied in long pulses (> 100s) with acceptable shine-through loads for a range of plasma densities and NB pulse durations at maximum power when operating in H and He plasmas [89, 90], and the key results are shown in figures 10 and 11, together with the expected H-mode thresholds for 5 MA/1.8 T and 7.5 MA/2.65 T in H and He plasmas. As shown in these figures, for both toroidal field values, significant power in addition to that from the HNB is required to access H-mode plasmas in H, while the required additional power is much lower for He. Access to H-mode for 7.5 MA/2.65 T in H will be possible with HNB and ECRH alone, but only by operating at relatively low densities and, thus, for NB power durations of less than 40 s.

Within the commissioning activities at the start of PFPO-2 the shine-through power deposition will be assessed with L-mode plasmas first in H and then in He, as described in section 3.2.5.2. If this assessment were to show that the predictions substantially overestimate the shine-through power deposition levels, this would enlarge the H-mode operational space for H plasmas at 1.8 T

and 2.65 T in ITER. On the other hand, if the predictions would underestimate the real level of shine-through loads this would eliminate the possibility of H-mode operation at 2.65 T in ITER for H plasmas. Refinement of shine-through losses for high energy NBI is therefore considered an important open R&D issue (see section 5.11.4). The experimental plan for PFPO-2 described below is developed according to the shine-through load levels as predicted and to the H-mode threshold levels described in [3-Appendix B]. The plan would, therefore, need to be adjusted depending on the experimental results concerning the H-mode access powers and the shine-through power loads determined by experiments in ITER itself.

Details of the deliverables from these plasmas and the rationale for the prioritization of the H-mode research are discussed below. The associated R&D that could be performed during ITER construction to refine the H-mode plans during PFPO-2 is discussed in section 5.3.

Motivation for H-mode scenarios during PFPO-2: H-mode operation during PFPO-2 aims at characterizing this scenario and developing the control schemes that will be required up to currents of ~7.5 MA, which are foreseen for the start of H-mode operation in FPO. During PFPO-2 all systems required to perform this research will be available in ITER in the final baseline configuration including heating and current drive, pellet fuelling, diagnostics (except most of the fast particle and some neutron diagnostics) and ELMCC. In elaborating the PFPO-2 plan, it is assumed that in PFPO-1: an initial assessment of the additional heating power level to access H-mode in ITER will be performed, H-mode operation at 1.8 T will be demonstrated in a reduced operational range, and initial studies of ELM control by pellet triggering will be performed. The availability of all the required systems in PFPO-2 will allow a wider exploration of H-mode plasmas in H and He to be performed in conditions closer to those in FPO, to perform a first systematic study of H-mode performance in ITER plasmas with $T_e \sim T_i$ and of the integration of core confinement and edge compatibility issues including radiative divertor operation and ELM control. These studies are essential to minimize the risks during initial FPO operation and are not possible during PFPO-1. The integration of core confinement and edge compatibility is particularly critical for the ITER mission since, for the conditions required for high-Q operation, unmitigated power fluxes are expected to exceed the power flux capability of the W divertor, excessive W production and core plasma contamination can lead to the loss of the H-mode and type-I ELMs are expected to cause melting of the plasma-facing components and cause significant W influxes that may also lead to the loss of the H-mode. Given the importance of demonstrating the compatibility of H-mode operation (with the required confinement level for high-Q operation) with acceptable edge plasma conditions (i.e., acceptable stationary and transient power fluxes and impurity sources), it is essential that this issue is addressed thoroughly and as soon as possible in the Research Plan and thus in PFPO-2. This will allow the development of mitigation strategies to be formulated and refined (e.g., development of other high confinement plasma scenarios in ITER alternative to the controlled-ELM H-mode, etc.) in advance of FPO should major issues be identified in the development of the plan described below.

Experimental plan and deliverables for H-mode scenarios in PFPO-2: The PFPO-2 experimental plan starts with similar H-mode plasmas to those that should have been obtained before the end of PFPO-1 and then expands the H-mode operational range towards 7.5 MA/2.65 T. Due to the high H-mode threshold of H plasmas at 2.65 T and the lack of a suitable heating scheme (for ICRF) or restrictions (NBI shine-through loads) in the application of the baseline heating systems, the reference research plan in PFPO-2 is to perform comparisons of

hydrogen and helium H-mode plasma behaviour at 1.8 T, with the main H-mode scenario development in He plasmas at 7.5 MA/2.65 T. Nevertheless, the plan includes an early assessment of the H-mode operational range that can be achieved in H plasmas at 7.5 MA/2.65 T so that the limitations expected for these plasmas can be corroborated experimentally (high shine-through power loads requiring high density for NBI and high H-mode threshold) and also includes dedicated studies to enlarge this operational range. Following the assessment and these studies, it should be possible to decide whether to conduct the main H-mode scenario development in He plasmas at 7.5 MA/2.65 T, or, alternatively, whether the program can be developed around H plasmas. The latter would obviously be advantageous for the extrapolation of the results obtained in PFPO-2 to FPO but, for the reasons explained above, this is not considered feasible with the experimental evidence currently available and the modelling performed for ITER to date. The exploration of H-mode operation will be developed in 6 stages, as discussed below.

(i) *H-mode operation to connect with PFPO-1, evaluate/mitigate TBM effects and to extend H-mode operation at 1.8 T:* The main objective of this phase is firstly to assess the effects of the TBMs on H-mode plasmas under the same plasma conditions as obtained in PFPO-1 at 5 MA/1.8 T, to mitigate these effects, if sizeable, and then to expand the operational range of 1.8 T plasmas, predominantly in H plasmas to take advantage of the increased additional heating power.

Building on results from operation at 1.8 T in PFPO-1, experiments in PFPO-2 will start in the conditions that provide type-I ELMy H-modes with high energy confinement. In principle, to provide a better assessment of the influence of the TBMs on H-mode plasmas, it is preferable to select plasma shapes whose separatrix-wall distance is as close to the reference ITER shape as possible while ensuring high energy confinement (if the -1.28% ripple level at the reference separatrix position turns out to degrade confinement unacceptably) and in H if possible (otherwise in He). The H-mode access experiments with power ramps (20 s ramp-up followed by 30 s stationary) would be repeated in PFPO-2, applying the same heating levels and schemes as in PFPO-1. Possible differences in relation to H-mode access and sustainment due to the presence of the TBMs will be documented and, if significant, schemes to mitigate these effects will be developed. These would be based on the optimization of n = 1 error field correction for H-mode plasmas with the EFCC plus the use of the ELMCC to fine tune static low-n error field correction and, possibly, to develop active correction schemes.

Once schemes to mitigate the effect of TBMs have been developed, the program will progress to the expansion of the H-mode operational range at 1.8 T by exploiting both the increased additional heating power available and the full ELM control capabilities with 3-D fields for both H and He plasmas. This will include experiments similar to those already performed in PFPO-1 over a range of currents of 3.5-5.0 MA and will address the scaling of H-mode confinement, pedestal/SOL plasma parameters with increasing input power and margin above the H-mode threshold power. The increased input power will also allow expansion of the operational range to higher plasma densities/ performance and an initial evaluation of the fuelling efficiency of gas versus pellet injection together with particle transport studies. These experiments will benefit from the nearly complete baseline diagnostic capabilities. From the evaluation in figure 10, it appears that H-mode operation should be possible for both H and He plasmas over the density range (n_e = 0.4 - 1.0×n_{GW}) with NBI and ECRH heating alone. The additional 20 MW of ICRF (assuming coupling issues are not important) would allow the achievement of both He and H

plasmas at a level of $P_{input}/P_{LH} \leq 2$, while He plasmas could be pushed towards levels of $P_{input}/P_{LH} \leq 3$ - 4 (if second harmonic H-minority heating is efficient) at 5 MA/1.8 T.

Together with the expansion of the type-I ELMy H-mode operational space, ELM control experiments with the ELMCCs will be performed. This will include exploration of a range of toroidal mode numbers (most likely from $n = 2$ to $n = 4$) and of poloidal spectra over the range of $q_{95} = 3.0$ - 4.3 at 1.8 T (i.e., $I_p = 3.5$ - 5.0 MA), as far as possible. In particular, optimization of the spectra to achieve the same level of ELM control/suppression to account for changes in q_{95}, $<n_e>$, β, and plasma rotation (that can be varied by adjusting the NBI power level) will be assessed thoroughly. The exploration will also assess the effects of 3-D fields on H-mode access and identify schemes for the time variation of the fields so that their impact on H-mode access is minimized while they provide the required level of ELM control during the stationary H-mode phase. This is an important step that should eventually conclude with the demonstration of ELM suppression for 1.8 T plasmas over the range $q_{95} = 3.0$ - 4.3, which will provide an assessment of the requirements for achieving ELM suppression more generally in ITER. As in PFPO-1, the back-up ELM triggering techniques provided by vertical plasma oscillations and pellet injection (now with 4 available injectors) will be applied to ensure that a minimum level of ELM control is maintained as the 3-D fields produced by the ELMCC are retuned for each of the conditions explored, particularly when q_{95} is varied.

The 1.8 T experiments described above will be shared between H and He plasmas. While priority will be given to operation in H, it is not possible to predict the operational sharing between the two species. If the potentially most pessimistic aspects of hydrogen H-mode operation at 1.8 T in ITER materialize, a significant proportion of the experiments would be performed in He. If this were not the case, operation in He would be restricted to the minimum required to provide:

- Assessment of the impact of TBMs on H-mode access and confinement, and exploration of mitigation measures (if the reference plasmas in PFPO-1 were performed in He), and
- Reference set of H-mode plasma conditions and requirements to control/suppress type-I ELMs at 5 MA/1.8 T for comparison with 7.5 MA/2.65 T He plasmas in PFPO-2.

Obviously, if this initial assessment of H-mode operation in H at 1.8 T also provided sufficient confidence that stationary type-I ELMy H-mode were feasible in H at 7.5 MA/2.65 T (e.g., lower H-mode threshold than expected and/or lower shine-through loads than calculated), then the helium operational period would be shortened or fully eliminated at this stage; but this would only be possible if the PFPO-1 reference H-modes providing a basis for the assessment of TBM effects had already been performed in H.

(ii) *Expansion of H-mode operation towards 7.5 MA/2.65 T in hydrogen:* These experiments will assess H-mode access at 2.65 T and will then explore H-mode operation with increasing power levels and ELM control, in a similar fashion to the 1.8T discussed above. As noted previously, the expected operational range of H-modes in H at 2.65 T is very narrow due to both the lack of an ICRF heating scheme with high SPA and the high NBI shine-through loads expected at low density. Therefore, these initial H experiments will be focussed towards the determination of the H-mode threshold in H plasmas at 2.65 T and the assessment of the possible operational range for stationary H-modes. From the analysis illustrated in figures 10 and 11, it should be possible to access the H-mode in H plasmas in ITER for densities in the range of 2.4 - 3.6×10^{19} m^3, but the H-mode phase would be limited to ~ 10 s when all available heating

power is applied (33 MW of NBI + 20 MW of ECRH). To minimize the probability of accidental melting of the W divertor during this exploration, experiments will start at 5 MA, where melting is not expected to occur (see [75]). At a current of 5 MA, $\langle n_e \rangle = 2.4\times10^{19}$ m^{-3} corresponds to $0.6\times n_{GW}$, and this density is expected to be achievable with pellet fuelling if required [166, 167]. The plasma current will then be increased in steps of 0.5 - 1.0 MA towards 7.5 MA, and the temperature of the divertor during ELMs will be monitored at each step. This scan will provide the scaling of the H-mode threshold at 2.65 T for H plasmas for comparison with that derived for 1.8 T plasmas in PFPO-1 and will potentially yield insight into the influence of q_{95} on H-mode access in low-ripple plasmas.

It is important to note that, as in PFPO-1 experiments, these operational conditions near the L-H threshold are likely to produce long ELM-free periods that may lead to a sudden transition back to L-mode due to W accumulation. Similarly, limitations on NBI heating arising from shine-through loads will restrict the possibilities for providing a soft landing of the H-mode by ramping the power down slowly in this phase. Therefore, significant effort will be required to ensure that these plasmas do not terminate abruptly. Maintaining ELM control throughout the H-mode entrance and exit phases will be a key measure in this respect, as demonstrated in present experiments [143]. This control will be most likely exploit the back-up ELM triggering schemes available for these plasmas (pellet injection and vertical plasma position oscillations), since developing an ELM control scheme with 3-D fields in marginal H-mode conditions is expected to be very challenging. Based on the evaluations in [3-Appendix C, 44, 34] for the low density range of the proposed scans, the divertor power loads for these H-mode plasma conditions will be sufficiently high to necessitate a consideration of applying impurity seeding to reduce the loads and W sputtering.

On the basis of the findings from these initial experiments, it would possible to assess whether the operational space of stationary H-modes at 2.65 T is consistent with the calculations shown in figures 10 and 11 (i.e., essentially non-existent or, at best, very narrow) or is indeed wider than predicted. This assessment would inform a decision point: experiments would either continue along the steps discussed immediately below (i.e., assuming no operational space for pure H plasmas at 2.65 T), or would move to a program discussed later (exploiting a wide operational space to pursue H-mode characterization and ELM control at 2.65 T in H plasmas). In the former case, the next step would be to investigate options for widening the H-mode operational space in predominantly H plasmas sufficiently to support the more extensive H-mode program in H plasmas discussed later. Two approaches can be considered:

- One approach would follow the line of study introduced in PFPO-1 by operating with ~10% He in H plasmas to decrease the H-mode threshold;
- An alternative approach explores the possibility of neon seeding of the H plasma to decrease the shine-through loads by more effective ionization of the injected neutrals, thus allowing longer pulses at low plasma densities, where the margin to the threshold should be largest.

For the first approach, it is assumed that injected He at levels of ~10% will decrease the H-mode threshold of H to intermediate values between H and He. Thus, the threshold for $\langle n_e \rangle = 3.5\times10^{19}$ m^{-3} predominantly H plasmas at 2.65 T would be in the range of ~35.7 - 41.5 MW, depending on the helium H-mode threshold value (and would allow a 30 - 40 s NBI heating pulse with acceptable shine-through loads). While some tests on the viability of this

approach will have been undertaken in PFPO-1 in 1.8 T plasmas (and possibly earlier in PFPO-2 if the reference pulse for the assessment of the H-mode impact of the TBMs were established with H + 10%He), it might not have been possible to exploit its full potential due to the relatively high ripple at 1.8 T. It is therefore proposed to study this operational scheme again at 2.65 T. The reduced H-mode threshold in mixed H-He plasmas can thus provide some operational range in type-I ELMy H-modes with 53 MW of total heating, particularly if the H-mode threshold is near the lower end of estimates. In addition, the presence of 10% He in the plasma decreases the shine-through loads approximately in proportion to the He concentration, so that a duration of 30 - 40 s for full power NBI in H+10%He plasmas with $\langle n_e \rangle = 3.5\times10^{19}$ m^{-3} ought to be conservative.

The second approach relies on increasing the density of impurities in the plasma, as this significantly enhances the effective ionization cross section of the plasma for fast NBI neutrals (charge-exchange capture by highly ionized impurities) and thus decreases the shine-through loads for a given value of $\langle n_e \rangle$. Drawbacks of this approach are that core radiative losses increase, which might cause a reduction in the edge power flow (which must be maximized for H-mode access), that higher W sputtering may result due to the additional impurities and the low density conditions and that the presence of a high level of impurities might impact the H-mode threshold itself [30, 31]. Simulations for ITER 7.5 MA/2.65 T plasmas show that seeding with neon can open a window for operation for H plasmas with full NBI + ECRH power during long pulses with acceptable shine-through loads, as shown in figure 12. For this purpose, medium-*Z* impurities are optimum as they are fully ionized in the ITER core plasma and thus do not contribute to an increase of the radiative losses.

The sharing among the three possible approaches (pure-H, H+10% He and H+1% Ne) will be determined by the results of the experiments themselves and by the degree of complexity of the scenario control issues (sudden H-L transitions, avoidance of long ELM-free periods, plasma radiative collapse etc.). These must be addressed when operating near the H-mode threshold and may be more difficult to resolve in some of the approaches than in others.

At this point of the experimental program a decision will be taken whether to proceed with the 2.65 T H-mode characterization and ELM control demonstration in H or H-dominant plasmas (i.e., going directly to the program discussed at stage (iv) below), or to perform these experiments in He. Given the reduced operational range predicted for H plasmas and predominantly H plasmas, the reference strategy is to switch to He plasmas at this stage. If this is not required, the development of helium H-mode access and initial characterization of H-mode behaviour, presented in stage (iii) immediately below, could be replaced by the expansion of the operational range of H plasmas towards high currents and fields described at stage (v).

(iii) *Expansion of H-mode operation towards 7.5 MA/2.65 T in helium:* If robust H-mode access and long-pulse type-I ELMy H-mode cannot be obtained at 2.65 T in H or H-dominant plasmas, He plasmas will be studied. The type of scans will be similar to those described in the preceding stage, starting with 5 MA/2.65 T plasmas to avoid melting of the W divertor by ELMs, and then increasing the current towards 7.5 MA. Given the much lower H-mode threshold, lower shine-through loads and the wider flexibility in heating mix (NBI, ICRF and ECRH) for He than is predicted for H plasmas, the range of plasma densities that can be explored will be considerably wider than in H (in principle, from the minimum density determined by mode-locking up to $\langle n_e \rangle \sim 6\times10^{19}$ m^{-3} = $n_{GW\text{-}7.5MA}$). In practice, the achievable range of $\langle n_e \rangle$ in H-mode is expected

to be limited to relatively low values of $<n_e>/n_{GW}$ due to the detachment of the divertor for He plasmas, which limits the separatrix density to 2.0 - 2.5×10^{19} m^{-3} for P_{SOL} = 40 - 60 MW (see [3-Appendix C]), due to the lack of pellet fuelling for these plasmas. Integrated simulations of ITER scenarios show that even with this limitation, and the possibility of gas fuelling only, stationary H-modes with $<n_e> \geq 0.5 \times n_{GW}$ should be achievable for 7.5 MA/2.65 T in He plasmas with the standard assumptions regarding particle transport in ITER [166, 168].

Operation in helium H-modes should thus allow studies of the q_{95} and density dependence of the power threshold in low ripple conditions (2.65 T), which is not expected to be possible in H plasmas. Otherwise, the same issues regarding the control of the plasma in these experiments will need to be faced as for H plasmas (e.g., avoidance of long ELM-free periods, etc.), but may be quantitatively different. For example, W sputtering by He will be larger than for H, due both to the higher mass and to the higher divertor plasma temperatures (for the same neutral pressures), as shown in [3-Appendix C]. This may restrict the minimum density that can be explored and require a more careful control of ELM-free periods. On the other hand, the ELM power pulses are expected to be longer in He than in H due to the longer ion transit time [169, 170], thus reducing the accidental risk of melting of the W divertor in these experiments. Similarly, the wider possibilities for additional heating in He will ease significantly the control of the plasma in the H-mode access and exit phases, thereby decreasing the risk of disruptions in these He experiments compared to that in H.

Depending on the range of parameters over which H-modes in He have already been characterized in PFPO-2, additional experiments on H-mode access at 1.8 T along the lines of those discussed at stage (i) above may be required at this stage to obtain a matching set of conditions at 1.8 T and 2.65 T (for example, with the same values of toroidal ripple).

(iv) *Characterization of H-mode operation up to 7.5 MA/2.65 T including ELM control and resolution of scenario integration issues:* The experiments described in stages (ii) and/or (iii) will provide an assessment of the power requirements for H-mode access and post-transition H-mode plasma evolution at 2.65 T, and will also determine which main ion species (H or He) will be used in the further characterization of stationary H-modes and ELM control. During this follow-up phase, the experiments will follow a similar strategy as that foreseen for 1.8 T at stage (i) above, but with a much wider scope. The objective of this phase of experiments is to provide a fully integrated H-mode scenario at 7.5 MA/2.65 T which can then be used as the starting point for H-mode experiments in deuterium plasmas during FPO.

The experiments will start at 5 MA/2.65 T, where melting of the divertor target during uncontrolled ELMs is not expected, and gradually increase (firstly) the heating power level and duration beyond the initial ~10 s stationary level demonstrated previously towards ~100 s of stationary heating power. For each power level the density will then be increased, which will allow the characterization of the changes to pedestal and SOL plasmas and overall H-mode confinement to be performed. Depending on whether the experiments are performed in H or He, a comparison of gas fuelling and pellet fuelling will be performed (only possible for H) at each level of the heating power. The anticipated level of heating for each density level will range from ~20% above the measured L-H threshold up to the maximum heating power allowed by shine-through loads (<73 MW at 5 MA).

ELM control with RMP fields will be developed building on the experience developed for 1.8 T plasmas over a range of q_{95} = 3.0 - 4.3. The effects of the RMP fields on ELM control/suppression, H-mode confinement, impurity exhaust and fast particle losses will be determined for a range of heating mixes with a varying level of NBI and optimized (both for effective ELM control versus confinement degradation and core W accumulation avoidance), while ensuring that fast particle power fluxes on plasma-facing components are acceptable. This will allow the development of RMP optimization schemes with varying levels of toroidal plasma rotation for each density level and/or to identify the level of toroidal plasma rotation/input NBI torque that is required for optimum confinement for a given level of ELM control. To ensure that ELMs remain controlled to the required level while ELM control schemes with RMPs are developed, the ELM back-up triggering schemes: vertical plasma oscillations and pellet pacing (if in H plasmas) will be applied. As these experiments will focus on ELM control with RMPs during the stationary heated flat-tops, the ELM back-up triggering schemes will be essential to ensure ELM control in the access and exit phases to/from stationary H-modes.

Once 5 MA/2.65 T stationary H-modes with ELM control have been developed, the plasma current level will be increased in steps of 0.5 - 1.0 MA towards 7.5 MA. Continuous monitoring of the divertor temperature during ELMs will be performed to ensure that no melting is caused by uncontrolled ELMs; this is expected to occur at the monoblock edges for currents of ~7.5 MA [75]. At each step, various levels of heating power and power mixtures will be applied and the density will also be varied (with gas and pellets if in H plasmas, but only with gas if in He). The optimization of the RMP fields applied for ELM control will be performed for each level of q_{95}, plasma parameters (chiefly β for the plasma response effects) and heating mix choice. This optimization is potentially time-consuming, and the sequence of steps will need to be carefully selected on the basis of previous experience in PFPO-1 and PFPO-2 to ensure that it can be performed with a reasonable investment of time. These experiments will provide an excellent characterization of H-mode confinement, pedestal characteristics and SOL plasma parameters with increasing level of plasma current and decreasing recycling neutral source (as the divertor/SOL ionization becomes more effective with increasing levels of plasma density). Similarly, if the increasing plasma β and decreasing q_{95} leads to the triggering of NTMs, control/suppression schemes using ECRH/ECCD will be implemented; this, together with the need to avoid central W accumulation, may restrict the range of heating mixes that can be explored above a given I_p.

For the lower core neutral sources expected at 7.5 MA, low density gradients are expected to appear in the pedestal (similar to DT operation). This should lead to profound changes to W impurity transport, as neoclassical screening dominates in the pedestal [67, 139, 171], which can affect the balance of W exhaust between ELMs and at the ELMs [68]. If these effects are identified at this level of plasma current, dedicated studies to determine the optimization of RMP fields to provide control of both power fluxes during ELMs and W exhaust will be performed. In these conditions with dominant pedestal impurity screening, increasing the ELM frequency and reducing ΔW_{ELM} may not provide W exhaust from the core plasma on longer timescales, as shown in figure 13 (in this modelled case for DT plasmas) [139].

With the expansion of the plasma scenarios towards 7.5 MA, transient ELM power fluxes to plasma-facing components, stationary power fluxes and the W sputtering source will all increase,

as the SOL power width is predicted to scale as I_p^{-1}. To ensure that stationary power fluxes remain within the ranges required for the W divertor target (see [3-Appendix C]) and to prevent core W contamination, injection of additional impurities is expected to be required to provide increased divertor radiation, thereby decreasing both divertor surface temperature (to prevent W recrystallization, see [3-Appendix C]) and the divertor plasma temperature. In addition, application of time-variation of the RMP perturbation [63] may be required to avoid the local power fluxes exceeding the specified limits. If necessary, therefore, the impact of RMPs on high density radiative divertor conditions and divertor power fluxes will be characterized at this stage. If not, dedicated experiments will be performed to assess the influence of RMPs on radiative divertor plasmas and on power fluxes in semi-detached divertor conditions. An additional goal would be to decrease off-separatrix localized power fluxes by time variation of the applied 3-D fields. Experiments to re-optimize the applied RMP perturbation and heating-mix would then be performed to identify the best compromise between core and edge integration in these plasmas. This will then guide the development of the ELM-controlled H-mode plasma scenarios in DT.

The experiments above will provide fully integrated and optimized stationary H-mode plasma scenarios in terms of plasma confinement, controlled stationary and ELM-generated power fluxes, and impurity exhaust via 3-D fields. The remaining set of experiments will aim at demonstrating the integration of ELM control, power fluxes and impurity exhaust during the H-mode access and exit phases with 3-D fields, and scenario elements which will be required for DT operation.

To address the control of H-mode access and exit with 3-D fields, two sets of experiments will be performed:

- At two levels of I_p (5 and 7.5 MA), 3-D fields will be applied before or just after the L-H transition and will be switched-off at, or just after, the H-L transition for a suitable range of plasma densities, levels of input power and heating mixture to be determined by the experiments above. The goal of these experiments is to demonstrate robust access from L-mode to a high confinement H-mode and controlled H-mode exit with control of ELMs, impurity exhaust and power fluxes to PFCs provided by 3-D fields.
- 3-D fields will be applied during the current ramp-phases (at 5 MA for a flat-top current of 7.5 MA) in which the L-H and H-L transition will be triggered by changes in additional heating. The switch-on and -off of the fields around the L-H and H-L transitions will follow the strategies developed in the previous experiments, and then the 3-D fields will be varied in time to provide ELM control through the current ramp-up/down H-mode phases in which q_{95} will be varying. The experiments will include a range of density and power waveforms and current ramp-up/down rates for which the 3-D fields will be optimized.

For these experiments, the back-up ELM triggering schemes (vertical plasma oscillation and pellet triggering (if in H plasmas)) will be used to provide the required level of ELM control while the applied 3-D fields are being optimized to provide ELM control. The results will provide fully integrated scenarios, including the H-mode access and exit phases, optimized in terms of plasma confinement, plasma fuelling as well as controlled stationary and ELM-driven power fluxes and impurity exhaust provided by 3-D fields. These will be used as templates for further development in D/DT and towards higher plasma currents in FPO.

(v) *Demonstration of long-pulse H-mode operation:* The last series of experiments in PFPO-2 will aim to provide a demonstration of a long-pulse H-mode scenario (potentially up to ~1000 s)

with the purpose of assessing issues related to processes that may evolve on very long timescales such as those related to changes in the current profile, etc.

These experiments will build on the results of the assessment of the current drive capabilities of the ITER systems described later in section 3.2.5.6, for which synergies with the experiments discussed in stage (iv) above will be exploited. Assuming that, in the experiments discussed in section 3.2.5.6, the current drive capabilities of the ITER NBI and ECRH systems are found to be in agreement with present estimates and that fast particle-related instabilities do not cause major effects in the plasma, it will be possible to achieve ~1000 s long pulses in 7.5 MA/2.65 T H-modes even without any significant use of the lifetime of the central solenoid. This is due to the predicted current drive efficiency of NBI in these plasmas, which is estimated to generate currents in the range ~2.5 - 3 MA [172, 173]. This, together with the pedestal bootstrap current, provides a non-inductive current component of 60% of the total plasma current, as shown in figure 14. A stationary H-mode of 1000 s is therefore feasible, even with a premagnetization current of 30 kA in the central solenoid (compared to the maximum value of ~45 kA), which makes a negligible contribution to the lifetime fatigue consumption; figure 15 summarizes the achievable flat-top durations for a range of plasma conditions versus premagnetization current. As described above, these demonstration experiments will focus on the determination of effects that may develop over very long timescales in ITER plasmas, such as those associated with the relaxation of the current profile which can affect plasma and impurity transport, long timescale evolution of processes related to plasma-wall interactions, etc., and to develop strategies for their control if required. However, at this point in the experimental program, the H-mode duration is likely to be limited by the pulse duration for which reliable high-power operation of the H&CD systems has been established; the development outlined here assumes that it has been possible to commission high-power operation of the required H&CD systems up to the necessary pulse lengths, or that the required extension of the pulse length can readily be achieved within the allocated experimental time.

For these plasma conditions, not only is a significant level of driven current predicted, but the fast ion populations, from NBI and ICRF, will also be significant. Therefore, the plasmas at the highest power levels may develop instabilities driven by fast particles or induced by the driven current profile. This might limit the extrapolability of these plasmas towards H-modes at higher plasma currents [173]. Details of experiments relevant to the use of the H&CD systems for current drive studies in preparation for the development of long-pulse operation, as well as the potential for research on fast particles in these plasmas is discussed in section 3.2.5.6.

(vi) *Option for low-ripple hydrogenic H-modes - H-modes in hydrogen at 3.0 or 3.3 T with plasma currents of up to 8.5 or 9.5 MA respectively:* An option exists for obtaining H-modes in H plasmas in regimes with low TF ripple by increasing the value of the toroidal field beyond 2.65 T to enable ICRF schemes with SPA based on the three-ion scheme [165], using ~10% ^{4}He and ~1% ^{3}He, following its demonstration in JET, Alcator C-Mod and ASDEX Upgrade [93]. Although the increase in toroidal field from 2.65 T to 3.0 - 3.3 T increases the H-mode threshold power by 10 - 20%, the possibility of utilizing ICRF heating at up to 20 MW and the possible reduction of the H-mode threshold by the presence of ~10% He, may provide access to predominantly hydrogenic H-mode plasmas at these higher fields. For example, for a H plasma with $\langle n_e \rangle = 4.5\times10^{19}$ m^{-3} and ~10% ^{4}He at 3.0 T, for which the application of NBI at full power is not restricted, the corresponding H-mode threshold could be in the range of 47 - 55 MW,

significantly less than the total available input power of 73 MW. Several issues need to be assessed before this option can be considered sufficiently viable to be added to those in the previous stages, or, indeed, to replace one of the strategies presented above. These include the experimental confirmation of the effect of quantities in the range of ~10% ^{4}He in decreasing the H-mode threshold in H and an assessment of the fast ion losses associated with the three-ion heating scheme with the ion species considered for ITER. This heating scheme specified produces very high energy ^{3}He ions and, for these fields in ITER, has a heating deposition profile which is well off-axis, so that there might be significant fast ion losses to the first wall. Preliminary modelling results show that the off-axis fast ^{3}He tail accelerated by the ICRF is well-confined, both at 3 T and 3.3 T [174], although the application of 3-D fields for ELM control may modify this. A further issue is the potential for W accumulation in the core with predominantly off-axis heating. This is not considered to be critical because the ICRF heating scheme also provides a significant central heating due to wave damping on electrons (~30 - 40% of the ICRF power). In addition, the ECRH deposition profiles for these fields are moderately peaked around the axis at 3.0 T in O-mode (170 GHz), although predominantly off-axis for 3.3 T. H-mode experiments combining central and off-axis ICRF heating have been performed in Alcator C-Mod without significant high-Z (molybdenum) accumulation [175], indicating that this may not be a problem in these ITER conditions. However, both the ICRF scheme and the issue of W accumulation in these ITER H-mode conditions need further assessment by modelling and experiment before this can be adopted as one of the main approaches for H-mode operation for PFPO-2.

Heat loads during divertor operation: While there are various options for H-modes at lower B_t and I_p, as noted above the lack of an ICRF coupling scheme at 2.65 T in H probably means recourse to 1.8 T, and thus lower I_p, or more exotic 3-ion absorption schemes at slightly higher B_t (3.0 - 3.3 T) for H-modes in H. High power H-modes in He, which should be possible at 7.5 MA/2.65 T, are attractive for first wall and divertor power load characterization, including the contributions of ELMs, but much less attractive for divertor heat load control, since the dynamics of divertor detachment differ substantially from those in hydrogenic plasmas due to the very different divertor radiation in He (see section 2.5.2). High power L-modes in H might therefore be preferred for the testing of impurity seeding for detachment control in this phase.

In general, PFC heat load experiments in PFPO-2 should follow the methodology of those in PFPO-1 (see section 3.2.4.4), studying L-mode power widths, divertor heat load spreading factors and general detachment behaviour for a larger range of I_p at higher input power and B_t. Such studies will benefit from the addition of the divertor Thomson scattering in PFPO-2. Characterization of inter-ELM and ELM divertor power loads and SOL widths can expand with the further development of H-modes at 1.8 T in H, as well as in He (and possibly in H) at 7.5 MA/2.65 T. One of the key aims here is to establish a firmer scaling for the SOL heat flux width over a wider range of I_p, with H-mode as a priority, but also recognizing the strong link between the L- and inter-ELM H-mode power widths (see section 2.5.2). As in PFPO-1, main chamber power loads should also be studied, but over the wider parameter range which will be available in PFPO-2, using scans in separatrix separation and plasma density to study profile broadening and possible links to detachment.

Methods for control of divertor power loads, first tested in PFPO-1, should be further developed at the higher power flux densities achievable in PFPO-2 L-modes with higher I_p and B_t. Neon seeding will be tested (and, if needed N_2), with the L-mode a more benign regime for such higher

power experiments. Nevertheless, SOL opacity will still be such as to require the use of core fuelling in conjunction with edge gas injection of fuel and impurity. These experiments must be conducted in H plasmas to be of relevance owing to the very different radiation distributions in He. Tests of the divertor plasma response to loss of divertor seeding and asymmetric toroidal divertor injection will be required.

Assuming a robust H target discharge is available at higher power in PFPO-2, more relevant, integrated detachment control of ELMy H-mode impurity-seeded plasmas can be further developed from the initial work in PFPO-1, but, should these plasmas have to be performed at low field and current, only a limited range in density will be accessible. Availability of the ELMCC in this phase should allow optimization of the 3-D spectrum and tests of rotation of the perturbation, so that further measurements of divertor heat load patterns can be performed, even if the density will be limited for low-I_p H-modes.

Deliverables for the H-mode scenario studies in PFPO-2: Consistent with the objectives of the initial H-mode operation in PFPO-1, the deliverables from H-mode operation in PFPO-2 are:

- *Quantifying power required for H-mode access and sustainment and characterization of H-mode plasmas in FPO-like conditions:* For PFPO-2, the operating scenarios and planned experiments are designed to confirm the assessment of the L-H transition power (P_{LH}) for both H and He together with the margin above this threshold for achieving H-mode confinement for at least two different toroidal fields. These experiments (particularly at 7.5 MA/2.65 T) will provide the first H-mode plasmas in FPO-like conditions (e.g., low core source of recycling neutrals) that will allow the development of optimization strategies for H-mode confinement in ITER (e.g., variations of additional heating mixtures). From these results it is also expected that the threshold power needed for H-mode access and sustainment in D and DT plasmas can be predicted with confidence. This will provide the final confirmation in advance of D/DT operation that the baseline H&CD level of 73 MW is appropriate to achieve ITER's $Q = 10$ goals and, if not, it should quantify the upgrade in power required.
- *ELM control:* ELM control studies in PFPO-2 are designed to verify the techniques to tune the applied RMP spectrum to optimize the control of ELMs for two values of the toroidal field and several edge safety factors using the full complement of power supplies for the internal coils. The range of q_{95} values (3.0 - 4.5) will span the values needed for the scenarios in the FPO campaigns over the range from 7.5 MA/2.65 T to high-Q operation including $Q = 10$ (15 MA/5.3 T) and long-pulse $Q = 5$ (11.2 - 12.5 MA/5.3 T). The ELM control validation with RMPs for multiple q_{95} values and during current ramps is very important for the detailed planning of H-mode operation in the first FPO campaign at higher field and current, for which unmitigated ELMs would cause melting of the PFCs. Similarly, the studies on ELM control with various heating mixtures will provide information regarding the influence of heating mix on ELM control and its optimization for minimum confinement deterioration. This can provide information regarding possible upgrades of the ITER H&CD systems to improve this optimization (e.g., provision of a 3rd HNB to increase torque input).

- *Document the effect of the TBMs on H-mode performance and develop schemes for their mitigation:* Plasma pulses produced in the presence of the TBMs in PFPO-2 will match those established in PFPO-1 without the TBMs and will allow documentation of the effects of the TBMs on H-mode performance, albeit at 1.8 T and most likely for the ITER reference plasma shape, which has a high level of ripple at this toroidal field value. Mitigation schemes for these effects (if significant) will be developed using the EFCC and the ELMCC at 1.8 T and applied to plasmas at 2.65 T, which have a much lower value of TF ripple.
- *Initial validation of predictions of SOL power width in ITER:* The variation of the plasma current for both hydrogen and helium H-mode plasmas planned for PFPO-2 will provide data to validate predictions of the width of the SOL power flux, i.e., that it scales inversely with current (linearly with poloidal field), but does not depend on the toroidal field. This data is important for the planning of high-power H-mode operation at high currents in FPO, in particular, to identify the need for schemes for divertor power load control with radiative divertor operation discussed in [3-Appendix C].
- *Assessment of scenario compatibility issues for ELM control with 3-D fields (pellet fuelling, impurity exhaust and radiative divertor):* The experiments in PFPO-2 will demonstrate these three key scenario compatibility issues of ELM control using 3-D fields, although marginally for pellet fuelling if experiments are performed in He plasmas. This assessment is required for the application of 3-D fields for ELM control in high-Q plasmas in FPO. The PFPO-2 experiments will provide guidance on how to use the large spectral flexibility of the ITER ELMCC for this fusion power demonstration.
- *An initial assessment of long-pulse H-mode operation:* The first demonstration of a long pulse (up to ~1000 s, if allowed by progress in the H&CD commissioning) 7.5 MA/2.65 T H-mode scenario with ~60% driven current would help to identify processes that may develop over long timescales in ITER affecting plasma confinement, impurity transport and MHD stability and the schemes required to control them. Guidance on control of such processes would be very valuable for preparation of the long H-mode pulses required for the demonstration of the $Q = 10$ and $Q = 5$ goals in FPO.

Assessment of diagnostic capabilities for performing H-mode research in PFPO-2: By PFPO-2 most of the ITER diagnostics will already be in their final configuration; the only diagnostics that will become available for FPO are those for additional neutron measurements (not essential for H and He plasmas) and for fast particle measurements. The latter are possibly the only systems which might be needed in PFPO-2 as the level of additional heating increases and, in particular, the use of NBI heating at high power levels starts. The triggering of fast particle driven MHD instabilities (see section 3.2.5.6), together with the application of 3-D fields for ELM control, might lead to increased fast particle losses, especially for NB-injected ions. If so, additional capabilities of the lost fast particle diagnostics would be useful for characterization of such losses. Nevertheless, if fast particle losses are non-negligible in PFPO-2 experiments, the associated local power fluxes to the first wall will be measured with the IR cameras. Therefore, an initial quantitative evaluation of the magnitude of the fast particle losses will be possible and the highest risk to plasma operation of such losses (localized first wall melting) can be avoided.

3.2.5.6 Long-pulse operation development in PFPO-2

Scenarios for long-pulse operation: Long-pulse operation is desirable in PFPO-2 (even in PFPO-1, time permitting) for commissioning all plant operations to meet FPO requirements. Of principal concern are the magnetic sensors and the H&CD systems. In addition, long pulses facilitate verification of the current drive efficiencies of the various H&CD systems, as these systems and the required diagnostics become available.

The IRP includes two basic scenarios for long-pulse operation in PFPO-2, both at 7.5 MA/2.65 T. The first is an L-mode scenario in H at 7.5 MA/2.65 T using reduced NBI energy/power and ECRH, with a flat-top length of ~100 s, which could be applied to fuel retention studies. The second is an H-mode scenario (in H or He) at 7.5 MA/2.65 T, with 33 MW of NBI and 20 - 40 MW of ECRH+ICRF, having a maximum potential flat-top length of ~1000 s. Both scenarios can be performed with 30 kA premagnetization and thus without significant consumption of the CS fatigue lifetime. Additional, specific issues related to the development of long-pulse Q ~ 5 scenarios for FPO are also considered in the following, although many of them do not necessarily require long pulses. Due to the availability of diagnostics (e.g., MSE) and H&CD (e.g., HNB and ICRF, in addition to ECRH), it is more appropriate to perform these studies and long-pulse H-mode operation in PFPO-2 than in PFPO-1. A detailed modelling analysis of the potential for the development of long-pulse operation has recently been completed [176].

Although not specifically mentioned in the discussion of the PFPO-1 experimental program, long-pulse scenarios are also possible in PFPO-1 and could be used for ECRH commissioning, diagnostic commissioning, etc. Given the relatively narrow operational space for H-mode operation in PFPO-1 (as discussed in section 3.2.4.5) and the reduced set of diagnostics at this stage (see Table 3), it would be more effective to perform such long discharges in hydrogen L-modes. The achievable flat-top durations for 5 MA plasmas with 20 MW of RF heating are in the range 200 - 700 s, depending on the value of the plasma density ($<n_e> = 0.2 - 1.0 \times n_{GW}$ - see figure 15) for 30 kA premagnetization and thus no significant consumption of CS fatigue lifetime. These L-mode plasmas would be a natural extension of the commissioning activities at 1.8 T discussed in section 3.2.4.3, if the reliability of the ECRH system is sufficient to attempt this long-pulse operation at that stage.

Establishing the operational basis for long-pulse experiments: Experimental operation during the FPO phase will rapidly lead to activation of the tokamak structures, implying that maintenance, repair and upgrade activities will require remote handling and are likely to be time consuming. To minimize in-vessel interventions, it is therefore essential for all operational systems to demonstrate that they are capable of operating as close to their performance and pulse length specifications as is feasible during PFPO-2. Due to limitations imposed by flux consumption, achieving long-pulse operation of up to 400 s, or longer, in PFPO-2 is likely to require operating at modest plasma currents of ~7.5 MA (e.g., figure 15). The program would likely involve both L- and H-mode plasmas, according to the system test involved, but, as discussed below, certain tests will benefit from H-mode operation. Further optimization of plasma scenarios may therefore be required to allow the exploitation of the maximum baseline power capability under relevant conditions, which provide the most demanding tests of the tokamak, auxiliary and plant systems. The PCS must also demonstrate as much of its advanced control

capabilities as possible in H/He plasmas to ensure that any modifications required of the actuators and diagnostic systems can be carried out prior to FPO. Similarly, critical plasma-related interlock and safety functions within CIS and CSS must be fully commissioned during PFPO-2. The pellet and gas fuelling systems must demonstrate adequate fuelling capability up to 15 MA operation, and so some elements of this program can be addressed within the 15 MA/5.3 T development discussed in section 3.2.5.7.

Once all H&CD systems have been commissioned to their rated power levels, operation at currents of at least 7.5 MA has been developed and reliable H-mode operation with acceptable ELM control has been established in PFPO-2, the long-pulse, heat management capabilities of the device will be tested under quasi-stationary long-pulse conditions. The pulse duration of high-power plasmas will be progressively extended to the maximum allowed by the available poloidal flux. Flat-top pulse lengths exceeding 100 s are possible (e.g., figure 15) according to the experimental time available for commissioning of the H&CD, fuelling, diagnostics, control systems, etc. to longer pulse lengths. To reach divertor heat flux levels approaching those expected in the DT phase of operation, maximum available power will be required in plasmas at the maximum current and field at which satisfactory H-mode operation can be sustained (see [3-Appendix C]). Monitoring of the heat handling capabilities of all critical systems (e.g., H&CD systems, in-vessel components, plasma-facing surfaces in the divertor) will be essential. Given that power densities are expected to be beyond those previously investigated in an actively cooled tokamak divertor, it is anticipated that this will be a demanding step, requiring, perhaps, several months, and longer if repairs or modifications are necessary. Operation in H-mode is preferred, since this will produce the most challenging combination of quasi-stationary and transient heat fluxes on the divertor, and feedback control of the edge radiation through impurity injection will be essential. These experiments will provide insight into the range of heat loads that may be expected in the future and verify the capability to measure these heat loads in real time and to take appropriate control actions on a routine basis. In addition, the output from this phase will provide valuable data for the assessment of divertor codes. With longer pulses, the heating of all components and structures inside and attached to the vacuum vessel will require careful monitoring.

The Tokamak Cooling Water System (TCWS) and cryoplant must also demonstrate the capability of maintaining sufficient cooling within prescribed limits at up to 73 MW of auxiliary heating power, both at high (preferably full) plasma current and for pulse lengths potentially up to several hundred seconds at lower current levels. The cooling capability must be demonstrated with sufficient margin to give confidence in the ability of these systems to handle the additional expected heat loads due to fusion power in the subsequent FPO phase. Indeed, a related issue is that the AC heat loads in the Magnet system must be characterized (and be within acceptable limits) to provide a basis for the extrapolation of plasma scenario demands to the $Q = 10$ and $Q = 5$ scenarios foreseen in DT operation. The combined heating and coil power supply systems must keep (pulsed) electrical grid demand within the 500 MW site limit and avoid excessive fluctuations on the grid for the most demanding emergency termination scenarios.

Deliverables from this phase of the PFPO-2 program with significant implications for the implementation of the FPO program include:

- ECRH, ICRF, and NB heating systems must demonstrate full power with pulse lengths limited only by the available experimental time for commissioning;

- Gas and pellet fuelling systems must demonstrate full fuelling capability (ultimately, as discussed in section 3.2.5.7, for 15 MA plasmas);
- Demonstration of satisfactory heat load control on first wall and divertor to full auxiliary heating power capability;
- Radiation and impurity profile control demonstrated up to full auxiliary heating power and available pulse length;
- TCWS and the cryoplant must demonstrate sufficient cooling capability at full auxiliary heating power and available pulse length to extrapolate to full fusion burn conditions;
- All systems must demonstrate that they operate within the 500 MW site power limit without excessive fluctuations on the grid up to the full auxiliary heating power for the most demanding emergency termination scenarios;
- CIS and CSS plasma-related interlock and safety functions must be fully commissioned.

Assessment of H&CD and diagnostic capabilities for performing current drive studies during PFPO-2: The primary goal of this research in PFPO-2 is to initiate demonstration of the essential components for the developments required to achieve the two long-pulse high-Q ITER goals. These are a stable long-pulse (target 1000 s, high non-inductive fraction $f_{NI} \sim 0.6$, $Q \sim 5$) and fully non-inductive steady-state pulse (target 3000 s, $f_{NI} = 1.0$, highest achievable Q, aiming at $Q \sim 5$) [177]. During these preliminary exploration stages in H/He, the research will concentrate on the assessment of non-inductive current drive efficiencies by various auxiliary systems (ECRH, ICRF and NBI) and plasma (bootstrap) means, and on the deployment of advanced real-time control techniques for maintaining plasma stability (β) as well as the desired current and kinetic profiles.

The experiments will be focussed on the range of $q_{95} = 3.6$ - 6. Scenario development at $q_{95} \sim 3.6$ will target long-pulse operation in hybrid discharges [178 - 181], while plasmas at $q_{95} \sim 4.5$ will provide the basis for development of (fully non-inductive) steady-state operation [182 - 184]. The capabilities of the baseline H&CD systems and of the diagnostics (in particular, those related to the determination of the current profile shape, such as polarimetry and MSE) already available at this phase of PFPO-2 will be fully exploited for this research. The overarching objective of the PFPO-2 experiments is to assess the current drive capabilities of the baseline H&CD systems in low-β L- and H-modes (He or H, although H is preferable) in this range of q_9. To allow these studies to be performed in H-mode plasmas, a toroidal field of 2.65 T has been selected (based on the rationale developed in section 3.2.5.5) with plasma currents in the range 5 - 6.3 MA. From the evaluation of the operational space in hydrogen H-modes with the baseline heating schemes at 2.65 T outlined in section 3.2.5.5, it is expected that most of the experiments in stationary H-modes will be performed in He. However, if the approaches discussed above are successful in expanding the H-mode operational space in H, it might be possible to perform those to be carried out at 6.3 MA/2.65 T with $q_{95} = 3.6$ in H plasmas.

To accomplish the goals of this phase the baseline H&CD systems must be fully operational. In addition, MSE, polarimetry and magnetic equilibrium calculations incorporating kinetic profiles are required to allow determination of the current profiles generated (including current drive experiments with individual H&CD systems). Moreover, it is essential that the diagnostic capability has achieved sufficient maturity and reliability to support successful implementation of the program. An additional requirement for this phase of operation is the availability of real-time control algorithms for plasma formation which maintain stability and robust H&CD actuator

control, supporting production of the desired target current profiles. The experiments will aim to establish stationary plasma conditions to produce relaxed $j(r)$ profiles. Therefore, density and ELM control systems must also be fully operational and demonstrated for H-mode plasmas, a capability which is foreseen in the PFPO-2 plan (as a result of the program discussed in section 3.2.5.5). Finally, application of ECRH/ECCD for NTM control might also be required.

As discussed in [185, 186], the flexibility of the baseline H&CD systems is not expected to be sufficient for high-Q operation in steady-state DT plasmas. Therefore, it is anticipated that a major activity during this initial scenario development will encompass evaluation of the capability of these systems to produce steady-state operation, to establish a firm physics basis for decisions on potential upgrades of these systems. It is anticipated that, even if fully non-inductive operation cannot be achieved with the baseline H&CD systems in this phase, it will be possible to sustain the required q-profile for sufficient duration ($t < t_{RESISTIVE}$) to allow assessments of the associated plasma performance, fuelling requirements, control needs, divertor compatibility and MHD plasma stability during PFPO-2. The results of these studies will provide first experimental evidence for the selection of upgrades to the baseline H&CD systems to ensure that the $Q \sim 5$ long-pulse and steady-state goals of ITER can be achieved in FPO. From the evaluations discussed in [185, 186], the foreseen upgrades are likely to include a 3rd HNB (to provide more current drive and input torque) and/or an additional 10 - 20 MW of ECRH/ECCD (to provide more heating and $j(r)$ control capability).

These experiments are designed to initiate the research program towards the production of a high non-inductive current fraction and, ultimately, fully non-inductive discharges with significant fusion power production. Efficient development of non-inductive steady-state plasmas will require a detailed assessment of the capabilities of the H&CD systems and the associated operating space during the H and D phases (the latter during FPO). Key issues to be addressed in this period are:

- Scans of the ECRH/ECCD power deposition at constant density in the current flattop of stationary;
  H-modes to evaluate heating and current drive;
- Scan of NBI beam sources (on-axis vs. off-axis) in the current flat-top of stationary H-modes and the assessment of NBI fast ion confinement;
- Attaining target $j(r)$ at the end of the current ramp-up phase (L-mode) using real-time control and its sustainment for at least 10 s (limited by shine-through loads).

Studies of energetic particle populations: Analysis of the evolution of energetic particle populations and their influence on MHD stability is likely to run as a parallel program to the H-mode studies program presented in section 3.2.5.5, the long pulse and current drive studies program, and the high current development program to be outlined in section 3.2.5.7. This will require commissioning of the relevant diagnostics which have already been installed prior to PFPO-2 (see Table 7). Additional points might need to be included in the foreseen experimental scans to characterize or control specific fast particle physics processes. A key physics issue which it would desirable to asses in this phase, if the available diagnostics allow, is whether confinement of fast beam-injected ions can be described by classical processes, or whether it is anomalous due to the presence of AEs or other MHD processes.

Detailed experimental plan for the initial studies of current drive efficiency, target q-profile formation and fast particle physics: The PFPO-2 program focuses on assessing current drive in low-β L-mode and H-mode plasmas (H or He) at q_{95} = 3.6 (6.3 MA/2.65 T) and q_{95} = 4.5 (5 MA/2.65 T). Specific objectives and the associated experimental activities planned include:

- Commissioning of the various H&CD systems for their respective current drive missions and identification of any restrictions on their application, if this has not been completed previously (e.g., shine-through for NBI, incomplete absorption of ECRH, etc.);
- Commissioning of start-up scenarios consistent with these limitations for 6.3 MA/2.65 T and 5 MA/2.65 T and commissioning of systems required for q-profile control during the ramp-up phase: Were MSE measurements to be incorporated in the q-profile control scheme in the ramp-up phase, the HNB energy would need to be substantially reduced to allow injection into the ramp-up; an alternative solution would involve short beam blips;
- Producing the target current profiles required for hybrid and non-inductive scenarios at the end of the ramp-up phase: This would include development for partially non-inductive hybrid discharges (q_{95} = 3.6) as well as for ultimately fully non-inductive, steady state scenarios (q_{95} = 4.5) in H-mode. The stability and confinement properties of the plasmas obtained should be assessed for a range of current and pressure, and (if NBI can be applied) rotation profiles;
- Assessing the ability to sustain the target current profile obtained at the end of the ramp-up during the current flat-top beyond the confinement time scale, e.g., up to at least 10 s (limited by shine-through): This will require tuning of the H&CD capabilities, as well as of the plasma density, to maintain the current profile control, particularly if access to H-mode were to be attempted at the start of the flat-top;
- Determining the EC current drive efficiency via scans of the EC deposition location by measuring the resulting $j(r)$ for q_{95} = 3.6 and 4.5 stationary L-mode and H-mode plasmas at a range of densities and temperatures (controlled by the application of NBI and ICRF);
- Determining the NB current drive efficiency via a scan of the NB deposition location by measuring the resulting $j(r)$ for q_{95} = 3.6 and 4.5 stationary H-mode plasmas over a range of densities and temperatures: The specific scans considered in this period rely on the use of one HNB on-axis and one off-axis. The scans will include an assessment of the heating and current drive of both beams separately and simultaneously in H-mode plasmas. This will include scans with similar total input power (i.e., using ICRF or ECRH to replace the reduced HNB power when one HNB is not used) and others in which the total power is scanned;
- Validating current drive models: For inductive operation, this will include an assessment of Spitzer versus neoclassical conductivity models. For non-inductive operation, neoclassical bootstrap models will be assessed, as well as whether neutral beam ion confinement is classical or anomalous due to the presence of AEs or other modes. The assessment of ICRF current drive will only be performed for He plasmas, for which an effective heating scheme at 2.65 T is available;
- Determining the experimental behaviour of fast ions and validating models for fast ion behaviour from studies of the fast ion populations arising from all heating systems: In

particular, determining the nature of any MHD instabilities observed (e.g., global TAE modes in the outer region of the plasma) [187];

- If AEs become unstable, investigating the influence of the various heating and current drive systems, in particular of their capabilities to affect AEs by local modification of plasma parameters (since heating influences the Landau damping experienced by these modes and also changes the spectrum of compressional and Alfvénic modes) [188]. If suitable actuators are established for AE control then development and refinement of AE control techniques and associated controllers could start at this stage;
- Determining and validating the effects of ELMCC on fast ion losses for plasmas with *q*-profiles, as required for hybrid and steady-state plasmas. This would be complementary to the experiments in PFPO-2 for the inductive scenario in section 3.2.5.5.

It is important to note that many of these activities may involve the same experimental conditions and do not require separate experiments. For instance, the experiments to determine the efficiency of ECRH/ECCD in H-modes with NBI (+ ICRF) heating are also likely to provide information regarding the possible use of ECRH/ECCD to affect AE stability if AEs are driven unstable by the NBI. In addition, other experiments carried out in PFPO-2 inductive H-mode scenarios may already have addressed some of the issues outlined above, or will provide guidance for experiments in this phase, thereby shortening the required experimental time. For example, the measurements of NB current drive efficiency may be already available from similar experiments where the heating mix will be varied to identify effects on H-mode performance and ELM control. Similarly, the effects of ELMCC on fast ion losses will have been characterized as part of the ELM control experiments within a range of q_{95} = 3 - 6, etc.

The main deliverables from this phase:

- Initial demonstration of fully integrated scenarios with q_{95} = 3.6 and 4.5 and $j(r)$ profiles required for advanced H-mode scenarios sustained for at least 10 s, including the formation of suitable $j(r)$ profiles in the ramp-up phase;
- Definition of control algorithms to achieve the target $j(r)$ profiles for q_{95} = 3.6 and 4.5 and to sustain these in L-mode, as well as initial attempt at H-mode plasmas;
- Assessment of NBCD in H-mode plasma conditions for q_{95} = 3.6 and 4.5 and $j(r)$ profiles required for advanced H-mode scenarios, which can substantiate the need for a third HNB to achieve the $Q \sim 5$ long-pulse goal;
- Assessment of ECCD in L-mode and H-mode for q_{95} = 3.6 and 4.5 and $j(r)$ profiles required for advanced H-mode scenarios, which can substantiate the need for additional ECRH/ECCD power to achieve the $Q \sim 5$ long-pulse goal;
- Assessment of $j(r)$ formation by application of ECRH/ECCD in the ramp-up for q_{95} = 3.6 and 4.5 scenarios foreseen for advanced H-modes, and of its flattop sustainment with ECRH/ECCD and other heating schemes;
- Assessment of the level of ECRH/ECCD required for NTM control for q_{95} = 3.6 and 4.5 with $j(r)$ profiles required for advanced H-mode scenarios, which might also identify a need for additional ECRH/ECCD to achieve the $Q \sim 5$ long-pulse goal;
- Assessment of the level of ECRH and ICRF needed for W control for q_{95} = 3.6 and 4.5 with $j(r)$ profiles required for advanced H-mode scenarios. This is expected to differ from the

reference inductive scenarios as core MHD is likely to change (e.g., less frequent or absent sawteeth), and could provide additional support to confirmation of a need for additional ECRH/ECCD to achieve the $Q \sim 5$ long-pulse goal;

- Assessment of the fast particle behaviour and its impact on MHD stability for $q_{95} = 3.6$ and 4.5 with $j(r)$ profiles required for advanced H-mode scenarios and identification of possible actuators to control this behaviour;
- Validation of models required to design hybrid and steady-state scenarios to be further developed in FPO.

3.2.5.7 Plasma operation at full technical performance (15 MA/5.3 T)

Once plasma operation, plasma control and, especially, the disruption management/mitigation capabilities are sufficiently reliable, the research program will address the extension of the operational space to full current ($I_p = 15$ MA), providing the first experience of high current plasmas in ITER in preparation for Fusion Power Operation (FPO). The principal aims of this phase are to develop the experimental basis for high current plasma scenarios and to provide the technical demonstration that ITER can operate at its baseline design parameters in terms of plasma current and toroidal field. It will assess the reliability of magnetic control, in particular vertical stability control, the robustness of the plasma current ramp-up and ramp-down, the efficiency of plasma fuelling with gas and pellets, as well as developing schemes for divertor heat flux management and control of W production and transport.

Continued commissioning of the heating systems and heating schemes will form an integral part of this activity. Further optimization of the DMS operation will, of course, be essential. This requires a well-developed disruption mitigation function (mitigation scheme, mitigation trigger) and effective disruption avoidance schemes, as well as a targeted operational campaign to demonstrate high current operation. Unmitigated disruptions at plasma currents above $I_p = 7.5$ MA should be avoided as far as possible to ensure more rapid progress towards FPO (i.e., by minimizing the risk of damage to in-vessel components); the measurements acquired in these events will be used to confirm the values extrapolated from lower currents using appropriate disruption models.

The operational campaign in this phase consists of several I_p/B_t steps along a path with approximately constant q_{95}. The extension to high current in PFPO-2 will be developed via L-mode operation in H, in view of the expected limitations in H-mode operation at currents and fields above 7.5 MA/2.65 T, for both H and He plasmas (see [3-Appendix B] and section 3.2.5.5). The target flat-top duration at full current and field for hydrogen L-mode operation is ~50 s. Operation at 15 MA/5.3 T requires the full capabilities of the central solenoid and optimization of the current ramp-up/down together with the use of additional heating. Scenario simulations of 15 MA/5.3 T plasmas shown in figure 15 indicate that, for ohmic plasmas, a flat-top of 10 s can be achieved, while 20 MW of RF heating (ECRH or ICRF) will allow the extension of the flat-top to 50 s. For lower values of the plasma current, similar or longer flat-top lengths can be achieved in heated L-mode plasmas but in this case at lower CS premagnetization currents ($\leq$30 kA) and, thus, with negligible consumption of fatigue lifetime.

Requirements: Prior to expansion of the operational space towards 15 MA/5.3 T in hydrogen L-mode plasmas, the following scenarios/technical demonstrations will have been performed:

- Demonstration of operation in hydrogen L-mode plasmas at both 7.5 MA/2.65 T and 7.5 MA/5.3 T using additional heating power levels of ~20 MW, in particular, with on- and off-axis ECRH heating. The off-axis case is essential to assess risks associated with off-axis heating of planned L-mode scenarios at intermediate fields between 2.65 and 5.3 T. Plasmas with off-axis heating can be prone to W accumulation (although this phenomenon is more likely in H-modes) and this can significantly increase the risk of disruptions;
- Operation at currents above 7.5 MA will significantly increase the potential for large electromagnetic forces at disruptions. Unmitigated disruptions should therefore be avoided in this research phase. As a consequence, this operational phase can start only when ITER operation has demonstrated a satisfactory capability for disruption avoidance and when the disruption mitigation function (mitigation scheme, mitigation trigger) has achieved a sufficiently high reliability;
- The H&CD systems will have been commissioned to adequate levels of power and duration to allow high I_p/B_t operation with flat-top durations of at least 50 s, which might also require heating of the plasma during the current ramp-up phase. Additional heating is essential to achieve the specified flat-top duration at 15 MA/5.3 T, since analysis of ohmic plasmas indicates that the flat-top will be limited to ~10 s (following a 65 s ramp-up), as illustrated in figure 15. At lower plasma currents, the use of plasma heating allows such flat-top lengths to be achieved at reduced values of CS premagnetization current for plasma breakdown, implying a substantial reduction in the consumption of CS fatigue lifetime in these experiments.
- Execution of this experimental program requires the availability of the full baseline fuelling capability (with H and impurity gas fuelling and 4 hydrogen pellet injectors), full axisymmetric PF control capabilities, the vertical stability systems VS1 and VS3, etc.
- By the beginning of PFPO-2, the ITER diagnostic set will be close to its final configuration (except for certain neutron and fast particle diagnostics) and therefore it is considered fully adequate for the planned L-mode experiments.

Experimental Plan: As outlined above, the plasma current will be increased in gradual steps from I_p = 7.5 to 15 MA. The gradual increase of I_p/B_t allows the establishment of robust scenarios at one current before proceeding to the next step in a process which aims to minimize potential problems at higher currents. At each step it will be necessary to verify that: (i) there are no operational limitations affecting the scenario feasibility, e.g., enough auxiliary power is available; (ii) the step is useful, i.e., it provides an appropriate stepping stone for operation at higher currents; and (iii) it provides relevant, new information and does not duplicate other experiments already performed within the IRP. Further details on the non-active operations scenarios can be found in [89].

The experimental plan is optimized to achieve the deliverables required for FPO, and particular care will need to be taken in this phase, as unmitigated disruptions at high currents can degrade in-vessel components. The choice of the intermediate B_t steps requires the optimization of two constraints related to the location of the ECRH resonance: firstly, if ohmic breakdown is not robust, ensuring that EC-assisted breakdown remains effective and, secondly, constraining the ECRH deposition profile to be ‘close enough’ to the plasma centre to prevent W accumulation. Failure to satisfy the latter requirement can lead to increase disruptivity and must therefore be

avoided when increasing I_p beyond 7.5 MA. An initial assessment of this issue for 7.5 MA/2.65 T plasmas with on-axis and off-axis heating is thus included in PFPO-1 (see section 3.2.4.4).

The detailed steps in the proposed increase of I_p/B_t to 15 MA/5.3 T depend, therefore, on the results of this ECRH on- and off-axis assessment and of the commissioning of the VS system for high current operation. It is planned to increase I_p/B_t at approximately constant q_{95} = 3 - 4: maintaining an approximately constant q_{95} from one I_p/B_t step to the next implies that MHD stability characteristics of the plasma are kept approximately constant as the value of I_p is increased. This is advantageous in minimizing the occurrence of disruptions, for which forces increase gradually as $\sim I_p \times B_t$. This strategy also reduces the need to redevelop the ramp-up/-down and heating termination scenarios for each step of the I_p/B_t, program, and these are usually the more critical phases of the discharge as far as disruptions are concerned (although the termination of heating may be less critical for these L-mode discharges than for later H-mode plasmas). The operational steps proposed within this program are shown in figure 8. Point 1 (7.5 MA/2.65 T) in the development path lies underneath point 2 - the difference between the two scenarios is the setting of the poloidal launch angles, such that for point 1 the ECRH deposition is as central as possible, and for point 2 it is tuned off-axis to match the innermost radial range accessible with ECRH at point 3 (9.5MA/ 3.3 T, the 2nd harmonic resonance moves to the low field side as the field is increased). Points 4 - 6 (9.5 - 10.5 - 12.5 MA/4.5 T) correspond to a similar radial range of off-axis heating using the fundamental resonance on the HFS. For points 7 (12.5 MA/5.3 T) and 8 (15 MA/5.3 T), the ECRH is deposited centrally again. Note that the centre of the ECRH heat deposition profile also depends on the temperature profile. The optimum values of the intermediate fields thus depend on the precise values of the plasma parameters obtained.

For each I_p/B_t combination, optimization of the current ramp-up/-down to minimize flux consumption while maintaining compatibility with an acceptable level of W concentration will be performed. This will include the use of the applicable heating systems (mostly of ECRH and ICRF) to heat the plasma in these phases. NBI could possibly be used, but at lower injection energy, and therefore reduced heating power, due to the low densities expected during the lower current phases of the ramp-up/-down. Gas fuelling and pellet fuelling scans will also be performed. Pellet fuelling is likely to be applied routinely for the unrestricted application of NBI in these hydrogen L-mode plasmas for which $\langle n_e \rangle \geq 4.5 \times 10^{19}$ m^{-3} is required [166]. The fuelling scans (including gas versus pellet comparisons and gas+pellet optimization) will also be performed for the flat-top phase in tandem with heating power scans (including variations of the heating mix). It is expected that, for high power levels (potentially up to 73 MW of power can be coupled to the plasma for the steps with $B_t \geq 4.5$ T) and/or low values of $\langle n_e \rangle$, the power load to the divertor will be significant and W sputtering may also need to be reduced/controlled. This will require the development of divertor load mitigation and W sputtering reduction schemes by establishing radiative divertor conditions with extrinsic impurity seeding in advance of the exploration of these plasma conditions.

Experiments in the PFPO-2 phase will, for first time, access heat loads approaching those possible during FPO when additional heating is supplemented by fusion power. In the course of this development program, L-modes in H with close to maximum P_{IN} (73 MW) and plasma currents approaching 15 MA could deliver values of P_{SOL} capable of driving separatrix parallel heat fluxes to values of up to ~50% of those to be expected in baseline burning plasmas, depending on the assumed values of SOL heat flux width (see [132]) and plasma density. At these

levels of $q_{||}$, divertor heat flux control becomes mandatory, depending on the divertor neutral pressure achieved, though the lack of ELM activity implies that the scenarios will not be equivalent to a high power H-mode in relation to the testing of power load control in a fully integrated sense in preparation for later operation in D and DT plasma.

The final goal of the experiments will be the demonstration, via the application of the additional heating and fuelling systems, of fully integrated L-mode scenarios, in terms of satisfactory W and divertor power load control (including ramp-up/-down), which minimize flux consumption and that are MHD stable (including VS) up to 15 MA/5.3 T. These scenarios will provide the basis for the subsequent development of the corresponding D and DT L-mode scenarios, from which the key H-mode scenarios will be developed.

In addition to the scenario development discussed above, these experiments will provide the first experimental assessment of core particle and energy transport and global plasma confinement at high I_p/B_t in ITER. The dependence on plasma density and fuelling schemes will certainly be assessed, as well as the influence of additional heating power level and mixture, within the overall experimental plan discussed above. For specific conditions, or for the assessment of specific physics effects, dedicated experiments will be performed beyond those strictly required for scenario development. Experiments of this type could include, for example, evaluation of the effect of injected torque on L-mode transport and confinement for NBI heating versus RF heating (i.e., ECRH, or ICRF, or ECRH+ICRF heating) and the evaluation of the influence on plasma confinement and transport of auxiliary power deposition profiles, etc.

It might turn out that not all the individual steps shown in figure 8 are feasible, for example, if ECRH is not effective in providing both plasma breakdown assist and control of W accumulation at all I_p/B_t combinations foreseen. As noted above, experiments to address this uncertainty are scheduled within the PFPO-1 program (and could, if necessary, be completed in an earlier phase of PFPO-2). For the moment, two options are retained for the path towards achieving the key milestone of demonstrating a 15 MA/5.3 T hydrogen L-mode plasma with a flat-top of ~50 s. These are summarized in Table 8, for the path assuming that off-axis ECRH heating can satisfy the required scenario needs, and in Table 9, for the last steps of the path (after 7.5 MA/2.65 T) which relies on maintaining on-axis ECRH heating, as far as possible, in most of the steps. For the latter it is assumed that control of W accumulation will be less efficient with off-axis ECRH heating and thus the number of pulses using off-axis ECRH is decreased to reduce the number of possible disruptions.

For both options, scenario #5 (in figure 8) is deemed to be unnecessary for the hydrogen L-mode phase. However, this will be developed in deuterium L-mode plasmas in preparation for deuterium H-mode experiments in the FPO phase, which will follow a more careful approach when increasing I_p/B_t (as discussed in section 3.3.2.1 and section 3.3.2.5): in this case as not only do disruption-induced electromagnetic forces increase, but the plasma thermal energy is also higher, which can lead to localized melting of first wall and divertor target plasma-facing components during transients.

The main deliverables of this operational phase are:

- Demonstration of first L-mode operation at full current and field (15 MA/5.3 T) with ~50 s flat-top in fully integrated plasma scenarios including plasma position and vertical stability control, power load control, W accumulation control, etc.;

- Demonstration of the intermediate I_p/B_t steps to be followed to achieve 15 MA/5.3 T L-mode plasmas along a path with q_{95} = 3 - 4, which will provide the basis for the further development of L-mode scenarios in D and DT (and for the corresponding H-mode scenarios) during FPO;
- Assessment of the effects of fuelling (via gas and pellet injection) and additional heating power level and mix on plasma transport and confinement in ITER L-mode scenarios with current and field up to 15 MA/5.3 T, including the ramp-up/-down phases;
- Optimization of flux consumption in L-mode ramp-up/-down phases by using the ITER systems' flexibility, in particular, in relation to the current ramp-rate as well as in the fuelling and heating capabilities.

3.2.5.8 Edge physics and PWI studies

Wall conditioning: The efficiency of H or He GDC and ICWC for removal of medium-*Z* impurities will be assessed in PFPO-2. It is expected that PFCs will have evolved with operational time and that significant co-deposition of impurities with Be eroded from the first wall will have occurred. Continuous follow-up of wall conditions and routine monitoring of impurity sources in reference pulses (see [3-Appendix D]) will therefore be pursued. Since ICRF will be available in PFPO-2, ECWC is not expected to be used on a routine basis (cf. section 3.2.4.7), though scenarios will have been made available in PFPO-1 and can be repeated for comparison with ICWC in PFPO-2.

During PFPO-2, the efficiency of ICWC as a method for the control of the in-vessel T-inventory during the FPO phase can be studied in detail. However, isotopic exchange between H and D with ICWC can only be quantified if D-trace experiments can be performed or if D-ICWC discharges are allowed. If so, this implies the development of half and full field ICWC scenarios at f/B_t = 7.0 - 10.5 MHz/T, in H as well as in in D, knowing that D-ICWC will be applied for control of the T-inventory in the FPO phase. As in PFPO-1, machine operation time will be required to optimize isotopic exchange efficiency vs. pressure, power, poloidal field patterns and duty cycle. The benefit of using the ICRF antennas at a higher frequency (55 MHz), as demonstrated in ASDEX-Upgrade [149] and JET-ILW [150], might also be assessed. In addition to torus pressure measurements and RGAs for the gas balance, partial regeneration (to ~100 K) of the cryopumps will allow the quantity of removed and retained isotopes to be measured using gas chromatography.

Fuel retention and material migration - (i) Dust generation and characterization: In addition to the limit on in-vessel tritium retention, there is also an inventory limit on the amount of dust inside the vacuum vessel: the maximum permitted amount of mobilizable dust in the vessel is 1000 kg. To prevent the risk of hydrogen explosion following the accidental ingress of air and water into the vessel, the amount of dust on hot surfaces must be kept below 18 kg (9kg Be, 9kg W). It is necessary, therefore, to be able to diagnose the vacuum vessel dust inventory and to ensure that safety limits are not exceeded.

Several mechanisms can contribute to dust formation, but the most significant are expected to be droplet ejection during transient events (especially from melting of the Be wall) and flaking of layers forming as a result of first wall erosion, material migration and subsequent deposition. Uncertainties remain as to how much dust can be generated during a disruption because it is

currently unclear how much of the melted material can be ejected in the form of droplets and what proportion of these droplets that can convert into dust. Recent simulations have shown, however, that this fraction (at least for disruption induced melting of the Be wall) is likely to be at a level lower than ~ 10% [189]. When applied to the case of disruption induced melting of the Be wall in JET ILW experiments, the same modelling approach has yielded very good agreement with experimental data [190]. Numerical analyses with the MIGRAINe dust transport code have also demonstrated, in fact, shown that droplets could be ablated into the disrupting plasma which would potentially reduce the dust formation rate [191]. Despite these recent modelling advances, it will be important to quantify the dust production rates in ITER, and to determine the characteristics of the generated dust (size distribution, composition) prior to the start of nuclear operations.

An endoscope-based dust monitor system is being designed to view and collect particles below the divertor (both on the cassette body and on the vacuum vessel floor). It is planned to bring the system into operation during PFPO-2, allowing regular inspections during the campaign. In parallel, regular monitoring of the wall erosion/damage will be possible using the In-Vessel Viewing System (IVVS), which has the capability to perform direct viewing and measurements of height changes (with ~85% coverage of the FW) on surfaces. Such inspections can be used to identify the locations of damage formation and inform the adaptation of plasma scenarios to prevent further damage. The IVVS will also allow the monitoring of excessive erosion, either due to direct sputtering/evaporation or due to material redistribution from melt layer motion. A full vessel inspection requires about 8 hours and can, in principle, be performed during short-term maintenance periods.

Deployment of the dust monitor and IVVS should probably occur after a disruption or sequence of disruptions in which camera observations show particles being released. No dedicated experimental time is required, but the required deployment time must be factored into the program planning. After PFPO-2, a complete dust collection through vacuum cleaning of the divertor may be performed to quantify the dust creation during the entire campaign. Dust collection on the vacuum vessel floor is not possible unless divertor cassettes are removed, so that if a cassette were removed for operational reasons (e.g. localized damage impacting operation), this would provide an opportunity to inspect the vessel floor in this location and possibly aspirate debris before active operations began.

Fuel retention and material migration - (ii) Post-campaign analysis of plasma-facing components: The divertor plasma-facing material in ITER will be exposed to unprecedented ion fluences and possibly to a very large number of heavy transient heat loads. Damage (melting, cracking) could occur early in operations, and it is important to document its occurrence and evolution. High resolution inspection of the high heat flux regions of the divertor targets will provide information on the surface morphology and on the occurrence of melting and melt motion. The planned Erosion Monitor (based on speckle interferometry) can be deployed at the end of each operation day and provides (at a single toroidal location) high resolution measurements of the surface morphology to characterize surface roughening (caused by melting or thermal shocking) but with a rather limited coverage.

A further concern with the tungsten divertor is the extent to which early operations, including experiments in He, will modify the W thermo-mechanical properties and how this might impede later higher power operation [73]. At present, no such characterization is foreseen in the IRP

unless this would be required for operational reasons. Removal and full inspection of a divertor cassette after PFPO-2 would be required to perform such characterization, and, as mentioned previously, would also contribute to the characterization of Be migration. Following such removal of a cassette, samples can be extracted (destructively) from the plasma-facing armour and sent for dedicated analysis. The results of this characterization would indicate whether the W material/components are still compatible with the expected loads during high power operations. Finally, as in PFPO-1, the First Wall Samples will be removed for analysis after PFPO-2 to determine erosion by charge exchange neutrals and retention by implantation.

Fuel retention and material migration - (iii) Ammonia formation during nitrogen-seeded H-modes: The higher auxiliary power available during PFPO-2 will necessitate the use of impurity seeding for exhaust power dissipation and will qualify the use of Ne for power exhaust in ITER H-modes with a view to its application in FPO. Should the power exhaust/plasma performance balance not meet the expectations with Ne, other options (including N_2 and Ar) will be explored. If nitrogen is retained as an option for impurity seeding, this would motivate the investigation of the ammonia formation rate. Since such discharges would be required for testing of divertor power load control, ammonia formation rates could probably be studied without the need for dedicated discharges. Assuming that plasmas executed during this phase will have higher divertor heat loads and higher wall fluxes, it should be possible to assess/confirm the role of these parameters on the ammonia formation rate. This will require analysis of the exhaust gas composition using RGAs. Calibration of these RGAs might require the injection of known amounts of ammonia into the empty vacuum vessel. In addition, complete regeneration of the cryopumps will be necessary to recover the ammonia trapped on the active charcoal, the amount of which can be determined by chromatography of the exhaust gas.

3.2.5.9 Experimental Risks in PFPO-2

The main physics/operational risks to the PFPO-2 program and their mitigation can be identified according to the main four areas addressed in this campaign.

Commissioning of systems with plasma and expansion of the operational space in L-mode to at least 7.5 MA/5.3 T: PFPO-2 shares similar risks to those in PFPO-1 related to commissioning of systems with plasma and to the expansion of operational space in L-mode to 15 MA/5. 3T. For PFPO-2 the risks to investment protection are greater due to the higher power, more diversified additional heating systems and higher plasma current, implying a significant increase in plasma energy. The strategy to minimize these risks in the execution of the IRP is similar to that in PFPO-1 with its details adapted to the different heating systems used for plasma operation and the plasma scenarios explored, as described in detail in previous PFPO-2 sections.

A specific PFPO-2 risk regarding the expansion of the operational space in terms of toroidal field concerns the development of breakdown scenarios at intermediate fields between 2.65 and 5.3 T, if EC-assist is found to be essential for reliable plasma start-up in ITER, since the location of ECRH deposition moves off-axis for such intermediate fields. To mitigate this risk additional experimental time might be required for the development of reliable plasma breakdown in these cases. If this is unsuccessful, the next mitigation measure would be to adjust the current and toroidal field levels for the intermediate I_p/B_t steps foreseen for the expansion of the operational range. In the worst possible case, the risk would be retired by performing all intermediate I_p steps at B_t = 5.3 T and thus with q_{95} varying from 6 to 3, the strategy already considered to retire the

PFPO-2 W accumulation risk should it materialize during off-axis ECRH experiments in PFPO-1.

Disruption mitigation: A key element of the risk mitigation strategy for disruption mitigation in PFPO-2 is the implementation of the PFPO-1 risk mitigation strategy described in section 3.2.4.8, which is designed to essentially eliminate the possibility that the risk of an inadequate disruption mitigation capability for the PFPO-2 experimental program materializes. As described in the IRP, the main objective of the PFPO-2 disruption mitigation program is to tune the parameters of the DMS system so that it provides efficient and effective disruption mitigation for the full operational space up to 15 MA/5.3 T in L-mode and up to, at least, 7.5 MA/2.65 T in H-mode. If this is not successful, further risk mitigation beyond PFPO-2 will depend on to what degree, risk mitigation measures have been implemented to upgrade the DMS as a result of the PFPO-1 experience. If such measures have not been implemented after PFPO-1, there would be an opportunity to implement them after PFPO-2, although this would probably imply a longer shutdown period than foreseen in the IRP. Specific open R&D issues related to disruption mitigation are described section 5.2.2.

H-mode operation up to, at least, 7.5 MA/2.65 T: The principal risks related to H-mode operation in PFPO-2 are:

- *Large power requirements for H-mode access/ sustainment:* The basic considerations related to this issue have been outlined in already in section 3.2.4.5 and are further discussed in [3-Appendix B], and an initial assessment of the power required for H-mode access will have been performed in PFPO-1 at 1.8 T (for H and He) and at 2.65 T for He. Nevertheless, due to the large ripple at the separatrix for 1.8 T, the low margin for 2.65 T H-mode access in He plasmas in PFPO-1 and the presence of the TBMs in PFPO-2, it is possible that deviations from the expected H-mode threshold power are identified at this stage that would require a modification of the PFPO-2 research plan. It should also be noted that the application of 3-D fields (particularly, with the alignment required for strong ELM mitigation or suppression) can significantly affect the H-mode threshold, as originally observed in DIII-D, MAST [192] and later in ASDEX-Upgrade [14]. It is also frequently observed that, to achieve high energy confinement, the edge power flow has to exceed the H-mode threshold by a given margin [9]. For ITER operation it is typically assumed that $P_{sep} > 1.2 - 1.5 \times P_{LH}$ is required to achieve an energy confinement time corresponding to the IPB98(y,2) scaling, although the confinement that will be achieved in H and He plasmas is expected to be lower than in D/DT plasmas. During PFPO-2 the available level of heating will make it possible to assess both the power requirements to access H-mode and the changes to H-mode energy confinement at a relevant margin of the edge power flow over the L-H transition at 1.8 T for H and He plasmas and at 2.65 T, though possibly only for He plasmas;

  If the assessment in PFPO-2 reveals that either the H-mode power threshold is higher than expected, or that a significant margin over the H-mode transition power is required to achieve high confinement H-modes in ITER, the extent to which the characterization of H-modes and the demonstration of edge-core integration can be performed in PFPO-2 will be constrained, thus postponing these studies until FPO and increasing experimental risks to

the successful implementation of later phases of the IRP. Moreover, an upgrade of the additional heating systems should be launched at this stage to minimize the risk that ITER will not achieve the level of plasma performance required to sustain high-*Q* operation in DT plasmas;

- *Conflicting requirements for stationary and ELM power load control and W contamination control:* Although an initial assessment of this issue may already be derived experiments during PFPO-1, it is only during PFPO-2 that the edge plasma parameters during H-modes will have sufficiently high values to provide access to the key features of H-mode operation in FPO. These features include the low core plasma neutral source, due to efficient ionization of neutrals in the divertor, SOL power e-folding lengths in the mm scale and edge power flows of up to 50 - 60 MW. The control of stationary power fluxes at these power levels in ITER is expected to require operation with high separatrix densities and, possibly, radiative power dissipation at the divertor, as discussed in [3-Appendix C]. This is expected, in turn, to prevent impurity penetration through the pedestal by providing impurity exhaust between ELMs [67], but may also reduce the efficiency of impurity exhaust during ELMs. The latter, together with the transient W influxes from the divertor following the ELMs and the need to avoid melting of the divertor target by ELMs, may restrict the range over which the integration of all requirements can be achieved at this stage [171]. Depending on the results obtained, this might imply that only suppressed ELM regimes (i.e., having no transient W influxes) are viable over some range of the plasma current/energy level to be explored in PFPO-2. The PFPO-2 plan minimizes this risk by the development of H-mode scenarios and stationary power/ELM control/W control schemes at low plasma current (≤5 MA). Risk minimization in these plasmas conditions is twofold: (a) stationary power fluxes are expected to remain low (under 10 MWm^{-2} toroidally averaged) in non-detached divertor conditions [44, 193]; (b) uncontrolled ELMs are not expected to cause W divertor melting [75]. Despite this, it may be the case that the natural ELM frequency in such plasmas is too low to prevent W accumulation [34] and active triggering of ELMs may be required. This risk is already significantly reduced within the IRP plan by the application of vertical plasma position oscillations, which are expected to be effective in triggering ELMs up to currents of at least 7.5 MA [140], and by exploitation of the four available fuelling pellet injectors, capable of injecting pellets from the LFS and HFS, as a back-up ELM control technique. In this application, it is expected that pellet frequencies of up to 64 Hz can be achieved over the range of H-modes explored, and this should be sufficient to mitigate the risk of W accumulation in low and medium plasma current H-modes. Should the PFPO-2 assessment show that this is insufficient for FPO scenarios, the mitigation of these actions would involve the addition of two further pellet injectors for ELM triggering prior to FPO operation.

  If the assessment in PFPO-2 reveals that only suppressed ELM regimes can provide a viable integrated scenario for H-mode operation at high currents in FPO, the PFPO-2 H-mode program would strongly focus on the development of such scenarios by the application of ELMCC to achieve ELM suppression. Should this not provide the level of integration required for the high-*Q* FPO scenarios (e.g., an inadequate level of energy confinement is achieved), alternative ELM-less plasma scenarios to the controlled/suppressed ELMy H-mode would be explored at this stage (QH-mode, I-mode, etc.). Performing this assessment

as soon as possible in the ITER experimental program (i.e., in PFPO-2, as considered here) will allow the implementation of early mitigation strategies to prevent this risk materializing in FPO;

- *Fuelling of He plasmas at 7.5 MA/2.65 T*: Fuelling of He plasmas can only be performed by gas injection and this is not an efficient approach to core fuelling in ITER due to the high ionization efficiency for neutrals in the SOL/divertor plasma. Moreover, pellet fuelling would imply H contamination of the helium H-modes, which might reduce their operational space. Integrated simulations that incorporate the limits imposed by divertor detachment on the separatrix density (see [3-Appendix C]) and anomalous core particle transport in ITER show that H-mode scenarios exist which allow unrestricted application of NBI in both the access phase and the stationary phase [172, 173]. If experiments at ITER were to deviate strongly from these simulations and lower density values were to be achieved (particularly in L-mode), the application of NBI in He plasmas would be more complex and the helium H-mode scenarios more difficult to develop, since only ICRF and ECRH might be possible in some scenario phases or even throughout the plasma pulse. Possible mitigation strategies consist of: (a) reducing the NBI energy, and thus power injected, to adapt to a lower plasma density while maintaining acceptable shine-through loads; and (b) triggering the L-H transition with ECRH+ICRF and subsequently applying NBI at full power once the density has increased in H-mode.

Specific open R&D issues related to PFPO-2 H-mode operation are described in section 5.3.

Initial studies of current drive efficiency, target q-profile formation and energetic particle physics: The major risks to these studies are associated with difficulties which the available H&CD systems and/or their integrated control might experience in providing the required H&CD to form and sustain the desired *q*-profile and/or to provide the expected current drive efficiency. Inadequacies in the scope of the fast particles diagnostic systems during this campaign might also pose a risk. Specific risks identified include:

- *H&CD systems or their control schemes cannot provide the required capabilities to produce and/or sustain the target j(r) required for the experiments:* Depending on whether or not these issues are related to specific features of the H/He plasmas, the mitigation strategy will vary. To mitigate this risk more experimental time could be allocated to refine the control schemes in PFPO-2. If the inefficiency in current drive or control results from the specific features of these H/He plasmas (e.g., T_e is too low for efficiency current drive, density control in helium H-modes does not allow a proper evaluation of CD efficiency, etc.), which are not expected to occur in D/DT plasmas, this operational period could be shortened, as it is unlikely to provide useful information. On the other hand, if the inefficiency in current drive is expected to affect D/DT plasmas, it will be necessary to ensure that this is mitigated prior to the start of the FPO phase, most probably by implementing an upgrade of the baseline H&CD systems;
- *Deficiencies in the diagnosis of specific plasma parameters may affect the execution or interpretation of the experimental results:* Possible issues are related to measurement of the current profile and of the characteristics of energetic particle populations. The first requirement is well covered by the available diagnostics in PFPO-2 (with no changes foreseen prior to FPO), but it may turn out that these are not sufficiently accurate. If so, an

upgrade of the back-end instrumentation might be required before proceeding to long-pulse experiments in FPO. In relation to fast particles, the measurement capabilities are more restricted in PFPO-2 than in FPO due to the lack of profile-resolved fast particle and neutron-related measurements (see Table 7). Fast particle studies will therefore mostly be based on diagnosis of their effects on the plasma (fast magnetics, SXR, ECE, interferometry and polarimetry) and measurements of fast particle losses via observation of first wall and divertor heat loads (see Table 7). This risk could be minimized by advancing installation and commissioning of the fast ion loss detectors, together with the neutron and gamma ray spectrometer cameras, to PFPO-2 (these are currently foreseen for FPO - see Table 10). The implementation of a charge exchange diagnostic upgrade at this stage (discussed in [3-Appendix H]) would also enhance the measurement capability in this area.

3.2.5.10 Principal outcomes from PFPO program

An ambitious experimental program is foreseen for the PFPO phase, advancing the facility operational capabilities from sustainment of the simplest plasma breakdown, with plasma currents of less than 1 MA, to fully integrated L- and H-mode plasma scenarios in the range 5-15 MA which exploit essentially all of the tokamak, auxiliary and plant systems. The overall objectives of this phase are to demonstrate essentially the full technical capability of the ITER systems (accepting that the limiting capability in areas such as heat loads, pulse length etc., might not be accessible until significant fusion power is produced), to achieve robust and routine plasma operation over the accessible L- and H-mode parameter range, to perform initial exploration of fusion plasma physics at the ITER scale, and to prepare the scientific, technical and operational basis for the transition to DT operation and significant fusion power production.

The PFPO research program will already allow extensive testing of many elements of the physics basis developed to support the ITER design and performance predictions. The values of key physics parameters such as collisionality and normalized Larmor radius, as well as ‘engineering parameters’ such as plasma current, major/minor radius etc., accessible during this phase will extend the tokamak physics basis very considerably and allow numerous comparative studies of predictions derived from the ITER physics basis in plasma transport and confinement, MHD stability, divertor and plasma wall interactions, heating and current drive efficiency, plasma control and scenario integration, and possibly also energetic particle physics (but still with anisotropic velocity distributions). Perhaps the key caveat in this respect is that, although a substantial program addressing H-mode physics (access conditions, energy and particle confinement, ELM characterization and control etc.) is planned, the extent to which key aspects of H-mode physics can be addressed adequately will probably depend on achieving satisfactory H-mode performance in H as well as in He - key physics tests in this area might otherwise await the transition to D operation in the FPO phase. Overall, therefore, and despite the inevitable emphasis on ‘commissioning with plasma’ activities within the presentation of the PFPO research program, this phase of ITER operation will provide significant opportunities for studies of fusion plasma physics at the ITER scale and will allow access to plasma and operational parameters substantially beyond those of current experiments.

The experimental program implemented during PFPO will also provide wide-ranging tests of much of the ITER technology under challenging conditions. It will, in particular, launch the first phase of the TBM testing program (see section 4), a central element of the ITER mission.

Operation of major systems and components such as the superconducting magnets, plasma facing components, heating and current drive systems, diagnostics, fuelling and vacuum systems, control systems, power supplies, the cryogenic system, tokamak and auxiliary cooling water systems (and even remote handling systems, which are required in this phase simply due to the scale of ITER components) will already yield an invaluable database on system performance and reliability over pulse lengths ranging from several tens to several hundreds of seconds. The upper limit of this range in pulse length will rely on successful commissioning and operation of the tokamak, auxiliary and plant systems, as well as successful implementation of the scientific research program, which will determine the rate of progress through the various performance milestones, potentially releasing time for commissioning of the key tokamak and facility systems, in particular, the H&CD systems, to extended pulse lengths of up to 1000 s.

The routine operation of plasma pulses with long durations during the PFPO phase would be a desirable, and significant, achievement, which would give additional confidence in operational reliability in advance of the FPO phase. This would be a major advantage in the preparation for the transition to DT operation and could be expected to shorten the experimental time required to achieve long-pulse operation at high fusion power in DT plasmas. Nevertheless, if all other elements were in place to allow a timely transition to D/DT operation, reliable L- and H-mode operation over a range of plasma scenarios with flat-top durations of up to 100 s would be an adequate criterion to support this transition, given the emphasis on ITER's role in demonstrating fusion power production as rapidly as possible.

Table 5 (section 3.2.4.1) and Table 6 (section 3.2.5.1) provide an overview of the experimental activities implemented in each of the PFPO phases and of the operational time estimated as necessary to meet the objectives defined for each phase. There are, of course, significant uncertainties in these estimates, given the complexity of some of the 'commissioning with plasma' activities which it is planned to implement during the PFPO phase and the reliability issues which might be encountered in commissioning plant and auxiliary systems for the first time. For comparison, the estimated experimental time required for PFPO-1 is 449 days (including the programmatic options considered) compared to an estimate of 470 operational days available (see Table 1), implying that there is little contingency in the estimated time schedule. For PFPO-2, the proposed program is estimated to require 457 days, as compared to the estimated 545 operational days available, and so the PFPO-2 program does include contingency against unexpected developments. This potentially offers opportunities, for example, to place a greater emphasis on the commissioning of H&CD systems to long-pulse operation and to exploit this capability in the experimental program.

Bringing all ITER systems from the initial phase of Integrated Commissioning to preparedness for DT operation, establishing the required range of plasma scenarios and demonstrating the necessary level of operational reliability to support the transition to the FPO phase within the scheduled period of experimental operation of ~40 months is, as noted above, ambitious. There is a range of risks, in terms of hardware reliability/performance and plasma performance (as discussed in preceding sections and consolidated in [3-Appendix J]), which, if encountered, will need to be addressed and resolved, or mitigated, rapidly to ensure that the schedule towards DT operation proposed within the Staged Approach is maintained. Key among the challenges and risks which might have to be addressed are: establishing reliable plasma breakdown over a range of currents and fields; developing reliable plasma operation under a robust (but complex) control

capability implemented in PCS; establishing highly reliable means for predicting, avoiding and, when necessary, mitigating disruptions over the entire range of operational space associated with ITER's mission; ensuring acceptable power loads (including energetic particle losses) on the first wall and divertor under stationary and transient conditions; demonstrating reliable operation of power integrated plasma scenarios at 15 MA/5.3 T with high power auxiliary heating; establishing H-mode operation with acceptable energy confinement, impurity content and plasma edge integration (with the required level of ELM control) over the widest possible parameter range in H and He plasmas; and exploiting the H&CD capabilities to extend the plasma pulse duration into the range of several hundred to one thousand seconds.

Many of these risks are being addressed in ongoing physics and technology R&D programs which are discussed in detail in section 5. Nevertheless, given the scale of the extrapolation from current devices to ITER, the associated uncertainties in the underlying physics basis, and the novelty of elements of ITER's integrated plasma scenarios, it is inevitable that expectations of plasma behaviour and performance, in particular, must be tested in the ITER environment. As indicated in the discussion in previous sections, a significant outcome of these tests and of measures to address the consequences of risks realized in the research program will be the specification of system upgrades required to improve operational reliability and assure the required plasma performance in later phases of the Research Plan.

3.3 Fusion Power Operation (FPO)

3.3.1 Objectives and Assumptions for FPO program

In this version of the Research Plan, only the first 3 experimental campaigns of the Fusion Power Operation phase are discussed in detail. The detailed research to be addressed in later campaigns, after FPO-3, depends to a large extent on the results obtained in the first three campaigns. Therefore, the discussion of the longer-term research program restricts itself in the present version of the IRP to an outline of likely areas of research.

The FPO-1 campaign involves both D and DT plasmas and focusses on the development of inductive plasma operation to fusion power production levels of several hundred megawatts, while in the FPO-2 and FPO-3 campaigns long-pulse operation is developed in inductive, hybrid and non-inductive DT plasma scenarios, with the aim of meeting the project's mission goals of $Q \geq 10$ for periods of 300 - 500 s, and $Q \geq 5$ in fully non-inductive operation for periods of up to 3000 s. Nevertheless, as illustrated in figure 3 (section 2.4), the DT experimental program will continue beyond these initial campaigns, preparing the science and technology basis for DEMO-class devices (the potential scope of such experiments is outlined in section 3.3.6) until the ITER Members conclude that the project exploitation phase should end.

During FPO, ITER will operate with all its baseline ancillary systems at full performance, including the T-Plant. Nevertheless, within the Staged Approach installation and commissioning program, commissioning of the T-Plant to full performance will occur in parallel with the final phase of PFPO and the initial phase of FPO (see figure 3). It is therefore assumed that the T-Plant will start to provide a significant throughput for DT operation (supporting a plasma concentration of at least 10% T in D for ~50 s) not later than one year after the start of D operation. The subsequent steady increase in DT throughput will allow an extended program of DT experiments to be launched. Final elements of the baseline diagnostic systems should be installed during

Assembly Phase IV to satisfy the measurement requirements for the FPO phase. Table 10 lists the neutron and fusion product diagnostic systems which will be completed in advance of FPO together with a range of upgrades under consideration, which would enhance the studies of burning plasma physics.

It would also be advantageous if upgrades identified as required to achieve the long-pulse/ steady-state goals were to be implemented before the start of FPO (e.g., additional ECRH power, 3rd HNBI, RWM control power supplies, etc.). Note that the possible upgrade of a 3rd HNB requires certain measures to be taken well before the start of FPO, in particular, the installation of captive components (see [3-Appendix G]), which are included in the staged approach. However, as the initial experimental activities will be focussed on the $Q \geq 10$ goal, and achieving this milestone is likely to extend beyond the first 2-year cycle of DT operation, an implementation of these upgrades that provides their functionality during FPO-2 is not likely to severely affect the development of the research program towards the $Q \sim 5$ goal.

To provide an adequate basis for the efficient development of D and DT plasma scenarios, it is assumed that fully integrated scenarios have been developed for L-mode plasmas up to 15 MA/5.3 T and for H-modes up to 7.5 MA/2.65 T (including ELM control, power load control, etc.), which will require retuning, but not full redevelopment, in D/DT. If this H-mode milestone is not achieved in PFPO, due to difficulties in accessing the H-mode regime in H/He plasmas, additional experimental time in D plasmas will be required to determine H-mode access conditions, assess H-mode plasma behaviour at the ITER scale and develop control schemes, as part of the integrated scenarios assumed for D/DT. Similarly, it is assumed that disruption mitigation and avoidance schemes have been developed in PFPO for the same range of scenarios and that retuning, but not full re-development, will be required for D/DT.

The FPO R&D activities discussed in the following sections (i.e., corresponding to campaigns FPO-1 to FPO-3 of figure 3) can be divided into four experimental phases.

Initial D and trace-T operation:

In this phase all ITER systems will be commissioned (or recommissioned) for nuclear operation and the target scenarios of PFPO-2 will be reproduced in D plasmas. This implies the recommissioning of the ITER H&CD for D operation (mainly the HNBs, for which the injected species will change to D, and the ICRF), diagnostics (chiefly the neutron-related diagnostics), fuelling (change to D), etc.

As soon as the H&CD systems achieve a sufficient level of performance (injected power and pulse length), plasma conditions achieved in H and/or He plasmas will be reproduced: L-mode operation will be expanded to 15 MA/5.3 T and H-mode operation will be explored up to 7.5 MA/2.65 T. The operational strategies and control schemes developed during PFPO will be applied and refined/ retuned to the higher plasma energies expected in D plasmas. This phase will provide first experimental confirmation of the plasma parameters expected in DT plasmas in this I_p range, as the plasma characteristics are expected to be similar in D and DT plasmas, except for those related to high fusion power production. Once D operation is reliably established, trace-T experiments will be performed with special focus on the 7.5 MA/2.65 T H-mode scenario, including also the L-mode phases. Tritium transport and fuelling experiments will be performed and the results will be used to optimize fuelling and mixture control strategies for DT.

The research program during this initial period will include studies to confirm the key ingredients of the long-pulse/ steady-state scenarios. For example, experiments similar to those performed in PFPO-2 will be performed to develop the target *q*-profiles in the ramp-up, to sustain them for at least 10 s in the flat-top and to determine the current drive efficiency of each of the H&CD systems (chiefly NBI and ECRH) in H-mode plasmas. The extent to which these aspects will be pursued will be determined by progress on the H-mode program and the availability of the T-Plant for DT plasma operation.

The main objectives of this experimental period are:

- Commissioning of plasma control, interlock and safety systems with plasma to the required level to support the experimental program;
- Commissioning of the additional diagnostic systems (particularly those related to neutrons), validation of data and integration into control/ interlock systems;
- Recommissioning of H&CD systems for D plasmas to their installed power level for at least 100 s;
- Extension of the capability for disruption prediction, avoidance and mitigation to parameters characteristic of the highest performance achievable in D plasmas;
- Demonstration of deuterium L-mode operation to 15 MA/5.3 T;
- Demonstration of robust NTM control in high confinement deuterium H-mode plasmas;
- Development of deuterium H-modes to 7.5 MA/2.65 T (~50 s) with reliable ELM control and stationary divertor power load control;
- Physics characterization (e.g., confinement, MHD stability, etc.) of ohmic, L-mode and H-mode plasmas in D;
- Performance of trace-T experiments in deuterium L- and H-mode plasmas to assess T transport and T fuelling requirements and schemes;
- Characterization of key aspects of plasma-wall interactions in the ITER environment in D plasmas;
- Preparatory studies of hybrid/ non-inductive scenarios in D plasmas;
- Preparatory studies of ‘burning plasma’ issues (e.g., He exhaust, fuel mixture control in trace T, etc.).

<u>Initial operation in DT plasmas during FPO-1 and early FPO-2:</u>

During this period, the daily tritium throughput of the T-Plant should allow operation with T concentrations in the range of 10-70% to sustain high-*Q* operation for up to ~50 s. This will allow the development of plasma scenarios with significant fusion energy production, and neutron measurements will become important, both for the evaluation of the fusion power and for the execution of the experimental program. As a consequence of the fusion energy production, the effects of neutron heating on the superconducting coils will start to be measurable and, although this is not expected to raise any issues for operational durations at high *Q* of ~50 s, the consequences for longer pulse operation at high *Q* will need to be evaluated at this stage. This may call for further optimization of the plasma scenarios to reduce AC losses. With the increased level of plasma thermal energy and exhaust power in DT H-modes, routine operation of plasma scenarios with ELM control and radiative divertors will be required. This is expected to

necessitate development and/or retuning of the control schemes developed at lower currents for D plasmas, and this will also apply to the disruption avoidance and mitigation schemes. The T throughput of the fuelling and exhaust systems will start to be non-negligible, and in this phase, therefore, T-retention measurements and removal schemes are expected to become an element of the operation cycle in preparation for their routine use in the subsequent DT operational phase.

The plasma regimes to be explored in this period start at 7.5 MA/2.65 T, and these plasmas will be characterized extensively, both in L- and H-mode, over a range of T concentrations. In these experiments, it will be possible to document the first effects of α-heating, adapt the density feedback control to the D/T fuelling requirements and identify possible new edge-core integration requirements that might arise due to the presence of T in the plasma. Once a fully integrated 7.5 MA/2.65 T H-mode scenario in DT has been developed, the plasma current/toroidal field will be increased in steps towards 15 MA/5.3 T with the aim of demonstrating a fusion gain of $Q = 10$ for ~50 s. For FPO-1, the target is to achieve a fusion power level of several hundred MW with $Q \geq 5$ for ~50 s, while establishing plasmas with $Q \geq 10$ initially for ~50 s and subsequently for 300 - 500 s, is foreseen for FPO-2. It is expected that the steps will be similar to those in the L-mode D program, except that additional steps in current/field will be added between 12 and 15 MA to account for the large change of plasma energy with I_p expected in H-mode operation. For each step, the T concentration will be scanned and fully integrated scenarios will be developed, including ELM control, fuelling and divertor power load control. It should be noted that the range of T concentrations that will be explored will decrease as I_p increases because the α-heating will become an essential part of the scenario to sustain the high confinement H-mode. It is expected that, in the expansion towards high-I_p/high-Q, control of MHD stability will become more challenging and significant time will have to be dedicated to the control of NTMs and sawteeth as part of the scenario development process.

Initial development of long pulse scenarios with high Q will also be undertaken. This will include current ramp optimization in DT L-modes and H-modes (during the ramp-up), as well as sustainment of the flat-top H-mode phase. It is likely that, in this first experimental phase with DT plasmas, the sustainment will be limited to a few tens of seconds with relatively low Q, due to limited operational time and the available H&CD schemes.

The main objectives of this experimental phase are:

- Commissioning of plasma control, interlock and safety systems with plasma to the required level to support the DT experimental program towards $Q = 10$;
- Commissioning of additional diagnostic systems (e.g., for fusion power and fusion products), validation of data and integration into control/ interlock systems, as required;
- Commissioning of ICRF heating scenarios for DT plasmas to installed power level for at least 100 s;
- Extension of the capability for disruption prediction, avoidance and mitigation to parameters characteristic of the highest performance in DT plasmas;
- Development of DT H-modes at 7.5 MA/2.65 T (~50 s) with reliable ELM control, NTM control and radiative divertor operation;
- Expansion of DT H-mode operational space from 7.5 MA/2.65 T, culminating in 12 - 15 MA/5.3 T DT H-mode operation with full feedback control at fusion powers of 200 - 300 MW for at least 50 s (in FPO-1);

- Extension of operation to 15 MA (if not completed in previous step) and optimization of fusion gain to demonstrate $Q \geq 10$ for at least 50 s (in FPO-2);
- Optimization of fuel mixture control, burn control and plasma-facing component protection in DT plasmas;
- Physics characterization of ohmic, L-mode and H-mode plasmas in DT;
- Exploration of options for current profile control in DT plasmas to identify most promising approaches for long-pulse/ steady-state operation.

Since experiments in 50:50 D/T plasmas will only be possible during the latter phase of the FPO-1 campaign (as determined by progress in the T-Plant commissioning), it is not expected that goal of $Q = 10$ will be achieved in the first DT campaign: the target foreseen for the end of FPO-1 is a fusion power of 200 - 300 MW with a fusion gain of $Q \geq 5$ sustained for ~ 50 s. Expanding this firstly towards a scenario with $Q \geq 10$ for 50 s and then further towards a burn duration of 300 - 500 s would be the principal goal of the FPO-2 campaign.

Further DT campaigns (mid/late FPO-2 and FPO-3):

During these campaigns, the $Q = 10$ scenario will be extended towards 300 - 500 s and the long-pulse and steady-state scenarios will be developed. The rate of progress of these developments will depend, of course, on the degree of success achieved within specific experiments and on the physics behaviour revealed by the studies of burning plasma, as well as on the availability of upgrades which may be required to achieve the $Q \sim 5$ goals (e.g., additional ECRH/ECCD, 3rd HNB, power supplies for RWM control, etc.). During this phase the T throughput will reach its design specification, routine measurements of T-retention will be undertaken and T-removal schemes will be applied routinely as part of the operations cycle. As the burning plasma duration is extended, neutron heating of the TF coils is likely to reach its maximum, and this may require re-optimization of the scenarios to limit, or decrease AC losses. Moreover, as burn length, fusion power/ power load to components and non-inductive current fraction increase, plasma control in general and event handling, in particular, are expected to become significantly more complex, and a substantial fraction of the operational time to extend the burn length is expected to be dedicated to solving such issues.

The main objectives of this experimental phase are:

- Development of DT plasma scenarios with $Q \geq 10$ at $P_{fus} \sim 500$ MW for 300 - 500 s;
- Characterization of key aspects of PWI in the ITER environment in high fusion power/ high gain plasmas;
- Developing a program of burning plasma studies around high fusion power/ high gain inductive plasmas;
- Demonstration of satisfactory T-accounting, T-retention measurements and T-removal techniques;
- Providing required support to the TBM testing program;
- Investigating optimization of fusion power with $Q > 10$ during quasi-stationary inductive conditions and characterizing plasma behaviour in these conditions;
- Identification of needs for upgrades to improve fusion performance, or to improve potential for non-inductive operation (e.g., further ECRH power, ELMCC power supplies for RWM control, if not previously implemented);

- Establishing robust current profile control techniques for DT plasmas;
- Developing DT plasma scenarios with current profile control and improved H-mode confinement allowing a burn duration of ~1000 s at several hundred megawatts of fusion power based on the hybrid/ improved H-mode scenario at $q_{95} \sim 3.6$;
- Establishing non-inductive plasmas with the longest sustainable pulse duration (>1000 s) and moderate fusion performance ($Q \sim 2$);
- Optimizing fusion gain and pulse duration to establish plasmas with durations beyond 1000 s and $Q \geq 5$;
- Optimizing Q in fully non-inductive DT plasmas towards $Q \sim 5$;
- Initiating the characterization of key aspects of PWI in the ITER environment over very long durations (e.g., impact on fuelling, erosion/ redeposition, fuel retention, etc.).

It should be noted that, depending on the suitability of the upgrades implemented by this phase and the need for additional measures to achieve the non-inductive goal, the latter part of the R&D activities detailed here might be implemented in the following phase of FPO.

Long-term DT fusion R&D research (FPO-4 and beyond):

In this phase, priority would be given to the completion of any outstanding milestones associated with ITER's fusion power goals (e.g., demonstration of $Q \geq 5$ for durations of up to 3000 s in fully non-inductive operation), to ensuring that the TBM testing program continues to receive adequate operational support and to continue studies of the performance of fusion-relevant technology (e.g., superconducting magnet systems, PFCs, T-Plant, cryogenic and cooling systems, etc.) in the burning plasma environment. With adequate progress on satisfying ITER's primary mission goals, it is expected that the operational focus would turn to R&D issues related to addressing the long-term goals of ITER towards DEMO. This is likely to require specific DEMO-related upgrades, which will be identified in the course of the research program and implemented during this phase of operations. Such upgrades may be undertaken in parallel with, or subsequent to, the completion of upgrades required to achieve the $Q \sim 5$ non-inductive goal and are considered further in section 3.3.6.

The main objectives of this experimental phase are:

- Completion of experimental program associated with achievement of ITER's primary fusion power goals;
- Conducting a program of burning plasma studies to characterize physics process in non-inductive DT scenarios;
- Performing systematic characterization of key aspects of PWI in the ITER environment over very long durations (e.g., impact on fuelling, erosion/ redeposition, fuel retention etc.);
- Provision of required support to the TBM testing program;
- Studying the operational reliability of major elements of fusion technology and plant systems under reactor-relevant conditions (in particular, long-pulse, high-Q burning plasma operation);
- Identification and implementation of options for further upgrades to prepare longer-term DEMO-targeted studies;
- Achieving the goal for average first wall neutron fluence of 0.3 $MW.yr.m^{-2}$.

3.3.2 Operational plan for D-phase experiments

An overriding aim in FPO will be to make the transition to full DT operation as quickly as is allowed by commissioning of the T-Plant. Nevertheless, the agreed schedule within the Staged Approach implies that commissioning of the T-Plant to the level of DT throughput at which it can support an extensive experimental program in DT plasmas will extend through approximately the first year of the FPO phase. To exploit this experimental time adequately to ensure a rapid development of high fusion power plasmas, a detailed program has been developed for operation in D plasmas (including plasmas with 'trace' levels of T). The thrust of this program is to extend L- and H-mode operation to performance levels significantly beyond those achieved during PFPO, to pursue detailed studies of physics processes at the ITER scale under conditions which are more 'fusion relevant' than in PFPO and to ensure the reliable operation of all auxiliary systems required for an efficient exploitation of DT plasmas. A summary of the experimental program, together with the ranges in experimental plasma parameters and estimates of corresponding time allocation, foreseen in D plasmas is given in Table 11 to provide a point of reference for the following discussion of the studies foreseen.

3.3.2.1 Plasma restart and commissioning

Plasma restart with H&CD and Diagnostic commissioning: The plasma restart in FPO should establish routine plasma operation in deuterium at 7.5 MA/2.65 T following completion of the final preparations for DT operation during Assembly Phase IV. This is the first time that diagnostics will see significant neutron fluxes; therefore, careful commissioning of the shape and current control, vertical position control, and first wall heat flux management systems must be carried out at the beginning of FPO. The main restart activity for the H&CD systems will be the commissioning of the NB systems for deuterium operation.

Plasma initiation in D will be slightly different from that developed in H and He plasmas in the previous phases, but optimization of the plasma initiation can be performed parasitically during other restart activities. An optimized (and robust) initiation sequence will be established at 2.65 T and 5.3 T over a range of CS precharge currents.

Recommissioning of the plasma shape, current and vertical position control will follow the procedures developed in the previous phases. The key issue is to examine whether effects of radiation-induced voltages in the sensors are evident. Precise shape control will be needed for recommissioning of the first wall heat flux protection, similar to the protocols developed in the previous phases. The milestone for this element of the restart is robust 7.5 MA/2.65 T operation.

Density control will need to be re-tuned to account for the different transport behaviour of D (compared to H and He) neutrals and ions. Moreover, the transition to nuclear operation with the launching of FPO implies that integrated use of the T-Plant for supplying the gas and pellet injectors is necessary. Fuel mix control will have been developed for ICRF and H-mode operation using H/He mixtures in previous phases, but this will need to be adapted for DT mix control (at the appropriate time), plus minority concentration control for ICRF heating.

The major restart activity for the H&CD systems will relate to commissioning of the HNB systems for D^0 injection. This will involve the first operation at 1 MeV acceleration voltage and, additionally, in the presence of significant neutron flux from the plasma. The change in working gas in both the beamline and the plasma will require requalification of the internal protection

systems in the beamline and port. The ICRF coupling control will also need to be re-optimized for deuterium, but no changes should be required for ECRH operation. All three systems should be recommissioned to at least 50 s operation in order to support the research program. In the event that the systems had been commissioned for longer pulses in PFPO-2, it would be beneficial to demonstrate that longer pulse capability again in the restart phase, if time permits. Once H&CD power in excess of 40 MW is available, the divertor heat flux management system will need to be recommissioned and the control loops will need to be re-optimized for the different behaviour of D neutral and ion transport.

New control issues associated with the introduction of significant self-heating such as entry to burn, exit from burn, and robust normal and off-normal termination schemes will be developed within the research phase of the campaign.

Advanced control commissioning in FPO: These activities will extend the advanced control capabilities beyond those exploited in previous operational phases to satisfy the demands of high performance operation in D and DT plasmas. Depending on the need for upgrades identified in PFPO and their implementation, there might be new or upgraded actuators requiring commissioning in the early phases of FPO. In addition, new diagnostics for fusion products are expected to be available and the additional fusion power will enhance plasma performance, requiring significant changes to advanced control schemes, particularly for kinetic control, MHD control, integrated control, and event handling. Neutron and gamma ray emission from fusion reactions may also impact some diagnostic measurements and actuators, so that additional commissioning of advanced control functions that depend on the impacted systems may be required.

An important aspect of advanced control commissioning involves the adaptation of control techniques (even those established in earlier operational phases) to plasmas with a significant α-particle population, which, of course, has substantial implications for plasma parameters, MHD stability, plasma-wall interactions, etc. Establishing robust control capabilities in this environment, and under the range of plasma scenarios envisaged, is likely to require ongoing studies, both to improve the physics basis for control and to fine-tune control algorithms, for some considerable time within the experimental program.

The deliverables for advanced control commissioning in the FPO phase include:

- Development of routine operation of first wall and divertor heat flux control with fusion power;
- Implementation of thermohydraulic, model-based, control of the superconducting coils with eddy current and nuclear heat loads and event handling;
- Establishing fusion burn control, β and stored energy control;
- Commissioning of temperature, pressure, rotation, and current density profile control;
- Establishing reliable ELM control in high fusion power plasmas;
- Demonstration of sawtooth control with fast α-particles;
- Establishing robust and routine NTM control in high fusion power plasmas;
- Development of AE control with fast α-particles;
- Commissioning of dynamic error field correction and RWM avoidance at high plasma performance (high fusion power, significant fusion gain).

3.3.2.2 Disruption management program in FPO

The DMS system must be recommissioned using reference pulses from PFPO-2 and any modified/ upgraded elements of DMS hardware that might have been installed during Assembly Phase IV must be commissioned. Early operation at 5.3 T will be necessary to demonstrate that runaway mitigation is maintained in deuterium.

During FPO disruption management will focus on monitoring disruption budget consumption and taking corrective actions when needed. This also involves monitoring the performance of the DMS in dealing with higher plasma stored energies and with potential additional RE seed mechanisms (tritium decay, Compton scattering). Priorities will be given to reducing disruption rates by appropriate event handling within PCS (see section 3.2.4.3) and by active MHD control (discussed below). The target success rate for thermal quench mitigation in FPO will be determined both by the need to limit thermal loads on in-vessel surfaces and by the need to suppress runaway formation that could potentially follow from strong tungsten influxes. Requirements for the target success rate for plasma current quench mitigation will already have been identified from the EM load and current quench heat load scalings derived during PFPO-2 experiments, but is expected to be close to 100% for FPO. Reliable current quench mitigation is expected to be very effective following the disruption detection methodology developed during PFPO-2 experiments.

Due to the thermal energies expected in FPO plasmas, there might be a need for further optimization of the mitigation sequence or mitigation species composition to achieve higher radiation rates, while limiting radiation peaking, and thus heat loads to the FW, to acceptable values. Improvements in plasma performance can also introduce new stability limits (e.g., pressure driven instabilities). This, together with possible changes in diagnostic capabilities, may necessitate adaptations in the disruption prediction schemes to ensure sufficiently long warning times to activate avoidance capabilities or the DMS.

3.3.2.3 Deuterium L-mode operation

Plasma scenarios and overall objectives: Development of L-mode scenarios in D mimics the earlier development program in H (section 3.2.5.7), with the same final target of 15 MA/5.3 T plasmas of ~ 50 s flat-top duration. As in the PFPO-2 H program, the L-mode development will start at 7.5 MA/2.65 T plasmas in D and will progress towards 15 MA/5.3 T I_p/B_t steps following a q_{95} = 3 - 4 path, with fuelling and power scans being performed at each step. This is expected to require retuning of the Plasma Control System (PCS), for density control and heat load control, and of the DMS and disruption avoidance schemes to reflect the experimental characteristics of deuterium plasmas. In parallel, some elements of the disruption management activities described in section 3.3.2.2 will be implemented. An additional program within this operational phase will assess the power threshold to access H-mode in D plasmas at 2.65 T. This will include the determination of the density dependence and possible q_{95} dependence of the H-mode threshold, in particular, at q_{95} = 3, where some experiments show an increased power threshold at high B_t compared to that at q_{95} = 2.7 or 3.3 [15].

A precise determination of the power required to access H-mode in D plasmas over a range of conditions is planned at this point, to perform a final check (in advance of DT operation) that the baseline power level is sufficient to achieve H-mode in DT plasmas at 15 MA/5.3T, as required

for the $Q \geq 10$ mission. Should this program not provide confidence that the baseline H&CD capability can assure robust H-mode operation under these conditions, it would be essential to proceed with the necessary H&CD upgrades. The proposed operations plan assesses this possible need early in D operations to limit the overall delay in the research program.

Experimental plan for deuterium L-mode development to 15 MA/5.3 T: The development plan for deuterium L-mode plasma development follows the same I_p/B_t sequence already shown in figure 8 for H plasmas, including scenario #5 (10 MA/4.5 T) to reduce the I_p/B_t step. Table 12 summarizes the scenarios to be explored in this phase: there is significant additional flexibility for heating of D plasmas, in comparison with H plasmas, because the lower density limit (~2.5×10^{19} m^{-3}) for unrestricted NBI use with tolerable shine-through loads in D is substantially less than that for H (~4.5×10^{19} m^{-3}) and because for low fields (below 3.3 T) a viable scheme for ICRF heating exists (H-minority). This is expected to make the issue of off-axis ECRH heating for W control in D plasmas less critical, as more heating mix possibilities exist. Otherwise, the experimental plan is similar to that for H plasmas (section 3.2.5.5), consisting of fuelling scans, power and power mix scans, etc., in the flat-top and in the ramp-up/down, with specific experiments to assess core transport and confinement properties of deuterium L-mode plasmas. Similarly, there will be experiments to optimize flux consumption for these scenarios and to control divertor power loads, as well as W production and W accumulation control in the main plasma; this may be already necessary at high additional heating levels (see [3-Appendix C]).

L-H transition experiments in D plasmas: This program to prepare for the subsequent exploration of H-mode operation in D plasmas, includes the scaling of the H-mode threshold with density and heating mix at 2.65 T and an assessment of the q_{95} dependence around $q_{95} \sim 3$, as some experiments show an increased H-mode power threshold at this precise value, the reference value for $Q \geq 10$ operation in ITER. An initial assessment of H-mode access at $q_{95} \sim 4.5$, which is a typical value for steady-state $Q = 5$ operation in ITER, will also be performed. The H-mode access assessment at $q_{95} \sim 3$ will be carried out around scenario #2 in Table 12 by varying the plasma current by up to ±10%. Table 13 provides an outline of the anticipated range in experimental conditions within this initial exploration of H-mode access in D.

Main deliverables of this operational phase:

- Demonstration of fully integrated L-mode plasma scenarios in D at full current and field (15 MA/5.3 T) with ~50 s flat-top, including plasma position and vertical stability control, power load control, W accumulation control, etc.
- Demonstration of the intermediate I_p/B_t steps required to achieve 15 MA/5.3 T L-mode operation in D plasmas along a $q_{95} = 3 - 4$ path; these will provide the basis for the subsequent development of high-I_p H-mode scenarios in D and DT;
- Assessment of the effects of gas and pellet fuelling and additional heating power level and mix on plasma transport and confinement in ITER L-mode D scenarios up to 15 MA/5.3 T, including ramp-up/down phases;
- Optimization of flux consumption in deuterium L-mode ramp-up/down phases by using the flexibility of ITER systems to optimize the current ramp rate and the exploitation of heating and fuelling systems;

- Assessment of the power required to access H-mode in 2.65 T D plasmas for a range of densities and for q_{95} = 3 - 5, with specific detail on the possible q_{95} dependence around q_{95} ~ 3.

3.3.2.4 Deuterium H-mode operation towards full performance

Plasma scenarios and overall objectives: The main aim of this first phase of H-mode development in D will be to assemble a complete H-mode scenario at 7.5 MA/2.65 T. The scenario will have to be reliable, robust to disruptions and MHD stable with controlled ELMs. It will be used as a 'working scenario' to explore the use and optimization of the additional heating schemes, the tools for ELM control, NTM stabilization, plasma fuelling and divertor heat load control in ITER H-modes. The H-mode operational range will then be expanded towards higher current and fields in pure D plasmas, although this expansion might already exploit plasmas with a significant (i.e., beyond trace) T concentrations should the T-Plant commissioning be sufficiently advanced.

Taking into account the time foreseen to:

a) Commission the required systems with plasma;
b) Develop the associated L-mode scenario and complete the H-mode access program prior to the establishment of quasi-stationary deuterium H-modes, and;
c) Commission the T-Plant.

The present plan considers that the expansion of the H-mode operational space in FPO beyond 7.5 MA/2.65 T will be performed in predominantly D plasmas (with T content in the several % level), rather than in pure D plasmas, to optimize operational time, as described in sections 3.3.3.2 and 3.3.3.3. If the T-Plant were not available, part of this program towards expansion of the H-mode operational range would be performed with pure D plasmas and could require a significant increase in the foreseen operational time (by up to a factor of ~3 - 4), depending on the I_p/B_t combination reached before the T-Plant became available.

A major part of the H-mode studies in the first campaign of FPO will be carried out in D plasmas at 7.5 MA/2.65 T (q_{95} = 3) and will explore the requirements for ELM control with in-vessel coils, building on the findings of PFPO-2 experiments. An alternative option is to perform the initial deuterium H-mode characterization and ELM control studies with 5 MA/1.8 T plasmas, where the risk of divertor melting by uncontrolled ELMs is very low (see [75]). Assuming robust ohmic plasma initiation at 1.8 T has been established, this option provides an H-mode development path at q_{95} = 3 and should therefore exhibit similar MHD stability behaviour to 7.5 MA/2.65 T plasmas. A third option would involve starting the development sequence at 5 MA/2.65 T, increasing the plasma current sequentially. However, q_{95} varies from 4.5 to 3 as the current is increased towards 7.5 MA and so the associated variation in MHD stability (in particular, as related to ELMs) would need to be addressed when developing the scenarios.

As noted previously, the reduced shine-through loads in D operation provide more flexibility for exploiting NBI in 5 MA deuterium H-modes than in PFPO-2 experiments: figure 16 shows the ratio of the FW shine-through heat load compared to the permitted value when applying 33 MW of NBI power, with the lower density threshold of 2.5×10^{19} m^{-3} (i.e., ~$0.6\times n_{GW}$ at 5 MA) indicated. It has been shown that this density can be achieved in L-mode with gas and pellet

fuelling [166]. The less restrictive conditions for application of NBI, together with the lower expected H-mode threshold range of 14 MW (1.8 T) to 19 MW (2.65 T) at the minimum density threshold for shine-through in D plasmas, are expected to simplify the issues related to access and sustainment of H-modes at this level of plasma current (an operating regime which should have been extensively studied in H/He plasmas during PFPO-2).

Similarly, if L-H threshold studies in D plasmas discussed in section 3.3.2.3 show that small deviations from q_{95} = 3 are required to optimize H-mode access, this will affect the exact value of the plasma current at which H-mode access is studied in the 2.65 T experiments and also inform a decision on the optimum value of q_{95} at which subsequent experiments should be performed. The choice of the 'optimum' value of q_{95} must also encompass the need to satisfy the scientific goals of the project in terms of fusion power and fusion gain. A full assessment will therefore require comprehensive plasma modelling, benchmarked on the experimentally determined performance at ~7.5 MA/2.65 T.

Experimental plan for H-mode development in D plasmas: Bearing in mind the considerations outlined above, it is planned to launch the experimental program with 5 MA plasmas and then progressively increase I_p towards 7.5 MA in steps of 0.5 - 1.0 MA, preferably following a path with approximately constant q_{95}, or, if this were not possible, a constant B_t = 2.65 T approach. In each step, insofar as ELM divertor power loads allow without edge monoblock melting, and degradation of the W surface by repetitive thermal cycling, characterization of H-modes with uncontrolled type-I ELMs will be performed, similar to the program foreseen in PFPO-2 for heating pulses of similar duration (~50 s). Methodologies developed in PFPO-2 for ELM control (using RMP fields), W impurity exhaust and control of stationary power loads with impurity seeding would then be re-tuned to D plasmas: due to differences in the recycling and atomic properties of D and H/He and the expected consequences for the pedestal plasma, ELM dynamics and overall H-mode confinement, the phenomenology of H-mode plasmas in D is expected to be quantitatively (and, in some aspects, possibly qualitatively) different from that in H/He plasmas.

This program builds on the experience gained in PFPO-2 and will include scans in power levels above the L-H transition, variations in power mixes, and gas versus pellet fuelling comparisons, to determine effects on H-mode confinement, pedestal and SOL plasma characteristics, etc., as detailed in the PFPO-2 program in section 3.2.5.7. This experimental period will conclude with an integrated demonstration of a 7.5 MA/2.65 T deuterium H-mode plasma scenario which fulfils all requirements expected of a (15 MA) Q = 10 scenario related to core confinement and core-edge integration issues, such as W impurity exhaust and controlled stationary and ELM transient power loads to PFCs.

Operation in deuterium H-mode plasmas raises issues that require specific experimental focus or different/additional experiments beyond those detailed for the corresponding phase of PFPO-2. These include:

- *Development of optimized additional heating strategies to maximize plasma confinement while maintaining global MHD plasma stability:* Operation in D is expected to lead to higher plasma energies (and β values) leading to a different plasma response to error fields. It is therefore probable that dedicated experiments will be required to retune the correction of error fields with the EFCC and to optimize the power mix as plasma β increases. The

potential need for DEFC by the in-vessel coils to optimize H-mode performance would also be explored, noting that, at this low range in I_p, there should be margin in the ELMCC system to provide both ELM control and a DEFC functionality (i.e., the current level expected for ELM control is ≤45 kAt whereas the maximum coil current capability is 90 kAt). Similarly, specific tests will be included for optimization of vertical stability control in the presence of ELMs, with abrupt l_i and β_p changes, and for the control of NTMs by ECRH/ECCD. In parallel, the DMS will be re-tuned to provide the required disruption mitigation capability as the plasma energy increases.

Additional heating optimization will include an assessment of specific issues related to the use of heating systems in D plasmas, such as:

a) control of the H minority concentration to provide reliable ICRF heating at 2.65 T, due to the very different recycling and pumping behaviour from that in He plasmas used in PFPO-2;
b) demonstration and optimization of ICRF coupling in the varying edge plasma conditions expected in deuterium H-mode plasma scenarios;
c) re-assessment of the NBI shine-through loads with D^0 NBI in deuterium H-mode plasmas;
d) optimization of the sharing of ECRH/ECCD power between equatorial and upper launchers to provide multiple actions such as W core transport control (W accumulation avoidance), NTM control, etc.

Certain H&CD issues, already confronted in PFPO-2, would arise if 5 MA/1.8 T plasmas were chosen as the first step of the deuterium H-mode program: e.g., ICRF would require second harmonic H-minority heating and ECRH would operate in third harmonic absorption, which may be ineffective in an ohmic target plasma. Nevertheless, the PFPO-2 experiments should already have indicated whether a satisfactory resolution of these challenges was possible (and the preferred resolution), providing an initial basis for this scenario development. In addition, the availability of D^0 NBI, with reduced shine-through compared to the H^0 beams used in the PFPO campaigns, would provide additional flexibility in the scenario development (see, e.g., [166, 194]): to limit shine-through losses the NB injection energy could be reduced (though limiting the injected power), or the NBI power and plasma density could be raised gradually, and advantage could be taken of the higher 3rd harmonic ECRH absorption of plasmas pre-heated by the beams.

- *Studies of plasma fuelling in the stationary H-mode phase and of H-mode access and exit phases with pellet and gas fuelling, including the density evolution during confinement and pellet transients:* These studies are key to validating predictions of the fuelling efficiency of gas fuelling and recycled neutrals in ITER D and DT plasmas (expected to be very low) to inform optimization of H-mode access and exit through control of the plasma density in these phases and to inform optimization of pellet fuelling. Some initial experimental evidence on these issues is expected from PFPO-2 in H (gas and pellet fuelling) and He (gas fuelling alone) H-mode plasmas. However, dedicated experiments in D are essential to provide a more quantitative assessment in view of DT operation, due to differences between H/He and D plasmas in edge and pedestal plasma parameters (that affect edge ionization

and transport) and in core transport. In addition, the restricted operational space for H-mode plasmas in H is likely to restrict the H-mode experiments in PFPO-2 and it is possible that no significant experimental assessment of these issues can be made in hydrogen H-mode plasmas during PFPO-2. The experimental program will explore the range of stationary H-mode operational conditions and the degree of control of the plasma density in the H-mode access and exit phases that can be obtained with gas fuelling, pellet fuelling and the combination of both, over ranges in I_p (5.0 - 7.5 MA), in the ratio P_{in}/P_{LH}, in pellet specification (size, frequency and injection velocity) and in pumping throughput (controlled through shot-to-shot variations of the cryopumps' opening valves). These experiments will perform a full exploration of the effects of various fuelling and pumping choices on ITER H-mode plasma scenarios, thus providing essential data to assess the accuracy of the particle transport physics models and to develop the best H-mode fuelling strategies for access to and exit from burn, i.e., data required for the development of the DT research program.

- *Exploration of various scenario options for entrance to and exit from high confinement H-modes, including H-mode entrance in the current ramp-up phase and exit in the ramp-down phase, as well as phasing of the pellet fuelling ramp-up/down versus the heating ramp-up/down:* These experiments will build up on the initial experience in PFPO-2 and will expand those results to relevant conditions with a view to their application to DT plasmas. The experiments will be carried out in plasmas with an I_p flat-top of 7.5MA and their main aim is to determine:
  a) the evolution of plasma parameters (including l_i and core W concentration) in the H-mode access/exit transient phases, and;
  b) the level to which these parameters can be controlled by the heating and fuelling waveforms.

  This is essential to initiate the development of higher I_p scenarios in DT: the ratio of auxiliary input power to the H-mode threshold power will be lower at higher values of I_p and B_t, and therefore optimization of α-heating will be necessary to ensure the development of robust schemes for access to and exit from burning plasma conditions, i.e., avoiding fast back transitions to L-mode and core accumulation of W [195]. In higher I_p scenarios in DT, the fine details of access to and exit from the burning H-mode plasma depend on the evolution of plasma parameters in the core and pedestal during the transient phases (e.g., pedestal plasma formation for the low edge ∇n conditions expected with gas fuelling). The knowledge of ELM control during these transient phases acquired during PFPO-2 will be applied and retuned to D plasmas. The final goal of these experiments will be to demonstrate an optimum scheme for ELM control with RMP fields under stationary conditions and throughout the H-mode access and exit phases. This scheme (or schemes) must be established both for the case in which these access/exit phases occur at the flat-top current of 7.5 MA and for cases in which access and exit occur during the current ramp-up/-down in the range of 5.0 - 7.5 MA, in which q_{95} varies over the range 3.0 - 4.5. Based on experience gained in PFPO-2 experiments, the ELM triggering back-up schemes (vertical plasma oscillations and pellet triggering) will be applied during the transient phases, when necessary, to ensure that ELM control is maintained.

- *Specific experiments to demonstrate a full edge-core integrated scenario at 7.5 MA/2.65 T with performance equivalent to that required for the achievement of Q = 10 in 15 MA/5.3 T plasmas:* These experiments will integrate the knowledge acquired in this phase regarding the control of ELM transient loads with 3-D fields, of W impurity exhaust and of stationary divertor exhaust using impurity seeding in both stationary H-mode conditions and H-mode access/exit phases, and will exploit this to demonstrate a robust H-mode scenario at 7.5 MA/2.65 T that can be extrapolated to the conditions required for $Q = 10$ operation. Basic elements of such a scenario should have been explored in PFPO-2, but it is likely that this exploration will only have been performed in helium H-mode plasmas (given that H-mode operation in H is likely to be marginal) and at relatively low β. Due to the significant changes expected in the SOL, pedestal and core plasma when operating in D, and the consequences for edge-core integration issues (ELM control by 3-D fields depends strongly on the plasma response, while pedestal W transport and λ_q are expected to depend on neoclassical-related effects, etc.), it is expected that significant differences will result in the optimization of the various schemes and strategies for D compared to those applied in PFPO-2. More specifically, operation in D will allow an appropriate assessment of the effect that the margin above the L-H transition threshold and the value of β have on the overall optimization of scenarios and on the achievable H-mode confinement: for D plasmas in these conditions, the ratio of the input power to the L-H threshold power can be varied over a wide range, $P_{in}/P_{LH} = 1.0 - 4.0$ for $\langle n_e \rangle = 0.4 - 1.0 \times n_{GW}$.

Heat loads and detachment control: It is only in the FPO phases that stationary first wall and divertor target heat loads can routinely attain engineering limits (with the exception of certain 'pathological' operating conditions). By the start of FPO, power load monitoring and control should have reached a level of maturity sufficient to allow the progressive increase of input power and current in H-mode which will be made possible by the switch to D. In fact, progression to high power H-modes beyond half current will not be possible until feedback schemes for divertor heat load control have been fully optimized and shown to be robust and reliable.

High input power ($P_{SOL} \gtrsim 40$ MW) deuterium H-mode plasmas without extrinsic seeding at 7.5 MA/2.65 T ($q_{95} = 3$) are expected to produce power flux densities in the strike-point regions close to steady-state power handling limits, and considerably above them at low neutral pressure (see [3-Appendix C]). Such operation will require active detachment control and can be performed at densities high enough for meaningful application of extrinsic seeding. This also corresponds to the conditions under which unmitigated ELM energy densities are expected to produce clear toroidal gap edge melting of the W divertor monoblocks [45, 75], leading to potential problems with ELM-driven W influxes, requiring that ELM mitigation, or suppression, be fully developed.

With the progressive increase of I_p in H-mode which will be possible in FPO, the database of inter-ELM $\lambda_{q,near}$ can be expanded beyond the lower power H-modes accessible in the PFPO phases, permitting evaluation of the extent to which the predicted $\lambda_{q,near} \propto 1/I_p$ scaling is preserved as plasma performance increases. Confirmation of this trend to the highest currents in ITER would imply that the requirements for detachment control would be even more stringent and that the operational window would likely be more constrained as I_p increased.

As in the PFPO phases, heat load characterization should proceed via L-mode plasmas (but now in D), to expand the PFPO database, while applying the detachment control techniques developed in PFPO-2. Application of 3-D fields at higher current and density in L-mode will allow the effect of divertor dissipation on the perturbed divertor target heat load distribution to be studied. Even 7.5 MA/2.65 T deuterium H-modes are likely to require integrated scenarios coupling ELM control with impurity seeding, thus requiring a detailed investigation of divertor heat load patterns in the presence of dissipation and of (potentially rotating) magnetic perturbations.

Divertor heat load characterization will thus be integrated with scenario development and may not require much dedicated experimental time. Some specific experiments will be necessary to study main chamber power loads, along the lines performed in PFPO-1 and PFPO-2 (e.g., effect of separatrix separation on steady-state loading at the top of chamber), though H-mode studies are likely to be limited by divertor constraints (e.g., analysis of the impact of unmitigated ELMs on the first wall will not be possible if such ELMs are incompatible with divertor power loads or W influxes).

This phase of experiments will, for the first time, allow heat flux control by impurity seeding in H-mode to be rigorously tested under relevant conditions. This would encompass tests of the response to loss of impurity injection, the effect of impurity injection through the main chamber and divertor gas inlets, and the detailed dynamics of the combination of divertor/main chamber fuelling with impurity seeding. An important outcome of this phase is the confirmation that Ne can provide the required power exhaust compatible with high confinement H-mode operation: until the advent of higher power H-mode operation in D, extrapolation of experimental results to burning plasma conditions may be problematic, as lower power hydrogen H-modes are expected to exhibit lower pedestal temperatures and densities (and helium H-modes are not relevant for addressing this question). Early H-mode experiments in D, prior to the introduction of T, should allow a much clearer assessment of whether, as indicated by plasma boundary simulations of ITER scenarios and JET experimental results (e.g., [51]), Ne can provide the required divertor radiation with high H-mode confinement. If this is not confirmed, other impurities (Ar, N_2) will be explored at this stage. We note that N_2 is less preferable for ITER due the formation of ammonia. Should the use of N_2 seeding prove to be essential it would be important to further quantify the rate of ammonia formation (section 2.5.2) in more relevant, higher power H-mode conditions (higher surface temperatures), for which studies may have already begun in PFPO-2.

The main deliverables for this phase are:

- A robust deuterium H-mode scenario at 7.5 MA/2.65 T, having $H_{98} = 1$ with integrated fuelling, error field correction, control of NTMs and of W accumulation, ELM control with 3-D fields (from in-vessel coils) which provides acceptable transient power loads and impurity exhaust, control of stationary power loads via a radiative divertor, and exhibiting low disruptivity, and with reliable and effective DMS operation when disruptions do occur. This provides the basis for predictive modelling and for the operational development of the 15 MA/5.3 T DT H-mode scenario to be demonstrated in FPO;
- Evaluation of the power level and power mix required to access and sustain high confinement H-modes in D plasmas. This will provide a high confidence estimate of the requirements for DT plasmas. If the baseline additional heating level is found to be insufficient for successful $Q = 10$ operation at this late stage, upgrades of the heating

systems could be implemented to ensure the achievement of the $Q = 10$ goal, although the high-Q DT research would need to be delayed until such upgrades were fully functional.

- First evaluation of key plasma behaviour in deuterium H-modes relevant to the optimization of plasma scenarios in D and DT plasmas. This includes the degree of control of pedestal and core plasma density, temperature and l_i which can be achieved by tuning the heating and fuelling schemes (and their waveforms) in both the transient H-mode access/exit phases and the stationary ELM-controlled H-modes;
- Confirmation of the ELM control capability that can be expected from in-vessel coils under relevant D plasma conditions during transient H-mode access/exit and stationary phases over a current range of 5 MA - 7.5 MA, allowing a high confidence evaluation of these capabilities for later high I_p operation in D and DT. If this is found to be insufficient, or marginal, an upgrade of the back-up ELM triggering scheme based on pellet pacing will be implemented at this stage (e.g., addition of two pellet injectors specially designed for pellet pacing);

In parallel with the development of the 'reference' deuterium H-mode scenario, hydrogenic retention studies, diagnostic validation and investigations of intrinsic and extrinsic impurity behaviour, etc., will have been performed.

Progress towards full current and field in deuterium H-modes: Demonstration of a reliable ELMy H-mode scenario at parameters as close as possible to 15 MA/5.3 T and with plasma characteristics extrapolating to high fusion performance in DT operation is a key step on the path to high fusion power production. Based on the considerations outlined above, it is planned to undertake that development program in plasmas containing some level of tritium, as discussed in more detail in section 3.3.3.1. In the following, an additional research program towards this target is outlined which would be implemented only if delays in the commissioning of the T-Plant should necessitate performing these studies in pure D plasmas.

From the integrated demonstration at 7.5 MA/2.65 T, the range of plasma currents and fields would be expanded towards 15 MA/5.3 T along an approximately constant $q_{95} \sim 3$ path, similar to the L-mode development plan (I_p = 9.5, 12.5 and 15 MA) in figure 8. Precise value of current and fields to be used at intermediate steps will be the subject of studies during the development, as they are expected to be determined by the need for central heating by ECRH and ICRF to avoid W accumulation while maintaining the capability for off-axis ECRH/ECCD to control NTMs, etc. Given the expected H-mode threshold in D plasmas and the maximum additional heating of 73 MW, it is likely that the maximum I_p/B_t combination where stationary H-mode operation can be sustained in D is ~12.5 MA/4.5 T, as shown in figure 17. Operation at higher plasma currents, where H-mode access may be marginal, will likely carry additional risks due to possible difficulties in controlling plasma behaviour, with the potential for disruptions at high I_p.

For each current level, a similar set of experiments to those at 7.5 MA/2.65 T, leading to a demonstration of an integrated H-mode scenario, is foreseen. This is not included in the plans for pure D and would only be implemented in case of delays in the T-Plant commissioning.

3.3.2.5 Edge physics and PWI studies in D plasmas

Wall conditioning: During the FPO phase, only D-ICWC is of relevance, either at half or full field with a frequency, f, corresponding to f/B_t = 7.0-10.5 MHz/T, depending on the IC frequency

applied. The efficiency of D-ICWC for the removal of medium Z impurities can be further evaluated in FPO whenever cleaning discharges are required for programmatic or operational needs. Dedicated trace-T removal experiments using isotopic exchange with D-ICWC can be also executed during the D phase. Gas balance studies will be performed, as before, using torus pressure measurements, RGAs and analysis by gas chromatography of the gas released from the partial regeneration of the cryopump (to ~100 K). Once experience has been gained on the operational parameters to be used (pressure, power, duty cycle and poloidal fields), D-ICWC can be applied to effectively control the T-inventory build-up in the vacuum vessel, expected to occur principally via Be co-deposition in the divertor.

Extrapolations from current devices, in particular, the JET-ILW, show that isotopic exchange in D-ICWC discharges could remove an amount of T comparable to that of the estimated retention per nominal DT pulse [77, 81]. However, this may only hold if these discharges are regularly applied before thick T-rich co-deposits accumulate. Only in this case will ICWC be able to contribute to mitigation of the T-inventory build-up (the so-called 'good housekeeping approach' [196]).

Fuel retention and material migration: Operations with pure D will increase the accuracy of gas balance measurements, allowing estimates obtained during PFPO phases to be further refined. In particular, characterization of D retention during H-mode operation with ELM control and a radiative divertor at high power will expand the existing database. The higher mass of D will cause an increase of the Be sputtering from the first wall, both between and during ELMs. Regular monitoring of material migration will therefore be important. This can be done parasitically during operations via visible spectroscopy and regular operation of the tritium and erosion monitors. In addition, routine execution of the reference pulse (see [3-Appendix D]) will allow for routine monitoring of impurity sources.

Most of the fuel retention characterization will be performed in parallel with the main scientific program, but it might be beneficial to perform a dedicated fuel removal experiment before the start of trace-T experiments. This would involve D-removal by hydrogen ICWC followed by a full bake of the PFCs. Since co-deposits will have accumulated during this phase, benchmarking of the fuel removal simulations can be performed with thicker deposits, allowing validation of the knowledge gained during the PFPO phases.

A similar strategy will be pursued during trace-T experiments (see section 3.3.2.6), where T-removal using isotopic exchange with D can be developed and validated. An important additional aim of that campaign will be to develop/validate the T accounting strategy, which relies on measurements performed in the T-Plant for global accounting (including decay), via gas balance measurements, to determine in-vessel retention, and neutron measurements, for determination of the burn-up fraction. Performing a further fuel removal exercise before the start of DT operations would also be desirable to validate earlier measurements. This would be of particular importance in informing a determination of the frequency with which these procedures will need to be employed during DT operations to ensure that the in-vessel T-inventory remains below regulatory limits.

3.3.2.6 Trace tritium H-mode experiments

Objectives and plasma scenarios: At this stage of the Research Plan, the T-Plant commissioning should be sufficiently advanced to support H-mode experiments in D plasmas

containing trace concentrations of T, i.e., with T concentrations of up to several percent, involving a much smaller T throughput (typically more than 100 times lower) than that required for $Q = 10$ operation in 300 - 500 s burn pulses. The basic scenario foreseen for these experiments is the integrated deuterium H-mode scenario at 7.5 MA/2.65 T ($q_{95} = 3$) developed in section 3.3.2.4, and the main research aims are to carry out fuelling and particle transport studies of T in deuterium H-modes and to perform an initial evaluation of T-retention under H-mode operation. In addition, the program will encompass initial commissioning of diagnostics required for the DT experimental phase, especially the 14.1 MeV neutron diagnostics, a key capability for investigation of core physics processes involving nuclear fuel (T transport, DT fuel mixture control, etc.), both in this phase and in later, full DT, experiments.

Experimental plan: Diagnostics for tritium measurements in the confined plasma are designed to measure T concentrations to the 1% level with a time resolution of 100 ms and 20% accuracy. However, the final capabilities of the diagnostics are dependent on plasma parameters and it may be the case that, for very low T concentrations, the viable time resolution exceeds 100 ms when 20% accuracy is required. Optimization of the trace-T level for accurate diagnostic measurements is, therefore, included as the first item in the experimental plan, which consists of the following steps:

- Optimization of the trace-T concentration (by T-doped deuterium pellet fuelling) into 7.5 MA/2.65 T plasmas in order to ensure the highest quality measurements and to allow the commissioning of other diagnostics required for the DT phase (i.e., beyond those required for determining the T concentration (e.g., 14.1 MeV neutron measurements));
- For at least two trace-T levels, fuelling experiments will be performed by injecting the trace-T by gas puffing and by T-doped deuterium pellets. DT mix control experiments will be performed both for stationary H-mode conditions and during the H-mode access and exit phases. The main goals of these experiments are:
  - Validation of predictions for T fuelling efficiency by gas fuelling and pellet fuelling derived from stationary deuterium H-mode plasmas;
  - Optimization of pellet fuelling for efficient core fuelling;
  - Validation of predictions for core T transport derived from stationary deuterium H-mode plasmas and identification of possible effects associated with the different masses of T and D on both anomalous and neoclassical transport [195, 197] and on ELM control; the trace-T gas/pellet fuelling schemes would be re-optimized accordingly;
  - Studies of T fuelling (most likely by pellets) in the transient H-mode access/exit phases to provide a basis for optimization of T throughput and for establishment of robust H-mode access/exit phases in DT plasmas. These experiments will address the requirements for (and effectiveness of) using T fuelling to change the DT mix (at the trace level) in the H-mode access/exit phases by varying the timing between the start/stop of tritium injection and the start/end of the H-mode for a range of deuterium L-mode densities (pre- and post-H-mode);
  - Experiments to diagnose T-retention, both by in-situ diagnostics and by gas balance, will be performed in parallel. This analysis will be accompanied by studies to demonstrate in-situ removal techniques, such as ICWC, between pulses.

The main deliverables for this phase are:

- First assessment of the T fuelling efficiency in ITER integrated H-mode scenarios (at 7.5 MA/2.65 T) and of the capabilities for DT mix control by gas and pellet fuelling both for stationary and transient phases;
- Essential data on T transport for benchmarking numerical models to be used to predict the schemes required to achieve DT mix control for optimum burn access/exit and stationary burn optimization;
- Initial assessment of T-retention in conditions relevant for DT operation to confirm the evaluation performed on the basis of D experiments and the effectiveness of between-shot T-removal techniques such as ICWC.

3.3.2.7 Initial development of hybrid/ advanced scenarios in D plasmas

Objectives and plasma scenarios: The overarching objective for this campaign is to optimize non-inductive current drive fraction in high-β, low collisionality, integrated q_{95} = 3.6 (hybrid) and q_{95} = 4.5 (candidate steady-state) scenarios. Note that, due to the constraints on plasmas with high non-inductive fraction in this phase of the research program (in particular, the negligible or limited contribution from α-heating), it may not be possible to establish fully non-inductive plasma operation. Throughout the discussion, therefore, plasmas designed to achieve the highest non-inductive current fraction will be referred to as 'candidate steady-state' scenarios.

The results from this campaign will establish the basis for those foreseen in the DT campaign, ultimately achieving highly, or fully, non-inductive discharges with durations of 1000 - 3000 s and with significant levels of fusion power production. Plasma scenarios with q_{95} = 3.6 and 4.5 at both 2.65 T (6.3 and 5 MA respectively) and 4.5 T (11 and 8.5 MA respectively) will provide the basis for these studies. Consistent with the strategy followed for deuterium H-modes in section 3.3.2.4, experiments performed at 2.65 T will most likely be performed in pure D plasmas while those at 4.5 T will most likely be performed with some level of T (a concentration of at least 10%), taking advantage of the availability of the T-Plant at this stage. Should the available T throughput not be sufficient, experiments at 4.5 T will also be carried out in D plasmas.

To accomplish these goals, it will be necessary to have full H&CD systems operational with pulse lengths of ~50 s, fast ion diagnostics and current profile measurements available, and real-time β, and current/pressure profile control developed. The DMS should be routinely available and fully functional. Stationary H-modes with robust ELM and density control and real-time divertor detachment control must have been established in 2.65 and 4.5 T plasmas with $\langle n_e \rangle / n_{GW} \geq 0.5$. This implies that the 2.65 T elements of this program rely on the successful completion of the corresponding H-mode program (section 3.3.2.4), while the program at 4.5 T will probably rely on scenario developments in the DT H-mode program discussed below (in section 3.3.3.3).

The major steps in this program are described below. However, it should be noted that they assume successful completion of earlier phases of the research plan, such as H-mode scenario development (section 3.3.2.4) and commissioning of advanced control schemes (section 3.3.2.1):

- Application of β/ $j(r)$/ $p(r)$ control algorithms using target current profiles for q_{95} = 3.6 and 4.5 at 2.65 T in stationary H-mode conditions;

- Optimization of performance and non-inductive current drive in 2.65 T discharges at q_{95} ~ 3.6 to 4.5 (I_p ~ 6.3 to 5 MA);
- Optimization of performance and non-inductive current drive in 4.5 T discharges at q_{95} ~ 3.6 to 4.5 (I_p ~ 11 to 8.5 MA).

Experimental plan: Given (i) that the detailed implementation of this program will rely on experience gained from preceding elements of the Research Plan and that (ii) there remains a range of physics uncertainties relating to the extrapolation of hybrid and fully non-inductive scenarios to ITER, it would be unrealistic to formulate a detailed specification for the plasma scenarios spanning the range q_{95} = 3 - 6 (focussed on q_{95} = 3.6 and 4.5) at 2.65 T and 4.5 T to be explored within this program. Nevertheless, it is possible to identify the specific experimental objectives to be pursued:

- Assessment of the diagnostic and control capabilities in longer-pulse plasmas to support the development of control techniques for accessing current profiles consistent with steady-state operation in ITER;
- Establishment of a basis for fully non-inductive plasma operation in ITER, including initial tests of closed-loop feedback capabilities;
- Development and sustainment of q_{95} = 3.6 hybrid scenarios with $H_{98} \geq 1$ which integrate all ITER operational requirements, including edge-core integration (fuelling, power loads, impurity exhaust, etc.), MHD control, etc., and evaluation of expected fusion performance in DT;
- Establishment of (~ 50 s) plasmas with optimized non-inductive current drive fraction integrating all ITER operational requirements, including edge-core integration (fuelling, power loads, impurity exhaust, etc.), MHD control, etc., and evaluation of expected fusion performance in DT;
- Assessment of MHD stability (NTM, AEs, etc.) and confinement properties of long-pulse q_{95} = 3.6 hybrid scenarios and candidate steady-state scenarios to determine the control requirements for stable operation;
- Development of disruption detection and avoidance schemes for highly non-inductive plasmas, and demonstration of disruption mitigation - these might well deviate from those for q_{95} = 3 - 4 plasmas. This will include an assessment of the need for RWM control, which will be explored within the installed capabilities of the ELMCC (90 kAt, 5 Hz rotation) and the coil current margin available beyond the level required for ELM control. For the I_p/B_t levels in these plasmas, the available current capability for RWM control is expected to be >45 kAt for 2.65 T and >15 kAt for 4.5 T plasmas;
- Assessment of the pedestal characteristic of hybrid and candidate steady-state plasma scenarios and of the coupled core and pedestal optimization at the expected operating points for hybrid and steady-state operation in DT. This is expected to require optimization of the heating power level and mix, torque input, fast particle content and, possibly, plasma density to determine the dominant physics process that leads to enhanced energy confinement (i.e., $H_{98} \geq 1$) in these scenarios;
- Completion of model validation for codes simulating ECRH, ICRF and NBI heating and current drive in D plasmas to enable extrapolation to the corresponding hybrid and steady-state plasmas in DT. The validation activity is also key to informing any decision to proceed

with an ECRH&CD upgrade at this stage. This is currently considered for the achievement of the $Q \sim 5$ DT steady-state operation goal [185, 186]. H&CD model validation must be given high priority throughout the IRP phases addressing steady-state scenario development, initially in PFPO-2 and, most importantly, in this first stage of FPO. Successful model validation will provide a powerful tool for planning experiments during later FPO DT campaigns, and, ultimately, will increase confidence in the extrapolation of steady-state scenarios achieved in ITER towards DEMO. In this context, it should be noted that the installation of a 3rd HNB is required for the achievement of the $Q \sim 5$ steady-state goal [185, 186];

- Analysis of the experimental behaviour of fast ions and validation of models for fast ion behaviour associated with energetic ion populations produced by the several heating systems in D plasmas. Differences are expected from behaviour observed in PFPO-2 plasmas because, *inter alia*, the HNBs inject D, rather than H, and the ICRF will exploit ^{3}He-minority heating at 4.5 T, while H-minority heating was applied at 2.65 T (see section 3.2.3). Determining the nature of any MHD instabilities observed (e.g., global TAE modes in the outer region of the plasma) [187] will be a particular focus of the experiments;
- If AEs become unstable, investigating the impact of the various H&CD systems, in particular, the capabilities of these systems to influence AE stability by local modifications of plasma parameters would be a key experiment (since such modifications influence the Landau damping experienced by these modes and change the spectrum of compressional and Alfvénic modes [188]). If suitable actuators for AE control were identified, experimental time could be allocated to further refinement of the control techniques and associated controllers [198];
- Analysis of the effects of ELMCC on fast ion losses for plasmas with q-profiles required for hybrid and candidate steady-state deuterium H-mode plasmas [199] and validation of simulation models. This would be complementary to experiments for the inductive scenario discussed in section 3.3.2.4.

The main deliverables required from this operational phase are:

- Assessment of the effect of the different fuel species (H/He/D) on the development of hybrid and non-inductive scenarios in H-mode;
- Establishment of a validated model basis for extrapolation of D plasma scenarios to long-pulse and steady-state DT operation;
- First assessment of β/ $j(r)$/ $p(r)$ control in deuterium H-modes and its consequences for plasma performance;
- First assessment of the current drive capabilities of the H&CD systems in long-pulse deuterium H-mode plasmas at $q_{95} \sim 3.6$ and 4.5 for two B_t values. This assessment will lead to (i) refinement in the application of the available H&CD, (ii) establishment of the upgrade requirements for control system sensors and actuators, including, potentially, an ECRH&CD upgrade for the development of long-pulse plasmas and/or NTM control and (iii) evaluation of the need to upgrade power supplies for active control of RWMs;
- Development of closed-loop feedback algorithms for control of core performance and edge-core integration (fuelling, power loads, impurity exhaust, etc.);

- Demonstration of integrated hybrid discharges at q_{95} = 3.6, having $H_{98} \geq 1$ and satisfying all ITER operational scenario requirements including edge-core integration (fuelling, power loads, impurity exhaust, etc.), MHD control, etc.;
- Demonstration of long-pulse (~50 s) plasmas with an optimized non-inductive current drive fraction and integrated with all ITER operational scenario requirements including edge-core integration (fuelling, power loads, impurity exhaust, etc.), MHD control, etc.

3.3.3 Operational plan for DT plasma experiments towards Q = 10

3.3.3.1 Objectives and plasma scenarios

From a basic integrated scenario at 7.5 MA/2.65 T, derived from D and D+trace-T experiments described in sections 3.3.2.4 and 3.3.2.6, further development of the DT program will proceed by increasing I_p and B_t in steps along a $q_{95} \sim 3$ trajectory (with I_p = 9.5, 12.5 and 15 MA, plus a possible intermediate step at 13.5 MA at constant B_t) while aiming to maintain a stationary H-mode duration of ~50 s. For each current level, the T concentration will be varied from trace levels to ≥60% to evaluate the influence of the increasing α-heating on plasma behaviour and to determine the optimum T concentration for maximum fusion power production. As discussed in section 3.3.2.4, it is expected that in D and D+trace-T plasmas the installed baseline heating power of 73 MW will be insufficient to support stationary H-mode operation beyond ~12.5 MA/4.5 T. At higher currents, maintenance of stationary H-mode conditions will likely require plasmas containing significant T concentrations: a higher T/D ratio will decrease the H-mode power threshold, due to the isotope mass scaling of the threshold, and the total input power benefits from the additional α-heating. Moreover, the use of higher T concentrations can mitigate risks related to changes in the ECRH and ICRF power deposition profiles at intermediate B_t values between 2.65 T and 5.3 T: in such cases, α-heating will remain centrally peaked and, even for the low Q values (~1 - 2) expected at low I_p levels, the resulting α-heating power will be in the range of tens of MW, which is sufficient to have an important influence on the W concentration, according to the ITER modelling analysis illustrated in figure 18 [195].

The DT research program towards achievement of the Q = 10 goal is divided into three main phases:

i. Characterization of H-mode access in DT, a thorough exploration of DT H-modes and the solution of operational issues in 7.5 MA/2.65 T H-modes;
ii. Expansion of the H-mode operational range to 15 MA/5.3 T, concluding with the demonstration of Q = 10 operation for burn durations of ~50 s;
iii. Developments required to increase the Q = 10 burn duration into the range 300 - 500 s, thereby concluding with the demonstration of the principal ITER scientific goal in inductive operation.

It is important to note that reaching the Q = 10 short pulse goal during the first operational campaign in FPO is very unlikely: this campaign, lasting 16 months, and corresponding to 415 operational days, will encompass significant commissioning and operational development activities associated with the start of D, and subsequently DT, operations. The present Research Plan therefore foresees that fusion power production at the level of ~250 MW for ~50 s with $Q \sim 5$ will have been demonstrated by the end of FPO-1. Definition of the plasma scenario in which this can be achieved will depend, of course, on results of the research performed within this initial

phase of FPO. Results of current modelling, illustrated in figure 19, suggest that candidate scenarios could include $I_p \sim 12.5$ MA at $\langle n_e \rangle \sim 10^{20}$ m^{-3} (i.e., $\langle n_e \rangle \sim n_{GW}$) and $I_p = 15$ MA at $\langle n_e \rangle \sim 0.7\times10^{20}$ m^{-3} (i.e., $\langle n_e \rangle \sim 0.6\times n_{GW}$) for values of τ_E predicted by the IPB98(y,2) scaling [200]. Table 14 provides an overview of the range of experiments and plasma parameters, together with estimates of the allocation of experimental time, which should be encompassed by the DT research program within FPO-1.

By the start of FPO-1, ITER should be equipped with the full contingent of diagnostics required for DT operation. Diagnostic-specific limitations are therefore not considered in the following sections. Should it turn out, however, that key diagnostics do not provide the required measurements with the specified accuracy, or if the measurement requirements prove to be inappropriate to the plasma parameters achieved in ITER during the implementation of the Research Plan, appropriate mitigation actions will have to be implemented.

It is also expected that all tools needed to characterize fuel retention and material migration will already have been validated and a good understanding of erosion/redeposition will have been attained. Measurements would then be integrated into a routine monitoring program to check the power handling capabilities and thermal response of PFCs, to ensure that FW erosion remains within allowable limits, and that fuel retention rates are as expected and do not change with time. One important aspect, as wall fluence and integrated material erosion accumulates, will be to monitor the occurrence of co-deposit flaking, which is known to occur when co-deposits become too thick. As mentioned earlier, this would represent a potential source of dust creation in the vessel and could be the dominant dust production mechanism when the disruption mitigation/avoidance system has reached its target for mitigation rates.

3.3.3.2 Optimization of DT plasma scenarios at 7.5 MA/2.65 T

Characterization of H-mode access: To prepare for the following DT H-mode operation, an assessment of the L-H power threshold will be performed in DT plasmas. This includes the scaling of the H-mode threshold with T concentration, plasma density and heating mix at 2.65 T and $q_{95} \sim 3$. An initial study of H-mode access at $q_{95} = 5$ in the current ramp-up will also be performed.

As soon as the T-Plant throughput allows, an assessment of the isotopic mass dependence of the H-mode threshold will be completed by exploring H-mode access in DT plasmas with up to 50% T concentration and by incorporating data from earlier D experiments. H-mode access in the current ramp will also be explored by accessing the H-mode at ~2/3 of the flat-top level (i.e., 5 MA). These elements are essential for the further development of H-mode scenarios in DT, where the optimization of the DT mix and the heating mix is required to ensure a robust H-mode transition for both the flat-top and the current ramp-up phases. Outlines of the foreseen experimental conditions covering the ranges to be explored are summarized in Tables 15 and 16 for stationary DT plasmas and for the current ramp-up experiments respectively.

Major experimental challenges for these studies include:

- Achievement of sufficiently reliable ELM control to avoid long ELM-free periods that can cause edge melting of the W divertor monoblocks and W accumulation in the main plasma. ELM control by in-vessel coils and by back-up ELM triggering schemes (pellet pacing and vertical position oscillation) will therefore be applied based on previous operational experience in PFPO-1, PFPO-2 (H/He plasmas) and FPO (D plasmas);

- Ensuring robust DT mixture control for experiments where the T concentration is scanned by gas fuelling and/or pellets.

Experimental plans for exploration of DT H-modes at 7.5 MA/2.65 T: The 7.5 MA/2.65 T D and D+trace-T plasmas should have been extensively explored and understood by this point, providing a basis from which H-modes scenarios with gradually increasing T content can be developed, producing greater levels of α-heating until the optimum T concentration is exceeded and the α-heating decreases. In principle, the modification of plasma characteristics with increasing T concentration is expected to be gradual, as the maximum level of α-heating at 7.5 MA/2.65 T will be moderate compared to the auxiliary heating sources (<20%) and the reduction in the H-mode power threshold from pure D to ~50/50 DT is expected to be ~20%. On the other hand, new physics phenomena may appear with the variation in D/T ratio. For example, if the level of core turbulence is low in ITER, neoclassical DT transport effects due to the different masses of D and T can cause density gradients to appear in the central plasma region which do not exist in D plasmas, and this can affect W transport [195], as shown in figure 20.

The experimental plan for this phase proposes a variation in the tritium concentration from levels of ~10% (well above the trace-T level) to levels in excess of 60 - 70%, which is expected to be well beyond the optimum concentration for fusion power production. Various levels of additional heating and additional heating mixes will be explored and the impact of the increasing T concentration on core/edge/boundary plasma characteristics will be characterized. Demonstration of capabilities to control the DT mix, derived from experimental results in D+trace-T plasmas, is a key ingredient to ensure the feasibility of this characterization. For the highest fusion powers some accumulation of thermalized He will occur, although probably at a level an order of magnitude lower than that in $Q = 10$ plasmas, but this should allow initial studies on the exhaust of He ash. To ensure that the core He concentration exceeds the measurement threshold of 1%, so that the time evolution of the core He concentration can be determined, the pumping throughput might need to be decreased, but this may need to be balanced against the pumping requirements for control of the density and fuel mixture.

During this phase, moderate pulse durations of several tens of seconds are likely to be required to assess long time-scale stability of established feedback algorithms, such as those required for the control of the DT mixture. Therefore, it is foreseen that the stationary phase of these plasmas should be at least 50 s long (i.e., $\sim 25\,\tau_E$). The final phase of the experimental program will concentrate on the optimization of fusion performance and its control. It is planned to use fuelling and additional heating schemes to develop strategies to be applied in later experiments at higher plasma currents and higher fusion power, where development of such schemes is more difficult due to the need to control the higher power loads to plasma-facing components in parallel with the scenario development.

The principal experimental activities foreseen are:

- Scans of the core plasma T concentration, starting at ~10% and progressing beyond the optimum DT mix, most likely by pellet fuelling, for various levels of additional heating power/ additional heating mix and stationary H-mode plasma density to assess the effects of increasing T concentration on:
  - The L-H power threshold, which is expected to decrease with increasing T concentration;

  - Edge pedestal plasma characteristics and ELM power loads (uncontrolled, if permissible): the pedestal pressure and the associated energy losses due to uncontrolled ELMs are expected to increase with increasing T-fraction;
  - MHD stability of the core plasma including fast particle effects in DT plasmas (from NBI, ICRF and fusion-produced α-particles);
  - Core He concentration and collateral effects (e.g., ICRF parasitic resonances, divertor PWI effects, etc.) and He exhaust via uncontrolled ELMs (if permissible) and controlled ELMs.
- Assessment and retuning of control schemes which depend on increasing T concentration and plasma energy (energy confinement is expected to follow T concentration), plus specific scenario control issues for DT plasmas (derived from preliminary developments in D and D+trace-T plasmas):
  - Optimization of T plasmas for stationary H-modes (pellet, size, injection velocity, etc.) and studies of burn control by fuelling;
  - Development of schemes for robust H-mode access/exit phases, including optimization of the associated density waveforms and evolution of the T concentration (e.g., reaching the target DT mix in L-mode and maintaining it through the H-mode, or increasing the T-fraction following the H-mode transition, etc.);
  - Re-optimization/ redevelopment of schemes to maintain stationary control of exhaust power by operating in the radiative divertor regime, and evaluation of the consequences for core plasma confinement (both W impurity production and transport are expected to be affected by increasing T concentration);
  - Re-optimization/ redevelopment of the 3-D fields applied by the in-vessel coils to provide ELM control - increasing T concentration is expected to increase the pedestal plasma pressure, and hence the ELM energy losses, necessitating this step. This re-optimization must integrate other scenario requirements such as radiative divertor operation, impurity control and He exhaust while limiting losses of fast particles in the applied 3-D fields;
  - Re-optimization of NTM control schemes, sawtooth control schemes, error field correction, disruption and runaway mitigation, etc., which may be required due to the increase in plasma β and changes in the current profile associated with an increased T-fraction (e.g., a higher pedestal pressure implies a higher edge bootstrap current, causing a lowering of l_i, etc.);
  - Re-optimization of the H&CD schemes to avoid W accumulation as the D/T ratio is varied.

In parallel with these studies, further studies on T-retention and removal (e.g., ICWC or ECWC) will be performed to quantify T-retention and the effectiveness of T-removal techniques in conditions very similar to those expected in $Q = 10$ plasmas.

The main deliverables of this experimental phase are:

- Determination of the variation of the H-mode power threshold with T concentration at 2.65 T, for both flat-top plasmas ($q_{95} = 3$) and during the current ramp-up ($q_{95} = 5$);
- Robust 7.5 MA/2.65 T DT H-mode scenarios with $H_{98} = 1$ over a range of densities and additional heating power, with integrated fuelling and DT mix control, NTM and W

accumulation control, error field correction, ELM control using 3-D fields from in-vessel coils to provide acceptable transient power loads and impurity exhaust (including He exhaust), stationary power load control through a radiative divertor while maintaining low disruptivity, but effective DMS operation when disruptions occur. This scenario would provide a benchmark for predictive modelling to be used to guide the operational development of the DT program towards the 15 MA/5.3 T, Q = 10 goal;

- Validated and optimized (i.e., minimized T throughput) schemes to control the DT mix in H-mode plasmas, including the (transient) H-mode access and exit phases;
- Documented experimental behaviour of DT H-mode plasmas, including their reaction to heating and fuelling actuators, an essential element in designing burn control strategies that will be required in the next step of the experimental program;
- Operational experience and experimental data to benchmark the procedure for re-optimization of control schemes for both ELM transient loads (via ELMCC) and stationary power loads (via fuelling and impurity seeding) with increasing β and T fraction, which should provide a basis for more rapid progress in the following, higher current, phase of the DT program;
- First evaluation of the magnitude of T-retention and of the efficiency of T-removal techniques (e.g., ICWC) in H-mode plasma conditions very similar to those expected for Q = 10 operation;
- Initial assessment of the magnitude of nuclear heating and AC losses in the TF coils during DT H-mode plasmas: this will provide a basis for evaluation of whether TF coil heating might constrain high current/high-Q operation, implying the need for a greater emphasis on minimizing AC losses during the next operational phase.

3.3.3.3 Optimization of fusion power in DT plasma scenarios towards 15 MA/5.3 T.

Building on the experience gained in the preceding program of experiments, the operational space of DT H-mode plasmas will be expanded towards the final demonstration of the ITER Q = 10 goal, initially for burn lengths of ~50 s. Following a program of commissioning/ recommissioning of auxiliary systems, PCS etc. at the start of FPO-2, achievement of this fusion gain target will follow a similar route to the development of high current L-mode plasmas discussed in section 3.3.2.3: I_p and B_t would be increased gradually, following the steps 7.5 MA/2.65 T, 9.5 MA/3.3 T, 12.5 MA/4.5 T, 12.5 MA/5.3 T and 15 MA/5.3 T, while keeping q_{95} ~ 3. This 'step-ladder' will, of course, be refined on the basis of the I_p/B_t steps finally found to be optimum for L-mode. Operation along this path exploits the flexibility of the ITER H&CD systems to maintain power deposition in the central part of the plasma, $r/a < 0.5$, which is beneficial for plasma performance and is expected to prevent W accumulation, an effect which should have been confirmed in L-mode experiments. In this respect, as α-heating increases in these experiments, the associated peaking of the heating profile should have a significant effect on W transport, potentially reducing the need for central localization of the ECRH and ICRF deposition profiles when operating at intermediate fields between 2.65 and 5.3 T. Nevertheless, if the α-heating contribution is insufficient to control W accumulation for certain I_p/B_t steps, an alternative approach to maintaining central ECRH/ICRF deposition would involve increasing I_p at constant B_t = 5.3 T, allowing q_{95} to vary.

Table 17 provides an overview of the principal research activities, the estimated experimental time allocation and the principal sets of plasma parameters encompassed by the major elements of the IRP within the FPO-2 campaign, which is intended to have the demonstration of $Q = 10$ as its initial focus. The overall structure of this first phase of the FPO-2 experimental program will follow the I_p/B_t step-ladder while tuning the H&CD power and mix and varying the T concentration until the $Q = 10$ goal is achieved at a stationary fusion power level of ~500 MW. The strategies and schemes developed for DT mix control, divertor power load control, ELM control, etc., in the experiments discussed in section 3.3.3.2 will be applied routinely during this phase as the uncontrolled stationary and transient loads at higher current will already be incompatible with the ITER PFC power handling capabilities and lifetime constraints, as discussed in [3-Appendix C].

As emphasized in section 3.3.2.4, the dependences on isotopic mass, plasma density and toroidal field embedded in the scaling for the H-mode power threshold implies that as I_p increases (requiring operation at higher B_t values), a significant T concentration will be required to increase α-heating and facilitate access to the H-mode. This trend will be reinforced by the need to sustain high density operation to achieve $Q = 10$ (the target value of volume average density is 10^{20} m^{-3}, or $\langle n_e \rangle = 0.85 \times n_{GW}$). The experimental strategy adopted streamlines the development of high current H-modes towards DT by integrating the development across the D and DT operational phases.

Within this experimental strategy, experimental results for 12.5 MA/4.5 T plasmas at $\langle n_e \rangle = 0.5 \times n_{GW}$ will be crucial to determining the optimum approach to higher I_p/B_t operation. This plasma scenario is expected to be dominated by gas fuelling, resulting in relatively low density gradients in the pedestal. Present integrated modelling estimates assuming that the transport reduction in the edge transport barrier is not influenced by density gradients indicate that a significant fusion performance can be achieved ($Q > 3$) [194, 200], as shown in figure 21, due to the high pedestal temperatures that can be sustained in these conditions within the calculated edge MHD stability limits. Experimental confirmation of this prediction would open an easier developmental route to high-Q operation (i.e., with a more gradual increase of α-heating with increasing current), exploiting operation at $\langle n_e \rangle \sim 0.5 \times n_{GW}$ as I_p increases - the conventional route relies on pellet fuelling to sustain $\langle n_e \rangle \sim 0.85 \times n_{GW}$. In the alternative approach, $P_{aux}/P_{LH} \geq 1.7$ can be maintained to 15 MA/5.3 T. Robust H-mode operation should therefore be more controllable with auxiliary heating and less reliant on optimization of the α-heating.

Success in this approach would then allow access to $Q = 10$ operation at 15 MA with $\langle n_e \rangle \sim 0.85 \times n_{GW}$ to be developed from a 15 MA scenario with $\langle n_e \rangle \sim 0.5 \times n_{GW}$ and $Q \sim 5$, using pellet fuelling to raise the density. Indeed, modelling of a scenario in which an initial H-mode phase with $\langle n_e \rangle \sim 0.5 \times n_{GW}$ is used to build up α-heating prior to increasing the density indicates that more robust access and exit phases to/from the burning plasma state can be established, both in terms of H-mode control and avoidance of W accumulation [143, 166, 195, 201, 202]. Figure 22 illustrates key aspects of this analysis. In contrast, direct access from L-mode to $Q = 10$ conditions at $\langle n_e \rangle \sim 0.85 \times n_{GW}$, relies on the use of the full additional heating power (73 MW) in all discharges [203], since $P_{aux}/P_{LH} \sim 1.0$ at this density level at 15 MA/5.3 T.

The experimental plan foresees experiments for each level of I_p/B_t and T-fraction using a range of plasma densities (at least three, $\langle n_e \rangle \sim 0.5, 0.7, 0.9 \times n_{GW}$) and two levels of additional heating,

one to match $\beta_N \sim 1.8$ and the other to match the expected P_{aux}/P_{LH} for $Q = 10$ plasmas. At each of these steps, the schemes previously developed to avoid, or control, limiting instabilities such as NTMs, sawteeth, etc., may need additional optimization time. Similarly, it is likely that at each step the schemes to control divertor power loads and to ensure ELM control will have to be re-tuned. The impact of impurity seeding (for control of divertor heat loads) and 3-D fields (for ELM control) on core plasma performance, and hence on fusion power production, might be more significant as the plasma current and fusion power increases, so that the retuning of integrated control of the plasma scenario may become more time-consuming as the high fusion power/high fusion gain program progresses.

The edge MHD stability limit in these plasmas may be determined by ballooning or peeling instabilities. Depending on which is more dominant, the pedestal pressure is expected to scale as $P_{ballooning,ped} \sim I_p^2$ or $P_{peeling,ped} \sim I_p \times B_t$ [200, 204]. If ballooning dominates, at 5.3 T an intermediate current point between 12.5 MA and 15 MA may be required to avoid large changes in the edge plasma parameters in progressing from one scenario to the next: excessively large steps would present challenges in ensuring that ELM control is maintained as I_p increases (since both q_{95} and edge pedestal pressure would then be subject to significant changes between 12.5 and 15 MA).

Note that the main considerations related to the approach to disruption management, avoidance, control and mitigation within FPO have been outlined in section 3.3.2.2 and will not be developed further here.

The main experimental activities foreseen for the implementation of this plan are:

- Develop integrated H-mode scenarios in DT at the first two I_p/B_t increments in the step-ladder (9.5 MA/3.3 T, 12.5 MA/4.5 T): The same type of experiments foreseen for the 7.5 MA/2.65 T DT H-mode program discussed previously will be performed for at least two levels of additional heating. This is intended to increase the α-heating in small steps, allowing retuning of the operational schemes to ensure that the plasma scenarios satisfy the compatibility requirements for ITER operation in terms of power loads, NTM and sawtooth control, etc.. As discussed above, as the α-population increases, a range of issues might emerge related to the influence of α-particles on MHD stability, to α-particle losses generated by α-induced MHD instabilities and by 3-D fields applied for ELM control, and to He exhaust. If so, experimental studies would likely be required to eliminate or mitigate any deleterious effects prior to progressing to higher current levels. In particular, the experimental results obtained for 12.5 MA/4.5 T plasmas at $\langle n_e \rangle \sim 0.5 \times n_{GW}$ will be crucial to determine the optimum way to proceed towards higher I_p/B_t in the next step, as discussed in detail above.
- Experimental results at 12.5 MA/4.5 T with $\langle n_e \rangle \sim 0.5 \times n_{GW}$ will provide critical insights for the further development of the program: in particular, the need for a significant α-heating contribution, both to facilitate H-mode sustainment and to limit W accumulation, will set a lower bound to the range in T concentration which can be explored. Within this reduced range in T concentration, two routes towards 15 MA/5.3 T, $Q = 10$ plasmas are considered feasible: the first is based on increasing I_p/B_t with $\langle n_e \rangle \sim 0.5 \times n_{GW}$, while the second develops scenarios with $\langle n_e \rangle \sim 0.7 - 0.9 \times n_{GW}$. A key point is that both approaches require to maintain scenario control in the q_{95} step (3.0 to 3.6) from 12.5 MA/4.5 T to 12.5 MA/5.3 T. Given the experience previously gained in adapting H-mode control

schemes (e.g., ELM control, NTM control) over a range in q_{95}, and the small increment in q_{95} involved, this is considered feasible, but the additional application of pellet-pacing to augment the ELM control capability would likely be advantageous.

- The lower density approach ($\langle n_e \rangle \sim 0.5 \times n_{GW}$) provides more 'head-room' for control of the H-mode scenario with additional heating, implying that the development of the next two I_p/B_t steps in the ladder (12.5 MA/5.3 T and 15 MA/5.3 T) is less dependent on the optimization of α-heating. This will allow exploration of a wider range in T concentration and a more gradual increase of the α-heating, which is expected to facilitate progress of the experiments. Nevertheless, the adaptation of scenario control schemes is expected to be more challenging with increasing current and additional power, and, of course, increasing α-power production. At some point from 12.5 MA/4.5 T onwards, burning plasma physics processes will become significant, and ultimately dominant, so that issues related to scenario control for $Q = 10$ plasmas must be addressed, but also that the burning plasma physics issues discussed in section 3.3.5 can be studied.

  Each step in additional heating power, T concentration and plasma current from 12.5 MA to 15 MA will require the development of a fully integrated H-mode scenario before proceeding to the next step, and this is expected to require significant experimental time. In principle, this procedure can be optimized by matching, as far as possible, the edge power flow of 12.5 MA plasmas with high T-fraction and that of 15 MA plasmas with lower T-fractions. Once the 15 MA, $Q \sim 5$ scenario has been achieved at $\langle n_e \rangle \sim 0.5 \times n_{GW}$, the plasma density would be raised in small steps towards the final goal of $\langle n_e \rangle \sim 0.85 \times n_{GW}$, $Q = 10$ while maintaining a T-fraction of ~50%.

  This strategy is not foreseen to entail particular difficulties in relation to the sustainment of stationary H-mode conditions since, under the specified conditions, the H-mode power threshold is expected to increase with $\langle n_e \rangle^{0.72}$ while the α-heating power increases approximately as $\langle n_e \rangle^{1.5}$, so that P_{tot}/P_{LH} increases approximately as $\langle n_e \rangle$. Therefore, if 5 steps in density are implemented, the step-by-step increase in α-heating can be limited to ~20% (e.g., if the α-power increases from 50 to 100 MW, as anticipated, the increment at each step would only be ~10 MW).

  This is to minimize the experimental activities associated with the development of a fully integrated H-mode scenario at each step in the program: each scenario must accommodate an increase in edge power flow due to the increase in α-heating, a higher rate of He exhaust, changes to pedestal parameters and edge stability (increasing n_{ped} and decreasing T_{ped}, etc.), increasing plasma β and possibly more strict requirements for NTM control, etc.. However, by choosing the density steps judiciously, this development could be simplified, as the changes to plasma parameters, α-population, etc., can potentially be made as gradual as required. Nevertheless, phenomena which only appear beyond a certain physics threshold (e.g., fast particle driven instabilities) might require dedicated experiments, possibly with finer parameter scans, for their study and for the development of mitigation or avoidance schemes (if necessary).
- The second approach ($\langle n_e \rangle \sim 0.7 - 0.9 \times n_{GW}$) requires a careful build-up of the α-heating to ensure that an appropriate margin of the edge power flow is maintained in each step to provide stationary H-mode operation. Satisfying this condition is expected to require

contributions from both auxiliary H&CD and α-heating, implying a need for additional experiments (compared to the first approach) to optimize DT mixture control and, hence, α-heating. In these scenarios, the key issue for the access to and exit from burning plasma conditions is the build-up/ramp-down of the α-heating with respect to that of the plasma density. If the density increases too rapidly after the L-H transition, the plasma might not sustain stationary H-mode conditions, as shown in figure 22(a). Additional experimental time is likely to be required relative to the lower density approach, therefore, to investigate and optimize this aspect of the scenarios (which will most likely rely on H-mode access/exit in the current ramp-up/down). The necessary experiments will include optimization of the fuelling waveform, the DT mix and the power waveform for access to/exit from H-mode in both the current flat-top and during the current ramp-up/down (typically with at I_p at ~2/3 of the flat-top value). Beyond 12.5 MA each increment in I_p , $<n_e>$, P_{aux} and T concentration (within the narrow range to be explored) will require the development of a fully integrated H-mode scenario. Given the potentially large increase in α-heating between 12.5 MA and 15 MA in these high density DT plasmas (a factor of ~2), it is likely that this approach will require at least one intermediate current point at 13.5 MA. The end point of this scenario development activity is essentially the same as that for the earlier approach: establishment of 15 MA, Q = 10 plasma conditions with $<n_e> \sim 0.85 \times n_{GW}$ for ~50 s.

It will only be possible to evaluate the relative advantages and disadvantages of these two approaches once experimental data is available from DT plasma operation in ITER: selection of the preferred approach will depend both on the results of physics processes (pedestal characteristics and achievable H-mode performance in gas-fuelling dominated plasmas, robustness of stationary H-mode operation with ELM control for $P_{tot} \sim P_{LH}$, etc.) and on the relative effectiveness of certain key control schemes (e.g., efficiency and time response of DT mix control, efficiency of ELM control in a variety of plasma conditions, etc.).

On the other hand, there are many operational and physics issues common to both approaches: e.g., the need to address a range of aspects of scenario integration, handling the transition to burning plasma conditions and exploiting the associated physics research opportunities. Both approaches will involve experiments on burning plasmas at various levels of α-heating to refine schemes for burn control and, if a robust stationary scenario can indeed be established at high current, will provide access to studies of transient high-Q phases (through additional heating step-down experiments) in which the behaviour of burning plasmas fully dominated by α-particles can be explored.

In relation to the challenges of scenario integration, an important issue is that, in the course of this program, many ITER systems will be approaching the upper limit of their operating range (e.g., maximum current in the ELMCC, maximum ECRH power demand due to sharing between control of NTMs and W accumulation, etc.). This may imply a need for additional experimental time to ensure that the scenario requirements can be matched by the hardware capabilities. Potential examples are:

a) Optimization of the plasma rotation profile by variation of the power mix to determine the minimum current requirements for ELM control, if experiments at 12.5 MA indicate that the ELMCC capability would be marginal for 15 MA operation;

b) Optimization of the power mix for W accumulation control, if insufficient ECRH power can be applied centrally due to the demands for off-axis NTM control;

c) Re-optimization of the current ramp-up/down rate and the stationary H-mode phases, if flux consumption and/or AC losses in the PF coils turn out to be excessive.

Whatever specific challenges of this nature emerge, the operational plan incorporates an allocation of time to perform the necessary experiments to ensure that the goal of maintaining $Q = 10$ for a duration of ~50 s can be achieved within the foreseen experimental period.

As α-heating increases, raising the plasma energy (thermal and total), the performance of key systems required to support $Q = 10$ operation will have to be verified, including the disruption mitigation system, the resilience of key diagnostics in a high neutron flux environment and (possibly) further calibration and cross-checks of neutron diagnostics at high neutron flux. In addition, confirmation of the satisfactory response of the superconducting coil systems to the combination of neutron heating pulses of ~50 s and AC losses associated with the high current scenarios is a key step before proceeding to longer duration high-Q pulses.

It is clear from the preceding discussion that, in the course of this first encounter with high current, high fusion power plasmas, a variety of challenges in the physics behaviour and control of the plasma scenarios might emerge, which will require dedicated experimental time and, quite probably, some ingenuity to resolve. It is anticipated, therefore, that the overall ($Q = 10$) goal of this phase is more likely to be achieved during the second DT operational campaign (i.e., FPO-2 - see figure 3), while a more practical target for the FPO-1 campaign is considered to be the demonstration of several hundred (200 - 300) megawatts of fusion power for ~50 s with $Q \sim 5$.

The principal deliverables from these experiments are:

- H-mode plasma scenarios integrated with all ITER operational constraints over a range of $I_p = 12.5$ - 15 MA ($q_{95} = 3.0$ - 3.6) delivering several hundred megawatts of fusion power, with burn control demonstrated for periods of ~50 s. This is a key step for both the development of the $Q = 10$ scenario towards 300 - 500 s burn duration and for preparing the development of the $Q = 5$, $t_{burn} > 1000$ s scenarios;
- A $Q = 10$ H-mode plasma scenario integrated with all ITER operational constraints at $I_p = 15$ MA ($q_{95} = 3.0$) delivering ~500 MW fusion power, with burn control demonstrated for periods of ~50 s by early FPO-2, laying the basis for the achievement of the ITER mission goal of maintaining $Q = 10$ for durations of 300 - 500 s by mid-to-late FPO-2;
- Initial studies in burning plasma conditions, providing validation tests of fusion product diagnostics, insight into the physics processes determining plasma behaviour and input to the validation/development of models applied in the expansion of burning plasmas scenarios in ITER;
- First results from TBM exposure to relevant neutron fluxes for high-Q operation (although at reduced fluences);
- Quantitative assessment of nuclear heating of the superconducting coils at high fusion power (up to ~500 MW) and of AC losses for a range of plasma scenarios with I_p up to 15 MA, data which provide key information for the further development of both the $Q = 10$/ $t_{burn} = 300$ - 500 s and $Q = 5$/ $t_{burn} > 1000$ s scenarios.

3.3.3.4 Extension of Q=10 scenario towards long-pulse operation (300 - 500 s).

Extension of the $Q = 10$ scenario to burn durations in the range 300 - 500 s is expected to develop naturally as a prolongation of the previous program phase, unless specific experimental activities need to be implemented to resolve issues which have emerged during the development of the 15 MA, $Q = 10$ scenario.

As the pulse duration increases, additional technical issues may well arise, e.g., implementation of exception handling in PCS, and control of the plasma termination will be more challenging, as the central solenoid will be operating close to its flux swing limit. While the short-pulse $Q = 10$ scenario will have provided a demonstration of a burning plasma scenario that integrates numerous processes related to power deposition control, α-particle physics, thermal and particle transport, DT mixture control, etc., some processes in ITER plasmas are expected to develop on longer timescales, such as:

- MHD instabilities sensitive to the current profile shape, which could lead to the triggering of tearing modes, AEs, etc., as the current profile evolves during the burn phase. The characteristic timescale for this process could range from 100 s to 1000 s, as illustrated in figure 23;
- Anomalous transport processes which are influenced by the evolving current profile shape. Integrated plasma simulations for ITER show that evolution in the magnetic shear can lead to the onset, or change in intensity, of turbulent transport (see figure 24) [205];
- Processes controlled by neoclassical particle transport, particularly in the central plasma region, where anomalous transport may be low in ITER. The neoclassical transport coefficients for D, T and W are very low for 15 MA/5.3 T plasmas, as shown in figure 25 [195, 206], implying that the typical timescale for evolution of the D, T and W profiles in the central plasma region is of the order of several tens of seconds. Thus, the fuel ion and W profiles might not be fully relaxed in $Q = 10/\ t_{burn} = 50$ s plasmas;
- There may be additional physics processes with characteristic timescales of several tens of seconds: e.g., sawteeth can be stabilized by fast particles and could exhibit repetition periods of ~50 s in ITER [207], as shown in figure 26.

Processes related to long timescale evolution of plasma-wall interactions observed in present devices are unlikely to occur in ITER, since the particle/power fluxes are much larger than in current experiments and the vessel and all in-vessel components are water cooled: in ITER, the typical timescale for in-vessel components to reach thermal equilibrium is several seconds. Nevertheless, additional issues might emerge in longer pulses, such as the accumulation of thick co-deposited beryllium layers, which might result in the overheating and/or detachment of the layers for $Q = 10/\ t_{burn} = 300$ - 500 s pulses, posing specific operational issues as the burn length is extended.

To ensure that such processes, or other operational limitations, do not increase the likelihood of disruptions, extension of the burn length will progress gradually (e.g., in steps of ~50 s), most likely starting at a lower value of Q: operation at lower Q, rather than at $Q = 10$, provides greater flexibility in the control of plasma behaviour using H&CD actuators. For example, $Q = 5$ could be obtained by operation with $\langle n_e \rangle = 0.5 \times n_{GW}$ at 15 MA/5.3 T, or at higher $\langle n_e \rangle / n_{GW}$ if T-fractions above 50% were used (lower T-fractions are excluded at 15 MA/5.3 T due to the increase in H-mode threshold). The experimental program would then work towards extending

the burn duration to a specified 'milestone' value at $Q = 5$, followed which the scenario would be developed towards achieving $Q = 10$, with the procedure repeated until the target of $Q = 10/ t_{burn} = 300 - 500$ s is established. In parallel, the burning plasma physics processes reviewed in section 3.3.5 would be studied and, where appropriate, dedicated experiments to characterize them will be interpolated into the program.

This phase of the program will conclude with a series of experiments studying approaches to higher fusion performance, beyond $Q = 10$, during both transient and stationary phases by taking advantage of the ITER H&CD flexibility and the favourable interaction of fast particle pressure with edge stability associated with the increased Shafranov shift (and possibly also through the direct influence on anomalous transport) [208, 209].

The T-Plant will, at this point, be producing the maximum T throughput for which it is designed. Therefore, routine characterization of T-retention and application of T-removal will necessarily have been integrated into ITER operation in parallel with the experimental program. T-removal schemes will be implemented between pulses, overnight, during routine maintenance periods (or other operational interventions) and possibly during dedicated phases of plasma pulses, to extract T retained within the vessel.

Consistent with the above overview, the main experimental activities will be:

- From a 15 MA/5.3 T, $Q = 5$ scenario with ~50 s burn, the burn duration will be increased by ~50 - 100 s while maintaining a fully integrated scenario, including control of stationary and ELM-related power fluxes, fuel, impurity and He exhaust, DT mix, burn stability, MHD stability, etc., over the longer timescales;
- From the extended $Q = 5$ scenario, the fusion gain will be developed towards $Q = 10$, retuning actuators as required. This sequence will be repeated until $Q = 10$ is sustained for 300 - 500 s. As the burn duration is increased, flux consumption will be monitored to ensure that there is sufficient current margin in the central solenoid to provide a robust (i.e., disruption-free) termination of the burn phase and of the discharge as a whole. This is likely to require re-optimization of the entry-to and exit-from the burn phases, and possibly also of the L-mode ramp-up/ramp-down phases;
- Within this program specific experiments will deal with aspects of the control of long-duration burning plasmas and with the characterization of burning plasma physics phenomena. For example, if the deleterious physics effects discussed above emerge as the pulse length is extended, dedicated experiments will be required to test and implement mitigation schemes: e.g., control of the current profile evolution by localized heating and/or current drive to avoid MHD instabilities; use of central H&CD to influence core particle transport and avoid W accumulation; suppression of AEs by exploitation of H&CD to modify the fast particle distributions, to influence the current profile shape locally, and to modify local plasma parameters; removal of retained T by implementing specially designed D phases within the high-Q discharges, or by interleaving D plasmas between high-Q discharges, etc;
- To conclude this phase of experiments, exploration of the possibility of achieving $Q > 10$ plasmas in 15 MA/5.3 T plasmas will be undertaken. One option involves exploiting transient phases with durations of several τ_E (i.e., tens of seconds at most) by gradually decreasing the additional heating power. Alternatively, the flexibility of the ITER H&CD

systems could be used to improve fusion performance in stationary conditions: for example, applying ICRF heating via the ^{3}He-minority scenario during the burn is expected to increase central ion heating, and thus the core reactivity and Q (an increase of up to $\Delta Q = 1.5$ is predicted [210]) - due to the scarcity of ^{3}He and the high consumption rate predicted for ITER, within current research planning the use of the ^{3}He-minority scheme has been limited to the H-mode access/exit phases.

A further possibility exploits the favourable relationship between Shafranov shift and edge stability, which is observed to improve plasma confinement in existing experiments. Auxiliary heating could be applied to maximize the central fast particle pressure (e.g., by injecting the beams as close to the plasma centre as possible) and thus the Shafranov shift, which might then generate improved confinement, resulting in a regime with $Q > 10$. Whether this concept can be exploited without triggering fast particle-driven MHD instabilities will have to be investigated.

In the longer-term perspective, research on approaches to operation at higher fusion power and fusion gain will be a recurring element within the ITER program, either to pursue specific aspects of burning plasma behaviour, or to provide higher neutron fluxes for TBM studies. However, once the primary fusion gain mission has been achieved, the immediate emphasis in the IRP will shift to the development of scenarios with a higher non-inductive current drive fraction (aiming towards fully non-inductive operation) and with enhanced confinement (i.e., $H_{98} > 1$), working towards the fulfilment of the $Q = 5/ t_{burn} \sim 1000$ - 3000 s mission, as discussed in section 3.3.4.

The main deliverables from this experimental phase are:

- Demonstration of robust, integrated H-mode scenarios achieving $Q = 5$ and $Q = 10$ for 300 - 500 s duration with a fusion power output of 400 - 500 MW, thus achieving the ITER fusion goal in inductive operation;
- Analysis and control of burning plasma physics processes occurring over timescales of hundreds of seconds. This is essential both for the achievement of the $Q = 10$ inductive goal and for the further development of $Q = 5/ t_{burn} > 1000$ s scenarios;
- Thorough exploration of burning plasma physics processes over long timescales;
- Demonstration of $Q > 10$ operation over a range of timescales (depending on scope of approaches to higher-Q which are successfully developed);
- Demonstration of routine operation with acceptable T-retention over long pulses and extended operational periods with high T throughput;
- Initial testing of the TBMs at high neutron fluxes and fluences.

It must also be remarked that attainment of quasi-stationary $Q = 10$ plasmas in ITER is likely to yield many insights into plasma behaviour in the burning plasma regime and to generate numerous new ideas for the optimization of fusion performance.

3.3.4 Operational plan for hybrid/ non-inductive DT plasma experiments

3.3.4.1 Objectives and plasma scenarios

Building on experimental results from the initial FPO campaign, candidate operating regimes will be identified with the potential for extension towards very long-pulse operation at high fusion power. Assuming that satisfactory progress is made towards the $Q = 10$ long-pulse goal in FPO-2, it can be expected that experiments will be undertaken in parallel with the later phase of the

$Q = 10$ program to develop candidate scenarios with substantial non-inductive current fractions, aiming towards pulse lengths beyond 1000 s. Based on analysis developed in the ITER Final Design Report (FDR) [1], ITER research planning has focussed on two lines of development: a 'hybrid' scenario, with $q_{95} \sim 4$, capable of supporting burning plasma phases with durations of up to 1000 s, and a fully non-inductive, steady-state scenario, with $q_{95} \sim 5$, capable of extending the burning plasma duration up to 3000 s. While fusion performance will certainly be a longer-term consideration, initial emphasis will be given to establishing a robust long-pulse operational scenario in which fusion power (and fusion gain) can be raised gradually. Once long-pulse, high-β_N operation has been demonstrated (initial target of $t_{burn} \geq 1000$ s, a high non-inductive fraction, say, $f_{NI} \geq 0.6$, and $Q \sim 2$ in FPO-2), the research program will focus on developing fully non-inductive steady-state operation (target of $t_{burn} \sim 3000$ s, $f_{NI} = 1.0$, optimized Q with an initial target of $Q \sim 2$ in FPO-2). The final targets for both long pulse and steady-state scenarios are those considered to be achievable by FPO-3.

Achievement of the final high-Q, long-pulse and steady-state goals will require the optimization of plasma energy confinement and non-inductive current drive (exploiting both bootstrap current and auxiliary current drive) while ensuring MHD plasma stability and plasma edge compatibility. The requirements for high energy confinement are less demanding for long-pulse operation (i.e., with non-inductive current fraction $f_{NI} < 1$) at high plasma currents. The long-pulse $Q = 5/\ t_{burn} \sim 1000$ s goal is expected to be achievable in ITER (potentially with even longer burn duration) with $H_{98} \sim 1.0$ - 1.1 for I_p in the range 13 to 15 MA ($q_{95} \sim 3.5$ - 3) [200] and low average densities ($\langle n_e \rangle \sim 0.5 \times n_{GW}$), as illustrated in figure 27 [211]. Long-pulse operation at lower currents, ~12.5 MA ($q_{95} \sim 3.6$), would require operation at higher plasma density and is more demanding with respect to energy confinement ($H_{98} \sim 1.25$), implying confinement values which are typical for 'hybrid' scenarios at $q_{95} \sim 3.6$ in present tokamaks [211]. Experiments within the development path towards the long-pulse $Q = 5$ scenario will therefore have to explore the trade-off between plasma current and energy confinement enhancement achievable in ITER. This will determine whether the 'hybrid' approach or the low-density 'conventional' H-mode approach provides the more promising basis for the initial long-pulse development program. The following discussion focusses on the hybrid approach towards the $Q = 5$ long-pulse goal since this is more relevant towards a DEMO reactor and has more synergies with the development path for the $Q = 5$ steady-state scenario: achieving $f_{NI} = 1.0$ will require even lower plasma current and higher energy confinement enhancement.

The development path for the $Q = 5$ steady-state goal ($f_{NI} = 1.0$) is subject to larger uncertainties associated with the achievable energy confinement, core density peaking (key to generating core bootstrap current), global MHD stability (which determines whether a sufficiently high value of β_N can be sustained to generate the required fusion power), edge MHD stability (key to providing high energy confinement and pedestal bootstrap current) and achievable current drive while also satisfying the demands of local current profile control. Of course, an acceptable combination of plasma parameters must be achieved while satisfying the normal constraints for long-pulse burning plasma operation, such as power and particle exhaust, fuel mixture control, burn control, etc.

Candidate operating scenarios satisfying the requirements for fully (or nearly so) non-inductive steady-state operation with $Q \sim 5$ have recently been revisited under current assumptions for the

H&CD capability, as well as possible upgrades which could be implemented early in the FPO phase [185, 186]. Figure 28 shows, as an example, the operational space of steady-state scenarios that can potentially be explored in ITER with I_p in the range 9 - 15 MA, 50 - 80 MW of H&CD power (up to 49.5 MW of NBI and up to 30 MW of ECRH) and a moderate core density peaking, characterized by the ratio $n_e(0)/n_{e,ped}$, taken as $R/L_n \sim 4$, with L_n the usual density scale length. As shown in the figure, using only the baseline H&CD capabilities (33 MW NBI, 20 MW ECRH), the achievement of $Q = 5$ requires $H_{98} = 1.7$ - 1.5 for $I_p = 9$ - 11 MA, with the required value of H_{98} falling slightly with increasing injected power. A more detailed review of the sensitivity of the steady-state scenario to H&CD power, required Q-value and small deviations from fully non-inductive operation can be found in [185, 186].

The experimental program in this phase will explore systematic variations in the main plasma parameters (e.g., density, plasma current, applied heating, current profile) while the edge conditions required for core-edge integration (e.g., divertor radiation for stationary power load control, ELM control, etc.) will be utilized to optimize performance towards the goal of fully non-inductive operation. During these scans, the control techniques developed previously in PFPO-2 and earlier in FPO will need to be adjusted in each case to optimize the control algorithms for the specific plasma conditions. Significant time will be required to optimize confinement and real-time MHD stability control in order to sustain operation near MHD stability boundaries.

It is important to note that while the $Q \sim 5$ long pulse operation scenario goal is expected to be achievable with the baseline configuration for H&CD and actuators (e.g., ELMCC), the achievement of the steady-state goal relies on the availability of upgrades to H&CD and plasma control (e.g., RWM control to limit disruptivity when operating close to MHD limits).

The overall research activities to be performed in this period are:

(i) Application of β/current/pressure profile control algorithms using target current profiles in stationary DT discharges: This research can, in principle, be carried out at any time within the $Q = 10$ DT development program in FPO-2 (e.g., if difficulties in developing that scenario were encountered);

(ii) Optimization of non-inductive current drive in 2.65 T discharges at $q_{95} \sim 3.6$ (hybrids) and assessment of the influence of isotope (D versus DT): As above, this activity can be pursued at any time within the $Q = 10$ DT development program in FPO-2;

(iii) Optimization of non-inductive current drive in 5.3 T discharges at q95 ~ 3.6 (hybrids): Once again, this research can, in principle, be carried out at any time within the Q = 10 DT development program in FPO-2;

(iv) Optimization of performance (with target $Q \geq 5$) and discharge length (up to 1000 s) in long-pulse full-field hybrids ($q_{95} \sim 3.6$);

(v) Demonstration of $q_{95} \geq 4.5$ steady-state (fully non-inductive) plasmas with duration of 3000 s and $Q \sim 2$;

(vi) Optimization of $q_{95} \geq 4.5$ steady-state (fully non-inductive) plasmas with duration of 3000 s and a target of $Q \geq 5$.

The initial, exploratory studies of long pulse operation with $Q \leq 2$ are expected to complete the FPO-2 program and are summarized in Table 17, while the major elements of the research program towards hybrid/fully non-inductive operation with $Q \geq 5$ are expected to form the principal focus of the FPO-3 campaign and are summarized in Table 18.

The major research focus within this phase will be given to the optimization of the core-pedestal coupling following the initial results from FPO experiments on this issue and the integration of the core-pedestal scenario with the ITER metallic wall. This will include the assessment of the role of fast particles and plasma rotation on the anticipated virtuous feedback loop between core and pedestal for high-β_N ITER plasmas with a large fraction of fusion-born fast α-particles [208]. In parallel, significant efforts to understand and optimize/control MHD instabilities triggered by fast particles and to reduce fast particle losses (by MHD instabilities or non-axisymmetric magnetic field effects) are likely to be necessary.

It is important to note that, should the long-pulse, high-β_N operation (target 1000 s, high non-inductive fraction, $f_{NI} \geq 0.6$, $Q \sim 5$) development encounter insurmountable difficulties, there exist alternatives to achieve the 1000 s, $Q = 5$ goal that do not require a very high inductive current drive fraction or enhanced confinement ($H_{98} > 1$), assuming that the remaining pedestal physics issues are resolved satisfactorily. These are based on the approach with $\langle n_e \rangle = 0.5 \times n_{GW}$ discussed in section 3.3.3.3, and are a natural extension of the $Q = 10$ scenario to lower densities and, therefore, to higher plasma temperatures, implying lower resistive flux consumption. Although this is a less attractive option from the perspective of fusion energy development towards DEMO, it remains a viable approach to the achievement of the 1000 s, $Q = 5$ goal in ITER.

3.3.4.2 Experimental plan for hybrid/ non-inductive operation at high fusion power

To provide a detailed experimental program for the achievement of the goals of the long-pulse (hybrid/ steady-state) program to the same level as that for $Q = 10$ (section 3.3.3) is not possible at this stage of the project as such details will depend critically on the research results of previous operational phases (PFPO-2 and the initial FPO campaigns) and on the upgrades of the H&CD and control systems (e.g., power supplies for RWM control) that should have been implemented in preparation for developing these elements of the IRP.

On the basis of the present analysis of long-pulse operation for ITER (see [185, 186, 3-Appendix E] for details), the experimental program must develop self-consistent scenarios, in terms of core and edge plasma confinement (e.g., pedestal MHD stability), which also satisfy the constraints on core and global MHD stability, to satisfy the project's mission goals. This will certainly require adjustment and control of the plasma current and pressure profiles using the available H&CD actuators and by exploitation of RWM stabilization to limit disruptivity when MHD limits are approached. Such scenarios will have to be established while satisfying the common requirements for ITER burning plasmas regarding core-edge integration (radiative divertor operation, ELM control and impurity exhaust) - these requirements are expected to give rise to specific issues associated with these novel scenarios due to the high edge power flows and the lower plasma currents and plasma densities expected. Similarly, fast particle physics and control of the associated MHD instabilities may require substantial experimental time, as the proportion of fast particles in these plasmas and their contribution to the total plasma pressure are expected to be larger than in the intermediate steps towards the $Q = 10$ goal described in section 3.3.3. This is due to the larger values of the ratio $P_{heat}/\langle n_e \rangle$ for the long-pulse high-Q scenarios than is obtained in conventional H-modes at similar I_p: an increase in $P_{heat}/\langle n_e \rangle$ should increase β_N, enhance plasma confinement (by the favourable core/pedestal/transport feedback loop generating improved confinement) and enhance the current drive needed for long-pulse operation.

It is anticipated that the experimental program towards achievement of the long-pulse high-Q goals will involve the development of a series of DT plasma scenarios at various levels of plasma current and field. In many of these scenarios (particularly at low values of I_p), the value of Q will be low, so that the influence of α-particles is not expected to be significant. During the initial scenario development, therefore, this should allow better control of the plasma behaviour by external actuators. A possible consequence, however, is that the effects of significant α-particle heating/fast α-particle densities might only be identified rather abruptly in the final steps of scenario development, i.e., when the highest values of Q (~5) are approached. Potentially, this could increase the risk of disruptions at high levels of plasma energy, e.g., if core modes are destabilized by the increased α-pressure, implying a possible need for significant scenario redevelopment/ retuning in the final steps towards high Q. The outline experimental program discussed below is intended to mitigate such deleterious effects.

At this stage of the operational program, it is assumed that the target current profiles for these scenarios, which require tuning of the current ramp-up phase (additional heating power, plasma density, ramp-up rate, etc.), have already been developed in the previous phases of FPO. If this is not the case or additional issues appear when the T concentration is increased, additional time will be required to address these issues; this is not included in the experimental plan below.

The envisaged program expands on the 6 points listed in section 3.3.4.1:

(i) Development and demonstration of β/current/pressure profile control algorithms using target current profiles in stationary DT discharges:

The aim will be to develop and demonstrate control algorithms with the available actuators (H&CD, fuelling, etc.) to control total plasma pressure and current/pressure profiles in DT plasmas for the range of plasma currents and magnetic fields foreseen in the development path of the high-Q, long-pulse scenarios. These experiments, exploiting plasmas with target current profiles optimized at the end of the ramp-up, will focus on the control aspects, rather than on the optimization of plasma confinement and pulse duration. Synergies exist with other elements of the DT program and these experiments could, in principle, be carried out at any time in the FPO program during the Q = 10 scenario development. However, various control actuators for these experiments are likely to have improved capabilities and/or versatility as result of H&CD upgrades in preparation for very long-pulse operation. It is considered more appropriate, therefore, to pursue this objective once a substantial research activity towards the achievement of the long-pulse, high-Q goals is launched.

(ii) Optimization of non-inductive current drive in 2.65 T discharges at q_{95} ~ 3.6 (hybrids) and assessment of the influence of isotope (D versus DT) in hybrid plasmas:

A hybrid scenario at 6.3 MA/2.65 T will have been developed during the D phase (see section 3.3.2.7), and this will serve as a basis for assessing the influence of the isotopic mix on discharge development during the DT phase, an aspect with substantial implications for subsequent developments at higher toroidal fields. The experiments will explore a range of D/T ratios (while demonstrating fuel mix control), plasma densities and H&CD mixes, and will aim to optimize current drive and overall plasma confinement for 2.65 T hybrid plasmas. The low value of the minimum density for acceptable shine-through loads in DT (~2.5×10^{19} m^{-3}) allows unrestricted application of NBI for $\langle n_e \rangle / n_{GW} > 0.6$ in these plasmas, facilitating the achievement of very large current drive fractions, even with moderate H-mode-like energy confinement. The resultant

current profiles might, however, pose issues for MHD stability (including fast particle effects). This, together with the use of ECRH for both heating and current drive and, possibly, ICRF for plasma heating, will allow systematic studies of current drive and an initial assessment of the influence of fast particles and plasma rotation on the enhancement over H-mode confinement that may be achievable in ITER hybrid plasmas. Due to the relatively low I_p values, it is expected that edge integration aspects (divertor power loads, W source and transport control, ELM control, etc.) will pose moderate demands on the scenario development activity, although dedicated experiments might be necessary at the highest levels of additional heating and lowest densities explored. Similarly, the effects of α-particle heating/fast α-particles in these plasmas are expected to be small due to the projected low values of Q. On the other hand, the influence of fast particles generated by the heating systems (NBI and ICRF) may be significant.

(iii) Optimization of non-inductive current drive in 5.3 T discharges at $q_{95} \sim 3.6$ (hybrids):

These experiments will extend the experience gained in operation at 6.3 MA/2.65 T to plasmas at ~12.5 MA/5.3 T. Although optimization of current drive at the levels of plasma current and toroidal fields required for the high-Q, 1000 s pulse goal will be emphasized, experiments in this phase will also perform an initial assessment to determine whether the findings relating to H-mode confinement optimization for hybrid plasmas at 2.65 T also apply at 5.3 T. It is important to note that the hybrid experiments for 5.3 T plasmas are expected to be significantly more complex than those at 2.65 T and will require more experimental time due to the following issues:

a) Operational experience of hybrid plasmas in D at 12.5 MA/5.3 T is unlikely to be available, as hybrid operation in D plasmas is only foreseen up to 10.5 MA/4.5 T, due to H-mode access issues. Therefore, an intermediate step at 4.5 T will be required before exploring these plasma conditions in DT at 5.3 T;

b) Due to the higher plasma currents, toroidal fields and additional heating levels, the edge integration issues (divertor power loads, W source and transport control, ELM control, etc.) will have to be addressed as an integral part of the scenario development. In addition to requiring additional experimental time, this may limit exploration of current drive at the highest plasma temperatures (i.e., emulating conditions expected for $Q \sim 5$ in this scenario), which require low density operation;

c) The α-heating expected in these experiments, although much smaller than the additional heating, may already be significant ($Q \geq 2$) and influence the development of the experiments themselves (e.g., triggering fast particle MHD instabilities that decrease current drive efficiency). This may impose restrictions on the range of DT isotopic mixes in which current drive efficiency can be explored and/or may have implications for the strategy followed in varying the isotope mix;

(iv)Optimization of performance (with target $Q \geq 5$) and discharge length (up to 1000 s) in long-pulse full-field hybrids ($q_{95} \sim 3.6$):

To a significant extent, the development of scenarios to achieve the $Q = 5$, 1000 s goal will be based on the results of the previous step at 11.2 MA: the experimental results at this step will indicate the plasma current level at which the $Q = 5$ goal is most likely to be achieved, based principally on the energy confinement and current drive efficiency obtained, but with consideration also given to possible (deleterious) MHD-related effects. An important aspect of the scenario development and performance optimization is the avoidance of large changes in Q

between experimental steps, to ensure a gradual tuning of the edge integration and MHD control schemes as plasma fusion performance increases. In this respect, it is important to note that, in the hybrid scenario, plasmas can be subject to positive feedback loops between core and pedestal confinement driven by α-heating and/or β_α that can potentially generate significant increments in Q as the scenario is developed towards higher Q values. Maintaining robust plasma control while sustaining fusion power production under such conditions will have to be developed and demonstrated. Depending on findings of the previous experimental step, two strategies can be considered to reach the Q = 5, 1000 s goal:

a) To develop a high confinement, MHD stable (most likely by active control), fully integrated and controlled, long burn (>1000 s) DT plasma scenario at 10.5 MA/4.5 T, while optimizing towards the highest achievable Q; subsequently to develop the equivalent scenario at 12.5 MA/5.3 T to demonstrate the final Q = 5, 1000 s goal; or
b) To develop an optimized scenario by initiating the development at 12.5 MA/5.3 T, or a different current level (depending on the previous findings), with the necessary adjustment of MHD control, edge integration schemes, etc., as the burn length and fusion performance increase.

Selection of the preferred option (or even a combination of the two) must await further experimentation in ITER. As noted above, an important operational issue is the potential generation of a positive feedback loop between core confinement and edge pedestal stability as fusion performance increases, leading to more substantial increments in Q than expected. One approach to avoiding this issue would be to optimize the scenarios initially in T-rich plasmas, taking advantage of the reduced fusion power (lower α-heating) and lower H-mode threshold in T-rich plasmas, followed by a progressive change in the D:T ratio towards 50:50, thereby increasing Q gradually. Note that a 'T-rich' strategy is preferable to a 'D-Rich' strategy due to the lower H-mode threshold power expected in the former case: e.g., for an 12.5 MA/5.3 T D plasma at $\langle n_e \rangle = 0.8 \times n_{GW}$, the H-mode power threshold is ~76 MW, which significantly reduces flexibility in the mix of H&CD systems that can be explored in developing the experimental path to the desired scenario.

(v) Demonstration of $q_{95} \geq 4.5$ steady-state (fully non-inductive) plasmas with duration of 3000 s and Q ~ 2:

Achievement of this fully non-inductive objective requires H_{98} of ~1.2 with Greenwald factors of ~0.85 [186]. However, development of this scenario would benefit from significant H&CD upgrades, including implementation of the 3rd HNB and an additional 20 MW of ECRH (e.g., case 12 in Table 3 of [186] with q_{95} = 5.7). The additional NBI injector is currently considered to be the most important component of the H&CD upgrade in this context: with the baseline H&CD, the Q value in fully non-inductive operation may fall to 1.3 for H_{98} ~ 1.2 (e.g., case 2 in Table 3 of [186] with q_{95} = 7.6).

While the operational experience in FPO and, in particular, within the research program for hybrid plasmas will have provided important input for this phase, significant issues will remain open and will have to be resolved to establish fully non-inductive operation. Maintaining fully non-inductive operation under essentially stationary conditions imposes significant requirements on the auxiliary current drive sources, which also inject substantial heating power and create significant fast particle densities (in particular, NBI). These affect both the current and pressure

profiles, which determine global MHD plasma stability ([185, 186] - internal modes rather than external ones are more likely in this case given the moderate total plasma β). Fast particle driven instabilities can also have an important influence on global plasma behaviour in these plasma scenarios. To achieve and maintain the required plasma conditions over the target duration of 3000 s, therefore, significant experimental time will have to be dedicated to the optimization of the current and pressure profiles via appropriate application of the H&CD and other actuators.

In principle, the level of energy confinement enhancement required for this plasma scenario is compatible with expectations for hybrid plasmas in present experiments, as well as in ITER. It is assumed, therefore, that this will have been demonstrated within the immediately preceding experiments exploiting the hybrid scenario. The main focus of this phase is production of an integrated scenario demonstrating the steady-state goal at a moderate value of Q (~2). Satisfying this goal will also require an increase in the fraction of self-driven bootstrap current. It is, moreover, expected that these experiments will provide the first empirical insight under ITER conditions into possible approaches to the optimization of plasma confinement and to the control of MHD stability in steady-state plasmas. Such experience will be essential for the development of the subsequent phase of the experimental program. It can be anticipated that the strategy followed for the development of moderate Q plasmas will be based on the DT hybrid scenario development, and will proceed either by starting from the 10.5 MA/4.5 T scenario, by increasing the field to 5.3 T and decreasing the current to 10 MA, or from the 12.5 MA/5.3 T scenario, by decreasing the current to 10 MA. If the resultant change in q-profile is found to cause difficulties for the development of this scenario in DT plasmas (e.g., control difficulties leading to disruptions), an alternative would be to start the development from a previously characterized D scenario at 8.5 MA/4.5 T (q_{95} = 4.5), discussed in section 3.3.2.7, redeveloping the scenario in DT and then increasing the current and field to 10 MA/5.3 T.

Edge integration issues for this scenario are not likely to be significantly more challenging than those for the Q = 5 hybrid plasmas developed previously. These fully non-inductive plasmas will require high auxiliary heating power (to increase plasma β and to contribute sufficient driven current to sustain fully non-inductive operation) and will have a lower plasma density than the hybrid plasmas (due to the lower plasma current), factors which are, in principle, more challenging for edge integration. This is compensated to a certain degree, however, by the lower α-heating levels targeted in this phase.

(vi) Optimization of $q_{95} \geq 4.5$ steady-state (fully non-inductive) plasmas with duration of 3000 s and a target of $Q \geq 5$:

As discussed in detail in [185, 186], achievement of this goal requires optimization of the use of the upgraded H&CD systems and other control schemes available in ITER to ensure full current drive and global MHD stability (implying avoidance of core MHD modes and active control/avoidance of RWMs to decrease disruptivity) while maintaining very high energy confinement (H_{98} ~ 1.7 - 1.5 for q_{95} = 4 - 5). Establishing such plasma conditions is expected to require a substantial experimental program, particularly for the achievement of the quoted energy confinement levels. The details of such a program will depend critically on the experience gained in the development of hybrid and the fully non-inductive Q ~ 2 scenarios discussed - results from these explorations will provide essential guidance on potential strategies for combining high-Q (~5) and fully non-inductive operation under burning plasma conditions.

It is important to note that if, ultimately, the achievable purely non-inductive and fully integrated plasma scenario (including all considerations regarding plasma fusion performance, MHD stability and edge integration) cannot attain the required fusion performance of $Q = 5$, other options with the potential to sustain $Q = 5$ for 3000 s can be explored. These correspond to plasmas with a high driven current fraction (but $f_{NI} < 1$), for which the burn duration can extend to 3000 s (very long, hybrid-like plasmas). In these scenarios the plasma current level is larger than for purely non-inductive operation, but lower than for hybrid plasmas. This reduces the value of H_{98} required to achieve $Q = 5$; more details on such scenarios can be found in [185].

Edge integration issues in these plasmas will have to be addressed simultaneously with the development of the scenario itself, irrespective of the value of f_{NI} finally achieved. This will be complex due to the lower plasma densities (lower edge currents) and high edge power flow (similar to those for the $Q = 5$ hybrid plasmas) expected in these scenarios. This integration aspect therefore represents a significant experimental challenge within this program.

Deliverables: This operational period, if successful, will satisfy the ITER $Q = 5$ mission goals in long-pulse (~1000 s) and fully non-inductive ('steady-state' of ~3000 s) operation with fully integrated scenarios. Even if not fully successful, it should elucidate the highest achievable values of Q in ITER for both scenarios, a key result for the further development of fusion energy. Specific deliverables for this campaign are:

- Understanding of the effect of the isotope mix on non-inductive scenario development in H-mode and on the development of plasmas scenarios incorporating this insight;
- Determination of the threshold for, and the consequences of, AE instabilities in long-pulse/steady-state plasmas with large α-particle populations and the control/mitigation of their effects as necessary;
- Assessment of the impact of the α-particle population on the scenarios obtained (stability and confinement);
- Development of fuelling techniques, DT mix control and burn control for long-pulse operation;
- Development of edge-core integration schemes to provide stationary and ELM power load control compatible with the high level of fusion performance (high confinement) required for these scenarios;
- Provision of input to the physics basis for the DEMO design and guidance on candidate operating scenarios.

As described earlier, upgrades of the heating and current drive systems will enable a broader range of candidate steady-state operation scenarios in ITER, in particular, those of relevance to DEMO design/operation. Due to the limited physics basis currently available for these scenarios, it is not straightforward to anticipate the specific research that will be carried out after the FPO-3 campaign. However, it is expected that the experience gained from existing devices before ITER operation and from the early phases of ITER operation will provide sufficient information for a detailed experimental plan, albeit incorporating a range of experimental options, to be developed prior to this phase. An important output of this program and, indeed, an issue which will be addressed further in subsequent experimental campaigns (FPO-4 and beyond) will be an assessment of the viability of, and requirements for, steady-state operation in DEMO. This topic is developed further in section 3.3.6.

3.3.5 Burning plasma physics studies

The range of plasma parameters achievable in ITER provides an opportunity to study the physics of toroidal burning plasmas in a new, currently inaccessible, regime where a significant population of fusion α-particles and self-heating are achieved simultaneously. This is particularly true of operation with Q > 5, when the plasma will be dominantly heated by the population of α-particles created as a result of the DT fusion process. It should be emphasized that, in this regard, ITER has considerable scientific value in providing validated models that will serve as a basis for DEMO design and operation, even if ITER itself may not provide an explicit experimental demonstration of DEMO scenarios.

The research program for the ITER burning plasma campaigns is likely to evolve as an improved understanding of key issues is developed within the fusion community during the Construction and early Operation Phases of ITER. However, there are certain research issues for which ITER may be expected to provide the primary contributions to the scientific understanding of the underlying physics. Some of these issues are shown in Table 19 and developed further in sections 3.3.5.1 to 3.3.5.5 below. This list is not intended to be exhaustive, but rather illustrative of the research opportunities available for burning plasma studies in ITER DT plasmas.

The initial phases of DT operation, as detailed in sections 3.3.3.1 - 3.3.3.3, will begin to address the issues associated with α-heating and increased power throughput, culminating in $Q \geq 10$ operation for a short pulse, of order (10 - 20)×τ_E (several tens of seconds). At this level, many of the essential burning plasma physics issues can be addressed. Subsequent experiments to extend the burn to the maximum inductive pulse length accessible within the Vs capability of the device in these 15 MA plasma conditions (300 - 500 s) will begin to encounter longer time scale phenomena. Broadly speaking, these include issues of particle transport and exhaust, resistive current diffusion, plasma material interactions (e.g., tritium retention and impurity generation), and infrequent off-normal events. While some of the long-pulse development prior to this phase may have provided relevant experience in most of these areas, the interaction with dominant self-heating and fast (and slowing down) α-particles will present new control challenges.

Specific issues to be addressed include:

- He ash build-up and exhaust, and control of the optimum fuel mix;
- Burn control in the context of time-varying energy, particle (fuel and impurity), and momentum transport as the *q*-profile evolves on the resistive timescale;
- Modification of MHD stability properties due to evolution of the *q*-profile driven by changes in the heating profile, including bootstrap current effects, affecting modes which then interact with the α's, including 'monster' sawteeth, fishbones, various types of AEs and NTMs;
- Interactions of escaping fast α's with first wall structures, potentially producing impurity sputtering;
- Intermittent or aperiodic relaxation phenomena driven by α-heating or instability drive, potentially leading to off-normal events (e.g., disruptions).

3.3.5.1 Energetic particle physics and influence of non-axisymmetry

Good confinement of α-particles generated in DT reactions is crucial for a fusion power plant. Classical single orbit α-particle confinement is well understood and, due to the use of

ferromagnetic inserts to correct the toroidal magnetic field ripple, α-particle loss is predicted to be relatively low in ITER plasmas. However, a high gradient of fast particle pressure in high-*Q* plasmas can drive collective instabilities that may cause α-particle loss. Collective modes of concern include different types of AEs, kinetic ballooning modes (KBM), and internal kink modes. In addition to these driven magneto-hydrodynamic modes, there are also energetic particle modes (EPMs) characterized by a strong dependence on the fast α-particle distribution function [212].

ITER plasma performance also relies on confinement of fast particles generated by auxiliary heating systems such as NBI and ICRF minority heating. The achievement of H-mode in H/He and D plasmas, as well as the transition to high-*Q* regimes in DT plasmas, is critically dependent on the efficiency of heating systems and their ability to deliver full power to the plasmas. Particle energy, pressure, and density of NBI- and ICRF-generated fast ions are expected to be comparable with those of α-particles in high-*Q* operation. It is expected that, by the beginning of DT operations, ITER experiments in the H/He and D phases will already have produced some information on the confinement of fast particles and on the influence of fast particles on the performance of ITER-scale plasmas. High-*Q* operation in the DT phase will provide a unique opportunity to study fast particle physics in reactor-relevant regimes.

Fast particle effects have been studied in many tokamak experiments using fast ion tails produced by NBI and ICRF plasma heating (e.g., [213; 214]), as well as fast α-particles in JET [215] and TFTR [216] DT experiments. However, direct extrapolation from these experiments to a burning plasma is limited, since the values of key characteristic dimensionless parameters and the isotropy of the distribution functions are different. For example, fast particles in ITER will have much smaller normalized gyro-radius and will have to be confined for a much greater number of bounce periods than fast particles in current experiments. Moreover, the distribution function of fast α-particles in a burning plasma will be nearly isotropic, whereas in present experiments, with fast particle distributions driven by auxiliary heating, distribution functions of fast particles are anisotropic.

Present models predict that the drive due to the α-particle pressure, β_α (<1%), in ITER inductive scenarios is comparable to that produced by neutral beam fast ions and leads to marginally unstable TAEs with n = 15 - 30 in the outer region of the plasma, $r/a > 0.4$, as shown in figure 29 [187]. Scenarios with high q_{95} and, in particular, with reversed magnetic shear are expected to be more prone to fast particle instabilities. Initial analysis of the non-linear dynamics of EPMs in configurations with reversed shear predicts rapid fast particle redistribution, albeit with a relatively small global particle loss.

Fast particles can transiently suppress the internal $m/n = 1/1$ MHD mode resulting in a large amplitude ‘monster’ sawtooth crash that redistributes fast particles and plasma parameters inside the affected zone - somewhat larger than the radius of the $q(r) = 1$ magnetic surface [116, 217]. This sawtooth crash can induce seed magnetic islands to initiate the growth of NTMs. On the other hand, fast particles can destabilize the internal $m/n = 1/1$ MHD mode through a resonant wave-particle interaction at the magnetic precession frequency of the trapped fast ions, resulting in fishbone oscillations that can also redistribute the fast particles within the central zone.

Given the large number of instabilities and the complexity of the problem, computational codes predicting α-particle-driven instabilities in burning plasma are unavoidably approximate and

sensitive to the detailed profiles of the scenarios. The development of predictive capabilities is therefore particularly challenging despite ongoing validation exercises against current experiments.

Physics research in the area of fast particles in burning plasmas will require additional measurements such as the profile of fusion power (e.g., neutron tomography), fuel composition, including D/T and He/D ratios and impurity concentrations, and MHD fluctuation in the range of Alfvén modes (30 - 300 kHz). If anomalous loss of fast α-particles is encountered, measurements of the energy spectrum of confined α-particles and the first wall flux of escaping α's may be required to understand the loss mechanism and to inform experiments to eliminate the cause. To avoid localized power loads on the FW - which is typical for fast particle loss - a monitoring of localized heat loads on the plasma-facing wall will be necessary, especially for high-*Q* operation. Whilst visible/IR cameras are sufficient for machine protection purposes, understanding the physics behind such loss channels requires dedicated fast ion loss detectors that can resolve more specific details of the lost fast ions, e.g., their pitch angle and energy. Such diagnostics are currently under investigation for implementation in the baseline, (see [3-Appendix H]).

In addition to non-axisymmetric effects arising from the presence of MHD phenomena, the application of 3-D magnetic fields to influence ELM behaviour will also have an impact on fast particle confinement. Detailed modelling, in which the important effect of the plasma response to the applied 3-D field is retained, has shown that, for the baseline scenario (15 MA) with maximum current in the ELMCC, the primary effect is additional fast ion power loading from NBI in the divertor region, as illustrated in figure 30 [218 - 220]. The ELMCC waveform can be optimized to reduce such losses at, in principle, similar level of ELM control [219. 220]. Therefore, this fast particle loss should be monitored during the experimental program as the various fast ion populations are increased and as various levels of current and relative phasing are explored in the ELMCC. Whilst the distribution of fast ion power loading in the divertor is largely determined by the geometry of the divertor structure, the loads on the first wall are determined by the applied 3-D spectrum. Optimization of the ELMCC current waveform to minimize these losses should be applied to reduce the associated loads to a tolerable level. If this cannot be achieved with static current waveforms, the flexibility within the ELMCC to change the applied field during a discharge will be exploited. This will allow the redistribution of the heat loads while satisfying the requirements for ELM control (e.g., by rigidly rotating a 'static' applied field).

3.3.5.2 Self-heating and thermal stability

Significant plasma self-heating by α-particles raises the issue of thermal stability of the operating point for burn. While one can conceive burn control simulation experiments in present devices, or in the earlier phases of ITER operation, in which a fraction of heating power is proportional to W_{th}^2 ($\propto P_{fus}$ in a power plant plasma), thermally stable operating modes for a power plant must be demonstrated in a plasma heated by fusion reactions. The plasma burn in ITER and DEMO is expected to be globally stable, with operation located near the stable (right) branch of the ignition curve where the power loss increases more rapidly with temperature than the fusion power [221]. An expected increase in fuel dilution by He ash with rising fusion power is an additional stabilizing factor. However, the consistency between the plasma pressure profile, the current density profile (including bootstrap current), and the plasma stability requirements may

raise multi-faceted feedback and profile control issues that could be important, especially for hybrid and steady-state scenarios, in which the power degradation of energy confinement is expected to be weaker than in conventional H-modes [222]. In such a case, a simple global control scheme may not be adequate and more sophisticated control of plasma current and pressure profiles may be required.

Possible actuators for fusion power control in ITER include auxiliary power, fuelling, and impurity injection. Even at $Q \approx 10$, substantial auxiliary heating power is required at the burn point, and a control strategy for regulating the fusion power by modulation of P_{aux} seems feasible. Actuators for particle control include gas puffing and cryogenic pellet injection. Reduction of the fuel ion density reduces the reactivity as $<n_{DT}>^2$, but the response to the fuelling source (primarily pellet injection) develops on the slower particle confinement timescale. More importantly, reduction in the core density tends to reduce the radiated power fraction, unless additional impurity seeding is provided simultaneously, thus aggravating the power exhaust challenge to the divertor.

Conversely, positive excursions in the density to counter a decrease in reactivity are bounded by the proximity to the density limit. A concept based on controlling the fuel mixture (ratio n_D/n_T) could be tested on ITER using independently timed pellet injectors for D and T fuelling.

Measurements of the various quantities of interest for control will be available in ITER. The fusion power (proportional to P_α) is itself observable with essentially zero time lag by monitoring the flux of 14.1 MeV neutrons. This is an important consideration, since the plasma response to variations in reactivity experiences a lag associated with the α-particle slowing down time and the energy confinement time, typically amounting to a delay of several seconds. Real-time spatial profiles of the kinetic quantities n_e, T_e, T_i, and to some extent of radiating impurities, are expected to be available on ITER using the foreseen diagnostic set. Real-time measurements of global quantities such as the plasma current, plasma pressure (β) and the plasma shape will be available from magnetic sensors. Measurement of the fuel mix at the plasma core, edge and the divertor region can be performed by neutral particle analyzers, neutron spectrometers, D and T neutral emission and by monitoring of the exhaust gas.

Although ITER's objective is the achievement of $Q \geq 10$, much higher Q values, and even ignition, are not precluded within the range of present uncertainties in projections of ITER plasma parameters (while remaining under a total fusion power of 700 MW). Optimization of operational scenarios with the aim of increasing Q will be an important part of the ITER research program during the FPO campaigns. An increase in Q to very high values will, of course, make plasma control more difficult, but it would provide a unique environment in which to develop plasma control schemes relevant to DEMO.

3.3.5.3 Macroscopic stability physics and control

Issues of macro-stability research to be addressed during the ITER DT phase operation are centred on four main topics:

- MHD activity driven by α-particles, as discussed in section 3.3.5.1;
- Confinement limiting instabilities, exemplified by NTMs in the core and pedestal stability and relaxation mechanisms in the edge;
- Ultimate pressure (β) limiting instabilities, such as internal modes and RWMs;

- Off-normal events, in particular disruptions.

These effects must be understood and dealt with in ITER for the facility to achieve its performance objectives. Moreover, research into these instabilities on ITER is essential to provide data in support of DEMO and reactor facilities, either by directly demonstrating relevant conditions or by validating theoretical extrapolations to parameters not achievable in ITER itself.

DT operation in ITER will provide a unique combination of β_α, a/ρ_α and $v_\alpha/v_{Alfvén}$ for the study of α-driven instabilities, especially AEs. While the projected value of β_α (<1%) in ITER is smaller than might be expected in a reactor, for example, the comparable value of ρ_α, as well as the isotropic source distribution and self-heated burn dynamics, make the ITER data an invaluable extension to the existing database in this area by providing a vital testbed for validation of linear and non-linear theoretical models of these phenomena. The ITER research program relating to α-driven instabilities would therefore incorporate:

- Validation of linear stability boundaries in the relevant range of parameter space;
- Validation of non-linear predictions of α-transport and redistribution in unstable regimes, including potential coupling to thermal plasma modes, either through direct excitation, e.g., generation of seed islands for NTMs, or modification of pressure or current profiles;
- Tests of active control or mitigation of α-driven instabilities.

Studies of NTM physics and application of ECRH/ECCD-based NTM control should have already begun during the PFPO and D phases of ITER operation. Control of these modes is expected to be required to allow achievement of the plasma pressure necessary for the target $Q \geq 10$ inductive operation, and thus a relevant demonstration of NTM suppression is required [102]. However, due to the limitations on available auxiliary power in the D phase it may be necessary for this demonstration to be conducted at less than full (dimensional and non-dimensional) parameters. While NTM physics has been extensively studied in smaller devices, validation of theoretical projections to reactor-scale ρ^* is a unique capability of ITER, as is the possible interaction of NTMs with α-driven modes and profile modifications associated with self-heating. The ITER research program into NTM physics during inductive operation in the DT phase would emphasize physics validation and control optimization in non-dimensional parameter regimes (β, ν^*, v/ω^*, ρ^*) not accessible during the D phase, and would identify and investigate issues associated with α-particle effects and self-heating. During hybrid mode operation, ITER research will investigate the beneficial role of saturated NTMs in maintaining $q_0 > 1$ at reactor-relevant β and in the presence of α-heating.

Non-inductive, high-β plasmas produced in support of the steady-state $Q \geq 5$ goal at high q_{95} are likely to present more stringent requirements on the NTM control algorithms, as a number of potentially unstable modes must be tracked and suppressed as the q-profile evolves. As the kink β-limit is approached, Δ' is increased, destabilizing the classical tearing mode, which can then grow as an NTM. To the extent possible, control algorithms will have been tested at similar β and q-profiles, but at reduced absolute parameters, during the PFPO and D phases. The extension to the burning plasma conditions during experiments in DT will introduce a unique combination of parameters, as well as confronting coupling of the self-heating to the pressure and current profiles. Optimization of the feedback/feedforward tearing mode control strategy will be essential to realization of the steady-state $Q \geq 5$ target. While neither the bootstrap fraction nor the achievable β in ITER will reach values anticipated for a steady-state DEMO based on advanced scenarios,

the interaction of self-heating and α-driven instabilities with NTM control represents an irreplaceable testbed for validation of models and control algorithms for extrapolation to DEMO and reactor conditions.

In the steady-state regime, ITER is expected to operate close to the no-wall β-limit and may therefore require control of RWMs. Much of the underlying physics associated with control of these modes is known (in principle), and has been, or will be, validated on medium-sized non-burning tokamaks. Some issues will remain, however, which can only be fully elucidated by experiments at the reactor scale. The first research problem to be confronted by high-β experiments on ITER is likely to be exploration and validation of models of the passive (rotational) stability boundary, below which active feedback is not required. Kinetic effects, due to thermal plasma and fast particles, are important elements of the MHD physics of wall stabilization, and, of course, in the absence of strong injected torque, the rotation will depend on transport phenomena. Therefore, experiments at ITER values of ρ^* and including fast ions (initially from MeV NBI in the D phase, then by the more isotropic α-particle distribution in the DT phase) will provide essential checks on the theory. A powerful tool supporting such experiments is the capability to diagnose the proximity to RWM instability by means of active MHD spectroscopy [223]. This could be achieved on ITER by using the in-vessel ELMCC to apply a rotating $n = 1$ perturbation while measuring the amplitude and relative phase of the plasma response and comparing (or fitting) to theoretical models.

The results of these experiments will need to be incorporated into the design of model-based controller algorithms for avoidance and stabilization when operating close to the wall-stabilized β-limit [224]. Specific control algorithms and actuators for steady-state operation will be tested in ITER, to the extent possible, prior to DT operation by accessing the relevant β at half-field, provided the auxiliary power is adequate in the absence of α-heating. Since the extrapolation in ρ^* to full field DT operation will be less than a factor of two, these experiments would provide confidence in the approach and methodology. The additional RWM physics associated with DT operation will arise primarily from the influence of an isotropic fast ion (α) distribution, and from the couplings associated with self-heating, which imposes additional constraints on pressure and current profiles, impacting the stability which may require a MIMO (Multiple-Input Multiple-Output) control strategy.

Upgrades to power supplies of the ELMCC so that they can provide RWM control to avoid high disruptivity with high β values may need to be considered to support extension of the ITER advanced scenario operational regime near to physics limits.

A particularly important stability issue for ITER is that of disruptions, due to the potential impact of disruptions on the research program [87] (see also section 2.5.4). In addition to the electromagnetic and thermal loads imposed on the tokamak internal structures, which can be estimated to some degree from experience on smaller devices, disruptions at the ITER scale are predicted to generate substantial avalanche runaway electron currents at levels not previously encountered. This prediction should be tested already during the PFPO phase on ITER, together with qualification of mitigation techniques. The technical demands on the mitigation system during the DT phase are expected to be only quantitatively, not qualitatively, different, due primarily to the increased stored thermal energy, except in conditions in which the additional sources of seed electrons in DT plasmas are sizeable [225]. Of course, the reliability of the

mitigation algorithm must be assured before DT operation and reconfirmed as full parameters are approached.

While disruption mitigation will be relied upon to prevent melting of the ITER plasma-facing components and the production of large electromagnetic forces on vessel and in-vessel component, the recovery time associated with even mitigated disruptions may represent a significant cost to the ITER research program, especially during the high-Q inductive DT phase. Moreover, while the consequences of such off-normal events in terms of lost research time are serious for ITER, the tolerance for such occurrences in a DEMO, or a reactor, will be orders of magnitude less. To this end, research on ITER should aim to develop both real-time control algorithms that avoid (as much as possible) instabilities that may lead to disruptions and control methods for stabilizing the responsible instabilities. The development of these control techniques and the assembly of information on the scaling of disruption effects with machine size will be extremely valuable in the design of the next-generation of fusion devices.

3.3.5.4 Multiscale transport physics

The physics governing magnetic fusion plasmas covers an enormous range of spatial and temporal scales. ITER will represent the first opportunity for the fusion community to assess plasma transport in a system with a reactor-relevant ratio of the ion gyro-radius to the system size (i.e., at very low ρ^*). Because ρ^* is the only dimensionless parameter governing plasma transport that cannot be matched in existing devices, the research conducted on ITER in this area will provide significant leverage in the scaling of present databases to future devices. A further important issue that ITER will help resolve is the impact of electron transport on overall confinement in reactor-like conditions in which the α-particle energy will primarily be coupled to the plasma electrons.

Detailed turbulence characterization studies will be more challenging on ITER than on current devices, but some diagnostics do appear capable of diagnosing turbulence in ITER (e.g., Beam Emission Spectroscopy fluctuation measurements) could be considered for incorporation into the baseline if required (see [3-Appendix H]). These diagnostics allow comparisons of plasma turbulence in ITER and those in smaller devices.

Plasma rotation will also be a critical issue for ITER. It is well established that increased plasma rotation can have beneficial effects on both transport and stability properties of tokamak plasmas. However, the likely level of rotation in ITER plasmas remains uncertain. The main source of external torque is limited to NBI (1 MeV energy) and self-generated torques may play a significant role in generating rotation. Measuring rotation and, more importantly, identifying the mechanisms responsible for the observed rotation should be a high priority research topic on ITER. Such research may point the way to optimization of a future device to take maximum advantage of self-generated plasma rotation.

A closely related topic is that of transport barrier formation, sustainment and, where appropriate, avoidance. Present knowledge suggests that these barriers can be induced by a combination of plasma rotation and compression of the magnetic field on the outboard side of the plasma. While ITER's tools for rotation control are limited, the significant current drive capability available should allow manipulation of the driven current profile over a wide range to assess the

practicality of generating transport barriers in the presence of significant α-particle heating. Such knowledge may be necessary to achieve the mission objectives of the long-pulse $Q \sim 5$ scenarios.

3.3.5.5 Physics of the plasma-boundary interface

ITER will represent a major step towards reactor-like edge conditions, simultaneously requiring a high pedestal temperature, dissipation of high heat fluxes, low tritium retention, and adequate exhaust of the He ash produced by the fusion process. While many aspects of the plasma boundary interface issues required for successful operation of ITER have been demonstrated individually in current devices, ITER experiments will play a crucial role in obtaining physics data for developing specifications for power and particle exhaust and plasma-wall interactions in DEMO.

Simulations of ITER performance suggest that the strength of the H-mode edge transport barrier will play a major role in the ability to achieve high-Q operation [226]. At present, a first-principles understanding of the structure of this edge region (i.e., pedestal) is still being developed. The operating conditions of ITER plasmas (low ρ^*, low collisionality, high pedestal density relative to the Greenwald density, moderate β, low neutral source) will be distinct from those accessible in current devices, providing an opportunity to develop more fully the physics understanding of the processes that determine the edge plasma structure. Integrally linked to this issue is the control of ELMs to reduce large transient heat fluxes to the divertor targets. Research to control the edge evolution and/or structure through the use of non-axisymmetric magnetic fields (resonant magnetic perturbations), or other means (for example pellet pacing, vertical plasma oscillations, etc.) will take on added importance in ITER as performance increases towards its design goals [63].

The study of the performance of PFCs constitutes a major activity within the Research Plan [132]. ITER research must demonstrate, to the extent possible, that most of the energy arriving in the divertor region can be radiated, that tritium retention can be kept within acceptable levels (i.e., below 1%), that adequate He exhaust can be provided, that acceptable core impurity concentrations can be maintained and that plasma-facing materials have a tolerable lifetime. In brief, having established an adequate mode of divertor operation that satisfies the requirements of ITER's fusion performance goals, the ultimate goal of the IRP in this area will be to explore the extent to which this mode of operation can be developed further to provide a divertor physics and technological solution basis adequate for a reactor.

Regarding tritium retention, R&D planning for the PFPO campaigns aims to ensure that an adequate knowledge base will have been acquired to allow a robust scheme for fuel retention management to be developed prior to DT experiments. Moreover, DT operations will benefit from the deployment and validation of the global tritium accounting scheme using tritium accounting through the T-Plant, determination of burned fuel through neutron rate measurements, gas balance measurements and local retention measurements using the planned tritium monitor, which first becomes available in PFPO-2 (see [3-Appendix H]). With the development of long-pulse DT discharges, both T retention and T permeation through components to the cooling water can be characterized. While permeation through Be is expected to be negligible, this is not the case for stainless steel components visible to the plasma (Diagnostic First Wall, TBM front surfaces, blanket module surfaces not completely covered by first wall panels, etc.), in which permeation

will probably occur during baking of in-vessel components and must be accounted for to close the tritium cycle. Although the dpa levels in ITER will be relatively modest compared to those expected in DEMO, ITER will provide valuable information for the next step on the evolution of the retention and permeation rates in neutron damaged materials (especially for W and steel) in the tokamak environment.

As operations progress towards DT and longer pulse durations, and as disruptivity requirements are tightened, it is anticipated that dust production mechanisms during FPO will evolve from melt-generated droplets to solid particles resulting from the delamination of thick co-deposit. Modelled Be deposition rates for ITER are in the range of ~0.15-0.9 $nm \cdot s^{-1}$ in the divertor [227, 228] This corresponds to thicknesses of up to several 100 μm that may be reached by the end of FPO-1. Monitoring the formation of thick co-deposits and their delamination will be important to avoid the creation of loose material on surfaces, which could, for example, be detrimental to plasma initiation.

Regular monitoring of first wall erosion will be important to validate earlier estimates of the first wall lifetime and inform the need for detailed adjustments of the magnetic equilibrium in case of pronounced localized wall erosion. In essence, it is expected that the wall erosion rate will be understood sufficiently well at this stage that the FPO phases will serve only for the validation of existing models, providing important input data for the design of the DEMO first wall in terms of erosion lifetime (though not on the erosion itself, since wall materials may be different). If, as expected, long-term wall erosion in DEMO-class devices is dominated by charge-exchange neutral impact, then ITER is likely to be the only device in which this can (at least partially) be verified, largely through the application of models together with the experimentally determined overall migration balance (though the latter requires routine long-pulse operation). Although experience gained through the PFPO phases will be helpful, it is likely to be only as a result of long-pulse fusion power operation that a proper assessment can be made of the need for (and timing of) replacement (including possible change of plasma facing material) to in-vessel components.

It is important to note that during FPO, the divertor material in the high heat flux regions will be regularly operated close to the tungsten recrystallization temperature. Such conditions are unlikely to be obtained, even with full power, in PFPO-2. Regular execution of a reference pulse (see [3-Appendix D]) will allow the evolution of the divertor power handling capabilities to be carefully characterized during operations. As the discharge duration is increased, the ion fluence onto the divertor (and, possibly, the number of mitigated ELMs) will also reach very high values. Analysis of divertor material exposed to FPO plasmas (following single or multiple divertor cassette replacements) will provide important information on modifications of the material thermal and mechanical properties, supplying guidelines for the possible development of advanced tungsten-based materials for DEMO. In general, it is expected that ITER will provide key information on the use of a divertor with solid targets (as opposed to liquid plasma-facing surfaces) at the reactor scale.

During the FPO phase, mixed He-D-T plasma interactions with tungsten at elevated temperatures will occur and surface morphology changes may be more likely than during pure He operation in PFPO [73]. He-induced morphology changes might strongly affect the surface emissivity, implying a requirement for regular calibration of the infrared and visible diagnostics

to account for this and to ensure that reliable measurements can be derived. At the same time, observations of emissivity changes will provide information on the formation/ evolution of any He-induced morphology changes.

3.3.6 Perspective to longer-term DT operation after FPO-3

The overall duration of the FPO Phase will be eventually determined by the ITER Members at an appropriate time.

The detailed research program for the FPO phase developed within the previous sections encompasses only the first 3 DT campaigns with the aim of presenting an experimental plan that can achieve the principal scientific goals and some elements of the fusion technology mission, to illustrate the issues and risks that will need to be addressed in establishing the necessary high fusion gain plasma scenarios, including areas where early upgrades to the baseline hardware capability could be advantageous to mitigate them, and to consider the key aspects of burning plasma physics to which ITER experiments will give access. Clearly, many details of this plan will evolve in response to the experimental results obtained during ITER operation and in the light of the experience gained in the study of burning plasmas following the introduction of DT fuel.

Given the ambitious scientific and technology goals for the ITER project detailed in section 1, fulfilment of the principal fusion gain goals will merely provide the baseline from which the overarching role of the project in the development of fusion energy will be fully developed. The attainment of high fusion power, high fusion gain and long duration burning plasmas will provide the 'tools' to enable wide-ranging studies of fusion science and technology in a reactor-relevant environment. Looking beyond the initial 3 FPO campaigns discussed in previous sections, there is, therefore, extensive scope for a significantly longer period of DT operation to prepare the science and technology basis for DEMO-class devices.

In this context, it should be emphasized that the ITER design accommodates substantial potential for upgrades to many auxiliary systems to facilitate the achievement of mission goals (e.g., should the baseline H&CD or fuelling capabilities prove inadequate to achieve the fusion power/ fusion gain or pulse duration goals), to extend the fusion performance of the device beyond the baseline requirements (e.g., towards higher Q in inductive and non-inductive operation), to more fully explore burning plasma operation under DEMO-relevant conditions (e.g., using more advanced plasma-facing materials currently under development for application in DEMO-class devices - the ITER design accommodates the possibility of changing the material of the entire first wall and replacing the divertor), to explore the performance of DEMO-relevant technology under burning plasma conditions (e.g., alternative or more advanced TBM concepts, H&CD or Diagnostic sub-systems, etc.), and to develop integrated plasma scenarios towards reactor-relevant conditions (e.g., exploiting the full potential for H&CD upgrades to significantly increase the total plasma loss power, requiring operation at higher radiated power fractions). A more extensive discussion of the potential scope of, and rationale for, upgrades to the ITER device can be found in [3].

It would be premature to develop a detailed prescription for the longer-term DT research program, given how much is likely to be learned from ITER experiments during the PFPO and FPO-1 to FPO-3 campaigns. Nevertheless, the current understanding of the role that ITER should play in the development of fusion energy provides a basis for anticipating the scope of the research

program beyond FPO-3. As already noted, on this timescale the capabilities and flexibility of the device could already have been expanded by the installation of a variety of upgrades, perhaps to take advantage of opportunities which have emerged from ITER experiments, or to resolve challenges identified *en route* to high fusion gain, and this process can be expected to continue during the latter periods of DT operation to further develop ITER's ability to address scientific and technology issues in support of the development of DEMO-class devices. Indeed, the ITER *Project Requirements* already specify a range of upgrades which the facility is designed to accommodate to enhance its potential for fully exploring high gain fusion operation and testing reactor-relevant technology:

- The installation of a 3rd NBI box, which, in combination with the 2 baseline NBI systems, would deliver a total of 50 MW of beam power;
- An increase of both the ECRH and ICRF H&CD systems to launch powers of 40 MW;
- The upgrade of the in-vessel coil power supplies for RWM control, etc.;
- An increase of the number of fuel pellet injectors from 4 to 6;
- The installation of a second tungsten divertor;
- Replacement of the beryllium first wall with a tungsten first wall;
- Upgrades to port-based systems such as diagnostics, disruption mitigation systems, etc.;
- The installation of improved TBM designs and, possibly, new TBS designs.

A significant fraction of these upgrades could be developed around DEMO-relevant technology, which would enhance ITER's contribution to the development of the design and operational basis for DEMO-class devices. Such options are developed further below.

Specific lines of research which might require significant allocations of experimental time in the later DT campaigns, in addition to a continuing program to deepen the understanding of burning plasma behaviour in various high fusion gain plasma scenarios, could include: optimization of fusion gain in very long pulse, in particular fully non-inductive, plasma scenarios (the trade-off between the achievable fusion gain and the approach to fully non-inductive operation might be of particular interest - but note that the limitation of the duration of ITER high fusion gain plasmas to durations of ~3000 s is associated with intrinsic aspects of the ITER design); fusion technology studies in burning plasma conditions, e.g., extended exposure of a range of TBMs to high neutron fluences, tests of DEMO-relevant plasma-facing materials and components, studies of the resilience of plant systems (cooling, cryo-systems, T-Plant, etc.) in long pulses at high fusion power; exploration of candidate plasma scenarios for DEMO operation, based both on ITER's operational experience and on new results which might emerge from the R&D activities in the Members' programs; tests of plasma operating concepts for DEMO-class burning plasmas in which plasma control systems, H&CD systems, Diagnostics, PFCs, etc. are constrained by DEMO-relevant considerations (e.g., using a slimmed-down Diagnostic set based on diagnostic concepts applicable in DEMO-class devices); and, as an overarching task, attainment of the lifetime average first wall neutron fluence of 0.3 MW.yr.m^{-2}, as required by the *Project Specification*.

It should be noted that, to the maximum extent possible, it would be the project's aim to satisfy this last requirement as an end result of the research program developed around the other themes. Nevertheless, analysis of a 'strawman' experimental program developed to understand the implications of the lifetime neutron fluence requirement has shown that this goal is achievable,

but is demanding in terms of fusion power production and sustained pulse duration. Such a program must also be consistent with technological constraints, such as the overall CS design limit of 30,000 full flux swings, the minimum duty cycle of 25%, which impacts the pulsing rate in very long pulse hybrid or fully non-inductive scenarios, but must also allow flexibility in adapting pulse parameters, target fusion power and pulse duration to the needs of experimental research. On the other hand, some credit can be taken for the gain in overall system reliability with operational experience and with gains from experimental research, such as a substantial reduction in disruption frequency, which will be essential for the pursuit of a viable research program at high fusion power. On the basis of these considerations, IRP analysis has concluded that in the course of the FPO-1, FPO-2 and FPO-3 campaigns the neutron fluence produced will be in the range of 20-30% of the lifetime target. This implies that a substantial programme of R&D in DT plasmas can be implemented in FPO-4 and subsequent campaigns before the lifetime neutron fluence goal is achieved.

Following a successful research program demonstrating the key fusion science goals of the project (say, within the period FPO-1 through FPO-3, as outlined here) and establishing the reliability of ITER's design and technology solutions in the burning plasma environment, a reasonable expectation is that the program's focus would turn more explicitly towards the preparations for DEMO. ITER can be expected to deploy improved plasma H&CD schemes, as well as components to test first wall and heat extraction technologies, which would be suitable for initial deployment on DEMO. These would comprise evolutionary updates to existing or planned H&CD systems to provide greater flexibility, reliability and survivability and/or higher power density.

Such H&CD upgrades would bring the level of installed power to the allowed maximum of 130 MW, of which ~110 MW would be available for simultaneous injection into plasmas (due to site power limitations). This expansion in H&CD capability, together with the upgrades for fuelling and first wall components described above, would make ITER an ideal test bed for integrating the technology and plasma regimes foreseen in DEMO. The upgrades would allow ITER to explore plasma operation with DEMO-like H&CD schemes and first wall divertor materials under DEMO-relevant plasma conditions: high P_{loss}/P_{LH}, high β_N, high P_{rad}/P_{tot}, high $\langle n_e \rangle / n_{GW}$, high Q ($\geq$10) and steady-state Q ($\geq$5), albeit not simultaneously and/or not at the highest currents. Given the uncertainty in the predicted H-mode threshold in ITER, an increase of the heating power level may also be required to access very high gain (Q significantly above 10), which would allow the study of quasi-self-sustained thermonuclear plasmas in ITER.

As a specific illustration of the ITER's potential to provide support to the development of DEMO-class devices, exploitation of the H&CD upgrades would allow the study of DEMO scenarios with significant levels of core/edge radiation that are currently foreseen to provide a solution to the stationary power exhaust problem for conventional divertor DEMO designs [229]. Such studies would most likely be restricted in Q in ITER and, thus, to plasmas with non-dominant α-heating (unlike DEMO). As an example, the range of achievable core radiation fractions in ITER and the resulting Q for 15 MA/5.3 T and 7.5 MA/2.65 T scenarios is shown in figure 31. These have been evaluated using extrapolations of integrated plasma simulations for 50 MW additional heating [66], together with a simple 0-D model with $H_{98} = 1$ and using the (optimistic) assumption of constant impurity and He fractions independent of core radiation. The

final performance of such ITER scenarios with high core radiation needs to be refined with integrated plasma simulations to quantitatively determine the range of available Q versus core radiation for high additional power operation in DT. It should be noted that if the performance in figure 31 can be realized for 15 MA/5.3 T plasmas with additional heating levels above 50 MW and high core radiation, this implies operation with 500 MW < P_{fus} < 700 MW. In turn, this would require prior assessment and authorization to proceed and may be restricted to shorter burn durations than operation at Q = 10 with P_{fus} = 500 MW. On the other hand, the increase in both auxiliary and α-heating under these conditions is compensated by core radiation, so that the power to the SOL (P_{SOL} ~ 100 MW) is the same as for Q = 10, P_{fus} = 500 MW operation, requiring similar levels of SOL+divertor power dissipation as for Q = 10 scenarios.

ITER can also make significant contributions to the testing of advanced DEMO-relevant first wall and divertor materials and structures, together with associated heat extraction technologies, in an integrated fusion environment (the first wall technology might be incorporated in more advanced versions of TBMs). Replacement of the first ITER divertor is foreseen in the FPO phase. As discussed in section 5.4.5, limits for divertor lifetime based on W recrystallization indicate that this could be reached by the end of FPO-3 [45, 73]. Depending on findings in the PFPO and early FPO campaigns and on the outcome of research for fusion reactor divertor materials and design, the second divertor could incorporate the use of advanced tungsten-based materials considered for DEMO [230], improved monoblock surface shaping or vertical target design based on operating experience at ITER, and modifications to the divertor geometry to address DEMO divertor physics and technology issues, within the constraints defined by interfaces with the divertor cassette structure. This could include modifications to the vertical target and dome geometry to widen the ITER operational space at high fusion power by increasing power dissipation and/or He exhaust, etc.

Similarly, a change of the first wall armour from beryllium to a reactor relevant material, while maintaining the interfaces with the blanket shield modules, in later phases of FPO would enable DEMO-relevant assessments of the compatibility of such a wall with high-Q scenarios to be performed in ITER. Of particular interest are the issues of core impurity and radiation control since wall-born impurities have a much higher probability of entering the core plasma than those originating from the divertor. Nevertheless, as identified in [67] and discussed in section 5.3.2.1, edge plasma screening in ITER is expected to be very efficient for medium- to high-Z impurities.

Further tests, in particular, those related to novel technologies linked to advanced TBMs, would focus on studying the synergetic effects of neutron irradiation and high plasma fluxes on the sputtering of advanced materials and on the tritium uptake, retention and diffusion through high performance helium-gas cooled first wall and divertor panels operating at elevated temperatures (higher than 600 °C). Attractive advanced plasma-facing/structural material combinations, such as tungsten joined to oxide dispersion strengthened, low-activation steel, could be tested. Such tests would be enhanced significantly by running a series of highly reproducible steady-state pulses during the latter phase of ITER operation.

As noted above, DEMO-relevant plasma operation could be explored by constraining auxiliary systems to reflect the contemporary thinking on the limitations inherent in the scope and operational capabilities of DEMO auxiliary systems, in particular, H&CD, Diagnostics, Fuelling, and by adapting control algorithms within the PCS to reflect such constraints (see, e.g., [231,

232]). When combined with a DEMO-relevant PFC environment and exploiting candidate plasma scenarios for long-pulse or steady-state DEMO operation, such experimentation could prepare an important basis for initial fusion power production in DEMO-class devices. Although experiments of this type might imply additional operational risks (e.g., can robust disruption detection, avoidance and mitigation be implemented reliably within this mode of operation?), such risks will have to be addressed and resolved within the fusion research program to ensure reliable operation of a DEMO.

3.3.7 Experimental Risks in FPO

The physics and operational risks to the successful implementation of the FPO phase evolve as the operational space opens from DD to DT high Q operation and are discussed below in terms of the major strands of research developed in preceding sections.

3.3.7.1 FPO DD and Trace-T operation

Many of the risks that impact this phase should be already retired by the PFPO programme to the extent that this is possible as a result of experiments in H/He plasmas. In this respect, the main operational risks concern the retuning of ELM control schemes for H-mode operation, DMS, divertor power load control, etc., to characteristics of the DD scenarios (higher plasma energy, temperature, power fluxes, etc.). Similarly, the H&CD systems must be commissioned for D plasmas; this impacts particularly the NBI which will operate in deuterium. However, since shine-through losses are lower in D plasmas with D^0 beams than in H/He plasmas with H^0 beams, the operational risk in D plasmas with D^0 NBI are reduced. This also applies to the intermediate scenario steps required to achieve 15 MA/5.3 T L-mode operation in D, since risks with such a strategy should have been retired by PFPO experiments or, if this were not possible, the strategy modified to avoid issues encountered during PFPO by the time of FPO.

In general, the strategy followed to mitigate operational/ physics risks in D plasmas is similar to that applied in the PFPO, i.e., start with plasma scenarios at low current and additional heating power in which the risks to investment protection are low and expand the scenario operational space gradually. The main physics risk in this phase is that, despite the assessment of this issue in PFPO, it may emerge that the additional heating power required for robust H-mode operation in D up to, at least, 7.5 MA/2.65 T or the power expected for $Q \geq 10$ operation is larger than that estimated from PFPO experiments (assuming that no power upgrade were required as a result of PFPO findings). If this were the case, the mitigation would involve the launching of an additional heating power upgrade at this stage before it is required to support the high-Q DT program.

Initial development of hybrid/advanced scenarios in D plasmas have common risks with the H-mode development program, but there are also specific risks to the hybrid/advanced scenarios. These are related to the capability of the ITER actuators and control loops to achieve the required level of plasma control and to uncertainties in the extrapolation of results from PFPO-2 to D plasmas:

- *Higher β operation leads to additional MHD-related phenomena affecting the scenarios:* The β of the D plasmas in this phase will be higher than that of the H/He plasmas in PFPO-2. This may lead to new MHD phenomenology affecting NB current drive and fast particle losses (e.g., AEs, enhanced losses with 3-D fields for ELM control due to larger

plasma response [92], etc.). Mitigation would require additional experimental time to characterize and control these phenomena, limiting their effects on the plasma;

- *Heating and current drive flexibility is not adequate to develop the scenarios:* Due to the increasing demands on the H&CD capabilities, sharing of missions among the systems will be challenging (e.g., ECRH/ECCD may be required for core W control, AE control, NTM control, etc.). If the demands cannot be met, an assessment of the implications for DT operation will be made and, if necessary, the upgrade(s) required for successful $Q \sim 5$ long-pulse operation identified and implemented at this stage;
- *Experience developed in PFPO-2 is not relevant:* D plasmas in these scenarios might differ significantly from the corresponding scenarios in H/He plasmas, so that operational recipes developed in H/He do not extrapolate: e.g., current ramp-up scenarios developed in hydrogen/helium L-mode plasmas might not be applicable to D plasmas due to the lower H-mode threshold in D, analogous to the experience in D and DT plasmas at JET [183]. This would necessitate a redevelopment of scenarios involving adjustments in the heating level, current ramp-up rate, density, etc.

In relation to the trace-T experiments the main physics and operational risks are:

- *Insufficient sensitivity in key diagnostic measurements:* At very low T concentrations (~1% T in D), the key diagnostics to determine the T concentration in the confined plasma, in the recycling fluxes or retained in the plasma-facing components might be found not to have the sensitivity required to determine trace amounts of tritium in 7.5 MA/2.65 T H-mode plasmas. Depending on the sensitivity problems and the diagnostics affected, this could be solved by performing the experiments at a higher T concentration (~10% T), if the required throughput can be provided by the T-Plant at this stage;
- *Modelling of T transport is not sufficiently mature at this stage to allow particle transport validation:* Modelling of multi-species particle transport in ITER-like plasmas is expected to be highly developed at this stage of the experimental program. This should allow its validation and fine tuning with the trace-T experiments and application of the corresponding numerical codes to the detailed planning of DT experiments. Should this expectation not be fulfilled, the impact on the trace-T experiments themselves would be limited, but the lack of an adequate simulation capability for the subsequent DT campaigns would be more significant: the DT campaigns would then have to be based fundamentally on experimental findings, which would slow the progress towards maximum fusion performance;
- *Trace-T experiments reveal that T-retention in ITER PFCs is larger than expected, or T-removal is less efficient than foreseen:* The impact on the trace-T program would be minimal, given the relatively small amounts of T involved, but this could have significant implications for the following DT campaigns. Obtaining relevant experimental data at an early point in FPO is therefore essential to inform potential actions to retire these risks prior to the transition to routine long-pulse DT operation, where they may become an issue.

3.3.7.2 FPO DT operation in inductive scenarios

This phase covers operation at ~ 50-50 DT starting from 7.5 MA/2.65 T H-mode plasmas up to the demonstration of $Q \geq 10$ operation for burn lengths of 300 - 500 s. A general discussion of

the risks to the achievement of ITER's Q ≥ 10 goal can be found in [3-Appendix J]. In the following, few specific risks to this phase of the experimental program are described in detail:

- *Nuclear heating and/or AC losses of the superconducting coils significantly exceed expectations:* This phase of the IRP will offer the first opportunity to address this issue quantitatively at parameters (current, field and fusion power) corresponding to the ITER design specifications. Since the approach to the long pulse (300 - 500 s) $Q \geq 10$ burn is gradual, the possible materialization of the risk will not be sudden. It is considered unlikely that any discrepancy with the predicted thermal load on the superconducting coils would limit operations in the initial $Q \geq 5$ experiments due to the short burn duration of ~50 s. However, if this risk materializes, it could have implications for the achievement of the ITER long burn, high-Q mission goals. The mitigation of the risk would require redevelopment of the plasma scenarios to reduce AC losses (the scope for reduction of the nuclear heating load is limited in view of the high fusion power, high fusion gain mission) and/or upgrades to the cryogenic plant;
- *Flux swing provided by the CS/PF system is marginal for H-mode operation at 15 MA:* The PFPO and FPO L-mode experiments at 15 MA should already provide data on flux consumption at high current, but a realistic evaluation of the flux consumption of the complete H-mode scenario, including the burn access and exit transitions, will only be available in this phase. If poloidal flux limitations were encountered in the high-Q DT experiments at 15 MA, further scenario optimization studies would be required within this program. Some aspects of such studies are, indeed, included in the research plan for this phase (e.g., H-mode access and exit at $2/3 \times I_{p,flat\text{-}top}$), but an expansion of measures to minimize flux consumption, particularly in the burn access/exit phases, would be required;
- *Predictive and interpretative modelling of particle and thermal transport (core to edge) and of α-particle behaviour is not sufficiently mature to provide a reliable basis for scenario development:* This would require a more empirical approach to high current, high fusion power scenario development, resulting in slower progress - increments in I_p/B_t, auxiliary power, T-fraction, etc., might be smaller than strictly required to ensure that plasma control requirements remain consistent with the operational/hardware capabilities, and that plasma scenarios remain MHD stable to ensure low disruptivity;
- *Edge-core integration requirements (ELM control, stationary power load control, etc.) prevent the achievement of $Q \geq 10$ or its sustainment over long operational periods:* This could be associated with excessive core plasma impurity contamination as a result of power load control, degraded confinement due to ELM control, insufficient control capability due to hardware limitations for $Q \geq 10$ operation with 15 MA plasmas, etc. Depending on how the risk materializes, mitigation strategies may involve: (a) hardware upgrades, such as increased ECRH power for central heating/impurity control, additional pellet injection for improved density control, etc.; (b) definition and monitoring of a divertor operational budget to ensure that its lifetime is used in accordance to the IRP objectives/priorities; (c) earlier development of the hybrid/advanced scenarios and their optimization for $Q > 5$, since they may have less demanding edge-core integration requirements; (d) development of alternative high confinement, ELM-less regimes such as QH-mode, I-mode, etc.

It should be noted that the IRP already includes mitigation strategies to minimize the edge-core integration risks as the operational space of DT H-modes expands towards high-Q operation at 15 MA. These include the usual gradual operational expansion, in terms of plasma current/field and additional heating power, utilized from PFPO onwards, together with specific choices of operational density steps, variations of T-fraction, etc. The latter are intended to optimize the way in which α-heating increases as the operational space widens and Q increases, so that large changes in α-heating, which may be challenging from the edge-core integration and fast particle stability control points of view, are avoided between successive operational scenario steps.

3.3.7.3 FPO DT operation in long pulse and steady-state scenarios

This phase covers operation at ~50:50 DT towards the demonstration of $Q \geq 5$, 1000 s long-pulse burn length and the exploration of steady-state operation up to $Q \geq 5$ with a 3000 s burn. Long-pulse and steady-state scenarios require fully integrated capabilities to control plasma scenarios. Failure to achieve a comprehensive level of scenario integration would affect the accomplishment of this aspect of the project's mission goals. The general risks to the $Q \geq 5$ long pulse and steady-state goals are registered in [3-Appendix J]. These are related to H&CD, including the impact of fast particles, to edge-core integration and to the achievable level of improved H-mode plasma confinement. The last is essential in these scenarios, both to achieve the required plasma performance for $Q \geq 5$ and to provide the required bootstrap current to sustain steady-state operation.

In addition to these issues, the major specific risk for this operation phase is that the scenarios developed for D plasmas (particularly in the ramp-up phase) may not be viable for DT plasmas due to the isotopic dependence of the H-mode power threshold, an effect already observed in JET [183]. This is linked to the issue that the H&CD requirements for establishing the required target current profile at the end of the current ramp-up must be compatible with sustaining the required plasma confinement regime during the ramp-up, e.g., if the ramp-up scenarios should require L-mode plasma profiles to achieve a given $j(r)$, but the H&CD level required to sustain the current profile formation were to cause the plasma to enter the H-mode. If this risk materialized, specific additional studies to those performed in D would be necessary, e.g., to suppress the H-mode to facilitate formation of the target $j(r)$ at the end of the current ramp-up.

3.3.8 Outcome of initial DT program to FPO-3

The plan presented in sections 3.3.1 - 3.3.5 initially emphasizes the development of (predominantly) inductive scenarios, in particular, the 'conventional' ELMy H-mode regime in D and DT plasmas, since this, at present, has the most developed quantitative physics basis for extrapolation to fusion power production in ITER. The primary focus of the initial D phase of operation is the development of DT-relevant scenarios in parallel with the continuing commissioning of the T-Plant and the gradual rise in T throughput, leading to the establishment of plasmas with a sufficient T concentration to initiate significant fusion power production (say, ~50 MW). As discussed in previous sub-sections, much can be learned from these experiments in D plasmas, not least in terms of scenario optimization, since they should allow easier access (i.e., lower threshold power) to H-mode operation than the H and He plasmas available during the PFPO phase. Nevertheless, a rapid transition to DT operation, if allowed by progress in the T-

Plant commissioning, would be favourable for the achievement of high fusion power/ high fusion gain and the associated studies of burning plasma physics, due to the additional heating power provided by the α-particle population and the further reduction in the H-mode power threshold expected. It should be emphasized that this focus on the conventional ELMy H-mode as the principal path towards the demonstration of $Q = 10$ plasmas in ITER will be kept under review in the light of results from the ongoing R&D programs in current devices and, indeed, in response to the results of initial operation of ITER: it is clear that ITER should exploit the most favourable plasma regime for the achievement of high fusion gain according to the understanding developed at the time of the implementation of the FPO phase.

Progress towards higher fusion power and fusion gain will require the integration of scenario elements such as fuel mixture control, burn control, heat load control, He exhaust and MHD stability control, providing capabilities which can be exploited as other burning plasma scenarios are developed. Several parallel programmatic threads are therefore likely to emerge within the DT experiments, as approaches to longer pulse operation are developed and specific aspects of burning plasma physics are explored. In the present version of the IRP, it is assumed that the important milestone of achieving fusion power levels of ~300 - 500 MW with $Q \sim 10$, even for 'short' burn durations of several tens of seconds, will take priority due to its wider implications for fusion energy development. Demonstration of this level of fusion performance would provide motivation for wide-ranging exploration of ITER's potential for fusion power production. This logic forms the basis of the detailed discussion of the early FPO campaigns developed in section 3.3, in which achievement of this initial milestone is followed by lines of research exploring several modes of long-pulse operation, from conventional ELMy H-mode, through hybrid/improved H-mode scenarios to fully non-inductive operation. The precise evolution of these lines of research will, of course, depend very strongly on results emerging from initial investigation of such modes of operation in the burning plasma regime. The preceding discussion has, therefore, proposed a strategy based on current expectations, but these expectations will evolve very significantly in the coming decades. Nevertheless, the achievement of significant fusion power production in ITER will open the path to an extensive exploration of viable plasma scenarios and to wide-ranging studies of the physics of burning plasmas.

In parallel with the scientific program towards high fusion power, high fusion gain, long-pulse operation and burning plasma studies, the technology R&D program will assume greater significance in the FPO phase, since this provides a first opportunity to investigate the performance of numerous DEMO-relevant technologies in the burning plasma environment with significant fluxes of 14.1 MeV neutrons (even if the ultimate neutron fluences in ITER will be significantly lower than in a DEMO device or fusion power plant). The progress towards long-pulse operation will provide insight into the reliability of many components and systems when operating at their performance limits over long durations of up to 3000 s. In addition, as presented later in section 4, the TBM program will make use of these early DT campaigns to test various aspects of TBM and ancillary system performance, leading to an integrated test of modules capable of breeding tritium and generating high grade heat. This will also be a significant milestone for the project, being the first practical demonstration of a novel technology critical for the realization of electricity production from DT fusion.

Table 20 summarizes the more detailed programmatic breakdown given in Tables 11, 14, 17 and 18 of research activities developed around D and DT plasmas within the first 3 FPO

campaigns, listing the estimated operational days required to achieve the key IRP objectives, corresponding, in particular, to satisfying the project mission goal of demonstrating long-pulse (300-500 s) operation at $Q \geq 10$ and to making significant progress towards the mission goal of fully non-inductive operation for durations of up to 3000 s with $Q \geq 5$. The estimates made for the duration of specific activities, particularly those related to the development of burning plasma scenarios, are necessarily uncertain, since ITER will furnish the first opportunity for the magnetic confinement program to establish and study this entirely new regime of fusion plasmas. The challenges likely to emerge in the development of fully non-inductive DT scenarios are particularly uncertain, given the present state of understanding of non-inductive operation in existing devices. As the discussion in section 5.13 illustrates, there is much that can be learned during ITER construction and the initial years of ITER operation, through collaboration with the international fusion community, to establish a stronger basis for the development of such scenarios. Nevertheless, it is clear from the time estimates derived for the DT research program that the achievement of these key scientific mission goals is likely to stretch over several FPO campaigns: the estimated duration of the proposed research program, 1245 days, essentially corresponds to the duration of the first 3 FPO campaigns (415 operational days per campaign - Table 1).

Achieving the mission goal of fully non-inductive operation at $Q \geq 5$ may also require upgrades to one or more of the ITER H&CD systems and, possibly, to the power supplies of the ELMCC for RWM control, to provide both the current drive capability and the flexibility required for the more complex control environment of fully non-inductive plasmas. Assuming that ITER were successful in meeting the principal mission goals during the first few DT campaigns (even if there were some deviation from the precise numerical targets established in the *Project Specification*), the later FPO experimental campaigns will provide opportunities to develop substantial physics and technology basis for the design and operation of DEMO devices. As outlined in section 3.3.6, further upgrading of the ITER tokamak and auxiliary systems could lead to a focussed program aiming to simulate burning plasma operation under DEMO-relevant constraints and with DEMO-relevant plasma-facing components, H&CD systems, Diagnostics, etc.

4. Technology Research Program

As outlined in section 1, the ITER project will carry out an extensive research program in fusion technology in fulfilment of its mission goals and in pursuit of its overall programmatic objective formalized within the *Project Specification*. Wide-ranging R&D activities have already been undertaken across the entire scope of key fusion technologies for ITER to provide the technical basis for the design and manufacturing of ITER's tokamak, auxiliary and plant systems, e.g., in superconducting materials and magnets, plasma-facing materials and components, heating and current drive systems, diagnostics, fuelling and vacuum technology, tritium handling, remote handling, control systems, power supplies, cryogenic and cooling systems, and an ambitious Test Blanket Module Program has been launched to develop and construct a series of tritium breeding blanket modules, together with the required ancillary systems, with key features relevant to a fusion reactor.

These technologies will be tested intensively during ITER operations, providing a technical basis for most of the fusion technology required for construction of a DEMO device. The research

program which will be undertaken in each of these technology areas will be developed in the coming years to ensure that a comprehensive definition is in place in advance of the ITER Operations Phase. As these plans become available, they will be integrated into the overall Research Plan in the course of its regular updating. At present, the analysis of the TBM testing program is considerably more advanced than that of other technology areas, as it is necessary to specify how the staged testing of various aspects of TBM technology will be integrated into the operations program (and on what timescale) to provide guidance to the TBM development program; this must deliver a sequence of TBMs through the operations program, leading to the integrated testing of tritium breeding and high grade heat extraction during the FPO phase.

The following discussion of the Technology Research Program is therefore limited, in the present version of the Research Plan, to the detailing of the TBM testing program, with an initial scope which extends from PFPO-2 to the end of FPO-2. The longer-term TBM Program might be expected to undergo significant evolution, as further developments of blanket concepts emerge in response to the Members' design studies of potential DEMO-class devices in support of the exploitation of fusion energy for electricity generation. In addition, it can be expected that the discussion in this section will be significantly expanded in future versions of the Research Plan to encompass the full scope of technology testing activities which will be implemented during ITER operations.

4.1 Test Blanket Module (TBM) Program

4.1.1 Introduction and Background

A Tritium Breeding Blanket (TBB) ensuring tritium breeding self-sufficiency is a compulsory element for a demonstration power reactor, such as DEMO, the next-step after ITER. Although a TBB is not required for ITER, since it will procure the tritium from external sources, a high-level project objective for ITER is the testing of mock-ups, denoted Test Blanket Modules (TBM), of various TBB concepts that would lead in a future reactor to tritium self-sufficiency, the extraction of high grade heat and electricity production. All activities related to this mission correspond to the so-called 'ITER TBM Program'. A successful ITER TBM Program represents an essential step for any fusion power development plan of all the seven ITER Members (IMs) [233 - 236].

In ITER it is planned to test a range of TBB systems, each formed by the in-vessel part, named TBM, and by the associated ancillary systems (i.e., the coolant system, the tritium extraction system, the coolant purification systems, the control and measurement system). Such complete TBB mock-ups are referred to as Test Blanket Systems (TBSs). The TBMs are installed in two Equatorial Ports, two TBMs per Port, allowing the simultaneous testing and operation of 4 independent TBSs. The initial configuration consists of two water-cooled TBS types (i.e., one using lithium-ceramic pebbles as the tritium breeder and beryllium as the neutron multiplier, and the other using a liquid lithium-lead alloy acting as both breeder and multiplier) and two helium-cooled TBS types, both using lithium-ceramic pebbles as the tritium breeder and beryllium as the neutron multiplier. These initial TBSs will start operation during the PFPO-2 campaign, the final experimental campaign of the non-active operation phase, and will continue for the initial campaigns of FPO, involving exposure to fusion power operation in DT plasmas. In later phases of FPO, further TBMs could be tested (using available TBS Ancillary Systems) and additional TBS concepts could be installed and operated.

The design of the infrastructures required for hosting of the 4 TBSs (i.e., port plugs frames, port cell common components, common maintenance tools and equipment) is in progress, with some components having already reached the final design stage. For example, the design of the TBS Connection Pipes system, which includes all pipes connecting TBS components located in different rooms of the Tokamak Complex, has reached its final phase, since these are 'captive components' and must be installed before ITER First Plasma.

The functional characteristics of the various TBSs are dictated by the operational conditions and requirements expected in the corresponding DEMO-TBB system and, in this sense, they differ from essentially all other ITER components, which are designed only on the basis of ITER-specific requirements. Of course, TBS integration and safety aspects must (and do) take into account that ITER is a French Nuclear Facility, designated INB-174 (*installation nucléaire de base*).

4.1.2 Overall Objectives of the Testing Program

ITER provides a unique opportunity for testing TBB mock-ups in a real fusion environment prior to the construction of a DEMO reactor. The TBS installation is planned so that the testing program can start in the final campaign of ITER's non-active phase, PFPO-2, and continues into the FPO phase, when the TBMs will be exposed to 14.1 MeV neutron emission from DT plasmas. This testing program ensures that:

(i) During PFPO-2: It should be demonstrated that an entire TBS can be routinely and correctly operated from the control room by using an efficient control system. It should be noted that a complete TBS is a first-of-kind system, i.e., a TBS has never been operated as an integrated system before in a (nuclear) fusion environment. In particular, the effects of relevant magnetic fields, relevant plasma regimes (e.g., H-mode), surface heat fluxes, hydrogen permeation in the TBM First Wall coolant, and disruption-induced loads will be assessed. This phase will also be essential for learning how to operate a TBS in a reliable and controlled way from the control room and for confirming several operational performance parameters that will be part of the ITER licensing file for nuclear operation;

(ii) During FPO: The effect of relevant neutron flux, volumetric heating, and tritium production, with corresponding tritium extraction, permeation, and transfer to the ITER exhaust system, and integrated heat and tritium management capabilities will be assessed.

Important characteristics of TBB testing in ITER concern the magnitude of the neutron flux and of the volumetric power density, which are lower than those expected in a DEMO/power reactor, and that ITER experimental operations feature relatively short pulse lengths (maximum burn length of 3000 s), implying, therefore, a shorter time at operating temperature compared to the quasi-continuous operation expected in a DEMO. The approach taken for the testing program is that, for each selected TBB concept, specific 'act-alike' TBMs have to be developed making use of 'engineering scaling' for testing during different ITER experimental campaigns. In this way different aspects of the TBM performances (neutronics, thermo-mechanics, thermo-hydraulics, etc.) can be addressed in association with a parallel development of modelling capabilities.

In addition, the expected neutron fluence in ITER is insufficient for the testing of long-term irradiation effects on materials: the lifetime average first wall neutron load of 0.3 $MW.yr.m^{-2}$ corresponds to an 'end of life' radiation damage of 3 dpa (displacements per atom) in ITER,

compared with ~50 - 70 dpa expected in a DEMO blanket during 5 - 10 years of operation. Such effects will therefore have to be investigated in complementary research programs.

Taking into account these limitations associated with ITER operation, the major overall testing objectives of the TBM Program are [233-236]:

1. Validation of structural integrity predictions under combined and relevant thermal, mechanical and electromagnetic loads;
2. Validation of tritium breeding and nuclear heating predictions;
3. Validation of the efficiency of the tritium recovery process and the evolution of T-inventories in the TBS materials;
4. Validation of thermal predictions for strongly heterogeneous breeding blanket concepts with volumetric heat sources;
5. Demonstration of the integral performance of the TBS, with its various sub-systems, in the ITER environment.

The 4 TBSs of the Initial Configuration must be installed prior to the PFPO-2 campaign and operated during this campaign with H/He plasmas to obtain certain necessary data during non-active operation. The principal specific results expected from the PFPO-2 phase testing are:

(i) Demonstration of the structural behaviour of the TBM-set structures and attachments during both normal operation and transient events, such as disruptions and VDEs;

(ii) Assessment of the impact of Reduced Activation Ferritic-Martensitic (RAFM) steel, from which the TBM structure is fabricated, on magnetic field distortion and the possible influence of such perturbations on H-mode plasma confinement and fast ion losses; such issues are particularly relevant for the FPO phase. RAFM steel magnetization (thus Maxwell force) can be also assessed (or demonstrated);

(iii) Demonstration of all the functionalities of the various TBS sub-systems;

(iv) Confirmation of essential data relevant for the TBS safety demonstration, a requirement for advancing to the nuclear phase of ITER operation (FPO) in conformance with all applicable regulations.

4.1.3 Initial Configuration for the Test Blanket Systems

As mentioned in section 4.1.1 the TBSs are located in two Equatorial Ports (EP), namely EP#16 and EP#18, providing the capability of testing up to 4 TBSs simultaneously. The 4 TBSs that will be installed and tested during PFPO-2 will form the so-called Initial Configuration. This configuration includes the following concepts, for which the conceptual design has already been approved:

Equatorial Port #16 (EP#16):

- TBS-1: Water-Cooled Lithium-Lead (WCLL) TBS [237], designed and procured by the EU. The main water-coolant operating conditions are a pressure of 15.5 MPa and inlet/outlet temperatures of 295/328 ºC; the Pb16Li loop is operated at ~340 ºC;
- TBS-2: Helium Cooled Pebble Ceramic (HCCP) TBS [238], jointly designed and procured by South Korea and the EU. The main helium-coolant operating conditions are a pressure of 8.0 MPa and inlet/outlet temperatures of 300/500 ºC.

Equatorial Port #18 (EP#18):

- TBS-3: Water-Cooled Ceramic Breeder (WCCB) TBS [239], designed and procured by Japan. The main water-coolant operating conditions are pressure of 15.5 MPa and inlet/outlet temperatures of 280/325 ºC;
- TBS-4: Helium-Cooled Ceramic Breeder (HCCB) TBS [240], designed and procured by China. The main helium-coolant operating conditions are pressure of 8.0 MPa and inlet/outlet temperatures of 300/500 ºC.

A 3-D model of this initial set of 4 TBSs located within the Tokamak Complex is shown in figure 32.

Following testing of the TBSs of this Initial Configuration during PFPO-2 and the initial FPO campaigns, a different configuration of TBSs (i.e., second configuration and beyond) might be adopted for testing during subsequent FPO campaigns. The testing program could include TBSs designed and procured by the other ITER Members, i.e., India, the Russian Federation and the US. The later configurations might encompass TBM concepts which are evolutionary developments of the initial concepts, but also entirely novel TBM concepts, and, in either case, it might be possible to make use of the existing ancillary systems. Alternatively different TBSs might be required, such as the Dual-Coolant TBS, which would imply the replacement/ upgrade of the ancillary systems of two TBSs, as two coolant systems would be required.

The main associated ancillary systems forming the TBS are as follows (note that not all of the listed systems are necessarily present in each TBS) [235]:

- Primary Cooling System: either Helium (HCS) or pressurised water (WCS) as in fission based Pressurized Water Reactors;
- Coolant Purification System (CPS);
- Tritium Extraction System (TES);
- Pb16Li system: a circulation loop of the tritium breeder (that could also be used simultaneously as the Primary Coolant);
- Tritium Accountancy System (TAS);
- Instrumentation & Control System (I&C);
- Neutron Activation System (NAS): this has the function of assessing the neutron flux and fluence locally within the TBM.

To ensure that the operation of the TBSs will not adversely impact ITER operations, it is necessary to minimise the risk of failures within each TBS which could cause significant shutdowns of the ITER device. To achieve this objective, most of the TBSs components have been classified at the highest level in the ITER facility Quality Assurance System (Quality Class-1). Due to the presence of tritium, most components are also classified as Protection Important Components, in particular Safety Important Class-2 for confinement (of radioactive inventories). As high-pressure coolant is used, most components, in particular those of the coolant systems, are classified as Pressure Equipment or, in cases where significant radioactive inventories are involved, as Nuclear Pressure Equipment.

Many the characteristics of the TBS sub-systems are shared among all of the TBSs. Some of the sub-systems might have more than one function (e.g., coolant and breeder). A detailed description of these sub-systems can be found in [235].

4.1.4 TBM Program Testing Strategy

Each TBS is functionally independent of the others. Two distinct TBSs will be tested in each of the two equatorial ports and, therefore, they will share the corresponding Port Plug (PP) and the Port Cell (PC) area. The TBM, the in-vessel element of the TBS facing the plasma, is attached to a TBM-shield to form a TBM-set. Two TBM-sets are installed in a water-cooled steel frame that acts as TBM-set support and as the interface with the ITER vacuum vessel. The two TBM-sets and corresponding frame form the TBM PP, as shown in figure 33.

For the Initial Configuration, tested over the period from PFPO-2 and into the early FPO campaigns, the TBS testing strategy for each TBB concept is to test a sequence of versions of the corresponding TBM concept. Each version will be adapted to the operational plan for a given ITER experimental campaign and will use different instrumentation to explore well-defined experimental aspect of the TBM performance in each campaign. This strategy implies that each TBM will have to be replaced several times, which will also require the removal and the re-installation of the TBS components located in the TBM Port Cells. The TBM replacement scheme which has been adopted involves the substitution of a complete TBM PP during the major shutdown periods of the ITER device, i.e., the ‘Long Term Maintenance’ shutdowns having typical duration of 8 months in FPO. Refurbishment of the extracted TBM PPs will be undertaken off-line in the Hot Cell (HC). This strategy implies that two frames must be available for each port. As a consequence, the design of the TBM PP must be Remote-Handling (RH) compatible, which imposes significant constraints on the PP design and operations. Each TBM PP will be leak-tested in the ITER Port Plug Test Facility before installation in the VV. If a replacement TBM-Set were not available, it would be replaced by a Dummy TBM to avoid impacting ITER availability.

The TBS components are located partially in the Port Cell area behind the bio-shield and partially in other rooms of the Tokamak Complex, as shown in figures 32 and 33. Components in the PCs are installed in a self-sustained steel structure denoted the Ancillary Equipment Unit (AEU). Since all the feed/return pipes are connected to the VV, these must be considered as extensions of the VV envelope (and therefore part of the first confinement barrier) until they reach the location of two in-series isolation valves per pipe located in the AEU. This bundle of pipes is accommodated in a self-sustained steel structure, the Pipe Forest (PF), which also supports the central bio-shield plug. Removal of the TBM PP therefore requires, firstly, removal of the AEU followed by extraction of the PF. These units are then transported to the HC. Reconfiguration of each PP-based system is subsequently achieved through the re-installation of the TBM PP, followed by the installation of a new PF and the re-installation of the original AEU.

4.1.5 TBM Experimental Program

The TBM experimental program can be divided in two main parts: 1) the TBM R&D program accompanying design and construction; and 2) the experimental program during Test Blanket System operation during the various ITER operation phases. These two aspects are discussed in detail in the following two sub-sections.

4.1.5.1 TBM R&D Program accompanying design and construction

Significant R&D will be performed during the TBS design phase and the TBS manufacturing phase. The major R&D topics concern: (i) development of the structural materials, namely the reduced-activation ferritic-martensitic steels; (ii) development of functional materials; (iii) development of instrumentation for data acquisition and control; (iv) development of modelling tools; and (v) validation of tritium processing technologies.

Some general aspects of these topics are discussed below. Note that, for all of these activities, 'development' includes the necessary qualification for use under ITER nuclear operating conditions.

(i) Structural materials for TBMs:

The TBMs are expected to use the same structural material as the corresponding DEMO breeding blankets. Reduced activation ferritic-martensitic (RAFM) steels are the only candidates for the TBMs designed for operation within the Initial Configuration. They have the capability to avoid the production of rad-waste with lifetime longer than 100 years, an aspect of fusion energy that is very important for public acceptance. Industrial batches of various RAFM steels have been produced by several ITER Members and a database of their properties has been developed to support TBM design and manufacturing.

However, further R&D will be needed during final design and manufacturing phases with the following objectives:

a) Consolidation of the material properties database up to radiation damage levels of at least 1 dpa, covering the radiation damage expected in ITER;
b) Completion of each RAFM database to support production of the PMA (Particular Material Appraisal) for conformity assessment, as required by the (Nuclear) Pressure Equipment regulations. This encompasses both base and joint materials, as well as various product forms (plates, tubes, etc.). In view of DEMO, it would be of interest to integrate each RAFM steel database in industrial Codes and Standards for the design of nuclear components, in particular the RCC-MRx (Design and Construction Rules for Mechanical Components of nuclear installations).

(ii) Functional materials for TBSs:

The functional materials in the TBMs are ceramic breeder pebbles (ternary lithium oxides such as Li_2TiO_3 or Li_4SiO_4), neutron-multiplier pebbles (beryllium or beryllides), and Pb-16Li, the eutectic alloy of Li and Pb that performs both the breeder and multiplier functions. Material properties for such functional materials must be determined for the same neutron fluences as for the RAFM steel structures of the TBM. Thermo-mechanical behaviour of pebble-beds must also be adequately tested and modelled for the various TBM versions, to correctly predict the thermal response of breeding zones to nuclear heating.

Further functional materials under development relate to TBS components and process equipment, such as seals, valves, getters, catalysts, etc.

(iii) Development of specific instrumentation:

The technical objectives of the TBM Program are based on the analysis of data collected during ITER operation. The deployment of instrumentation capable of collecting the required data is therefore an essential part of the system design.

The TBM instrumentation is specific to each phase of the IRP and, therefore, its development will continue during the fabrication of the TBMs intended for installation in PFPO-2 to provide the technical basis for instrumentation to be incorporated in subsequent versions and configurations, which will be tested in FPO. The general parameters that are foreseen to be measured (directly or indirectly) in the TBS are: (i) magnetic field; (ii) electrical currents; (iii) force/strain; (iv) displacement/position; (v) vibration; (vi) temperatures; (vii) pressure; (viii) flow rate; (ix) flow field (fluid velocity); (x) tritium concentration; (xi) chemical composition; (xii) neutron field parameters (flux, spectra); (xiii) secondary photon field parameters (flux, spectra); (xiv) tritium production rate; and (xv) tritium release rate.

Most of the instrumentation must exhibit adequate radiation hardness. Specific electronic, electrical, and electro-mechanical (EEE) parts, e.g., isolation valves, must be qualified through a rigorous testing program which also encompasses mechanical parts. Based on the relevancy of the operating conditions, the materials selected and technologies adopted for the main components, some of the instrumentation developed for the ITER TBSs might also be applicable to DEMO. Operation in ITER will, moreover, contribute to the assessment of the accuracy and reliability of the required instrumentation in an integrated fusion environment.

(iv) Modelling

A fundamental requirement for the achievement of the TBM test program objectives is the development (when not yet available) and validation of computer simulation tools that reproduce the behaviour of the TBSs during ITER operation. These tools must, of course, be based on computational models of the physical phenomena involved.

The following areas require further research to refine the design and operation of TBSs:

- thermohydraulic analysis, magnetohydrodynamic analysis and chemistry of lead-lithium alloy Pb16Li;
- tritium transport in solids, liquids, gases and across interfaces;
- structural analysis of selected TBS components, including the thermomechanical response of pebble beds;
- electromagnetic analysis of magnetic structures and reaction forces for critical areas;
- thermohydraulics of high pressure helium;
- TBS and TBS sub-system operational procedures (normal and maintenance, interfaces);
- neutronics analyses, including activation and corrosion products in process fluids and effluents;
- Safety studies and supporting R&D.

The main objective for the development of these simulation tools is to support the analysis of the experimental data collected during ITER operation and to provide tools to tailor the testing plan. In addition, the ITER simulation tools will constitute the basis for developing new tools to be applied to the design of the DEMO Breeding Blanket. To ensure an accurate analysis of the measurements obtained during ITER operation, the physics and geometry embedded in the modelling tools must be sufficiently detailed. This is necessary to ensure that the behaviour of the various TBS components is described at a level of detail allowing the mapping, in space and time, of all the physical parameters measured during the TBS experimental campaigns.

At the same time, to serve as a design tool, the physics embedded in the models should be sufficiently general to apply in a wide range of operating conditions beyond those to be explored in ITER. The numerical schemes adopted should be extensible and robust enough to allow their application to more complex systems, such as the DEMO BB.

(v) Validation of tritium processing technologies

Validation of the 'tritium processing technologies' is a major objective of the TBM Program implementation, as it is a highly relevant 'return on experience' (RoX) element for a DEMO breeding blanket. 'Tritium processing technologies' refer essentially to the tritium extractor from Pb16Li, tritium sensor in Pb16Li (when present), tritium extraction and concentration for helium purge (getters and adsorption beds), tritium sensors in helium and water, and tritium permeation barriers.

4.1.5.2 Experimental program during ITER operation for the Test Blanket Systems

The overall structure of the TBM testing program within the Staged Approach was introduced in section 4.1.1 and is illustrated schematically in figure 3 in section 2.4. The first set of TBMs within the Initial Configuration will be exposed only to H and He plasmas, while subsequent TBM versions will be exposed to a range of plasma scenarios in D (primarily in FPO-1) and DT, implying, of course, that these versions must be fully nuclear compliant. As discussed in section 4.1.5.1, the TBS testing strategy for each breeding blanket design concept is to test a sequence of versions of each TBM concept, each version adapted to the operational plan of ITER while taking into account the required specific instrumentation and sensors required to meet the corresponding experimental objectives for the TBM testing program. This strategy, illustrated in figure 3, implies that each TBM will have to be replaced several times, requiring the removal and the re-installation of the TBS components present in the TBM Port Cells.

Within this strategy, successful operation of the tokamak and execution of the accompanying physics experiments is essential to ensure that the performance of the TBSs can be fully assessed. The TBM Program must therefore be sufficiently flexible to adjust, when necessary, to the operational needs of the overall ITER program. This includes start-up and shutdown, and the accommodation of unscheduled down-times.

The approach adopted for the TBM testing program is to consider it as an independent experimental activity, where the TBMs will be exposed to a series of ITER plasma discharges without impact on plasma operation and on the goals of specific physics experiments. This approach requires the TBM teams to work closely with the operational teams implementing the experimental program to achieve the objectives of the IRP; satisfying this last constraint is also essential to the success of the TBM testing program. One example of the link between the TBM Program and the IRP is the identification by the TBM Program of the benefits of implementing (whenever possible) an experimental program of at least six days of back-to-back high-Q plasma pulses. This would allow a satisfactory quasi-equilibrium of the tritium-related parameters in the TBM to be established and facilitate quantitative measurements of relevant tritium-related performance data.

(i) Testing objectives in the final non-active phase (PFPO-2 TBM):

The PFPO-2 TBMs are installed for operation during the final campaign of the non-active operation phase (i.e., only a negligible neutron load is expected). Installation is followed by the TBS Commissioning and Integrated Commissioning, prior to full operation.

The main technical objectives specific to the PFPO-2 TBM and associated ancillary systems are:

- Validation of the assessment of the impact of ferromagnetic structures on plasma performance (error fields and their correction, plasma confinement and fast ion losses - see also sections 3.2.4.5 and 3.2.5.5). Because of the use of ferromagnetic RAFM steel as structural material, the presence of TBMs induces localized magnetic field perturbations in the TBM Port area. Tests in presently operating tokamaks have shown a limited impact of such localized phenomena on plasma performance once the associated error fields have been corrected [241 - 244]. However, their extrapolation to ITER is inherently limited and predictions will have to be confirmed as soon as possible in the test program by comparing PFPO-2 plasma performance with reference PFPO-1 plasmas (no TBMs are installed in PFPO-1);
- Obtaining essential data relevant for the safety files, allowing confirmation of the assumptions made, in order to obtain authorization to proceed with the nuclear phase of ITER operation;
- Validation of Maxwell forces due to the magnetisation of RAFM steel;
- Verification of the integrated TBS operation in the ITER operational environment, in particular sub-systems operation (including instrumentation and control) and assembly sequences (including remote handling) in Port Cell and Hot Cell. Both types of activities are inherently coupled with the TBM design. It is therefore essential that the whole TBS is installed to verify the integrated system operation;
- Verification of the TBS response and the margins for control under off-normal events, such as plasma disruptions, VDEs and power excursions;
- Verification of the operational margins assumed in the design analysis, in particular, in relation to the structural integrity of the TBM box during off-normal events (disruptions and VDEs);
- Validation of tritium recovery process efficiency (e.g., using deuterium);
- Validation of the TBM box basic instrumentation lay-out and functions as foreseen in the later TBM versions, and verifying operability of the NAS;
- To address remaining ITER/TBS interface issues, in particular, in relation to mechanical tolerances with adjacent components and interferences with the operation of ITER systems that interface with the TBS.

(ii) Testing objectives for the nuclear phases (FPO-1 TBM, FPO-2 TBM and beyond):

The first TBMs for the nuclear phases are installed for operation during FPO-1 and other TBMs versions will follow in subsequent phases. These later TBMs could exploit either the same, or a different, breeding blanket concept (especially after FPO-2). The testing objectives for each FPO campaign depend on the plasma characteristics and operating conditions for each phase and on the instrumentation that has been integrated in each TBM version.

Initially in FPO, it is expected to have plasma pulses with significant fusion power ($Q \geq 5$), but for relatively short periods (≥ 50 s). Eventually, once ITER fusion power goals of $Q \geq 10$ for 300 - 500 s and long pulse/steady-state operation with burn durations of 1000 - 3000 s with $Q \geq 5$ have been achieved, experimental phases dedicated to the TBM testing program are envisaged. For example, a campaign with several days (> 6) of continuous back-to-back operation with $Q \geq 5$ is envisaged during FPO-3, or beyond.

The principal technical objectives which the TBM Program would expect to satisfy during the FPO campaigns evolve as a function of the achieved plasma performance, but they encompass:

- Verification of the operation and of the calibration of neutron sensors. Supporting data (such as sensor operating temperature) are provided by the TBM box basic instrumentation;
- Preliminary validation of the TBM neutronic response, by measuring the neutron flux and its energy distribution by specific sensors and by exploiting the NAS. Supporting data (mainly temperature distributions) are provided by the TBM box basic instrumentation. The measured data are compared to modelling predictions to validate the simulation models and tools used in design analysis;
- Validation of tritium production by measuring the local tritium production rate (TPR) using, e.g., modified Single Crystal Diamond (SCD) sensors or other Li-based detectors under development. These sensors can be designed with high sensitivity to optimize operation in the relatively short burning pulses of FPO-1 and to take advantage of the lower operating temperature, so they will be installed specifically in the TBM version operating in this campaign. Depending on their specification, a subset may also be considered for the following TBM versions. Supporting data (mainly temperature distributions) will be provided by the TBM box basic instrumentation. The measured data will be compared to modelling predictions to validate the simulation models and tools which will be used for the assessment of the DEMO breeding blanket tritium breeding ratio (TBR);
- Validation of tritium recovery process efficiency and assessment of evolution of T-inventories in the TBS materials;
- Verification of the operation of the TES and of the calibration of instrumentation and systems dedicated to the measurement and control of tritium in the TBS sub-systems, including the TAS;
- Verification of the operation and of the calibration of micro-fission chambers (MFC) when present; completion of the calibration of other neutrons sensors foreseen for deployment in subsequent versions of the TBM;
- Validation of the TBM neutronic response by measuring the neutron flux and its energy distribution using all the neutron diagnostics developed for the TBM, possibly including NAS, Self-Powered Neutron Detector (SPND), SCD, Micro-Fission Chamber (MFC) and others. Supporting data (mainly temperature distributions) will be provided by the TBM box basic instrumentation. The measured data will be compared to modelling prediction to validate the simulation tools used in design analysis;
- Operation of the TES/TAS, and continuation of the validation of tritium production started in FPO-1 by measuring the tritium production rate (TPR), if sensors compatible with the operating conditions expected in FPO-2 are available in the FPO-2 TBM;

- Validation of the thermo-mechanical response of the TBM box under DEMO relevant loads, including volumetric heat deposition, by measuring local temperatures and strain of internal components (in addition to the FW already implemented) and the strain on the attachments. Additional sensors measuring local temperatures and mechanical response (strain, displacement, vibration) will be installed in selected locations of the FPO-2 TBM using the same technology as is used for the TBM box basic instrumentation. The measured data will be compared to modelling predictions to validate the simulation tools used for the corresponding DEMO breeding blanket design;
- In the case of the Pb16Li-based TBM, validation of the effect of magnetohydrodynamic (MHD) phenomena on the TBM performance, started in PFPO-2, and including volumetric heat and tritium transport will continue. This will be performed by measurement of the local physical parameters of Pb16Li (temperature, pressure and flow rate) but relying only on the TBM box and system basic instrumentation. The measured data will be compared to modelling predictions to validate the simulation models and tools for DEMO breeding blanket thermo-hydraulics (including MHD) and tritium transport;
- Preliminary validation of the technologies and design solution of sub-system components by assessing their performance with basic instrumentation. The measured data will be compared to modelling predictions to validate the simulation tools used for design;
- Assessment of materials activation, measured during Post-Irradiation Examination (PIE) activities. The measured data will be compared to modelling predictions to validate the simulation tools used in safety analysis and waste assessment;
- Continuing validation of the thermo-mechanical response of the TBM box under DEMO relevant loads and the extension of the reliability and operational performance database for materials and components of the breeding blanket under DEMO-relevant operating conditions for an extended period of time;
- Validation of tritium control and recovery in the TBS by measuring local tritium concentrations in the process fluids, and transfers through the TAS, while taking into account all coupled multi-physics effects in the TBM and sub-systems. The measured data will be compared to modelling predictions to validate tritium transport simulation tools. For the Pb16Li based TBS, the local tritium concentration in the Pb16Li loop will also be measured;
- Parametric analysis on the impact of the functional parameters (process fluid mass flows, heat transfers, and chemistry) on the global tritium system performance to obtain relevant information for extrapolation to a DEMO;
- Validation of technologies and design solutions for subsystem components, and extension of the reliability and operational performance database by assessing their performance with the subsystem's basic instrumentation;
- Establishment of the neutronic response using the in-line sensors and NAS to validate the radiation dose levels in all TBMs, key data for the preparation and execution of the post-irradiation testing.

All measured data will be compared to modelling predictions to validate the simulation models and tools used for design.

4.1.6 Summary and Conclusions

The overarching objective of the ITER TBM Program is to operate and test mock-ups of candidate DEMO breeding blanket systems. These TBSs use high-temperature/high-pressure coolants similar to those needed in DEMO and requiring a high thermal efficiency.

The TBM Program is split into two principal phases:

(i) Testing of four TBSs for the Initial Configuration, starting in PFPO-2 and continuing during the first campaigns of FPO. This phase of the TBM Program is expected to provide information required for the design, manufacture and operation of one (or more) DEMO breeding blankets;

(ii) In the subsequent FPO campaigns, it is foreseen to continue the testing of four TBSs in a Second Configuration to produce additional information for the design, manufacture and operation of DEMO breeding blankets. This includes topics such a reliability aspects of the TBSs previously tested in FPO, operation/testing of improved TBM designs and, possibly, operation/testing of new TBS designs.

5. Required R&D during construction to support the Research Plan

5.1 Introduction

Elaboration of the IRP has led to the identification of issues for which further experimental and modelling R&D is required to support the Plan's refinement or consolidation. The issues identified cover a wide range of areas and are described in detail in [245]. These areas include:

- R&D for design completion, particularly for the Disruption Mitigation System;
- Disruption characterization, prediction and avoidance;
- Stationary H-mode plasmas, impact of ELMs, ELM control and its impact on H-mode access, sustainment and performance;
- Characterization and control of stationary power fluxes;
- Plasma-materials/components interactions, including consequences for ITER operation;
- Start-up, ohmic and L-mode scenario development;
- Conditioning and fuel inventory control;
- Basic scenario control schemes and commissioning of control systems;
- Transient phases of scenarios and their control;
- Complex scenario control actions during stationary phases;
- Validation of scenario modelling and analysis tools;
- Heating and Current Drive and fast particle physics;
- Long pulse/enhanced confinement scenario issues.

Results from the R&D activities implemented in these areas can influence the further development of the IRP in a variety of ways. Their potential impact encompasses (ordering the impact from major to minor): (a) reconsideration of the experimental strategy and/or, potentially, the objectives in each phase; (b) modification of significant details of the experimental strategy designed to achieve each phase's objectives; or (c) optimization of finer details of the experimental strategy in each phase by providing relevant inputs/experience.

The following discussion highlights specific issues in some of the areas listed above where the outcome of R&D can significantly impact the IRP (e.g., ranges (a) and (b) above).

5.2 Disruption Management

5.2.1 Disruption load characterization

Unmitigated, or partially mitigated, major disruptions and vertical displacement events generate significant thermal and electromagnetic loads and could lead to the formation of runaway electrons in ITER. In fact, the risk of RE formation can be increased as a consequence of attempts to mitigate thermal and electromagnetic loads. Quantification of these loads is essential for Disruption Management in ITER [85]. As discussed in section 2.5.4, each unmitigated, or partially mitigated, disruption event in ITER will be characterized in terms of its disruption budget consumption, which describes the reduction in lifetime of tokamak components depending on the type and magnitude of the loads in disruptions. A precise forecast of the DBC is the basis on which target values of the disruption rates and the mitigation success rates can be defined for the various phases of ITER operation. Achievement of the target disruption rates requires the development of avoidance and prevention strategies, while the ability to attain the target mitigation rates depends on the development of reliable prediction schemes and an effective mitigation process. The aim of the R&D in this area is, therefore, to establish a solid basis for the accurate planning of the disruption budget within the IRP, which includes the confirmation of its basis in the initial PFPO operation.

5.2.1.1 Disruption thermal loads

Thermal loads arise during the fast loss of thermal energy at the thermal quench, but also during the current quench when the plasma is vertically displaced, but the poloidal magnetic energy which has not dissipated via radiation is lost through the halo region interacting with the plasma facing PFCs. The thermal quench losses are driven by MHD, and the heat flux footprint has, to date, only been described approximately by a broadening factor that reflects the impact of magnetic field stochastization on the heat flux profiles in this phase. The experimental database for extrapolation to ITER of both the duration of the heat flux and the spatial heat flux distribution on the PFCs during the thermal quench is rather sparse, and very few experiments have been carried out since the original work reported by [246] to quantitatively characterize these loads (e.g., [247 - 249]). To quantify the contribution of the thermal quench power fluxes to the DBC, a more accurate experimental characterization of the heat flux distributions on PFCs is required. This would allow a more solidly based evaluation, over a wide range of plasma scenarios, of both the peak heat fluxes expected in ITER during the thermal quench and of the sharing of the energy deposition among the various PFCs. This is important because the PFC material at the ITER divertor (W) and first wall (Be) have different melting thresholds under transient loads. An improved physics-based evaluation of thermal quench fluxes would allow a more precise identification of the plasma conditions for which melting is expected under unmitigated thermal quenches for wall and divertor target and an improved evaluation of the magnitude of the melting that these PFCs will experience. This is essential for the quantification of the DBC for the wall and divertor independently. It is important to note that, although heat fluxes during the thermal quench are expected to cause substantial surface melting in ITER, significant erosion of the first

wall due to melt movement and splashing is not expected in single events: the short duration of the thermal quench leads to shallow and short-lived melting, despite significant Lorentz forces on the melt layer due to eddy currents during the quench (Be has a low thermionic emission). Be melt dynamics during the thermal quench remain, however, an open R&D topic.

Heat loads during the current quench have, on the contrary, much longer timescales and thus a higher potential for material erosion when melting occurs. In this phase of the disruption, the forces acting on the material, caused by current flows produced by the disruption, are larger than during the thermal quench. Since both (conducted and convected) heat fluxes to PFCs during the current quench and halo current flows are intimately linked, it is essential to develop an experimentally validated understanding of the plasma parameters in the halo region, including their spatial distribution, to evaluate the DBC for the current quench over a range of ITER scenarios [250]. Present state-of-the-art modelling indicates that melting of the divertor and first wall would be avoided during the current quench of major disruptions in ITER at plasma currents of up to ~7 MA [124]. This determines the operational range in which disruption load characterization and the development of mitigation schemes can be undertaken with low impact on the DBC due to the avoidance of melting. This is critical for the later development of the IRP and requires further confirmation/ refinement, including the validation in present experiments of models used for ITER.

An overview of the ITER operational space over which disruptions do, or do not, contribute to the DBC from the perspective of PFC melting due to transient thermal loads is shown in figure 5 (section 2.5.4). Mitigation is required for disruptions that contribute to the DBC, either to nullify or to reduce their DBC contribution, whereas no mitigation is required for disruptions not contributing to the DBC.

It should be noted that it is not possible to develop a detailed specification of the DBC based simply on PFC melting limits being exceeded. The DBC must also account for the impact of such transient events on the heat load handling capability for those PFCs exposed to substantial heat fluxes during stationary operation. For example, significant W cracking can take place in events generating thermal loads which remain under the melting threshold when operating with PFCs below the Ductile to Brittle Transition Temperature (DBTT) [251], which is typical of PFPO plasmas [44]. This can potentially degrade the W divertor power handling capabilities, even when operating plasmas in ITER in which melting does not occur during disruptions. This subtlety must be understood to ensure that the DBC defined for ITER also accounts appropriately for disruptive events which remain under the melting threshold.

5.2.1.2 Disruption electromagnetic loads

Disruptions and VDEs cause mechanical loads to tokamak components, either due to eddy currents induced during fast current decays, or due to halo currents in the open field line region during the vertical displacement of the plasma column. Mechanical loads in these ITER components can reach their design limits for high current plasmas either by too fast current quenches (eddy currents) caused by the introduction of too many impurities during mitigation attempts or by large halo currents during insufficiently mitigated or unmitigated disruptions. These loads have been quantified so far for ITER with free-boundary equilibrium solvers such as DINA [252] supported by empirical scalings to quantify 3-D plasma effects and can be used to formulate an initial DBC associated with lifetime consumption due to electromagnetic loads.

However, it is well known that such formulation is oversimplified and needs to be refined. Unmitigated current quenches with low levels of radiated power in ITER have current decay times similar to or larger than the characteristic resistive vacuum vessel time. This leads to field penetration across the vacuum vessel that can potentially cause the destabilization of large kink-like MHD modes that make the plasma strongly deviate from a 2-D picture and cause large asymmetries in the EM loads which can be amplified by the rotation of the plasma during the disruptive phase [253]. Additionally, the 3-D nature of the tokamak structures has a direct impact on the current paths during disruptions and thus on the EM loads on components.

An accurate prediction of EM loads in ITER requires the application of non-linear MHD codes that can describe accurately the 3-D behaviour of the plasma itself as well as of the exchange of currents with tokamak conducting structures during disruptive events [254 - 256]. R&D is therefore required to validate these codes against well diagnosed experiments that are, as far as possible, similar to ITER (e.g., similar ratio of the current decay time to the resistive vacuum vessel time [257], with low and high radiated power during the current quench, etc.).

5.2.1.3 Runaway electron loads

Runaway electrons in ITER can result in highly localized energy deposition, in the worst case causing failure of the water cooling pipes of the impacted PFCs. Although RE-induced damage of PFCs (including first wall melting) has been observed in tokamaks (e.g., [136, 258, 259]), as illustrated in figure 34, data characterizing the spatial distribution of runaway impact and its timescales are very rare. This imposes significant uncertainties in the estimates for the evaluation of PFC melt thresholds and the possible damage caused by REs in ITER.

RE beams in ITER are vertically unstable [260], resulting initially in energy deposition on the PFCs during scraping-off of the RE beam against them and eventually due to MHD events leading to full or partial loss of the RE population to the PFCs. Depending on the timescale and nature of these events, a substantial fraction of the magnetic energy carried by the RE beam can be transferred into kinetic RE energy increasing the total energy deposited onto PFCs by runaways by up to an order of magnitude in ITER [225, 246]. Therefore, high quality experimental data for RE energy deposition (time and space resolved) for a range of magnetic to kinetic energy conversion is required to provide guidance to the assumptions to be made for ITER. This should be supported by the development of 3-D non-linear MHD models for simulations of disruptions including REs and their validation against such experimental data.

5.2.2 Disruption mitigation

The mitigation concept for ITER relies on material injection through Shattered Pellet Injection (SPI) to reduce heat and electro-magnetic loads, suppress the formation of runaway electrons, and mitigate their possible impact on component lifetime [261, 262]. This is based on the injection of solid pellets made of hydrogen, neon or mixtures of the two, which are shattered into fragments before entering the plasma, to radiate the plasma thermal and magnetic energy and to avoid runaway formation or to dissipate the energy of already formed runaway electron plasmas. A broad R&D programme has been launched through the ITER Disruption Mitigation System Task Force (DMSTF) to improve the physics basis for design choices for the Disruption Mitigation System (DMS) and to adapt the required technology to ITER needs. Dedicated SPI experiments

at various tokamaks [263 - 268] and accompanying modelling activities [269] in this R&D programme aim to assess:

- The adequacy of the injection locations;
- The efficiency of multiple simultaneous injections and associated synchronisation requirements;
- The efficacy of runaway electron avoidance and mitigation schemes;
- The optimum fragment size and velocity distributions for highest assimilation;
- The required quantities, pellet compositions, and injection sequences.

ITER's DMS baseline design has a total of 24 injectors in 3 equatorial ports (12 in one port and the other 12 distributed in two groups of 6) and 3 additional injectors in 3 upper ports, as shown in figure 35. This provides the ITER DMS with significant capabilities to inject a large amount of material, to allow massive multiple injections simultaneously or sequentially, to explore the effects of injection location on mitigation of thermal/magnetic/RE loads and to vary the composition of the pellets (from pure hydrogen to pure neon) to optimize the various mitigation functions and to provide redundancy to the system to meet these functions.

Extensive R&D is, therefore, needed to explore possible schemes for optimizing SPI injection, especially with respect to the avoidance of runaway electrons while mitigating the thermal and electro-magnetic loads. In addition, R&D effort on the technology side is also required to improve the understanding of SPI technology and to ensure that key components are compatible with ITER requirements. The key activities under this technology R&D program are:

- Systematic tests and optimization of the pellet formation and release process to ensure reproducible high-quality pellets;
- Development and testing of shattering units to deliver the required fragment sizes;
- Development of a pellet launching unit consisting of optimized fast valve and punch mechanisms;
- Development of effective pellet trajectory control to achieve the successful delivery of unguided and intact pellets;
- Development of optical pellet diagnostics to diagnose pellet alignment, pellet integrity and pellet parameters;
- Development of shattering simulation tools to optimise the shattering unit;
- Large scale testing to ensure high reliability of the DMS.

While the ITER DMSTF programme focuses on short term activities to ensure the best design choices for the ITER DMS, a long term R&D programme is also required in this area to minimize risks during the commissioning phase of the DMS and to ensure that alternative mitigation schemes are available should the present strategy show deficiencies during PFPO or already during the preparatory experimental and modelling activities.

As described in section 3.2.4.6 (PFPO-1) and section 3.2.5.4 (PFPO-2), the commissioning of the DMS will be performed in parallel to the stepwise increase in plasma performance. Especially the increase of plasma current poses a risk for accidental runaway electron formation since the avalanche multiplication is expected to increase by a factor of 10 for each additional mega-ampere in plasma current. It will be essential to understand the margins to RE formation for the various injection scenarios that have to be tested and optimised in terms of pellet quantities and compositions. Preparatory R&D will be essential, making use of SPI systems on tokamaks as

close as possible to the ITER DMS configuration together with 3-D MHD modelling activities. Here, full simulations of the pre-thermal quench, the thermal quench and the current quench phases will be required to assess the overall mitigation performance. Such simulations may become possible on affordable timescales, as the computing power will increase over the next years. These simulations would ideally be coupled to kinetic solvers to describe the RE formation phase during the thermal quench and can make use of RE fluid models during the avalanche phase. The inclusion of synthetic diagnostics that are relevant to quantify the mitigation efficiency in ITER will be essential in these models. The aim of such R&D is to minimise the risk of RE formation in ITER, but also to allow efficient commissioning of the DMS by limiting the required number of tests during PFPO.

Significant uncertainties exist on whether SPI can avoid RE formation in all phases of ITER operation and at the highest performance parameters, especially at the highest current and during the FPO phase. Although present R&D aims to address this issue, it is possible that deficiencies of this mitigation scheme may only materialize once the DMS is being commissioned in PFPO. Therefore, R&D is required to assess possible alternative material injection schemes, but especially also mitigation strategies based on mechanisms other than material injection. Such R&D may comprise bringing technologies to a level of maturity to be applicable in present tokamaks for exploration and, at a later stage, to be compatible with the ITER environment.

Possible alternative RE mitigation strategies could be based on the interaction of REs with kinetic instabilities or MHD driven perturbations. The loss of RE seeds due to field stochastization during the thermal quench can prevent the formation of a substantial RE population in present day devices. Correlations between thermal quench MHD activity and RE beam formation were indeed seen in experiments [270]. However, the avalanche multiplication in ITER is so high that for this scheme to be efficient a virtually complete loss of RE seeds would be required. Additionally, during FPO RE seeds from tritium decay and Compton scattering will play a dominant role and these sources are independent of MHD. Therefore, means to induce RE losses also during the current quench phase are required. Kinetic instabilities excited during the current quench phase have been seen to prevent the formation of RE beams [271]. Either actively driven or induced currents in in-vessel coils during a disruption can generate perturbed fields that enhance the loss of runaway electrons. Note that such techniques are feasible in ITER only if the available in-vessel conductors and power supplies are sufficient, within the capabilities for their main functions (namely vertical plasma position stabilization, ELM control and Resistive Wall Mode control). Earlier assessments of RE de-confinement using the ELMCC were not favourable [272, 273]. These may be revised in the light of possible new findings. Finally, should a RE beam have formed, whistler modes may provide an additional energy dissipation mechanism [274]. Possible excitation of these modes depends on the characteristics of the companion plasma to the runaway beam and additional means may be necessary to access the relevant parameter range.

Recently, large-scale MHD modes have been found beneficial for benign RE beam termination following SPI injection [275, 276] and these are being considered as a possible RE mitigation scheme to be applied in ITER.

Some of the mechanisms outlined above may work independently of material injection or be an integral part of a material injection based scheme. The aim of the R&D exploring alternative RE mitigation strategies must identify from those strategies the one feasible for ITER and bring any required technologies to a maturity level that would allow starting design activities for the

integration of these in ITER should that be required at some point during the execution of the research plan.

5.2.3 Disruption prediction and avoidance

The effectiveness of disruption mitigation schemes is intrinsically linked with that of the schemes aiming to prevent the effects of disruptions and avoid them; the mitigation schemes need to be more accurate and effective for operation with larger disruptivity (i.e., a higher fraction of the discharges disrupt), which is associated with poor effectiveness of disruption prevention and/or avoidance [84, 85, 87]. Currently a considerable research effort is devoted to the prediction and detection of disruptions, aimed at providing a trigger for the disruption mitigation system, as discussed in section 5.2.2.

It is, however, important to distinguish the triggering of such mitigation schemes from control schemes that aim to prevent disruptions or to avoid the effects of disruptions when not prevented, i.e., to ensure that they do not happen or that, when they happen, they do not significantly affect plasma operation. The latter are actions by the plasma control system (PCS), such as, for example, the initiation of a ramp-down of the plasma current or a reduction of the magnetic and kinetic energy, prior to a disruption while avoidance would mean the transitioning of the scenario to a more stable operating point.

Sustaining a low disruptivity tokamak plasma is, fundamentally, a plasma control problem. Beginning with a minimally disruptive target scenario, continuously-operating algorithms in the PCS must be able to maintain the plasma at a desired operating point, with passive stability to as many potentially disruptive modes as possible. Any remaining potentially disruptive modes must be actively and robustly stabilized. In addition to quantifiably robust continuous algorithms, the control system must be able to detect and respond asynchronously to hardware faults and off-normal plasma conditions [277]. Hence, disruption prevention and avoidance schemes are a key part of the ITER PCS [278]. R&D to support the IRP should focus on developing and testing control schemes and ITER operation scenarios that can be incorporated directly into the ITER PCS for this purpose.

The R&D in this field to support the IRP should, thus, be focused on the following objectives:

(i) To improve understanding of events leading to potentially disruptive instabilities and methods for forecasting the approach to disruptive states with sufficient early warning to enable their avoidance.

(ii) To identify methods to improve ITER scenario trajectories toward maximizing robustness against disruptions by carrying out experimental and simulation studies to identify disruption-free operating points. To quantify uncertainties in operating point evolution and proximity to the relevant boundaries. To identify operational boundaries for various disruption causes.

(iii) To develop and study methods and control algorithms to actively regulate the proximity to key controllability/stability boundaries, and couple these with scenario evolution. To implement them into simulations and on control systems in existing devices followed by analysis of results and comparison of simulation and experimental data. It is important to study the effectiveness and robustness of these schemes during routine operation and their possible application on ITER.

(iv) To extrapolate the results to the expected uncertainties and performance in ITER using modelling and simulation. To assess the relevance of the proposed stability boundaries and control solutions for ITER. This will allow the identification of further experiments and analysis needed to improve understanding and of the extrapolation capability of the schemes proposed for ITER and beyond.

The successful execution of this R&D will allow the reduction of the ITER operational time necessary to develop robust scenarios during the execution of the IRP to reduce significantly disruptivity from PFPO-1 to the very low values required for ITER high performance operation in FPO.

5.3 Open H-mode Issues

5.3.1 H-mode access and sustainment in PFPO

Access and sustainment of H-modes in PFPO have specific issues associated with the plasma species used in this phase (hydrogen, helium and their mixtures) and the specific features of the available H&CD systems, in particular, the power that can be coupled to the plasma in the two PFPO phases, considering plasma absorption for RF heating schemes and shine-through losses for NBI. This section deals with open H-mode physics R&D issues for PFPO while the issues specific to H&CD are discussed in section 5.11.

The general issues regarding uncertainties in the prediction of the power required for H-mode access in ITER (e.g., impact of divertor configuration, wall/divertor material, plasma rotation, edge physics and neutral processes, etc.) are of obvious interest for all phases of the IRP. In addition, the main open issues regarding H-mode access itself in this phase concern the impact of plasma species on the power required to access H-mode and the optimum density for minimum H-mode threshold power. The latter is particularly important in this phase since the available level of additional heating is comparable to the expected value of the H-mode power threshold itself.

The IRP quantifies the impact of plasma species on the H-mode power threshold through a simple multiplier compared to that for deuterium ($P_{LH,D}$) provided by the multi-machine scaling [9]. This scaling provides a positive and near linear dependence of the H-mode power threshold on plasma density, toroidal field and plasma surface area. In particular, for the IRP it is assumed that $P_{LH,H} = 2 \times P_{LH,D}$ for H plasmas and that $P_{LH,He} = 1.4 \times P_{LH,D}$ for He plasmas, based on experimental findings in [10] and [11], respectively. While these proportionality factors provide a reasonable guidance for the IRP, significant deviations from them are seen in various experiments, for instance for high plasma densities [13, 279 - 281]. It is therefore important for the refinement of the IRP to elucidate the processes that determine the impact of plasma species on the H-mode power threshold and their extrapolation to ITER, since they have a major implications for the H-mode plasma operational scenarios that can be explored in PFPO.

Of specific interest for hydrogen H-mode plasmas is the understanding of the H-mode power threshold dependence on mixed-species plasmas. Experiments from JET show that the behaviour of the H-mode threshold in mixed H-D and H-He plasmas is non-linear [15]. The detrimental effect of H was identified already in ASDEX Upgrade for He plasmas [14]. However, the impact of a heavier species (He or D) on the H-mode threshold of H plasmas is more complex. The JET results indicate a significant effect reducing the H-mode power threshold when there is a concentration of 10-20% of D or He in H plasmas, whereas in ASDEX Upgrade such effects do

not take place at these concentration levels [17], while in DIII-D substantial effects are seen at He concentration levels of 20-25% [16]. As described in section 5.3.1.2, this reduction of the H-mode threshold by some amount of He could potentially be beneficially exploited to expand the range of ITER H-mode operation in hydrogen-dominant plasmas. It is, thus, important to determine which reduction of the L-H transition could be expected by adding some amount of He to a H plasma for the further refinement of the IRP.

In general P_{LH} is found to deviate from the near linear increase with density that is seen above a given density ($n_{LH,min}$). For densities under this value P_{LH} is found to strongly increase with decreasing density, i.e. an opposite trend to that predicted by the scaling. This determines the optimum density for H-mode access and this is of particular importance for PFPO given the reduced margin above the L-H threshold with the available heating in this phase. The physics determining this minimum value is not yet fully understood and includes changes to the nature of the turbulence with collisionality (which depends on density) and stabilization of the underlying turbulence by the radial electric field shear [282], which itself depends on gradients of electron and ion temperatures/ densities and, thus, on the sharing of the edge power flux between ions and electrons [18]. To plan the IRP, $n_{LH,min}$ is evaluated with a physics model put forward on the basis of ASDEX Upgrade [18] assuming that this minimum density is determined by the role of the edge ion power fluxes in triggering the L-H transition. For dominantly electron heated plasmas, such as those in ITER, equipartition to heat the ions by the electrons is less efficient at low densities and thus increases the heating power required to achieve a given edge ion power flux at low densities thus determining the minimum threshold for H-mode access. Although this physics picture describes well the values found in other tokamaks of different size, such as Alcator C-Mod [283], for other tokamaks such as JET its applicability is less clear and other physics mechanisms related to the presence of impurities may be at work [15, 30, 279]. Similarly, the value of the turnover density as well as the power threshold in the vicinity of this density can depend on the divertor configuration [15, 31, 284], presence of impurities [29], ion species [13, 279 - 281, 285] and plasma rotation [286], which are not simply described by the equipartition picture above. It is, therefore, important to understand the physics processes that determine the existence of $n_{LH,min}$ and thus its expected value in ITER, particularly for hydrogen, helium and mixed hydrogen-helium plasmas since this impacts the density range accessible in H-mode in these plasmas, for which the H-mode operational range is expected to be rather restricted.

5.3.1.1 Hydrogen and He-doped hydrogen H-mode plasmas

Hydrogen H-modes: As described in sections 3.2.4.5 (PFPO-1) and 3.2.5.5 (PFPO-2), hydrogen H-modes are expected to have a narrow operational space both in PFPO-1 and PFPO-2. In PFPO-1, where H-mode plasmas at 1.8 T are considered, the main limitation comes from the available level of ECRH power and the specific issues associated with low density operation and 3rd harmonic heating discussed below and in section 5.11 respectively. For PFPO-2, the availability of NBI heating opens the operational space for these 1.8 T plasmas by allowing operation at higher plasma density with low NBI energy injection (540 keV) [33]. In this case the main open R&D issue concerns whether the NBI shine-through would be sufficiently low to allow H-mode durations of at least 100 s and this is discussed further in section 5.11.

The only viable scenario for H-mode operation in PFPO-2 hydrogen plasmas at higher fields than 1.8 T, which allows H-mode duration of at least 100 s, relies on low density operation near

$n_{LH,min}$ with Ne seeding to decrease shine-through losses [90, 168]. The main open issues for the viability of such a scenario and its operational range concern the required level of Ne to reduce the shine-trough losses to the required level, the impact of neon on the core radiative losses directly and indirectly through the impact of neon on divertor tungsten sputtering and ensuing core plasma contamination. Similarly, the compatibility of the required core Ne levels for shine-through loss reduction with divertor power flux exhaust is an open issue, since a high level of core Ne could lead to total divertor detachment and thus loss of the H-mode and follow-up radiative collapse and disruption of the plasma.

Helium-doped hydrogen plasmas: As seen in some tokamak experiments, the addition of a fraction of He (~10%) can have sufficient impact on the required power for H-mode access and sustainment, as to enable hydrogen dominant H-mode operation in PFPO. For PFPO-1, the impact on H-mode scenarios is rather straightforward and directly linked with the reduction of the H-mode power threshold and the open issues in this respect are covered above. The impact of the main plasma species on the access to H-mode at 1.8 T is illustrated in figure 36. With the baseline 20 MW of ECRH power for PFPO-1, robust H-mode access ($P_{input}/P_{LH} > 1.5$) should be possible in He plasmas at currents of up to 5 MA in scenarios with $\langle n_e \rangle = 0.5 \times n_{GW}$, while H-mode access may be possible at these levels for H plasmas with a He concentration of 10% He, but not for pure H plasmas. If the ECRH power level were increased to 30 MW, this would allow robust H-mode access for H plasmas H with 10% He and ensure H-mode access for H plasmas to plasma currents of 5 MA with $\langle n_e \rangle = 0.5 \times n_{GW}$.

For PFPO-2 the impact of He doping is more complex, since it allows operation at higher densities, which decreases NBI shine-through losses, and enables specific ICRF heating schemes (3-ion heating) that are not available for pure hydrogen plasmas. The open R&D issues for these PFPO-2 H-mode scenarios are described in the following subsections.

Helium doped hydrogen plasmas with NBI + ECRH in PFPO-2: The reduction of the H-mode threshold by the addition of a fraction of helium (~10%) enables access to higher density operation in PFPO-2. This, together with the presence of He in the plasma, reduces shine-through losses and increases the NBI power coupled to the plasma. Such effects, in combination with ECRH heating (particularly if upgraded to a total of 30 MW from PFPO-1 onwards) significantly widen the operational space for helium-doped hydrogen plasmas compared to pure H plasmas at 7.5 MA/2.65 T, as shown in figure 37. The main open issues regarding this plasma scenario, in addition to the quantitative reduction of the shine-through losses discussed in section 5.11, concern the edge-core compatibility of such a scenario, since the additional He may increase W sputtering and core radiation losses and thus reduce the H-mode operational space. Similarly, if Ne impurities need to be injected to control divertor power fluxes or to reduce divertor temperature and associated W sputtering, this may reduce the H-mode operational space due to increased core radiative losses.

Helium doped hydrogen plasmas with NBI + ECRH + ICRF in PFPO-2: Doping pure H plasmas with He allows additional ICRF schemes (based on the 3-ion approach) to the usual minority scheme, which is not applicable to H plasmas at ~2.65 T. These ICRF schemes are based on the use of ^{4}He at ~10 - 15% level, together with ^{3}He at levels lower than 1%, and operation at a toroidal field level of 3.0 - 3.3 T. This combination enables H-mode operation with up to 73 MW of total heating (NBI, ECRH and ICRF) for $q_{95} = 3$ scenarios in the range of

8.5 - 9.3 MA/3.0 - 3.3 T, taking advantage of the high available heating and the reduction of H-mode threshold due to the He level of ~11%. These H-mode scenarios have specific open issues associated with the 3-ion ICRF scheme for these plasmas (discussed in section 5.11) and those related to edge-core integration similar to those for the scenarios discussed above using NBI+ECRH. In addition, the main open issue for such H-mode scenarios concerns the impact of the ICRF power deposition profile on plasma behaviour, particularly on core plasma transport, including that of W impurities. As shown in figure 38, the modelled 3-ion ICRF power deposition profiles are expected to peak in the range of ρ = 0.5 - 0.7, depending on the value of the field [287]. Since ICRF represents <30% of the total heating, this is not expected to modify core plasma transport significantly, but this issue does need to be studied since, in addition to the deposition of power, ICRF produces a significant population of off-axis fast particles and these can also impact main plasma transport and W impurity transport.

ECRH-heated H-mode plasmas in PFPO-1: In addition to the general H-mode issues for PFPO plasmas described above, ECH heated plasmas pose specific issues due to the low available heating power in the PFPO-1 phase (20 MW of ECRH with an additional 10 MW of ECRH upgrade under discussion), exclusively heating the electrons and the low value of the absolute density of such plasmas. The latter is determined by the available power only allowing H-mode operation at 1.8 T and thus plasmas with $I_p \leq 5$ MA at low densities, $n_{LH,min} = 1.4\times10^{19} \leq \langle n_e \rangle \leq 2.0\times10^{19}$ m^{-3}. Such a reduced density range poses specific issues regarding core transport physics in these H-mode scenarios related to the low effectiveness of equipartition in these plasmas exclusively heated by ECRH.

As shown in figure 39 and figure 40 [34], this is expected to lead to plasmas with very large central electron temperatures (similar to those in FPO plasmas) with low ion temperatures, which are not found in other phases of the IRP. Understanding plasma transport in these H-mode conditions (including impurity transport) is required to determine the expected characteristics of these initial H-mode plasmas and the focus of H-mode research in PFPO-1. We note that H-mode research in PFPO-1 should be aimed at minimizing risks in later phases of the IRP rather than on the characterization of PFPO-1 H-mode specific issues.

Edge-core integration may also pose specific challenges in particular regarding W sputtering and core plasma radiation. Given the low values of density that are compatible with H-mode access and sustainment, relatively high divertor plasma temperatures and significant tungsten sputtering may take place for these H-mode plasmas even if the power heat flux level is very moderate compared to the divertor power handling capabilities [34, 44]. While the impact on the core plasma depends on the level of prompt W redeposition, present results indicate that W contamination of the core plasma may limit the operational space of H-mode plasmas in PFPO-1 [34, 288], particularly for He plasmas due to the higher sputtering as described in section 5.3.1.2. It is, therefore, required to study these integration issues in similar conditions to those expected in these PFPO-1 H-mode plasmas to evaluate their operational space and to explore approaches (e.g., Ne seeding in hydrogen-dominant H-modes) to widen it.

It is important to note that the issues above are expected to be less critical for 5 MA/1.8 T H-modes in later phases of the IRP since the higher available power allows operation at higher densities in H-mode and access to divertor conditions with lower temperatures and lower W sputtering, as well as higher electron equipartition in the core plasma.

5.3.1.2 Helium H-mode plasmas

Helium H-mode access and sustainment: From the point of view of margin above the H-mode threshold, helium H-mode access should be simpler both in PFPO-1 and in PFPO-2. In PFPO-1 this is solely due to the lower H-mode threshold of He plasmas in comparison to H plasmas. In PFPO-2, He plasmas will also allow for more effective heating since the NBI shine-through density is ~3.1×10^{19} m^{-3} and efficient ICRF heating schemes using H as minority in first harmonic for 2.65 T and second harmonic at 1.8 T are available. Both ICRF heating schemes have been demonstrated in present experiments and no issue is expected regarding their application to ITER. The main open issues regarding helium H-mode plasmas for the IRP concern edge-core integration issues that can affect sustainment of the H-mode plasmas and plasma-wall interaction issues discussed in section. 5.4.3. The former are associated with the larger sputtering of tungsten by helium both during stationary phases and during ELMs and pedestal specificities of tungsten transport physics in helium plasmas. The latter are related to the specificities of helium interactions with tungsten and the possible modification of its thermo-mechanical properties.

The edge-core integration issues are illustrated with modelling results in figure 41, showing that already for very moderate ELM energy losses (~0.3 MJ) the post-ELM core plasma transient radiation can reach levels comparable to the additional heating level foreseen for 7.5 MA/2.65 T helium H-modes of 53 - 73 MW if prompt redeposition during ELMs is low [67]. Similarly, neoclassical transport in the pedestal with low density gradients, as expected in ITER, is less favourable regarding W screening [67]. For a given set of pedestal density, pedestal temperature and pedestal widths, higher separatrix densities are required in He plasmas to screen W impurity influxes in the pedestal when compared to hydrogenic plasmas, as shown in figure 41, which may reduce the operational space for He plasmas due to increased core W contamination in ITER. Since both of these integration issues depend on the complex interaction of physics processes that are highly non-linear, an experimental assessment and validation of the models applied is required to quantify their impact for ITER scenarios.

ELM control in helium H-modes: A key objective of H-mode operation in PFPO is to develop ELM control schemes. In this respect, it is important to understand the qualitative and quantitative differences regarding ELM control for helium H-modes and R&D is required in this field.

The use of pellet pacing for ELM control is a well-established technique in D plasmas in present experiments [289] and DIII-D [290] and is foreseen to be explored in helium H-modes in ITER by the injection of H_2 pellets, since no H solid pellets can be formed. The principle that this technique can trigger ELMs in helium H-modes has been demonstrated in DIII-D [291]. However, the issues associated with the introduction of H by pellets into helium H-modes remain to be understood since dilution of the He plasma by H can increase the L-H power threshold, resulting in a back transition to the L-mode, as seen in experiments [14]. Initial modelling of dilution of He by H due to ELM pacing was considered for ITER H-modes in [292] and found not to reach levels that would substantially modify the L-H threshold, but this needs to be demonstrated experimentally in detail. R&D on this topic should focus on:

(a) identifying quantitative differences regarding the H pellets required to trigger ELMs in helium H-modes compared to D pellets in deuterium H-mode plasmas (size, injection velocity, geometry);

(b) determining the effect of H dilution by pellet injection into the sustainment of helium H-mode stationary phases.

Similarly, ELM control and suppression by 3-D fields will be explored in helium H-modes in ITER. Present experiments have shown that it is possible to achieve ELM suppression in helium H-modes [291], but the operational space is different and more restricted than for deuterium H-modes. R&D is required to determine if the observed differences are:

(a) due to the different plasma characteristics that can be achieved in helium vs. deuterium H-modes in present experiments (density, collisionality, etc.) caused by technical issues, such as inefficient He pumping that will not apply to ITER;
(b) associated with intrinsic features of He plasmas (lower ion content for same electron content, higher resistivity, etc.) which will be relevant for ITER.

Since the purpose of ELM control and suppression by 3-D fields in ITER helium H-modes is to develop the schemes to be applied in D and DT plasmas, resolving these outstanding issues is of great importance to define the appropriate PFPO programme in helium H-modes and the expected transfer of knowledge to be acquired in PFPO to deuterium and deuterium-tritium H-modes in FPO.

5.3.2 H-mode integration issues

5.3.2.1 Pedestal parameters and impurity exhaust

An important integration issue for H-modes in ITER concerns impurity exhaust from the core plasma. This involves He produced by fusion reactions, extrinsic impurities for power exhaust as well as those produced by plasma wall interactions and their exhaust from the core plasma through the pedestal to the divertor.

Regarding pedestal impurity transport, ITER H-mode scenarios are expected to operate with low pedestal density gradients given caused by high separatrix densities due to high power exhaust [293]. This implies that, if transport in the pedestal remains such that pedestal plasmas are peeling-ballooning limited, temperature gradients in the pedestal are the main contributor to the pedestal gradient, which is itself limited by MHD. This has a deep impact on impurity transport in the pedestal when it is dominated by neoclassical transport in ITER, as found in present experiments [294]. In such conditions, temperature screening is dominant and leads to an outwards impurity pinch. In these plasmas, the pedestal impurity density is lower than at the separatrix [67], which is unlike H-mode plasmas in present experiments. This effect depends very non-linearly on impurity charge and, thus, is minor for He, more sizeable for Ne and very large for W. An example of the edge impurity profiles for a PFPO-1 H-mode illustrating this effect, which is of general relevance to all ITER H-mode scenarios including DT plasmas in FPO, is shown in figure 42.

The strong screening of impurities in the pedestal of ITER H-modes has obvious positive implications for the achievable core plasma purity in ITER and it is, thus, very important to have it validated by experiments. Although the edge plasma parameters to achieve these ITER-like conditions are very challenging to achieve in present experiments in stationary conditions, the validation of this effect even in transient conditions would be of great value to consolidate ITER H-mode scenario predictions.

In addition, strong pedestal impurity screening can also have direct implications on impurity exhaust by ELMs in ITER. The MHD instability associated with ELMs leads to the mixing of the plasmas in flux tubes from inside the pedestal region through to the SOL and, in doing so, to transient radial particle fluxes. For the main plasma ions and for impurities in the usual conditions in present experiments (impurity accumulation in the pedestal), this ELM-driven flux tube mixing leads to a net radial outwards particle flux and thus impurity expulsion. On the contrary, in ITER where impurity screening is expected to dominate, the impurity density from the pedestal inwards increases after the ELM and thus a net inwards impurity influx can result from ELMs, as evaluated from non-linear MHD simulations of the ELM crash [68] shown in figure 43.

The result of impurity screening between ELMs and a net impurity influx by ELMs in ITER leads to the impurity exhaust having opposite phases in time compared with present experiments: outflux of impurities between ELMs and influx during ELMs. This can lead to limits on the maximum ELM frequency associated with unacceptable plasma contamination in ITER [66, 171].

The strong screening of impurities in the pedestal of ITER H-modes and its impact on impurity exhaust between ELMs and during ELMs have obvious implications for the achievable core plasma purity in ITER. It is thus very important to have this physics picture validated by experimental results. Although the edge plasma parameters to reach these ITER-like conditions are very challenging to achieve in present experiments in stationary conditions, the validation of these effects even in transient conditions would be of great value to consolidate the predictions of impurity exhaust in ITER H-mode plasma scenarios.

Screening of impurities in the pedestal can impact the possibility to control minority and 3-ion heating schemes for ICRF and injection of impurities for diagnostic purposes. Therefore, further studies of the impurity transport in the pedestal are also required to analyse the possibility of control of impurities for such purposes as well.

5.3.2.2 Power exhaust and impurity impact on pedestal plasmas

Divertor power exhaust by access to radiative semi-detached divertor plasma conditions is essential to maintain divertor power fluxes within acceptable ranges for sufficient divertor lifetime in ITER [45]. Since impurity radiation by intrinsic impurities (Be and W) is not an option in ITER, extrinsic impurities are required. The choice of impurity to provide radiative divertor power exhaust can impact not only the divertor plasma parameters, but also those of the pedestal plasma and, thus, the achievable level of plasma confinement in radiative H-mode conditions. Most current experimental evidence shows that use of N_2 provides the highest pedestal pressure and plasma confinement for radiative H-mode plasmas compared to other species such as Ne and Ar, particularly when the input power is comparable to the H-mode power threshold power [295 - 298], as will be the case in ITER. However, the use of N_2 in ITER has drawbacks related to its chemical reactivity with hydrogen and the production of ammonia that can lead to increased T retention and is not, therefore, a favoured option for divertor power exhaust compared to Ne.

Modelling results of present experiments (JET and ASDEX Upgrade) and ITER indicate that the favourable effects of N_2 compared to Ne regarding power exhaust are related to the physical dimensions of the divertor, compared to the ionization location of main ions and impurities, and to the variation of the edge density and temperature values with device size [51]. As a result, for devices of larger size, the differences between N_2 and Ne are small; this includes impurity compression at the divertor, as shown in figure 44, and the resulting divertor radiation. This,

combined with the higher pedestal temperatures in larger devices, leads to N_2 and Ne being comparable in terms of optimization for divertor radiative conditions in high confinement H-modes for large scale devices such as ITER. However, most of the simulation work to date has assumed gas fuelling and impurity injection from the main chamber. Use of the gas lines under the divertor cassettes, which would provide a more toroidally symmetric gas influx, is now preferred, but the full impact of this choice on divertor conditions has not yet been assessed and may be significant, particularly at high power.

Recent experimental results from JET [50] in conditions as close as possible to ITER (2.5 MA/2.7 T and $P_{aux} \geq 30$ MW) have shown that radiative divertor operation with Ne can meet and exceed the results obtained with N_2 in terms of integrating divertor radiative operation with high confinement H-mode operation, in line with the above predictions. R&D is required to quantitatively determine the size scaling effects on radiative divertor operation and H-mode confinement to optimize its application to ITER scenarios. This includes the exploration of other radiators suitable for ITER, such as Ar, together with the impact of the X-point radiation on H-mode confinement for strongly detached divertor conditions. X-point radiation is found to have a minor effect on H-mode confinement in smaller scale devices [55, 296], but the possible scaling with machine size is not yet clear.

A further area requiring R&D studies concerns the compatibility of stationary power exhaust with pellet fuelling. The latter leads to unavoidable edge density transients associated with the outwards transport of particles deposited by the pellet. Since pellet deposition in ITER in H-modes is rather peripheral due to the high pedestal temperatures [299], these transients can be substantial. For radiative divertor conditions, modelling finds that oscillations of the separatrix density associated with pellet fuelling can cause large changes to divertor detachment in ITER. These can eventually give rise to a thermal instability of the edge plasma, leading to a disruption if the density transient exceeds a value for a given level of stationary divertor radiation [300]. The triggering of such thermal instabilities depends on the competition between the increased edge particle transport and thermal transport following the ablation of the pellet into the plasma [301]. Therefore, edge thermal and energy transport after pellet injection need to be characterized and extrapolated to ITER-like plasma conditions to optimize pellet fuelling with respect to radiative divertor operation.

5.3.2.3 Plasma fuelling and DT mixture control.

To optimize the fusion power production, $P_{fus} \sim n_D n_T$ in ITER plasmas, it is necessary to deliver D and T ions to the hot plasma centre to provide a ratio of D:T ~ 50:50% and DT fuel at a rate sufficient for replenishment of the burnt fuel. The DT ratio and densities, n_D, n_T, depend on the ionization sources and sinks, S_D, S_T, as well as on the particle transport in the core, in the H-mode pedestal, SOL and divertor areas. D and T ion sources in ITER originate from penetration of D and T neutrals from the edge, neutrals injected by NBI, and neutrals delivered by pellets. ITER predictions [299, 302] show that edge opacity to neutrals in H-mode plasmas is very large, implying that DT core plasma fuelling and DT mixture control will rely on pellet fuelling.

Experimental and modelling R&D is therefore required to quantitatively determine the physics of neutral fuelling of the edge plasma, including isotope effects, to evaluate/confirm the negligible contribution of edge recycling to core fuelling in ITER H-modes.

Regarding core fuelling by pellets, it is necessary to understand the differences in transport between D and T ions, since the efficiency of DT mixture control with pellets in ITER can be very non-linear [303]. This is due to the formation of non-monotonic density profiles at the edge, which can significantly impact particle transport [304, 305]. In addition, the core transport predicted for D and T depends on the profiles of plasma parameters, including the mutual impact of D and T concentrations in the core [197, 306], so that their fluxes could propagate in opposite directions. This implies that the DT ratio for the source provided by the pellet system in ITER may deviate significantly from the 50:50 ratio to achieve an optimum ~50:50 DT mix in the core plasma to maximize fusion performance.

R&D is therefore required to validate modelling prediction of density and temperature profiles on core particle transport including DT isotopic effects, with special focus on the specific issues related to pellet fuelling (pellet ablation and mass relocation [307]) and the resulting non-monotonic density profiles. R&D is also required on the impact of ELM control schemes on plasma fuelling and DT mixture control. ELM control schemes rely on the increase of edge transport whether stationary (ELM suppression by 3-D fields) or by increased ELM frequency (pacing of ELMs by pellet injection, vertical plasma position oscillations, or increased ELM frequency via 3-D fields). Understanding and quantifying the fuelling needs for controlled ELM H-mode regimes in ITER is thus required. This includes the specific impact of ELM control techniques on the efficiency of pellet fuelling and on the edge isotopic mix, such as those in the presence of islands and ergodic field lines at the edge of plasmas to which 3-D fields are applied for ELM control.

5.4 Plasma-material interactions

5.4.1 Power fluxes to castellated PFCs

This particular issue has received a great deal of attention given that the IRP considers operations with a full W divertor from PFPO-1 [45]. In the case of carbon, which was the original choice for the high heat flux (HHF) areas of ITER's first divertor [308], small misalignments between neighbouring monoblocks (MB) comprising the plasma-facing components would, to a large extent, be eliminated by the plasma itself during operation. In the case of metals, the same does not apply and even relatively small edges exposed to parallel heat flux will drive significant melting and melt damage under ITER stationary and transient (particularly ELM) loading conditions at high performance. Driven by the ITER choice, much has been learned about the dynamics of castellation gap loading [75, 309], melt damage and melt motion (see e.g., [310 - 313], particularly in the case of W. This has supported and confirmed the further decision [74] to ensure the protection of poloidal gap (PG) edges (i.e., between toroidally neighbouring units) in the HHF regions by adding a toroidal bevel to the top surface of the ITER divertor MBs.

Even with the toroidal bevelling, extremely localized heat loads to PG edges (referred to as 'optical hot spots' [75]) are not completely avoided as a result of penetration of particles following the magnetic field through toroidal gaps (TG). These hotspots are minute impact regions on the leading edges of MBs in which heat flux is highly focussed and are an unavoidable consequence of the gaps between components which must be present in an actively cooled divertor. As shown in figure 45, they have been experimentally observed on WEST equipped with ITER-like W MB plasma-facing units (PFU) [251, 314]. The toroidal MB surface bevelling likewise does nothing

to prevent excessive ELM-induced loading on the TG sides. For reasons explained in detail in [309], it is not possible on ITER to find a MB top surface shaping solution which protects all gap edges, at both inner and outer divertor targets, from transient loading.

Detailed ion orbit calculations for ITER [75], in combination with the most recent scaling for the peak parallel unmitigated type-I ELM energy density at the outer divertors of the JET, ASDEX Upgrade and MAST tokamaks [64] (confirmed also on COMPASS [315] and HL-2A [316]), can be used to illustrate the importance of this ELM-induced TG loading in the context of the IRP. In figure 46, for any operating point lying within or below the shaded region, unmitigated type-I ELMs would be expected to lead to either top surface or TG edge melting. Evidently, whilst surface melting should not occur until burning plasma conditions are achieved, TG edge melting is marginally avoided for 5 MA H-mode operation and is likely to be an issue already in 7.5 MA H-modes, if ELM mitigation is not rapidly developed early in the IRP. Unfortunately, the ELM energy deposition scaling in [64] is driven strongly by the pedestal pressure and first indications for RMP mitigated ELMs reported in [64], demonstrate that the reduction in ELM energy fluence found in this case is due only to the decrease in pedestal pressure during the RMP phase. Thus, if this scaling is also found on ITER, mitigation alone will not reduce the ELM target energy densities if pedestal pressure is unaffected by the mitigation, which is preferable for high confinement H-modes.

A confirmation that TG loading is a real effect was first obtained in COMPASS, but only for stationary loading conditions (thus with low energy ions with small Larmor radius) and in a limiter plasma configuration [317]. Making similar measurements at the strike points of divertor plasmas, during ELMs, is extremely challenging. A very recent experiment on ASDEX Upgrade has succeeded in clearly demonstrating ELM induced TG loading, confirming the picture that this is driven by finite ion orbits, but was restricted to indirect measurements using erosion of marker layers [318]. More work in this area is desirable to support quantitative evaluations for ITER, in particular, if possible, direct measurement of the ELM TG loading using ultra-high resolution IR cameras such as those being attempted on the WEST tokamak [319].

Since the orbit effect has been confirmed experimentally, it is also important to assess the consequence of TG edge melting should it occur on ITER. If it does, it should take place all along the TG length. Since the ELM energy densities required to induce this TG melting can only be accessed on ITER, there is no possibility to produce this damage in current tokamaks, but tools are now becoming available with which to simulate this melt and melt evolution with subsequent plasma exposure, and R&D in this direction is required. It may also be possible to insert pre-damaged components into an operating tokamak to study the power loading compared with undamaged geometries (see section 5.4.6).

Given the importance of the divertor in handling the majority of the ITER exhaust power and the high impact of W plasma contamination, it is clear that the vast majority of R&D on PFC castellation interactions has to date focused on W. Nevertheless, the ITER First Wall (FW), comprising water cooled panels made up of individual Be flat tiles bonded to cooling substrates, is a ~650 m^2 surface with ~4×10^6 castellation edges. Unlike in the HHF regions of the divertor, these tiles are not shaped and the gaps between FW castellations are in some cases significantly wider than for the W MBs.

In the case of ELM impact on the FW, the situation is somewhat different to the divertor in the sense that wall loading will occur as a result of discrete ELM filament interactions, rather than

the direct connection to the pedestal plasma which seems to characterise the ELM heat pulse at the divertor targets. As a result, filaments reaching the wall may not carry the highest particle energies characteristic of the pedestal top, but there is strong experimental evidence from JET that ion temperatures in these filaments may still nevertheless be considerably higher than the background SOL plasma [320] and thus carry memory of their pedestal origin. Ion orbits may thus be sufficient to drive edge loading, particularly since gaps between FW Be tiles will generally be larger than between MBs in the divertor. There has not, however, yet been a systematic assessment of the ELM-induced castellation edge loading of the kind described in [75] for the divertor. Such an assessment has been made for ELM filament impact on the top surfaces of the Be tiles in ITER in the key region of the secondary divertor where the worst impacts are expected to occur [69]. For ELM energy losses (ΔW_{ELM}) consistent with the avoidance of melting the top surface (but not TG edges) of W MBs in the divertor, this will also be avoided on the FW, but analysis is required for the edge loading, including both PG and TG sides, since no Be tile top surface shaping will be implemented on ITER. In this context, it is also desirable for more R&D to focus on the measurement of ELM filament energy deposition on tokamak main chamber walls, allowing the ELM filament propagation models used to assess this power loading on ITER [69] to be benchmarked.

Melting under stationary limiter plasma conditions and due to VDEs and runaway electron events has been clearly seen and reported on bulk Be castellated structures on JET [136, 258] - see also section 5.2.1.3. Since JET is the only tokamak using Be PFCs, this is the principal source of information on the impact of castellation edge melting on this material. Although this data can only ever be obtained from post-mortem inspection, and is therefore usually the result of multiple exposures over long campaigns, high resolution photography and post-mortem destructive analysis of components extracted from the device can be used to build up an improved appreciation of the various types of damage that can occur in the vicinity of castellations. Modelling using the same tools developed for W melting simulations can then also be applied to specific cases to provide benchmarks for predictive ITER work. Such efforts have already been successful, for example, in the case of simulations of the VDE-induced melt flow cascades and melt splashing seen on the JET Be upper dump plates [190, 313] but specific gap edge melting has not yet been addressed and is necessary to evaluate the consequences of such edge power loads on the ITER Be FW.

5.4.2 W erosion under controlled ELMs

To remain below divertor target stationary power handling limits, partial detachment using seed impurities will be mandatory during burning plasma operation on ITER. Under such conditions, W sputter erosion between ELMs is expected to be extremely low due to the low energies of fuel particles impacting the targets. By virtue of their higher mass and charge state, any W release that does occur is likely to be dominated by impurity ions, such as Be or seeded species, in the impacting flux [171]. Moreover, any sputtering in the inter-ELM period will be associated with a very high prompt redeposition fraction, so that the net erosion is negligible. During ELMs, however, the potentially higher particle energies brought to the target by the transient (see for example the measurements on JET reported in [321]) mean that even if the total duration of the ELM impact is a small fraction of the inter-ELM power deposition, the W source and sputter erosion are dominated by the ELMs and the prompt redeposition physics is more complex [322].

In this case, the fuel ions contribute a significant fraction of the sputtering [323] and might be expected to be the dominant factor at high pedestal temperatures in ITER.

Given the higher ELM-induced gross erosion, the magnitude of the prompt redeposition fraction is key in terms of the impact of the enhanced W source on plasma operation, both in terms of core W contamination and on the prompt radiative heat losses at the ELM [171]. As shown in figure 47, this fraction is critical with regard to W core contamination and resulting radiation. Already at an ELM energy loss level of $\Delta W_{ELM} \sim 0.7$ MJ, the ensuing W erosion and core plasma contamination following the ELM is sufficient to lead to the loss of the H-mode and to the radiative collapse of the plasma for 7.5 MA/2.65 T helium H-modes if W redeposition were not to take place during the ELM. On the other hand, when a 50% prompt W redeposition during the ELM is assumed, the plasma remains in stationary conditions with a very low core W concentration and associated radiation.

Regarding total ELM-induced erosion of W, without high prompt redeposition fractions numbers can be quite significant for ITER if full ELM suppression is not achieved. The JET study in [325] on divertor erosion, migration and screening under unseeded, deuterium type-I ELMy H-mode conditions found, for a total exposure time of ~900 s, a gross erosion of ~50 g for the outer target (the majority due to ELM-induced sputtering). This was for a ~1 m^2 wetted area and ~3×10^4 ELMs. This JET exposure, requiring ~150 discharges, is roughly equivalent to a single ITER FPO $Q = 10$ H-mode pulse in terms of ion flux, ion fluence and energy loads. Based on this JET result, a very rough extrapolation to the whole of the ITER FPO phases 1 - 3 (~8×10^6 s [45]), assuming, for simplicity, deuterium only impact, mitigated ELMs at $f_{ELM} = 40$ Hz and a total divertor affected area of ~3 m^2, gives an erosion depth of ~8 mm, which exceeds the ITER divertor MB W thickness above the cooling channel (the numbers will be higher if tritium impact is also accounted for). Fortunately, the measured prompt redeposition factor of ~95% in the JET experiment, if it also applied on ITER, would reduce this 8 mm to a net erosion of only ~0.4 mm. It is, therefore, essential to understand the mechanisms causing prompt redeposition during ELMs to determine their expected role in ITER.

Measurements of prompt redeposition factors, especially during ELMs, are rare, with the approach of Optical Emission Spectroscopy on JET in [323, 325] to observe W atoms (WI) and the first ionization stage (WII) coupled with post-mortem analysis of W marker tiles, being the first real demonstration of a viable technique to establish ELM-resolved gross and net erosion. When supported by local erosion migration modelling, as in [325, 326], it is a powerful tool for extrapolation to ITER, and further measurements and modelling of this type would be extremely valuable, particularly in the sense of application to a broader range of plasma conditions. In view of the ITER PFPO phases, measurements of prompt redeposition fractions during ELMs in helium H-modes are especially encouraged, given the higher W sputtering that will occur due to the higher He ion mass. In this case, it is not net target erosion that is at stake, since the total He plasma duration will not be significant in comparison to the burning plasma operation phases, but more the impact of the increased W source on core plasma contamination and on the prompt radiative losses at the ELM as discussed in section 5.3.1.2 (see also figure 47).

A further important issue, linked also to the general question of ELM-induced material damage (see also section 5.4.5), is the extent to which the ELM energy transient may be buffered by the divertor or SOL plasma before striking the targets. Very little R&D has been reported in this area,

but it is clearly important from the point of view of ELM-induced W erosion and the general question of the required levels of ELM control, to study the maximum ELM energy loss which may be permitted before the transient is able to burn through the cold divertor plasma and impact the W targets. On the basis of reported experience, notably at JET [327] and ASDEX Upgrade [328], ELM buffering is moderate for medium-*Z* impurities (e.g., N, Ne), but can be achieved (with reduction factors of up to 80%) with Ar seeding. The results suggest that what is required is an impurity that radiates efficiently at electron temperatures characteristic of the pedestal plasma, consistent with the picture of the ELM as a transient heat pulse originating from the pedestal region. More R&D is required in this area, particularly since it can be difficult to disentangle the effects of the radiating impurity on the ELM parameters at source and the buffering effect. If some degree of buffering could be combined with ELM mitigation, this might be a viable alternative to complete suppression on ITER if the latter proves difficult.

Finally, given the intended use of magnetic perturbations for ELM control (section 5.12), R&D is required on the W redeposition fractions at the divertor targets in the presence of 3-D fields. This is evidently tightly linked to the key issue of whether or not dissipative divertor conditions can be achieved under such conditions (section 5.12.5) since if this is possible, it is likely that prompt redeposition factors will be similar to those found in normally partially detached plasmas without 3-D fields. This is an important open R&D issue that impacts the technical application of 3-D fields in ITER to ensure both acceptable divertor power loads as and net erosion. It also has implications for lifetime consumption of the ELMCC during the execution of the IRP, due to $j \times B$ cyclic forces with the main toroidal field, [63].

5.4.3 Helium plasma-wall interactions

Helium plasma interactions with ITER PFCs, especially those at the W divertor targets, have specific features that can potentially impact component lifetime [73]. Tungsten exposure to a He plasma can lead to the formation of He bubbles [329] and, at elevated temperatures, surface modification by the growth of a fibre-form nano-structure referred to as ‘fuzz’ [330]. In addition, it can also impact the thermo-mechanical and recrystallization properties of W, which are a key driver for the ITER divertor lifetime [73]. It should be noted, however, that He effects on metals are strongly temperature dependent and it is not expected that pure He plasma operation in the PFPO phases will produce divertor power fluxes sufficient to provoke any significant degradation of lifetime in advance of the FPO phases, in which He will be present in the divertor plasma fluxes (see section 5.4.4). It is nevertheless possible that the He-plasma induced embrittlement caused by the formation of a porous sub-surface structure (populated by a large fraction of voids and bubbles) and associated reductions in the thermal conductivity of the surface [331], could lead to a reduction in the threshold for transient-induced damage (due, in particular, to ELM impact). Opposed to this, however, is the observation in electron beam facilities that the energy density threshold for W surface cracking under ITER-relevant cycle numbers (~10^6) of ELM-like heat pulses is extremely low [332]. Thus, although surface cracking might appear sooner in the case of He ELMy H-mode operation, it appears likely to occur anyway in later phases. The question is then what the long term impact might be on the W surface of crack networks occurring early on in ITER operation (see also section 5.4.5).

A more pressing issue for pure He operation on ITER is that of erosion of Be from the first wall. This will be much larger than for H (or D) plasmas and could therefore lead to a much higher

deposition of Be on the divertor targets. Such effects have already been seen in ASDEX Upgrade during a pure He campaign in 2015, where it was found that the outer divertor target switched to an area of net deposition from the usual net erosion found in D plasmas [35]. More specifically, thick boron coatings were found on samples installed on the outer divertor target manipulator, originating from enhanced boron sputter erosion of structures around the ICRH antenna and/or of coatings on the first wall deposited by boronization.

Much heavier deposition of Be on the ITER divertor targets during pure He plasmas would lead to an 'effective Be target', which could significantly alleviate some of the operational issues related to W release during the PFPO phases (e.g., ELM-induced sputtering) and reduce the longer term impact of He PWI on the divertor material. Since the peak divertor target surface temperatures will be much lower in the PFPO phases than during burning plasma operation, it is unlikely that thick Be coatings that may develop can be easily removed by the plasma.

It is thus the quantification of this modified material erosion and migration during He plasmas (e.g., how much, where does the Be migrate to preferentially, how much time is required to develop substantial coatings?) that is the key outstanding R&D issue to resolve in view of future pure He operation in PFPO on ITER. Experiments to address this fully can only be conducted on JET with the ITER-Like Wall. Data from these experiments would be important input to benchmarks of migration modelling codes that have now reached a rather high level of sophistication and that are being applied to make predictions for ITER plasma operation, including operation in pure He (see, e.g., [333]).

5.4.4 Impact of helium on plasma-material interactions (DT)

The FPO-1 phase, will be the first time mixed He-D-T plasma interactions with W at elevated temperatures will take place on ITER. It is only under these conditions that fuzz formation would be expected to occur in some regions of the W divertor HHF regions and really the key outstanding question is whether or not fuzz will be formed, and if it is, how thick might such layers grow and what would be the consequences. Applied to ELMy H-mode ITER burning plasma divertor conditions, the fuzz growth-annealing model in [334] predicts the achievement of an equilibrium fuzz thickness at which the growth rate is compensated by ELM-induced annealing. This thickness is far smaller (a few microns at most) than would be expected in the absence of ELMs and is dependent on the assumed ELM energy density (being largest for smaller ELMs). If this model applies, saturation of the thickness would occur in tens to hundreds of seconds, depending on the ELM frequency. In the absence of annealing transients (as for example in the case of ELM suppressed regimes), the fuzz thickness would increase with a typical $t^{1/2}$ time dependence.

Although there are a great many laboratory experiments that have addressed different aspects of fuzz growth dynamics, what is missing are observations under tokamak conditions, with simultaneous bombardment with H/D/T and He, preferably with Be impurity, to test the models and investigate the importance of Be deposition or ELM erosion in suppressing the fuzz growth. Such experiments are possible on JET with the ITER-Like Wall, using the fact that the inertially cooled divertor targets can be heated by H-mode plasma operation to a range ($900\ \mathrm{K} < T_{surf} < 2000\ \mathrm{K}$) at which fuzz is expected to grow. This would also be a useful test of the ability of in-situ diagnostics (such as optical emission spectroscopy or IR thermography) to detect the formation/ destruction and, in the case of IR, to investigate whether or not the He plasma

exposure (independent of fuzz growth) leads to modifications in the surface thermal conductivity (using the T_{surf} response to ELM transients).

Even if fuzz does not ultimately form on ITER, the consequences of He implantation (and in general for all processes leading to dislocations, voids, bubbles etc.) for the thermo-physical properties of the W near surface may be potentially important. In particular, very significant reductions in the thermal conductivity, down to 20 - 30%, have been found in several experiments and numerical simulations - see, e.g., [331, 335]. Even for relatively shallow affected layers (~tens of μm), such reductions could have a profound impact on melt thresholds under transient impact. Experiments on current devices could be designed in which in-situ melting on pre-irradiated and pristine W PFCs is induced, combined with pre- and post-mortem analysis. The findings should then be benchmarked against melt simulations to check if the measurements are consistent with reduced top surface thermal conductivity.

5.4.5 Impact of power/particle fluxes on tungsten PFC performance

There are a great deal of effects of plasma irradiation on W PFCs that may impact the short and long term performance of W components (see [73] and references therein). In addition to the specific issues related to He plasma exposure discussed in sections 5.4.3 and 5.4.4, particularly important outstanding R&D areas may be summarised as follows:

- W surface modifications under high plasma fluence exposure;
- Consequences for W MB performance after sustained operation above recrystallization temperature;
- Impact of plasma transients on surface cracking and subsequent evolution.

Many aspects have been the subject of intense laboratory studies in recent years (e.g., electron beam exposures [332]), but the principal difficulty lies in performing assessments under realistic tokamak plasma operating conditions (high fluence, small angles of incidence of plasma fluxes to the surface, simultaneous impact of stationary and transient heat fluxes, relevant incident plasma species mix, etc.). Until this is achieved, no quantitative assessment of the likely performance - essentially a lifetime assessment - will really be possible for ITER.

The situation is, however, changing with, for example, the advent of devices such as Magnum-PSI, which has completed the first ever exposure of ITER-like W MBs to ITER lifetime ion fluences (10^{30} - 10^{31} m^{-2}) under stationary plasma conditions [336]. Separate exposures combining stationary loading with mitigated ELM-like transient energy densities (produced by laser irradiation) at the level of 10^6 events, corresponding to a few tens of ITER $Q = 10$ baseline discharges, have also been performed [337]. Similarly, the WEST tokamak platform, intended as a major testbed for ITER divertor PFCs, is now operating routinely [338] and will begin Phase 2 operations in 2022 targeting the full long pulse/high fluence capability (10 MW input power, 1000 s discharge duration) on an ITER-grade actively cooled lower divertor.

First results from both the Magnum-PSI experiments [336] and WEST Phase 1 exposures [339] demonstrate that there are no apparent adverse impacts of high fluence stationary exposure on specifically arranged pre-damaged components. These experiments are providing the first glimpses of the synergies and particularities that appear in terms of, for example, material cracking when transients and plasma stationary loading are combined.

A particularly interesting observation for ITER has been the finding on WEST [251] that even relatively low amplitude transients, comparable to very small (mitigated) ELMs that ITER must target as a minimum, can provoke rather significant micro-cracking on W surfaces operating below the Ductile to Brittle Transition Temperature (DBTT). This is expected to be the case for a significant fraction of the ITER PFPO phases, since power fluxes to the divertor will be insufficient to raise the temperature of the divertor MBs above the DBTT, particularly for PFPO-1 [44]. An important question then arises as to whether or not extensive MB surface cracking experienced near the beginning of ITER operations will have any impact on long term material evolution, particularly in view of the fact that small cracks may act as seeds for deeper cracks under the fatigue action of high stationary plasma load cycles and millions of small scale transients [332].

Even if such early phase cracking is avoided on ITER, it seems likely impossible to avoid it in the long term, particularly in view of the very large numbers of small scale transients that will almost certainly occur over the first divertor lifetime and the known impact of embrittlement and increased stress in the W material when exposed to plasma flux [73]. All tokamaks operating (or soon to operate) long pulses on actively cooled W divertor PFCs, such as EAST, KSTAR and WEST, are encouraged to make as many efforts as possible to monitor the long term evolution of components.

Recrystallization is a well-recognized issue for W PFCs and a number of studies have focussed on its consequences. In particular, the appearance, in electron beam tests, of macro-cracks in the centre of some of the MBs exposed to high cyclic thermal loads (20 MWm^{-2}), a factor of ~2 higher than the nominal peak stationary power load for which the MBs are qualified [72, 340, 341]. Such loads are entirely possible in the HHF regions of the ITER vertical targets and could occur transiently under conditions of divertor reattachment in the case, for example, of loss of detachment control [45]. Also referred to as ‘self-castellation’, this macro-cracking is the most serious possible consequence of recrystallization identified to-date. Avoiding it, by setting an operating constraint on the allowed maximum stationary surface temperature (and hence the power flux density) has been proposed as a criterion determining sufficient lifetime for the first ITER divertor [45, 73]. In fact, this macro-cracking in itself does not necessarily imply that the power handling capability of the MB is compromised, even if the crack propagates through the entire MB W thickness to the cooling interface [341]. What is also clear from laboratory tests is that surface damage under small scale, rapid transients (cracking, localized melting and grain ejection) is much more pronounced on recrystallized surfaces [342].

A key aspect that can hopefully be resolved by R&D in tokamaks before high power ITER operation begins, is how large macro-cracks evolve under realistic cyclic, high fluence plasma exposure, particularly with particle fluxes at near grazing incidence and under high heat flux conditions in the presence of rapid transients. The concern is that the very wide openings (similar to the gaps between poloidally adjacent MBs) occurring during self-castellation may become sites of intense erosion and melting, leading to potentially serious further degradation and/or plasma pollution, especially since such cracks open preferentially in the centre of MBs where thermal stresses are highest as a result of the MB geometry. In this case, the MB top surface bevelling, designed to protect leading edges at PGs in ITER would not be effective at hiding the crack. Experiments in tokamaks are thus required in which pre-damaged (hence macro-cracked) W PFCs are exposed to high fluence, high power loads, preferably in the presence of large numbers of

ELM transients. This should be combined with in-situ monitoring of the component surfaces, together with assessment of impact on plasma performance and post-mortem surface/destructive analysis.

An ultimate test of the ITER divertor target lifetime would require that a large number of PFCs be pushed, under relevant power densities and plasma exposure conditions, to high enough temperatures for times sufficient to achieve recrystallization through a significant depth of material. This is the basis of the ITER divertor lifetime constraints on surface power flux density referred to earlier and proposed in [45, 73]. Such an experiment would clearly be sacrificial in the sense that once recrystallization occurs, it is irreversible. Moreover, the exposure time required for a true test of ITER lifetime cannot be attained in any operating tokamak. Nevertheless, even if only shallower recrystallization depths can be obtained (as a consequence of shorter integral exposure durations), important statistical information can be obtained (assuming sufficient in-situ and ex-situ monitoring is available). Whilst a positive outcome would not prove that the required lifetime of the first ITER W divertor will be obtained, negative consequences would provide extremely important input with regard to operational constraints on the permissible ITER divertor power fluxes.

5.4.6 Tokamak operability with damaged tungsten PFCs and PFC melting

The issue of how ITER operation maybe affected by damaged PFCs is extremely difficult to assess in current devices, since all experiments to-date have been restricted to relatively localized damage. Whilst disruption-induced Be PFC melting is expected to occur on ITER [124], and has been experienced on JET [136, 258], the ITER plasma is orders of magnitude more tolerant to Be and transient damage to the ITER First Wall will not always occur in regions that are subject to high stationary power loads [124]. In contrast, if significant damage does occur on ITER divertor W MBs, there is a good chance this occurs in HHF regions where power handling is at a premium.

In the case of W PFCs, melting on current tokamaks can only occur on misaligned edges since no operating device can attain the transient energy densities (ELMs and disruptions) possible on ITER by virtue of its elevated stored energy. Tokamak experiments deploying deliberately misaligned PFCs have been used extensively in support of ITER [310, 311, 343] to study the dynamics of melt motion and to benchmark simulations [313, 344, 345]. These studies are, however by definition restricted to just a single misaligned edge, either in locations not normally solicited by high power fluxes [310, 343], or on manipulator systems allowing the damaged component to be removed once the experiment is performed [311]. Despite significant melting, melt motion, and even droplet formation, no noticeable perturbation on the core plasma was reported in these ‘leading edge’ experiments.

A variation on this theme of deliberately misaligned edges has been the ‘W pin’ experiments on ASDEX Upgrade, in which a small W rod, a few mm long, was exposed to ELMy H-mode discharges such that melting and droplet emission occurred [346]. Here the emphasis was on the study of droplet dynamics and screening in the divertor plasma rather than melt motion on a local surface. In this case, notable perturbations to the core W concentration accompanied droplet ejection events in the divertor and droplets were observed to survive over quite long durations and to travel over large distances in the divertor plasma (as a result of the various forces acting on the droplets).

More extreme examples of ‘leading edge’ interactions have occasionally been reported from tokamaks (Alcator C-Mod [347], ASDEX Upgrade [348] and EAST [349]) using W PFCs in divertor target regions. In these cases, edges are not deliberately exposed, but are the result either of assembly misalignment [348] or accidental events which lead to misalignment during operating campaigns [347, 348]. Observations here are varied: on ASDEX Upgrade, rather severe, but localized melting on 4 outer target inertially cooled, misaligned edges produced no effect on the core plasma and the device operated for ~800 plasma discharges without impact. In Alcator C-Mod, an entire (inertially cooled) PFC was lost in a row of W blocks in the outer divertor, leading to a very severe leading edge which did not heal with subsequent discharges and on which strike points could not be placed without plasma disruption (as a result of significant droplet production). On EAST, misaligned edges on adjacent cassettes of the full-W, ITER-like upper divertor (thus with water cooled MBs of the ITER design), initially led to plasma disruptions due to W ingress, but then appeared to heal somewhat with further plasma operation. One conclusion in this case is that melted W moved poloidally out of harm’s way and re-solidified on adjacent cooled surfaces from where it was not subsequently mobilised.

Only qualitative conclusions can be drawn for ITER from these various (deliberate and accidental) experiments: in the case of edge melting, if this is restricted to very localized regions and droplets do not form in significant quantities, then plasma operation may not be compromised, but this will also depend sensitively on the type of operation (e.g., cold detached divertor plasmas with lower peak target power fluxes). Since PG edges in the ITER divertor are protected in the HHF areas by the top surface bevelling, only TG edges, which can be loaded even without misalignment and which cannot be protected everywhere, will be expected to melt if ELMs beyond a given amplitude are not avoided (section 5.4.1). Unfortunately, no current device has sufficient transient energy density to melt TG edges, so it is extremely difficult to study this effect experimentally other than to expose pre-damaged TG edges, as proposed in section 5.4.1, or to approach the problem through melt code simulations.

Based on the Alcator C-Mod observation, should an entire MB be lost, or become seriously misaligned in HHF areas on ITER, then it is very likely that plasma operation would be completely compromised. However, such failure modes are extremely unlikely in the ITER divertor concept.

Unlike in current devices, entire top surface MB melting can readily occur on ITER in the case of unmitigated ELMs and disruptions, and even in steady state, if control of divertor heat flux is lost even for a short time at very high performance. In this case, the very rapid melt motion of W (due to strong thermionic emission and subsequent Lorentz drive [74, 344], means that even for very short lived transients, shallow melt layers can move material poloidally across TGs. Since it is known that splashing from PFC edges is likely to constitute the dominant instability responsible for material ejection and droplet production in situations without clear protruding leading edges [190, 350], further investigations (experimental and simulation) in this general area of melt gap bridging is thus a very high priority for ITER. Does splashing occur when an accelerated W melt layer encounters a castellation gap? Or does the gap simply fill with re-solidified material (as seen on JET in the case of Be upper dump plate melting [258], or on protruding edges in the EAST upper divertor [349].

Given the fact that loss of control events (e.g., of stationary plasma loads or ELM mitigation/suppression) can very quickly lead to quite significant top surface MB melting on

ITER, it is also important to assess the long term impact of operation on melt damaged surfaces other than exposed edges. It is clear that, given the remarks in section 5.4.5 on the importance of avoiding recrystallization, all efforts need to be made during ITER operation to maintain MBs below a given operating temperature. Nevertheless, off-normal events cannot be excluded, and, if in sufficient number, they could radically change the surface topology of certain MBs, not to mention the material thermo-physical properties. Here again, experiments in which pre-damaged W components (i.e., having undergone extensive top surface melting) are installed in tokamak divertors and exposed to high fluence, high power plasma fluxes, can provide valuable input as to the possible further degradation of the component under long term exposure as well as permitting an assessment of any global impact on plasma operation.

5.5 Plasma Initiation

5.5.1 Ohmic plasma initiation

The plasma initiation process in larger super-conducting tokamaks, such as ITER has a narrower operation range than in present tokamaks. It is well known that due to voltage limitations on the superconducting central solenoid, the larger device size and the highly conducting vessel, ITER will have a smaller maximum breakdown electric field than in most presently operating tokamaks ($\leq$0.3 Vm^{-1}). This limits the range of possible pre-fill pressures for hydrogenic ionization, which is further restricted by the criteria to burn-through impurity radiation, providing a pressure window for plasma breakdown in the range of 0.5 to 1 mPa [88]. This is impacted by the vessel volume, which is larger during ITER First Plasma operation for which the blanket is still absent, leading to a significantly larger amount of neutrals being ionized to achieve main-species burn-through [88].

It is clear that the delicate ITER plasma initiation process needs to be well-understood to optimally prepare for ITER plasma operation and R&D is required for this. It is important to account for the fact that the plasma initiation process is more than just the breakdown or ionization of a neutral gas and turning it into a plasma. Moreover, the current through the plasma should be raised continuously and eventually become feedback controlled. This requires a constant drop in the plasma resistance and thus increasing electron temperature. Hence, plasma heating should overcome the losses, and importantly burn-through radiation losses from main-species and impurity line-emission. Raising the current will eventually create closed magnetic flux surfaces that improve the confinement of the fragile early plasma. It is also important to initiate the control of the plasma position, possibly its shape, and importantly the plasma density. Fine-tuning the early density control will have to avoid burn-through failure, density limits and a radiative collapse, while at the same time avoiding too low a density, that may result in the formation of runaway electron discharges during the plasma initiation process [351]. The aim is to eventually control the plasma such that a stable diverted plasma shape can be created and the current and density can be ramped-up further to the desired operation value.

The physics of the broader plasma initiation process is reasonably well-understood and a number of good simulation codes exist that have been validated against experiments. A standard Townsend avalanche process is assumed for the first part of the breakdown process. Thereafter, these codes predominantly simulate the plasma burn-through process, taking into account changes in the plasma confinement (e.g., flux surface formation), various energy loss processes, while

often self-consistently calculating the particle balance and impurity content from plasma-surface interactions [352]. Auxiliary plasma heating can be added to aid the burn-through process as described later.

A number of aspects of the plasma initiation process have been identified that would benefit from further research and development, in preparation for ITER plasma operation. The plasma initiation process is usually described and modelled as a zero-dimensional process. One assumes a constant plasma size or volume, with constant values of plasma parameters over the volume. However, it is experimentally observed that during this stage the plasma volume is rather dynamic. Assuming spatially and time-varying density, temperature and current density profiles rather than constant parameters, could alter the overall dynamics of the process and thus the simulations for ITER. Including a dynamic volume size, profiles and thus internal transport processes, greatly complicates the simulation codes. Recently efforts have started to understand the Townsend avalanche process in a 3-D tokamak. Thus, instead of only taking into account the electron acceleration and the results of collisions along the field-lines such as done in the standard theory [88], one should assume the full particle motion in the three-dimensional tokamak configuration [353]. This alters the speed at which this process can take place. R&D to characterize in detail the plasma breakdown process and its evolution to a fully ionized tokamak plasma with closed flux surfaces is required to validate models to predict plasma breakdown used for ITER, as well as to optimize this phase of the discharge to ensure reproducible and reliable plasma start-up in ITER.

Another important issue relates to the formation of runaway electrons during the plasma initiation process. This is a well-known phenomenon since the early days of tokamak research, and the impact of a high number of energetic runaway electrons can, if they are lost, do damage to in-vessel components. For long, the occurrence of such runaway electrons was attributed to the use of a too low pre-fill pressure. However, the process is more complex and linked to the detailed dynamics of the electron density, toroidal electric field and the plasma current [351]. It is also known that even though the electric field is above the critical electric field to allow runaway electrons to be present, significant runaway loss can occur during the current ramp-up. This means that accurate simulation of the runaway electron generation process during plasma start-up in ITER with validated models also requires a detailed understanding and modelling of the runaway loss processes in this phase. The development and validation of the models require further experimental research to identify in detail the runaway electron generation processes as well as the loss processes during plasma initiation and start-up. The validated runaway electron models are then to be included in existing plasma initiation codes allowing the integrated simulation of the combined process of plasma start-up and runaway electron generation, which will be used to aid the preparation of ITER plasma operation and the optimization of the plasma start-up phase.

5.5.2 EC-assisted plasma initiation

A further aspect that requires supporting R&D relates to assisting plasma initiation by applying high power electromagnetic waves, such as ECRH, which will be used at ITER [354]. This scheme assists the plasma initiation process in two distinctly different ways: (a) EC waves can provide auxiliary heating that aids the burn-through process and (b) ECRH can also pre-ionize the neutral gas.

The first process can be accurately simulated and thus its effect is rather well understood for ITER. Key in the effectiveness of the ECRH burn-through assist is the fraction of the power that is absorbed by the plasma. The low plasma densities and temperatures at this early stage in the tokamak discharge means that only a small part of the power is absorbed. The exact quality of ECRH absorption may further depend on the exact geometry of the injected EC-wave beam, the possibility that it passes multiple times through the plasma by reflecting against the inner walls and also the harmonic and polarization of the waves that are used. Detailed simulations of burn-through assist by ECRH show that second harmonic extraordinary polarized waves will not be able to extend the ITER pre-fill range, while this is possible using first harmonic ordinary polarized waves [355]. This can be understood by the fact that the absorbed power by second harmonic extraordinary modes is only a small fraction of the total injected power and that it scales linearly with the electron density and temperature, while the radiated power increases with the square of the density [88]. Thus, it is difficult for the EC absorbed power at the 2nd harmonic with extraordinary mode polarization to overcome the radiation losses. For 3rd harmonic ECRH (required for 1.8 T operation) the issues are more serious in ITER and EC-assisted start-up is not considered viable.

On the contrary, ECRH pre-ionization is not well understood. Recent theoretical work, using a single electron approach, has derived criteria for the minimum wave power density needed to achieve direct ionization of the neutral gas by ECRH [356]. It is, however, not clear yet to what extent the acceleration of single electrons, localized to where the ECRH beam intersects the EC resonance in the vessel, will aid the overall plasma initiation. Further research is needed to determine the ECRH requirements for the pre-ionization process to effectively assist the tokamak discharge initiation, taking again into account the exact geometry of the injected EC-wave beams in ITER along the lines of studies such as those in [357].

5.5.3 ICRF-assisted plasma initiation

ITER PFPO includes operation at 1.8 T to achieve H-mode at low current. This will allow commissioning of the plasma control system in H-mode scenarios and to test ELM mitigation techniques, as described in section 5.3.1. However, breakdown at 1.8 T is more difficult to achieve in ITER than at higher fields. In the first place, the connection length of magnetic field lines is shorter than for half or full toroidal field. In addition, and more importantly, as mentioned above, pre-ionisation does not work with the third ECH harmonic of 170 GHz waves at 1.8 T. Since, as described in section 5.5.2, even at 2.65 T and 5.3 T, ohmic plasma initiation in ITER may only succeed for a narrow prefill pressure range, it is possible that at 1.8 T ohmic breakdown is difficult to achieve reliably in ITER. Thus, if ohmic breakdown is unsuccessful in ITER, 1.8 T operation will require a specific set of lower frequency or dual frequency gyrotrons to support plasma start-up (third harmonic ECRH heating issues are described in section 5.11.1). Alternatively, ICRF-assisted plasma initiation is an option that can be considered to provide breakdown assist at 1.8 T in ITER for PFPO-2 operation.

A robust ICRF-assisted breakdown scenario with ITER relevant electric field was developed at JET, both with D and H fuelling, at 2.3 T and 33 MHz, and with D fuelling at 1.7 T and 29 MHz. The ICRF pre-ionisation discharges are similar to ICWC plasmas with monopole toroidal strap phasing [358]. The low, but uniform, density allowed the optimal neutral gas pressure range for the Townsend avalanche to be provided while maintaining a constant and high

gas throughput. More work is needed to develop and characterise such ICRF-assisted breakdown in present devices, at ITER relevant loop voltage, toroidal field and RF frequency, to assess its possible application in ITER as an alternative/complement to EC-assisted breakdown where the application of ECRH may be ineffective. This is the case when there is not a suitable harmonic/ polarization providing good pre-ionization/absorption for a given value of the toroidal field or, possibly, after the use of the DMS, where residual impurities may remain relatively high, to assist in maintaining the pulse repetition rate. In the latter case there may be issues related to unabsorbed EC power during several seconds of low n_e-T_e plasma because of high impurity radiation, which can narrow the application of EC power for burn-through assist.

5.6 Wall conditioning

The toroidal magnetic field in ITER, generated by superconducting magnets for which the number of large electromagnetic cycles is limited, excludes use of DC glow discharges for wall conditioning and fuel removal during the ITER operational campaigns [150]. As discussed in section 2.5.3, the use of ICWC and ECWC is therefore foreseen to provide wall conditioning in the presence of the magnetic field, i.e., during an experimental campaign between pulses or between operational days. In JET, after the installation of the ITER-like wall, inter-pulse wall conditioning is not found to be a necessity. However, ICWC and ECWC may be needed at ITER to recondition the device after the use of the DMS, to assist fuelling gas changes and possibly to control the T inventory. Hence the efficiency and operational boundaries of ICWC and ECWC need to be studied in present devices supported by modelling in preparation for ITER operation.

5.6.1 Electron cyclotron wall conditioning

EC-generated plasmas for wall conditioning are currentless discharges, without equilibrium and partially ionized, produced by resonant absorption of EC power. ITER foresees heating by EC waves at a level of, at least 20 MW from PFPO-1 onwards. The main open issues relation to the preparation of ECWC operation in ITER concern the required EC power for efficient neutral gas breakdown and to maintain the quasi-stationary plasma, including the role of multi-pass absorption and the expected levels of stray radiation. In addition, the particle fluxes to the PFCs and their efficiency for fuel and impurity removal need to be characterized, including the influence of discharge parameters such as poloidal field maps and EC launch parameters on the achievable plasma. This requires a multi-machine study to allow extrapolations from present devices to ITER. Here JT-60SA can play a major role, as the largest tokamak equipped with ECRH and superconducting coils. In addition, it is proposed to start the commissioning phase with a, mostly, metallic wall. Tokamak experiments are to be complemented by the further development of models for EC-assisted breakdown discussed in section 5.5.2, and for the quasi-stationary plasma phase, described below.

The removal of hydrogen isotopes and impurity species from PFC surfaces is determined by the particle fluence, hence an ECWC pulse scenario in ITER, like those developed for W7-X [359], requires sufficient plasma duration, at least several hundred milliseconds per pulse. Minimizing stray radiation in such pulses requires short breakdown times, as well as optimal stationary plasma parameters, since resonant absorption of EC power depends strongly on n_e and T_e. Recently, the potential of modelling ECWC plasmas using a fluid approach has been

demonstrated successfully with the TOMATOR-1D code [360]. The model reproduces the density profiles of ECWC plasmas in TCV using conventional assumptions on anomalous diffusion and outward convection, and provides insight on the fraction of absorbed EC power, which remained below 25%. However, the model is intrinsically 1-D, and several enhancements are required to address the outstanding research questions in which 2-D effects are central. The trapped particle configuration, a poloidal field configuration having open field lines, but with the open ends curved toward the HFS, was shown to improve the EC-generated plasma parameters in KSTAR [361]. Similarly, a quadrupole-like poloidal field map maximized the particle flux to the HFS in TCV [362]. These 2-D effects need to be understood in detail by modelling to optimize the field configuration to be applied in ITER.

Experimental inputs, in particular, from metallic devices such as ASDEX Upgrade, EAST and KSTAR (and possibly WEST in the near future) equipped with an ECRH system and metallic PFCs are key to preparing ECWC for ITER. On the other hand, devices with carbon based PFCs already allow for systematic studies of ECWC to be carried out. In this respect, plasma characterization will benefit from dedicated diagnostic developments such as, but not limited to, high resolution Thomson scattering systems and camera tomography for these specific plasma conditions. Finally, devices with superconducting magnets are particularly well suited to demonstrate the effectiveness of ECWC for isotopic changeover and the recovery of operational conditions after the use of massive material injection for disruption mitigation.

5.6.2 Ion cyclotron wall conditioning

ICWC is being developed to contribute to T recovery by isotopic exchange and impurity removal after DMS events in ITER. A conservative estimate of the upper limit for its use indicates that it might be applied after every mitigated disruption and, in addition, on a daily basis during FPO-1, or after every few DT pulses during FPO-2 and FPO-3 (and beyond, if experience confirms the desirability/necessity of this frequency of use). Experiments in present devices show that ICWC can be effective for these purposes at the ITER scale [150]. To better understand the underlying mechanisms of its efficiency and to plan its use in ITER, however, a better characterization of ICRF-generated plasmas in present devices is required. This encompasses, notably, the density profiles in front of the IC antenna and the particle fluxes to the PFCs, using dedicated diagnostics such as, but not limited to, electrostatic probes, pre-characterized surface samples and low energy neutral particle analysers.

ICWC in ITER will use the ICH&CD antenna system, operating in the 40 - 55 MHz frequency band, to first initiate the conditioning discharge by the strong vacuum electric fields in the vicinity of the antenna and then to maintain the stationary homogeneous plasma by coupling ICRF power to both electrons and ions, mainly via non-resonant processes. Both phases need to be studied numerically and experimentally. Monte Carlo simulations show that, in a 1-D toroidal approximation, the ionization rate in the IC breakdown phase is lower at the higher frequencies and the larger torus size of ITER [363]. Therefore, the minimum antenna excitation required to allow breakdown as a function of ICRF frequency needs to be studied both experimentally, for well characterized IC antennas in present devices, and numerically. Using such a benchmarked model, the same minimum excitation can be studied for the ITER antenna structure, respecting the maximum peak voltage of 45 kV permitted in the antenna system, at the relevant frequency range and common toroidal phasings of the antenna straps. Ideally, such a study should take into

account the complex, 3-D pattern of the ICRF field in vacuum and the prescribed shaped poloidal field.

IC-generated discharges are successfully initiated and sustained over a large range of toroidal magnetic field values (0.1 to 3.8 T) and frequencies (5 to 48 MHz) in present devices. To ensure ICWC operation in ITER, the ICRF power requirement in the stationary discharge phase and the ability of the antennas to couple this power to the plasma must be studied. This requires experimental input on density and temperature profiles from present devices to benchmark self-consistent models that describe collisional processes and anomalous transport in the toroidal plasma (e.g., the TOMATOR-1-D code [360]), extended with wave excitation and dissipation descriptions that carefully treat the possible occurrence of the lower hybrid resonance in the plasma [364].

Finally, devices with superconducting magnets can best contribute to the development of the operation scenario for ICWC in ITER, by studying the optimal pulse duty cycle for fuel and impurity removal and by identifying diagnostic requirements and operational challenges.

5.7 Error fields and correction

5.7.1 Development of error field criteria (n = 1, 2, resonant, non-resonant)

Non-axisymmetric components of tokamak magnetic fields with low toroidal mode number, *n*, (error fields), degrade plasma confinement and can cause a disruption [5, 207]. In ITER, these error fields are caused by misalignments and deviations in the manufacture and assembly of the superconducting TF, CS and PF coils as well as magnetized ferromagnetic components of the machine (e.g., TBMs) and its ferromagnetic surroundings (e.g., rebar reinforcing the building concrete structures).

Error fields have been categorized based on their impacts on plasma performance [365]:

(i) core-resonant error fields that lead to locked modes (LMs) and disruptions;
(ii) edge-resonant error fields that degrade particle and energy confinement near and in the pedestal region;
(iii) non-resonant error fields that apply torque and degrade plasma toroidal momentum confinement.

The study of critical values of error fields for ITER has been performed since the beginning of the ITER design activities with the support of the ITPA (initially ITER Physics Expert Groups) in the Topical Group on MHD, Disruptions and Control [5, 207, 365 - 370].

This effort led to the development of a criterion on $n = 1$ core-resonant error fields leading to LMs and disruptions, evolving from the initial '3-mode' definition (metric) of the error field based on vacuum fields to the present 'overlap' definition (metric) of the error field, which uses linear, ideal MHD modelling [365 - 370]. The metric used is the amount of overlap between an error field and the spectrum that drives the largest linear ideal MHD resonance, i.e., error field component that triggers the dominant resonant magnetic perturbation response. This metric, which takes into account both the external field and plasma response, is scaled against experimental parameters known to be important for the inner layer physics and has led to the LM 'overlap' error field criterion for the critical value of the magnetic field for the growth of the $n = 1$ mode, B_{ovlp} [366]. This is currently used to guide the assembly of the ITER tokamak through its practical implementation described in [358]:

$$\frac{B_{ovlp}}{B_0} = 4.5 \times 10^{-3}(n_e^{1.4\pm0.13} B_0^{-1.8\pm0.16} R^{0.81\pm0.24} \beta_N^{-0.86\pm0.14} \qquad (2)$$

where B_0(T) is the toroidal magnetic field value at the plasma centre (B_0 = 5.3 T for ITER at R = 6.2 m), n_e (10^{19} m^{-3}) the plasma density, R (m) the tokamak major radius and β_N the value of normalized β.

Further experimental and modelling R&D is required to refine this criterion, when needed, but most importantly to develop similar approaches for higher values of n, in particular, for n = 2. This is already in progress and an initial guidance for locked mode triggering by core-resonant n = 2 error fields has been produced [368] that requires further development.

It is important to implement further experiments and modelling to understand the effect of core-resonant error fields for n = 1 and n = 2 not only regarding LMs in stationary phases but also during transient phases of the plasma (e.g., L-H/H-L transitions) and in relation to non-resonant error field effects. A knowledge of the impact of error fields on ITER operation, in particular, the critical values for n = 1 and n = 2 error fields, provides the criteria on acceptable deviations of the TF, CS and PF coil current centrelines from their ideal shape and position as a result of manufacturing and positioning tolerances, key information which is being used to guide tokamak assembly. This knowledge will also be used to optimize error field correction by exploiting the EFCC and ELMCC in the course of executing of the IRP.

5.7.2 Optimization of error field identification and correction

Correction of error fields needs to be optimized so that the spectrum applied by the correcting field compensates, as much as possible, that of the intrinsic error fields, both for resonant and non-resonant components, without the introduction of additional components that degrade the final plasma symmetry. This is particularly challenging for error fields produced by sources located at the HFS of a tokamak (e.g., caused by misalignments of the current centrelines of the TF coil inner legs or deviations of the CS coils from their ideal positions). These intrinsic error fields produce spectra that differ significantly from those produced by the error field correction coils located on the plasma LFS in ITER and do not resonate strongly with the dominant kink mode, i.e., they have a low ‘overlap’ component and significant non-resonant components. Non-resonant components reduce plasma toroidal rotation through NTV torque [154] (see section 3.2.5.3), resulting in significantly degraded plasma performance, possibly even causing a disruption during transient confinement phases (e.g., after the L- to H-mode transition) [371 - 374].

Development of optimum error field correction schemes that optimize both correction of resonant and non-resonant components, such as the quasi-symmetric error field correction scheme [371], should be developed for ITER to take advantage of the capabilities of the EFCC and ELMCC sets, both having equatorial, upper and lower toroidal rows of coils. This R&D involves both experimental and modelling studies to provide a solid physics-based guideline for application in ITER and should include both stationary and transient plasma phases.

Before error field correction is applied in ITER, it is necessary to identify the sources and magnitude of the intrinsic error fields. This requires the study of a range of plasmas in which different possible sources of error fields are scanned (e.g., using a range of current level ratios in

the PF Coils, various values of TF field (and thus TF ripple), etc.) so that the resulting error fields can be identified, especially the low-*n* resonant error fields leading to LMs. Since the plasma processes generating LMs which are associated with the error fields include the plasma response, a range of plasma scenarios must be included in the error field identification experiments to be performed within the IRP, and this range of scenarios must be optimized to generate the required data. Schemes for error field identification must be developed for ITER. The classical 'compass scan' [375] to identify low-*n* resonant error fields relies on the triggering of LMs as a result of low density operation, which typically ends in a disruption. Since disruption loads on plasma facing components, even at low current, can be significant and cause surface melting [124], the use of schemes that rely on unmitigated disruptions for error field identification will be very limited in ITER. It is, therefore, of very high priority for the successful execution of the IRP to develop schemes for error field identification that avoid disruptions. In this respect, it should be noted that the first steps in error field identification will take place in PFPO-1, for which the only available heating scheme is ECRH. Therefore, schemes that rely on increasing torque input (e.g., increasing the toroidal rotation by NBI injection) are not applicable for PFPO-1 and, in general, are of very restricted application in PFPO-2 because of shine-through limitations. Since error field identification should be completed by PFPO-2, the availability of a robust and reliable error field identification scheme with no or minimum disruptivity is a high priority R&D activity for ITER.

5.8 Controlled termination of H-mode scenarios

5.8.1 General open issues on H-mode termination in ITER

The termination of H-mode plasmas and the current ramp-down phase of ITER plasmas need to be designed considering a range of aspects, including plasma physics, tokamak design and plasma control constraints to ensure a reliable termination of the plasma discharge. ITER will be the first fusion device that will require the termination of the plasma discharge starting from burning conditions. Since, for high-*Q* operation, α-heating is comparable to, or higher than, the auxiliary heating power, the dynamic evolution of the total heating power in ITER high-*Q* plasmas will differ significantly from present tokamak plasmas. Currently, control of the auxiliary heating systems allows a reasonably robust control of the H-mode termination and ramp-down phase by tuning of the H-L mode transition. To design the H-mode termination and ramp-down phases in ITER high-*Q* plasmas, specific models must be developed and these will be tested and validated prior to FPO by dedicated experiments in PFPO such that a complete model can be progressively assembled in preparation for high performance operation in DT. In addition to these scenario modelling tools, control schemes need to be developed that ensure that ITER H-mode terminations remain within stability and control limits, while ensuring the ramp-down follows the optimum path downward.

While the ultimate test of the scenario modelling tools and control schemes will be performed in ITER, the development of models and control schemes for the termination phase and their testing against experiment should already be undertaken in present tokamak devices by dedicated R&D with focus on the specific aspects described below.

Integrated modelling of termination scenarios and experimental validation: The basic strategy considered for ITER H-mode plasma termination is to reduce the plasma size and elongation in parallel with the reduction of the plasma current, while maintaining a diverted

plasma configuration until the plasma current becomes sufficiently low. This is necessary to avoid excessive power loads to plasma facing components, given the lower power handling capability of the first wall compared to that of the divertor: figure 48 [376] provides an example of this termination strategy. The reduction in elongation improves plasma vertical stability, given the increased internal inductance which develops during current ramp-down, complicating vertical stability control. Of course, this is not the only aspect of the plasma evolution that must be controlled in this phase: the density must be controlled to avoid approaching a density limit, as must stationary and ELM-generated transient power fluxes and impurity accumulation, especially if the plasma is maintained in H-mode during part of the ramp-down phase.

The physics mechanisms associated with the H-mode termination and ramp-down processes depend on the coupled dynamics of magnetic and thermal plasma energy, which have their characteristic time scales determined by the plasma resistive time and energy/ particle confinement times respectively. Since these characteristic times do not scale with device dimensions in a proportional way, the robustness of the proposed ITER terminations can only be assessed by performing integrated modelling of the plasma dynamics and control [376]. These integrated models need to be applied to predict terminations in present experiments and validated by dedicated experiments targeting ITER-like H-mode termination scenarios. Recent modelling studies of the ITER plasma termination from an H-mode [186, 377] has shown that the exit from H-mode must be optimized while considering various physics and operational aspects. On the one side, designing an early H-L confinement transition at high plasma current is beneficial for avoiding density limits, since the decay of plasma density during the H-mode phase could be slower than that of the plasma current. On the other side, allowing an extended H-mode during the current ramp-down is beneficial for vertical stability, since β_p remains high while l_i is lower than that in L-mode [378]. A slow variation of dW/dt during the extended H-mode and late H-L transition is also beneficial to control divertor power fluxes and to avoid W accumulation [377, 379], as discussed in the next section. An extended H-mode during the current ramp-down also has the advantage that if a disruption is triggered by the H-L transition, the resulting loads will be lower, given the reduced plasma current and energy, and their mitigation easier to achieve [87].

It is, therefore, important to perform experimental and integrated modelling R&D for the key physics processes in H-mode termination plasmas, since many of them (e.g., H-L transition, pedestal and impurity dynamics) are subject to large uncertainties and cannot be scaled empirically to ITER. In this respect, the transfer of many of the operational aspects from present experiments to ITER (e.g., optimum H&CD mix and power waveform, including plasma shape evolution, ELM control schemes to avoid low frequency type-I ELMs or a long final ELM-free phase, etc.) [376] can only be undertaken on the basis of a strong integrated modelling activity connected to such experiments.

Advanced control schemes and experimental validation: In addition to the use of reference scenarios improved through the enhanced integrated modelling activities discussed above, a reliable ITER plasma termination from H-mode will require advanced control of multiple parameters. It is significantly more challenging to achieve a controlled ramp-down of a plasma parameter than to maintain a specified constant value. This is exacerbated by the fact that many plasma parameters are coupled in a complex way during the termination phase. The aim of the advanced control schemes is to ensure that the ramp-down of all plasma parameters avoids stability and operational limits. Moreover, such schemes can possibly be used to determine the

optimal path during this phase. In this respect, important aspects of termination scenario control include control of the plasma current and density ramp-down, control of the plasma shape, of vertical stability, of plasma radiation, of detachment and divertor heat load, as well as ELM control, impurity accumulation avoidance, the timing and plasma energy evolution during the H-mode back-transition, and the avoidance of MHD stability limits, while taking into account actuator limits and their availability (e.g., H&CD power is impacted by plasma shape and position, plasma density, etc.).

To guide the development of such advanced multi-variable control schemes, there are several control requirements which must be investigated for ITER plasma terminations and which have to be supported by targeted activities to develop and test the relevant control schemes in present experiments. For example, the requirements for plasma shape and elongation control need to be assessed in terms of the vertical stability margin and vertical forces on the CS coils. Reducing the elongation too quickly during the current ramp-down, to maintain vertical stability [376], may involve the approach to vertical force limits on the CS coils, if this is implemented too early during the extended H-mode phase [380]. Similarly, control requirements on the density, impurity and radiative power during the entire current ramp-down phase need to be developed and optimized while taking into account ITER's fuelling capabilities and the impact of impurity accumulation during this phase. In addition, divertor heat load and detachment control requirements must be developed to incorporate potential changes in the ELM and impurity dynamics in this phase. The requirements to control the H-L mode transition need to be further investigated for various termination scenarios to avoid loss of vertical stability and radial plasma position control. Control of H&CD schemes to avoid impurity accumulation in the termination phase must also be further developed, given the strong impact of plasma shape evolution and plasma density on heating effectiveness (coupling of ICRF, central ECRH deposition, excessive NBI shine-through, etc.).

Since many of the control requirements are mutually coupled when several plasma parameters are ramped simultaneously in the termination phase, an advanced approach with several supervisory layers that determine the priorities and sharing of actuators will have to be developed and tested in present experiments with targeted ITER-like H-mode termination scenarios.

Development of validated physics models: To improve candidate termination scenarios for ITER using integrated modelling tools, as well as to develop advanced controls for robust plasma termination, it is very important to develop a range of physics models of key processes in the plasma termination phase and to validate them against experiment. For example, particle transport and density decay during the current ramp-down from H-mode are not well understood. It is often found that the density decay is significantly slower than the reduction in the plasma current in present experiments. However, this could be influenced by different recycling dynamics in ITER and requires a detailed, validated physics model to make reliable predictions for ITER. Similarly, a better understanding of the behaviour of the H-mode pedestal in dynamic situations is required (e.g., along the lines discussed in [63, 202]) to develop robust ITER terminations [376] including the impact of plasma parameters on the α-power evolution. Understanding the behaviour of divertor parameters, including detachment, in H-mode transient phases and the development of models to be used in integrated modelling simulations is also necessary, since, without specific control, power loads in the H-mode termination phase can be significant.

In ITER, the H-mode termination phase is expected to remain at relatively low q_{95} due to the elongation reduction associated with maintaining vertical stability. This is not a common strategy in present devices and leads to the plasma evolution tracing the upper boundary of the l_i-q stability diagram [376], which may lead to specific MHD stability issues. The plasma may also approach ideal MHD β-limits for the steady-state scenario, if the enhanced confinement of the burning plasma phase is maintained during the extended H-mode termination phase [185, 186]. The impact on MHD stability of such termination conditions needs to be assessed with validated models to optimize control during this phase of the scenarios.

While a key step for the validation of these models will come from the experimental programme to be executed during PFPO in ITER, it is important that the models are well developed and validated, to the extent possible, in present experiments to ensure the efficient implementation of the IRP.

5.8.2 Tungsten accumulation control in H-mode terminations

H-mode terminations raise specific issues regarding the control of ELMs and of W accumulation, which make this phase of the scenario particularly critical in ITER. It is commonly observed in present experiments that lack of adequate ELM control, together with the natural density peaking that occurs in the H-mode termination phase, can frequently lead to W accumulation and plasma disruptions [377]. This must be avoided in ITER. It therefore requires sufficient control of ELMs to exhaust W from the edge, as well as controlling the plasma density and temperature to avoid conditions prone to core W accumulation. Open R&D issues on ELM control in transient phases are discussed in section 5.12, while the analysis here concentrates on core W accumulation which can occur in this phase even if the pedestal W level remains low.

Modelling and experimental studies have shown that core W accumulation in ITER is not likely to occur, since ITER plasmas are predominantly electron heated and the core particle source from NBI is very low [195, 206, 381]. However, the termination phase of H-modes in ITER is more challenging due to the formation of peaked density profiles. This is driven by the relatively fast adjustment of the pedestal parameters to the varying conditions (e.g., if pellet fuelling is reduced) compared to slower evolution of the central part of the plasma in which anomalous transport is low [195]. As discussed in section 5.8.1, termination of H-mode plasmas presents specific challenges due to the relatively slow timescale for control of the radial position of ITER plasmas compared to that for the decrease of the plasma energy, a mismatch in timescales that can lead to contact between the plasma and the HFS first wall during these phases [63, 376]. Optimum radial position control requires a slow decrease of the plasma energy in the H-mode termination phase, which can be achieved by extending the time that the plasma remains in H-mode. This requires sustainment of a margin in edge power flow above the L-H transition threshold which remains as high as possible for as long as possible [63, 376]. This condition can be achieved by switching-off pellet fuelling, thus reducing plasma density, when the ramp-down of the additional heating starts and by subsequently maintaining some lower level of additional heating. The strategy also favours the sustainment of high P_α in the H-mode termination phase, since the core plasma temperature remains high [63, 376, 380].

Simulations of W transport for the exit phase of $Q \sim 10$ H-modes show that, while this strategy is very effective in minimizing the rate of change of the plasma energy, it can lead to W

accumulation in the core due to the steep density gradients formed in the plasma core after pellet fuelling stops (see figure 49) [195]. On the other hand, reducing pellet fuelling in a more gradual way is sufficient to avoid W accumulation while still providing a slow decrease of plasma energy in this phase (figure 50). It should be emphasized that, as mentioned earlier, the key to avoiding W accumulation is to maintain a low density gradient in the central plasma region during the H-mode termination phase. The most effective way to achieve this is to decrease the value of the plasma density itself to $<n_e>/n_{GW} \sim 0.5$ before the H-mode termination phase starts. This is found to effectively prevent W accumulation for a slow ramp-down (i.e., with a characteristic timescale of ~20 s) of the heating power for $Q = 10$ plasmas even when pellet fuelling is switched-off at the start of the power ramp-down, as shown in figure 50. This robust strategy to avoid W accumulation in the termination phase implies a reduction of the $Q = 10$ burn length by 20 - 30 s (i.e., <6%).

It is, therefore, of key importance for the design of ITER scenarios to develop H-mode terminations that are robust to W accumulation. This requires the use of models that have been validated against experiments for the specifically complex processes involved in W transport and accumulation during such transient phases. It should be noted that these validating experiments need to be carefully planned to be ITER-like during the termination phase and must, therefore, also address other issues that require appropriate matching of resistive and main species energy and transport timescales. This specifically involves the sustainment of ELM control in the H-mode termination phase, as well as the avoidance of a significant core particle source from NBI, since this is known to be the major driver for W accumulation in present experiments, but will not be a significant influence in ITER.

5.9 Complex control of ITER scenarios

Control of the plasma in ITER will require complex schemes that integrate acceptable edge/plasma wall interaction with high performance core burning plasmas. In this section, we consider the R&D required for two such complex control topics, while others that are directly linked to specific aspects of scenarios are discussed in the relevant sections.

5.9.1 Divertor detachment control with ITER schemes

Control of power fluxes to the ITER divertor will be necessary on a routine basis for a wide range of ITER scenarios, specifically in those foreseen for high-Q operation. This requires operation in radiative divertor conditions with detached divertor plasmas. Control of the divertor power load, but also of the radiation location in the divertor channel, which is associated with the degree of detachment, is thus required. Loss of detachment control can lead to full divertor detachment and to the formation of a highly radiative zone in the X-point region. This may potentially impact plasma confinement and lead to an H-L transition [296, 298] and disruption, especially in ITER plasma scenarios, since the margin above the L-H transition power threshold is $(P_\alpha + P_{aux})/P_{LH} \leq 2$ - 3 over the foreseen H-mode scenarios. Loss of detachment control can, of course, also lead to transient divertor re-attachment, with power fluxes that exceed, by a factor of several, the stationary power handling capabilities of the ITER divertor [382] a situation which must be avoided.

Control of divertor detachment relies on similar actuators as in present experiments, namely gas fuelling, extrinsic impurity seeding and additional heating power level. However, in ITER their use for control purposes can differ significantly from present experiments because of device physical dimensions (e.g., length of the gas fuelling pipes) or plasma timescales (e.g., energy confinement time) that lead to very different timescales for the actuators in ITER compared with the SOL timescales regulating plasma detachment. As an example, modelling of ITER plasma behaviour when re-attachment is detected shows that it is possible to re-establish the semi-detached plasma conditions in less than 8 ms by D+Ne gas fuelling, once the gas arrives at the divertor, as shown in figure 51. However, arrival of the gas to the divertor typically takes 0.40 - 0.45 s and it requires ~0.6 - 1.0 s to reach 2/3 of the set point for the flow [382]. Similarly, control schemes based on heating systems in ITER have to take into account that the edge power flow will evolve on timescales of ~1 s (dictated by the energy confinement time), unless specific actions are taken to increase edge deposition (e.g., use of peripheral ECRH heating using the upper launchers).

In addition, the sensors used in present experiments to control detachment are not expected to be routinely available in ITER. For example, Langmuir probes used both in the first detachment control experiments and in more recent studies [52, 383] are not considered for ITER due to possible limitations of the probe lifetime. The sensors for detachment control in ITER will be based on plasma spectroscopy with support from thermography and bolometer measurements, with some similarities to those used in [49, 54, 55, 384, 385]. These may be complemented by measurements of thermoelectric currents, which are routinely used for detachment control in present experiments [386], if the ITER sensors for measuring divertor current flow can be used. R&D on this specific aspect is currently on-going.

The successful execution of the IRP relies on efficient schemes to control divertor power fluxes and plasma detachment. This requires the development of control schemes and supporting plasma models, together with their validation by ITER-relevant experiments. These models and experiments should incorporate the relevant characteristics and timescales of ITER plasmas, actuators and sensors. An important point is that this development and the experimental validation must include both stationary plasma conditions and the transient phases of ITER scenarios. As described in section 5.8, the termination phase of ITER scenarios relies on the sustainment of H-mode plasma conditions with varying density, additional heating level, plasma current, etc. Radiative divertor conditions will need to be maintained in these transient phases to ensure acceptable divertor power loads. This is shown to be feasible by integrated modelling for ITER [377], as shown in figure 52, but the detachment control aspects of these transient scenario phases remains an open R&D issue.

5.9.2 Burn control

Burn control is essential in ITER high-Q scenarios, both in stationary phases and in transients, such as in the entrance to and exit from burn, since α-heating is key to maintaining the plasma in H-mode. Regulating the amount of fusion power produced by ITER will require precise control of the plasma density and temperature and of the DT fuel mix. For example, poor density control in the entrance to burn can lead to the plasma not reaching a stationary $Q = 10$ burn in ITER due to insufficient α-heating during the entrance phase, as shown in figure 53 [377].

Due to the non-linearly coupled dynamics of the plasma parameters, feedback control of the burn condition will be necessary to avoid undesirable transient excursions and to respond to changes in plasma confinement, impurity content and operation conditions that could significantly alter the burn. This requires the development of controllers that utilize multiple actuators simultaneously, such as auxiliary heating schemes and DT fuelling to control the burn [387, 388] while taking into account other necessary actions such as ELM control and power flux control [389]. Such control schemes must include the constraints of actuator sharing. In addition to maintaining a stationary burn when perturbations of the plasma parameters or malfunction of some actuators occur, the controllers should be capable of following conditions in which the fusion power evolves in time, such as during entrance and exit from burn phases.

To make progress in the design of the robust control schemes required for ITER, it is essential to develop fast and accurate models of actuators and sensors (diagnostics) that take into account the ITER specificities. These diagnostic and actuator models will be used to determine if the information provided by the measurement systems can be used for burn control in a direct way, or if additional real-time estimates of parameters that are not easily measured need to be developed for optimum burn control. For example, the concentration of T in the fuelling lines may vary from the initial (90% T + 10% D) for long pulse operation and this may not be measurable in real time in ITER. This requires the design of advanced non-linear controllers that take this uncertainty into account and can optimize plasma parameters to maintain the fusion power at the required level despite any variation of the T concentration in the fuelling lines [390].

These advanced control schemes should then be validated and optimized against specific experiments where timescales for plasma processes and those of actuators and sensors are matched to those of ITER. Experiments of this type include, for example, burn control experiments in which part of the additional heating power is fed back on plasma parameters (e.g., plasma energy), or isotopic control experiments with deuterium and hydrogen with feedback on the DD neutron rate.

5.10 Development and validation of scenario modelling and analysis tools

As mentioned in several previous sections, the effective planning and execution of the IRP relies on the development of models for plasma behaviour and for diagnostics and actuators. All these models must be developed at several levels of sophistication to allow their use for a wide range of applications, ranging from high fidelity simulations of ITER scenarios, through efficient ITER scenario design, to real time plasma control applications. Similarly, analysis tools beyond the production of data from individual diagnostics need to be developed to support the effective execution of the Research Plan. Such tools should provide best estimates of plasma parameters from multi-diagnostic measurements or multi-diagnostic processing. Their implementation should also cover a range of applications from sophisticated computationally intensive, lengthy post-pulse analysis, along the lines of [391, 392], through inter-pulse analysis, to real time applications for plasma control.

The models must also be tested and validated in an integrated way with dedicated experiments in present fusion facilities. This includes use of the models to design plasma scenarios and their control (including sensor and actuator modelling), their validation against experiments in routine application and the validation of experimental analysis tools.

To achieve the goals of this research, it is essential that both modelling and experimental data use a common representation. In addition, individual models for physics processes, actuators, sensors, etc., should be easily interchangeable when used as part of the integrated modelling and analysis approach required to design, control and analyse experimental data from ITER scenarios. For this purpose, the ITER Organization with support from fusion institutions in the Members has developed the Integrated Modelling and Analysis Suite (IMAS) [393] The adaptation of existing plasma physics models and scenario modelling tools, as well as models for actuators, diagnostics and analysis tools, to IMAS and the development of new models and tools operating in this framework is a key R&D activity to support the development and execution of the Research Plan. The outcome of this activity will be the best possible set of tools to design ITER scenarios, optimize their control and interpret the results from experiments [394 - 396]. This set of tools must be validated, and it requires, in addition to the dedicated R&D activities described in this and other sections, that the experimental data from such experiments is readily available in the IMAS data format. This allows seamless implementation of the simulation and analysis tools and the comparison of their results against experiments while avoiding device-specific prescriptions. This minimizes the effort required and the possibilities for errors in the validation process when using experimental data from several devices.

5.11 H&CD application in ITER scenarios and fast particle issues

5.11.1 Use of 3rd harmonic ECRH for 1.8 T plasmas

H-mode operation in PFPO-1 is considered an important risk mitigation measure in the Research Plan since it allows early determination of the power requirements for H-mode operation and the commissioning of ELM control schemes. If H-mode scenarios can be established in PFPO-1, this will serve as a reference to identify possible effects on plasma performance of the Test Blanket Modules (TBMs) in PFPO-2 (beyond those leading to mode-locking discussed in section 5.7) and to optimize the correction schemes (EFCC and, possibly, ELMCC) to minimize them. Since, in PFPO-1, only a limited power will be available from the ECH system (20 MW, with a possible upgrade to 30 MW under discussion), H-mode operation (i.e., beyond L-H threshold identification) will only be possible at low values of the plasma current and field, namely at 1.8 T with plasma currents up to 5 MA. To minimize the required power, as described in section 5.3.1, low plasma densities will be explored in these H-mode plasmas typically in the range of 40% and 50% of the Greenwald density. These same plasmas can then be further explored in PFPO-2 at the same and higher power levels with different heating mixes to determine the effects of TBMs on H-mode plasmas. Therefore, these scenarios have been developed for the two PFPO phases: a study has been carried out to address whether these H-mode scenarios at 5 MA/1.8 T can be achieved and sustained in ITER, taking into account all physics and technical considerations, and to determine which parameters such plasmas will have [33, 34].

The main outstanding question related to H&CD application concerns EC heating of 1.8 T plasmas, since the ITER gyrotron frequency of 170 GHz corresponds to 3rd harmonic absorption. Heating of ohmic plasmas at 1.8 T with the 3rd EC harmonic is not efficient when ECRH power is initially applied, since the plasma temperature is of the order of 2 - 3 keV, which is too low for efficient 3rd harmonic absorption, as evaluated with the GRAY code [397]. To determine if there

is a viable scheme for 3rd harmonic heating of 1.8 T plasmas, simulations accounting for the self-consistent interplay between the EC deposition and plasma kinetic profiles using self-consistent transport modelling have been performed with the JINTRAC code [398], as described in [33] Due to the interplay between ECRH and plasma transport, the central plasma temperature evolves rapidly after the application of the EC power, leading to an increased absorption and further increase in the plasma temperature in a positive feedback loop, as previously observed in 3rd harmonic EC heating experiments [399, 400]. This results in a very high level of 3rd harmonic absorption on timescales of less than 1 - 2 s for an EC power of 10 MW or higher after start of heating for PFPO-1 L-mode 5 MA/1.8 T plasmas, as shown in figure 54 [33].

Since H-mode operation in PFPO-1 is important for the Research Plan, it is important to confirm these modelling findings for the further development of ITER scenarios by specific experimental and modelling R&D. This concerns the quantitative evaluation of ECH absorption modelling predictions as well as the validation of the models that describe plasma transport and density and temperature evolution in the transient phase from low absorption/low temperature ohmic plasma conditions to high absorption/high temperature heated conditions with 3rd harmonic ECRH heating.

A remaining open issue concerns plasma start-up at 1.8 T. If ohmic start-up at 1.8 T were found not to be sufficiently robust in ITER (as discussed in section 5.5.1), some lower frequency (~110 GHz) gyrotrons may be required to assist plasma start-up at 1.8 T. These would also facilitate the efficiency of 3rd harmonic ECRH in later phases of the discharge. A decision on whether to install such gyrotrons is expected to be taken following the operational experience obtained during the First Plasma and Engineering Operations campaign.

5.11.2 Application of ICRF heating to PFPO-2 scenarios

Several effective absorption schemes are available in H and He plasmas at magnetic fields of 5.3 T, 2.65 T and 1.8 T, in the ITER ICRF frequency range 40 - 55 MHz, except for H operation at 2.65 T, as reported in [287]. The most promising schemes are:

- In helium plasmas:
  - At 5.3 T: Fundamental ^{3}He-minority heating, with ^{3}He concentration of the order of 5%, leading to a Single Pass Absorption (SPA) of ~80%. Note that pure He operation is only considered in the IRP in the context of H-mode development for the toroidal field range of 1.8 - 2.65 T.
  - At 2.65 T:
    - Fundamental H-minority heating with an H concentration of 2 - 8%, leading to an SPA of ~100%, which is the reference scheme for the IRP;
    - 2nd harmonic ^{4}He-majority heating, leading to an SPA of ~80%. This scheme could be used as back-up in case of severe deleterious effect of H-minority on He H-mode performance.
  - At 1.8 T: 2nd harmonic H-minority heating, if needed, leading to an SPA of ~100%. Good 2nd harmonic minority heating at cyclotron harmonics is unusual, but can be achieved thanks to the beneficial $1/B_0^2$ scaling of the finite Larmor radius absorption [401].
- In hydrogen plasmas:
  - At 5.3 T:

- Fundamental ^{3}He-minority heating in a ^{4}He-H mixture (3-ion heating scheme) with a ^{4}He concentration of the order of 10% and ^{3}He concentration below 1%, leading to an SPA of ~95%.
- Fundamental ^{4}He-minority heating accounting for the ^{9}Be concentration (3-ion heating scheme) or not (2-ion scheme), with a ^{4}He concentration of 0.1 - 2%, leading to an SPA between 60% and 80%. The ^{4}He concentration has to be adjusted according to the ^{9}Be concentration: the ^{4}He concentration must be lower for high ^{9}Be concentration, for an optimized absorption.
- Fundamental ^{3}He-minority heating with a ^{3}He concentration of 2 - 4%.

- At 2.65 T: scheme with very reduced efficiency (R&D is on-going to increase ELD/TTMP damping);
- At 1.8 T: 2nd harmonic H-majority heating, leading to an SPA of ~100%.

The lack of an efficient ICRF scheme at 2.65 T in hydrogen may be compensated by optional schemes at 3 - 3.3 T with fundamental ^{3}He-minority heating in a H-^{4}He mixture (3-ion heating scheme). However, this scheme leads to off-axis absorption (at r/a ~ 0.7 and 0.5 respectively) that can impact core transport, as described in section 5.3.1.1. Furthermore, it requires specific plasma parameters (low density and fine-tuned plasma composition) and antenna configuration (a lower toroidal mode number, corresponding to the 00ππ toroidal strap phasing instead of the 0ππ0 reference phasing for ITER).

Specific issues for which R&D is required to optimize the use of these ICRF heating schemes concern the interaction of the ICRF waves with ion species in the plasma (beyond the minorities foreseen for the scheme), since these impact ICRF deposition and, potentially, plasma transport [152]. In relation to H minority in He plasmas, the application of ICRF together with NBI causes a redistribution of the NBI absorption [402], decreasing electron heating in the plasma centre, as shown in figure 55, and this may affect inwards transport of W [381].

For the 3-ion heating scheme in an H plasma with ^{4}He doping ($c_{4He} = n_{4He}/n_e$) and 0.1% of ^{3}He minority, the main issue is the impact of the Be concentration naturally present in the plasma. This Be concentration affects the SPA of this scheme and requires fine tuning of the ^{4}He concentration and its monitoring must be maintained in real time to ensure a good SPA. The same issue applies to the full-field ^{3}He minority heating scheme ($c_{3He} \approx 3\%$), since the ICRF absorption by the ^{3}He minority degrades with increasing contamination by Be, and so tuning of the ^{3}He minority is required to ensure a good SPA.

The understanding and control of all these effects requires further R&D, including simulations of scenarios integrated with particle and heat transport simulations, as well as supporting experimental verification.

5.11.3 ICRF schemes for Fusion Power Operation

The two main ICRF schemes foreseen for the ITER FPO phase are fundamental ^{3}He-minority heating and 2nd harmonic T-majority heating (see, e.g., [403]). The two schemes can be associated because their resonances are at the same central location for an IC frequency of ~53 MHz. From the physics of wave-particle absorption in the IC frequency range, fundamental minority heating is efficient at low temperature while higher cyclotron harmonics are more efficient at intermediate ion energies. Hence, it is foreseen to first inject ^{3}He in the plasma for a limited time, until the ion temperature increases to a level such that the 2nd harmonic T heating becomes efficient enough to

take over and become the main absorption mechanism. Such schemes have been experimentally demonstrated at JET [404, 405] However a quantitative demonstration of their efficiency in ITER-like plasma conditions, including the dynamics of the transition between the two heating schemes, remains to be performed. For FPO, 3-ion schemes can potentially be applied, such as those based on T - ^{9}Be - D and T - fast-D - D, which have the advantage of not requiring the injection of a specific minority into the plasma [406]. It is important to demonstrate the effectiveness of these schemes and their sensitivity to the 3rd ion concentration, namely the fast-D and ^{9}Be levels, since it will not be possible to control these in ITER to high accuracy. The fast-D density will result from the influence of background plasma populations influencing the slowing-down of high energy D ions produced by the NBI. ^{9}Be ions, on the other hand, will result from plasma-wall interactions, which will need to be controlled. However, the main driver for plasma-wall interaction control will be the needs of core-edge integration, rather than the aim of maintaining the core ^{9}Be concentration within a given range for efficient ICRF heating.

5.11.4 Validation of shine-through loads at high NBI energy

The Neutral Beam Injection of H^0 and D^0 is considered as the most powerful tool for plasma heating, application of torque and production of non-inductive current drive in ITER [3]. As discussed previously, the baseline configuration consists of two beamlines injecting 33 MW, while an upgrade option of a 3rd beam line, providing a total injected power of up to 49.5 MW, is foreseen. In present tokamaks, such as ASDEX Upgrade, DIII-D, EAST, JET, KSTAR, etc., the NBI energies, E_b, span the range over 20 - 120 keV, which provides NBI absorption in the core of plasma. For such energies, the dominant processes for ‘stopping’ of the injected neutrals are charge-exchange with thermal ions and ionization by electrons. For reactor parameters, such as ITER, the opacity of the plasma to NBI penetration increases significantly, requiring an increase of the NBI energy into the range 500 - 1000 keV [5] for efficient core plasma heating and current drive. In this range of energies, the dominant NBI stopping process is multi-step ionization. The analytical fits to the stopping cross-sections derived for a certain limited number of impurity species are presented in [407, 408] to facilitate the extraction of numerical data for use in other applications. This data was used for the assessment of the NBI absorption profiles in ITER plasmas [90], which influences plasma performance and affects plasma control, as well as to estimate the fraction of non-absorbed power (NBI shine-through).

The main impact of shine-through loads on the execution of the Research Plan occurs during the PFPO-2 campaign, since the NBI neutrals are hydrogenic and the plasma majority ion species are H and He. Shine-through loads on the first wall restrict the operational density range at which NBI can be applied over extended fractions of the pulse. Since the H-mode density limit in tokamaks is found to increase with the plasma current, during PFPO-2 the plasma current range in which NBI heating is possible is restricted by shine-though loads [33, 89, 90]. This range can be enlarged by decreasing the NBI energy, but this comes at the price of a significantly reduced injected power, since, as discussed in section 3.2.5.5, to maintain beam perveance matching, $P_{NBI} \sim E_{NBI}^{2.5}$. Alternatively, the use of He injected into H plasmas to lower the H-mode power threshold, or of Ne to enhance radiation of the plasma exhaust the power, can significantly decrease the shine-through loads [90]. This can be used to extend the operational range of hydrogen-dominant H-modes, provided that integration with edge plasma requirements can be maintained [324].

Since, for fixed geometry, shine-through loads depend exponentially on the ionization probability of NBI neutrals crossing the plasma, it is very important to compare modelling predictions quantitatively with experimental measurements. In this respect, the only existing confirmation comes from JT-60U, in which shine-through measurements for a neutral hydrogen beam with E_b = 350 keV/amu injected into JT-60U plasmas appeared to be in a good agreement with the calculations [408]. However, further R&D is required both to extend the theoretical considerations, including the impurities expected in ITER (such as W, Ne, etc.) and in future fusion reactors. This assessment of the accuracy of the shine-through calculations (i.e., of the neutral stopping cross-sections) should also be extended to higher, and more ITER relevant energies, ($E_b \geq$ 500 keV). In this respect, future experiments in the JT-60SA tokamak can provide unique experimental evidence [409].

5.11.5 Fast particles in ITER plasma scenarios

The confinement of DT burning plasmas in which α-particle heating dominates all other forms of heating will open up new areas of fusion research in the realms of α-particle confinement and heating, as well as allowing studies of α-particle driven instabilities. Whilst experimental indications to date indicate that α-heating can be expected to be classical in nature [410, 411], the large size and strong magnetic fields of ITER mean that the most unstable TAEs are expected to have a much higher toroidal mode number, $n \sim 30$, than in present devices [187]. For the ELMy H-mode sawtoothing baseline scenario with a flat q-profile in the core just above unity, this leads to a dense population of many overlapping modes, particularly in the outer region of the plasma, that may lead to a change in the nature of energetic particle transport.

There is a sparsity of modes in the vicinity of the q = 1 surface, as shown in figure 56, with the exact distribution being very sensitive to small changes in the magnetic shear. The high temperatures in the plasma core also give rise to significant thermal ion Landau damping; this implies that only the modes in the outer region, where fast-α densities are lower, but fast ion densities produced by NBI are higher, are expected to be unstable.

Since such AEs have the potential to increase fast ion transport, and even lead to losses, specific R&D is needed to study the stability of AEs in H, He, D and DT plasmas in the presence and absence of energetic ions to develop and validate predictive models that are applicable throughout the different phases of ITER operation. Validation can take the form of observations of unstable modes, particularly their appearance at marginal stability, as well as direct measurements of the damping rates of stable modes using active excitation systems. Knowledge derived from such studies for various plasma species would allow preparations to be made for experiments in PFPO-2 that could help prepare for FPO and establish the need for any mitigation strategies, including attempting to control the unstable spectrum of AEs.

To prepare for the situations in which AEs lead to unacceptable fast ion transport or losses, research is needed to establish and demonstrate control techniques with ITER-like actuators (e.g., ECRH/ECCD [412 - 415]) over a range of ITER-relevant plasma conditions. Of particular importance is to determine the physics processes behind the control achieved in present experiments and assess their extrapolation to ITER, where the plasma regimes are expected to be very different. This includes whether the control is achieved through local modifications of the current profile or of the plasma parameters and/or their gradients by affecting the AE instability

directly or by increasing damping mechanisms, since their applicability to ITER strongly depends on this (i.e., whether ECRH or ECCD is required at $r/a > 0.5$).

Modelling fast ion stability requires appropriately accurate descriptions of the distribution of fast ions in real and velocity space. Predictive assessments of fast ion stability in ITER (and interpretive simulations in existing devices) would benefit from validated techniques to reconstruct fast ion distributions. Devices that can generate significant populations of fast particles and have ITER-relevant diagnostics could contribute to the development such techniques. Measurements of fast ion distributions in ITER are very challenging and additional approaches to those foreseen could be considered. In particular, the populations of confined and lost fast ions have been observed to create a rich spectrum of Ion Cyclotron Emission (ICE) in multiple devices [416 - 418]. This spectrum, which it might be possible to measure on ITER, encodes information about the fast ion distribution, but its systematic-quantitative interpretation remains outstanding. The limited possibilities for directly measuring the fast ion population in ITER motivates further research into extracting quantitative information on the confined and lost fast ions from the observed ICE spectrum in present experiments to determine whether this technique is a viable scheme for fast ion measurements in ITER.

The application of 3-D magnetic fields for ELM control is expected to influence the confinement of fast ions in the edge plasma region where, as shown above, a multitude of high-n TAEs are expected to be unstable. Validated fast particle stability analysis tools capable of describing the combined influence of these effects and other MHD phenomena, such as NTMs, besides those linked to the direct impact of the edge magnetic geometry on fast ion losses described in section 5.12.6, are required for ITER and motivates a community effort to develop and test such device-independent analysis tools well in advance of PFPO-2.

In this respect, significant fast ion pressures will be achieved in high-power NBI heated PFPO-2 scenarios and this will give a first indication of fast ion stability in FPO [152]. Using a combination of experiments and modelling, an assessment to establish the fast particle instabilities expected in hydrogen H-modes at 7.5 MA/2.65 T ($q_{95} \sim 3$) with 33 MW of H^0 beam injection (870 keV) is required to determine the nature of fast particle instabilities occurring and guide the need for the development of AE control techniques already from PFPO-2.

An emerging area of research in recent years is the interaction between fast ions and micro-turbulence and, in particular, the beneficial influence attributed to populations of energetic ions upon turbulent transport [419, 420]. Given the unique nature and strength of the fast ion populations in FPO burning plasmas, the development of validated models describing these interactions would enable such effects to be accounted for in the plasma scenarios prepared as part of the IRP, since this could be an important ingredient to achieve enhanced confinement together with long pulse operation in ITER, as described in section 5.13.1.

5.12 3-D field controlled-ELM H-mode as integrated ITER scenario

Given the impact of ELM loads on plasma facing component lifetime, ELM control is mandatory in ITER before accessing the high current/ high plasma energy conditions required for high-Q operation. Active triggering of ELMs by pellet injection will provide a level of ELM control that may be suitable for the development of the first H-mode scenarios in PFPO, but does not appear sufficient for later FPO scenarios and, in particular, in plasmas with high Q. For this

reason, ITER is equipped with a set of 27 in-vessel ELM control coils to provide an appropriate level of ELM control and to suppress ELMs over a wide range of ITER scenarios, including those at high Q. However, the application of ELM control by in-vessel coils leads to the formation of a 3-D edge magnetic field structure which also poses unresolved scenario integration issues. Therefore, specific R&D is required to address these integration issues beyond that targeted at understanding the physics processes that lead to the effects on ELM control when 3-D fields are applied and how these processes extrapolate to ITER.

5.12.1 3-D field ELM control and low torque input and impact on plasma performance

The application of 3-D fields for ELM control can have an impact on plasma rotation and plasma pressure that can potentially be detrimental for the achievement of high-Q plasmas in ITER and thus needs to be understood and optimized.

3-D fields interact with the plasma and apply a net torque through three mechanisms: Maxwell stress, neoclassical toroidal viscosity and Reynold stress. Since the normalized input torque provided by the high energy beams in ITER is low compared to present experiments, even a relatively small negative torque from the 3-D ELM control fields can slow the core plasma and lead to a disruption. This behaviour can be observed in present experiments when the magnitude of the field applied exceeds a given threshold and is typically more pronounced when the toroidal symmetry of the applied perturbation is low (n = 1, 2) than when it is high (n = 3, 4) as foreseen in ITER. This is not, however, a universal picture and, as an example, results from the EAST tokamak show a similar impact on plasma rotation for n = 2 and n = 4 in the suppressed ELM regime, as shown in figure 57 [421]. Similarly, predictions for ITER [422] show that the effects of 3-D fields on plasma rotation in ITER strongly depend on the spectrum applied for ELM control. For n = 3, 4 3-D field perturbations optimized for ELM control in ITER, the decrease of plasma rotation remains localized at the plasma edge and is very moderate at the location of the q = 2 surface. In some cases, the application of 3-D fields for ELM control can actually lead to a net increase of plasma toroidal rotation, rather than to its decrease, as shown in figure 58.

Since, in ITER, it is essential to maintain a very low disruptivity and simultaneously achieve a high degree of ELM control (aiming at full suppression) for high-Q operation, targeted R&D is required to understand in detail the physics processes leading to the torque applied in the plasma by 3-D fields. Key issues are to identify how these processes depend on plasma parameters and to validate the models that describe these processes against experiments. These models will then be used to evaluate such effects in ITER plasmas and to optimize the current waveforms applied to the ELMCC to maximize their effectiveness in ELM control while minimizing the detrimental effects on plasma rotation through the torque applied to the plasma.

The application of 3-D fields for ELM control also impacts plasma performance. This is associated with the decrease of the plasma density (the so-called ‘density pump-out’), but a decrease of plasma pressure, and thus fusion performance in ITER, can also occur. The effect on plasma density poses specific challenges to ITER plasma fuelling in the presence of the 3-D fields required for ELM suppression, and these challenges are discussed in section 5.12.4. In the following, the impact of the applied fields on plasma pressure is considered.

In general, the application of 3-D fields for ELM control (mitigation and suppression) leads to a decrease of edge plasma pressure compared to that observed in a type-I ELMy H-mode.

However, the magnitude of this decrease and its impact on overall confinement can vary significantly from experiment to experiment, whether in the same tokamak or across tokamaks. Regarding the pedestal plasma, the symmetry of the applied perturbation is found to influence the decrease of edge plasma pressure, with higher-*n* symmetries causing a smaller decrease [421]. However, even with the same applied *n*, the impact on plasma pressure depends on the pedestal plasma properties themselves, as shown in figure 59 [423]. Similarly, the impact on overall plasma energy confinement of the 3-D ELM control fields results from a complex balance of several effects that involve both plasma transport and the change in power deposition profiles and equipartition caused by the density pump-out mentioned above. R&D is required to understand and model in detail the effects leading to the limitation of pedestal pressure by 3-D fields and its impact on overall plasma confinement. This will allow an analysis of whether they are likely have a similar impact on ITER pedestal and core plasma conditions to that observed in present experiments and, if so, what the magnitude of such an impact would be. These validated models will also be used to guide the optimization of 3-D fields to provide ELM suppression in ITER while minimizing, or completely eliminating, such deleterious effects. In this respect, recent R&D has opened a way to successfully tackle this optimization in KSTAR experiments [424]. It is important to pursue this, or similar approaches, to confirm that they are generally applicable to existing experiments and, subsequently, to ITER plasmas.

5.12.2 ELM control in transient phases

In ITER scenarios, ELM control is not only required in the stationary phases, but also during transients. These include the transition from L- to H-mode and the exit phase from H-mode, as well as during phases of H-mode scenarios in which the plasma current is ramped, as foreseen in ITER high-*Q* scenarios [377, 380].

Regarding ELM control with 3-D fields in L-H and H-L phases, it has been observed in present experiments that the magnitude and the detailed spectra of the applied 3-D field can have a significant impact on the power requirements to access and sustain the H-mode. In this respect, applying resonant fields of the magnitude required to suppress ELMs are found to have the largest effects on the H-mode threshold power, while non-resonant fields and resonant fields of lower magnitude have no sizeable effect [21, 425 - 429]. Thus, the application of 3-D fields for ELM control can have a significant impact on the plasma behaviour in the transient phases from L- to H-mode and vice-versa, with the potential for preventing access to H-mode altogether, if not properly optimized. In this respect, and on the basis of the experimental evidence, for ITER two strategies have been conceived: (a) the first is to apply 3-D fields optimized for ELM control either at a low level, or not to apply them at all, in the L- to H-mode access phase and, once the plasma is in H-mode, to ramp their magnitude to the desired value for ELM suppression; this exploits the relatively long time scale for the pedestal pressure build-up expected in ITER (~1 s) compared to the time to establish the 3-D fields (50 ms); (b) the second strategy is to apply the 3-D fields at the required magnitude for ELM control, but with a de-optimized spectrum for this purpose, and once the plasma is in H-mode to change to the optimum spectrum. For the H- to L-mode transition phase, similar strategies could be applied. R&D is required to identify the optimum approach to switching on and off the 3-D fields for ELM control in the H-mode access and exit phases, with the objective to ensure smooth transitions without large type-I ELMs.

Regarding H-mode phases with varying plasma current, the issue concerns the sustainment of the optimum spectrum for ELM control in such phases since it depends on q_{95} and this varies strongly during such phases. It is, therefore, necessary to ensure that the applied 3-D fields remain within the resonant windows for which ELM control can be maintained as q_{95} varies. Technically, this will be easier in ITER than in present experiments due to the long timescales for plasma processes with respect to that for applying 3-D fields, unless a high degree of spectrum optimization is required for the varying q_{95}. In addition, for the ramp-down phase, the elongation of ITER plasmas will be reduced to maintain vertical stability. This decreases the effectiveness of the contribution of the upper row of ELMCC to the resonant field formation. R&D is required to understand the optimization of the 3-D spectrum for ELM control for varying q_{95} phases, both concerning the alignment of the perturbation to the edge magnetic field (perturbation poloidal spectrum) [422] and in the determination of the parameter space over which the resonant condition is achieved (error in the perturbation poloidal spectrum) [430 431]. In addition, studies in which the plasma shape is changed are required to determine how to optimize the applied 3-D fields as the upper row of coils becomes ineffective in the plasma current ramp-down phase, along the lines of the initial findings in [432].

5.12.3 Impurity exhaust with 3-D fields

Efficient impurity exhaust from the core plasma is commonly observed when 3-D fields are applied [433 - 435]. This allows the sustainment of H-mode plasmas with low concentrations of W in the core, even in conditions for which density pump-out is very large. These, post pump-out, low density conditions have a high divertor plasma temperature which produces a sputtering source of W in the divertor [434, 435]. While the empirical extrapolation of these results to ITER is very favourable with regards to helium exhaust and intrinsic and extrinsic impurity control, whether the observed impurity exhaust can be extrapolated to ITER on a purely empirical basis must still be understood. Several factors can potentially lead to the increased impurity exhaust by 3-D fields applied for ELM control in current experiments: 1) increased impurity screening at the plasma edge and divertor because of the associated 3-dimensional plasma structure, with ergodic field lines [60] created by the 3-D fields (see section 5.12.5); 2) improved impurity screening due to the influence of changes in the edge density and temperature profiles caused by the density pump-out; 3) improved screening at the pedestal because of the modified edge electric field as a result of particle orbits in the 3-D fields causing a stronger neoclassical screening [436]; 4) the increase of outwards edge turbulent transport [437, 438]. Depending on the dominant mechanism, the observed behaviour in present experiments may, or may not, be directly extrapolated to ITER. For example, if the effects are mostly due to changes in pedestal density and temperature profiles, these will be of no relevance to high-Q operation in ITER since the density and temperature at the pedestal will need to remain in a narrow range of values, even when 3-D fields are applied for ELM control, to ensure that the required value of Q can be sustained. R&D is, thus, required to determine which the leading physics mechanism causing the improved impurity exhaust in present experiments is, so that physics-based quantitative evaluations of impurity exhaust can be performed for ITER.

5.12.4 Compatibility of ELM suppression with high density and pellet fuelling

The achievement of ELM suppression is observed to be limited to a range of densities in present experiments, with the upper limit typically lower than 60% of the Greenwald density [434, 435, 439]. Increasing this density beyond this value, by either gas or pellet fuelling, leads to the return of mitigated ELMs [421, 434, 440, 441]. If ELM suppression in ITER were to be restricted to the range of densities reported from present experiments, this would not be suitable for high-Q operation. From the ITER reference operation scenarios, only the 15 MA scenario at $\langle n_e \rangle \sim 0.5 \times n_{GW}$ with $Q = 5$ [66] would be compatible with ELM suppression, if the present results are extrapolated purely on an empirical basis. On the other hand, the physics of the density limitation for ELM suppression remains uncertain and it is, therefore, not clear whether this will be applicable to ITER. In the initial experiments on ELM suppression, this density limitation was attributed to a pedestal collisionality limit, rather than to a density limit and, thus, implied no such limitation on ELM suppression in ITER [442], since pedestal collisionality in ITER H-modes is very low. Later experiments showed this picture to be oversimplified and the limit to be linked to density, and not to collisionality as such [434, 435, 439]. However, the physics processes that determine this limit are not yet fully understood. Some experiments and modelling indicate that the penetration of the applied 3-D fields for ELM control at the plasma edge may play a leading role in ELM suppression [430, 439]. On this basis, access to ELM suppression for the nominal parameters of the $Q = 10$ scenario is expected for the nominal plasma density, $\langle n_e \rangle \sim 0.9 \times n_{GW}$ [431, 443]. Other experiments indicate that the density limitation is associated with increased edge turbulent transport caused by 3-D fields being insufficiently strong to compensate for the increased edge source at higher densities [438], which leads to the triggering of ELMs. Therefore, focused R&D is required to understand the physics processes that determine the limit in density for ELM suppression and how such a limit extrapolates to ITER pedestal plasma conditions.

Independent of the issue above, fuelling of ITER H-mode plasmas will rely on pellet fuelling because gas fuelling is ineffective in providing a core particle source in ITER [66, 302]. Pellet fuelling will also be required to compensate the potential density pump-out that may occur in ITER due to enhanced edge transport resulting from the edge ergodic field [60], enhanced turbulence [437, 438] or neoclassical effects [444]. The injection of pellets in H-mode plasmas is found to trigger growth of MHD modes due to local modification to the pressure profile. When this modification is of sufficient intensity, it can grow non-linearly and lead to the triggering of ELMs. Modelling of ITER plasmas shows that pellets of the size used for fuelling are expected to trigger ELMs when 3-D fields are not applied [141]. If this applies to ELM suppressed H-modes in ITER, it can potentially lead to the triggering of ELMs for each fuelling pellet injected. Such ELMs can cause power loads that can melt the tungsten divertor for high-Q operation [75]. Present experiments have demonstrated that, for some plasma conditions, ELM suppression can be maintained following the injection of pellets [421, 440], as shown in figure 60. For such experiments, low frequency pellet injection is applied to ensure that the plasma density remains under the values required to maintain ELM suppression. The injection of pellets leads to MHD and power load transients in these ELM suppressed H-modes, but with different characteristics from those of ELMs, as originally identified in initial experiments [445]. R&D is, therefore, required to understand if ELM suppression will be compatible with pellet fuelling in ITER and how to optimize the pellet injection characteristics (size, velocity and injection location), together

with the applied 3-D field spectrum and magnitude, to ensure an efficient fuelling of the plasma while maintaining ELM suppression. Similarly, the characterization of the power and particle fluxes to PFCs following pellet injection in suppressed ELM regimes (e.g., time and spatial resolution) is necessary to determine their characteristics in ITER. These fluxes may need to be taken into account in the optimization of pellet fuelling if they approach material degradation limits (melting, cracking), or if impurity generation in such events reaches levels detrimental to the sustainment of H-mode plasmas in ITER.

5.12.5 Radiative divertor operation with 3-D fields

A critical aspect of ITER operation, especially for later phases of the Research Plan when the heat load on the divertor targets is expected to exceed the engineering design load of 10 MWm^{-2}, is the ability to access and sustain radiative divertor operational scenarios. It has long been established (see [45, 446] and references therein] that the preferred means to avoid high heat loads on the divertor targets in ITER will be through partial divertor plasma detachment by means of impurity puffing. Extensive research, both experimental and computational, has been performed, and is still being undertaken, on the topic of detached plasmas. Questions arise as to the nature and quantity of the radiating impurity (or mixture of impurities) that could be used, the best injection location for these impurities, the location of the radiation front, and the compatibility of the radiating divertor scenarios with core confinement requirements and pumping of He ash. However, most of the existing research has been restricted to toroidally symmetric cases, in which the power and particle load pattern on the divertor targets is toroidally uniform. When applying 3-D fields for ELM control, the power deposition pattern on the divertors splits into several lobes with a distinct 3-D structure and varying connection lengths to the core plasma from whence energetic particles will flow. This poses specific challenges to divertor power exhaust and may lead to different optimization of plasma conditions to achieve radiative divertor operation than those evaluated for 2-D conditions.

For example, achievement of detached divertor conditions near the plasma separatrix does not automatically ensure that divertor power loads will remain under power handling limits across the divertor. This is due to 3-D effects leading to different behaviour of the plasma near the separatrix (nearly toroidally symmetric) and in the lobes (toroidally asymmetric), as originally identified in [449] and reproduced by modelling for ITER [61], shown in figure 61. ITER modelling [62] and current experiments [421] indicate that the edge ergodic magnetic field structure plays a key role in the achievement of high density, low temperature plasma conditions across the divertor (near the separatrix and in the lobes). A narrower penetration of ergodic field lines into the confined plasma favours a behaviour of power fluxes closer to that of 2-D divertors when plasma density is increased [421], as shown in figure 62.

In addition to its impact on the plasma density to access radiative divertor conditions, the 3-D field structure can also impact the optimization of the impurity species and fuelling rates required to increase divertor radiation, which may be different from those adopted for 2-D plasmas (see section 5.3.2.2). In this respect, modelling shows that 3-D fields significantly impact plasma flow [60] and, thus, impurity entrainment in the divertor differs from that modelled for 2-D plasma configurations. This can influence both the optimum impurity species for effective radiation (due to impurity entrainment in the divertor) and the role of device size in such optimization, which can differ from that evaluated for 2-D divertors [51, 448].The higher temperatures and lower

densities found in the lobes compared to those at the separatrix may also require the use of impurity mixes to achieve highly radiating divertor conditions in ITER when 3-D fields are applied: medium-*Z* impurities, such as neon, are not found to be an effective radiator in the lobes for ITER, at least for PFPO-1 H-modes [62].

Dedicated experimental and modelling R&D is, therefore, required to understand the physics determining the power fluxes to plasma facing components when 3-D fields are applied for ELM control, their relation to the 3-D magnetic field structure and their impact on impurity dynamics. This will allow the development of a basis to optimize the applied 3-D fields to achieve both ELM control and satisfactory divertor power exhaust in ITER. This is particularly challenging for ITER high-*Q* scenarios, where transient loads during ELMs and stationary loads between ELMs both challenge the power handling capabilities of the ITER divertor PFCs. It should be noted that, if it is not possible to achieve a 3-D radiative divertor which reduces power loads at both the separatrix and the lobes, an alternative solution to the power flux handling problem with 3-D fields does exist in ITER. This relies on the rotation of the 3-D structure by a periodic variation of the current in the ELMCC with frequencies of several Hz, which is sufficient to reduce the average power flux in the divertor lobes to under 10 MWm^{-2} [63]. While this is technically viable and considered for the ELMCC design in ITER, it implies a high number of stress cycles for these coils. Therefore, its use should be restricted as far as possible to maintain an adequate lifetime for these coils to support the scientific exploitation foreseen in the Research Plan.

5.12.6 Impact of 3-D fields for ELM control on fast particle losses

The application of 3-D fields for ELM control is found to lead to increased fast ion losses from NBI in present experiments [449 - 452]. Such losses can potentially decrease the heating efficiency of ITER H&CD schemes, as well as that of the α-particles, and cause localized power fluxes to PFCs. Initial studies for ITER showed that the effect of 3-D fields on fast particle losses was larger for NBI than for other schemes that are associated with fast ion generation in the core plasma (ICRF and α-particles), since NBI particles enter from the plasma edge [453, 454]. The effects associated with such fast particle losses could be substantial and lead to high power fluxes in the under-dome structure of the divertor [455]. Later studies using a more appropriate representation of the 3-D magnetic field structure [218, 456], namely including plasma response (unlike the calculations in [453, 454]), showed that such losses and power fluxes persist, but at much lower amplitude as illustrated in figure 30.

The losses of fast ions and localized power fluxes caused by 3-D fields are due to two effects: (a) the trajectories of the ions in the 3-D fields themselves and the associated issues for trapped and passing particles in the field wells created; and (b) the formation of an edge ergodic layer that allows fast ions to reach spatial positions not accessible within the usual tokamak closed magnetic surfaces. Studies have been launched to optimize ELM suppression in ITER while reducing to a minimum the associated fast particle losses (especially from NBI) and ensuing localized power fluxes. Initial modelling for ITER $Q = 10$ plasmas ([219]) shows that there is significant margin to optimize the fast particle losses by adjusting the 3-D field spectrum in configurations that should provide a similar level of ELM control, as illustrated in figure 63. This includes the optimum absolute phase of the perturbation with respect to the location of the NBI injection ports in ITER, as well the poloidal spectrum of the applied 3-D field.

Experimental and modelling R&D along the lines of [219] is required to determine how to optimize the applied 3-D field to minimize fast particle losses while maintaining the required level of ELM control. This requires detailed experimental measurements of fast particle losses, localized power fluxes and of the magnetic field structure (including plasma response), supported by extensive modelling. The experiments and associated modelling should consider plasma conditions that are relevant to the foreseen scenarios in the IRP (especially the high-Q scenarios). The validated models will be then used to optimize the application of ELM control by 3-D fields in ITER as well as to define further experiments to validate these optimization strategies in advance of high-Q operation in ITER.

5.13 Long-pulse and enhanced confinement scenarios

5.13.1 Enhanced confinement and role of fast particles, toroidal rotation, pedestal-core feedback, core fuelling and effective ion heating

Long pulse operation (1000 s burn) and steady-state ITER scenarios with $Q \geq 5$ and $I_p \leq 13.5$ MA rely on access to confinement regimes with $H_{98} > 1$ [200, 211, 457]. Common features to the long pulse scenarios, including steady-state operation [185] in ITER, are:

- Flat or weakly reversed q-profiles in the central part of the plasma with $q_{min} > 1$;
- Large contribution of fast particle pressure to the central plasma pressure;
- High toroidal rotation in absolute value, but moderate when normalized to the Mach number.

Plasmas meeting the energy confinement required for long pulse and steady-state operation are obtained in present experiments [458 - 461], but the empirical extrapolation of these results to ITER remains questionable as discussed below. Some open questions concern both the long pulse and steady-state scenarios while others are specific to only one. For example, understanding the mechanisms that modify current diffusion in some present experiments [462, 463], but not in others [180, 463], is required to achieve stationary operation with relaxed current profiles in long pulses [464]. On the other hand, fine control of the current profile is required to ensure MHD stability for steady-state plasmas [185] and specific experimental and modelling R&D is required to address such issues.

Present experiments show that a large fast particle content, high toroidal plasma rotation, increased MHD edge pedestal stability, core fuelling and central ion heating play an important role in achieving plasmas with high energy confinement. Fast particles are found to have a significant effect on plasma confinement by their direct effect on plasma turbulent transport (increased Shafranov shift, dilution of thermal ions, etc.) and through the MHD instabilities that fast particles can trigger [419, 420]. Understanding the relevant physics processes in detail is required to determine what will be the impact of fast particles in ITER, since the positive impact of fast particles on thermal transport may be compensated by increased fast particle diffusion due to overlapping AEs, leading to a less effective plasma heating [187].

Plasma turbulent transport is predicted to be reduced by the toroidal velocity shear. Turbulent transport modelling predicts that the torque provided by NBI heating, with the boundary conditions determined by intrinsic torque, can create a large enough sheared rotation to reduce turbulent transport noticeably, even for $Q = 10$ baseline plasmas with a high density [465, 466]. These predicted values are in good agreement with simple modelling of plasma momentum [90,

467] combined with empirical assumptions [468. For long pulse and steady-state plasma scenarios, the absolute toroidal rotation level is expected to be higher than for $Q = 10$ baseline scenario, since plasma density is lower while momentum confinement is expected to be similar. This has the potential to significantly reduce anomalous transport in these plasma scenarios. Indeed, correlation of energy confinement improvement with increasing shear of toroidal rotation is reported in many tokamak experiments [181, 465, 469]. However, it is not clearly understood whether such effects will eventually play a role in ITER. In contrast to present experiments, in which NBI systems provide strong ion heating and a toroidal momentum source, NBI in ITER provides a momentum source similar to that in present tokamaks (somewhat lower because of the higher beam energy), resulting in low normalized torque and predominantly electron heating. Since confinement is better in ITER than in present devices, a high absolute rotation level is found in ITER plasmas, similar to JET, but, due to ITER's larger size and higher plasma temperature, this results in a lower normalized toroidal rotation ($\Omega = V_{tor}/R$ and Mach number = V_{tor}/C_s, with Ω the toroidal angular rotation frequency, V_{tor} the toroidal rotation velocity and C_s the ion sound speed). Experimental and modelling studies are required to determine the physics basis for the impact of rotation in ITER-like plasma conditions namely, with high electron and ion temperatures, significant electron heating and at comparable V_{tor} and Mach numbers for the toroidal plasma flow.

The magnitude of the pedestal pressure is expected to have a major impact on ITER confinement, so that the fusion gain increases significantly with pedestal pressure [226]. In particular, a high pedestal pressure is essential to achieve high confinement long pulse and steady-state plasma scenarios in ITER. Reduced anomalous transport and a high fast particle pressure increase the core plasma pressure and, thus, the Shafranov shift. This in turn increases the pedestal pressure range that can be sustained in MHD stable equilibria and improves plasma confinement. This positive feedback loop has been found to play a critical role in the access to high confinement in present experiments [208]. However, it is not clear if such a feedback loop will be effective in ITER high-Q plasmas. This is due to the different pedestal density/temperature structure in ITER plasmas compared to present experiments. As discussed in section 5.3.2.3, edge neutral opacity in ITER leads to relatively shallow gradients in the ITER pedestal, which, in turn, impacts the level of bootstrap current driven by a given pressure gradient and the limiting MHD instability for a given value of the pedestal pressure (a dominantly peeling instability versus a dominantly ballooning one). This may lead to a different core-pedestal stability-confinement feedback loop, particularly for long pulse/steady-state scenarios in ITER [470]. These different physics processes in the core-pedestal feedback loop impact the expected increase of overall confinement in ITER plasmas. Further R&D is required to investigate the core-pedestal stability-confinement feedback loop in conditions as close as possible to those in ITER, namely with pedestal plasmas at low collisionality and with low density gradients, to understand if the high levels of energy confinement observed in present experiments, where this mechanism plays an important role, will be achievable in ITER.

Enhanced confinement plasmas in present experiments are largely NBI dominated at low densities and have effective core fuelling and ion heating, leading to peaked density/pressure profiles and ion temperatures higher than the electron temperature in the central plasma region. While density profiles are expected to be peaked in ITER, due to anomalous transport processes

[471], they are not expected to be as peaked as those in present experiments, since the NBI particle source is a significant contribution to density peaking in present experiments at low collisionalities [472, 473]. Similarly, although ion heating is expected to increase for $Q \geq 5$ long pulse operation/steady state plasmas in ITER compared to $Q \geq 10$ inductive baseline plasmas, because of the higher plasma temperatures, overall, high-Q ITER plasmas remain electron heating dominated, unlike present experiments with enhanced confinement. R&D is required to understand to which degree core density peaking and ion heating play a role in the observed increased confinement and, thus, what are the expectations associated with these factors for ITER.

5.13.2 ELM suppression in high-q_{95}/high-β_N plasmas and edge-core compatibility issues

In addition to requiring greater than conventional H-mode energy confinement, long pulse and steady-state plasma scenarios in ITER pose specific challenges regarding ELM control and edge-core compatibility issues. In relation to the latter, the main issue is to achieve acceptable divertor power loads, since the edge power outflux for $Q \geq 5$ scenario plasmas is similar to that for $Q \geq 10$ plasmas, while the plasma density is significantly lower (by up to a factor of 2 for steady-state plasmas) [185]. This implies a more demanding optimization of the radiation by impurities, as well as the associated plasma contamination, since lower density operation requires a higher density of impurities at the divertor to radiate the same amount of power. How much more challenging this optimization is compared to that for $Q \geq 10$ plasmas remains an open issue, since specific physics effects can favour this integration for $Q \geq 5$ plasmas despite the lower densities. The first physics factor is the high pedestal temperature expected in $Q \geq 5$ plasmas in ITER [185] which, together with the low density, provides a higher impurity neoclassical screening in the pedestal than for $Q \geq 10$ plasmas. A second factor concerns the edge transport level, which, in H-modes, is expected to scale as $1/I_p$ [39, 40] and the longer connection lengths, which should provide a wider e-folding length for the edge power flow, thus decreasing the divertor power flux compared to $Q \geq 10$ plasmas. It should be noted, however, that this higher edge transport level at lower I_p may not apply in ITER if edge transport is dominated by different turbulence mechanisms from those in present experiments, as found in modelling studies [41, 42]. In that case, the level of edge transport would be lower for long pulse/steady-state $Q \geq 5$ scenario plasmas than for inductive $Q \geq 10$ plasmas at 15 MA, which would exacerbate the divertor power dissipation issue, as discussed above. Experimental and modelling R&D is, thus, required to address the specific aspects of radiative divertor operation in ITER-like $q_{95} = 3.5$ - 5.0 scenarios with enhanced confinement to assess its optimization in comparison with that of $q_{95} = 3$ conventional H-modes.

ELM control for long pulse/steady-state $Q \geq 5$ plasmas also exhibits some specificities which, in this case, may be qualitatively different for steady-state plasmas. Higher q_{95} operation implies that the poloidal spectrum of the 3-D fields for ELM control needs to be optimized in a different way from that for $q_{95} = 3$ to stay aligned with the edge magnetic field lines. The variation of the optimum spectrum with q_{95}, which is obtained by varying the relative phase of the current waveforms in the three rows of ELMCC, is smooth in the range of $q_{95} = 3$ - 5. However, rapid changes can appear around the q_{95} values foreseen for steady-state operation [422], which may pose specific challenges to maintain the required level of ELM control. In fact, the modelled impact of 3-D fields on pedestal behaviour is found to be different for $Q \geq 10$ plasmas at 15 MA from that foreseen for steady-state operation with $Q \geq 5$ at 10 MA, due to the much larger

normalized pressure in the latter and its impact in amplifying the plasma response to the applied 3-D fields. While 'conventional ELM suppression' is modelled to occur for $Q \geq 10$, for $Q \geq 5$ steady-state plasmas a 'QH-mode like' behaviour is obtained when 3-D fields for ELM control are applied [434]. Similarly, a low density pump-out by ELM suppression is predicted for $Q \geq 10$ plasmas at 15 MA, while this is much larger for $Q \geq 5$ at 10 MA [413]. Experiments have shown that the higher β, at the level required for long pulse/steady-state scenarios in ITER, impacts the plasma response to 3-D fields and introduces differences in ELM control behaviour compared to that in conventional lower q_{95} H-modes. The impact of ELM control on plasma confinement is also different for high-β/high-q_{95} plasmas [460, 474]. ELM control has a negligible impact on energy confinement for high-β/high-q_{95} plasmas [460, 474], which is a very positive aspect for ITER $Q \geq 5$ long pulse/steady-state scenarios, if the same physics processes apply. Further experimental R&D in a range of tokamaks and supporting modelling are required to optimize ELM control for long pulse/steady-state scenarios, including possible effects on edge pressure and energy confinement. In this respect, as discussed in section 5.13.1, understanding the impact of ELM control on pedestal pressure is critical, since access to the high energy confinement required for long pulse/steady-state scenarios is based on the positive feedback loop between core confinement and edge stability, and this may be more limited when ELM control is applied.

6. Conclusions and Perspectives

The ITER Research Plan (IRP) provides a guide to the overall research activities to be undertaken within the framework of the ITER Project, including physics and technology research, to achieve the Project's goals. In the version described in this paper the focus is on physics R&D and on the R&D and testing program of the (tritium breeding) Test Blanket Modules (TBM) consistent with the Staged Approach. As the project evolves, the IRP will be updated in order to provide a complete overview of the research scope and plans of the project in all the physics and technology areas addressed by the ITER program.

The IRP defines the objectives of each operational phase within the Staged Approach and outlines the detailed experimental strategy to achieve the first set of Project objectives in a time-effective way, proceeding from First Plasma to the demonstration of ITER's three high-Q reference operational scenarios and the TBM Program goals: (a) $Q = 10$ inductive scenarios with burn length 300 - 500 s, (b) $Q = 5$ long pulse scenario with 1000 s burn, (c) $Q = 5$ steady-state scenario with 3000 s burn, and (d) to provide experimental tests of prototype tritium breeding modules which would inform the design, manufacture and operation of DEMO breeding blankets. In addition, the IRP identifies the risks of the proposed experimental strategy for each phase, mitigation measures and options for taking the research program forward if such risks materialize. These mitigation measures and options include both operational and experimental aspects, as well as planning and implementation of upgrades of ITER systems, within the capabilities of the design of the ITER tokamak and its ancillary systems.

The achievement of the first set of IRP objectives described in (a) to (d) above requires a total of six experimental campaigns (FP+EO, PFPO-1, PFPO-2, FPO-1 through to FPO-3), of which half are performed in H/He plasmas and the other half in D and DT plasmas. The major objectives and activities foreseen for each phase are:

- First Plasma (FP): achievement of the First Plasma milestone of plasma breakdown in hydrogen or helium with at least 100 kA of plasma current for at least 100 ms; during the subsequent Engineering Operation phase commissioning of the Magnet systems to full current will take place;
- Pre-Fusion Power Operation 1 (PFPO-1): extensive 'commissioning with plasma' activities to establish diverted plasma operation in hydrogen/helium in L-mode up to at least 7.5 MA/5.3 T with ECRH power of up to 20 MW. This is supported by a commissioning program for plasma control, diagnostics and ECRH, together with the systematic development of a disruption management/ mitigation capability to prepare for operation at higher currents. H-mode access and sustainment at toroidal fields of up to 2.65 T, supported by ECRH, will be also explored;
- Pre-Fusion Power Operation 2 (PFPO-2): commissioning of the HNB, DNB and ICRF heating systems to full power, together with the necessary plasma control capability, to support the subsequent program. The plasma scenarios to be demonstrated include: (a) H-mode operation in hydrogen up to, at least, 7.5 MA/2.65 T, incorporating reliable ELM control and divertor heat flux control, with helium as back-up should H-modes prove unsustainable in hydrogen plasmas; and, (b) L-mode operation to demonstrate the full technical capability of the device (i.e., operation at 15 MA/5.3 T). In this campaign systematic studies of plasma-wall interactions and issues such as erosion of plasma-facing components, redeposition, dust production, fuel retention and fuel removal would also be pursued in preparation for the nuclear phase of operation;
- Fusion Power Operation (FPO) up to FPO-3: the initial aim of the first campaign is to demonstrate operation of high-power H-modes in deuterium to prepare plasma scenarios for DT operation. Beginning with trace tritium experiments, a gradual transition to full DT operation would be undertaken as the fuel reprocessing throughput of the Tritium Plant increases. The goal of the first campaign of DT operation is the demonstration of fusion power production of several hundred MW for at least 50 s at $Q \geq 5$. In subsequent experimental campaigns, the fusion gain will be optimized to achieve $Q \geq 10$, and the pulse duration in inductive plasma scenarios would be extended towards the target range of 300 - 500 s burn required by the ITER *Project Specification*; hybrid and fully non-inductive scenarios will also be developed to achieve burn durations in the range 1000 - 3000 s with $Q \sim 5$;
- Fusion Power Operation (FPO) from FPO-4 onwards: Following the achievement of the first set of IRP objectives, the Research Plan is foreseen to evolve into a DEMO-focused programme leading also to the demonstration of the average first wall neutron fluence goal of 0.3 MW.yr.m^{-2} defined in the *Project Specificatio*n. The details of the R&D programme in this phase cannot be defined at this stage, but it is likely to require specific upgrades, which can be accommodated by the design, relating to, e.g., H&CD, fuelling systems, TBMs, divertor, first wall, etc.

The plan for each of the phases is based on a series of key research issues around which an experimental program has been developed to commission systems with plasma, to develop certain control capabilities, to establish specific plasma scenarios, to address uncertainties in the physics of plasmas at the ITER scale and in the burning plasma regime, and finally to perform detailed

scientific studies of burning plasmas while optimizing their fusion performance. The details of the later phases of the IRP are, obviously, subject to larger uncertainties, since the results derived from earlier phases are expected to dominate the final planning of subsequent phases and, in addition, ITER is the first experiment which will provide access to the study of burning plasmas.

Much can be learned about the behaviour of fusion plasmas at the ITER scale from the initial experiments in hydrogen and helium plasmas presented in earlier sections. However, the overarching goal of the ITER project is the production of several hundred MW of fusion power at high fusion gain in long pulse operation to: (i) allow the detailed study of the physics processes determining the behaviour of burning plasmas and (ii) to provide the physics basis for the design and operation of DEMO-class fusion reactors. The testing of prototype tritium breeder modules (and of much of the reactor-relevant technology incorporated in ITER) is a key complementary aspect (and benefit) of these physics goals which responds to the technical goals of the ITER mission statement. To ensure the success of the initial phases of the IRP, supporting a rapid transition to DT plasma operation with high fusion power production, it is critical to continue the refinement of the physics basis for ITER operation by pursuing the R&D activities outlined in section 5, making use of the current fusion facilities. The R&D needs discussed in the previous section are considered as a ‘risk mitigation’ strategy in preparation for ITER operation: continued studies to address the physics and control issues developed in section 5 can make a significant contribution to the successful implementation of the IRP and to the production of high fusion power on the foreseen timescale.

As the project moves towards the Operations Phase, it is essential to maintain a regular review of the ITER Research Plan, as results from the accompanying R&D program and, later, from the experimental exploitation of ITER itself, become available. The IRP is thus to be viewed as a living document that evolves with the project. In addition, the IRP serves as a baseline from which the consequences of design or planning changes, or of unforeseen events, on the achievement of the ITER mission can be determined.

Acknowledgements

We wish like to acknowledge the many colleagues in the ITER Organization, Domestic Agencies and in the international fusion research community, particularly the participants in the International Tokamak Physics Activity, for numerous enlightening discussions on ITER system capabilities and on current progress in fusion physics research, which provided invaluable support to the development of the ITER Research Plan.

ITER is the Nuclear Facility INB-54. This publication is provided for scientific purposes only. The ITER Organization as nuclear operator is not constrained by the information presented here. The views and opinions expressed herein do not necessarily reflect those of the ITER Organization.

References

[1]ITER Technical Basis 2002 ITER EDA Documentation Series No. 24, IAEA, Vienna

[2]Bigot B. 2019 *Nucl. Fusion* **59** 112001

[3]ITER Organization 2018 ITER Research Plan within the staged approach (Level III—provisional version) *ITER Technical Report* ITR-18-003 (www.iter.org/technical-reports)

[4]Van Houtte D., Okayama K. and Sagot F. 2010 *Fusion Eng. Des.* **85** 1220

[5]ITER Physics Basis Editors *et al* 1999 *Nucl. Fusion* **39** 2137 (and subsequent articles in this issue)

[6]Progress in ITER Physics Basis Editors *et al* 2007 *Nucl. Fusion* **47 S1** (and subsequent articles in this issue)

[7]Connor J.W. and Wilson H.R. 2000 *Plasma Phys. Control. Fusion* **42** R1

[8]Bourdelle C. 2020 *Nucl. Fusion* **60** 102002

[9]Martin Y.R. *et al* 2008 *J. of Phys. Conf. Series* **123** 012033

[10] Righi E. *et al* 1999 *Nucl. Fusion* **39** 309

[11] McDonald D.C. *et al* 2004 *Plasma Phys. Control. Fusion* **46** 519

[12] Ryter F. *et al* 2009 *Nucl. Fusion* **49** 062003

[13] Gohil P. *et al* 2012 Assessment of the H-mode Power Threshold Requirements for ITER *Preprint: 2012 IAEA Fusion Energy Conf. (San Diego, USA, 8-13 October 2012)* [ITR/P1-36]

[14] Ryter F. *et al* 2013 *Nucl. Fusion* **53** 113003

[15] Hillesheim J.C. *et al* 2016 Role of Stationary Zonal Flows and Momentum Transport for L-H Transitions in JET *Preprint: 2016 IAEA Fusion Energy Conf. (Kyoto, Japan, 17-22 October 2016)* [EX/5-2]

[16] Schmitz L. *et al* 2022 *Nucl. Fusion* **62** 126050

[17] Plank U. *et al* 2020 *Nucl. Fusion* **60** 074001

[18] Ryter F. *et al* 2014 *Nucl. Fusion* **54** 083003

[19] Andrew Y. *et al* 2008 *Plasma Phys. Control. Fusion* **50** 124053

[20] Tobita K. *et al* 1995 *Nucl. Fusion* **35** 1585

[21] Gohil P. *et al* 2011 *Nucl. Fusion* **51** 103020

[22] JET Team 1993 *Plasma Physics and Controlled Nuclear Fusion Research 1992 (Proc. 14th Int. Conf., Würzburg, 1992)* Vol 1, IAEA, Vienna 429

[23] Urano H. *et al* 2011 *Nucl. Fusion* **51** 113004

[24] Delabie E. *et al* 2015 *42nd European Physical Society Conf. on Plasma Physics (EPS) (Lisbon, Portugal, 22-26 June 2015)* ECA vol. 39E O3.113 (http://ocs.ciemat.es/EPS2015ABS/pdf/O3.113.pdf)

[25] Horton L.D. *et al* 1999 *Nucl. Fusion* **39** 17

[26] Ma Y. *et al* 2012 *Nucl. Fusion* **52** 23010

[27] Maggi C.F. *et al* 2012 *39th European Physical Society Conf. on Plasma Physics (EPS) (Stockholm, Sweden, 2-6 July 2012)* ECA vol. 36F O3.108 (http://ocs.ciemat.es/epsicpp2012pap/pdf/O3.108.pdf)

[28] Neu R. *et al* 2013 *J. Nucl. Mater.* **438** S34

[29] Takizuka T. *et al* 2004 *Plasma Phys. Control. Fusion* **46 A**227

[30] Bourdelle C. *et al* 2014 *Nucl. Fusion* **54** 022001

[31] Maggi C.F. *et al* 2014 *Nucl. Fusion* **54** 023007
[32] McKee G.R. et al 2009 Nucl. Fusion **49** 115016
[33] Schneider, M. *et al* 2019 *Nucl. Fusion* **59** 126014
[34] Loarte, A. *et al* 2021 *Nucl. Fusion* **61** 076012
[35] Hakola A. *et al* 2017 *Nucl. Fusion* **57** 066105
[36] Loarte A. *et al* 2000 *Contrib. Plasma Phys.* **40** 508
[37] Pitts R.A. *et al* 2003 *J. Nucl. Mater.* **313-316** 777
[38] Wischmeier M. *et al* 2003 *J. Nucl. Mater.* **313-316** 980
[39] Eich T. *et al* 2013 *Nucl. Fusion* **53** 093031
[40] Goldston R.J. 2012 *Nucl. Fusion* **52** 013009
[41] Chang C.S. *et al* 2017 *Nucl. Fusion* **57** 116023
[42] Chang C.S. *et al* 2021 *Phys. Plasmas* **28** 022501
[43] Xu X.Q. *et al* 2019 *Nucl. Fusion* **59** 126039
[44] Park J.S., Bonnin X. and Pitts R.A. 2021 *Nucl. Fusion* **61** 016021
[45] Pitts R.A. *et al* 2019 *Nucl. Mater. Energy* **20** 100696
[46] Krasheninnikov S.I., Kukushkin A.S. and Pshenov A.A. 2016 *Phys. Plasmas* **23** 055602
[47] Leonard A.W. 2018 *Plasma Phys. Contr. Fusion* **60** 044001
[48] Kallenbach A. *et al* 2010 *Plasma Phys. Control. Fusion* **52** 055002
[49] Kallenbach A. *et al* 2012 *Nucl. Fusion* **52** 122003
[50] Giroud C. *et al* 2021 High Performance ITER-Baseline Discharges in Deuterium with Nitrogen and Neon-Seeding in the JET-ILW *Preprint: 2020 IAEA Fusion Energy Conf. (Virtual Event, 10-15 May 2021)* [EX/P3-9]
[51] Rozhansky V. *et al* 2021 *Nucl. Fusion* **61** 126073
[52] Guillemaut C. *et al* 2017 *Plasma Phys. Control. Fusion* **59** 045001
[53] Eldon D. *et al* 2017 *Nucl. Fusion* **57** 066039
[54] Xu G.S. *et al* 2020 *Nucl. Fusion* **60** 086001
[55] Bernert M. *et al* 2021 *Nucl. Fusion* **61** 024001
[56] Ravensbergen T. *et al* 2020 *Nucl. Fusion* **60** 066017
[57] Carralero D. *et al* 2015 *Phys. Rev. Lett.* **115** 215002
[58] Carralero D. *et al* 2017 *Nucl. Mater. Energy* **12** 1189
[59] Garcia O.E. *et al* 2016 *Phys. Plasmas* **23** 052308
[60] Schmitz O. *et al* 2016 *Nucl. Fusion* **56** 066008
[61] Frerichs H. *et al* 2020 *Phys. Rev. Lett.* **125** 155001
[62] Frerichs H. *et al* 2021 *Nucl. Fusion* **61** 126027
[63] Loarte A. *et al* 2014 *Nucl. Fusion* **54** 033007
[64] Eich T. *et al* 2017 *Nucl. Mater. Energy* **12** 84
[65] Gunn J.P. *et al* 2017 *Nucl. Mater. Energy* **12** 75
[66] Polevoi A.R. *et al* 2018 *Nucl. Fusion* **58** 056020
[67] Dux R. *et al* 2014 *Plasma Phys. Control. Fusion* **56** 124003
[68] van Vugt D. *et al* 2019 *Phys. Plasmas* **26** 042508
[69] Kocan M. *et al* 2015 J. *Nucl. Mater.* **463** 709
[70] Loarte A. *et al* 2008 Power and Particle Fluxes at the Plasma Edge of ITER: Specifications and Physics Basis *Preprint: 2008 IAEA Fusion Energy Conf. (Geneva, Switzeerland, 13-18 October 2008)* [IT/P6-13]

[71] Pintsuk G. *et al* 2015 *Fusion Eng. Des.* **98-99** 1384
[72] Panayotis S. *et al* 2017 *Fusion Eng. Des.* **125** 256
[73] De Temmerman G. *et al* 2018 *Plasma Phys. Control. Fusion* **60** 044018
[74] Pitts R.A. *et al* 2017 *Nucl. Mater. Energy* **12** 60
[75] Gunn J.P. *et al* 2017 *Nucl. Fusion* **57** 046025
[76] Hirai T. *et al* 2018 *Fusion Eng. Des.* **127** 66
[77] Shimada M. and Pitts R.A. 2011 *J. Nucl. Mater.* **415** S1013
[78] Lyssoivan A. *et al* 2012 *Plasma Phys. Control.* Fusion **54** 074014
[79] Kogut D. *et al* 2016 *Phys. Scr.* **2016** 014062
[80] Kwon M. *et al* 2011 *Nucl. Fusion* **51** 094006
[81] Brezinsek S. *et al* 2013 *Nucl. Fusion* **53** 083023
[82] Douai D. *et al* 2016 Development of Helium Electron Cyclotron Wall Conditioning on TCV for the Operation of JT-60SA *Preprint: 2016 IAEA Fusion Energy Conf. (Kyoto, Japan, 17-22 October 2016)* [EX/P8-31]
[83] Wauters T. *et al* 2022 *Phys. Scr.*. **97** 044001
[84] de Vries P.C. *et al* 2016 *Fusion Sci. Technol.* **69** 471
[85] Lehnen M. *et al* 2016 Plasma Disruption Management in ITER *Preprint: 2016 IAEA Fusion Energy Conf. (Kyoto, Japan, 17-22 October 2016)* [EX/P6-39]
[86] Hollmann E.M. *et al* 2015 *Phys. Plasmas* **22** 021802
[87] Lehnen M. *et al* 2015 *J. Nucl. Mater.* **463** 39
[88] de Vries P.C. and Gribov Y. 2019 *Nucl. Fusion* **59** 096043
[89] Kim S.H. *et al* 2017 *Nucl. Fusion* **57** 086021
[90] Singh M.J. *et al* 2017 *New J. Phys.* **19** 055004
[91] Lukash V.E. *et al* 2017 *44th European Physical Society Conf. on Plasma Physics (EPS) (Belfast, United Kingdom, 26-30 June 2017)* ECA vol. 41F P5.152 (http://ocs.ciemat.es/EPS2017PAP/pdf/P5.152.pdf)
[92] Kurki-Suonio T. *et al* 2017 *Plasma Phys. Control. Fusion* **59** 014013
[93] Kazakov Y. *et al* 2018 Recent Advances in ICRF Heating of Mixture Plasmas: Survey of JET and AUG Experiments and Application for JET-DT and ITER *Preprint: 2018 IAEA Fusion Energy Conf. (Gandhinagar, India, 22-27 October 2018)* [EX/8-1]
[94] Jackson G.L. *et al* 2010 *Phys. Plasmas* **17** 056116
[95] Pitts R.A. *et al* 2022 *Nucl. Fusion* **62** 096022
[96] Laqua H.P. *et al* 2021 *Nucl. Fusion* **61** 106005
[97] Goumiri I.R. *et al* 2017 *Phys. Plasmas* **24** 056101
[98] Buttery R.J. *et al* 2000 *Nucl. Fusion* **40** 807
[99] Luxon J.L. *et al* 2003 *Nucl. Fusion* **43** 1813
[100] Lang P.T. *et al* 2004 *Nucl. Fusion* **44** 665
[101] Baylor L.R. *et al* 2013 *Phys. Rev. Lett.* **110** 245001
[102] Degeling A.W. *et al* 2003 *Plasma Phys. Control. Fusion* **45** 1637
[103] Lang P.T. *et al* 2004 *Plasma Phys. Control. Fusion* **46** L31
[104] de la Luna E. *et al* 2010 Effect of ELM mitigation on confinement and divertor heat loads on JET *Preprint: 2010 IAEA Fusion Energy Conf. (Daejeon, Republic of Korea, 11-16 October 2010)* [EXC/8-4]

[105] La Haye R.J. *et al* 2006 *Nucl. Fusion* **46** 451
[106] Maraschek M. *et al* 2007 *Phys. Rev. Lett.* **98** 025005
[107] La Haye R.J., Isayama A. and Marascheck M. 2009 *Nucl. Fusion* **49** 045005
[108] Sauter O. *et al* 2010 *Plasma Phys. Control. Fusion* **52** 025002
[109] Austin M.E. 2011 *Fusion Sci. Technol.* **59** 647
[110] Reich M. *et al* 2012 *Fusion Sci. Technol.* **61** 309
[111] van den Brand H. *et al* 2012 *Plasma Phys. Control. Fusion* **54** 094003
[112] van den Brand H. *et al* 2013 *Nucl. Fusion* **53** 013005
[113] Rapson C. *et al* 2014 *Fusion Eng. Des.* **89** 568
[114] Mück A. *et al* 2005 *Plasma Phys. Control. Fusion* **47** 1633
[115] Graves J.P. *et al* 2005 *Plasma Phys. Control. Fusion* **47** B121
[116] Chapman I.T. *et al* 2007 *Plasma Phys. Control. Fusion* **49** B385
[117] Graves J.P. *et al* 2009 *Phys. Rev. Lett.* **102** 065005
[118] Chapman I.T. *et al* 2009 *Nucl. Fusion* **49** 035006
[119] Goodman T.P. *et al* 2011 *Phys. Rev. Lett.* **106** 245002
[120] Kim D., Goodman T.P. and Sauter O. 2014 *Phys. Plasmas* **21** 061503
[121] Humphreys D.A. *et al* 2015 *Phys. Plasmas* **22** 021806
[122] Raupp G. *et al* 2017 *Fusion Eng. Des.* **123** 541
[123] Treutterer W. *et al* 2017 *Fusion Eng. Des.* **115** 33
[124] Coburn J. *et al* 2022 *Nucl. Fusion* **62** 016001
[125] Mitteau R. *et al* 2011 *J. Nucl. Mater.* **415** S969
[126] Kocan M. *et al* 2015 *Nucl. Fusion* **55** 033019
[127] Nunes I.M. *et al* 2012 Be Tile Power Handling and Main Wall Protecttion *Preprint: 2012 IAEA Fusion Energy Conf. (San Diego, USA, 8-13 October 2012)* [FTP/2-1Rb]
[128] Arnoux G. *et al* 2013 *Nucl. Fusion* **53** 073016
[129] Goldston R.J. 2015 *J. Nucl. Mater.* **463** 397
[130] Horacek J. *et al* 2016 *Plasma Phys. Control. Fusion* **58** 074005
[131] Mitteau R. *et al* 2015 *J. Nucl. Mater.* **463** 411
[132] Pitts R.A. *et al* 2011 *J. Nucl. Mater.* **415** S957
[133] Horacek J. *et al* 2015 *J. Nucl. Mater.* **463** 385
[134] Harris G.R. 1990 Comparisons of the current decay during carbon-bounded and beryllium-bounded disruptions in JET *Report JET-R(90)07, JET, Abingdon*
[135] Reux C. *et al* 2015 *Nucl. Fusion* **55** 093013
[136] Matthews G.F. *et al* 2016 *Phys. Scr.* **2016** 014070
[137] De Temmerman G. *et al* 2017 *Nucl. Mater. Energy* **12** 267
[138] Kolesnikov R.A. *et al* 2013 *Nucl. Fusion* **53** 083021
[139] Polevoi A.R. *et al* 2016 Integrated Simulations of H-Mode Operation including Core Fuelling, Divertor Detachment and ELM Control *Preprint: 2016 IAEA Fusion Energy Conf. (Kyoto, Japan, 17-22 October 2016)* [EX/P6-44]
[140] Gribov Y. *et al* 2015 *Nucl. Fusion* **55** 073021
[141] Futatani S. *et al* 2014 *Nucl. Fusion* **54** 073008
[142] de Vries P.C. *et al* 2016 Multimachine Analysis of Termination Scenarios, Providing the Specifications for Controlled Shutdown of ITER Discharges *Preprint: 2016 IAEA Fusion Energy Conf. (Kyoto, Japan, 17-22 October 2016)* [EX/P6-41]

[143] Köchl F. *et al* 2016 Evolution and Control of Tungsten Transport in the Termination Phase of JET H-Mode Discharges and Implications for ITER *Preprint: 2016 IAEA Fusion Energy Conf. (Kyoto, Japan, 17-22 October 2016)* [EX/P6-15]
[144] Goldston R.J. 2011 *Nucl. Fusion* **52** 013009
[145] Baylor L.R. *et al* 2015 Pellet injection technology and applications on ITER *Preprint: IEEE 26th Symposium on Fusion Engineering (SOFE) (Austin, USA, 31 May-04 June 2015),* DOI: 10.1109/SOFE.2015.7482362
[146] Maruyama S. *et al* 2015 ITER disruptions mitigation technologies and beyond *Preprint: IEEE 26th Symposium on Fusion Engineering (SOFE) (Austin, USA, 31 May-04 June 2015),* DOI: 10.1109/SOFE.2015.7482363
[147] Luce T.C. *et al* 2021 Progress on the ITER DMS Design and Integration *Preprint: 2020 IAEA Fusion Energy Conf. (Virtual Event, 10-15 May 2021)* [TECH/1-4Ra]
[148] Pautasso G. *et al* 2016 Generation of Runaway Mitigation Trigger: Developing a Preliminary Design for ITER *Preprint: 2016 IAEA Fusion Energy Conf. (Kyoto, Japan, 17-22 October 2016)* [EX/P6-38]
[149] Lyssoivan A. *et al* 2014 *AIP Conference Proceedings* **1580** 287
[150] Wauters T. *et al* 2020 *Plasma Phys. Control. Fusion* **62** 034002
[151] De Temmerman G. private communication
[152] Polevoi A.R. *et al* 2021 *Nucl. Fusion* **61** 076008
[153] Shaing K.C., Ida K. and Sabbagh S.A. 2015 *Nucl. Fusion* **55** 125001
[154] Zhu W. *et al* 2006 *Phys. Rev. Lett.* **96** 225002
[155] Garofalo A.M. *et al* 2008 *Phys. Rev. Lett.* **101** 195005
[156] Jones T.T.C. *et al* 2001 *28th European Physical Society Conf. on Controlled Fusion and Plasma Physics (EPS) (Funchal, Portugal, 17-22 June 2001)* ECA vol. 25A 1197 (http://ocs.ciemat.es/EPS2001/html/pdf/P3.073.pdf)
[157] Noterdaeme J.-M. *et al* 2003 *Nucl. Fusion* **43** 202
[158] Mayoral M.-L. *et al* 2004 *Phys. Plasmas* **11** 2607
[159] Shimomura K. *et al* 2007 *Fusion Eng. Des.* **82** 953
[160] Hawryluk R.J. *et al* 2015 *Nucl. Fusion* **55** 053001
[161] Sabbagh S.A. *et al* 2006 *Phys. Rev. Lett.* **97** 045004
[162] Sabbagh S.A. *et al* 2013 *Nucl. Fusion* **53** 104007
[163] Van Zeeland M.A. *et al* 2009 *Nucl. Fusion* **49** 065003
[164] Garcia-Munoz M. *et al* 2015 Impact of Localized ECRH on NBI and ICRH Driven Alfven Eigenmodes in the ASDEX Upgrade Tokamak *Preprint: Proc. 14thIAEA TM on Energetic Particles in Magnetic Confinement Systems (Vienna, Austria, 1-4 September 2015)*
[165] Kazakov Ye.O. *et al* 2015 *Nucl. Fusion* **55** 032001
[166] Militello Asp E. *et al* 2016 ITER Fuelling Requirements and Scenario Development for H, He and DT through JINTRAC Integrated Modelling *Preprint: 2016 IAEA Fusion Energy Conf. (Kyoto, Japan, 17-22 October 2016)* [TH/P2-23]
[167] Garzotti L. *et al* 2016 *43rd European Physical Society Conf. on Plasma Physics (EPS) (Leuven, Belgium, 4-8 July 2016)* ECA vol. 40A O4.113 (http://ocs.ciemat.es/EPS2016PAP/pdf/O4.113.pdf)
[168] Polevoi A.R. *et al* 2013 *Nucl. Fusion* **53** 123026
[169] Loarte A. *et al* 2003 *Plasma Phys. Control. Fusion* **45** 1549

[170] Eich T. *et al* 2003 *J. Nucl. Mater.* **313-316** 919
[171] Dux R. *et al* 2017 *Nucl. Mater. Energy* **12** 28
[172] Polevoi A.R. *et al* 2012 *39th European Physical Society Conf. on Plasma Physics (EPS) (Stockholm, Sweden, 2-6 July 2012)* ECA vol. 36F P4.032 (http://ocs.ciemat.es/EPSICPP2012PAP/pdf/P4.032.pdf)
[173] Maget P. *et al* 2013 *Nucl. Fusion* **53** 093011
[174] Joly J. *et al* 2017 Fast ions produced by ICRF three-ion species during the non-active phase of ITER *Preprint: 22nd Topical Conf. on Radiofrequency Power in Plasmas (Aix-en-Provence, France, 30 May-2 June 2017)* EPJ Web of Conferences vol. 157
[175] Rice J.E. *et al* 2002 *Nucl. Fusion* **42** 510
[176] Polevoi A.R. *et al* 2023 *et al* 2013 *Nucl. Fusion* **63** 076003
[177] Gormezano C. *et al* 2007 *Nucl. Fusion* **47** S285
[178] Luce T.C. *et al* 2003 *Nucl. Fusion* **43** 321
[179] Staebler A. *et al* 2005 *Nucl. Fusion* **45** 617
[180] Joffrin E. *et al* 2005 *Nucl. Fusion* **45** 626
[181] Hobirk J. *et al* 2012 *Plasma Phys. Control. Fusion* **54** 095001
[182] Kamada Y. *et al* 1994 *Nucl. Fusion* **34** 1605
[183] Söldner F.X. *et al* 1999 *Nucl. Fusion* **39** 407
[184] Wolf R.C. 2003 *Plasma Phys. Control. Fusion* **45** R1
[185] Polevoi A.R. *et al* 2020 *Nucl. Fusion* **60** 096024
[186] Kim S.H. *et al* 2021 *Nucl. Fusion* **61** 076004
[187] Pinches S.D. *et al* 2015 *Phys. Plasmas* **22** 021807
[188] Lauber Ph. 2015 *Plasma Phys. Control. Fusion* **57** 054011
[189] Vignitchouk L. et al 2023 *Nucl. Fusion* **63** 016004
[190] Vignitchouk L. *et al* 2022 *Nucl. Fusion* **62** 036016
[191] Vignitchouk L. et al 2018 *Nucl. Fusion* **58** 076008
[192] Fenstermacher M.E. *et al* 2010 ELM Control by Resonant Magnetic Perturbations: Overview of Research by the ITPA Pedestal and Edge Physics Group *Preprint: 2010 IAEA Fusion Energy Conf. (Daejeon, Republic of Korea, 11-16 October 2010)* [ITR/P1-30]
[193] Militello Asp E. *et al* 2022 *Nucl. Fusion* **62** 126033
[194] Romanelli M. *et al* 2015 *Nucl. Fusion* **55** 093008
[195] Loarte A. *et al* 2016 Evaluation of Tungsten Transport and Concentration Control in ITER Scenarios *Preprint: 2016 IAEA Fusion Energy Conf. (Kyoto, Japan, 17-22 October 2016)* [PPC/2-1]
[196] Counsell G. *et al* 2006 *Plasma Phys. Control. Fusion* **48** B189
[197] Belli E.A. and Candy J. 2021 *Phys. Plasmas* **28** 062301
[198] Van Zeeland M.A. *et al* 2016 *Nucl. Fusion* **56** 112007
[199] Garcia-Munoz M. *et al* 2013 *Nucl. Fusion* **53** 123008
[200] Polevoi A.R. *et al* 2015 *Nucl. Fusion* **55** 063019
[201] Köchl F. *et al* 2014 Modelling of Transitions between L- and H-mode Including W Behaviour in ITER Scenarios *Preprint: 2014 IAEA Fusion Energy Conf. (St Petersburg, Russian Federation, 13-18 October 2014)* [TH/P3-24]
[202] Koechl F. *et al* 2017 *Nucl. Fusion* **57** 086023
[203] Kessel C.E., Koechl F. and Kim S.H. 2015 *Nucl. Fusion* **55** 063038

[204] Snyder P.B. *et al* 2011 *Nucl. Fusion* **51** 103016
[205] Parail V. *et al* 2013 *Nucl. Fusion* **53** 113002
[206] Loarte A. *et al* 2015 *Phys. Plasmas* **22** 056117
[207] Hender T.C. *et al* 2007 *Nucl. Fusion* **47** S128
[208] Garcia J. *et al* 2015 *Nucl. Fusion* **55** 053007
[209] Urano H. *et al* 2016 Global Stabilization Effect of Shafranov Shift on the Edge Pedestal Plasmas in JET and JT-60U *Preprint: 2016 IAEA Fusion Energy Conf. (Kyoto, Japan, 17-22 October 2016)* [EX/3-4]
[210] Wagner F. *et al* 2010 *Plasma Phys. Control. Fusion* **52** 124044
[211] Luce T.C. *et al* 2014 *Nucl. Fusion* **54** 013015
[212] Gorelenkov N.N., Pinches S.D. and Toi K. 2014 *Nucl. Fusion* **54** 125001
[213] ITER Physics Expert Group for Energetic Particles, Heating and Current Drive *et al* 1999 *Nucl. Fusion* **39** 2471
[214] Fasoli A. *et al* 2007 *Nucl. Fusion* **47** S264
[215] Sharapov S.E. *et al* 1999 *Nucl. Fusion* **39** 373
[216] Nazikian R. *et al* 1997 *Phys. Rev. Lett.* **78** 2976
[217] Campbell D.J. *et al* 1988 *Phys. Rev. Lett.* **60** 2148
[218] Akers R.J. *et al* 2016 High Fidelity Simulations of Fast Ion Power Flux Driven by 3D Perturbations on ITER *Preprint: 2016 IAEA Fusion Energy Conf. (Kyoto, Japan, 17-22 October 2016)* [TH/4-1]
[219] Sanchis L. *et al* 2021 *Nucl. Fusion* **61** 046006
[220] Ward S.H. *et al* 2022 *Nucl. Fusion* **62** 126014
[221] Rebhan E. and Vieth U. 1997 *Nucl. Fusion* **37** 251
[222] Challis C.D. *et al* 2015 *Nucl. Fusion* **55** 053031
[223] Chapman I.T. *et al* 2009 *Plasma Phys. Control. Fusion* **51** 055015
[224] Liu Y.Q. *et al* 2009 *Nucl. Fusion* **49** 035004
[225] Martín-Solís J.R., Loarte A. and Lehnen M. 2017 *Nucl. Fusion* **57** 066025
[226] Mukhovatov V. *et al* 2003 *Plasma Phys. Control. Fusion* **45** A235
[227] Schmid K. *et al* 2015 *Nucl. Fusion* **55** 053015
[228] Khan A. *et al* 2019 *Nucl. Mater. Energy* **20** 100674
[229] Zohm H. *et al* 2021 *Fusion Eng. Des.* **166** 112307
[230] Pintsuk G. *et al* 2019 *Fusion Eng. Des.* **146A** 1300
[231] Biel W. *et al* 2022 *Fusion Eng. Des.* **179** 113122
[232] Morris A.W. *et al* 2022 *Plasma Phys. Control. Fusion* **64** 064002
[233] Giancarli L. *et al* 2012 *Fusion Eng. Des.* **87** 395
[234] Giancarli L. *et al* 2016 *Fusion Eng. Des.* **109-111** 1491
[235] Giancarli L. *et al* 2018 *Fusion Eng. Des.* **136** 815
[236] Giancarli L. *et al* 2020 *Fusion Eng. Des.* **158** 111674
[237] Aubert J. *et al* 2020 *Fusion Eng. Des.* **160** 111921
[238] Zmitko M. *et al* 2018 *Fusion Eng. Des.* **136** 1376
[239] Tanigawa H. *et al* 2018 *Fusion Eng. Des.* **136** 1221
[240] Wang X.Y. *et al* 2019 *Nucl. Fusion* **59** 076019

[241] Snipes J.A. *et al* 2010 *37th European Physical Society Conf. on Plasma Physics (EPS) (Dublin, Ireland, 21-25 June 2010)* ECA vol. 34A P1.1093 (http://ocs.ciemat.es/EPS2010PAP/pdf/P1.1093.pdf)
[242] Schaffer M.J. *et al* 2011 *Nucl. Fusion* **51** 103028
[243] Reimerdes H. *et al* 2012 Rotation Braking and Error Field Correction of the Test Blanket Module Induced Magnetic Error Field in ITER *Preprint: 2012 IAEA Fusion Energy Conf. (San Diego, USA, 8-13 October 2012)* [EX/P4-09]
[244] Lanctot M.J. *et al* 2017 *Nucl. Fusion* **57** 036004
[245] Required R&D in Existing Fusion Facilities to Support the ITER Research Plan *ITER Technical Report* ITR-20-008 (www.iter.org/technical-reports)
[246] Loarte A *et al* 2011 *Nucl. Fusion* **51** 073004
[247] Arnoux G. *et al* 2009 *Nucl. Fusion* **49** 085038
[248] Hollmann E.M. *et al* 2011 *J. Nucl. Mat.* **415** S27
[249] Hollmann E.M. *et al* 2018 *Phys. Plasmas* **25** 102502
[250] Coburn J. *et al* 2021 *Nucl. Mater. Energy* **28** 101016
[251] Gunn J.P. *et al* 2021 *Nucl. Mater. Energy* **27** 100920
[252] Sugihara M. *et al* 2007 *Nucl. Fusion* **47** 337
[253] Schioler T. *et al* 2011 *Fusion Eng. Des.* **86** 1963
[254] Clauser C.F., Jardin S.C. and Ferraro N.M. 2019 *Nucl. Fusion* **59** 126037
[255] Artola F.J. *et al* 2022 *Nucl. Fusion* **62** 056023
[256] Krebs I. *et al* 2020 *Phys. Plasmas* **27** 022505
[257] Pautasso G., Herrmann A. and Lackner K. 1994 *Nucl. Fusion* **34** 455
[258] Jepu I. *et al* 2019 *Nucl. Fus.* **59** 086009
[259] Saint-Laurent F. *et al* 2013 *Fusion Sci. Technol.* **64** 711
[260] Lukash V.E. *et al* 2013 *40th European Physical Society Conf. on Plasma Physics (EPS) (Espoo, Finland, 1-5 July 2013)* ECA vol. 37D P5.167 (http://ocs.ciemat.es/EPS2013PAP/pdf/P5.167.pdf)
[261] Lehnen M. *et al* 2018 R&D for Reliable Disruption Mitigation in ITER *Preprint: 2018 IAEA Fusion Energy Conf. (Ahmedabad, India, 22-27 October 2018)* [EX/P7-12]
[262] Baylor L.R. *et al* 2019 *Nucl. Fusion* **59** 066008
[263] Jachmich S. *et al* 2021 Shattered Pellet Injection Experiments at JET in Support of the ITER Disruptions Mitigation System Design *Preprint: 2020 IAEA Fusion Energy Conference (Virtual Event, 10-15 May 2021)* [EX/5-1Ra]
[264] Shiraki D. *et al* 2021 DIII-D and International Research towards Extrapolating Shattered Pellet Injection Performance to ITER *Preprint: 2020 IAEA Fusion Energy Conference (Virtual Event, 10-15 May 2021)* [EX/5-2Ra]
[265] Kim J. *et al* 2021 Disruption Mitigation by Symmetric Dual Injection of Shattered Pellets in KSTAR *Preprint: 2020 IAEA Fusion Energy Conference (Virtual Event, 10-15 May 2021)* [EX/5-3Ra]
[266] Chen Z. *et al* 2021 Disruption Mitigation by Shattered Pellet Injection on J-TEXT *Preprint: 2020 IAEA Fusion Energy Conference (Virtual Event, 10-15 May 2021)* [EX/P5-23]
[267] Papp G. *et al* 2020 ASDEX Upgrade SPI: design, status and plans *Preprint: IAEA Technical Meeting on Plasma Disruptions and their Mitigation (Virtual Event, 20-23 July 2020)* (https://nucleus.iaea.org/sites/fusionportal/disruptions/SitePages/Home.aspx)

[268] Heinrich P. *et al* 2022 Characterization of the ASDEX Upgrade Shattered Pellet Injector *Preprint: 2nd IAEA Technical Meeting on Plasma Disruptions and their Mitigation (St Paul-lez-Durance, France, 19-22 July 2022)* (https://conferences.iaea.org/event/281/)
[269] Nardon E. *et al* 2021 Theory and Modelling Activities in Support of the ITER Disruption Mitigation System *Preprint: 2020 IAEA Fusion Energy Conference (Virtual Event, 10-15 May 2021)* [TH/6-1]
[270] Zeng L. *et al* 2013 *Phys. Rev. Lett.* **110** 235003
[271] Lvovskiy A. *et al* 2018 *Plasma Phys. Control. Fusion* **60** 124003
[272] Aleynikov P.B. *et al 37th European Physical Society Conf. on Plasma Physics (EPS) (Dublin, Ireland, 21-25 June 2010)* ECA vol. 34A P1.1004 (http://ocs.ciemat.es/EPS2010PAP/pdf/P1.1004.pdf)
[273] Papp G. *et al* 2011 *Nucl. Fusion* **51** 043004.
[274] Pavel Aleynikov and Boris Breizman 2015 *Nucl. Fusion* **55** 043014
[275] Reux C. *et al* 2021 *Phys. Rev. Lett.* **126** 175001
[276] Paz-Soldan C. *et al* 2019 *Plasma Phys. Control. Fusion* **61** 054001
[277] Strait E.J. *et al* 2019 *Nucl. Fusion* **59** 112012
[278] Snipes J.A. *et al* 2017 *Nucl. Fusion* **57** 125001
[279] Yan Z. *et al* 2017 *Nucl. Fusion* **57** 126015.
[280] Maggi C.F. *et al* 2018 *Plasma Phys. Control. Fusion* **60** 014045
[281] Solano E.R. *et al* 2021 *Nucl. Fusion* **61** 124001
[282] Bourdelle C. *et al* 2015 *Nucl. Fusion* **55** 073015
[283] Schmidtmayr M. *et al* 2018 *Nucl. Fusion* **58** 056003
[284] Andrew Y. *et al* 2006 *Plasma Phys. Control. Fusion* **48** 479
[285] McDonald D.C. *et al* 2010 JET Helium-4 ELMy H-mode Studies *Preprint: 2010 IAEA Fusion Energy Conf. (Daejeon, Republic of Korea, 11-16 October 2010)* [EXC/2-4Rb]
[286] Gohil P. *et al* 2008 *Journal. Phys. Conf. Ser.* **123** 012017
[287] Schneider M. *et al* 2017 *EPJ Web of Conferences* **157** 03046
[288] Militello Asp E. *et al* 2018 *Proc. 60th Annual Meeting of the APS Division of Plasma Physics (Portland, USA, 5-9 November 2018)* p UO5.00008
[289] Lang P.T. *et al* 2005 *Nucl. Fusion* **45** 502
[290] Baylor L.R. *et al* 2012 *39th European Physical Society Conf. on Plasma Physics (EPS) (Stockholm, Sweden, 2-6 July 2012)* ECA vol. 36F O4.113 (http://ocs.ciemat.es/epsicpp2012pap/pdf/O4.113.pdf)
[291] Evans T.E. *et al* 2017 *Nucl. Fusion* **57** 086016
[292] Polevoi A.R. *et al* 2011 *38th European Physical Society Conf. on Plasma Physics (EPS) (Strasbourg, France, 27 June-1 July 2011)* ECA vol. 35G P4.109 (http://ocs.ciemat.es/EPS2011PAP/pdf/P4.109.pdf)
[293] Pacher H.D. *et al* 2015 *J. Nucl. Mater.* **463** 591
[294] Pütterich T. *et al* 2011 *J. Nucl. Mater.* **415** S334
[295] Hughes J.W. *et al Nucl. Fusion* **51** 083007
[296] Loarte A. *et al* 2011 *Phys. Plasmas* **18** 056105
[297] Giroud C. *et al* 2012 *Nucl. Fusion* **52** 063022
[298] Kallenbach A. *et al* 2013 *Plasma Phys. Control. Fusion* **55** 124041
[299] Polevoi A.R. *et al* 2017 *Nucl. Fusion* **57** 022014

[300] Garzotti L. *et al* 2019 *Nucl. Fusion* **59** 026006
[301] Valovic M. *et al* 2008 *J. Phys. Conf. Ser.* **123** 012039
[302] Kukushkin A.S. *et al* 2011 *J. Nucl. Mater.* **415** S497
[303] Polevoi A.R. *et al* 2018 *45th European Physical Society Conf. on Plasma Physics (EPS) (Prague, Czech Republic, 2-6 July 2018)* ECA vol. 42A P5.1050 (http://ocs.ciemat.es/EPS2018PAP/pdf/P5.1050.pdf)
[304] Loarte A *et al* 2013 *Nucl. Fusion* **53** 083031
[305] Garzotti L. *et al* 2014 *Plasma Phys. Control. Fusion* **56** 035004
[306] Tokar M.Z. and Moradi S. 2011 *Nucl. Fusion* **51** 063013
[307] Pegourie B. *et al* 2009 *Plasma Phys. Control. Fusion* **51** 124023
[308] Pitts R.A. *et al* 2009 *Phys. Scr.* **2009** 014001
[309] Gunn J.P. *et al* 2019 *Nucl. Fusion* **59** 126043
[310] Coenen J.W. *et al* 2015 *Nucl. Fusion* **55** 023010
[311] Krieger K. *et al* 2018 *Nucl. Fusion* **58** 026024
[312] Thorén E. *et al* 2021 *Plasma Phys. Control. Fusion* **63** 035021
[313] Ratynskaia S. *et al* 2020 *Nucl. Fusion* **60** 104001
[314] Diez M. *et al* 2020 *Nucl. Fusion* **60** 054001
[315] Adamek J. et al 2017 *Nucl. Fusion* **57** 116017
[316] Gao J.M. *et al* 2021 *Nucl. Fusion* **61** 066024
[317] Dejarnac R. *et al* 2018 *Nucl. Fusion* **58** 066003
[318] Krieger K. *et al* 2023 *Nucl. Fusion* **63** 066021
[319] Grosjean A. *et al* 2020 *Nucl. Fusion* **60** 106020
[320] Pitts R.A. *et al* 2006 *Nucl. Fusion* **46** 82
[321] Guillemaut C. *et al* 2016 *Phys. Scr.* **2016** 014005
[322] Chankin A.V., Coster D.P. and Dux R. 2014 *Plasma Phys. Control. Fusion* **56** 025003
[323] Den Harder N. *et al* 2016 Nucl. Fusion **56** 026014
[324] Militello Asp E. *et al* 2021 Global JINTRAC Simulations for ITER PFPO Scenarion Development *Preprint: 2020 IAEA Fusion Energy Conf. (Virtual Event, 10-15 May 2021)* [TH/1-1]
[325] Brezinsek S. *et al* 2019 *Nucl. Fusion* **59** 096035
[326] Kirschner A. *et al* 2019 *Nucl. Mater. Energy* **18** 239
[327] Rapp J. *et al* 2004 *Nucl. Fusion* **44** 312
[328] Komm M. *et al* 2023 *Nucl. Fusion* **63** 126018
[329] Sandoval L. *et al* 2018 *Acta Materialia* **159** 46
[330] Kajita S. *et al* 2009 *Nucl. Fusion* **49** 095005
[331] Cui S. *et al* 2018 *J. Nucl. Mater.* **511** 141
[332] Wirtz M. *et al* 2017 *Nucl. Mater. Energy* **12** 148
[333] Romazanov J. *et al* 2022 *Nucl. Fusion* **62** 036011
[334] De Temmerman G., Doerner R.P. and Pitts R.A. 2019 *Nucl. Mater. Energy* **19** 255
[335] Wang Y. and Zhao J. 2021 *J. Nucl. Mater.* **543** 152601
[336] Morgan T.W. *et al* 2020 *Phys. Scr.* **2020** 014065
[337] Morgan T.W. *et al* 2021 *Nucl. Fusion* **61** 116045
[338] Bucalossi J. *et al* 2022 *Nucl. Fusion* **62** 042007
[339] Richou M. *et al* 2022 *Nucl. Fusion* **62** 056010

[340] Hirai T. *et al* 2016 *Nucl. Mater. Energy* **9** 616
[341] Gavila P. *et al* 2015 *Fusion Eng. Des.* **98-99** 1305
[342] Loewenhoff Th. *et al* 2015 *Nucl. Fusion* **55** 123004
[343] Corre Y. *et al* 2021 *Phys. Scr.* **96** 124057
[344] Thorén E *et al* 2018 *Nucl. Fusion* **58** 106003
[345] Ratynskaia S. *et al* 2021 *Phys. Scr.* **96** 124009
[346] Krieger K. *et al* 2011 *Phys. Scr.* **2011** 014067
[347] Lipschultz B. *et al* 2012 *Nucl. Fusion* **52** 123002
[348] Herrmann A. *et al* 2017 *Nucl. Mater. Energy* **12** 205
[349] Lei Y. *et al* 2021 *Nucl. Mater. Energy* **27** 100997
[350] Ratynskaia S., Vignitchouk L. and Tolias P. 2022 *Plasma Phys. Control. Fusion* **64** 044004
[351] de Vries P.C. *et al* 2020 *Plasma Phys. Control. Fusion* **62** 125014
[352] Kim H.T. *et al* 2013 *Plasma Phys. Control. Fusion* **55** 124032
[353] Chew J. *et al 2021 Plasma Phys. Control. Fusion* **63** 045012
[354] Stober J. *et al* 2011 *Nucl. Fusion* **51** 083031
[355] Ricci D. *et al* 2016 *43rd European Physical Society Conf. on Plasma Physics (EPS) Leuven, Belgium, 4-8 July 2016)* ECA vol. 40A O5.140 (http://ocs.ciemat.es/EPS2016PAP/pdf/O5.130.pdf)
[356] Farina D. 2018 *Nucl. Fusion* **58** 066012
[357] Sinha J. *et al* 2022 *Nucl. Fusion* **62** 066013
[358] Sun H.J. *et al* 2023 *Plasma Phys. Control. Fusion* **65** 095009
[359] Goriaev A. *et al* 2020 *Phys. Scr.* **2020** 014063
[360] Wauters T. *et al* 2020 *Plasma Phys. Control. Fusion* **62** 105010
[361] Lee J. *et al* 2017 *Nucl. Fusion* **57** 126033
[362] Douai D. *et al* 2018 *Nucl. Fusion* **58** 026018
[363] Tripský M. *et al* 2017 *Nucl. Fusion* **57** 126043
[364] Maquet V., Druart A. and Messiaen A. 2021 *J. Plasma Phys.* **87** 905870617
[365] Park J.-K. *et al* 2017 MDC-19 Report Assessment of Error Field Correction Criteria for ITER *ITPA MHD topical group (private communication)*
[366] Park J.-K. *et al* 2008 *Nucl. Fusion* **48** 045006
[367] Amoskov V.M. *et al* 2019 *Fusion Eng. Des.* **148** 111271
[368] Logan N.C. *et al* 2020 *Nucl. Fusion* **60** 086010
[369] Logan N.C. *et al* 2020 *Plasma Phys. Control. Fusion* **62** 084001
[370] King J.D. *et al* 2015 *Phys. Plasmas* **22** 072501
[371] Park J.-K. *et al* 2021 Quasi-Symmetric Error Field Correction in Tokamaks *Preprint: 2020 IAEA Fusion Energy Conf. (Virtual Event, 10-15 May 2021)* [EX/4-3]
[372] Markovic T. *et al* 2018 High-field side error field effects on H-mode plasma performance and their correction in ITER-like experiments on COMPASS *Preprint: 45th European Physical Society Conf. on Plasma Physics (EPS) (Prague, Czech Republic, 2-6 July 2018)* O3.108
[373] Ferraro M.N. *et al* 2019 *Nucl. Fusion* **59** 086021
[374] Paz-Soldan C. *et al* 2015 *Nucl. Fusion* **55** 083012
[375] La Haye R.J. *et al* 1992 *Phys. Fluids B* **4** 2098
[376] de Vries P.C. *et al* 2018 *Nucl. Fusion* **58** 026019

[377] Koechl F. *et al* 2020 *Nucl. Fusion* **60** 066015
[378] Portone A. *et al* 2005 *Fusion Eng. Des.* **74** 537
[379] Köchl F. *et al* 2018 *Plasma Phys. Control. Fusion* **60** 074008
[380] Kim S.H., Casper T.A. and Snipes J.A. 2018 *Nucl. Fusion* **58** 056013
[381] Angioni C. *et al* 2017 *Nucl. Fusion* **57** 056015
[382] Bonnin X. *et al* 2017 *Nucl. Mater. Energy* **12** 1100
[383] Loarte A. *et al* 1998 *Nucl. Fusion* **38** 331
[384] Eldon D. et al 2019 *Nucl. Mater. Energy* **18** 285
[385] Ravensbergen T. *et al* 2021 *Nature Comm.* **12** 1105
[386] Kallenbach A. *et al* 2015 *Nucl. Fusion* **55** 053026
[387] Schuster E., Krstic M. and Tynan G. 2002 *Fusion Eng. Des.* **63-64** 569
[388] Schuster E., Krstic M. and Tynan G. 2003 *Fusion Sci. Technol.* **43** 18
[389] Boyer M.D. and Schuster E. 2014 *Plasma Phys. Control. Fusion* **56** 104004
[390] Pajares A. and Schuster E. 2019 *Nucl. Fusion* **59** 096023
[391] Fischer R. and Dinklage A. 2008 Integrated Data Analysis for Nuclear Fusion *Preprint: Computational Intelligence In Decision And Control - Proc. 8th Int. Flins Conf.* (World Scientific Proceedings Series On Computer Engineering And Information Science Book 1) 37
[392] Svensson J. and Werner A. 2007 Large Scale Bayesian Data Analysis for Nuclear Fusion Experiments *Preprint: 2007 IEEE International Symposium on Intelligent Signal Processing (Alcala de Henares, Spain, 3-5 October 2007)* 1
[393] Imbeaux F. *et al* 2015 *Nucl. Fusion* **55** 123006
[394] Schneider M. *et al* 2021 *Nucl. Fusion* **61** 126058
[395] Lauber P. *et al* 2021 Energetic Particle Dynamics Induced by Off-Axis Neutral Beam Injection in ASDEX Upgrade, JT-60SA and ITER *Preprint: 2020 IAEA Fusion Energy Conf. (Virtual Event, 10-15 May 2021)* [TH/P1-20]
[396] Pinches S.D. *et al* 2021 Integrated Modelling &Analysis Suite : Developments to Address ITER Needs *Preprint: 2020 IAEA Fusion Energy Conf. (Virtual Event, 10-15 May 2021)* [TH/P2-22]
[397] Farina D. 2007 *Fusion Sci. Technol.* **52** 154
[398] Romanelli M. *et al* 2014 *Plasma Fusion Res.* **9** 3403023
[399] Alberti S. *et al* 2005 *Nucl. Fusion* **45** 1224
[400] Höhnle H. *et al* 2011 *Nucl. Fusion* **51** 083013
[401] Porkolab M. 1994 *AIP Conference Proceedings* **314** 99
[402] Bilato R. *et al* 2018 *45th European Physical Society Conf. on Plasma Physics (EPS) (Prague, Czech Republic, 2-6 July 2018)* ECA vol. 42A P1.1070 (http://ocs.ciemat.es/EPS2018PAP/pdf/P1.1070.pdf)
[403] Bergeaud V., Eriksson L.-G. and Start D.F.H. 2000 *Nucl. Fusion* **40** 35
[404] Start D.F.H. *et al* 1998 *Phys. Rev. Lett.* **80** 4681
[405] Start D.F.H. *et al* 1999 *Nucl. Fusion* **39** 321
[406] Kazakov Ye.O. *et al* 2021 *Phys. Plasmas* **28** 020501
[407] Janev R.K., Boley C.D. and Post D.E. 1989 *Nucl. Fusion* **29** 006
[408] Suzuki S. *et al* 1998 *Plasma Phys. Control. Fusion* **40** 2097
[409] JT-60SA Research Unit 2016 JT-60SA Research Plan version 3.3

[410] Taylor G. *et al* 1996 *Phys. Rev. Lett.* **76** 2722
[411] Thomas P.R. *et al* 1998 *Phys. Rev. Lett.* **80** 5548
[412] Van Zeeland M.A. *et al* 2008 *Plasma Phys. Control. Fusion* **50** 035009
[413] Sharapov S.E. *et al* 2018 *Plasma Phys. Control. Fusion* **60** 014026
[414] Garcia-Munoz M. *et al* 2019 *Plasma Phys. Control. Fusion* **61** 054007
[415] Kim J. *et al* 2022 *Nucl. Fusion* **62** 026029
[416] Cottrell G.A. *et al* 1993 *Nucl. Fusion* **33** 1365
[417] McClements K.G. *et al* 2015 *Nucl. Fusion* **55** 043013
[418] Ochoukov R. *et al* 2018 *Rev. Sci. Instrum.* **89** 10J101
[419] Di Siena A. *et al* 2019 *Nucl. Fusion* **59** 124001 and Corrigendum: Di Siena A. *et al* 2020 *Nucl. Fusion* **60** 089501
[420] Mazzi S. *et al* 2022 *Nature Phys.* **18** 776
[421] Jia M. *et al* 2021 *Nucl. Fusion* **61** 106023
[422] Li L. *et al* 2022 *Nucl. Fusion* **62** 096008
[423] Nazikian R. *et al* 2014 Recent Advances in the Understanding and Optimization of RMP ELM Suppression for ITER *Preprint: 2014 IAEA Fusion Energy Conf. (St Petersburg, Russian Federation, 13-18 October 2014)* [EX/1-1]
[424] Kim S.K. *et al* 2022 *Nucl. Fusion* **62** 026043
[425] Leonard A.W. *et al* 1991 *Nucl. Fusion* **31** 1511
[426] Kirk A. *et al* 2011 *Plasma Phys. Control. Fusion* **53** 065011
[427] Kaye S.M. *et al* 2011 *Nucl. Fusion* **51** 113019
[428] Ryter F. *et al* 2012 *Nucl. Fusion* **52** 114014
[429] In Y. *et al* 2017 *Nucl. Fusion* **57** 116054
[430] Hu Q.M. *et al* 2021 *Phys. Plasmas* **28** 052505
[431] Hu Q. *et al* 2021 Role of Resonant Magnetic Field Penetrations in ELM Suppression and Density Pump-Out in DIII-D ITER-Like Plasmas *Preprint: 2020 IAEA Fusion Energy Conf. (Virtual Event, 10-15 May 2021)* [TH/2-1]
[432] In Y. *et al*. 2022 *Nucl. Fusion* **62** 066014
[433] Grierson B.A. *et al* 2015 *Phys. Plasmas* **22** 055901
[434] Suttrop W. *et al* 2018 *Nucl. Fusion* **58** 096031
[435] Sun Y. *et al* 2021 *Nucl. Fusion* **61** 106037
[436] Reynolds-Barredo J.M. *et al* 2020 *Nucl. Fusion* **60** 086017
[437] Tamain P. *et al* 2010 *Plasma Phys. Control. Fusion* **52** 075017
[438] Leuthold N. 2020 Experimental investigation of enhanced particle transport due to magnetic perturbations on ASDEX upgrade *PhD Thesis LMU Munich*
[439] Paz-Soldan C. *et al* 2019 *Nucl. Fusion* **59** 056012
[440] Valovič M. *et al* 2020 *Nucl. Fusion* **60** 054006
[441] Baylor L.R. *et al* 2008 ELMs triggered from deuterium pellets injected into DIII-D and extrapolation to ITER *General Atomics Report General Atomics GA-A26143*
[442] Evans T.E. *et al* 2008 *Nucl. Fusion* **48** 024002
[443] Becoulet M. *et al* 2022 *Nucl. Fusion* **62** 066022
[444] Liu Y. *et al* 2020 *Nucl. Fusion* **60** 036018

[445] Evans T.E. *et al* 2008 Operating Characteristsics in DIII-D ELM-Suppressed RMP H-modes with ITER Similar Shapes *Preprint: 2008 IAEA Fusion Energy Conf. (Geneva, Switzeerland, 13-18 October 2008)* [EX/4-1]
[446] Kukushkin A.S. *et al* 2011 *Fusion Eng. Des.* **86** 2865
[447] Li J. *et al* 2013 *Nature Phys.* **9** 817
[448] Sytova E. *et al* 2019 *Nucl. Mater. Energy* **19** 72
[449] Van Zeeland M.A. *et al* 2015 *Nucl. Fusion* **55** 073028
[450] McClements K.G. *et al* 2018 *Plasma Phys. Control. Fusion* **60** 095005
[451] Garcia-Munoz M. *et al* 2013 *Plasma Phys. Control. Fusion* **55** 124014
[452] Kim K. *et al* 2018 *Phys. Plasmas* **25** 122511
[453] Shinohara K. *et al* 2012 *Nucl. Fusion* **52** 094008
[454] Tani K. *et al* 2012 *Nucl. Fusion* **52** 013012
[455] Oikawa T. *et al* 2012 Effects of ELM Control Coils on Fast Ion Confinement in ITER H-mode Scenarios *Preprint: 2012 IAEA Fusion Energy Conf. (San Diego, USA, 8-13 October 2012)* [ITR/P1-35]
[456] Varje J. *et al* 2016 *Nucl. Fusion* **56** 046014
[457] Polevoi A.R. *et al* 2010 *37th European Physical Society Conf. on Plasma Physics (EPS) (Dublin, Ireland, 21-25 June 2010)* ECA vol. 34A P2.187 (http://ocs.ciemat.es/EPS2010PAP/pdf/P2.187.pdf)
[458] Challis C.D. *et al* 2015 *Nucl. Fusion* **55** 053031
[459] Petty C.C. *et al* 2016 *Nucl. Fusion* **56** 016016
[460] Petty C.C. *et al* 2017 *Nucl. Fusion* **57** 116057
[461] Bock A. *et al* 2017 *Nucl. Fusion* **57** 126041
[462] Petty C.C. *et al* 2009 *Phys. Rev. Lett.* **102** 045005
[463] Burckhardt A. *et al* 2021 Experimental Evidence of Magnetic Flux Pumping at ASDEX Upgrade *Preprint: 2020 IAEA Fusion Energy Conf. (Virtual Event, 10-15 May 2021)* [EX/4-1]
[464] Kim S.H. *et al* 2016 *Nucl. Fusion* **56** 126002
[465] Chrystal C. *et al* 2017 *Phys. Plasmas* **24** 056113
[466] Chrystal C. *et al* 2020 *Nucl. Fusion* **60** 036003
[467] Li L. *et al* 2019 *Nucl. Fusion* **59** 096038
[468] de Vries P.C. *et al* 2008 *Nucl. Fusion* **48** 065006
[469] Solomon W.M. *et al* 2013 *Nucl. Fusion* **53** 093033
[470] Oosterbeek W. *et al* 2020 *Phys. Plasmas* **27** 092502
[471] Angioni C. *et al* 2009 *Plasma Phys. Control. Fusion* **51** 124017
[472] Fable E. *et al* 2019 *Nucl. Fusion* **59** 076042
[473] Tala T. *et al* 2019 *Nucl. Fusion* **59** 126030
[474] Nazikian R. *et al* 2018 *Nucl. Fusion* **58** 106010

Annex A. Contributors to ITER Research Plan within the Staged Approach not included in main author list

P. Andrew, IO
I. Bandyopadhayay, IN DA (IN)
R. Barnsley, IO
B. Beaumont, IO
L. Bertalot, IO
C. Bourdelle, CEA/IRFM (EU)
A. Chakraborty, IPR (IN)
D. Chandra, IPR (IN)
M. Clough, IO
C. Darbos, IO
M. De Bock, IO
G. De Temmerman, IO
E. Lerche, ERM/KMS (EU)
D. Douai, CEA/IRFM (EU)
X. Duan, SWIP (CN)
J. Elbez-Uzan, IO
M. Fenstermacher, LLNL (US)
A. Fossen, IO
J. Graceffa, IO
M. Graham, IO
J. Gunn, CEA/IRFM (EU)
S.-H. Hong, NFRI (KO)
G. Huijsmans, EC (EU)
Y.-K. In, NFRI (KO)
A. Isayama, QST (JA)
S. Kaye, PPPL (US)
Y. Kazakov, ERM/KMS (EU)
F Kazarian, IO
A. Khan, IO
N. Kirneva, NRCKI (RF)
M. Kocan, IO
S. Konovalov, NRCKI (RF)
V. Leonov, NRCKI (RF)
T. Suzuki, QST (JA)
S. Lisgo, IO
X. Litaudon, EUROfusion (EU)
R. Maingi, PPPL (US)
S. Maruyama, IO
Y.-S. Na, Seoul Nat Uni (KO)
R. Neu, IPP (EU)
Y.-K. Oh, NFRI (KO)
F. Rimini, UKAEA (EU)
A. Romannikov, NRCKI (RF)
R. Rotella, IO
S. Sabbagh, Columbia Uni (US)
V. Safronov, RF DA (RF)
G. Saibene, F4E (EU)
R. Sartori, F4E (EU)
K. Schmid, IPP (EU)
B. Schunke, IO
M. Singh, IPR (IN)
G. Sips, EC (EU)
A. Sirinelli, IO
J. Stober, IPP (EU)
J. Stober, IPP (EU)
L. Svensson, IO
Y. Takase, Uni Tokyo (JA)
H. Takenaga, QST (JA)
E. Tsitrone, CEA/IRFM (EU)
V. Udintsev, IO
H. Urano, QST (JA)
D. Van Eester, ERM/KMS (EU)
E. Veshchev, IO
M. Walsh, IO
C. Watts, IO
T. Wauters, IO
S. Willms (IO)
S.-W. Yoon, NFRI (KO)
L. Zabeo (IO)
G. Zhuang, HUST EDU (CN)

Annex B. Contributors to previous versions of the ITER Research Plan not included in main author list

M. Bell, PPPL (US)
D. Babineau, IO
A. Costley, IO
V. Chuyanov, IO
M. Glugla, IO
R. Hemsworth, IO
N. Holtkamp, IO
L. Horton, IPP and EFDA (EU)
W. Houlberg, IO
S. Ide, JAEA (JA)
G. Janeschitz, IO
H. Jhang, ITER Korea (KO)
Y. Kamada, JAEA (JA)
O. Kaneko, NIFS (JA)
W. C. Kim, NFRI (KO)
P. Lomas, UKAEA (EU)
S. Milora, ORNL (US)
V. Mukhovatov, IO
Y. K. Oh, NFRI (KO)
T. Oikawa, IO
N. Oyama, JAEA (JA)
S. Putvinski, IO
G. Saibene, F4E (EU)
R. Sartori, F4E (EU)
M. Shimada, IO
G. Sips, IPP and EFDA (EU)
E. Synakowski, LLNL (US)
Y. Takase, Uni Tokyo (JA)
A. Tanga, IO
C. Taylor, IO
D. Thomas, IO
D. van Houtte, IO
M. Wade, GA (US)
B. Wan, ASIPP (CN)
A. Winter, IO
S. Wolfe, MIT (US)

ITER Research Plan within the Staged Approach - Tables

Table 1. Overview of experimental days within the Research Plan campaigns

Campaign	Days
First Plasma Campaign (nom. 1 month)	25
Pre-Fusion Power Operation 1 (18 months)	470
Pre-Fusion Power Operation 2 (21 months)	545
Fusion Power Operation 1 (nom. 16 months)	415
Fusion Power Operation 2 (nom. 16 months)	415
Fusion Power Operation 3 (nom. 16 months)	415
Fusion Power Operation n ($n \geq 4$) (nom. 16 months)	415

Table 2. Overview of minimum measurement requirements and installed diagnostic systems for the First Plasma and Engineering Operation campaign*

Measurement Requirement	**Installed Diagnostic Systems**
Magnetics for plasma current, plasma position, velocity, shape and MHD mode structure	• Magnetics System Electronics & Software • Continuous External Rogowski • Outer Vessel Coils • Steady State Sensors • Flux Loops • Inner Vessel Coils • Diamagnetic Sensors
Plasma density measurements	• Density Interferometer (single channel)
Runaway electron detection (hard X-rays)	• Hard X-ray Monitor
Impurity identification and influxes (visible and near UV spectroscopy including H_α and visible bremsstrahlung)	• H_α/Visible in EPP12 (partial system) • Vacuum Ultra-Violet Survey • Visible Spectroscopy Reference System • X-Ray Crystal Spectrometer
Visible/IR TV viewing (spectroscopically filtered), partial coverage	• Visible/IR Equatorial in equatorial ports (temporary/partial)
Torus pressure (torus pressure gauges)	• Pressure Gauges (temporary)
Toroidal Field (TF) Mapping	• Temporary set of Nuclear Magnetic Resonance probes for TF mapping
Machine protection	• Tokamak Structural Monitoring System (partial) • Stray ECW detector
In-vessel inspection	• In-vessel Lighting (for test purposes)

** See [3-Appendix H] for further discussion of scope of systems labelled as 'temporary' or 'partial'.*

Table 3. Overview of measurement requirements and diagnostic systems available for the PFPO-1 campaign*

Measurement Requirement	**Installed Diagnostic Systems**
Magnetics for plasma current, position, velocity, shape, MHD mode structure and halo currents	• Magnetics System Electronics & Software • Continuous External Rogowski • Outer Vessel Sensors • Steady State Sensors • Flux Loops • Inner Vessel Sensors • Diamagnetic Sensors • High Frequency Sensors • Divertor Sensors • Divertor & Blanket Rogowski Sensors • Divertor Shunts
Core profiles of n_e and T_e (TS, ECE)	• Core Plasma Thomson Scattering (partial, 1 laser) • Electron Cyclotron Emission • Toroidal Interferometer Polarimeter • Density Interferometer Polarimeter
T_i and High-Z impurity content (XRCS and Radial SXR Cameras)	• X-Ray Crystal Spectrometer • Radial Soft X-Ray Camera
Impurity identification and influxes, Z_{eff} (visible and near UV spectroscopy, including H_α and visible bremsstrahlung, He, Be, Ne, Kr, Ar, W emission)	• H_a Visible (partial - some cameras missing) • Core Imaging X-ray Spectrometer • X-Ray Crystal Spectroscopy Edge • Visible Spectroscopy Reference System • Vacuum Ultra-Violet Edge • Divertor Impurity Monitor (partial - some spectrometers missing) • VUV Divertor • VUV Survey • X-ray Crystal Spectrometer
Radiated power distribution (Bolometry)	• Bolometry System
Neutrons (Micro Fission Chambers, Neutron Flux Monitors, Divertor Neutron Flux Monitors, Neutron Activation System)**	• Microfission Chambers • Neutron Flux Monitor Systems • Neutron Activation System • Divertor Neutron Flux Monitors • Neutron Calibration (2.5 MeV) (partial; simple calibration planned) • Neutron Facility Area
Divertor plasma characterization (including divertor duct pressure and gas composition)	• Langmuir Probes • Pressure Gauges (cassette)

	• Residual Gas Analyzers (partial, 2 channels)
Visible/IR TV viewing (full coverage)	• Visible/IR Equatorial Ports • Visible/IR Upper Ports
PWI/Heat Load characterization	• First Wall Samples • Divertor IR Thermography • Thermocouples (Divertor) • Calorimetry
Data for gas balance measurements	• Pressure Gauges
Runaway electron detection (hard X-rays)	• Hard X-ray Monitor
Machine protection/ monitoring	• Tokamak Structural Monitoring System • Stray ECRH detector
In-vessel inspection	• In-vessel Lighting • In-vessel Viewing System

** Table lists the diagnostic systems planned to be available during PFPO-1 to meet the specified measurement requirements.*

*** Neutron measurements are required to monitor neutron production during the PFPO campaigns.*

Table 4. Availability and characteristics of H&CD systems in the four stages of the Research Plan

Stage	First Plasma	PFPO-1	PFPO-2	FPO-1
Main Ion	H	H, ^{4}He	H, ^{4}He	D, DT
ECRH*	Only UL 170 GHz (7 gyrotrons) **5.8 MW**	Full system, 170 GHz **20 MW**	Full system, 170 GHz **20 MW**	Full system, 170 GHz **20 MW**
ICRF	None	None	Full system 2 antennas 40 - 55 MHz **20 MW**	Full system 2 antennas 40 - 55 MHz **20 MW**
HNB	None	None	Full system, 2 injectors ≤870 keV H^0 beams **≤33 MW**	Full system, 2 injectors ≤1 MeV D^0 beams **≤33 MW**
Max H&CD**	**5.8 MW**	**20 MW**	**≤73 MW**	**≤73 MW**

** A 10 MW upgrade for the ECRH system is under consideration to allow for wider operational space of hydrogen H-modes in PFPO, possibly removing the need for helium plasmas to achieve H-mode in this phase.*

*** Note that this assumes that possible upgrades to the H&CD systems will be implemented for operation in FPO-2 at the earliest*

Table 5. Overview of experimental activities, estimates of required operational days, and ranges in plasma current and toroidal field within the research program for PFPO-1

Experimental Activities	**Days**	I_p **(MA)**	B_{TF} **(T)**
Plasma control/ Plasma scenario development	**155**		
• PF Null/ Breakdown optimization with CS currents up to 30 kA (and 40 kA if 10 MA operation is carried out)		• 0.5 - 1.0	• 1.8 - 5.3
• Commissioning of gas and pellets for density/impurity control		• 1.0 - 7.5	• 2.65
• Scenario development/ plasma magnetic control to 3.5 MA Limiter		• 1.0 - 3.5	• 2.65
• Scenario development/ plasma magnetic control at 3.5 MA/2.65 T Divertor		• 3.5	• 2.65
• Scenario development/ plasma magnetic control from 4 to 7.5 MA/2.65 T Divertor		• 4.0 - 7.5	• 2.65
• Scenario development/ plasma magnetic control at 7.5 MA/5.3 T Divertor		• 3.5 - 7.5	• 2.65 - 5.3
• Scenario development/ plasma magnetic control at 5 MA/1.8 T Divertor		• 3.5 - 5	• 1.8
Disruption management	**64**		
• Disruption load validation		• 1.0 - 7.5	• 2.65 - 5.3
• Commissioning/ Optimization of disruption prediction/ detection		• 1.0 - 7.5	• 2.65 - 5.3
• Commissioning/ Optimization of disruption mitigation		• 1.0 - 7.5	• 2.65 - 5.3
Commissioning of auxiliary systems	**56**		
• Diagnostics		• 1.0 - 7.5	• 2.65 - 5.3
• ECRH commissioning (170 GHz first and second harmonic heating, including plasma initiation)		• 3.5 - 7.5	• 2.65 - 5.3
• ECRH commissioning (170 GHz third harmonic heating)		• 3.5 - 5	• 1.8
Commissioning of advanced control systems	**79**		
• Advanced control functions (wall/divertor protection, MHD control etc.)		• 3.5 - 7.5	• 2.65 - 5.3
• Termination scenarios, exception handling, shared actuator management		• 3.5 - 7.5	• 2.65 - 5.3
Divertor and Plasma-Wall Interaction studies	**39**		
• Divertor/wall heat loads in divertor configuration and detachment control		• 3.5 - 7.5	• 1.8 - 5.3
• Limiter heat loads		• 1.0 - 3.5	• 2.65 - 5.3

• Disruption heat loads		• 1.0 - 7.5	• 2.65 - 5.3
• Electron Cyclotron Wall Conditioning		• -	• 2.65 - 5.3
• Plasma-Wall Interaction studies		• 3.5 - 7.5	• 2.65 - 5.3
H-mode studies	**44**		
• H/He H-mode access and operational space characterization (including ELM control)		• 3.5 - 5.0	• 1.8 - 2.65
• Studies related to TF ripple effects on H-modes (preparation for TBM effects)		• 3.5 - 7.5	• 1.8 - 2.65
• Assessment of H-mode power threshold variation with B_t		• 3.5 - 7.5	• 1.8 - 2.65
Extension of plasma operation to 10 MA	**12**	• 7.5 - 10.0	• 2.65 - 5.3
Total	**449**		

Table 6. Overview of experimental activities, estimates of required operational days, and ranges in plasma current and toroidal field within the research program for PFPO-2

Experimental Activities	**Days**	I_p **(MA)**	B_{TF} **(T)**
Plasma control/ Plasma scenario development	**95**		
• Plasma restart and assessment/mitigation of TBM error field effects up to 7.5 MA/2.65 T		• 1.0 - 7.5	• 2.65
• Axisymmetric magnetic control Commissioning		• 7.5 - 15.0	• 2.65 - 5.3
• MHD and error field control commissioning (Error Field Correction, ELM control, etc.)		• 3.5 - 15.0	• 1.8 - 5.3
• Basic plasma kinetic control commissioning (density control, divertor power flux, etc.)		• 3.5 - 15.0	• 1.8 - 5.3
• Scenario development/ plasma magnetic control of H-mode plasmas up to at least 7.5 MA/2.65 T		• 3.5 - 7.5	• 1.8 - 2.65
• Scenario development/ plasma magnetic control of L-mode plasmas up to the nominal 15 MA/ 5.3 T		• 3.5 - 7.5	• 2.65 - 5.3
Disruption management	**27**		
• Disruption load validation		• 7.5 - 15.0	• 2.65 - 5.3
• Commissioning/ Optimization of disruption prediction/ detection		• 7.5 - 15.0	• 2.65 - 5.3
• Commissioning/ Optimization of disruption mitigation		• 7.5 - 15.0	• 2.65 - 5.3
Commissioning of auxiliary systems	**100**		
• Diagnostics		• 1.0 - 15.0	• 1.8 - 5.3
• ECRH commissioning		• 3.5 - 15.0	• 1.8 - 5.3
• ICRF commissioning		• 3.5 - 15.0	• 1.8 - 5.3
• Heating and Diagnostic NBI Commissioning		• 5.0 - 15.0	• 1.8 - 5.3
Commissioning of advanced control functions	**34**		
• Advanced plasma kinetic control (density, temperature, current profile control, NTM control, fusion burn, etc.)		• 7.5 - 15.0	• 2.65 - 5.3
• Termination scenarios, exception handling, shared actuator management		• 5.0 - 15.0	• 1.8 - 5.3
Divertor and Plasma-Wall Interaction studies	**40**		
• Divertor/wall heat loads in divertor configuration and detachment control		• 3.5 - 15.0	• 1.8 - 5.3
• Disruption heat loads		• 1.0- <15.0	• 2.65 - 5.3
• Fuel retention and material migration		• 3.5 - 7.5	• 1.8 - 2.65

• He plasma-wall interaction effects		• 3.5 - 7.5	• 1.8 - 2.65
• Wall conditioning		• -	• 1.8 - 5.3
H-mode studies	**120**		
• H-mode 5 MA/1.8 T studies (TBM effects)		• 3.5 - 5.0	• 1.8
• Expansion of H-mode operation up to, at least, 7.5 MA/2.65 T including ELM control		• 3.5 - 7.5	• 1.8 - 2.65
• Development of long-pulse H-modes		• 7.5	• 2.65
Development of 15 MA/5.3 T L-mode	**25**	• 7.5 - 15.0	• 2.65 - 5.3
Current drive efficiency, target *q*-profile formation and fast particle effects	**16**	• 4.5 - 6.5	• 2.65
Total	**457**		

Table 7. Overview of measurement requirements and diagnostic systems available for the PFPO-2 campaign*

Measurement Requirement	Installed Diagnostic Systems
Magnetics for plasma current, plasma position, velocity, shape, MHD mode structure and halo currents	• Magnetics System Electronics & Software • Continuous External Rogowski • Outer Vessel Sensors • Steady State Sensors • Flux Loops • Inner Vessel Sensors • Diamagnetic Sensors • High Frequency Sensors • Divertor Sensors • Divertor & Blanket Rogowski Sensors • Divertor Shunts
Core profiles of n_e and T_e (TS, ECE, Reflectometry)	• Core Plasma Thomson Scattering • Electron Cyclotron Emission • Toroidal Interferometer Polarimeter • Density Interferometer Polarimeter • Poloidal Polarimeter • Reflectometry (Low Field Side) • Reflectometry (High Field Side)
T_i and High-Z impurity content (XRCS. Radial SXR Cameras, CXRS)	• X-Ray Crystal Spectrometer • Radial Soft X-Ray Camera • Charge Exchange Recombination Spec. (Core)
Edge profiles of n_e, T_e and T_i (TS, ECE, Reflectometry, CXRS)	• Edge Thomson Scattering • Charge Exchange Recombination Spec. (Edge) • Charge Exchange Recombination Spec. (Pedestal) • Reflectometry (Low Field Side) • Reflectometry (High Field Side)
Impurity identification, profiles and influxes, Z_{eff} (visible and near UV spectroscopy, including H_α and visible bremsstrahlung, He, Be, Ne, Kr, Ar, W emission)	• H_a Visible • Core Imaging X-ray Spectrometer • X-Ray Crystal Spectroscopy (Edge) • Visible Spectroscopy Reference System • Vacuum Ultra-Violet (Edge) • Divertor Impurity Monitor • Vacuum Ultra-Violet (Divertor) • Vacuum Ultra-Violet Survey • X-ray Crystal Spectrometer

	• Charge Exchange Recombination Spec. (Edge)
Radiated power distribution (Bolometry)	• Bolometry System
Neutrons (Micro Fission Chambers, Neutron Flux Monitors, Divertor Neutron Flux Monitors, Neutron Activation System)**	• Microfission Chambers • Neutron Flux Monitor Systems • Neutron Activation System • Divertor Neutron Flux Monitors • Neutron Calibration (2.5 MeV) (complete) • Neutron Facility Area
Divertor plasma characterization (including divertor duct pressure and gas composition)	• Langmuir Probes • Pressure Gauges (cassette) • Residual Gas Analyzers • Divertor Thomson Scattering
Current profile measurements	• Poloidal Polarimeter • Motional Stark Effect
Fuel species	• Charge Exchange Recombination Spec. (Core) • Neutral Particle Analyzers (NPAs) • Neutron Spectrometers
Visible/IR TV viewing (full coverage)	• Visible/IR Equatorial Ports • Visible/IR Upper Ports
PWI/Heat Load characterization	• First Wall Samples • Divertor IR Thermography • Thermocouples (Divertor) • Calorimetry • Dust Monitor • Erosion Monitor • Tritium Monitor (commissioning)
Data for gas balance measurements	• Pressure Gauges
Runaway electron detection (hard X-rays)	• Hard X-ray Monitor • Gamma Ray Spectrometer
Machine protection/ monitoring	• Tokamak Structural Monitoring System • Stray ECRH detector
In-vessel inspection	• In-vessel Lighting • In-vessel Viewing System

** Table lists the diagnostic systems planned to be available during PFPO-2 to meet the specified measurement requirements.*

*** Neutron measurements are required to monitor neutron production during the PFPO-2 campaign.*

Table 8. Path to 15 MA/5.3 T (in hydrogen) with ECRH off-axis (in #3, #4 and #6)

#	I_p/B_t	Available heating		
		P_{ECRH} (MW)	P_{ICRF} (MW)	P_{HNB} (MW)
2	7.5 MA/2.65 T	20	0	10-33*
3	9.5 MA/3.3 T	20	0	> 10**
4	9.5 MA/4.5 T	>13	20	> 10**
6	12.5 MA/4.5 T	>13	20	33
7	12.5 MA/5.3 T	>13	20	33
8	15 MA/5.3 T	>13	20	33

** These NBI power ranges have been calculated for different assumptions on Greenwald density fraction (see [86]; see also section 3.2.5.5).*

*** NB heating above 10 MW shall be possible for all scenarios with a proper adjustment of the acceleration voltage and power modulation to limit shine-through losses. These will determine the level of NBI heating applicable in these cases and remains to be evaluated.*

Table 9. Path to 15 MA/5.3 T (in hydrogen) with ECRH on-axis

#	I_p/B_t	Available heating		
		P_{ECRH} (MW)	P_{ICRF} (MW)	P_{HNB} (MW)
4	9.5 MA/4.5 T	>13	20	>10*
6	12.5 MA/4.5 T	>13	20	33
7	12.5 MA/5.3 T	>13	20	33
8	15 MA/5.3 T	>13	20	33

** NB heating above 10 MW shall be possible for all scenarios with a proper adjustment of the acceleration voltage and power modulation to limit shine-through losses. These will determine the level of NBI heating applicable in these cases and remains to be evaluated.*

Table 10. Overview of neutron and fusion product diagnostic systems available for the FPO campaigns

Measurement Requirement	**Installed Diagnostic Systems**
Neutrons (Micro Fission Chambers, Neutron Flux Monitors, Divertor Neutron Flux Monitors, Neutron Activation System)	• Microfission Chambers • Neutron Flux Monitor Systems • Neutron Activation System • Divertor Neutron Flux Monitors • Neutron Calibration (2.5 - 14 MeV) (complete) • Neutron Facility Area
Fusion products	• Radial Neutron Camera • Vertical Neutron Camera • Radial Gamma Ray Spectrometer (including runaway electron detection)* • Lost Alpha Monitor* • High Resolution Neutron Spectrometer* • Vertical Gamma Ray Spectrometer* • Tangential Neutron Spectrometer* • Collective Thomson Scattering

** These fusion product diagnostics are planned upgrades of the ITER Baseline.*

Table 11. Overview of experimental activities, estimates of required operational days, and ranges in plasma current and toroidal field within the research program in D plasmas during FPO-1

Experimental Activities	**Days**	I_p **(MA)**	B_t **(T)**
Plasma control/ Plasma scenario development/ Commissioning	**47**		
• Plasma restart, recommissioning and assessment of impact of D on start-up		• 1.0 - 7.5	• 2.65
• Advanced MHD and error field control commissioning (Error Field Correction, ELM control, etc.)		• 3.5 - 15.0	• 1.8 - 5.3
• Advanced plasma kinetic control commissioning (DT mix control, fusion burn control, β control, etc.)		• 3.5 - 15.0	• 1.8 - 5.3
• Scenario development/control of D L-mode plasmas up to 7.5 MA/2.65 T		• 3.5 - 7.5	• 1.8 - 2.65
Commissioning of auxiliary systems	**25**		
• Diagnostics (particularly for fusion products)		• 1.0 - 15.0	• 1.8 - 5.3
• ICRF commissioning (for D and DT operation)		• 3.5 - 15.0	• 1.8 - 5.3
• Heating and Diagnostic NBI commissioning (operation in D and DT plasmas)		• 5.0 - 15.0	• 1.8 - 5.3
Disruption management in D/DT plasmas	**11**		
• Commissioning/ Optimization of disruption prediction/ detection		• 7.5 - 15.0	• 2.65 - 5.3
• Commissioning/ Optimization of disruption mitigation		• 7.5 - 15.0	• 2.65 - 5.3
Divertor and PWI studies in D plasmas (incl. Trace-T)	**12**		
• Wall conditioning (ICWC and ECWC)		• -	• 2.65 - 5.3
• Fuel retention and material migration		• 7.5 - 15.0	• 2.65 - 5.3
Deuterium plasma scenario development and studies (incl. Trace-T)	**84**		
• Development of D plasma scenarios in L-mode up to 15 MA/5.3 T		• 7.5 - 15.0	• 2.65 - 5.3
• Determination of L-H transition power level in D plasmas		• 5.0 - 7.5	• 2.65
• Development of D H-mode plasma scenarios		• 5.0 - 7.5	• 1.8 - 2.65
• Trace-T H-mode experiments		• 7.5	• 2.65

Initial development of long pulse/ steady-state scenarios in Deuterium plasmas	**40**		
• Application of β/current/ pressure control schemes in D H-modes plasmas at 2.65 T		• 4.5 - 6.5	• 2.65
• Optimization of performance and non-inductive current drive at 2.65 T		• 4.5 - 6.5	• 2.65
• Optimization of performance and non-inductive current drive at 4.5 T		• 7.5 - 11.0	• 4.5
Total	**219**		

Table 12. Path to 15 MA/5.3 T (in deuterium)

#	I_p/B_t	**Available heating**		
		P_{ECRH} (MW)	P_{ICRF} (MW)	P_{HNB} (MW)
2	7.5 MA/2.65 T	20	20	33
3	9.5 MA/3.3 T	20	20	33
4	9.5 MA/4.5 T	20	20	33
5	10.5 MA/4.5 T	20	20	33
6	12.5 MA/4.5 T	20	20	33
7	12.5 MA/5.3 T	20	20	33
8	15 MA/5.3 T	20	20	33

Table 13. L-H transition scenarios (in deuterium)

I_p FT (MA)	B_t (T)	Density (f_{GW} %)	Heating mix	q_{95}	
7.5	2.65	40	NBI+ICRF+ECRH	3	Density scan
7.5	2.65	80	NBI+ICRF+ECRH	3	
7.5	2.65	40	NBI	3	Heating mix scan
7.5	2.65	40	ECRH+ICRF	3	
7.5-10%	2.65	40	NBI+ICRF+ECRH	3+10%	q_{95} scan
7.5+10%	2.65	40	NBI+ICRF+ECRH	3-10%	
7.5-10%	2.65	80	NBI+ICRF+ECRH	3+10%	
7.5+10%	2.65	80	NBI+ICRF+ECRH	3-10%	
4.5	2.65	40	NBI+ICRF+ECRH	5	Density scan for H-mode access at q_{95} of steady state scenario
4.5	2.65	80	NBI+ICRF+ECRH	5	

Table 14. Overview of experimental activities, estimates of required operational days, and ranges in plasma current and toroidal field within the DT-plasma research program during FPO-1

Experimental Activities	**Days**	I_p **(MA)**	B_t **(T)**
Optimization of DT H-mode plasmas at 7.5 MA/2.65 T	**66**		
• Determination of H-mode threshold and dependence on D/T ratio and plasma density		• 5.0 - 7.5	• 2.65
• Exploration of DT H-mode operation at 7.5 MA/2.65 T at a range of D/T ratios including: optimization of plasma performance and development of integrated scenarios		• 7.5	• 2.65
Demonstration of $Q \geq 5$ burn for burn lengths of at least 50 s	**130**		
• Expansion of H-mode DT operation from 7.5 MA/2.65 T up to at least 12.5 MA/5.3 T including DT mix optimization and development of fully integrated scenarios		• 7.5 - 12.5	• 2.65 - 4.5
• Optimization of fusion performance to demonstrate $Q \geq 5$ for burn lengths of at least 50 s		• 12.5 - 15.0	• 2.5 - 5.3
Total	**196**		

Table 15. DT scenarios for L-H transition studies during the current flat-top

I_p FT (MA)	B_t (T)	Density (f_{GW} %)	Heating mix	q_{95}	
7.5	2.65	40	NBI+ICRF+ECRH	3	Density scan with 10% T
7.5	2.65	80	NBI+ICRF+ECRH	3	
7.5	2.65	40	NBI+ICRF+ECRH	3	Density scan with 50% T
7.5	2.65	80	NBI+ICRF+ECRH	3	
7.5	2.65	40	NBI	3	Heating mix scan with 50% T
7.5	2.65	40	ECRH+ICRF	3	

Table 16. DT scenarios for L-H transition studies during the current ramp-up

I_p (MA)	B_t (T)	Density (f_{GW} %)	Heating mix	q_{95}	
5	2.65	40	NBI+ICRF+ECRH	4.5	Density scan with 50% T
5	2.65	80	NBI+ICRF+ECRH	4.5	

Table 17. Overview of experimental activities, estimates of required operational days, and ranges in plasma current and toroidal field within the research program for FPO-2

Experimental Activities	**Days**	I_p **(MA)**	B_t **(T)**
Plasma control/ Plasma scenario development/ Commissioning	**45**		
• Plasma restart and recommission of previously installed systems		• 1.0 - 15.0	• 2.65 - 5.3
• Commissioning of new ancillary systems and associated control and interlock systems		• 7.5 - 15.0	• 2.65 - 5.3
• Commissioning of new control systems to facilitate high-Q long burn duration operation: MHD control, kinetic control, Disruption mitigation, etc.		• 7.5 - 15.0	• 2.65 - 5.3
Demonstration of Q = 10 for burn duration of at least 50 s	**50**		
• Expansion of high-Q operation with burn duration of at least 50 s from $Q \sim 5$ to $Q = 10$		• 12.5 - 15.0	• 4.5 - 5.3
Demonstration of Q = 10 for burn duration of 300-500 s	**85**		
• Expansion of operation for $Q > 10$ for transient burn durations of tens of seconds		• 15.0	• 5.3
• Increase of Q from 5 to 10 at burn durations of 300 - 500 s		• 15.0	• 5.3
Exploration of $Q > 10$ operation	**15**		
• Wall conditioning (ICWC and ECWC)		• -	• 2.65 - 5.3
• Optimization of H&CD and plasma confinement to achieve $Q > 10$ for burn lengths of 300 - 500 s		• 7.5 - 15.0	• 2.65 - 5.3
Development of long pulse operation with $Q \leq 2$ for burn durations of 1000 s	**120**		
• Application of control schemes for b, current and pressure profile in stationary DT plasmas at 2.65 T and 5.3 T with q_{95} = 3.5 - 4.0		• 5.5 - 12.5	• 2.65 - 5.3
• Development of long-pulse scenarios at 2.65 T with q_{95} = 3.5 - 4.0		• 5.5 - 6.5	• 2.65
• Development of long-pulse scenarios at 5.3 T with q_{95} = 3.5 - 4.0 and fusion power optimization up to $Q \sim 2$ with 1000 s burn duration		• 5.5 - 12.5	• 2.65 - 5.3
Development of steady-state operation up to $Q \leq 2$ for burn duration of 3000 s	**100**		
• Development of steady-state scenarios with q_{95} = 4.5 - 5.0 and fusion power optimization up to $Q \sim 2$		• 7.5 - 10.0	• 2.65 - 5.3

• Optimization of fusion power and non-inductive current fraction at 5.3 T with q_{95} = 4.5 - 5.0 up to the achievement of Q ~ 2 with 3000 s burn duration		• 10.0 -12.5	• 5.3
Total	**415**		

Table 18. Overview of experimental activities, estimates of required operational days, and ranges in plasma current and toroidal field within the research program for FPO-3

Experimental Activities	**Days**	I_p **(MA)**	B_t **(T)**
Plasma control/ Plasma scenario development/ Commissioning	**60**		
• Plasma restart and recommission of previously installed systems		• 1.0 - 15.0	• 2.65 - 5.3
• Commissioning of new ancillary systems and associated control and interlock systems		• 7.5 - 15.0	• 2.65 - 5.3
• Commissioning of new control systems to enable $Q \geq 5$ and long pulse/steady-state operation: MHD control, kinetic control, Disruption mitigation, etc.		• 7.5 - 15.0	• 2.65 - 5.3
Demonstration of $Q \geq 5$ (long pulse) for burn duration of 1000 s	**155**		
• Expansion of long pulse operation (1000 s burn) from $Q \sim 2$ to $Q \geq 5$: optimization of confinement, current drive and control of MHD plasma stability		• 9.0 - 15.0	• 4.5 - 5.3
• Determination of maximum Q ($Q > 5$) achievable in long pulse scenarios with 1000 s burn length		• 11.0 - 15.0	• 5.3
Demonstration of $Q \geq 5$ (steady-state) for burn duration of 3000 s	**200**		
• Expansion of steady-state operation (3000 s burn) from $Q \sim 2$ to $Q \geq 5$: optimization of confinement, current drive and control of MHD plasma stability		• 7.5 - 10.0	• 4.5 - 5.3
• Determination of maximum Q ($Q > 5$) achievable in (non-steady state scenarios) with 3000 s burn duration		• 10.0 - 12.5	• 5.3
Total	**415**		

Table 19. New phenomena in DT plasmas and expected effects

New phenomena expected in DT	**Expected effects and potential issues**	**Experience from ITER H/He and D phases and present devices**	**Required additional dedicated experimental study during DT phase**
Significant increase of plasma heating power: ~150 MW in DT vs 73 MW in D	Higher heat loads in divertor, ELM control, divertor performance, effect on plasma core confinement, H-mode	Similar or higher power densities have been achieved in present experiments for short pulses	Explore high-$Q > 10$ regimes consistent with low divertor load, low tritium retention
He ash accumulation	Plasma dilution, reduction of fusion power	Externally introduced He	Investigate He profiles in the core plasma; study of He exhaust
Self-heating by fusion α-particles	Burn control issues such as transients in fusion power, profile control, etc.	Model experiments with $P \sim W^2$ possible	Plasma control with minimized auxiliary power
Fast α-particle population in the plasma core	Additional drive for AE instabilities can cause α-particle loss, reduction of heating, localized heat loads on FW; expect AE phenomena to be enhanced in long-pulse plasmas with higher q; effect of α-particles on MHD phenomena; additional wall erosion by α's	AEs driven by NBI and ICRF minority fast ions in other devices, as well as in ITER H/He and D phases	Exploration of stability limits; investigation of loss/redistribution vs plasma parameters
Isotope effect on plasma confinement and edge plasma performance	Positive effect on plasma confinement and L-H transition is expected; scenario adjustment and optimization could be required	Experience with H, He, D, DT and T plasmas in other devices and in the previous phases of ITER	Extend ρ^* scaling experiments to DT operation

Table 20. Overview of experimental activities and estimates of required operational days for the first 3 campaigns of the FPO research program

Activity	Days
D Plasmas	**219**
Plasma scenario and control commissioning (FPO-1)	47
Auxiliary system commissioning	25
Disruption management	11
Divertor and PWI studies	12
Experimental studies in D plasmas	124
DT Plasmas	**1026**
Plasma scenario and control commissioning (FPO-2, FPO-3)	105
Optimization of DT H-mode plasmas as 7.5 MA/2.65 T	66
Development of DT H-mode plasmas towards $Q \geq 5$ for ≥50 s	130
Development of DT H-mode plasmas towards $Q \geq 10$ for ≥50 s	50
Extension of DT H-mode operation towards $Q \geq 10$ for 300 - 500 s	85
Exploration of high fusion gain operation in DT with $Q > 10$	15
Initial development of DT long pulse scenarios with $Q \leq 2$ for ~1000 s	120
Initial development of DT (non-inductive) steady-state scenarios with $Q \leq 2$ for	100
Expansion of DT long pulse scenarios towards $Q \geq 5$ for ~1000 s	155
Exploration of DT (non-inductive) steady-state scenarios towards $Q \geq 5$ for	200
Total	**1245**

ITER Research Plan within the Staged Approach - Figures

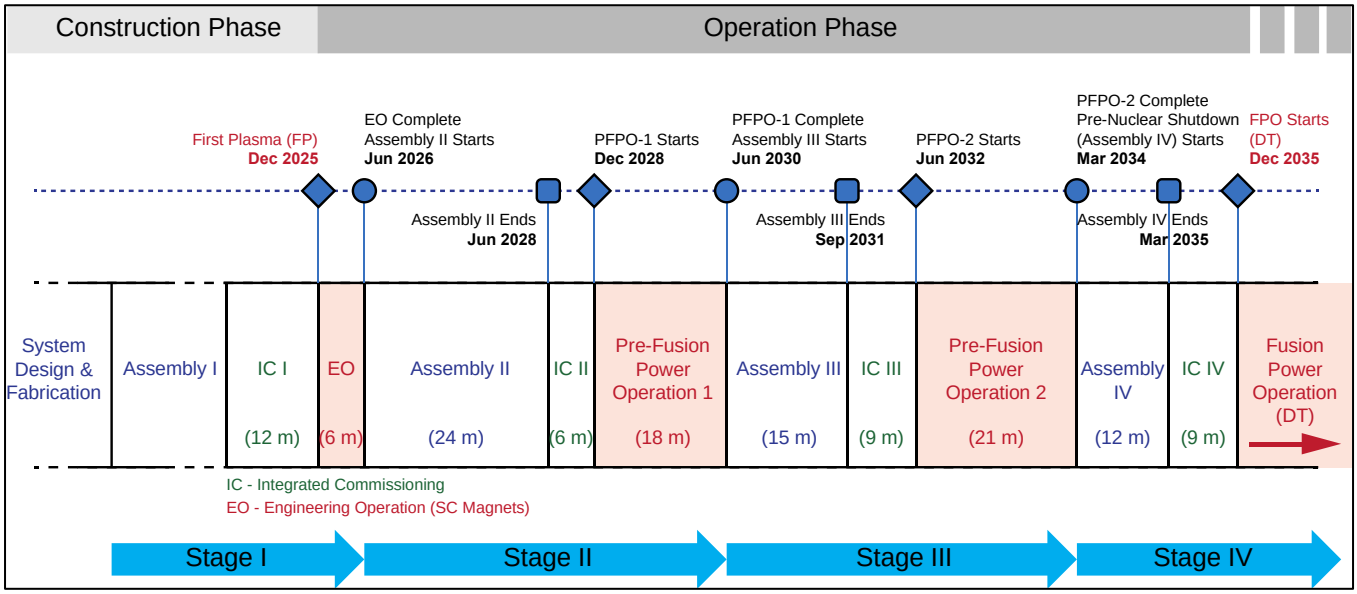

Figure 1. Schematic overview of the 'Staged Approach' strategy for the ITER Construction and initial Operations Phases. The diagram illustrates the transition from Construction via Integrated Commissioning to First Plasma and the subsequent sequence of Assembly, Commissioning and Operations periods as the facility is brought to its full capability for fusion power studies in deuterium-tritium plasmas during the Fusion Power Operation phase. Note that the dates shown for the sequence of events during the Operation Phase are based on the Baseline Schedule developed in 2016.

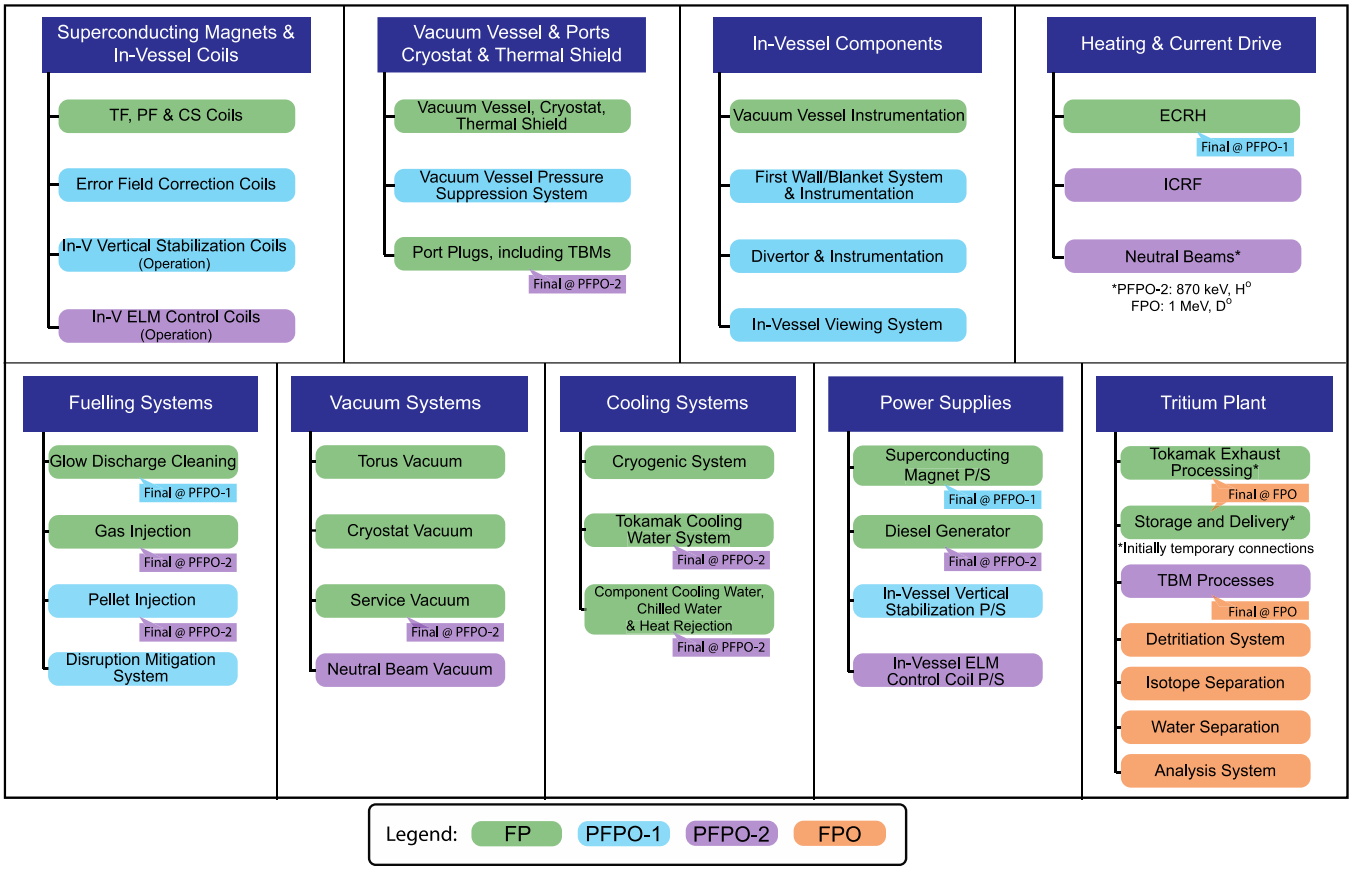

Figure 2. Schematic of the ITER 'Plant Configuration' at each phase of the Staged Approach, with the colour code indicating the stage at which each system becomes fully operational.

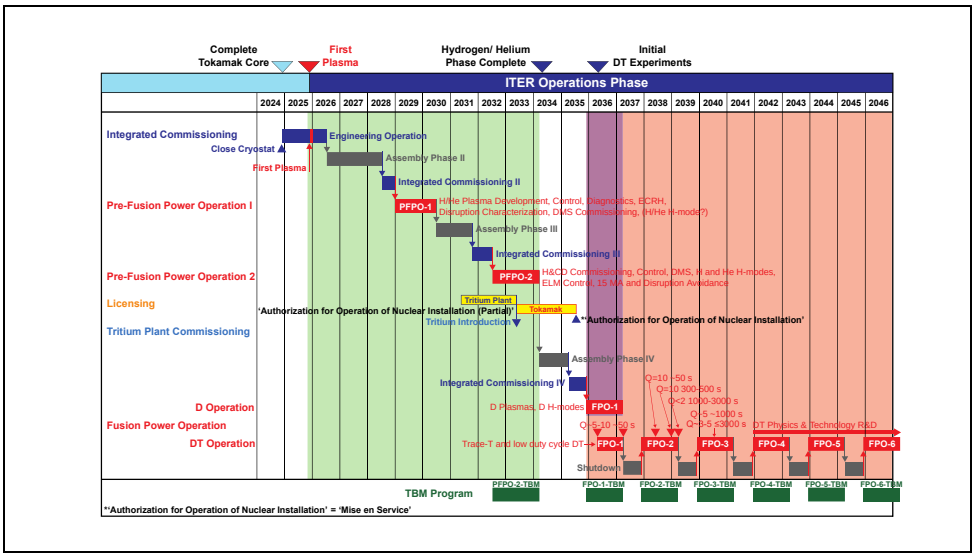

Figure 3. Schematic overview of the major experimental campaigns during the first 20 years of the ITER Research Plan within the Staged Approach integrated with the foreseen sequence of Assembly, Commissioning and Shutdown (Maintenance/ Upgrade) periods. The timing of the major milestones within this plan, in particular, First Plasma and the transition to DT operation, reflect the revised ITER Baseline Schedule endorsed by the ITER Council in November 2016 and may be subject to revision. The blocks labelled 'TBM Program' at the bottom of the figure indicate successive phases of the testing program for tritium breeding modules which will involve both variation in the functionality of the TBMs and evolution in the TBM concepts under test, as discussed in Section 4. Note that the dates shown for the sequence of events during the Operation Phase are based on the Baseline Schedule developed in 2016 and may be subject to revision.

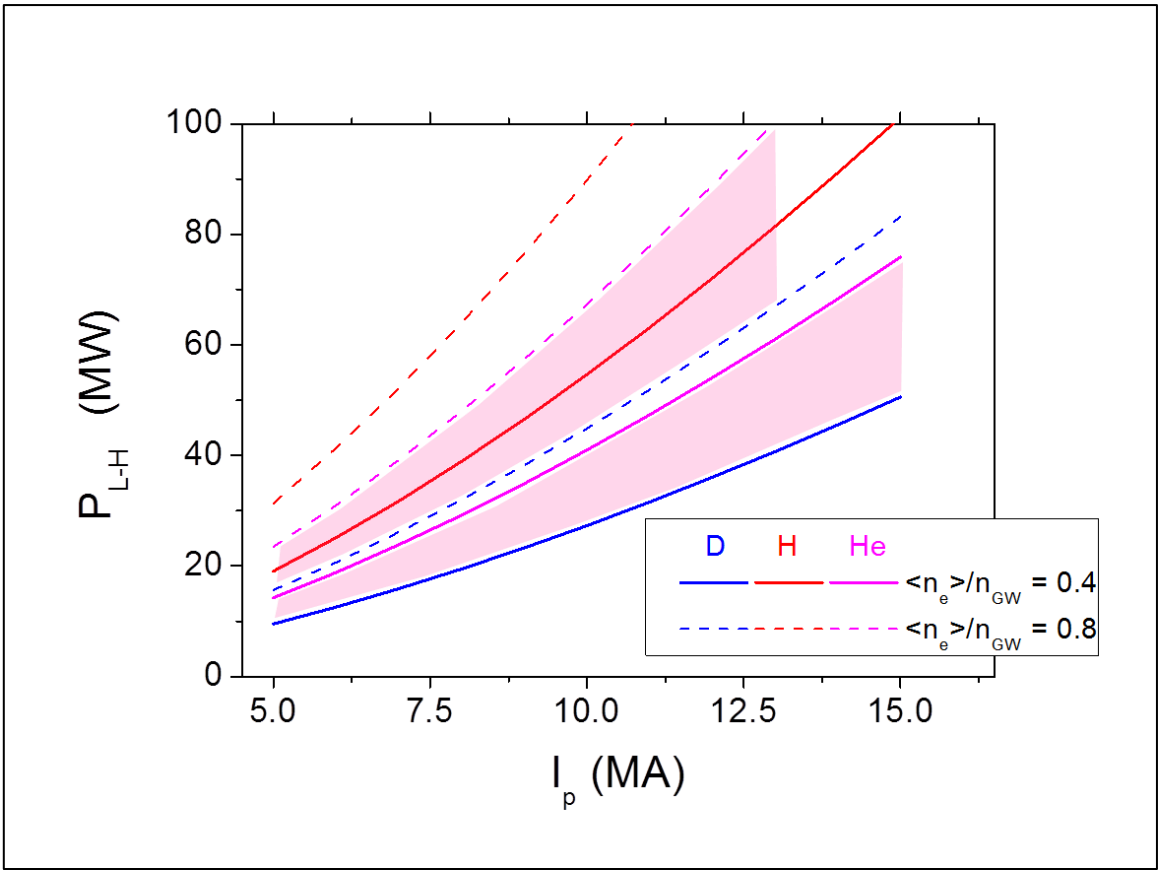

Figure 4. Expected L-H threshold power on the basis of the scaling of Eq. (1) for H, He and D plasmas in ITER over a range of plasma currents at q_{95} = 3 and for two values of the plasma density. For He plasmas the range $P_{th,He} = [1\ to\ 1.5] \times P_{th,D}$ is shown.

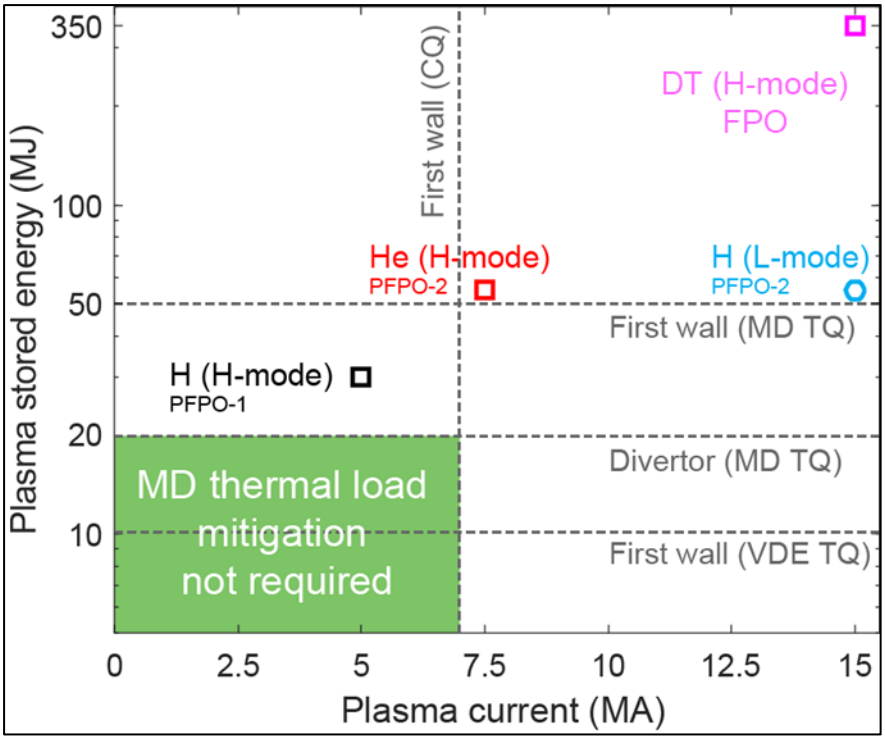

Figure 5. Predicted disruption loads over the operational range of ITER in terms of thermal plasma energy and plasma current, illustrating the operational space over which disruption mitigation is, or is not (green shaded area), required. Thermal load limits during the thermal quench are indicated by horizontal dotted lines and during the current quench by the vertical dotted line. The green area indicates the parameter range for which melt damage from unmitigated disruptions is not expected. The symbols indicate the target values for the planned operational scenarios associated with key IRP plasma target milestones (NB: loads associated with loss of runaway electrons are not included; updated from original version in [87]).

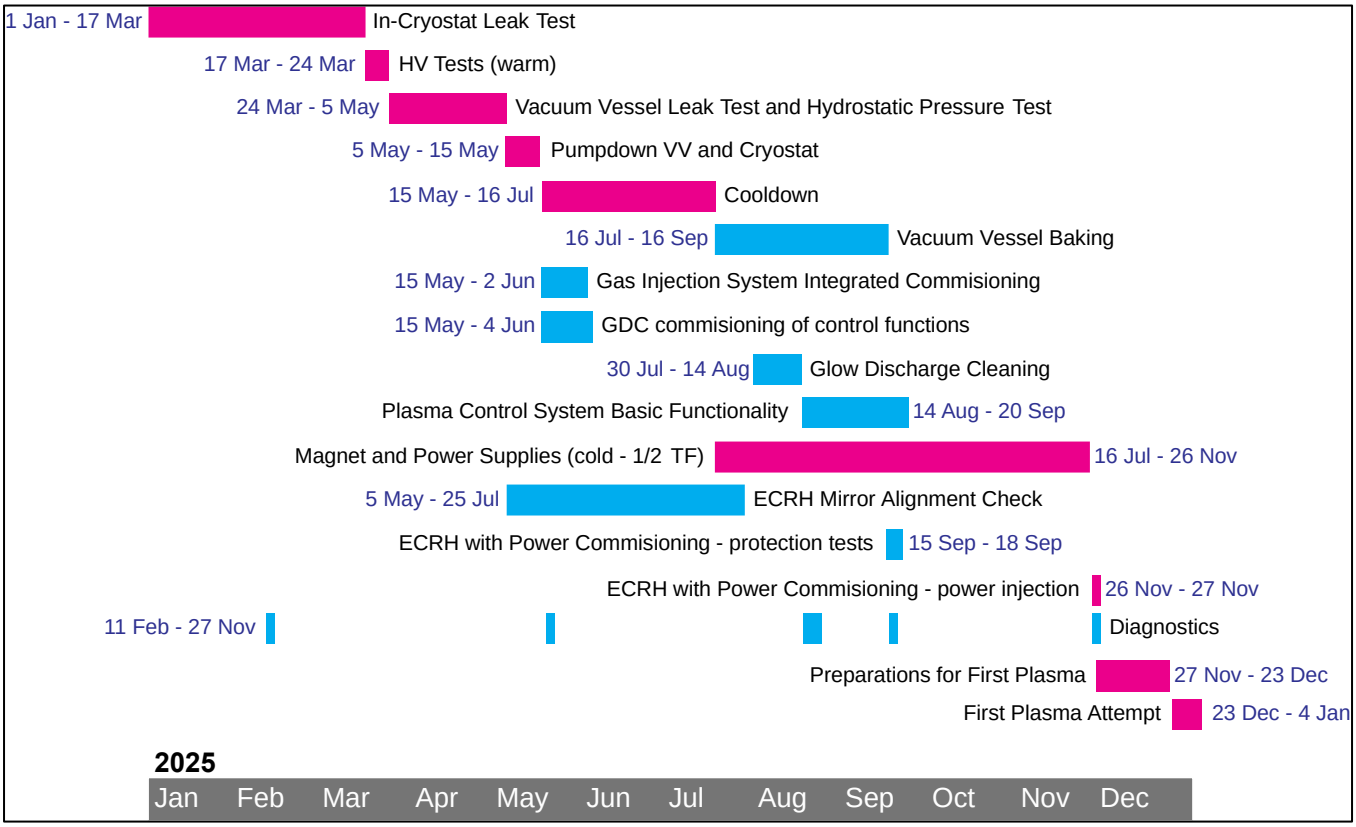

Figure 6. Schematic of the sequence of events during: Integrated Commissioning, First Plasma and Engineering Operation.

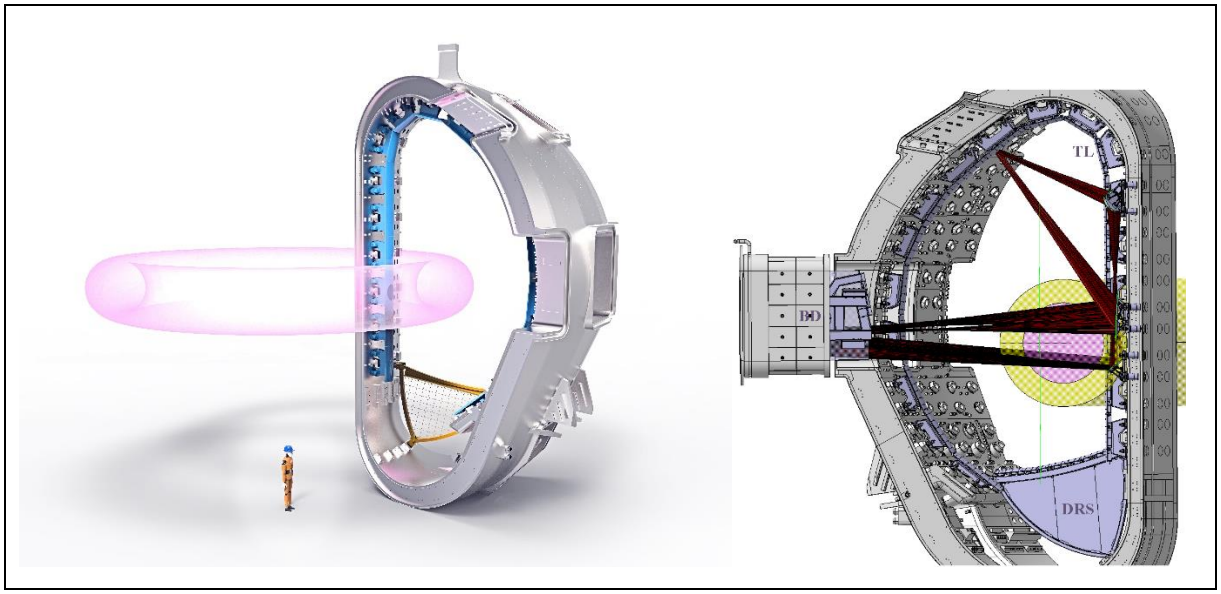

Figure 7. Schematic of the First Plasma Protection Components which will be installed in the ITER vacuum vessel to protect the vacuum vessel during the First Plasma campaign including 4 Temporary Limiters, Divertor Replacement Structure and ECRH mirrors and dump. The Divertor Replacement Structure a is installed in the lower part of the vacuum vessel, blocking the entrance to the divertor sub-volume, at a different toroidal location to the 4 Temporary Limiters.

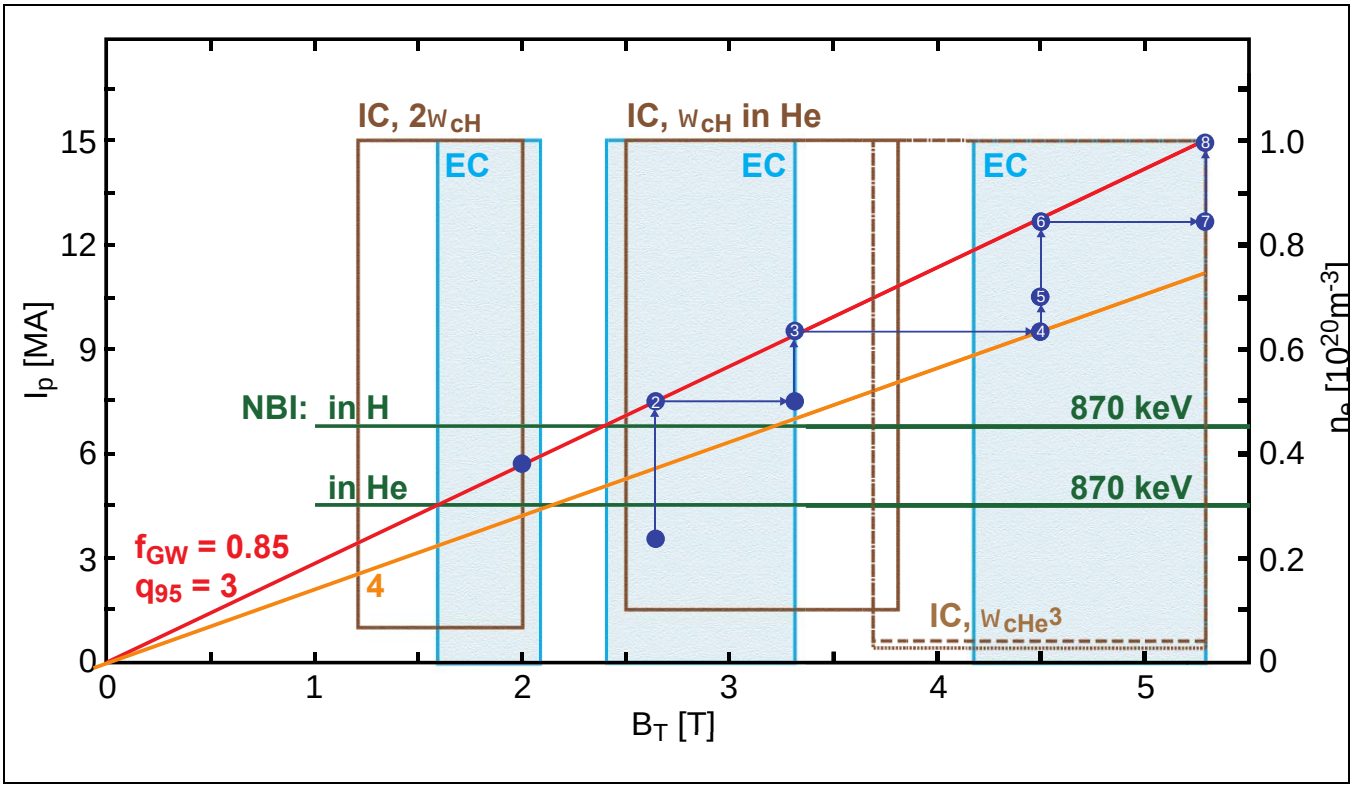

Figure 8. Operational range of H&CD systems over the relevant B_T, I_p and density range in ITER for H and He plasmas in PFPO and for DT plasmas in FPO. The red line corresponds to 0.85×n_{GW} at the corresponding current value. EC, IC and NBI operation ranges are in blue, brown and green respectively. The highlighted points and arrows indicate possible operational paths (in I_p, n_e versus B_T space) from 7.5 MA/2.65 T plasmas towards 15 MA/5.3 T L-mode operation.

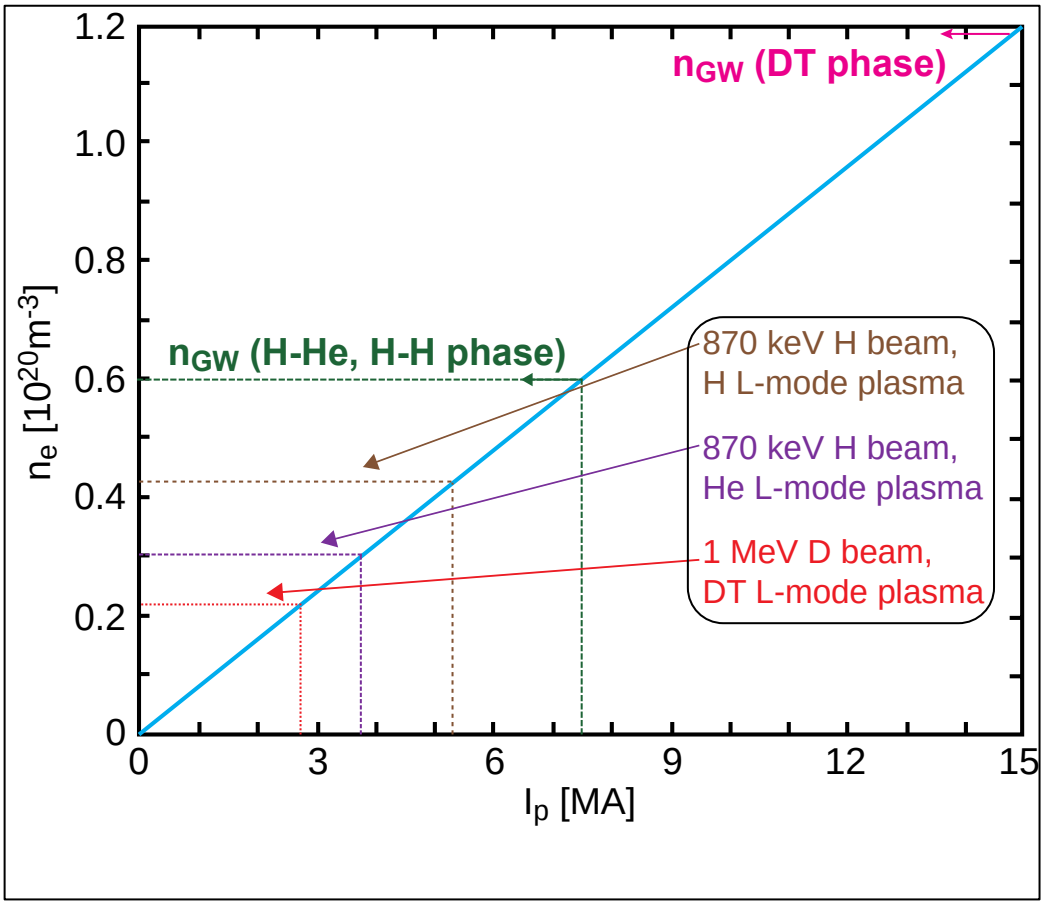

Figure 9. Shine-through limits for a range of densities, n_e, and plasma current, I_p, and various HNB beam energies and species (870 keV H beams for H/He plasmas and 1 MeV D beams for D/DT plasmas).

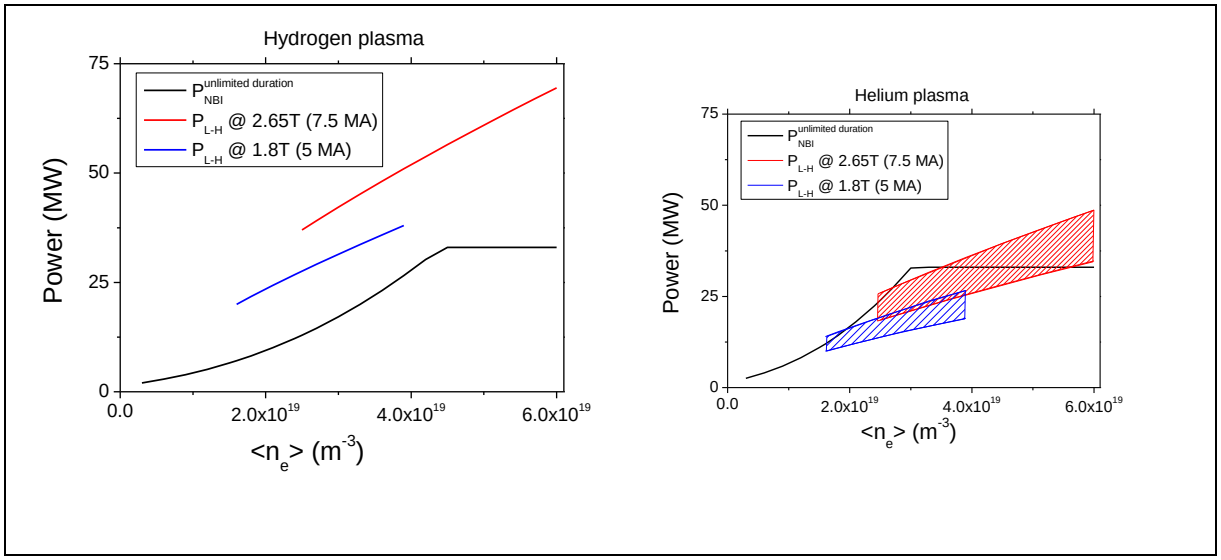

Figure 10. Maximum heating power which can be applied with unlimited duration versus plasma density with acceptable are shine-through loads for plasmas at 5 MA/1.8 T and 7.5 MA/2.65 T in (left) hydrogen and (right) helium. The red and blue lines (or shaded areas) show the expected H-mode threshold power for these plasma conditions and the density range of n_e = 0.4 - 1.0×n_{GW}, where n_{GW} (5 MA) = 4.0×10^{19} m^{-3} and n_{GW} (7.5 MA) = 6.0×10^{19} m^{-3}.

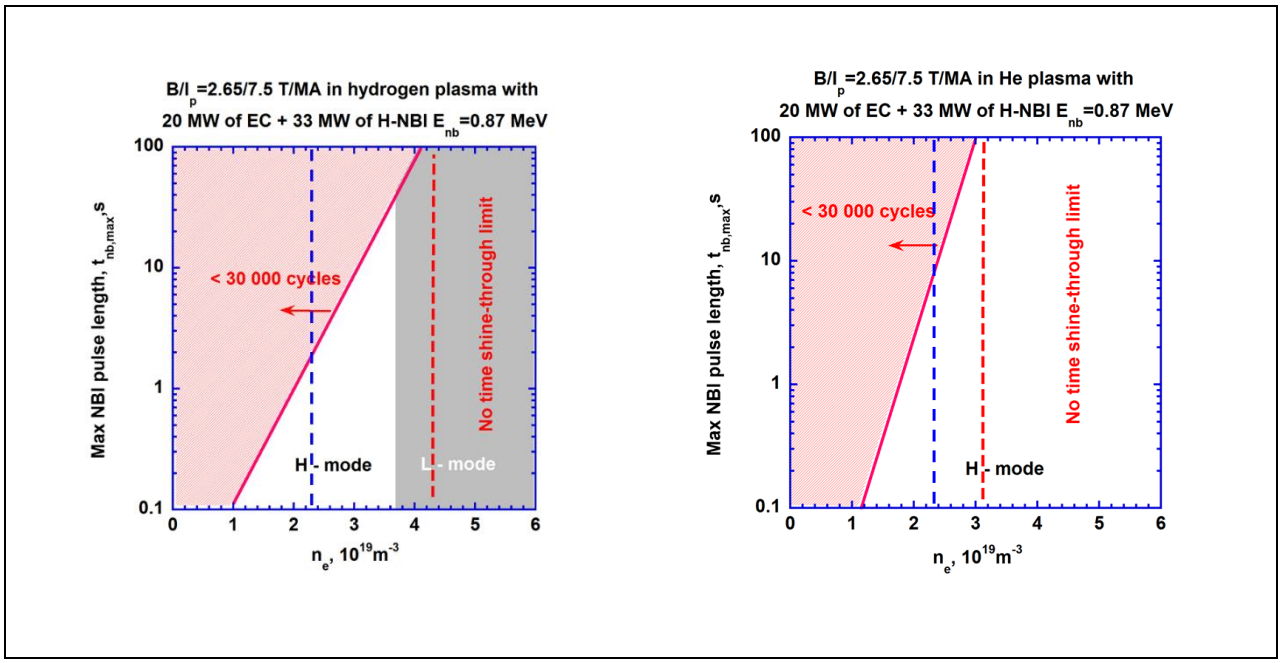

Figure 11. Duration of the NBI heating pulse at maximum power (33 MW at 870 keV) versus plasma density with acceptable shine-through loads for (left) hydrogen and (right) helium plasmas at 7.5 MA/2.65 T. The vertical red dashed line corresponds to the density for which NBI at full power can be applied without any limitation in heating pulse length and the vertical blue line to $n_e = 0.4 \times n_{GW}$; for densities lower than these, the scaling providing the H-mode threshold power in ITER is not expected to be valid.

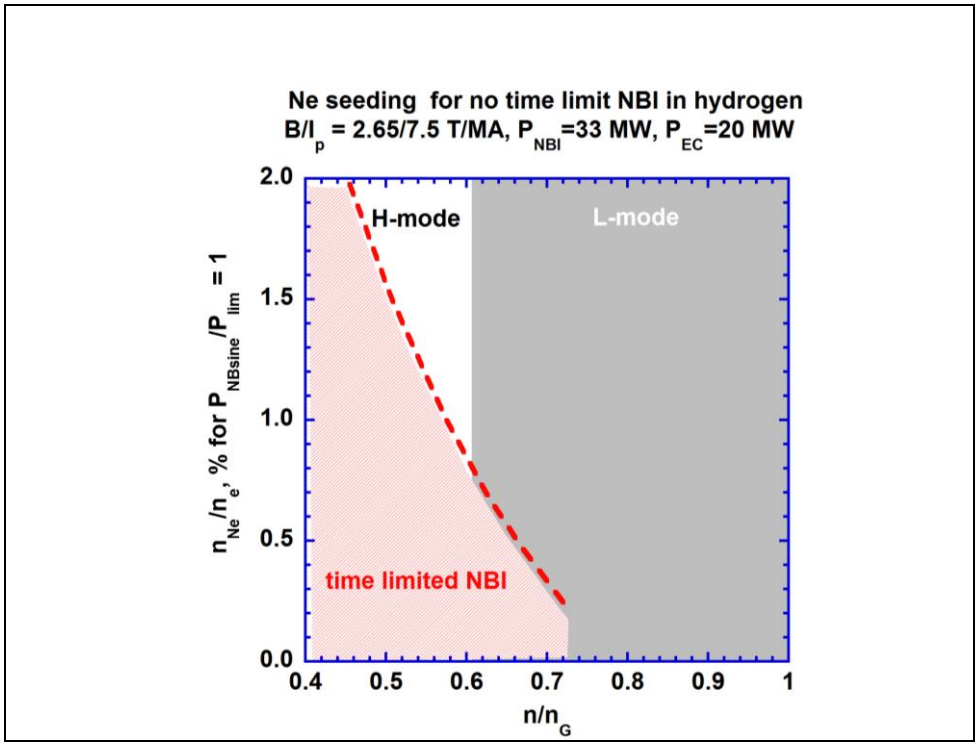

Figure 12. Required neon concentration, n_{Ne}/n_e, for unlimited application of full power NBI heating with acceptable shine-through loads in hydrogen at 7.5 MA/2.65 T vs. plasma density normalized to Greenwald density, n/n_G, showing the density range in which H-mode access is possible.

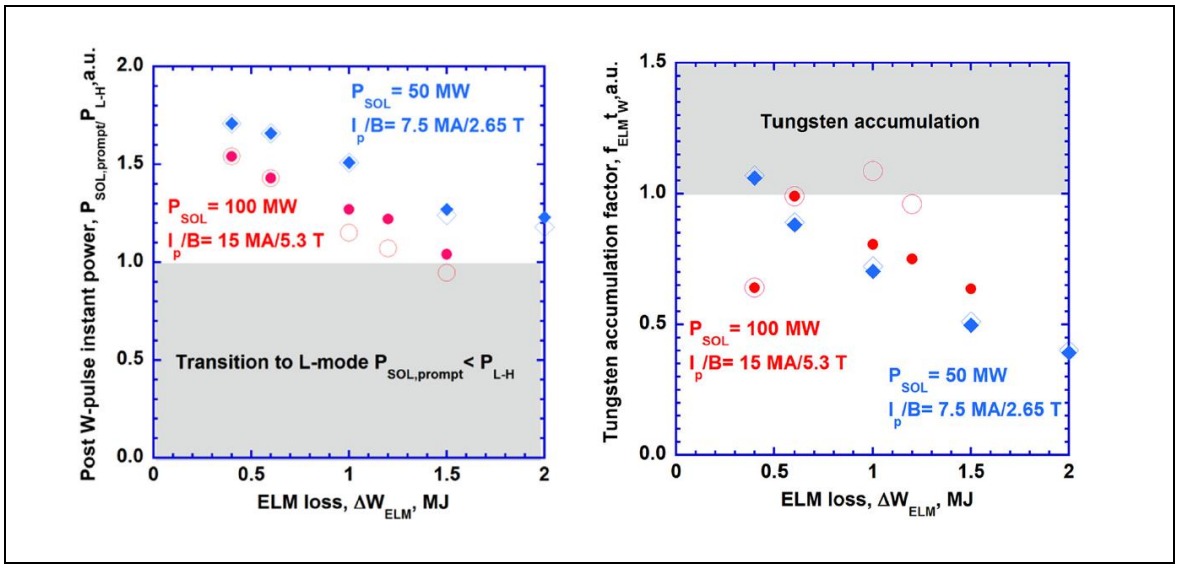

Figure 13. H-mode operating space for I_p/B_t = 15 MA/5.3 T with separatrix power, P_{SOL} = 100 MW, and for I_p/B_t = 7.5 MA/2.65 T with P_{SOL} = 50 MW, assuming no prompt W redeposition at the divertor during ELMs ($P_{ELM} = f_{ELM}\times\Delta W_{ELM} = 0.2\times P_{SOL}$). Open symbols correspond to a diffusive ELM transport model, while filled symbols correspond to a convective model. The ratio of power to the SOL, $P_{SOL,prompt}$, which decreases due to the post-ELM W influx, to the L-H power threshold is shown on the left. Sustainment of H-mode conditions w/o hysteresis, $P_{SOL,prompt}/P_{LH} > 1$, restricts the ELM size at the level $\Delta W_{ELM} \leqslant 1.2$ MJ for the model for the ELM. The tungsten accumulation factor, $F_{W,a} = f_{ELM}\times t_W$ (where t_W includes the time duration of the W impurity influx from ELMs and the timescale for its decay after ELMs) is shown on the right. W accumulation is predicted to occur when $F_{W,a} = f_{ELM}\times t_W \geqslant 1$, conditions which are shown in grey.

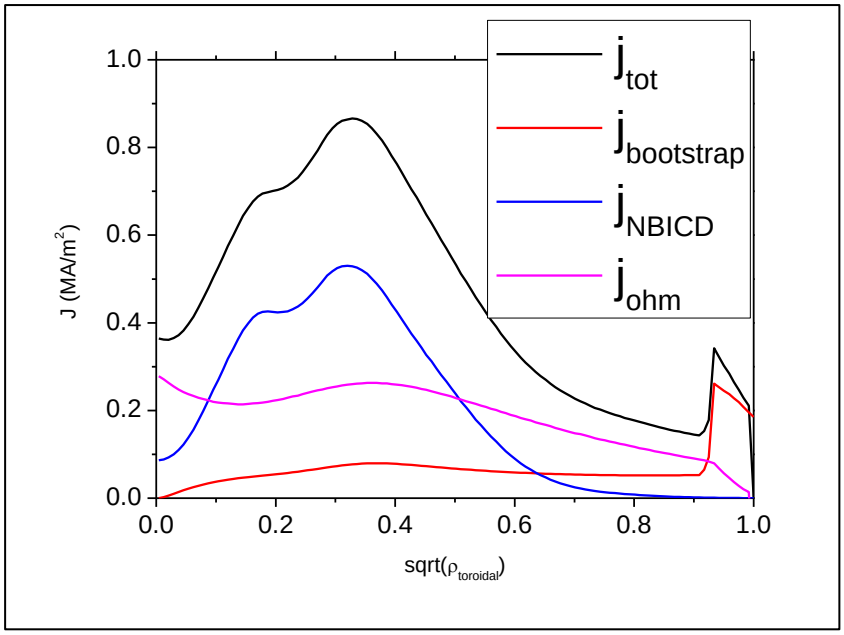

Figure 14. Radial current profile, *j*, as a function of the normalized toroidal flux, sqrt($\rho_{toroidal}$), for a 7.5 MA/2.65 T He H-mode with 33 MW of NBI, 20 MW of ECRH and 20 MW of ICRF showing the main contributions to the total current (bootstrap, NBICD and ohmic).

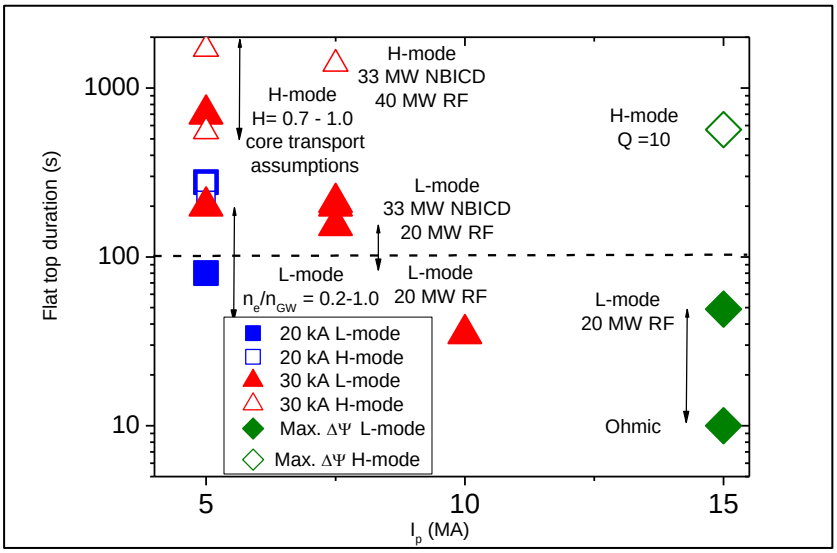

Figure 15. Flat-top duration versus plasma current, I_p, for a range of premagnetization currents and scenarios for each current level.

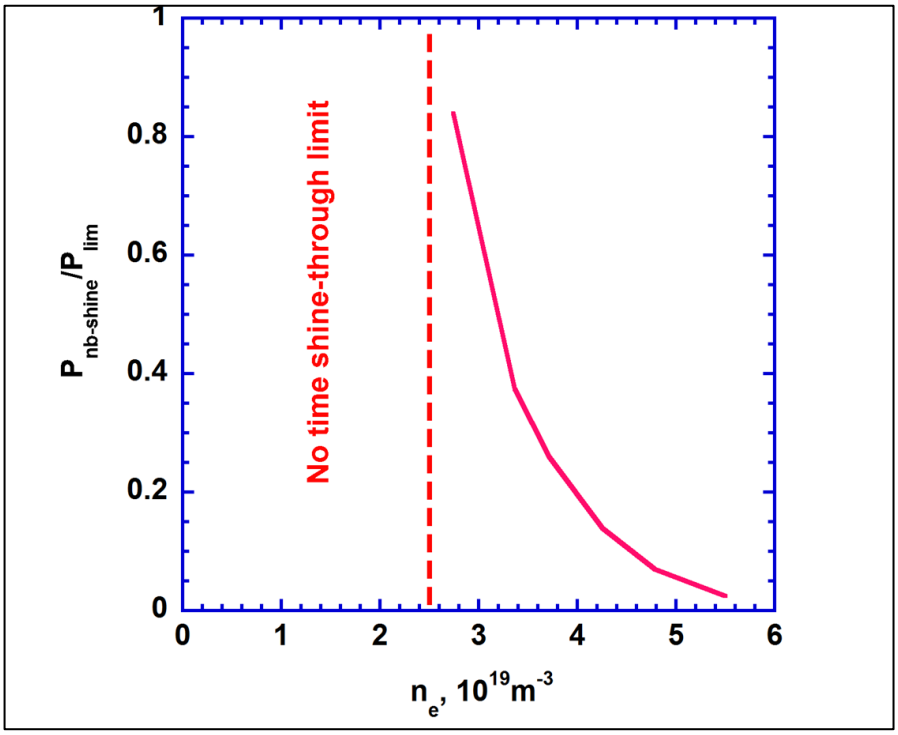

Figure 16. Normalized NBI shine-through loads (i.e., ratio of FW heat load due to shine-through to the value required for unlimited application of 33 MW of NBI power) for 1 MeV D^0 beams in D plasmas versus plasma density.

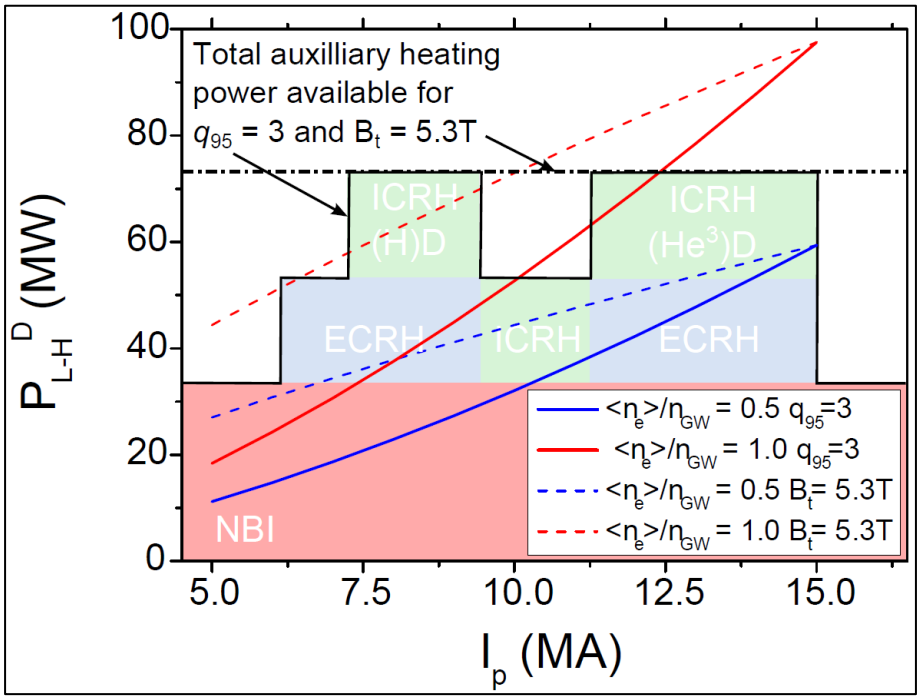

Figure 17. Dependence of the L-to-H power threshold, $P_{L\text{-}H}$, in D plasmas versus current, I_p. The available heating power with central deposition profiles ($\rho < 0.5$) for operation at q_{95} = 3 and B_t = 5.3 T is also shown.

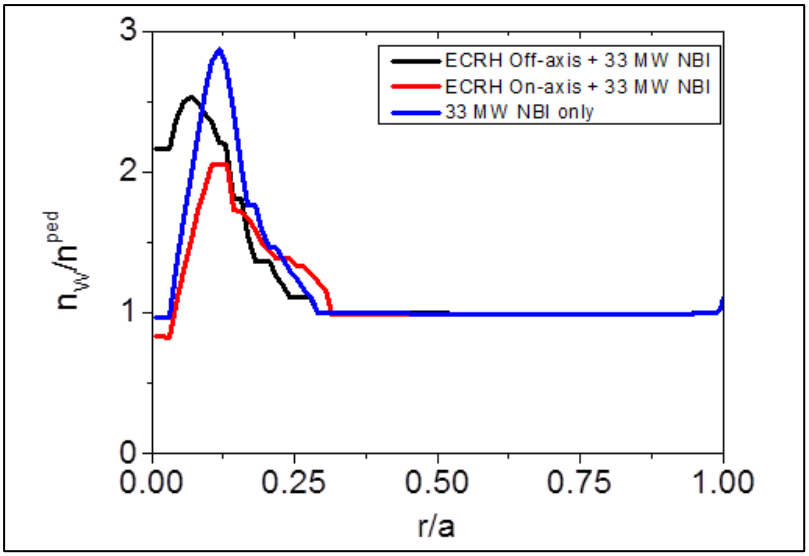

Figure 18. W density profiles, normalized to the pedestal value, n_W/n_{ped}, as a function of normalized minor radius, r/a, for DT 7.5 MA/2.65 T plasmas in ITER with 33 MW of NBI and 0/20 MW of RF for a range of heating schemes modelled with ASTRA. Where anomalous transport is negligible, core particle and energy transport assumptions are those of neoclassical transport for DT ions and electrons [195].

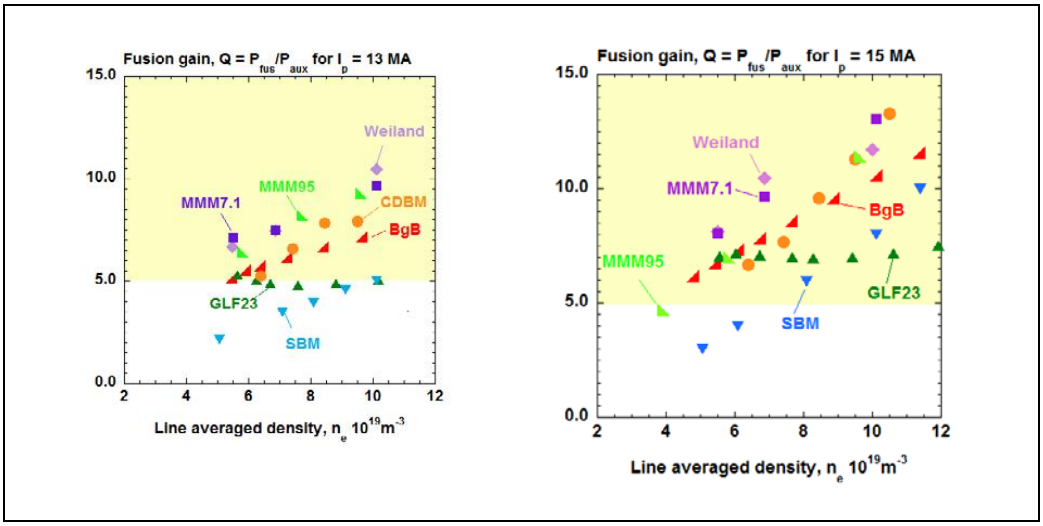

Figure 19. Fusion gain factor, *Q*, predicted by different core transport models for ITER 13 MA (left) and 15 MA (right) DT plasmas with P_{aux} = 50 - 53 MW. The predictions with the scaling based model (SBM) correspond to $H_{98}(y,2)$ = 1 [200].

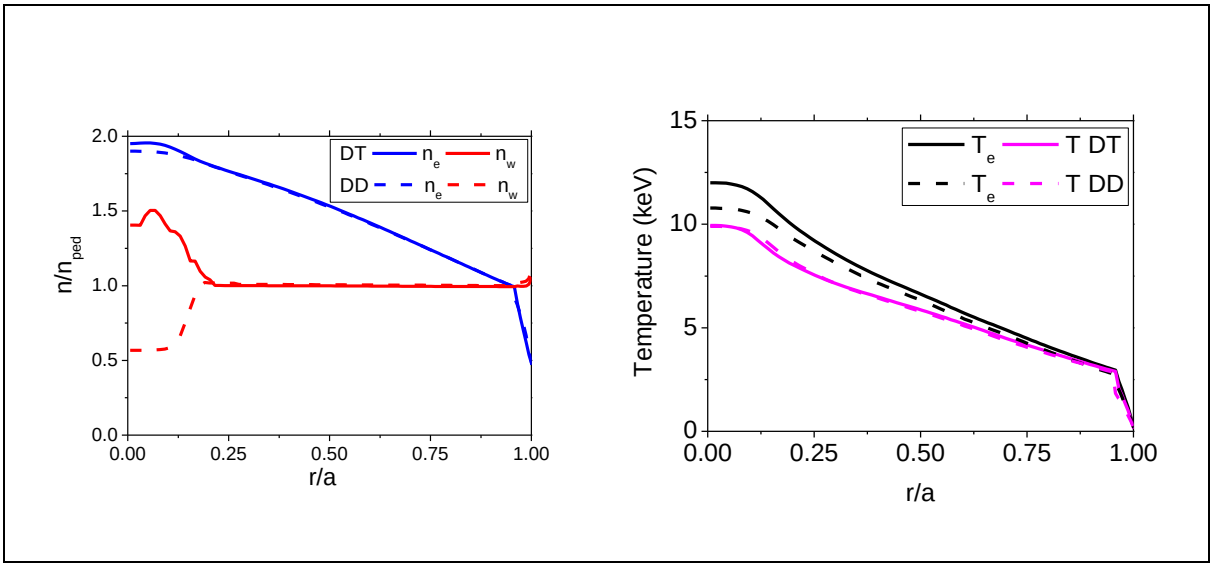

Figure 20. Simulated plasma density and W profiles normalized to the corresponding pedestal values, n_{ped}, (left) and electron and ion temperature profiles (right) plotted against normalized minor radius, r/a, for two 7.5 MA/2.65 T plasmas in ITER with P_{aux} = 50 - 53 MW, one in D and the other in DT. Due to neoclassical transport effects associated with the different masses of D and T, the density profiles are more peaked for DT than for D plasmas in the central plasma region, leading to an increased W peaking in DT compared to D plasmas [195].

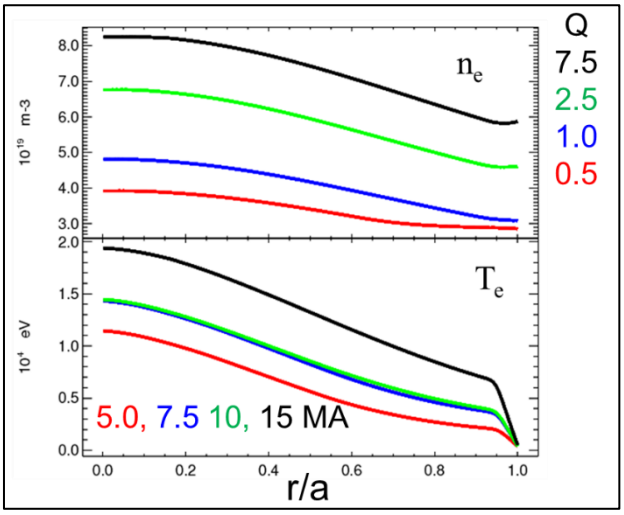

Figure 21. JINTRAC modelling of gas-fuelled DT H-mode plasmas for a range of plasma currents, with P_{NBI} = 33 MW, P_{ECRH} = 20 MW using the GLF23 core transport model. Note the low density gradients in the pedestal, the high pedestal and overall plasma temperatures, and achieved Q values. (a) Electron density (top) and temperature (bottom) profiles for the maximum DT gas puff rates that could be applied at 5 MA (red), 7.5 MA (blue), 10 MA (green) and 15 MA (black) without reaching full divertor detachment [194].

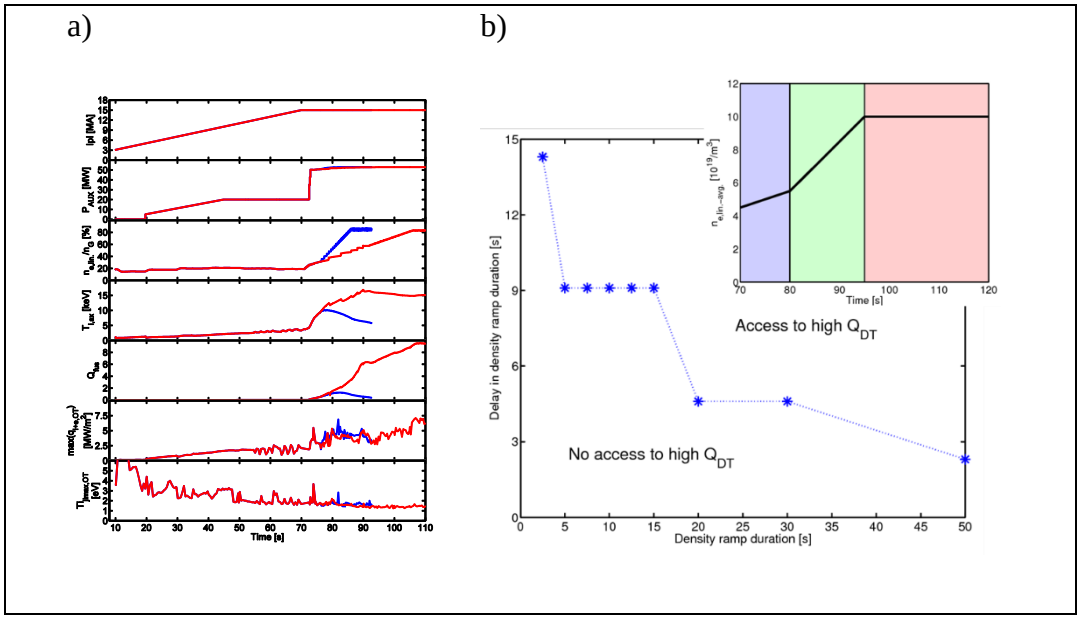

Figure 22. (a) Modelled current ramp-up for ITER DT baseline scenario with L-H transition at 15 MA, with slow (red) and fast (blue) pellet density ramp after the transition. From top to bottom: plasma current, I_{pl}, auxiliary heating level, P_{AUX}, line-average density, $n_{e,lin}$, central ion temperature, $T_{i,ax}$, fusion gain, Q_{fus}, and maximum divertor power flux, max($q_{i+e,OT}$) and ion temperature at the outer divertor target, $Ti_{jimax,OT}$. The divertor power flux does not exceed 10 MWm^{-2} in the H-mode access phase. (b) Operational space for the achievement of a transition to high-$Q_{DT} \sim 10$ for 15 MA/5.3 T H-modes with $P_{AUX} = 53$ MW in terms of the duration of the pellet fuelled ramp to the nominal density (green phase in inset) and of the delay in pellet fuelling with respect to the start of the high heating power, indicated by the blue phase in inset (adapted from [166] and [202]).

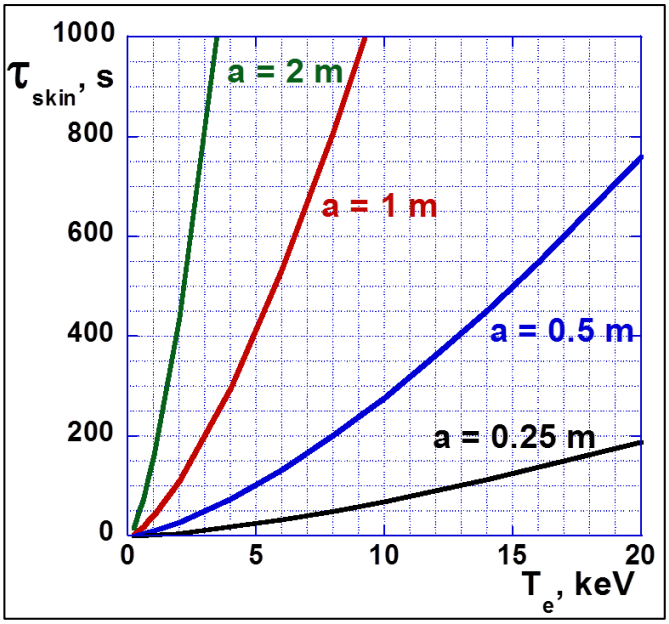

Figure 23. Current relaxation time in ITER, as characterized by the skin time, $\tau_{skin} = \mu_0 a^2/\rho_{par}$, with Spitzer resistivity and $Z_{eff} = 1.2$) for several values of the plasma minor radius as a function of electron temperature, T_e.

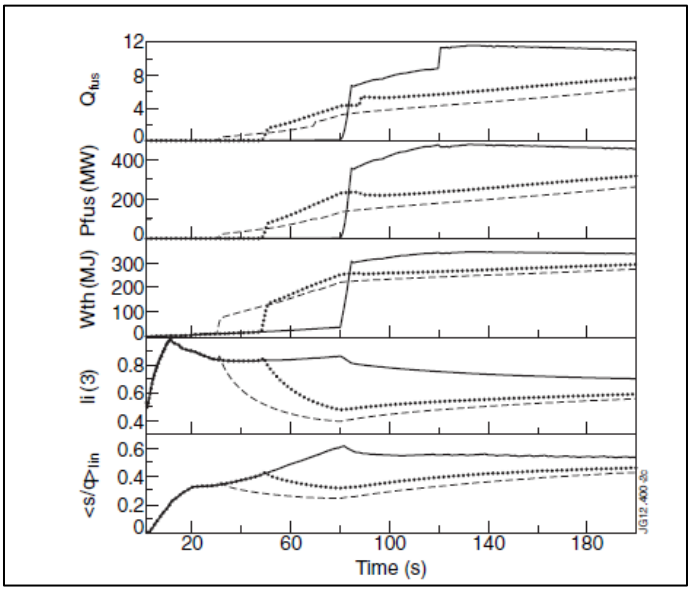

Figure 24. From top to bottom: fusion gain, Q_{fus}, fusion power, P_{fus}, plasma thermal energy, W_{th}, plasma internal inductance, $l_i(3)$ and line-averaged ratio of magnetic shear to safety factor, $\langle s/q \rangle$, as a function of time for ITER JINTRAC simulations of the entrance to burn, showing: a reference case with the L-H transition at 15 MA (solid), and two simulation cases with early L-H transition, at 10 MA (dotted) and 7 MA (dashed), showing the long-term evolution of the fusion power over timescales exceeding 50 s as the current profile shape relaxes. In the last case a Greenwald density fraction of 60% was applied to avoid the NB shine-through limit after the transition [205].

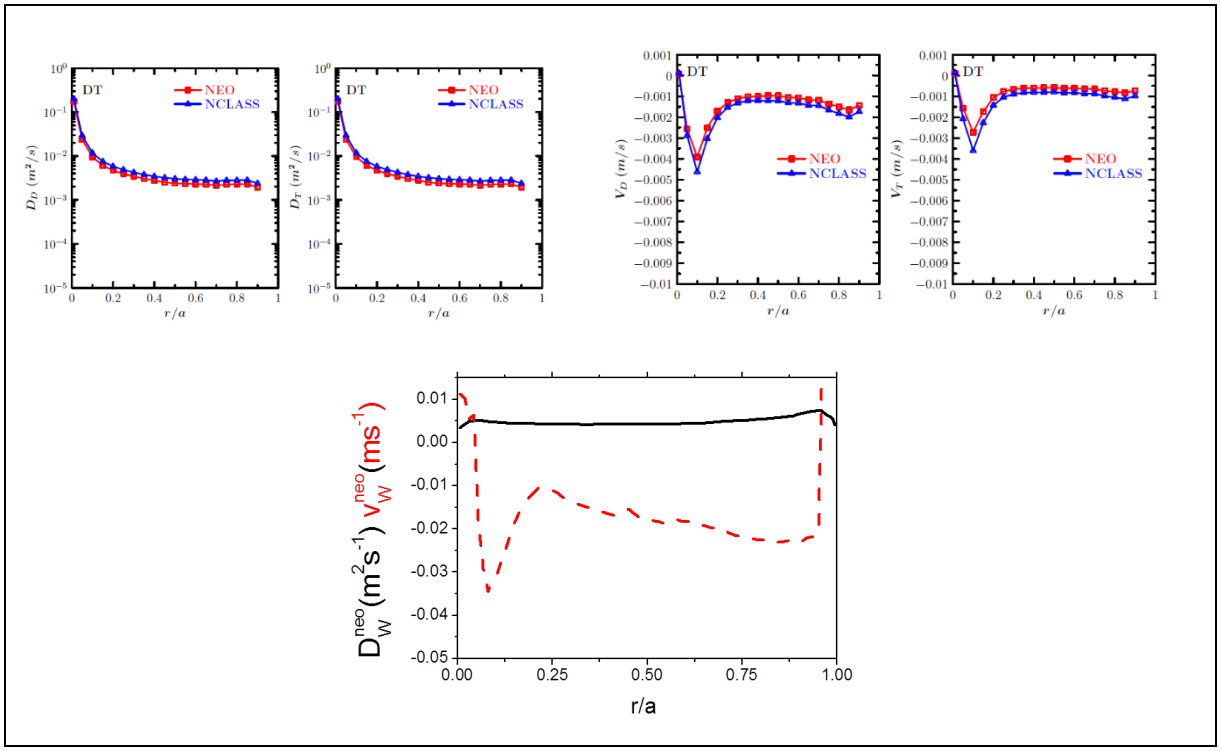

Figure 25. Top: Radial profiles of neoclassical diffusion coefficients and pinch velocities for D (D_D, v_D) and T (D_T, v_T) as calculated by the NCLASS and NEO codes; Bottom: Radial profiles of neoclassical diffusion coefficient and pinch velocity for W (D_W^{neo}, v_W^{neo}) calculated by NCLASS. Both D-T and W coefficients are for 15 MA/5.3 T, Q = 10 plasmas [195, 206].

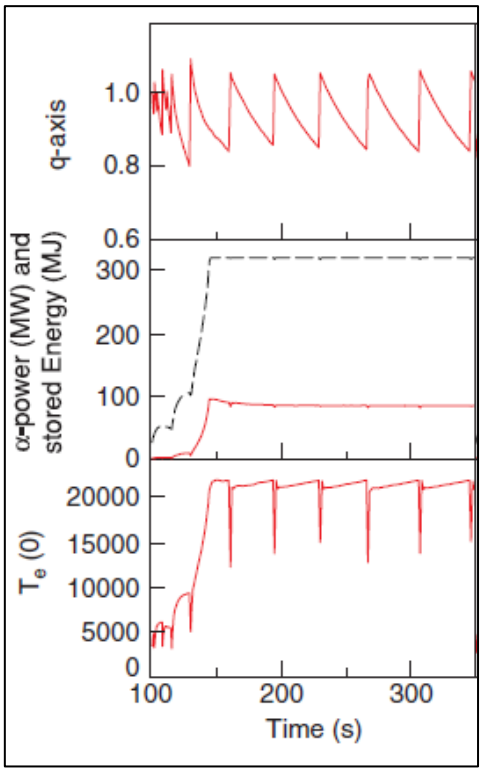

Figure 26. Simulation of an ITER DT scenario using the GLF23 transport model and the complete reconnection model for sawteeth, illustrating the evolution of various plasma parameters as a function of time in a 15 MA, $Q = 10$ plasma. Top: axial q value; Middle: the α-power (solid line) and plasma stored energy (broken line); Bottom: central electron temperature, $T_e(0)$ [207].

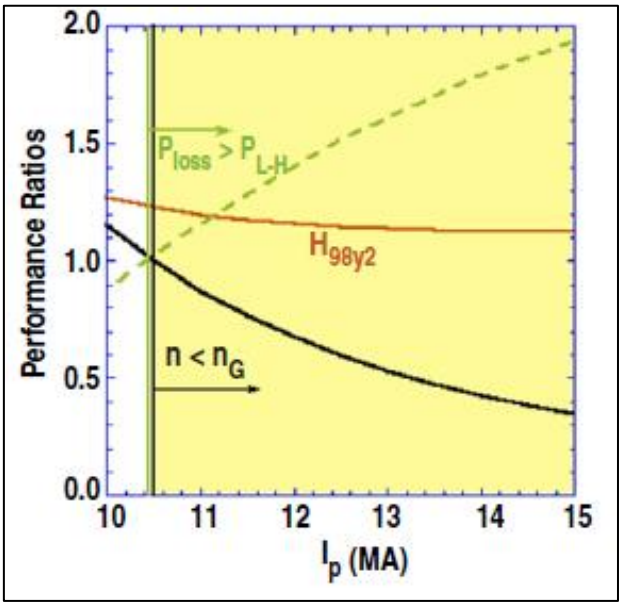

Figure 27. ITER operational space diagram for advanced inductive operation at the nominal ITER toroidal field of B_t = 5.3 T with P_{aux} = 50 MW and burn duration of 3000 s. The black curve is the ratio of the density to the Greenwald value, n/n_G, the green curve is the ratio of the loss power to the predicted L-H threshold power, $P_{loss}/P_{L\text{-}H}$, and the red curve is the confinement enhancement factor relative to the IPB98(y,2) H-mode scaling, H_{98y2} [211].

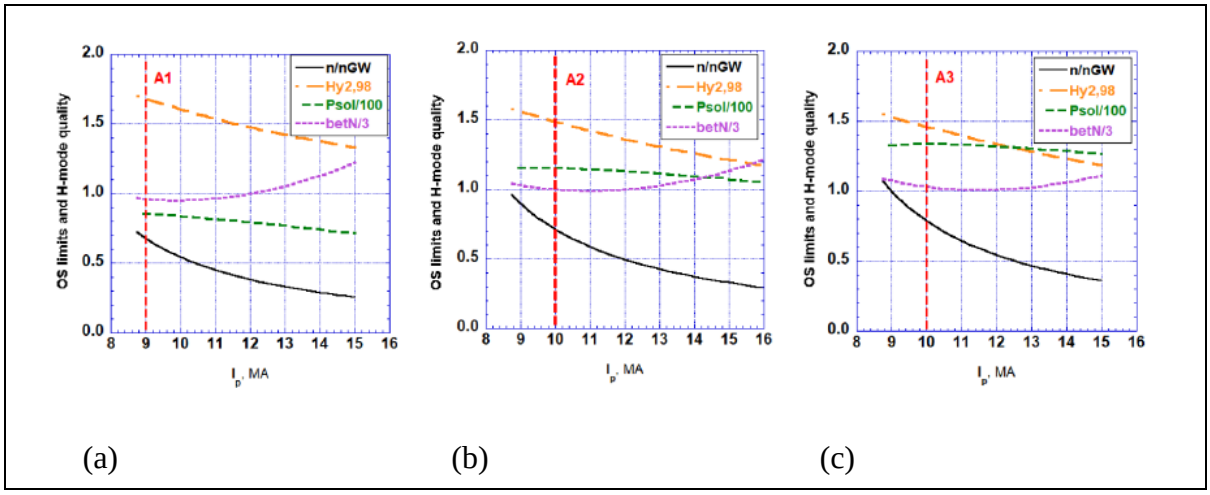

Figure 28. Potential operational space for fully non-inductive ITER steady-state $Q = 5$ plasmas in terms of plasma density normalized to the Greenwald density, $\langle n \rangle / n_{GW}$, energy confinement normalized to the IPB98(y,2) scaling, $H_{y2,98}$, edge power flow, P_{sol}, (in 100 MW) and $\beta_N/3$ with: (a) 33 MW NBI, 20 MW ECRH; (b) 49.5 MW NBI, 20 MW ECRH; (c) 49.5 MW NBI, 30 MW ECRH. The points A1, A2, A3, highlighted in red, were selected for more detailed transport and stability analysis using the ASTRA/KINX code combination (see [185] for more details).

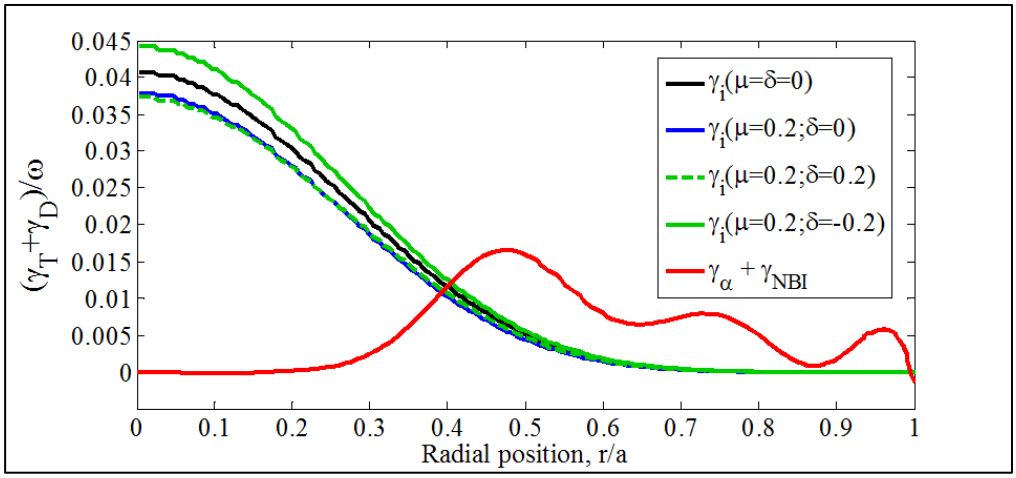

Figure 29. The sum of α-particle and beam drives (red) compared with the primary AE damping mechanism (ion Landau damping), as a function of normalized radius, r/a. The effects of the DT fuel mix ($\delta = 1 - n_T/n_D$) and depletion ($\mu = 1 - (n_D + n_T)/n_e$) on the damping are also depicted [187].

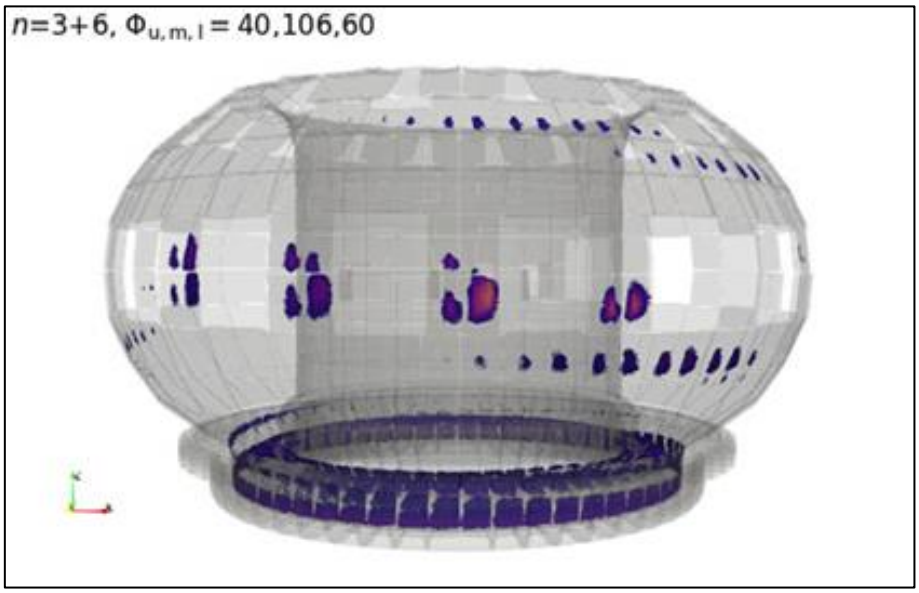

Figure 30. Fast ion power loading to the ITER first wall and divertor components, viewed from outside the ITER vacuum vessel (rendered semi-transparent), for 33 MW of 1 MeV NBI into a 15 MA flat-top H-mode with 90 kAt of $n = 3$ ELM control coil field applied (including the $n = 6$ side-band and plasma response). The wall panels closest to the viewing point are located opposite to the ITER HNB ports [220].

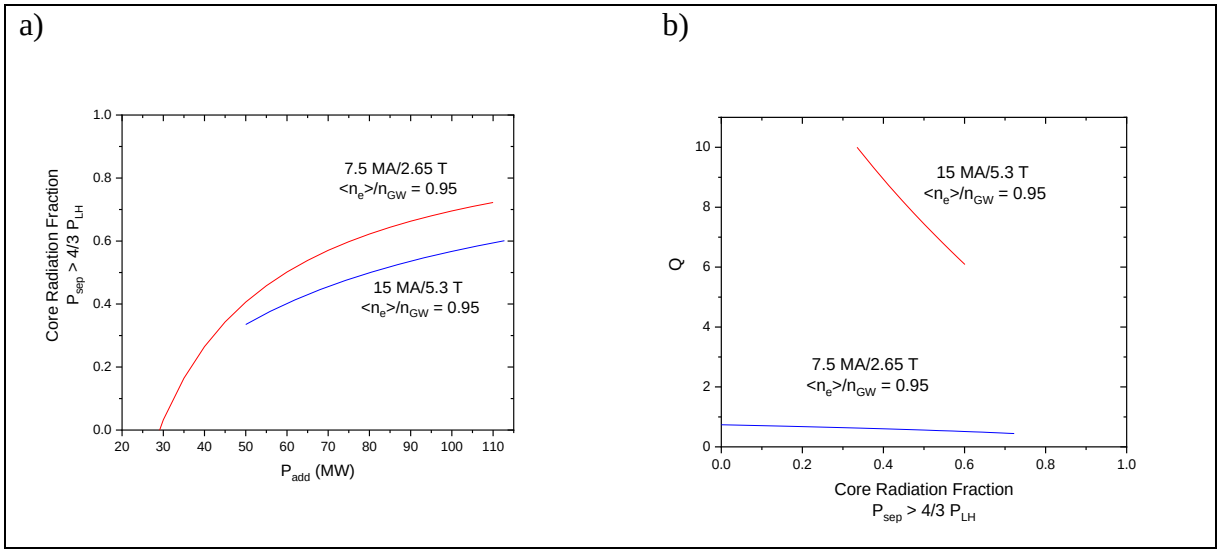

Figure 31. a) Level of core radiation fraction versus additional heating power, P_{add}, for $\langle n_e \rangle / n_{GW} = 0.95$ in DT plasmas with 15 MA/5.3 T and 7.5 MA/2.65 T (extrapolated from integrated plasma simulations for 50 MW additional heating and a simple 0-D model with $H_{98} = 1$ plus constant impurity and helium fractions independent of radiation fraction level). b) Fusion gain, Q, for the two cases as a function of the core radiation fraction.

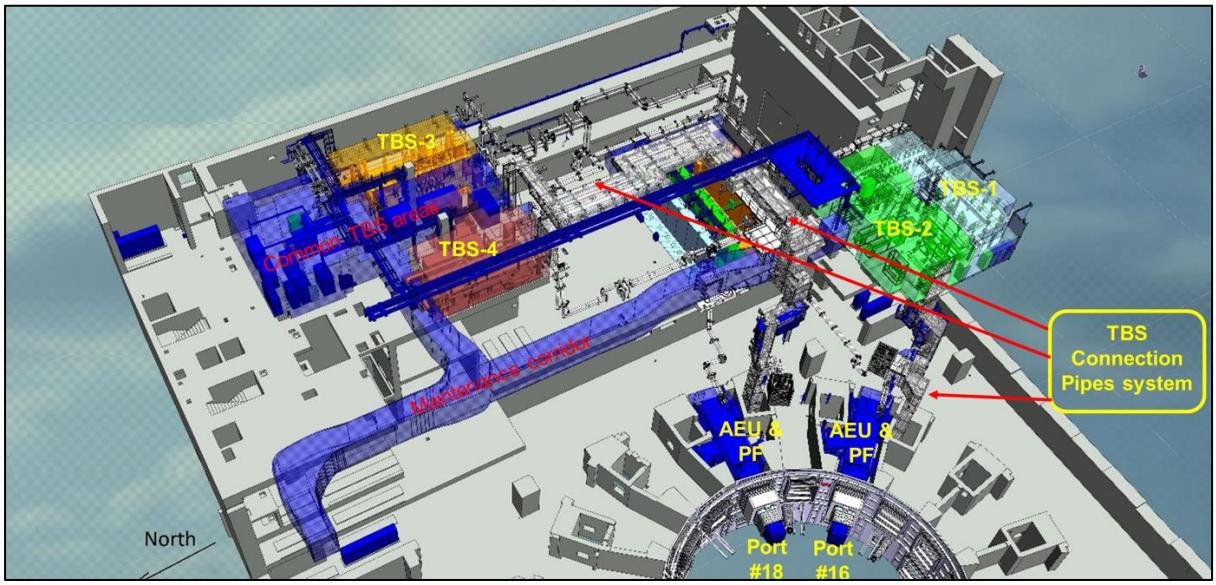

Figure 32. 3-D Model of the 4 TBS showing the location of the various TBS components in the Tokamak and Tritium Buildings.

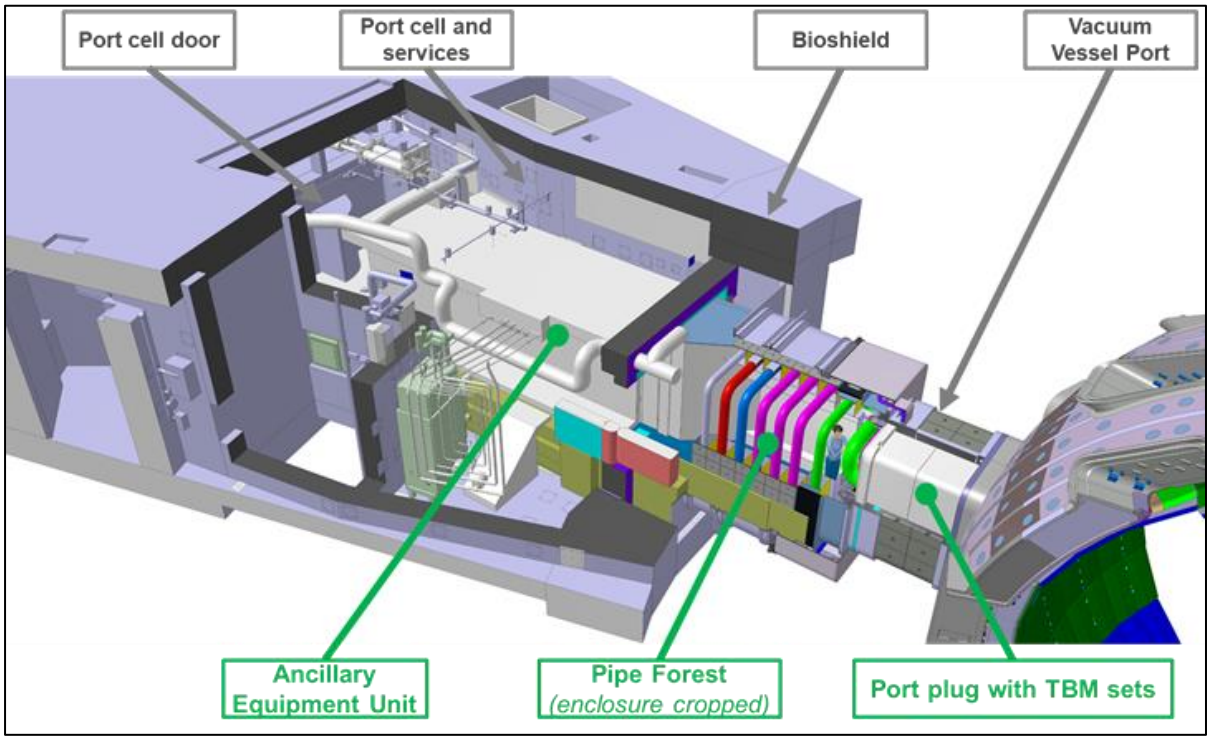

Figure 33. 3-D Model of an Equatorial Port Plug and Port Cell showing the location of the various TBS components.

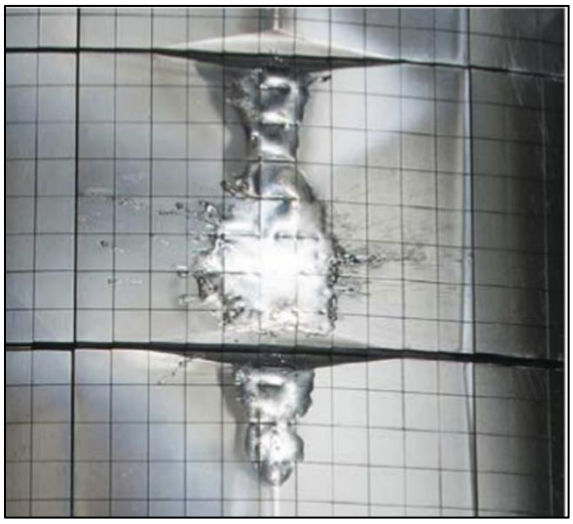

Figure 34. Be melt damage caused by runaway electron impact on the inner wall protection tiles at JET [136, 258].

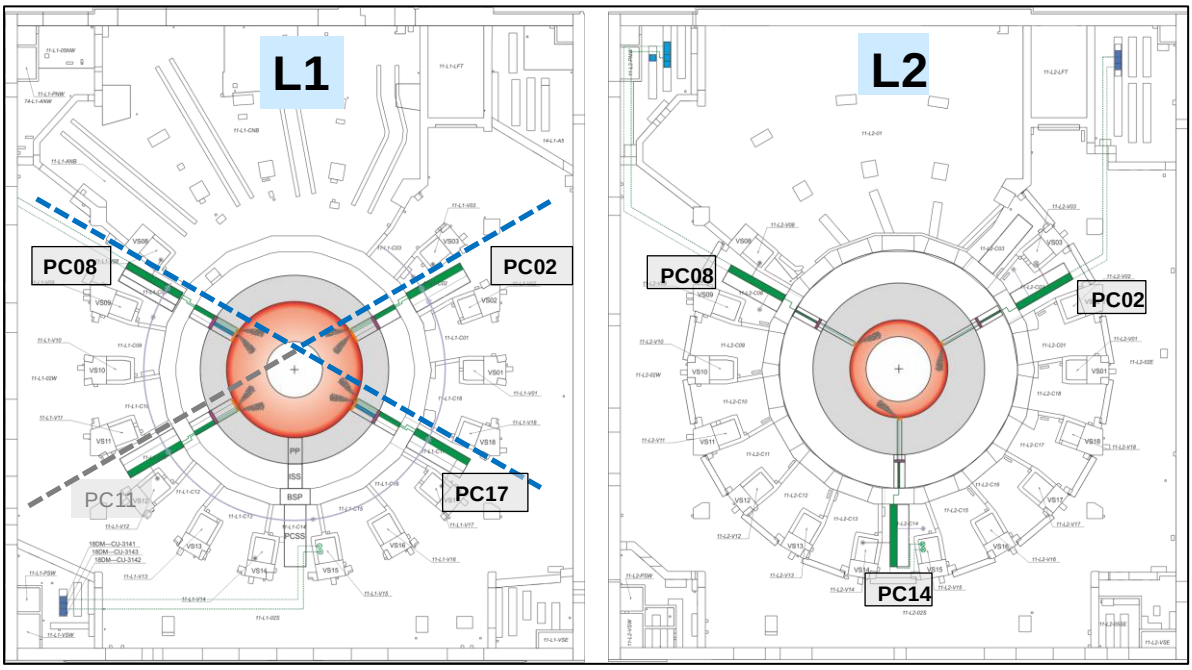

Figure 35. ITER DMS configuration on the L1 level (equatorial) and L2 level (upper). Note that there are 12 injectors in Equatorial Port #2 (PC02) and 6 injectors in EPs #17 (PC17) and #8 (PC08) respectively. The baseline configuration includes the possibility of a later upgrade by installing 6 injectors at EP #11 (PC11), but these are not included in the initial baseline configuration. The baseline DMS also has three injectors (one per port) installed at three Upper Ports (PC02, PC08 and PC14).

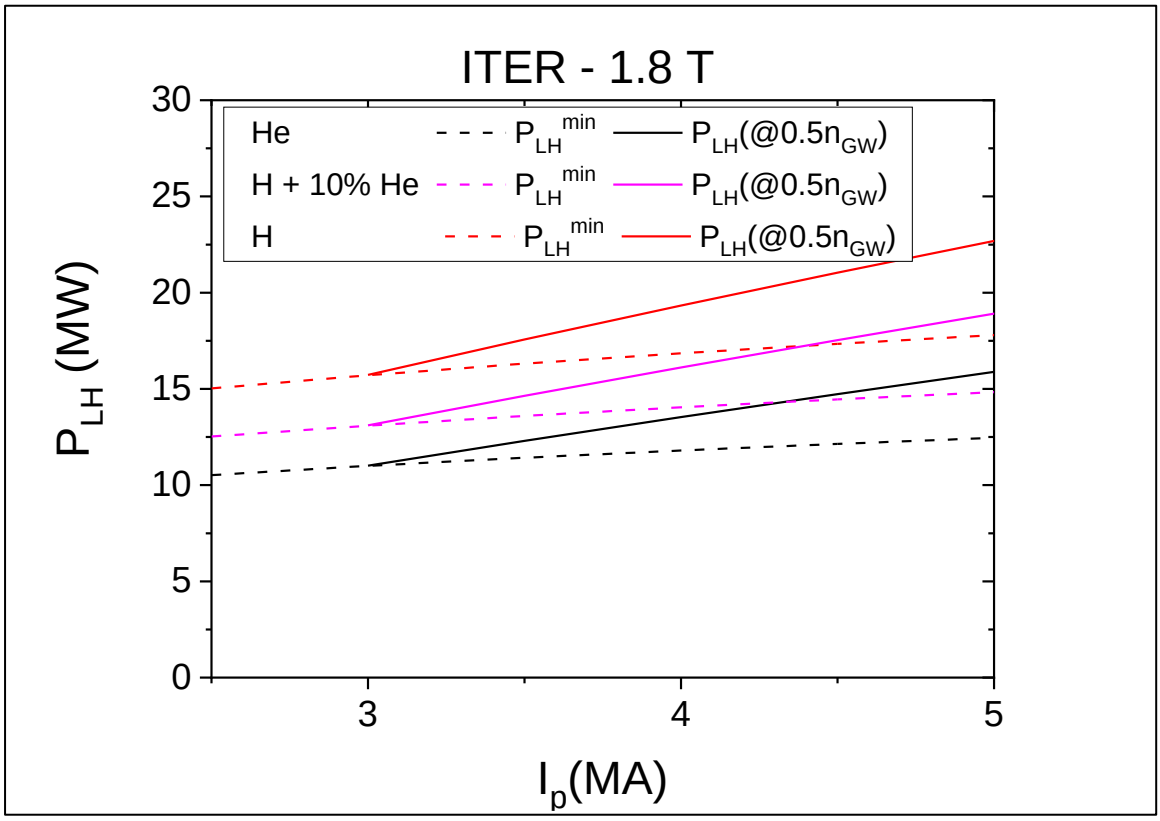

Figure 36. Expected H-mode threshold, P_{LH}, for H, He and H+10%He plasmas at 1.8 T in ITER versus plasma current, I_p, for the minimum density according to [18] and for $\langle n_e \rangle = 0.5 \times n_{GW}$.

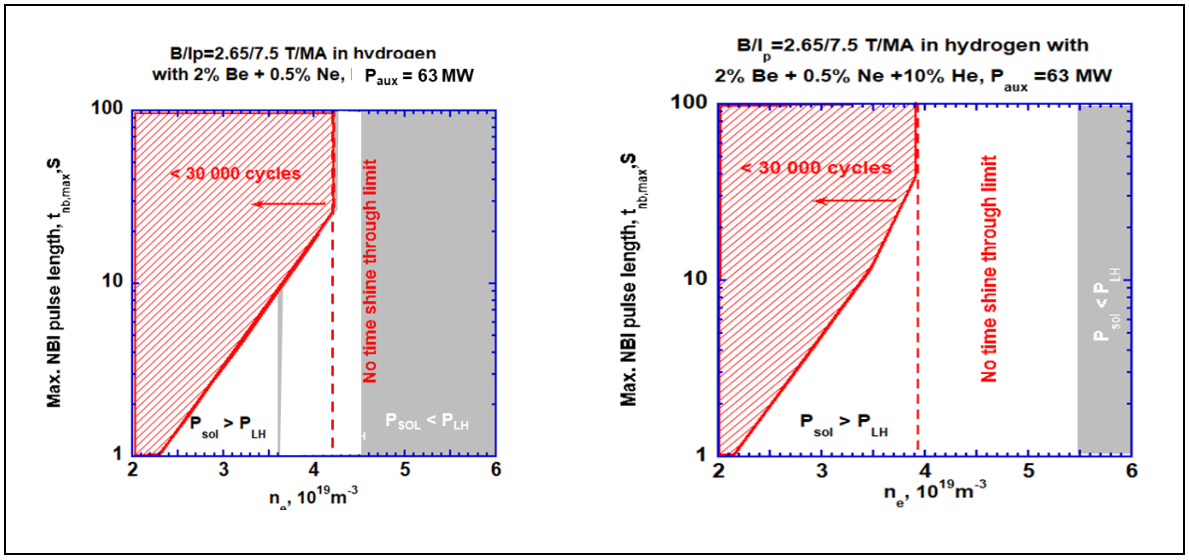

Figure 37. H-mode operational space for 7.5 MA/2.65 T plasmas heated by 33 MW NBI + 30 MW ECRH: (Left) Pure H plasmas, (Right) He-doped (10%) H plasmas. The red line indicates the maximum NBI duration due to shine-through limits on the ITER first wall blanket shield modules and the grey area corresponds to conditions in which H-mode access is not possible at this power level due to excessive plasma density.

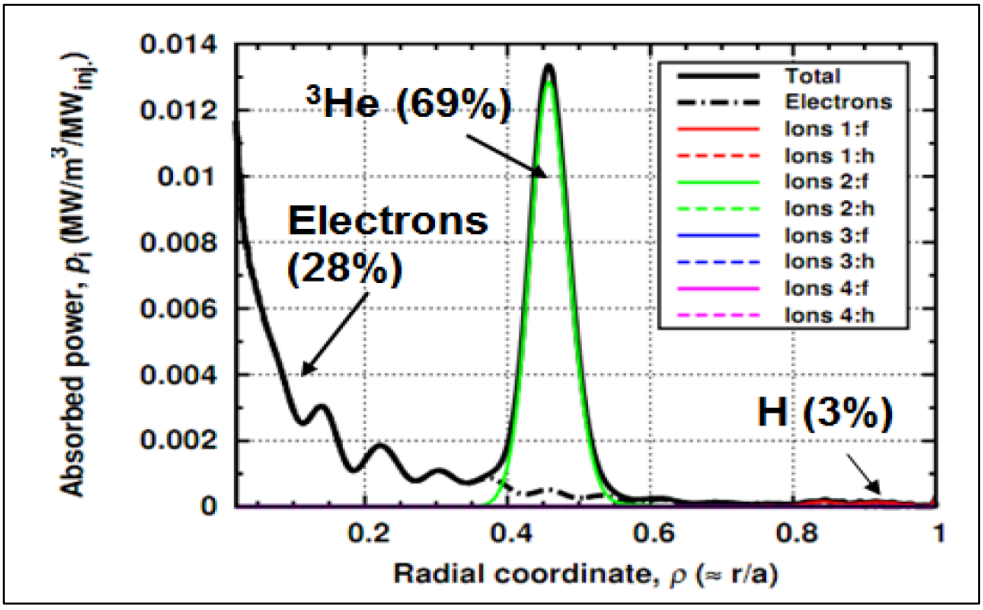

Figure 38. ICRF power deposition profiles for the 3-ion heating scheme at 3.3 T in a H: ^{4}He mix [287].

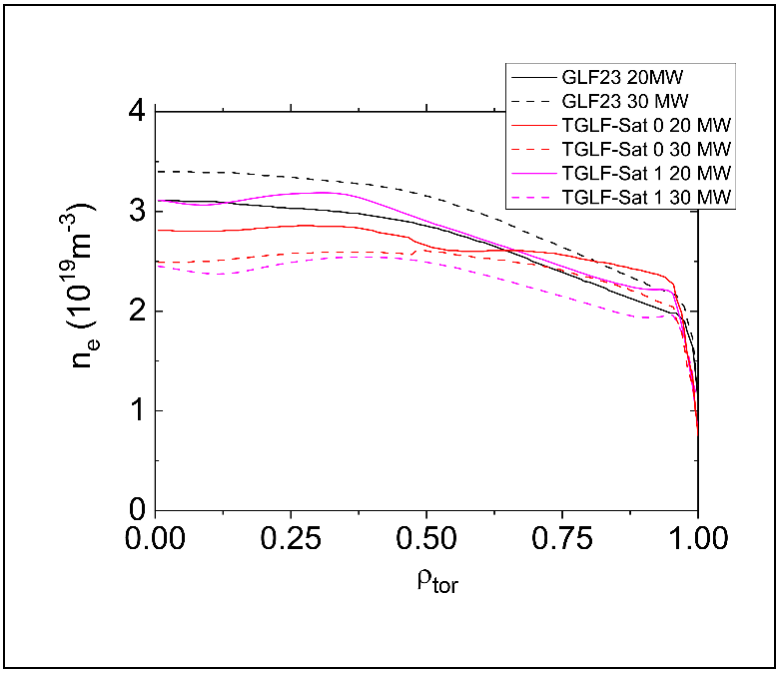

Figure 39. Plasma density profiles, n_e, as a function of normalized toroidal flux, ρ_{tor}, for 20 and 30 MW ECRH power level for ASTRA simulations with three models for anomalous transport GLF23, TGLF not including multi-scale effects (SAT-0 saturation rule) and TGLF including multi-scale effects (SAT-1 saturation rule) [34].

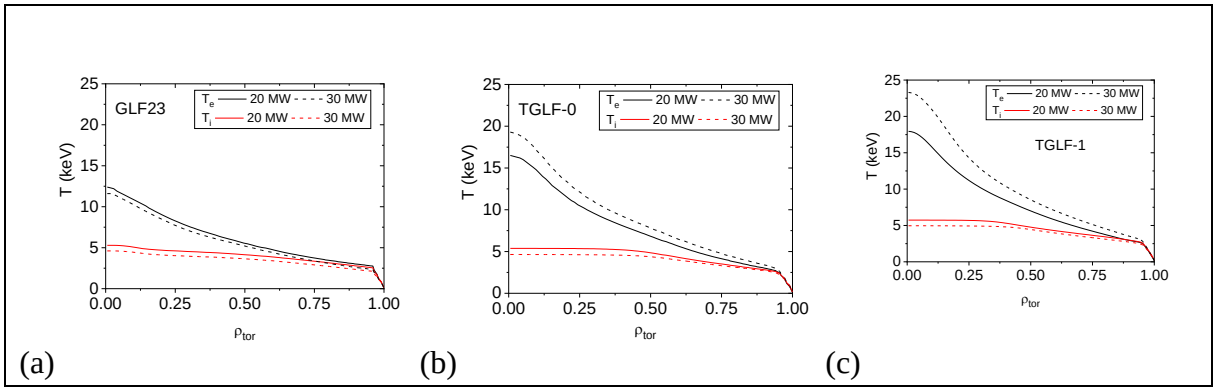

Figure 40. Plasma electron and ion temperature profiles, *T*, as a function of normalized toroidal flux, ρ_{tor}, for 20 and 30 MW of central ECRH power for ASTRA simulations with three models for anomalous transport: (a) GLF23, (b) TGLF not including multi-scale effects (SAT-0 saturation rule), (c) TGLF including multi-scale effects (SAT-1 saturation rule) [34].

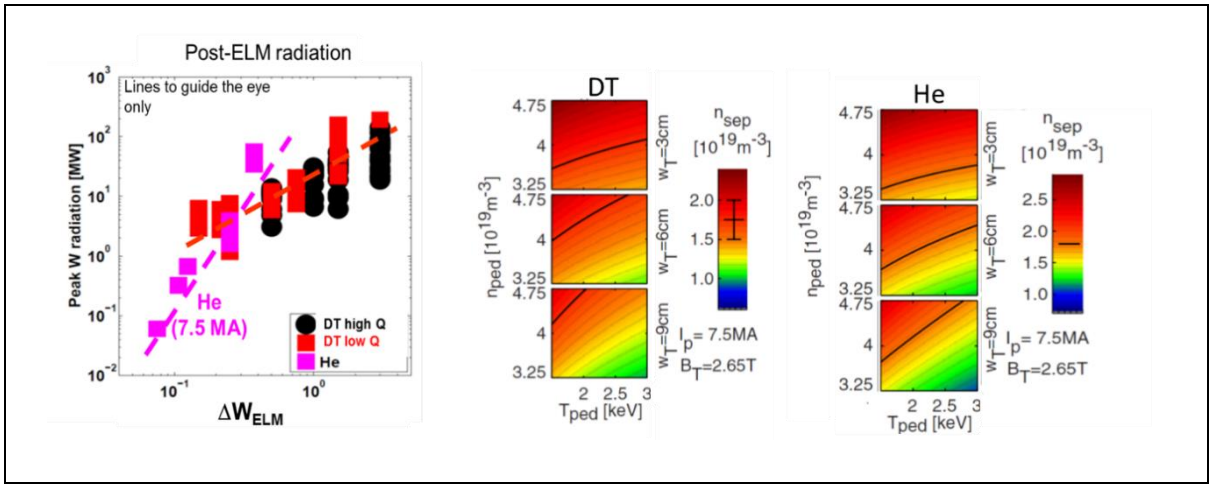

Figure 41. (Left) SOLPS+ASTRA modelled transient core plasma radiation following ELMs versus ELM energy loss for He and DT plasmas in ITER [171]. (Right) Separatrix densities leading to equal tungsten densities at the edge and the pedestal top for a range of pedestal densities (for a pedestal density width of 6 cm) and pedestal temperatures/ pedestal widths in 7.5 MA/2.65 T DT and He H-modes in ITER. For higher n_{sep} values, neoclassical transport leads to well screened tungsten profiles in the pedestal (hollow tungsten profiles) and vice-versa [67].

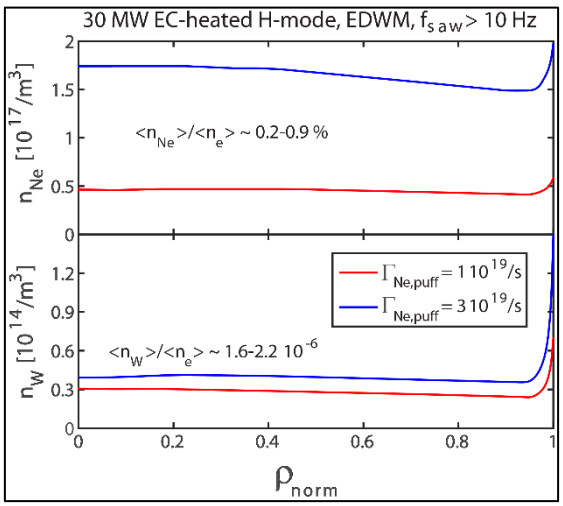

Figure 42. Neon and tungsten profiles in the core plasma for the JINTRAC simulations of 5 MA/1.8 T hydrogen H-mode plasmas with the EDMW transport model [288] with 30 MW of central ECRH.

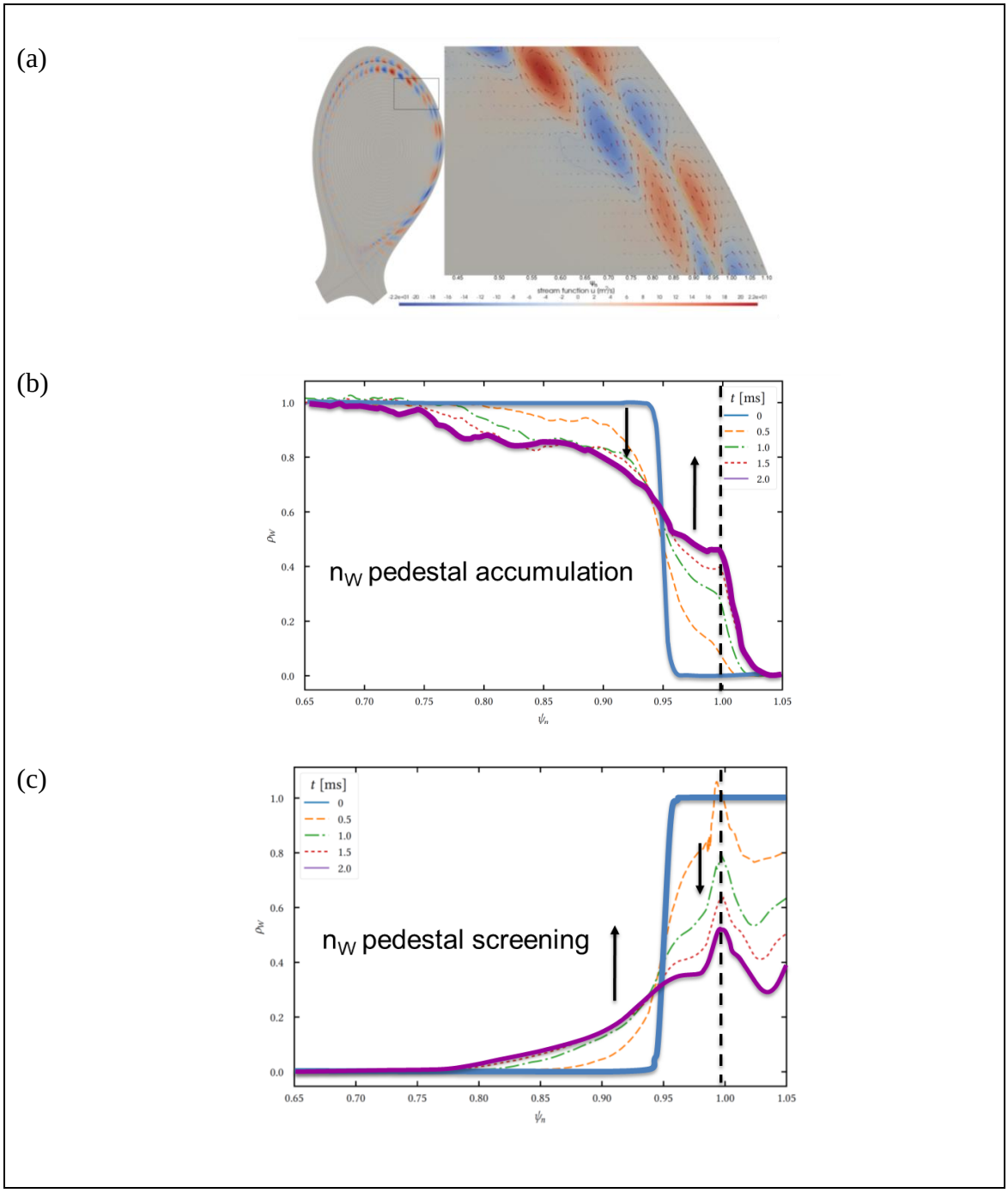

Figure 43. (a) Velocity stream function, *u*, of the ELM fields with the inset also showing the ***E***×***B*** drift of particles in an ELM. Arrows indicate the direction of the drift, with the colour indicating the magnitude. (b) W impurity distribution before and after the ELM when impurity accumulation dominates in the pedestal. (c) W impurity distribution before and after the ELM when impurity screening dominates in the pedestal [68].

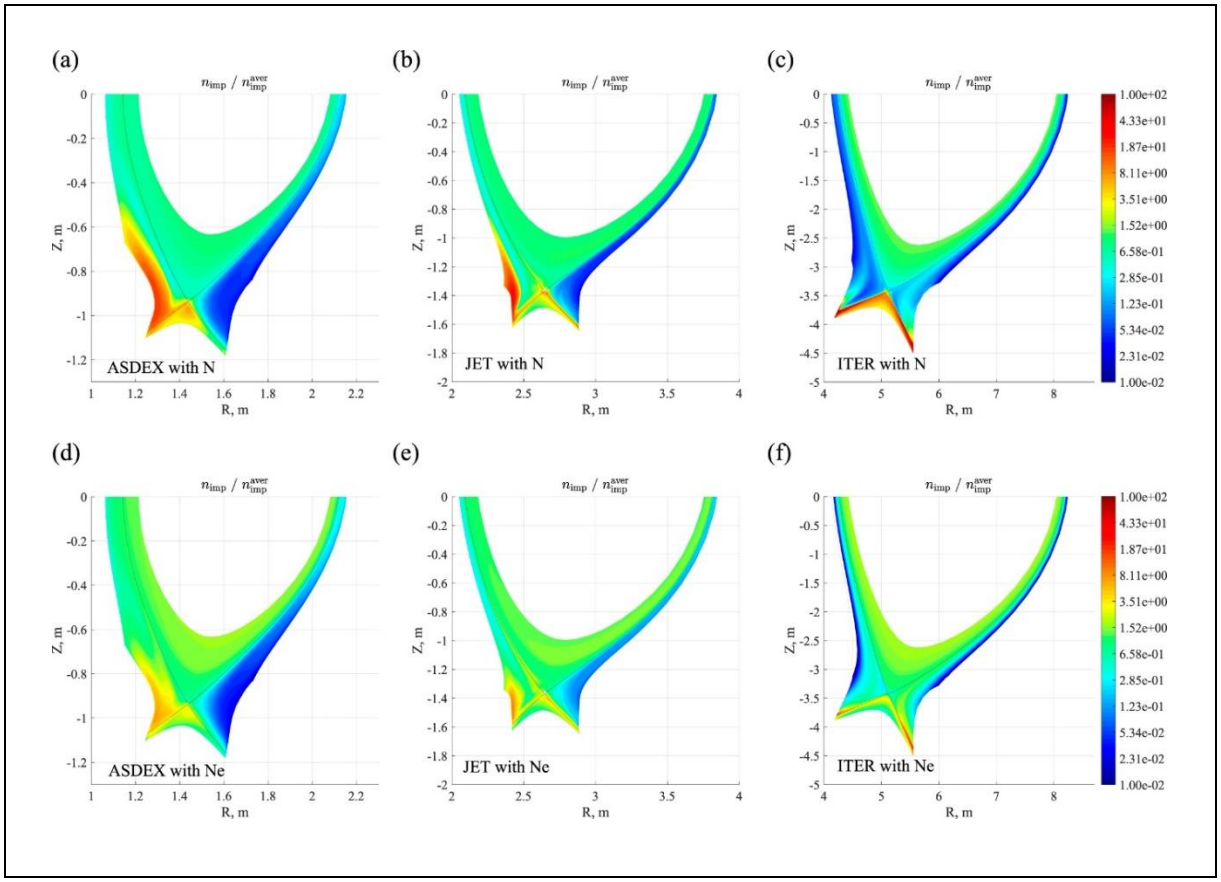

Figure 44. Distribution of impurity density (normalized to the average impurity density) for: (a) AUG with N_2; (b) JET with N_2; (c) ITER with N_2; (d) AUG with Ne; (e) JET with Ne; (f) ITER with Ne.

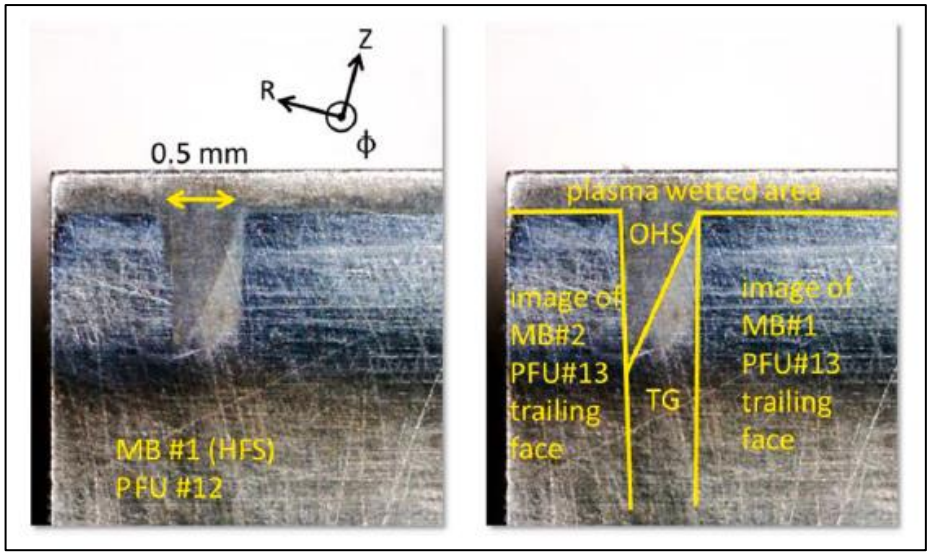

Figure 45. Direct evidence of optical hotspots on the leading edges of ITER-like monoblocks in the WEST lower divertor. The plasma heat flux is directed into the page. The image on the left is repeated on the right with the yellow lines indicating the MB edges to guide the eye. The optical hotspot is the triangular region. The hot spots were created by relatively low heat fluxes in WEST L-mode plasmas compared to what will be experienced on ITER at high performance and the long-time impact of loading on the W in these minute regions is unknown [251].

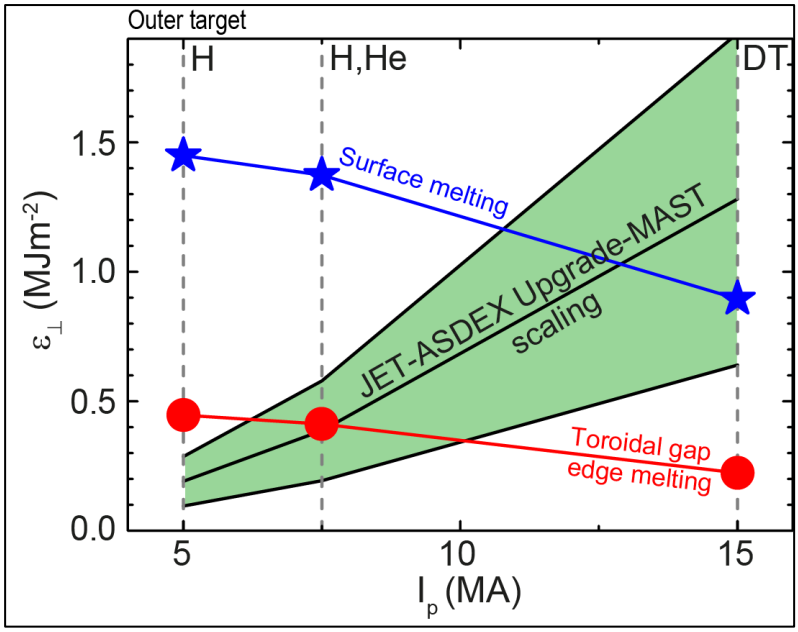

Figure 46. Outer target ELM energy fluences ($\varepsilon_\perp$) which lead to monoblock top surface and toroidal gap edge melting at 3 representative operating points within the IRP, corresponding to non-active H-modes at 5 MA/1.8 T in H, 7.5 MA/2.65 T in He or D and 15 MA/5.3 T in DT. The values are computed from ion orbit modelling, including a full thermal model of the monoblock subject to appropriate inter-ELM heat loads at these operating points. The expected $\varepsilon_\perp$ from the empirical type-I ELM energy deposition scaling in [64] is also included for ΔW_{ELM} = 5.4% (as in [64]), with the associated factor 3 spread of the experimental data about the regression (shaded area).

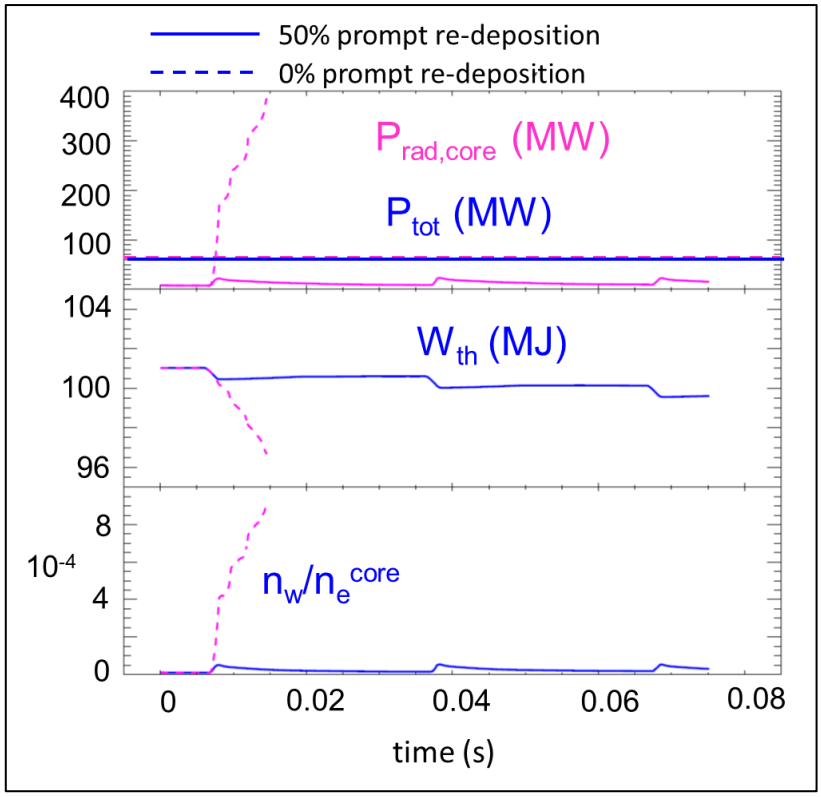

Figure 47. Core-edge integrated simulations of a PFPO-2 ITER ELMy H-mode He plasma at 7.5 MA/2.65 T with 63 MW of additional heating and controlled ELM frequency f_{ELM} = 33 Hz. One simulation assumes 50% prompt W re-deposition during ELMs (full lines) and the other no prompt W re-deposition during ELMs (dashed lines). From top to bottom: heating power, P_{tot} , and core plasma radiation, $P_{rad,core}$, plasma energy, W_{th}, and core W concentration, n_W/n_e^{core}. For the no prompt re-deposition case, the plasma collapses radiatively after the first ELM due to the associated W influx and ensuing core plasma radiation [324].

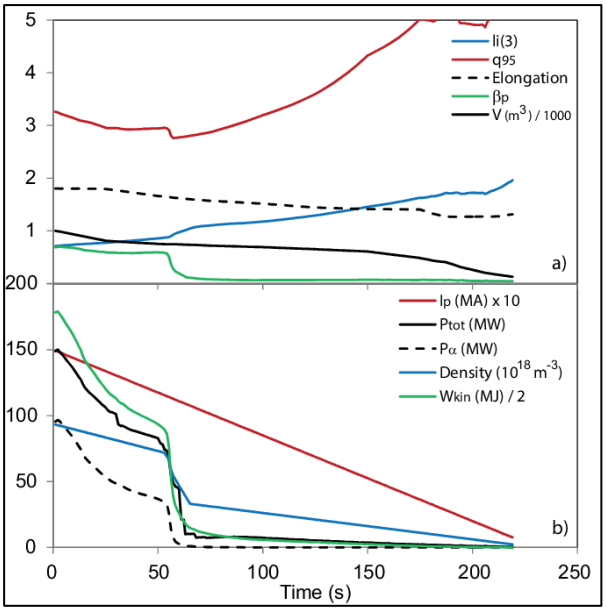

Figure 48. A modelled ITER termination from I_p = 15 MA at full Q = 10 performance (W_{kin} = 350 MJ, P_α = 100 MW) taking approximately 220 s. Shown are time traces of: a) internal inductance, l_i, value of, q_{95}, elongation, κ, poloidal β, and plasma volume, V (10^3 m^3); b) plasma current, I_p (in units of 10^2 kA), total input power, P_{tot} (MW), the α-heating power, P_α (MW), electron density (10^{18} m^{-3}) and kinetic energy, W_{kin} (MJ). The H-L back transition is visible as fast drop in β_p and W_{kin} at around t = 60s [376].

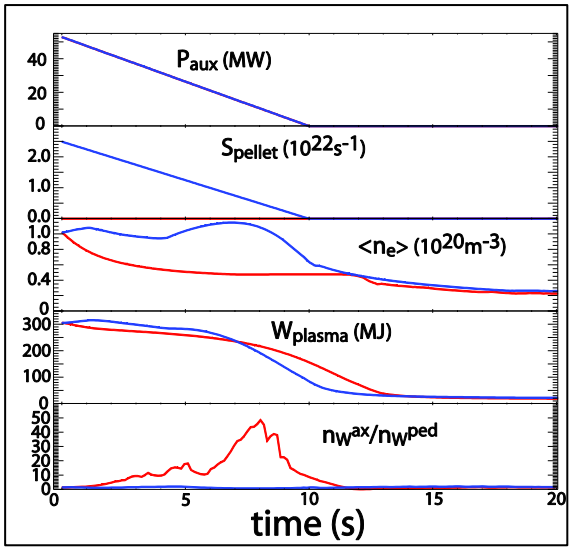

Figure 49. Evolution of auxiliary heating power, P_{aux}, pellet fuelling, S_{pellet}, and plasma parameters (density, $\langle n_e \rangle$, energy, W_{plasma}, and W peaking factor, n_W^{ax}/n_W^{pdx}) in the termination phase of ITER Q = 10 plasmas for a 10 s ramp of the auxiliary heating power and two fuelling pellet waveforms (immediate switch-off and 10 s ramp-down) [195].

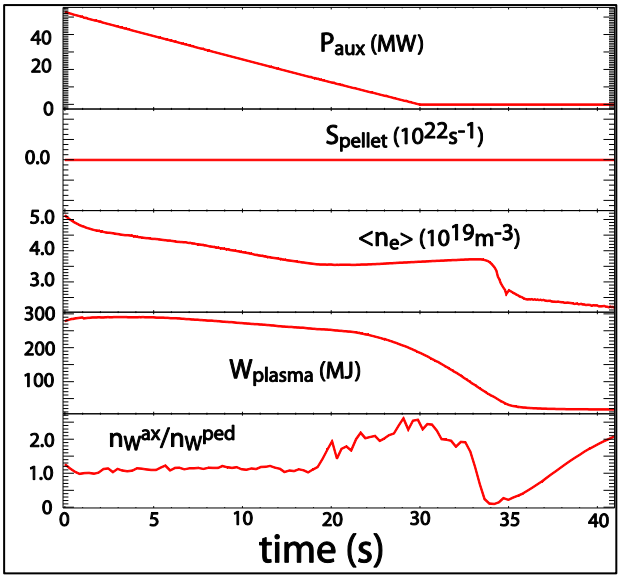

Figure 50. Evolution of auxiliary heating power, P_{aux}, pellet fuelling, S_{pellet}, and plasma parameters (density, $<n_e>$, energy, W_{plasma}, and W peaking factor, n_W^{ax}/n_W^{pdx}) in the termination phase of an ITER Q = 5 plasma ($<n_e>/n_{GW}$ = 0.5) for a 30 s ramp of the auxiliary heating power and immediate pellet fuelling switch-off [195].

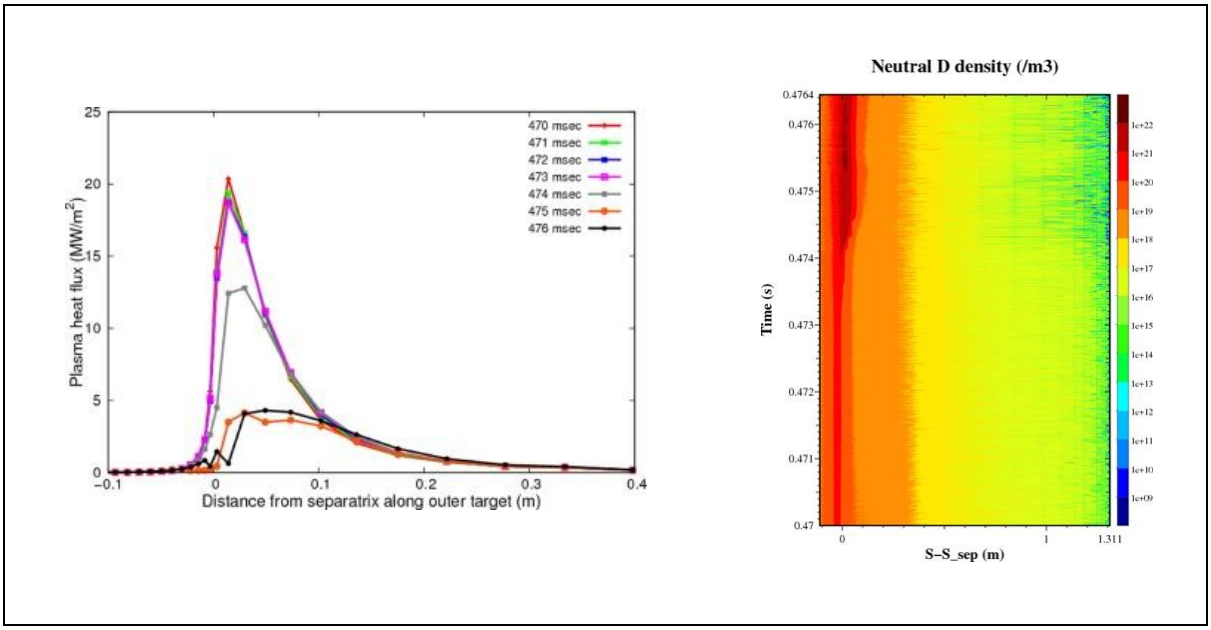

Figure 51. (Left) Total power flux on the ITER outer divertor target as a function of time. The arrival time of the gas injection is 0.4685 s. The injection set-point is 10 Pa•m^3s^{-1} for Ne, and 50 Pa•m^3s^{-1} for D_2. (Right). Neutral deuterium density along the outer divertor target for the same conditions showing the large increase of neutral density from 0.474 s onwards, marking the start of the recovery of semidetached plasma conditions [382].

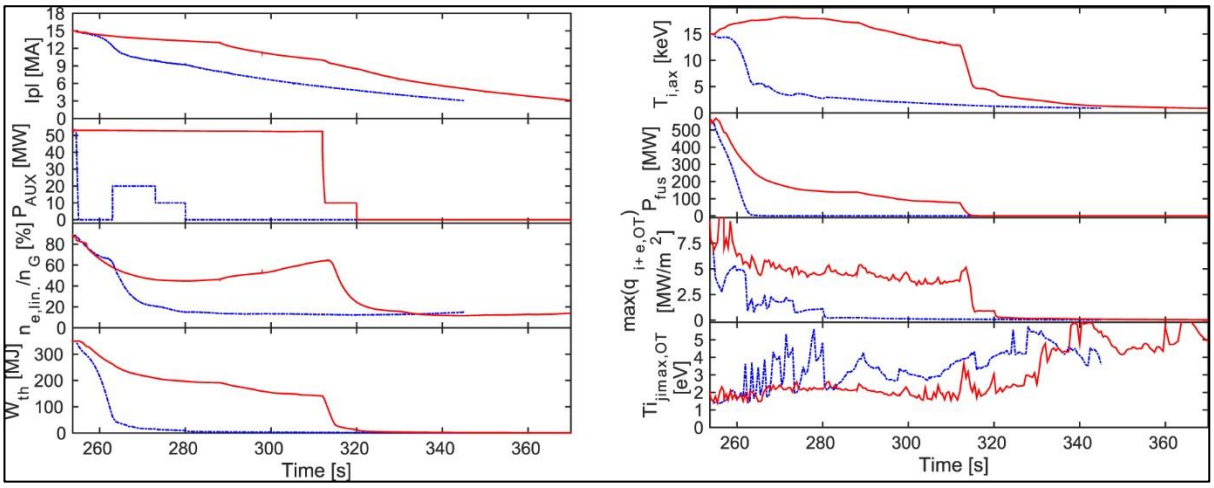

Figure 52. (Left) Time evolution of plasma current, I_{pl}, auxiliary power, P_{AUX}, Greenwald density fraction, $n_{e,lin}/n_G$, thermal energy content, W_{th}. (Right) time evolution of ion temperature on axis, $T_{i,ax}$, fusion power, P_{fus}, maximum power density at the outer target, max($q_{i+e,OT}$) and ion temperature at the outer target location with the maximum absolute value of ion flux, $Ti_{jimax,OT}$, during the high-Q_{fus} exit and current ramp-down for $I_{pl} = 15 \rightarrow 3$ MA for an H-L transition at $I_{pl} \sim 15$ MA (blue dash-dotted) and $I_{pl} \sim 10$ MA (red solid) [377].

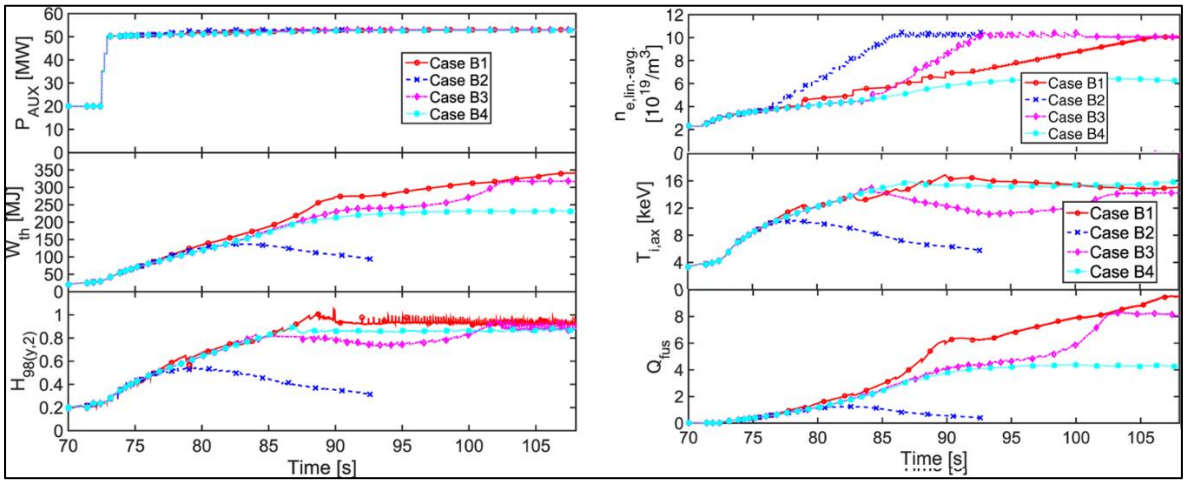

Figure 53. (Left) time evolution of auxiliary power, P_{AUX}, thermal energy content W_{th}, and $H_{(98,y2)}$ factor. (Right) Time evolution of line-averaged electron density, $n_{e,lin\text{-}avg}$, the ion temperature on axis, $T_{i,ax}$, and fusion gain Q_{fus}, from the end of ramp-up at 15 MA, for various temporal waveforms for the plasma density [377].

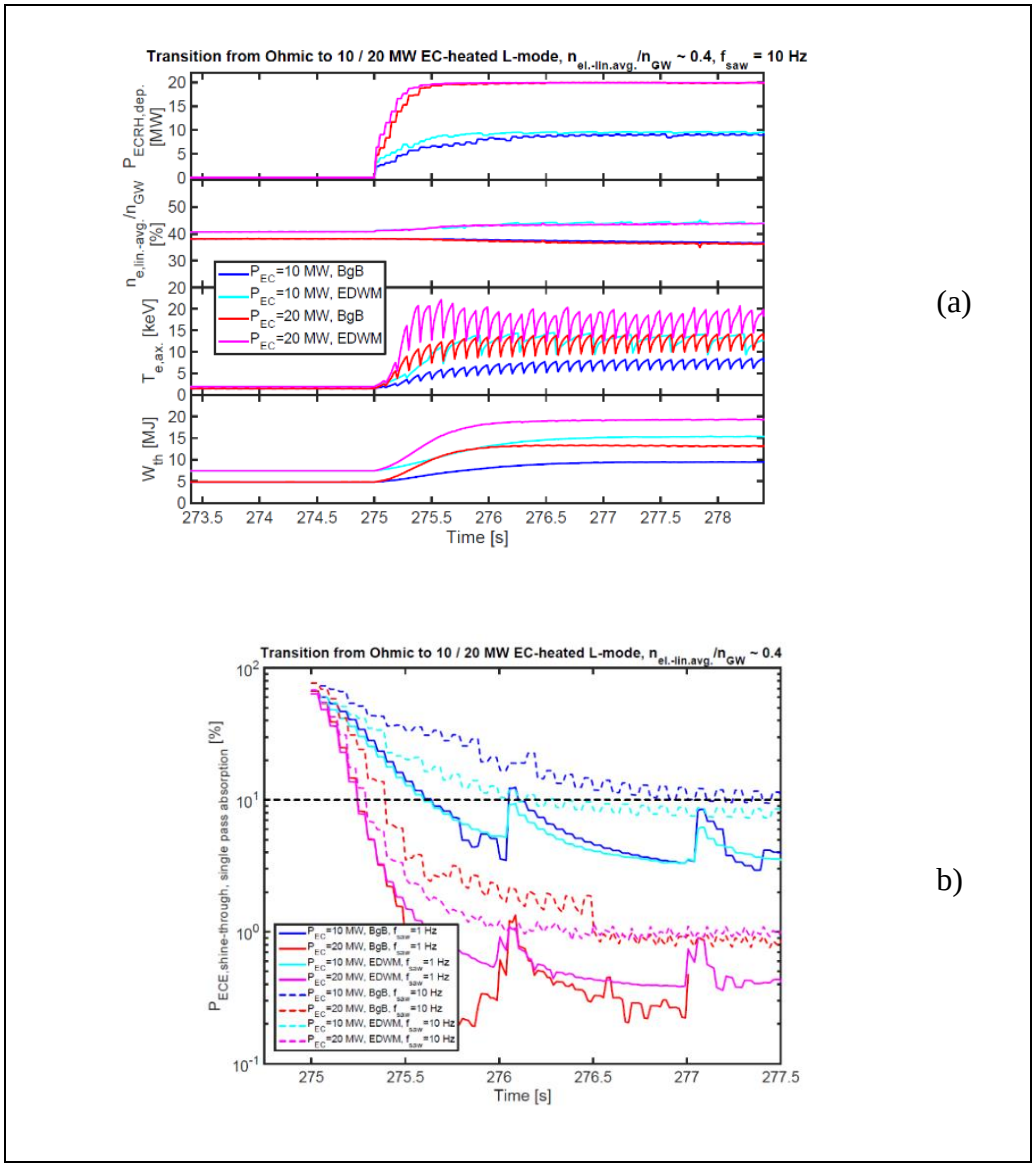

Figure 54. (a) Evolution of the single-pass absorbed ECRH power, $P_{ECRH,dep}$, (normalized) average plasma density, $n_{e,lin}/n_{GW}$, central electron temperature, $T_{e,ax}$, and plasma energy, W_{th}, following the injection of 3rd harmonic ECRH heating power (injected power of 10 and 20 MW) into a 5 MA/1.8 T $\langle n_e \rangle \sim 0.4 \times n_{GW}$ ohmic plasma in ITER for two transport models (Bohm-gyroBohm and EDWM with an assumed sawtooth frequency of 10 Hz). (b) Evolution of the single pass non-absorbed ECRH power following the injection of 3rd harmonic EC heating power for the same plasmas as in (a) for two assumed sawtooth frequencies of 1 and of 10 Hz. The line at 10% determines the acceptable limit for non-absorbed stationary ECRH power in single pass for these plasma conditions [33].

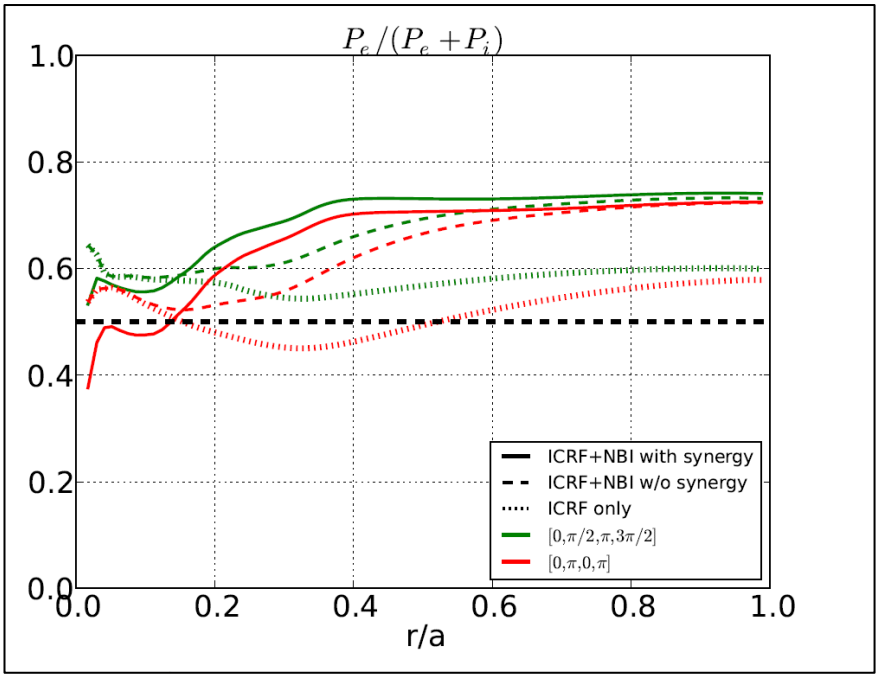

Figure 55. Ratio of electron heating power to total integrated power, $P_e/(P_e+P_i)$, for ICRF heating versus normalized radius, r/a, for a helium H-mode with NBI heating at an injected power of 33 MW, 22 MW of ECRH power and 22 MW of ICRF power (at a frequency of 40 MHz with a 5% H concentration) [402].

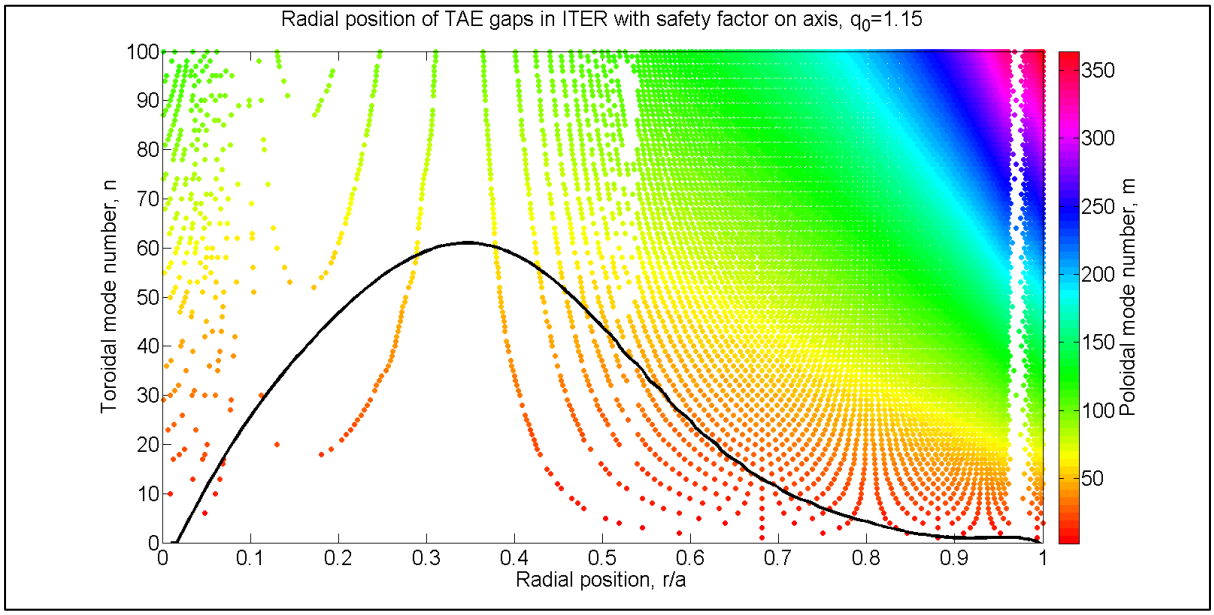

Figure 56. Radial localisation of TAE gaps in a 15 MA/5.3 T ITER Q = 10 plasma for modes with toroidal mode number, n. The solid line shows the α-particle pressure gradient.

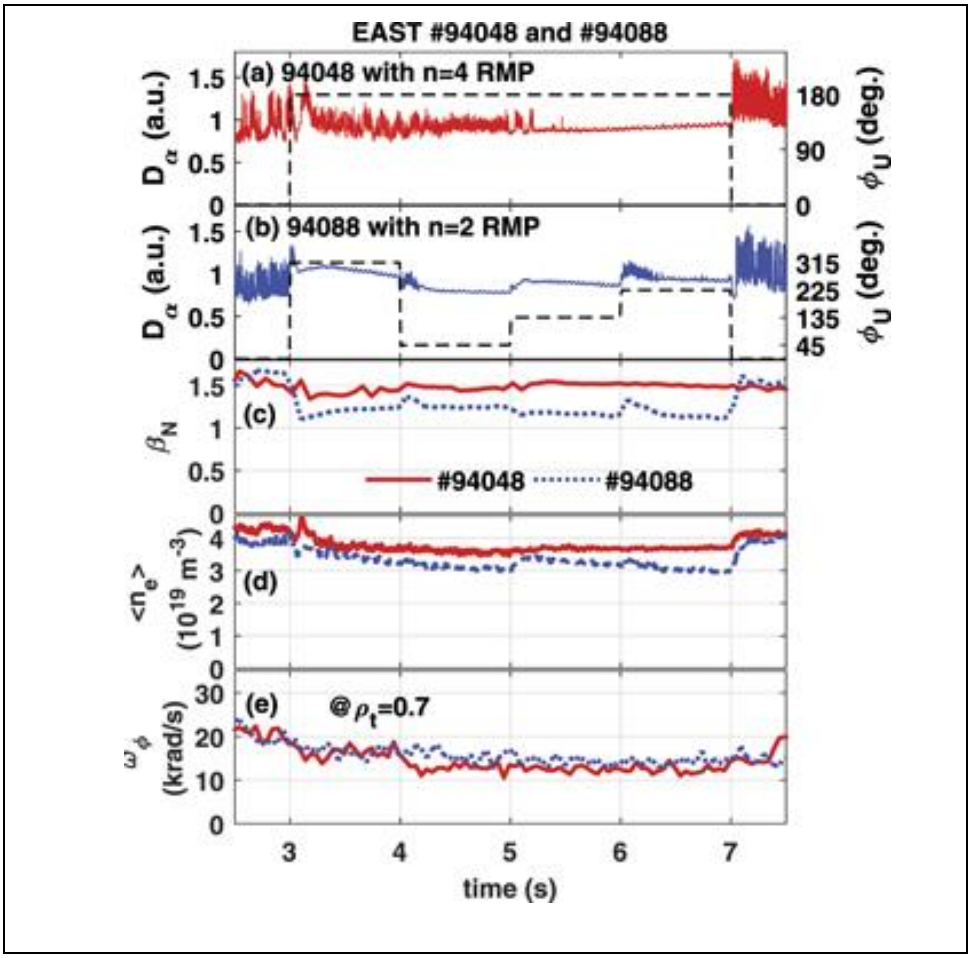

Figure 57. Impact of 3-D fields applied for ELM suppression in low torque input EAST tokamak H-mode plasmas. Temporal evolution of (a) the D_α emission (red solid line) and the upper coil current phase, ϕ_U, of the applied $n = 4$ RMP field (black dashed line) of shot #94088; (b) the D_α emission (blue solid line) and the upper coil current phase, ϕ_U, of the applied $n = 2$ RMP field (black dashed line) of shot #94048, (c) β_N; (d) line averaged density, $<n_e>$; and (e) toroidal rotation, ω_ϕ, at the normalized toroidal flux surface $\rho_t = 0.7$. In (c)-(e) two shots #94048 and #94088 are represented by red solid lines and blue dotted lines respectively [421].

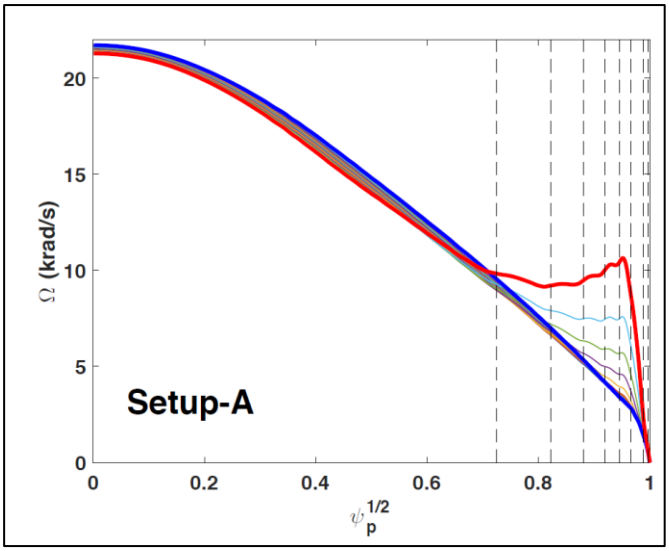

Figure 58. MARS-Q quasi-linear initial value simulation for the time evolution of the plasma toroidal rotation profile results for the ITER 15 MA/5.3 T Q = 10 scenario. The applied n = 3 RMP field corresponds to that obtained with maximum current in the ELM control coils and toroidal phasing optimized for maximum X-point response, which favours ELM suppression. The thick red lines indicate the profiles at the end of simulations (~380 ms for this scenario) [422].

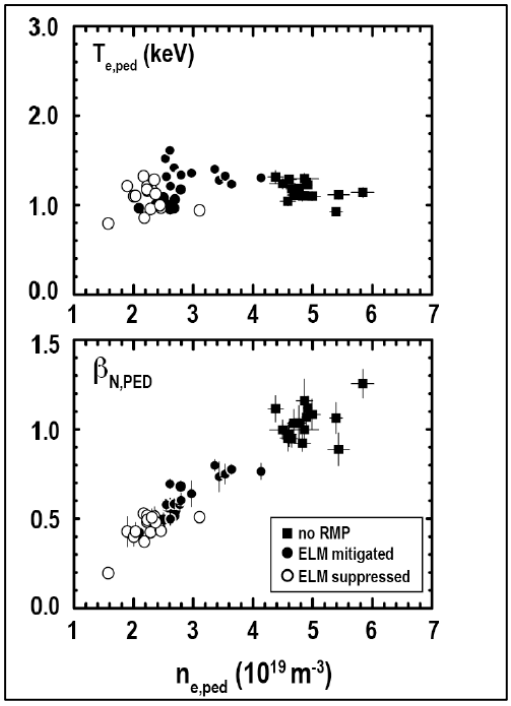

Figure 59. (a) Pedestal electron temperature, $T_{e,ped}$, (b) pedestal normalized beta, β_N, for ELM suppressed (open circles), ELM mitigated (closed circles) and ELMy plasmas with no RMP in DIII-D. The plasma configuration is the ITER-similar shape and $n = 3$ even parity RMPs are applied with the ELM control coils [423].

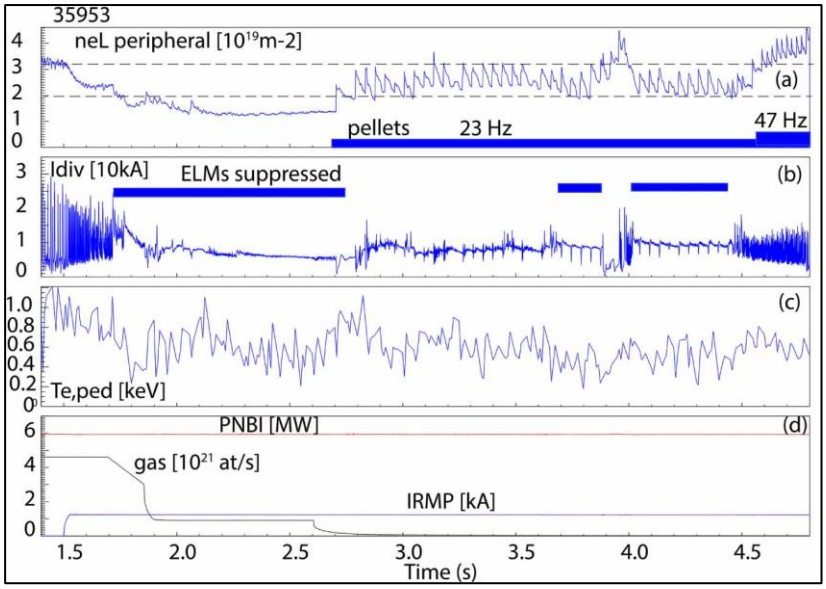

Figure 60. Pellet fuelling of H-mode plasma with ELM suppression by 3-D fields in ASDEX-Upgrade: (a) Line integral density from the interferometer on peripheral chord $\rho_{pol} > 0.8$, *nel.peripheral*; (b) Divertor tile current, *Idiv* — ELMs indicator; (c) electron temperature at pedestal top ($\rho_{pol} = 0.92$) by Thomson scattering, *Te,ped*; (d) NBI power, *PNBI*, gas puff rate, *gas*, and RMP current, *IRMP* [440].

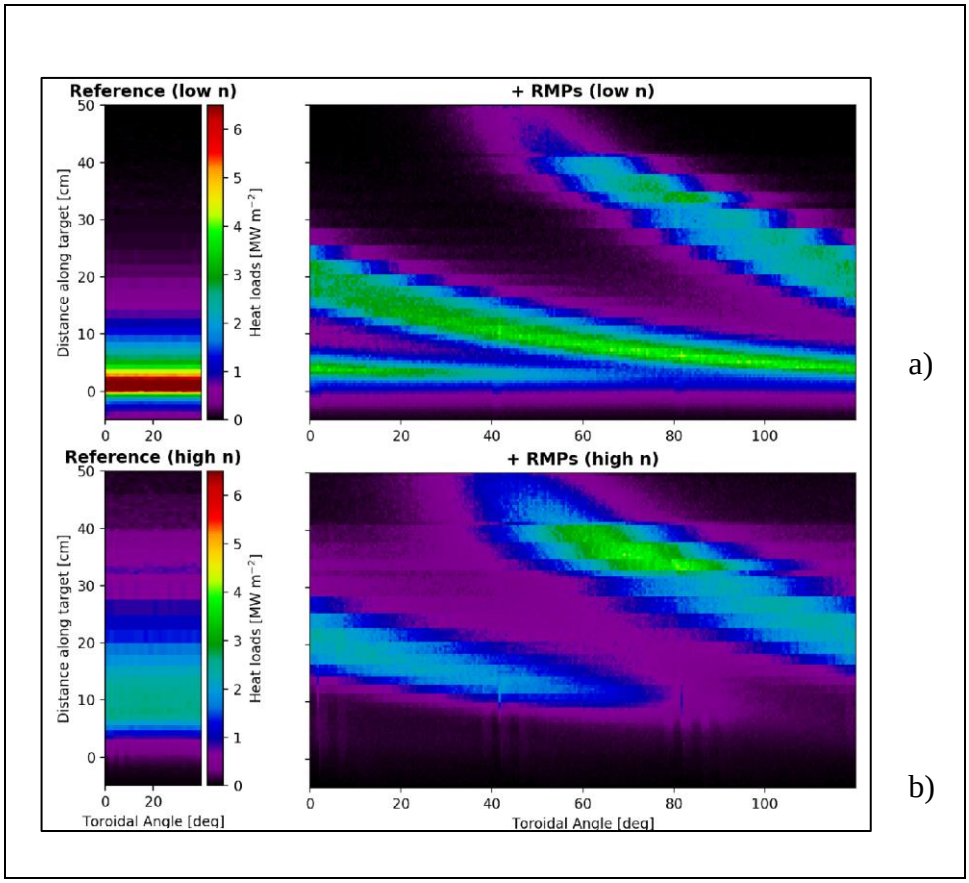

Figure 61. Power fluxes to the ITER outer divertor plasma at low and high plasma density (radiative divertor conditions) for PFPO-1: (a) 2-D toroidally symmetric plasma; (b) 3-D edge plasma with magnetic field modified by ELM control coils [61].

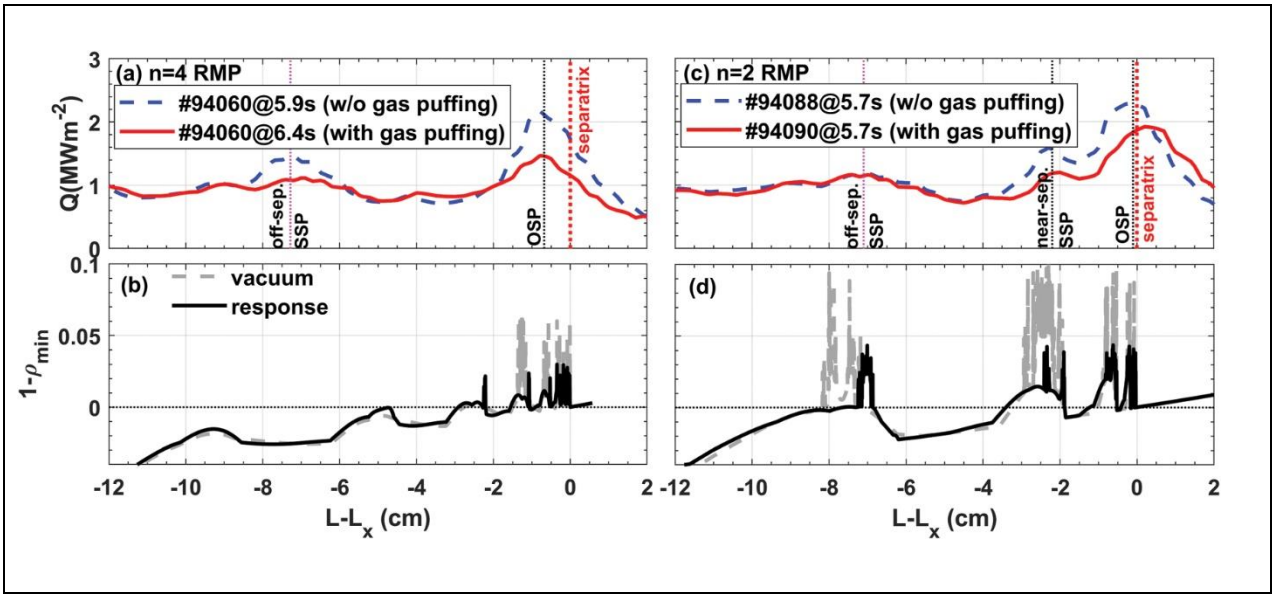

Figure 62. Comparison of the EAST divertor heat flux profiles without (blue dashed line) and with (red solid line) gas puffing for (a) $n = 4$ and (b) $n = 2$ RMPs. The divertor field line penetration depth at the corresponding toroidal angle, modelled by TOP2D in the vacuum approximation (grey dashed line) and taking into account the plasma response calculated by MARS-F (black solid line), is shown in (b) and (d) respectively for the two values of n, showing that the deeper field penetration with $n = 2$ is associated with no reduction of the heat flux for lobes away from the separatrix when the density is increased by gas puffing (while maintaining ELM suppression). L-L_X is the distance to the separatrix at the outer divertor target with negative values corresponding to the SOL and positive values to the private flux region. 1-ρ_{min} quantifies field penetration into the (2-D) separatrix associated with the application of RMPs with negative values corresponding to the SOL and positive values to inside the (unperturbed) 2-D plasma separatrix [421].

a)

Case	Φ_L - Φ_M [deg]	Φ_U - Φ_M [deg]
1	200	140
2	30	305
3	200	270
4	80	100
5	180	6
6	315	180

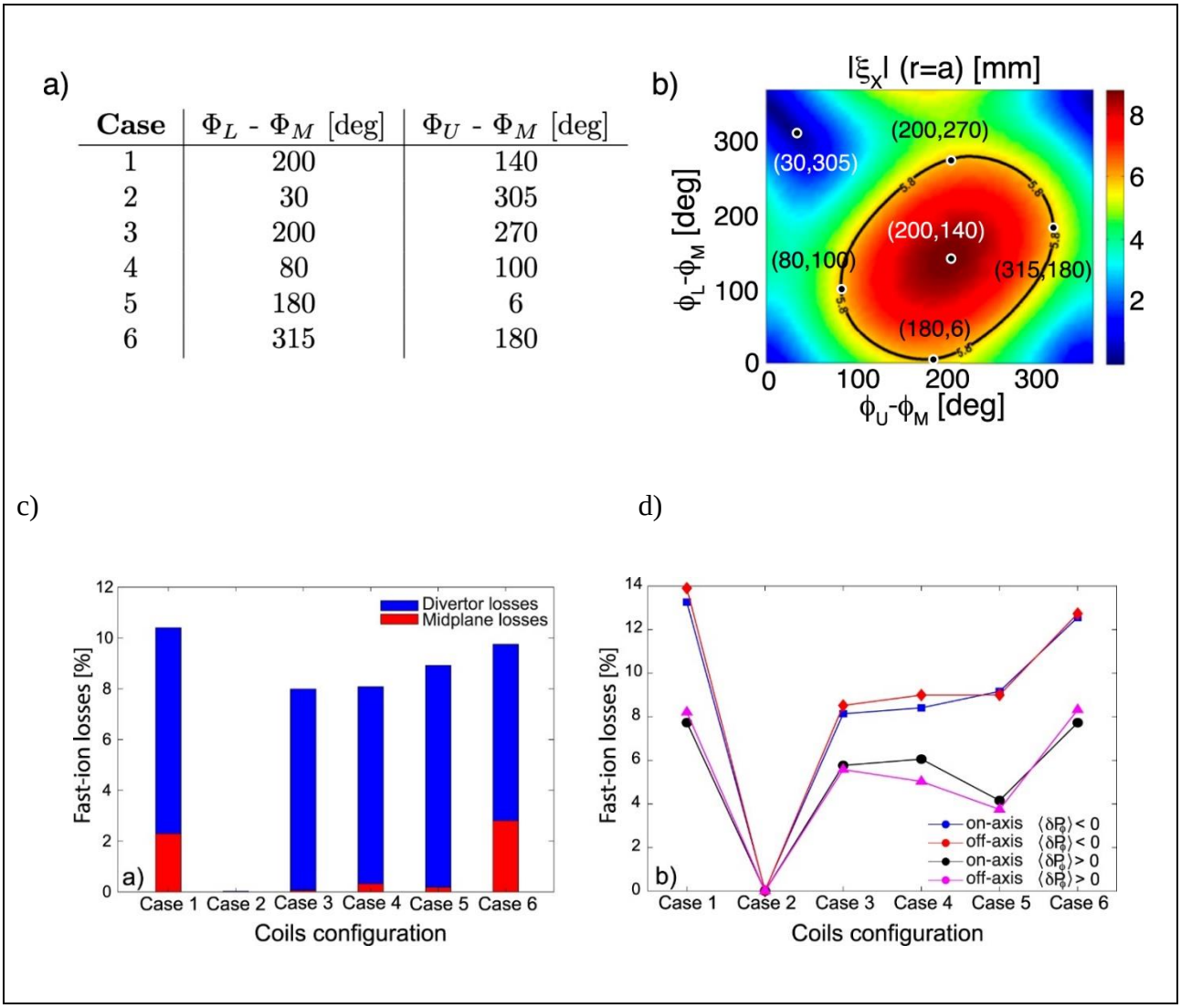

Figure 63. a) Differential phase shift of the upper (Φ_L-Φ_M) and lower (Φ_U-Φ_M) set of ELM control coils with respect to the coils in the middle row in ITER. b) MARS-F computed plasma surface displacement, ξ_X, near the X-point for an ITER $Q = 10$ plasma and maximum coil current; the relative toroidal phase shifts correspond to those shown in (a). Case 1 provides the best spectrum for ELM control while case 2 is the worst. Cases 3 - 6 have similar spectra regarding provision of ELM control. (c) Distribution of the fast-ion losses between the mid-plane and the divertor for the on-axis beam injection case with the absolute toroidal phases leading to the overall minimum losses ($\langle \delta P_\phi \rangle < 0$). (d) Fraction of lost fast-ions as a function of the perturbation poloidal mode spectra, including the on- and off-axis beam injections for the toroidal phase, leading to maximum or minimum losses $\langle \delta P_\phi \rangle < 0$ and $\langle \delta P_\phi \rangle > 0$ respectively) [219].

Disclaimer

The views and opinions expressed herein do not necessarily reflect those of the ITER Organization.

References

This ITER Technical Report may contain references to internal technical documents. These are accessible to ITER staff and External Collaborators included in the corresponding ITER Document Management (IDM) lists. If you are not included in these lists and need to access a specific technical document referenced in this report, please contact us at ITR.support@iter.org and your request will be considered, on a case by case basis, and in light of applicable ITER regulations.